

Natural Balancing of the Three-phase 2-cell and 3-cell Multicell Converters

By

Isaac Mahijoko Salagae

*Dissertation presented in fulfilment of the requirements for the
degree of Doctor of Philosophy in Engineering
at Stellenbosch University*



Promotor: Prof H. Du T. Mouton
Department of Electrical and Electronic Engineering

Co-promotor: Dr R.H. Wilkinson
Department of Electrical Engineering, Cape Peninsula University of Technology

March 2010

Declaration

By submitting this dissertation electronically, I declare that the entirety of the work contained therein is my own, original work, that I am the owner of the copyright thereof (unless to the extent explicitly otherwise stated) and that I have not previously in its entirety or in part submitted it for obtaining any qualification.

March 2010

Summary

The multicell inverter, being a widely used multilevel converter, has received much attention in recent years due to problems associated with cell capacitor voltage. In this dissertation we study the balancing problem with a focus on steady-state unbalance. This is achieved by systematic and mathematically rigorous study of the natural balancing mechanisms of the three-phase 2-cell and 3-cell multicell converter, undertaken by using dynamic modelling of the multicell converter, Bennet's geometric model, steady-state and time constant analysis. Space vector analysis is also performed for the three-phase 2-cell multicell converter. The theory is verified by comparing theoretical results with simulation results.

Opsomming

Die multisel omkeerder as algemeen-gebruikte meervlakkige omsetter het die afgelope jare groot belangstelling gewek op grond van die probleme wat met selkapsitor stroomspanning geassosieer word. In hierdie proefskrif word die balanseringsprobleem met die klem op die ewewigswanbalans bestudeer. Dit is verrig deur 'n sistematiese en streng wiskundige studie van die natuurlike balanseringsmeganismes van die drie-fase 2-sel en 3-sel multisel omsetter te maak. Dit is gedoen deur die gebruik van dinamiese modellering van die multisel omsetter, Bennet se geometriese model, ewewigtoestand tydkonstante analises, en ruimtevektoranalise is vir die drie-fase 2-sel multisel omsetter gedoen. Die teorie word bevestig deur die teoretiese resultate met die simuleringsresultate te vergelyk.

Acknowledgements

I would like to thank God almighty, ... *Bless the Lord, O my soul, And forget not all His benefits;.... Psalm 103:2*

I would also like to acknowledge and express my heartfelt gratitude to the following people and institutions:

My supervisors Prof. H. du T. Mouton and Dr R.H. Wilkinson for their extraordinary patience in guiding and supporting me; and for giving me the opportunity to do this project.

Rre eleng Gaetshelwe Salagae, yo mmogo le moswi mme Sikhi ba nnileng le bopelotelele, lorato le thotloetso e kgolo mo dithutong tsa me.

Bo nkgonne eleng Kanatu, Rabaki, Modukanele, Elija le kgaitsadiaka Magorogotlho ba kemonokeng ya bone e nnileng tlhwatlhwa kgolo mo diphitlhelelong tsa dithuto tsa me.

My wife Ncumisa for her patience, support and prayers.

My relatives and friends for their support during difficult times.

Morahe wa Ga-Maidi ko motseng wa Manthe le metsana ya one. Ba ba nthutile gore phitlhelelo ya a le mongwe, ke phitlhelelo ya morahe.

The members of the Power Electronics Research Group of the University of Stellenbosch for their support. In particular I would like to thank Francois Koeslag, Daleen Kleyn and the Serdyn brothers Neel and Jaco.

Andrew Mellon Foundation for their financial support.

Contents

1	Introduction	1
1.1	Multilevel Converters	1
1.1.1	Cascaded multicell	2
1.1.2	Diode-clamped converters	2
1.1.3	Capacitor-clamped converter	3
1.2	Research Objective	4
2	Literature Review	6
2.1	Meynard et al.'s Model	6
2.2	Barbi et al.'s Model	9
2.3	Ruderman et al.'s Model	12
2.4	Holmes et al.'s Model	14
2.5	Wilkinson et al.'s Model	17
2.6	Summary	18
3	Circuit and Spectral Analysis	19
3.1	Introduction	19
3.2	Operation of Multicell Converter	20
3.3	2-cell Multicell Converter	21
3.3.1	Circuit analysis	21
3.3.2	Equivalent circuit	22
3.4	Circuit Analysis of 3-Cell Multicell Converter	25
3.4.1	Circuit analysis	25
3.4.2	Equivalent circuit	26
3.5	Interleaved Switching	29
3.5.1	Switching functions of a single-cell converter	29
3.5.2	Switching functions of 2-cell converter	34
3.5.3	Switching functions of 3-cell converter	50
3.6	Summary	61

4	Steady State Analysis	62
4.1	Introduction	62
4.2	Steady State Balancing of 2-cell Converter	62
4.3	Steady State Balancing of 3-Cell Multicell Converter	76
4.4	Summary	92
5	Time Constant Analysis	93
5.1	Introduction	93
5.2	2-Cell Multicell Converter	94
5.2.1	Time Constant	94
5.2.2	Simulations	99
5.3	3-Cell Multicell Converter	105
5.3.1	Time constant	105
5.4	Summary	117
6	Space Vector Analysis	118
6.1	Introduction	118
6.2	Switching Vectors	118
6.3	Duty Cycles	122
6.3.1	Duty cycles for Sector I	123
6.3.2	Waveforms of V_{refa} , V_{refb} and V_{refc}	130
6.4	Simulations	133
6.4.1	Boundary for Regions A, B, C and D	133
6.4.2	Combination of switching states	135
6.4.3	Simulation results	136
6.5	Summary	141
7	Summary and Conclusions	142
7.1	Contributions and conclusions from this study	142
7.2	Conclusion	143
7.3	Future Work	143
A	Fourier Coefficients	152
A.1	Fourier Coefficients Calculations	152
A.2	Properties of Fourier Coefficients	156
B	Newton-Raphson Simulation	158
B.1	Theoretical Background	158
B.1.1	Newton Raphson Theory	158
B.1.2	Shift in time	159

B.2	Newton-Raphson Method for Simulation of a 2-cell Converter	159
B.2.1	Derivation of the spectrum for the switching function $s_{a1}(t)$	160
B.2.2	Derivation of the spectrum for the switching function $s_{a2}(t)$	164
B.2.3	Derivation of the spectrum for the switching function $s_{da}(t)$	168
B.2.4	Derivation of the spectrum for the switching function $s_{ta}(t)$	170
B.2.5	Derivation of the spectrum for the switching function $s_{b1}(t)$	173
B.2.6	Derivation of the spectrum for the switching function $s_{b2}(t)$	177
B.2.7	Derivation of the spectrum for the switching function $s_{db}(t)$	180
B.2.8	Derivation of the spectrum for the switching function $s_{tb}(t)$	182
B.2.9	Derivation of the spectrum for the switching function $s_{c1}(t)$	184
B.2.10	Derivation of the spectrum for the switching function $s_{c2}(t)$	188
B.2.11	Derivation of the spectrum for the switching function $s_{dc}(t)$	192
B.2.12	Derivation of the spectrum for the switching function $s_{tc}(t)$	194
B.3	Newton-Raphson Method for Simulation of a 3-cell converter	196
B.3.1	Derivation of the spectrum for the switching function $s_{a2}(t)$	196
B.3.2	Derivation of the spectrum for the switching function $s_{a3}(t)$	200
B.3.3	Derivation of the spectrum for the switching function $s_{b2}(t)$	204
B.3.4	Derivation of the spectrum for the switching function $s_{b3}(t)$	208
B.3.5	Derivation of the spectrum for the switching function $s_{c2}(t)$	212
B.3.6	Derivation of the spectrum for the switching function $s_{c3}(t)$	216
C	Phasor Diagrams	221
C.1	2-cell Multicell	221
C.1.1	For frequency modulation index $m_f = 3k$	221
C.1.2	For frequency modulation index $m_f = 3k + 1$	239
C.1.3	For frequency modulation index $m_f = 3k + 2$	253
C.2	3-cell Multicell	267
C.2.1	For frequency modulation index $m_f = 3k$	268
C.2.2	For frequency modulation index $m_f = 3k + 1$	289
C.2.3	For frequency modulation index $m_f = 3k + 2$	307
D	Duty Cycles for Other Five Sectors	325
D.1	Duty Cycles for Sector II	325
D.1.1	Region IIA	325
D.1.2	Region IIC	327
D.1.3	Region IIB	327
D.1.4	Region IID	328

D.2	Duty cycles for Sector III	329
D.2.1	Region IIIA	329
D.2.2	Region IIIC	330
D.2.3	Region IIIB	331
D.2.4	Region IIID	332
D.3	Duty cycles for Sector IV	332
D.3.1	Region IVA	332
D.3.2	Region IVC	334
D.3.3	Region IVB	334
D.3.4	Region IVD	335
D.4	Duty cycles for Sector V	336
D.4.1	Region VA	336
D.4.2	Region VC	337
D.4.3	Region VB	338
D.4.4	Region VD	339
D.5	Duty cycles for Sector VI	339
D.5.1	Region VIA	339
D.5.2	Region VIC	341
D.5.3	Region VIB	341
D.5.4	Region VID	342
E	Switching Combinations	343
E.1	Sector I	343
E.1.1	Region A	343
E.1.2	Region B	345
E.1.3	Region C	348
E.1.4	Region D	350
E.2	Sector II	352
E.2.1	Region A	352
E.2.2	Region C	354
E.2.3	Region B	355
E.2.4	Region D	357
E.3	Sector III	359
E.3.1	Region A	359
E.3.2	Region C	361
E.3.3	Region B	362
E.3.4	Region D	364
E.4	Sector IV	365
E.4.1	Region A	366

E.4.2	Region C	367
E.4.3	Region B	369
E.4.4	Region D	370
E.5	Sector V	372
E.5.1	Region A	372
E.5.2	Region C	374
E.5.3	Region B	375
E.5.4	Region D	377
E.6	Sector VI	379
E.6.1	Region A	379
E.6.2	Region C	381
E.6.3	Region B	382
E.6.4	Region D	384
E.7	Combination of switching states	386
E.7.1	First Combination for reference vector moving through regions C, B and D	386
E.7.2	Third Combination for reference vector moving through regions C, B and D	388
E.7.3	First Combination for reference vector moving through region A . .	391
E.7.4	Third Combination for reference vector moving through region A .	392

List of Figures

1.1	Cascaded multicell	2
1.2	Five level diode-clamp converter	3
1.3	2-cell 3-phase multicell converter	4
2.1	Commutation cell	6
2.2	Spontaneous cell capacitor current control loop	9
2.3	Half-bridge three-level capacitor-clamping converter	10
2.4	Single-phase three-level Flying Capacitor Converter with an RL load	13
2.5	DC modulation and corresponding switch states	13
2.6	Three phase flying capacitor converter	14
3.1	Multilevel commutation cell	20
3.2	Two-port circuit	20
3.3	2-cell 3-phase multicell converter	21
3.4	Phase A of 2-cell 3-phase multicell converter without load.	22
3.5	Equivalent circuit of Figure 3.4	24
3.6	Equivalent circuit for 2-cell 3-phase multicell converter	24
3.7	3-cell 3-phase multicell converter	25
3.8	Equivalent circuit for 3-cell 3-phase multicell converter	28
3.9	Generation of interleaved switching for cell 1 of phase A of 2-cell multicell converter	30
3.10	Construction of the background function $F(h, t)$	30
3.11	Construction of the background function $F(h, t)$	31
3.12	Top view of the three-dimensional background function	32
3.13	Generation of interleaved switching 2-cell multicell converter	34
3.14	Generation of interleaved switching 2-cell multicell converter	34
3.15	Top view of the background function of $s_{a1}(t)$ and $s_{a2}(t)$	36
3.16	Phasor representation for phase A of 2-cell converter	37
3.17	Phase B background function after $\frac{T_0}{3}$ phase-shift.	39
3.18	Generation of interleaved switching 2-cell multicell converter $m_f = 3k + 1$ for s_{b1}	39

3.19	Phase C background function after $\frac{2T_0}{3}$ phase-shift	41
3.20	Generation of interleaved switching 2-cell multicell converter $m_f = 3k + 2$ for s_{c2}	42
3.21	Top view of the background functions for the case of (a) $m_f = 3k + 1$ and (b) $m_f = 3k + 2$	43
3.22	Amplitude spectrum of $S_{da}(\omega)$ generated using (a) Newton-Raphson sim- ulation and (b) Theory	45
3.23	Phase spectrum of $S_{da}(\omega)$ generated using (a) Newton-Raphson simulation and (b) Theory	46
3.24	Amplitude spectrum of $S_{ta}(\omega)$ generated using (a) Newton-Raphson sim- ulation and (b) Theory	46
3.25	Phase spectrum of $S_{ta}(\omega)$ generated using (a) Newton-Raphson simulation and (b) Theory	47
3.26	Phase spectrum of $S_{db}(\omega)$ generated using (a) Newton-Raphson simulation and (b) Theory	47
3.27	Phase spectrum of $S_{tb}(\omega)$ generated using (a) Newton-Raphson simulation and (b) Theory	48
3.28	Phase spectrum of $S_{dc}(\omega)$ generated using (a) Newton-Raphson simulation and (b) Theory	48
3.29	Phase spectrum of $S_{tc}(\omega)$ generated using (a) Newton-Raphson simulation and (b) Theory	49
3.30	Generation of interleaved switching 3-cell multicell converter	51
3.31	Generation of interleaved switching 3-cell multicell converter	52
3.32	Generation of interleaved switching 3-cell multicell converter	53
3.33	Top view of the background functions for the case of (a) $m_f = 3k$ and (b) $m_f = 3k + 1$	55
3.34	(a)Harmonics of $S_{da1}(\omega)$ derived from simulation (b)Harmonics of $S_{da1}(\omega)$ derived from theory	59
3.35	(a)Harmonics of $S_{ta}(\omega)$ derived from simulation (b)Harmonics of $S_{ta}(\omega)$ derived from theory	59
3.36	(a)Harmonics of $ S_{da1}(\omega) S_{ta}(\omega) $ derived from simulation (b)Harmonics of $ S_{da1}(\omega) S_{ta}(\omega) $ derived from theory	60
4.1	Equivalent circuit of 2-cell 3-phase multicell converter	63
4.2	(a)Amplitude spectrum of $ B_{al} $ and (b)Amplitude spectrum of $ D_{al} $	72
4.3	(a)Amplitude spectrum of $ A_{al} $ and (b)Amplitude spectrum of $ D_{al} B_{al} $.	72
4.4	(a)Amplitude spectrum of $ B_{al} $ and (b)Amplitude spectrum of $ D_{al} $	73
4.5	(a)Amplitude spectrum of $ A_{al} $ and (b)Amplitude spectrum of $ D_{al} B_{al} $.	73
4.6	(a)Amplitude spectrum of $ B_{al} $ and (b)Amplitude spectrum of $ D_{al} $	74

4.7 (a)Amplitude spectrum of $|A_{al}|$ and (b)Amplitude spectrum of $|D_{al}| |B_{al}|$. 74

4.8 Equivalent circuit of 3-cell 3-phase multicell converter 76

4.9 (a)Amplitude spectrum of $|B_{al}|$ and (b)Amplitude spectrum of $|D_{a1l}|$. . . 89

4.10 (a)Amplitude spectrum of $|A_{al}|$ and (b)Amplitude spectrum of $|D_{a2l}|$. . . 89

4.11 (a)Amplitude spectrum of $|D_{a1l}| |B_{al}|$ and (b)Amplitude spectrum of $|D_{a2l}| |B_{al}|$ 90

4.12 (a)Amplitude spectrum of $|B_{al}|$ and (b)Amplitude spectrum of $|D_{a1l}|$. . . 90

4.13 (a)Amplitude spectrum of $|A_{al}|$ and (b)Amplitude spectrum of $|D_{a2l}|$. . . 91

4.14 (a)Amplitude spectrum of $|D_{a1l}| |B_{al}|$ and (b)Amplitude spectrum of $|D_{a2l}| |B_{al}|$ 91

5.1 Equivalent circuit of the 2-cell three-phase multicell converter with voltage source short-circuited 94

5.2 Exponential decay of $V_{\delta a}$, $V_{\delta b}$ and $V_{\delta c}$ for modulation index of 0.6 without balancing circuit. The blue curve is obtained using Simplorer simulation and the red curve is obtained from theoretical results. 99

5.3 Exponential decay of $V_{\delta a}$, $V_{\delta b}$ and $V_{\delta c}$ for modulation index of 0.8 without balancing circuit. The blue curve is obtained using Simplorer simulation and the red curve is obtained from theoretical results. 100

5.4 Exponential decay of $V_{\delta a}$, $V_{\delta b}$ and $V_{\delta c}$ for modulation index of 1 without balancing circuit. The blue curve is obtained using Simplorer simulation and the red curve is obtained from theoretical results 100

5.5 Balancing circuit 101

5.6 2-cell multicell converter with a balancing circuit connected 101

5.7 The frequency response plot for the RLC balance booster circuit 102

5.8 Effect of the quality factor 103

5.9 Exponential decay of $V_{\delta a}$, $V_{\delta b}$ and $V_{\delta c}$ for modulation index of 0.6 with balancing circuit. The blue curve is obtained using Simplorer simulation and the red curve is obtained from theoretical results 104

5.10 Exponential decay of $V_{\delta a}$, $V_{\delta b}$ and $V_{\delta c}$ for modulation index of 0.8 with balancing circuit. The blue curve is obtained using Simplorer simulation and the red curve is obtained from theoretical results 104

5.11 Exponential decay of $V_{\delta a}$, $V_{\delta b}$ and $V_{\delta c}$ for modulation index of 1 with balancing circuit. The blue curve is obtained using Simplorer simulation and the red curve is obtained from theoretical results 105

5.12 Equivalent circuit of 3-cell three-phase multicell converter with voltage source short-circuited 105

5.13 $V_{\delta a1}$ for modulation index of 1 without balancing circuit. The blue line=Simplorer simulation and the red line= theoretical simulation 113

5.14 $V_{\delta a1}$ for modulation index of 0.8 without balancing circuit. The blue line=Simplorer simulation and the red line= theoretical simulation 114

5.15 $V_{\delta a1}$ for modulation index of 0.6 without balancing circuit. The blue line=Simplorer simulation and the red line= theoretical simulation 114

5.16 $V_{\delta a1}$ for modulation index of 0.4 without balancing circuit. The blue line=Simplorer simulation and the red line= theoretical simulation 115

5.17 $V_{\delta a1}$ for modulation index of 1 with balancing circuit. The blue line=Simplorer simulation and the red line= theoretical simulation 115

5.18 $V_{\delta a1}$ for modulation index of 0.8 with balancing circuit. The blue line=Simplorer simulation and the red line= theoretical simulation 116

5.19 $V_{\delta a1}$ for modulation index of 0.6 with balancing circuit. The blue line=Simplorer simulation and the red line= theoretical simulation 116

5.20 $V_{\delta a1}$ for modulation index of 0.4 with balancing circuit. The blue line=Simplorer simulation and the red line= theoretical simulation 117

6.1 Switching vectors of a three-level Multicell converter 119

6.2 Regions of vector modulation of the 2-cell multicell converter in the first sector 123

6.3 PWM for duty cycles of region IA1 124

6.4 PWM for Duty cycles of Region IA2 125

6.5 PWM for Duty cycles of Region IB1 126

6.6 PWM for Duty cycles of region IB2 127

6.7 PWM for duty cycles of Region IC 128

6.8 PWM for Duty cycles of Region ID 129

6.9 Waveform of reference vectors V_{refa} , V_{refb} and V_{refc} for the six sectors of the 2-cell multicell converter passing through regions C and D for $m_a = \sqrt{2}$ 130

6.10 Waveform of reference vectors V_{refa} , V_{refb} and V_{refc} for the six sectors of the 2-cell multicell converter passing through regions C, B and D for $m_a = \frac{2}{\sqrt{3}}$ 131

6.11 Waveform of reference vectors V_{refa} , V_{refb} and V_{refc} for the six sectors of the 2-cell multicell converter passing through region A for $m_a = \frac{1}{\sqrt{6}}$ 132

6.12 Waveform of reference vectors V_{refa} , V_{refb} and V_{refc} for the six sectors of the 2-cell multicell converter passing through region B for $m_a = \sqrt{\frac{2}{3}}$ 133

6.13 Sector I with coordinates for each region 134

6.14 (a)Phase voltage and (b)Line voltage for reference voltage vector in regions C, B and D 136

6.15 (a) Switching functions of $s_{da}(t)$ and (b) $s_{ta}(t)$ in time domain for reference voltage vector in regions C, B and D 137

6.16 (a) Harmonics of $S_{da}(\omega)$ and (b) $S_{ta}(\omega)$ for reference voltage vector in regions C, B and D 137

6.17 (a)Phase voltage and (b)Line voltage for reference voltage vector in regions C and D 137

6.18	(a) Switching functions of $s_{da}(t)$, $s_{da}(t)$ and (b) $s_{da}(t) \cdot s_{da}(t)$ in time domain for reference voltage vector in regions C and D	138
6.19	(a) Harmonics of $s_{da}(t)$, $S_{da}(\omega)$ and (b) $S_{da}(t) \cdot s_{da}(\omega)$ for reference voltage vector in regions C and D	138
6.20	(a) Phase voltage and (b) Line voltage for reference voltage vector in regions A and B	138
6.21	(a) Switching functions of $s_{da}(t)$ and (b) $s_{ta}(t)$ in time domain for reference voltage vector in regions A and B	139
6.22	(a) Harmonics of $S_{da}(\omega)$ and (b) $S_{ta}(\omega)$ for reference voltage vector in regions A and B	139
6.23	(a) Phase voltage and (b) Line voltage for reference voltage vector in region B	139
6.24	(a) Switching functions of $s_{da}(t)$ and (b) $s_{ta}(t)$ in time domain for reference voltage vector in regions B	140
6.25	(a) Harmonics of $S_{da}(\omega)$ and (b) $S_{ta}(\omega)$ for reference voltage vector in regions B	140
6.26	Natural balancing for reference voltage vector (a) in region A and (b) in region B.	141
6.27	Natural balancing for reference voltage vector (a) in regions A and B and (b) in in regions C, B and D	141
A.1	Generation of interleaved switching single-cell multicell converter	152
B.1	Geometry behind Newton Raphson method	158
B.2	Newton-Raphson method of switching function $s_{a1}(t)$	160
B.3	Negative Pulse shift process by $t_{01} + \frac{W_1}{2}$	162
B.4	Positive Pulse shift process by $t_{02a1} + \frac{W_{2a1}}{2}$	163
B.5	Amplitude spectrum of $S_{a1}(\omega)$ generated using (a) Newton-Raphson simulation and (b) Theory	164
B.6	Phase spectrum of $S_{a1}(\omega)$ generated using (a) Newton-Raphson simulation and (b) Theory	164
B.7	Newton-Raphson method of switching function $s_{a2}(t)$	165
B.8	Phase spectrum of $S_{a2}(\omega)$ generated using (a) Newton-Rapson simulation and (b) Theory	168
B.9	Newton-Raphson method of switching function $s_{da}(t)$	168
B.10	Amplitude spectrum of $S_{da}(\omega)$ generated using (a) Newton-Rapson simulation and (b) Theory	170
B.11	Phase spectrum of $S_{da}(\omega)$ generated using (a) Newton-Raphson simulation and (b) Theory	170
B.12	Newton-Raphson method of switching function $s_{ta}(t)$	171

B.13 Amplitude spectrum of $S_{ta}(\omega)$ generated using (a) Newton-Raphson simulation and (b) Theory	172
B.14 Phase spectrum of $S_{ta}(\omega)$ generated using (a) Newton-Raphson simulation and (b) Theory	172
B.15 Newton-Raphson method of switching function $s_{b1}(t)$	173
B.16 Phase spectrum of $S_{b1}(\omega)$ generated using (a) Newton-Raphson simulation and (b) Theory	176
B.17 Newton-Raphson method of switching function $s_{b2}(t)$	177
B.18 Phase spectrum of $S_{b2}(\omega)$ generated using (a) Newton-Raphson simulation and (b) Theory	180
B.19 Newton-Raphson method of switching function $s_{db}(t)$	181
B.20 Phase spectrum of $S_{db}(\omega)$ generated using (a) Newton-Raphson simulation and (b) Theory	182
B.21 Newton-Raphson method of switching function $s_{tb}(t)$	183
B.22 Phase spectrum of $S_{tb}(\omega)$ generated using (a) Newton-Raphson simulation and (b) Theory	184
B.23 Newton-Raphson method of switching function $s_{c1}(t)$	184
B.24 Phase spectrum of $S_{c1}(\omega)$ generated using (a) Newton-Raphson simulation and (b) Theory	188
B.25 Newton-Raphson method of switching function $s_{c2}(t)$	188
B.26 Phase spectrum of $S_{c2}(\omega)$ generated using (a) Newton-Raphson simulation and (b) Theory	192
B.27 Newton-Raphson method of switching function $s_{dc}(t)$	192
B.28 Phase spectrum of $S_{dc}(\omega)$ generated using (a) Newton-Raphson simulation and (b) Theory	194
B.29 Newton-Raphson method of switching function $s_{tc}(t)$	194
B.30 Phase spectrum of $S_{tc}(\omega)$ generated using (a) Newton-Raphson simulation and (b) Theory	196
B.31 Newton-Raphson method of switching function $s_{a2}(t)$	197
B.32 Phase spectrum of $S_{a2}(\omega)$ generated using (a) Newton-Raphson simulation and (b) Theory	200
B.33 Newton-Raphson method of switching function $s_{a3}(t)$	200
B.34 Phase spectrum of $S_{a3}(\omega)$ generated using (a) Newton-Raphson simulation and (b) Theory	204
B.35 Newton-Raphson method of switching function $s_{b2}(t)$	204
B.36 Phase spectrum of $S_{b2}(\omega)$ generated using (a) Newton-Raphson simulation and (b) Theory	208
B.37 Newton-Raphson method of switching function $s_{b3}(t)$	208

B.38 Phase spectrum of $S_{b3}(\omega)$ generated using (a) Newton-Raphson simulation and (b) Theory	212
B.39 Newton-Raphson method of switching function $s_{c2}(t)$	212
B.40 Phase spectrum of $S_{c2}(\omega)$ generated using (a) Newton-Raphson simulation and (b) Theory	216
B.41 Newton-Raphson method of switching function $s_{c3}(t)$	216
B.42 Phase spectrum of $S_{c3}(\omega)$ generated using (a) Newton-Raphson simulation and (b) Theory	220
C.1 Phasor representation for phase A of 2-cell converter	224
C.2 Phasor representation for phase B of 2-cell converter for $n = 3p$ or $n = -3p$	229
C.3 Phasor representation for phase B of 2-cell converter for $n = 3p + 1$ or $n = -(3p + 2)$	230
C.4 Phasor representation for phase B of 2-cell converter for $n = 3p + 2$ or $n = -(3p + 1)$	231
C.5 Phasor representation for phase C of 2-cell converter for $n = 3p$ or $n = -3p$	236
C.6 Phasor representation for phase C of 2-cell converter for $n = 3p + 1$ or $n = -(3p + 2)$	237
C.7 Phasor representation for phase C of 2-cell converter for $n = 3p + 2$ or $n = -(3p + 1)$	238
C.8 Phase B phasor representation of 2-cell converter for $n = 3p$ or $n = -3p$. .	243
C.9 Phasor representation for phase B of 2-cell converter for $n = 3p + 1$ or $n = -(3p + 2)$	244
C.10 Phasor representation for phase B of 2-cell converter for $n = 3p + 2$ or $n = -(3p + 1)$	245
C.11 Phasor representation for phase C of 2-cell converter for $n = 3p$ or $n = -3p$	250
C.12 Phasor representation for phase C of 2-cell converter for $n = 3p + 1$ or $n = -(3p + 2)$	251
C.13 Phasor representation for phase C of 2-cell converter for $n = 3p + 2$ or $n = -(3p + 1)$	252
C.14 Phasor representation for phase B of 2-cell converter for $n = 3p$ or $n = -3p$	257
C.15 Phasor representation for phase B of 2-cell converter for $n = 3p + 1$ or $n = -(3p + 2)$	258
C.16 Phasor representation for phase B of 2-cell converter for $n = 3p + 2$ or $n = -(3p + 1)$	259
C.17 Phasor representation for phase C of 2-cell converter for $n = 3p$ or $n = -3p$	264
C.18 Phasor representation for phase C of 2-cell converter for $n = 3p + 1$ or $n = -(3p + 2)$	265

C.19 Phasor representation for phase C of 2-cell converter for $n = 3p + 2$ or $n = -(3p + 1)$ 266

C.20 Phasor representation for phase A of 3-cell converter 271

C.21 Phasor representation for phase B of 3-cell converter for $m = 3k$ 277

C.22 Phasor representation for phase B of 3-cell converter for $m = 3k + 1$ 278

C.23 Phasor representation for phase B of 3-cell converter for $m = 3k + 2$ 279

C.24 Phasor representation for phase C of 3-cell converter for $m = 3k$ 286

C.25 Phasor representation for phase C of 3-cell converter for $m = 3k + 1$ 287

C.26 Phasor representation for phase C of 3-cell converter for $m = 3k + 2$ 288

C.27 Phasor representation for phase B of 3-cell converter for $m = 3k$ 295

C.28 Phasor representation for phase B of 3-cell converter for $m = 3k + 1$ 296

C.29 Phasor representation for phase B of 3-cell converter for $m = 3k + 2$ 297

C.30 Phasor representation for phase C of 3-cell converter for $m = 3k$ 304

C.31 Phasor representation for phase C of 3-cell converter for $m = 3k + 1$ 305

C.32 Phasor representation for phase C of 3-cell converter for $m = 3k + 2$ 306

C.33 Phasor representation for phase B of 3-cell converter for $m = 3k$ 313

C.34 Phasor representation for phase B of 3-cell converter for $m = 3k + 1$ 314

C.35 Phasor representation for phase B of 3-cell converter for $m = 3k + 2$ 315

C.36 Phasor representation for phase C of 3-cell converter for $m = 3k$ 322

C.37 Phasor representation for phase C of 3-cell converter for $m = 3k + 1$ 323

C.38 Phasor representation for phase C of 3-cell converter for $3k + 2$ 324

D.1 Regions of vector modulation of the 2-cell multicell converter in the second sector 325

D.2 Regions of vector modulation of the 2-cell multicell converter in the third sector 329

D.3 Regions of vector modulation of the 2-cell multicell converter in the fourth sector 333

D.4 Regions of vector modulation of the 2-cell multicell converter in the fifth sector 336

D.5 Regions of vector modulation of the 2-cell multicell converter in the sixth sector 340

E.1 Regions of vector modulation of the 2-cell multicell converter in the first sector 343

E.2 Regions of vector modulation of the 2-cell multicell converter in the second sector 352

E.3 Regions of vector modulation of the 2-cell multicell converter in the third sector 359

E.4 Regions of vector modulation of the 2-cell multicell converter in the fourth sector 365

E.5 Regions of vector modulation of the 2-cell multicell converter in the fifth sector 372

E.6 Regions of vector modulation of the 2-cell multicell converter in the sixth sector 379

List of Tables

3.1	Values for t_x , c and h of background function for 2-cell multicell converter .	43
3.2	Observation from phasor diagrams for Phase A	44
3.3	Observation from phasor diagrams for Phase B	44
3.4	Observation from phasor diagrams for Phase C	44
3.5	Simulation parameters	45
3.6	Values for t_x and c of background function for 3-cell multicell converter . .	54
3.7	Values for t_x and c of background function for 3-cell multicell converter . .	54
3.8	Observation from phasor diagrams for Phase A	55
3.9	Observation from phasor diagrams for Phase B with $m_f = 3k$	56
3.10	Observation from phasor diagrams for Phase C with $m_f = 3k$	56
3.11	Observation from phasor diagrams for Phase B with $m_f = 3k + 1$	57
3.12	Observation from phasor diagrams for Phase C with $m_f = 3k + 1$	57
3.13	Observation from phasor diagrams for Phase B with $m_f = 3k + 2$	58
3.14	Observation from phasor diagrams for Phase C with $m_f = 3k + 2$	58
4.1	Different classes of harmonics	67
5.1	Simulation parameters	99
6.1	Zero switching vectors	120
6.2	Medium switching vectors	120
6.3	Large switching vectors	121
6.4	Small switching vectors	121
6.5	Small switching vectors	122
6.6	Simulation parameters	136
C.1	Values for t_x , c and h of background function for 2-cell multicell converter .	221
C.2	Values for t_x and c of background function for 3-cell multicell converter . .	267
C.3	Values for t_x and c of background function for 3-cell multicell converter . .	267

Glossary

Abbreviations

- DC : Direct current
- HVDC : High voltage direct current
- PWM : Pulsewidth modulation
- SVM : Space vector modulation

Symbols

C	: Filter capacitance
C_b	: Balancing circuit capacitance
C_d	: Cell capacitor
d	: Duty cycle
D_T	: Duty cycle
Δt	: The period that the particular vector is selected
f_0	: Fundamental frequency
f_r	: Reference frequency
f_s	: Switching frequency
ϵ	: Eigenvalue
i_a, i_b and i_c	: Phase currents
i_{ca}, i_{cb} and i_{cc}	: Cell capacitor currents for 2-cell converter
i_{ca1}, i_{cb1} and i_{cc1}	: Cell capacitor currents for 3-cell converter for the first cell
i_{ca2}, i_{cb2} and i_{cc2}	: Cell capacitor currents for 3-cell converter for the second cell
J	: Bessel function
L	: Output filter Inductor
L_b	: Balancing circuit inductance
m_a	: Modulation index
m_f	: Frequency modulation ratio
R	: Load resistor
R_b	: Balancing circuit resistance
\Re	: Real part of a complex number
s	: Switching function
s_{a1}, s_{a2} and s_{a3}	: Switching functions of phase A.
S_{a1}, S_{a2}, S_{a3} and S_{a4}	: Switches for phase A of Diode-Clamp converter.
S_{a5}, S_{a6}, S_{a7} and S_{a8}	: Switches for phase A of Diode-Clamp converter.
S_{a1t}, S_{a2t} and S_{a3t}	: Top switches for phase A of Multicell converter.
S_{a1b}, S_{a2b} and S_{a3b}	: Bottom switches for phase A of Multicell converter.
s_{b1}, s_{b2} and s_{b3}	: Switching functions of phase B.
S_{b1t}, S_{b2t} and S_{b3t}	: Top switches for phase B of Multicell converter.
S_{b1b}, S_{b2b} and S_{b3b}	: Bottom switches for phase B of Multicell converter.
s_{c1}, s_{c2} and s_{c3}	: Switching functions of phase C.
S_{c1t}, S_{c2t} and S_{c3t}	: Top switches for phase C of Multicell converter.
S_{c1b}, S_{c2b} and S_{c3b}	: Bottom switches for phase C of Multicell converter.

s_α , and s_β	: Switching functions in the $\alpha\beta$ -plane.
s_{da} , s_{db} and s_{dc}	: Difference switching function of each phase for 2-cell three-phase converter
s_{db1} and s_{db2}	: Difference switching function of phase B for 3-cell three-phase converter
s_{dc1} and s_{dc2}	: Difference switching function of phase C for 3-cell three-phase converter
s_{ta} , s_{tb} and s_{tc}	: Total switching functions.
t	: Time
τ	: Time constant
θ	: The angle position of a vector
T_r	: Reference period
T_s	: Switching period
v_{ab} , v_{bc} and v_{ac}	: Line voltages
v_{an} , v_{bn} and v_{cn}	: Phase voltages
v_{c1} , v_{c2} and v_{c3}	: Cell capacitor voltages for 2-cell converter
v_{ca1} , v_{cb1} and v_{cc1}	: Cell capacitor voltages for 3-cell converter for the first cell
v_{ca2} , v_{cb2} and v_{cc2}	: Cell capacitor voltages for 3-cell converter for the second cell
$V_{\delta a}$, $V_{\delta b}$ and $V_{\delta c}$: Cell capacitor voltage difference of each phase for 2-cell three-phase converter
$V_{\delta a1}$ and $V_{\delta a2}$: Cell capacitor voltage difference of phase A for 3-cell three-phase converter
$V_{\delta b1}$ and $V_{\delta b2}$: Cell capacitor voltage difference of phase B for 3-cell three-phase converter
$V_{\delta c1}$ and $V_{\delta c2}$: Cell capacitor voltage difference of phase C for 3-cell three-phase converter
v_{pa} , v_{pb} and v_{pc}	: Voltages across the load
V_t	: DC-bus voltage
V_r	: Reference voltage vector
V_{refa} , V_{refb} and V_{refc}	: Reference voltage vectors for the three phases
X_0	: Zero switching vector
X_1 , X_2 and X_3	: Small switching vectors
X_7 , \dots , X_{12}	: Medium switching vectors
X_{13} , \dots , X_{18}	: Large switching vectors
ω_0	: Fundamental angular frequency
ω_r	: Reference angular frequency
ω_s	: Switching angular frequency
Z	: Load impedance

Chapter 1

Introduction

This chapter introduces the reader to what motivated the present research into natural balancing of three-phase multicell converters. We begin this chapter by giving an overview of the development of multicell converters. However work done on natural balancing of multicell converters is treated separately in chapter 2. Furthermore we provide the research objective and the outline for achieving this objective.

1.1 Multilevel Converters

The need for high power ratings and reduction of harmonic content of generated voltage and current waveforms led to the design of different multilevel converter topologies. These converters use voltage clamps to equally share the input voltage between the series connected devices and supply a multilevel output voltage [1], [13], [14], [15], [16], [50]. The multilevel converter structure was introduced as a means of eliminating the need for the step-up transformer in high-voltage drives and reducing the output waveform harmonic content [17], [18].

The multilevel converter topology attempts to address some of the limitations of the standard two level converter. Because of their modular and simple structure, they can be stacked up to almost unlimited number of levels [51]. Motor damage and failure caused by adjustable-speed drive converters' high-voltage change rates(dv/dt)[16] was overcome by multilevel converters because their individual devices have a much lower (dv/dt) per switching and they operate at high efficiency because they can switch at a much lower frequency than PWM-controlled converters.

Increasing the output voltage meant raising the DC-bus voltage, which leads to significant problems with voltage sharing among switching devices connected in series during turn-on and turn-off [52],[53], thus limiting the number of devices to a maximum of five. This problem is avoided by employing multilevel converters because as the DC-bus voltage is raised, the voltage stress on each switching device can be held constant by adding more

levels to the converter. This helps in reducing the harmonics, because the increase in voltage levels leads to improved harmonic performance without increased switching loss and also reduces the filter size. Multilevel converters are used extensively in high-power applications with medium-voltage levels. Applications include laminators, mills, conveyors, pumps, fans, blowers and compressors [15]. The three most often used topologies for multilevel converters are briefly discussed in the following subsections.

1.1.1 Cascaded multicell

Cascaded multicell was not fully realised until Lai and Peng patented and presented its advantages in 1997. The interest in its research development ranges from small-power applications such as hybrid electric vehicles to very-high-power applications such as STATCOM and FACTS controllers. A cascaded multicell with separate DC source consists of half-bridge converter units connected in series as shown in Figure 1.1 [16], [70], [54]. Figure 1.1 depicts a cascaded multicell converter.

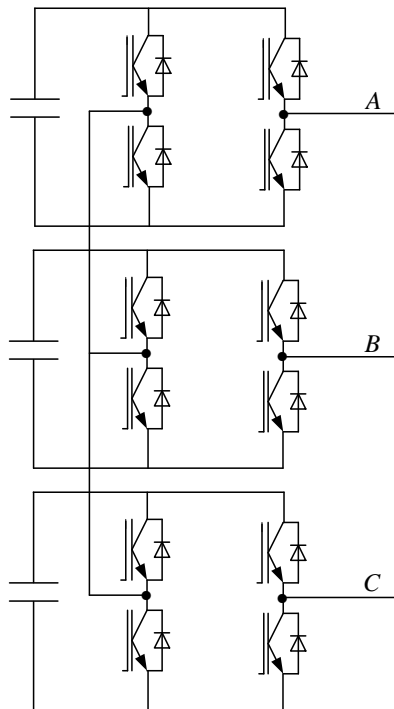


Figure 1.1: *Cascaded multicell*

1.1.2 Diode-clamped converters

This converter appeared in several papers including the study of vector control [19], [20] and of PWM strategy [55]. The topology consists of two capacitors that divide the DC-bus in half. Each phase leg consists of a number of switches in series connected via diode

to the tap points, which are connected to the neutral point between the two DC-bus capacitors as shown in Figure 1.2. Advantages of this converter include the improved quality of the output waveform and higher DC-bus voltage. Though initially intended for use in the reduction of current harmonics caused by nonsinusoidal voltage feeding that caused power losses, electromagnetic interferences and pulsating torques in ac motor drives [21], its applications now include a static var compensation system [22], [53], a high-voltage direct-current(HVDC) transmission system [23], [1], active filtering [23] and power conditioning systems for superconductive magnetic energy storage [23]. Figure 1.2 shows a five level diode-clamp converter.

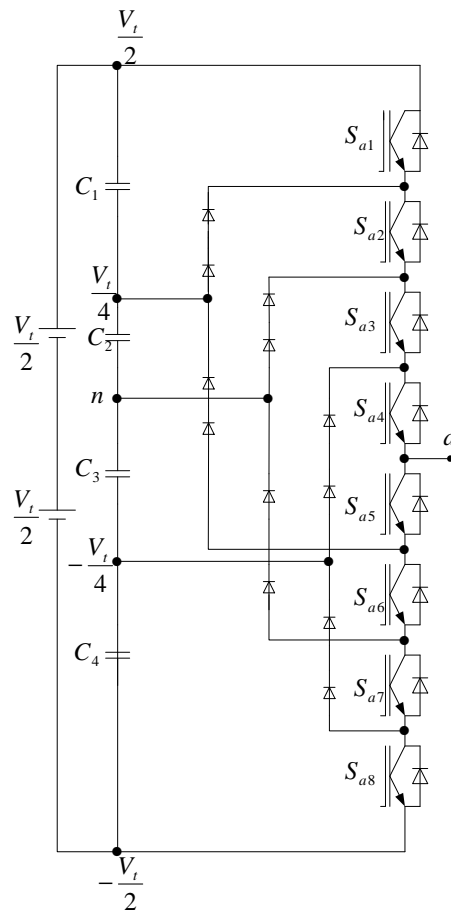


Figure 1.2: *Five level diode-clamp converter*

1.1.3 Capacitor-clamped converter

This converter, also known as a flying capacitor and multicell converter [50],[14],[24], consists of independent capacitors clamping the device voltage to one capacitor voltage level, allow an increase in the commutation voltage as well as the apparent frequency and having application in high-voltage DC transmission. Figure 1.3 shows a 2-cell 3-phase

multicell converter.

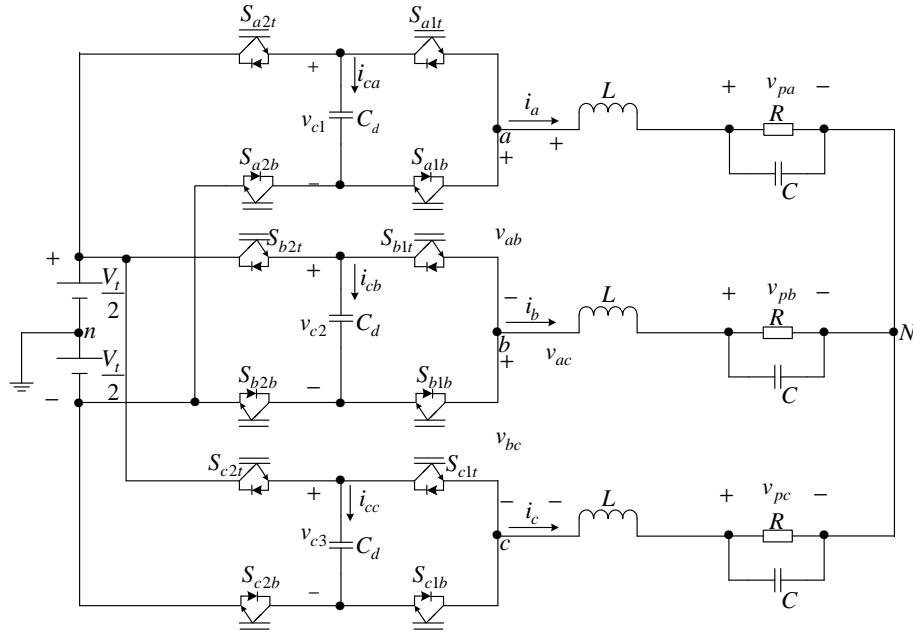


Figure 1.3: 2-cell 3-phase multicell converter

1.2 Research Objective

Natural balancing has been successfully applied in a series-stacked converter [71], a three-level NPC converter [25], [72], [56] and a single-phase p-cell multicell converter [73]. Though work has been done in the natural balancing of three-phase multicell converters [57], it has not been proved that their capacitor voltages naturally balance. This dissertation provides an insight into natural balancing of capacitor voltages of three-phase multicell converters. The work is divided into the following chapters:

Chapter 2 Literature Review

This chapter briefly reviews the work done by other authors in the natural balancing of capacitor voltages of multicell converters.

Chapter 3 Circuit and Spectral Analysis

This chapter analyses the switching functions of 2-cell and 3-cell three phase multicell converters using interleaved switching. It uses Bennet's geometric technique and Bowe's double Fourier series method to calculate the coefficients of the switching functions. Theoretical results are then verified with simulation results.

Chapter 4 Steady State Analysis

This chapter derives steady-state equations and uses them to describe the balancing of the cell capacitor voltages. This is done by mathematically modelling the coefficients of the switching functions to obtain the steady-state behaviour of the 2-cell and 3-cell three-phase multicell converter.

Chapter 5 Time Constant Analysis

This chapter calculates the time constants associated with the rebalancing of the DC-bus voltages. These time constants are then used to plot the exponential decay of the capacitor voltages. The results are then verified with simulations.

Chapter 6 Space Vector Analysis

This chapter studies the natural balancing of a 2-cell multicell converter under space vector modulation. It computes the switch combination sequences of 2-cell multicell and plots the waveform of the reference vector when in different regions of the six sectors. It then proves, using simulations, that a 2-cell multicell converter naturally balances under space-vector modulation.

Chapter 7 Conclusion

This chapter provides a summary and describes the contribution of this dissertation.

Chapter 2

Literature Review

In this chapter we review the work carried out on natural balancing of the cell capacitor voltages of multicell converters. Though progress has been made in the natural balancing of capacitor voltages, there is still opportunity for further investigation.

2.1 Meynard et al.'s Model

This model represents the self-balancing property of the imbricated cells of multilevel converters [24]. It focuses on the harmonic content of the cell capacitor currents which are modelled as functions of duty-cycles over the cells.

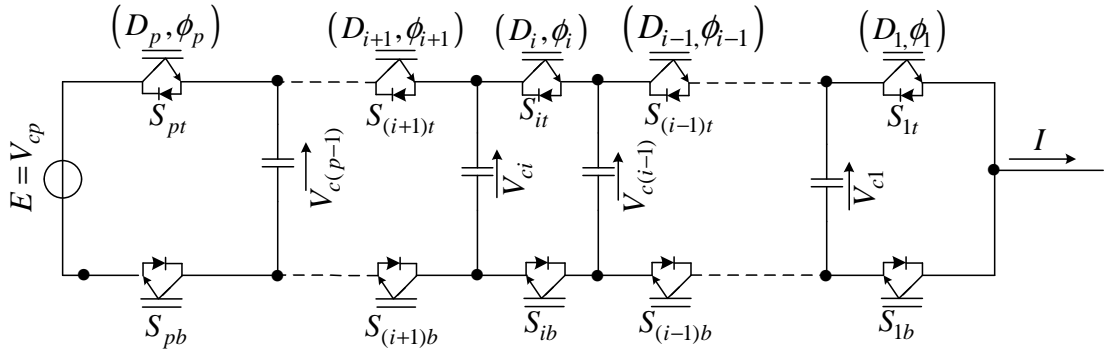


Figure 2.1: *Commutation cell*

Figure 2.1 consists floating interconnected capacitors and series connected switching devices. These floating capacitors act as DC-sources and thus have to be charged to the correct voltage. The voltage across each capacitor is determined by the input voltage and the number of cells. The sum of the instantaneous voltage across the switches is equal to the voltage E . The equation that describes the voltage across each cell capacitor is given by equation 2.1.

$$V_{ck} = i \cdot E/p, \quad i = 0, \dots, p. \quad (2.1)$$

The equivalent circuit is developed where each blocking switch is replaced with a voltage source and each conducting switch is replaced with a current source. The following assumptions were made:

- The switches are ideal; that is the on-state voltage, off-state currents, delays and switching times are zero.
- Dead times are zero.
- The floating capacitors are designed to limit the variations of the voltage applied to each commutation cell.
- The load has a time constant which is less than the switching period so that at each switching period, the load current is the steady state current.

The n th harmonic of a zero to one square signal with phase ϕ and duty cycle D is given by:

$$H_n = \frac{2}{n\pi} \sin(nD\pi) e^{jn\phi} \quad (2.2)$$

The n^{th} harmonic for the chopped voltage is given by:

$$V_s^n = \sum_{i=1}^p \frac{2}{m\pi} \sin(mD\pi) (V_{ci} - V_{ci-1}) e^{jn\phi_i} \quad (2.3)$$

The n^{th} harmonic for the load current is given by:

$$I^n = |I^n| e^{j\psi^n}$$

The average current in the top i^{th} switch S_{it} generated by the n^{th} harmonic of the load current is given by:

$$I_{S_{it}}^n = \frac{|I^n|}{n\pi} \cos(\psi^n - n\phi_i) \sin(nD_i\pi) \quad (2.4)$$

where ψ^n is the phase of the n^{th} harmonic of the load current.

The quantity G_i^n is given by:

$$G_i^n = \frac{1}{n\pi} \sin(nD_i\pi) e^{jn\phi_i} \quad (2.5)$$

Since $i_c = C \frac{dV_c}{dt}$ it follows that:

$$\dot{V}_{c_i}^n = \frac{1}{C_i} I_{C_i}^n \quad (2.6)$$

where $\dot{V}_{c_i}^n$ is the variation of the cell capacitor voltage over one switching period and $I_{C_i}^n$ is the average cell capacitor current over one switching period.

Rewriting $I_{C_i}^n = I_{S_{(i+1)t}}^n - I_{S_{it}}^n$ results in:

$$\dot{V}_{c_i}^n = \frac{1}{C_i} \Re e \left\{ \overline{G_{i+1}^n} - G_i^n I^n \right\} \quad (2.7)$$

With $I^n = \frac{V_s^n}{Z^n}$ the above equation is rewritten as:

$$\dot{V}_{C_i}^n = 2\Re e \left\{ \left[\frac{1}{C_i} \overline{G_{i+1}^n - G_i^n} \right] \frac{1}{Z^n} \left([\dots G_i^n - G_{i+1}^n \dots] [V_{C_i}^n] + G_p^n V_t \right) \right\} \quad (2.8)$$

Writing the above equation in the general form $\dot{X} = A \cdot X + B \cdot U$ with

$$X = V_{C_i}^n \quad (2.9)$$

$$U = V_t \quad (2.10)$$

$$A = \Re e \left\{ \left[\frac{1}{C_i} \overline{G_{i+1}^n - G_i^n} \right] \frac{1}{Z^n} [\dots G_i^n - G_{i+1}^n \dots] \right\} \quad (2.11)$$

$$B = \Re e \left\{ \left[\frac{1}{C_i} \overline{G_{i+1}^n - G_i^n} \right] \frac{1}{Z^n} G_p^n \right\} \quad (2.12)$$

Taking r harmonics into account equation 2.8 becomes:

$$[\dot{V}_{C_i}^n] = \sum_{n=1}^r 2\Re e 2\Re e \left\{ \left[\begin{array}{c} \vdots \\ \frac{1}{C_i} \overline{G_{i+1}^n - G_i^n} \\ \vdots \end{array} \right] \frac{1}{Z^n} \left([\dots G_i^n - G_{i+1}^n \dots] [V_{C_i}^n] + G_p^n V_t \right) \right\} \quad (2.13)$$

This results in a model

$$\dot{V}_{C_i} = A(D_i)V_{C_i} + B(D_i)V_t, \quad i = 1, \dots, p-1 \quad (2.14)$$

with

$$A = -2\Re e \left(\left[\begin{array}{ccc} \frac{G_1^1 - G_2^1}{C_1} & \dots & \frac{G_1^r - G_2^r}{C_1} \\ \vdots & \ddots & \vdots \\ \frac{G_{p-1}^1 - G_p^1}{C_{p-1}} & \dots & \frac{G_{p-1}^r - G_p^r}{C_{p-1}} \end{array} \right] \cdot \left[\begin{array}{ccc} \frac{G_1^1 - G_2^1}{Z^1} & \dots & \frac{G_1^r - G_2^r}{Z^1} \\ \vdots & \ddots & \vdots \\ \frac{G_{p-1}^1 - G_p^1}{Z^r} & \dots & \frac{G_{p-1}^r - G_p^r}{Z^r} \end{array} \right] \right) \quad (2.15)$$

$$B = 2\Re e \left(\left[\begin{array}{ccc} \frac{G_1^1 - G_2^1}{C_1} & \dots & \frac{G_1^r - G_2^r}{C_1} \\ \vdots & \ddots & \vdots \\ \frac{G_{p-1}^1 - G_p^1}{C_{p-1}} & \dots & \frac{G_{p-1}^r - G_p^r}{C_{p-1}} \end{array} \right] \cdot \left[\begin{array}{c} \frac{G_p^1}{Z^1} \\ \vdots \\ \frac{G_p^r}{Z^r} \end{array} \right] \right) \quad (2.16)$$

The following are the conclusions reached by the model:

- A static and dynamic model of multicell converters must take into account phenomena that occur within a switching period.
- Model techniques based on average values cannot represent the characteristics of a multicell converter.
- The harmonic content of the current is used to calculate the DC current in the cell capacitor currents which is used to construct an equivalent circuit that is used to derive state-equations of the model representing the converter.
- The model can be used to determine the steady-state as well as the dynamic response of the capacitor voltages.

2.2 Barbi et al.'s Model

This model is focussed on the self-balancing property of the cell capacitor voltages in a multicell converter [26]. The inverter is in a steady state in terms of cell capacitor voltages as long as the DC component of the current flowing through the clamping capacitor is zero. If this DC component deviates from zero, the cell capacitor will be charged or discharged, leading to load voltage variation, load current variation and in turn DC component variation in the cell-capacitor current. This model uses sub-harmonic PWM modulation, also known as interleaved switching, and it was observed that DC component variation will discharge or charge the cell capacitor until the DC component in the cell capacitor current returns to zero. The spontaneous cell capacitor current control loop is shown in Figure 2.2.

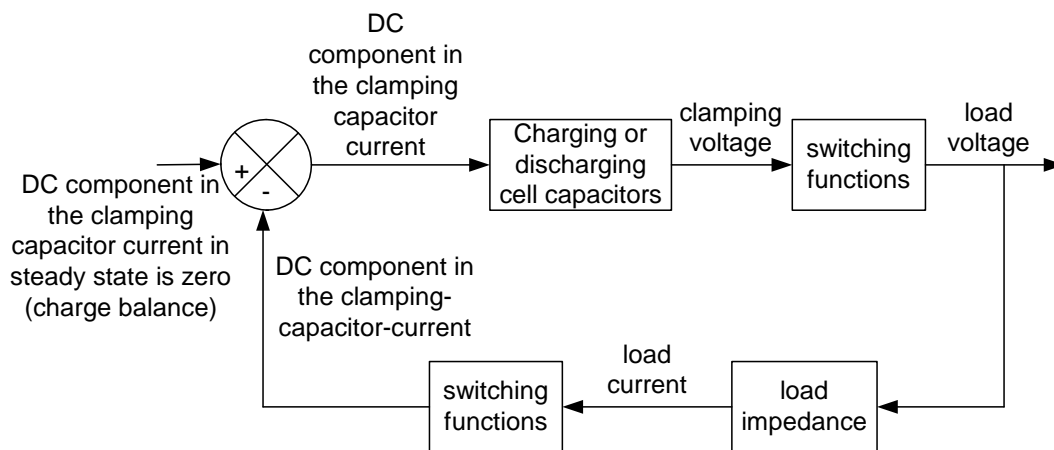


Figure 2.2: *Spontaneous cell capacitor current control loop*

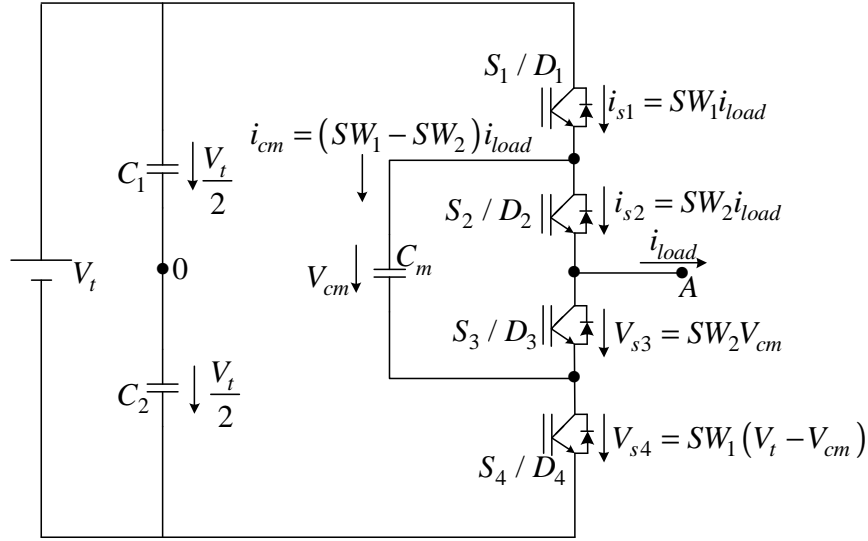


Figure 2.3: Half-bridge three-level capacitor-clamping converter

Figure 2.3 shows the structure of a half-bridge three-level capacitor-clamping converter. The switching functions generated using subharmonic modulation are expressed in Fourier form as follows:

$$\begin{aligned}
 s_1 &= \frac{1}{2} + \frac{M}{2} \sin(\omega_m t) + \sum_{m=1,3,5,\dots}^{\infty} (-1)^{\frac{m+1}{2}} \frac{2J_0^{\frac{mM\pi}{2}}}{m\pi} \sin(m\omega_c t - \frac{\pi}{2}) \\
 &+ \sum_{m=1,3,5,\dots}^{\infty} \sum_{n=\pm 2, \pm 4, \dots}^{\pm \infty} \frac{2J_n^{\frac{mM\pi}{2}}}{m\pi} \sin(\frac{m\pi}{2}) \cos[(m\omega_c t + n\omega_m t) - m\pi] \\
 &+ \sum_{m=2,4,\dots}^{\infty} \sum_{n=\pm 1, \pm 3, \dots}^{\pm \infty} \frac{2J_n^{\frac{mD\pi}{2}}}{m\pi} \cos(\frac{m\pi}{2}) \sin[(m\omega_c t + n\omega_m t) - m\pi] \quad (2.17)
 \end{aligned}$$

$$\begin{aligned}
 s_2 &= \frac{1}{2} + \frac{M}{2} \sin(\omega_m t) - \sum_{m=1,3,5,\dots}^{\infty} (-1)^{\frac{m+1}{2}} \frac{2J_0^{\frac{mM\pi}{2}}}{m\pi} \sin(m\omega_c t - \frac{\pi}{2}) \\
 &- \sum_{m=1,3,5,\dots}^{\infty} \sum_{n=\pm 2, \pm 4, \dots}^{\pm \infty} \frac{2J_n^{\frac{mM\pi}{2}}}{m\pi} \sin(\frac{m\pi}{2}) \cos[(m\omega_c t + n\omega_m t) - m\pi] \\
 &+ \sum_{m=2,4,\dots}^{\infty} \sum_{n=\pm 1, \pm 3, \dots}^{\pm \infty} \frac{2J_n^{\frac{mM\pi}{2}}}{m\pi} \cos(\frac{m\pi}{2}) \sin[(m\omega_c t + n\omega_m t) - m\pi] \quad (2.18)
 \end{aligned}$$

where M is the modulation index, ω_m is the modulating angular frequency, ω_c is the carrier angular frequency and J_n is the Bessel function of the first kind.

The load voltage variation in response to the deviation of the clamping-capacitor-voltage away from its steady state value is given by:

$$\begin{aligned} \Delta V_{A0} = & (V_{cm.steady} - V_{cm}) \left\{ \sum_{m=1,3,5,\dots}^{\infty} (-1)^{\frac{m+1}{2}} \frac{4J_0^{\frac{mM\pi}{2}}}{m\pi} \sin(m\omega_c t - \frac{\pi}{2}) \right. \\ & \left. + \sum_{m=1,3,5,\dots}^{\infty} \sum_{n=\pm 2, \pm 4, \dots}^{\pm \infty} \frac{4J_n^{\frac{mM\pi}{2}}}{m\pi} \sin(\frac{m\pi}{2}) \cos[(m\omega_c t + n\omega_m t) - m\pi] \right\} \end{aligned} \quad (2.19)$$

where $V_{cm.steady}$ is the steady state value of the cell capacitor voltage.

The load current variation resulting from the load voltage variation is given by:

$$\begin{aligned} \Delta i_{load} = & (V_{cm.steady} - V_{cm}) \left\{ \sum_{m=1,3,5,\dots}^{\infty} (-1)^{\frac{m+1}{2}} \frac{4J_0^{\frac{mM\pi}{2}}}{m\pi z_{m\omega_c}} \sin(m\omega_c t - \frac{\pi}{2} - \phi_{m\omega_c}) \right. \\ & \left. + \sum_{m=1,3,5,\dots}^{\infty} \sum_{n=\pm 2, \pm 4, \dots}^{\pm \infty} \frac{4J_n^{\frac{mM\pi}{2}}}{m\pi(z_{m\omega_c} + n\omega_m)} \sin(\frac{m\pi}{2}) \cos[(m\omega_c t + n\omega_m t) - m\pi - \phi_{m\omega_c} + n\omega_m] \right\} \end{aligned} \quad (2.20)$$

The corresponding cell capacitor current variation is given by:

$$\Delta i_{cm} = \Delta i_{load}(s_1 - s_2) \quad (2.21)$$

Substituting 2.17, 2.18 and 2.20 into 2.21, the DC component in the cell capacitor current variation is written as follows:

$$\Delta i_{cm.dc} = (V_{cm.steady} - V_{cm}) G \quad (2.22)$$

where

$$\begin{aligned} G = & \frac{1}{2} \left\{ \sum_{m=1,3,5,\dots}^{\infty} \left(\left[(-1)^{\frac{m+1}{2}} \frac{4J_0^{\frac{mM\pi}{2}}}{m\pi} \right]^2 \frac{1}{z_{m\omega_c}} \cos(\phi_{m\omega_c}) \right) \right. \\ & \left. + \sum_{m=1,3,5,\dots}^{\infty} \sum_{n=\pm 2, \pm 4, \dots}^{\pm \infty} \left[\frac{4J_n^{\frac{mM\pi}{2}}}{m\pi} \sin(\frac{m\pi}{2}) \right]^2 \frac{1}{(z_{m\omega_c} + n\omega_m)} \cos[\phi_{m\omega_c} + n\omega_m] \right\} \end{aligned} \quad (2.23)$$

Since the DC component in the cell capacitor current at steady state is zero, the cell capacitor voltage transient is given by:

$$V_{cm} = V_{cm.steady} + [V_{cm}(0) - V_{cm.steady}] e^{-\frac{t}{C_m G}} \quad (2.24)$$

where $V_{cm}(0)$ is the initial value of the cell capacitor voltage during transient, C_m is the capacitance of the cell capacitor, and $\frac{C_m}{G}$ is the time constant of the transient.

From the above equations except for the case of when the load is purely reactive, the DC component in the cell capacitor current variation, caused by cell capacitor voltage deviation, counteracts such deviation until the DC component in the cell capacitor current variation becomes zero and the cell capacitor voltage returns to its steady state. This phenomenon is called the self-balancing of the cell-capacitor voltage.

This model reached the following conclusions:

- cell capacitor voltage self-balances under sub-harmonic PWM modulation when the load is not purely reactive.
- the time constant of the cell capacitor voltage transient increases with the capacitance of the cell capacitor, the load impedance amplitude and angle, and decreases with modulation index.
- to deal with small loads, reactive load and a low modulation index there is a need for balance boosters to enhance self-balancing.

2.3 Ruderman et al.'s Model

This model uses switched systems to analyse the flying capacitor converter [58]. The analysis is performed in the time domain, treating the flying capacitor converter as a switched system. The subsystems are the various configurations obtained for each state of the circuit switches, and the switching law is determined by the modulation. Consider m continuous-time system described by:

$$\dot{x}(t) = f_i(x(t)), \quad i = 1, \dots, m. \quad (2.25)$$

where $x(\cdot) \in \mathfrak{R}^n$ is the state vector, and $f_i(\cdot) : \mathfrak{R}^n \rightarrow \mathfrak{R}^n$ describes the dynamics of system i . A switched system is a mathematical model in the form:

$$\dot{x}(t) = f_{\sigma(t)}(x(t)), \quad (2.26)$$

where $\sigma(\cdot) \in \{1, \dots, m\}$ is the switching law. The switching-law determines which subsystem is active at which time instant.

Switched systems provide suitable models for electric circuits that contain on and off switches. Each possible configuration of the set of switches induces a continuous time dynamics of the state variables. The dynamics of the system changes every time a switch opens or closes, that is, the modulation of the switches determines the switching law.

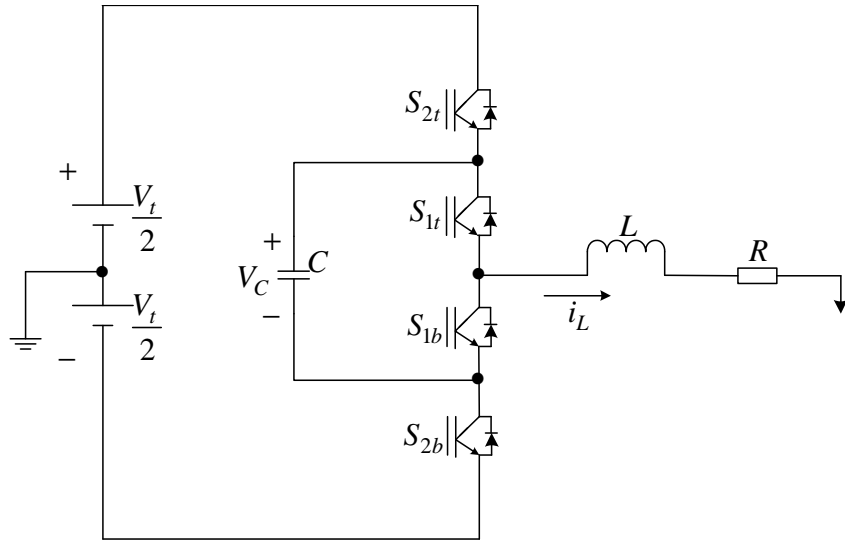


Figure 2.4: Single-phase three-level Flying Capacitor Converter with an RL load

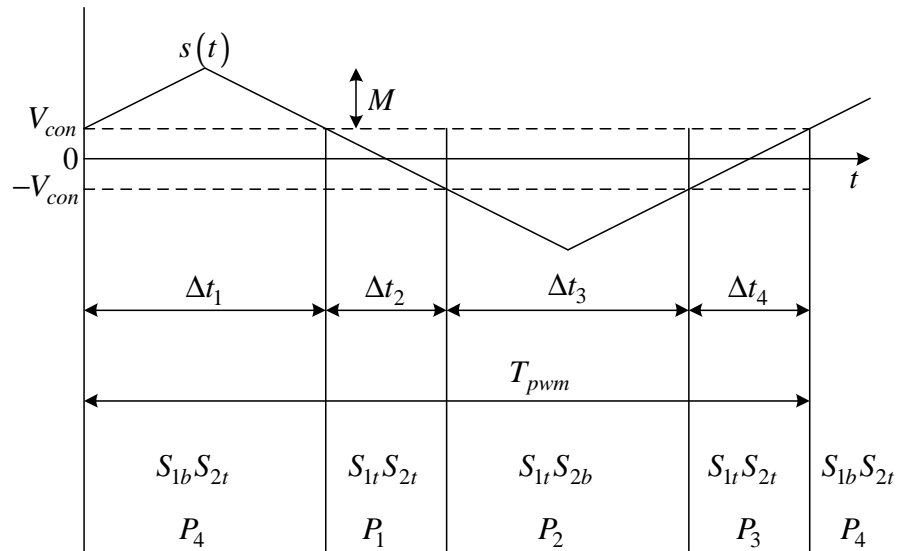


Figure 2.5: DC modulation and corresponding switch states

Figure 2.4 shows a flying capacitor converter with the switching states determined by equations 2.27 and 2.28.

$$S_1 = \begin{cases} on & \text{if } s(t) < V_{con} \\ off & \text{if } s(t) > V_{con} \end{cases} \quad (2.27)$$

$$S_2 = \begin{cases} on & \text{if } s(t) > -V_{con} \\ off & \text{if } s(t) < -V_{con} \end{cases} \quad (2.28)$$

where $V_{con}(t) = V_{con}$ is a constant signal compared to triangular signal $s(t)$ when using DC-modulation strategy. The resulting modulation is periodic and the flying capacitor

converter switches between the four possible phases P_1 , P_2 , P_3 , and P_4 as shown in Figure 2.5. Now let T_p denote the time of one period and Δt_i the time spent in phase P_i during one period such that $T_p = \sum_{i=1}^4 \Delta t_i$. In the AC-modulated case equations 2.27 and 2.28 are written as shown in equations 2.29 and 2.30.

$$S_1 = \begin{cases} on & \text{if } s(t) < M \sin(\eta t) \\ off & \text{if } s(t) > M \sin(\eta t) \end{cases} \quad (2.29)$$

$$S_2 = \begin{cases} on & \text{if } s(t) > -M \sin(\eta t) \\ off & \text{if } s(t) < -M \sin(\eta t) \end{cases} \quad (2.30)$$

From the performed simulations it was observed that the average value of the capacitor voltage converges exponentially to the desired value $\frac{V_t}{2}$, and then the converter operates as expected. This was found to be true for various initial conditions and for both DC and AC modulations. The time domain approach was then used to analyze the converter by combining the effects of the subsystems that correspond to the various switching configurations. The analysis provided information on the circuit behaviour and natural balancing property.

2.4 Holmes et al.'s Model

This model presents a strategy for the analytic determination of the natural voltage balancing dynamics for three phase flying capacitor converters [27], [28], [29], [57], [59]. It uses a double Fourier series representation of the modulation process to construct a linearized state-space model of the converter operation.

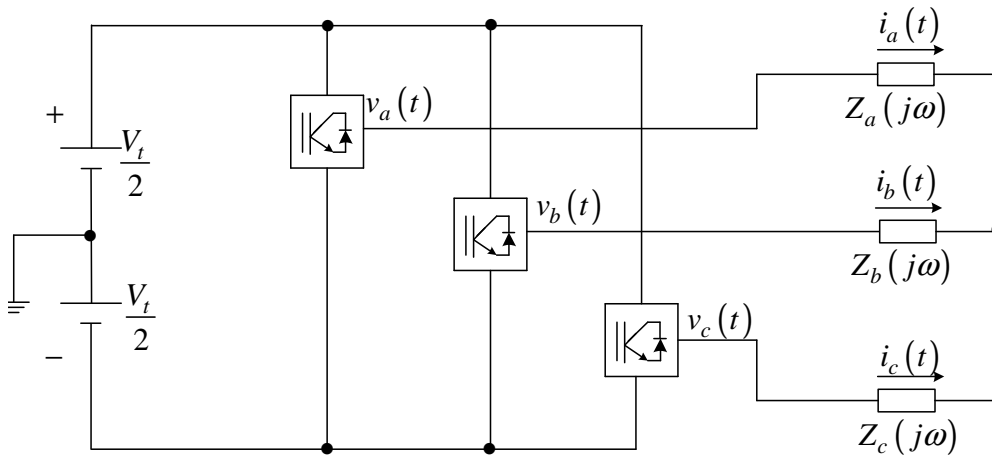


Figure 2.6: Three phase flying capacitor converter

Using Figures 2.6 and 2.1 the capacitor current is given by:

$$C_k \frac{dv_{x,k}}{dt}(t) = [S_{x,k+1}(t) - S_{x,k}(t)] i_x(t) \quad (2.31)$$

where the switching function $S_{x,k}(t) \in \{0, 1\}$, $x \in \{a, b, c\}$ and $k = 1, 2, \dots, p-2$

The phase leg output voltages are given by:

$$v_x = [2S_{x,p-1}(t) - 1] \left[\frac{V_t}{2} \right] - \sum_{k=1}^{p-2} [S_{x,k+1}(t) - S_{x,k}(t)] v_{x,k}(t) \quad (2.32)$$

and $v_{x,k}(t)$ is the capacitor voltage.

Using double Fourier series the difference switching functions in 2.31 becomes:

$$[S_{x,k+1}(t) - S_{x,k}(t)] = \sum_{m=1}^{\infty} \sum_{n=-\infty}^{\infty} [A_{mn} \cos(\omega_{mn} + \theta_{x,k}^{m,n})] \quad (2.33)$$

$$[S_{x,N-1}(t) - 1] = \sum_{m=1}^{\infty} [B_{0n} \cos\{(\omega_0 t + \phi_x)\}] + \sum_{m=1}^{\infty} \sum_{n=-\infty}^{\infty} [A_{mn} \cos(\omega_{mn} + \gamma_x^{m,n})] \quad (2.34)$$

where

$$\omega_{mn} = m\omega_c + n\omega_0$$

$$A_{mn} = 2 \sin\left(\frac{m\pi}{p-1}\right) C_{mn}$$

$$B_{mn} = 2C_{mn}$$

$$C_{mn} = \frac{2}{m\pi} \sin\left\{(m+n)\frac{\pi}{2}\right\} J_n\left(\frac{mM\pi}{2}\right)$$

$$\gamma_x^{m,n} = m\phi_{p-1} + n\phi_x$$

and

$$\theta_{x,k}^{m,n} = n\phi_x + m \left[(2k-1) \frac{\pi}{N-1} \right] \frac{\pi}{2}$$

Now, writing the capacitor voltage derivative in matrix form results in:

$$\dot{\mathbf{V}}_c(t) = \mathbf{A} \mathbf{V}_c(t) + \mathbf{B} V_t \quad (2.35)$$

where

$$\mathbf{A} = \begin{bmatrix} A_{aa} & A_{ab} & A_{ac} \\ A_{ba} & A_{bb} & A_{bc} \\ A_{ca} & A_{cb} & A_{cc} \end{bmatrix}, \quad A_{xx} = - \sum_{m=1}^{\infty} \sum_{n=-\infty}^{\infty} \Re e \left\{ \frac{\mathbf{C}^{-1} (\Lambda_x^{mn})^* (\Lambda_x^{mn})^T}{3|Z_{mn}| e^{j\psi_{mn}}} \right\},$$

$$A_{xy} = - \sum_{m=1}^{\infty} \sum_{n=-\infty}^{\infty} \Re e \left\{ \frac{\mathbf{C}^{-1} (\Lambda_x^{mn})^* (\Lambda_y^{mn})^T}{3|Z_{mn}| e^{j\psi_{mn}}} \right\}$$

$$\mathbf{B} = \begin{bmatrix} B_{aa} & B_{ab} & B_{ac} \\ B_{ba} & B_{bb} & B_{bc} \\ B_{ca} & B_{cb} & B_{cc} \end{bmatrix}, B_{xx} = -\sum_{m=1}^{\infty} \sum_{n=-\infty}^{\infty} \Re e \left\{ \frac{\mathbf{C}^{-1}(\Lambda_x^{mn})^* \Psi_x^{mn}}{3|Z_{mn}|e^{j\psi_{mn}}} \right\},$$

$$B_{xy} = -\sum_{m=1}^{\infty} \sum_{n=-\infty}^{\infty} \Re e \left\{ \frac{\mathbf{C}^{-1}(\Lambda_x^{mn})^* \Psi_x^{mn}}{3|Z_{mn}|e^{j\psi_{mn}}} \right\}$$

$$\text{and } \mathbf{C} = \text{diag}[C_c \dots C_{N-2}], \Psi_x^{m,n} = B_{mn}, \Lambda_x^{m,n} = A_{mn} [e^{j\theta_{x,1}^{m,n}} \ e^{j\theta_{x,2}^{m,n}} \ \dots e^{j\theta_{x,N-2}^{m,n}}]$$

A root locus analysis strategy is used to illustrate the potential of the modelling technique. The analysis investigates the capacitor voltage, balancing dependence on modulation index, carrier frequency and load resistance. This was done by plotting the loci of the system poles using the eigenvalues of the state-space matrices and recalculating the coefficients of the matrices at a number of points. The root-locus was plotted as a function of modulation index, carrier frequency, load resistance and load inductance.

2.5 Wilkinson et al.'s Model

Natural balancing was successfully studied for single phase p-cell converters [73], [30], [31]. The work used a mathematical model to derive equivalent circuits in d and t parameters and then analysed the switching functions of single to p-cell cases of single phase multicell under interleaved switching.

Now using Figure 2.1 and double Fourier analysis the following equation under steady state conditions was derived:

$$\begin{aligned}
 & \begin{bmatrix} \frac{V_{d_1}}{V_t} \\ \frac{V_{d_2}}{V_t} \\ \vdots \\ \frac{V_{d_{p-1}}}{V_t} \end{bmatrix} = \\
 & -\frac{1}{p} \begin{bmatrix} 2\Re \left\{ \sum_{l=1}^{p-1} \lambda_l \right\} & 2\Re \left\{ \sum_{l=1}^{p-1} e^{j\frac{2\pi l}{p}} \lambda_l \right\} & \cdots & 2\Re \left\{ \sum_{l=1}^{p-1} e^{j\frac{2\pi l(p-2)}{p}} \lambda_l \right\} \\ 2\Re \left\{ \sum_{l=1}^{p-1} e^{-j\frac{2\pi l}{p}} \lambda_l \right\} & 2\Re \left\{ \sum_{l=1}^{p-1} \lambda_l \right\} & \cdots & 2\Re \left\{ \sum_{l=1}^{p-1} e^{j\frac{2\pi l(p-3)}{p}} \lambda_l \right\} \\ \vdots & \vdots & \ddots & \vdots \\ 2\Re \left\{ \sum_{l=1}^{p-1} e^{-j\frac{2\pi l(p-2)}{p}} \lambda_l \right\} & 2\Re \left\{ \sum_{l=1}^{p-1} e^{-j\frac{2\pi l(p-3)}{p}} \lambda_l \right\} & \cdots & 2\Re \left\{ \sum_{l=1}^{p-1} \lambda_l \right\} \end{bmatrix} \\
 & \begin{bmatrix} 2\Re \left\{ \sum_{l=1}^{p-1} \alpha_l \right\} \\ 2\Re \left\{ \sum_{l=1}^{p-1} e^{-j\frac{2\pi l}{p}} \alpha_l \right\} \\ \vdots \\ 2\Re \left\{ \sum_{l=1}^{p-1} e^{-j\frac{2\pi l(p-2)}{p}} \alpha_l \right\} \end{bmatrix} \tag{2.36}
 \end{aligned}$$

where

$$\begin{aligned}
 \lambda_i &= \int_{m=pk+i} \frac{|S_{d_1}(\xi)|^2}{Z(\xi)} d\xi \\
 \alpha_i &= \int_{m=pk+i} \frac{S_t(\xi) \overline{S_{d_1}(\xi)}}{Z(\xi)} d\xi
 \end{aligned}$$

and V_{d_1} to $V_{d_{p-1}}$ are voltages difference in the cell capacitor, V_t is DC-bus voltage, S_{d_1} is the difference switching function, S_t is the total switching function and Z is the load impedance.

It was found that under steady-state conditions natural balance was guaranteed under the following conditions:

- When the switching frequency is sufficiently higher than the reference frequency such that there is no overlapping of the harmonics.
- When the reference signal does not contain a high frequency which results in aliasing of the harmonics.
- When the load impedance is reactive ($\Re Z(\omega) > 0$).

2.6 Summary

This chapter offers a brief review of the work done on the natural balancing of multicell converters. Natural balancing of capacitor voltages for single and three-phase converters has been studied using different approaches. However, opportunities for further investigation in both the single and three phase multicell still exists.

Chapter 3

Circuit and Spectral Analysis

3.1 Introduction

In this chapter we analyse the 2-cell and 3-cell three-phase multicell converter. This we do by analysing the switching functions and deriving the equivalent circuits of the 2-cell and 3-cell three-phase multicell converters. These circuits make it easier for us to undertake steady-state analysis in the next chapter. Furthermore we analyse the switching functions of the three-phase multicell converter using interleaved switching strategies in order to prove the natural balancing of cell-capacitor voltages.

We use Bennet's geometric technique and Bowe's double Fourier series method to calculate the coefficients of the switching functions. We then employ the derived results [73] of Fourier series expansions of the switching functions to plot the harmonics of the switching functions using the Matlab and Maple packages. Newton Raphson simulations and calculations of the switching functions are dealt with in detail in Appendices B and C; in this chapter we only refer to the results. The theory developed will be used in the next chapters to prove that the difference in cell-capacitor voltages v_δ decays to zero under steady-state conditions.

3.2 Operation of Multicell Converter

Figure 3.1 shows the p -cell structure of a single phase multicell converter topology. The switches of the i^{th} cell are arranged in pairs with the top switch denoted by S_{it} and the bottom switch by S_{ib} . The top and bottom switches of a cell must never conduct nor block simultaneously.

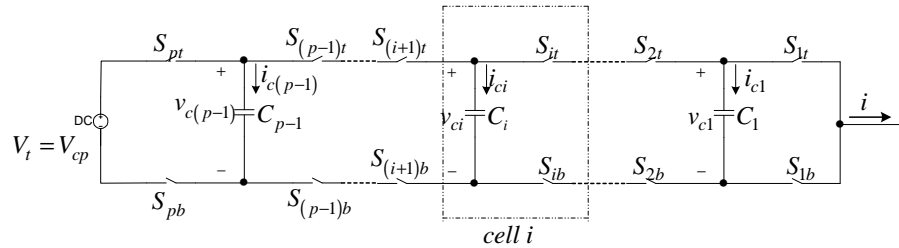


Figure 3.1: *Multilevel commutation cell*

The cell capacitor is denoted by C_i . The p^{th} or last cell is directly connected to the DC-bus.

The following assumptions are used when modelling the multicell converter circuit:

- Ideal switches are used, that is, on-state voltage, off-state current, dead-times, delays and switching times are zero.
- All passive components are ideal and linear.
- The DC-bus is assumed to be infinitely stiff and connected to two equally split voltage sources.

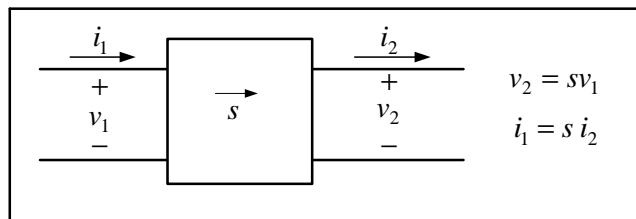


Figure 3.2: *Two-port circuit*

Figure 3.2 shows the two-port switching circuit which was first introduced in [71]. We will be using this two-port switching circuit in our analysis. The arrow points from port 1 to port 2. The relations between voltages v_1 and v_2 and the currents i_1 and i_2 are given by:

$$v_2 = sv_1 \quad (3.1)$$

$$i_1 = si_2 \quad (3.2)$$

where s is the switching function and assumes the values -1 and 1 .

The two-port circuit will be used in the next two sections for deriving the equivalent circuits of 2-cell and 3-cell 3-phase multicell converters.

3.3 2-cell Multicell Converter

Figure 3.3 depicts a 2-cell multicell converter. It consists of the following:

- a DC-voltage V_t split into two series DC-voltages of $\frac{V_t}{2}$ each with the centre-point grounded;
- two cells in each phase; and
- a low-pass filter and load resistor.

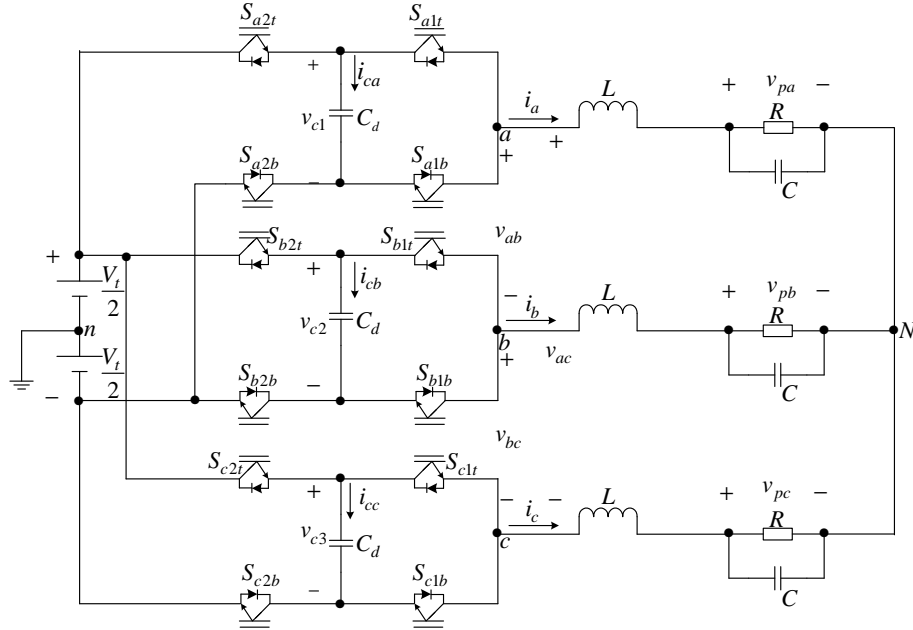


Figure 3.3: 2-cell 3-phase multicell converter

3.3.1 Circuit analysis

Let s_{a1} and s_{a2} represent the switching functions of phase A defined as follows:

$$s_{a1} = \begin{cases} 1 & \text{if } S_{a1t} \text{ is closed} \\ -1 & \text{if } S_{a1b} \text{ is closed} \end{cases} \quad (3.3)$$

$$s_{a2} = \begin{cases} 1 & \text{if } S_{a2t} \text{ is closed} \\ -1 & \text{if } S_{a2b} \text{ is closed} \end{cases} \quad (3.4)$$

The switching functions s_{b1} , s_{b2} , s_{c1} and s_{c2} of phases B and C are defined in a similar manner. Now let us consider Figure 3.3, excluding the load for the moment, that is, considering Figure 3.4 for phase A and similarly for the other phases.

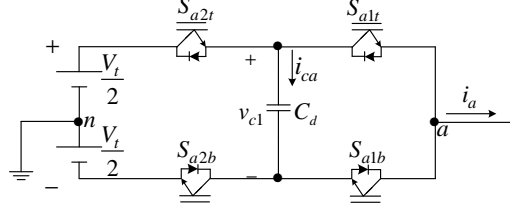


Figure 3.4: Phase A of 2-cell 3-phase multicell converter without load.

Expressing v_{an} , v_{bn} and v_{cn} in terms of the a, b and c switching functions results in

$$\begin{bmatrix} v_{an} \\ v_{bn} \\ v_{cn} \end{bmatrix} = \begin{bmatrix} s_{a2} \\ s_{b2} \\ s_{c2} \end{bmatrix} \frac{V_t}{2} + \frac{1}{2} \begin{bmatrix} s_{a1} - s_{a2} & 0 & 0 \\ 0 & s_{b1} - s_{b2} & 0 \\ 0 & 0 & s_{c1} - s_{c2} \end{bmatrix} \begin{bmatrix} v_{c1} \\ v_{c2} \\ v_{c3} \end{bmatrix} \quad (3.5)$$

and the cell capacitor currents are given by:

$$\begin{bmatrix} i_{ca} \\ i_{cb} \\ i_{cc} \end{bmatrix} = \frac{1}{2} \begin{bmatrix} s_{a2} - s_{a1} & 0 & 0 \\ 0 & s_{b2} - s_{b1} & 0 \\ 0 & 0 & s_{c2} - s_{c1} \end{bmatrix} \begin{bmatrix} i_a \\ i_b \\ i_c \end{bmatrix} \quad (3.6)$$

The differential equations describing the system are given by equation 3.7:

$$\begin{bmatrix} \frac{dv_{c1}}{dt} \\ \frac{dv_{c2}}{dt} \\ \frac{dv_{c3}}{dt} \end{bmatrix} = \frac{1}{2C_d} \begin{bmatrix} s_{a2} - s_{a1} & 0 & 0 \\ 0 & s_{b2} - s_{b1} & 0 \\ 0 & 0 & s_{c2} - s_{c1} \end{bmatrix} \begin{bmatrix} i_a \\ i_b \\ i_c \end{bmatrix} \quad (3.7)$$

3.3.2 Equivalent circuit

We now define the differences between the required voltages of a cell capacitor and the actual voltage across the cell capacitor. This is important for the study of the capacitor voltage balance. We define the voltage difference for phases A, B and C by $v_{\delta a}$, $v_{\delta b}$ and $v_{\delta c}$:

$$v_{\delta a} = \frac{V_t}{2} - v_{c1} \quad (3.8)$$

$$v_{\delta b} = \frac{V_t}{2} - v_{c2} \quad (3.9)$$

$$v_{\delta c} = \frac{V_t}{2} - v_{c3} \quad (3.10)$$

We also define the difference switching functions s_{da} , s_{db} and s_{dc} as a scaled difference between the switching function of cell 2 and cell 1 of phases A, B and C respectively as follows:

$$s_{da} = \frac{1}{2} \{s_{a2} - s_{a1}\} \quad (3.11)$$

$$s_{db} = \frac{1}{2} \{s_{b2} - s_{b1}\} \quad (3.12)$$

$$s_{dc} = \frac{1}{2} \{s_{c2} - s_{c1}\} \quad (3.13)$$

In the same way we define the total switching function as the scaled sum of the switching function of cell 2 and cell 1 as follows:

$$s_{ta} = \frac{1}{2} \{s_{a1} + s_{a2}\} \quad (3.14)$$

$$s_{tb} = \frac{1}{2} \{s_{b1} + s_{b2}\} \quad (3.15)$$

$$s_{tc} = \frac{1}{2} \{s_{c1} + s_{c2}\} \quad (3.16)$$

We rewrite matrix equations 3.5, 3.6 and 3.7 in terms of d and t parameters as shown in matrix equations 3.17, 3.18 and 3.19 respectively.

$$\begin{bmatrix} v_{an} \\ v_{bn} \\ v_{cn} \end{bmatrix} = \begin{bmatrix} s_{ta} \frac{V_t}{2} + s_{da} v_{\delta a} \\ s_{tb} \frac{V_t}{2} + s_{db} v_{\delta b} \\ s_{tc} \frac{V_t}{2} + s_{dc} v_{\delta c} \end{bmatrix} \quad (3.17)$$

$$\begin{bmatrix} i_{ca} \\ i_{cb} \\ i_{cc} \end{bmatrix} = \begin{bmatrix} s_{da} i_a \\ s_{db} i_b \\ s_{dc} i_c \end{bmatrix} \quad (3.18)$$

$$\begin{bmatrix} \frac{dv_{\delta a}}{dt} \\ \frac{dv_{\delta b}}{dt} \\ \frac{dv_{\delta c}}{dt} \end{bmatrix} = -\frac{1}{C_d} \begin{bmatrix} s_{da} i_a \\ s_{db} i_b \\ s_{dc} i_c \end{bmatrix} = -\frac{1}{C_d} \begin{bmatrix} i_{ca} \\ i_{cb} \\ i_{cc} \end{bmatrix} \quad (3.19)$$

Using equations 3.17, 3.18, 3.19, and the two-port circuit shown in Figure 3.2, we obtain the equivalent circuit of Figure 3.4 given by Figure 3.5. Figure 3.5 shows the two-port circuits and their direction.

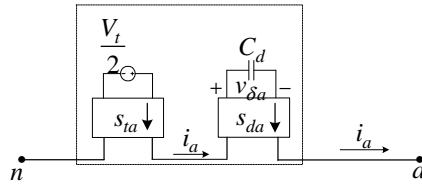


Figure 3.5: *Equivalent circuit of Figure 3.4*

We obtain similar equivalent circuits for phase B and C. Substituting these equivalent circuits into Figure 3.3 we obtain the equivalent circuit to the 2-cell 3-phase multicell converter, shown in Figure 3.3, as given by Figure 3.6. Z denotes the impedance of the filter and load.

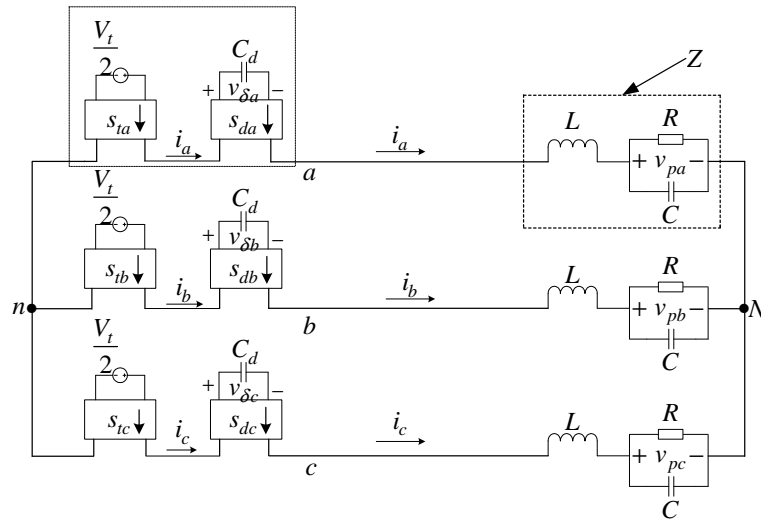


Figure 3.6: *Equivalent circuit for 2-cell 3-phase multicell converter*

3.4 Circuit Analysis of 3-Cell Multicell Converter

Figure 3.7 illustrates a 3-cell 3-phase multicell converter.

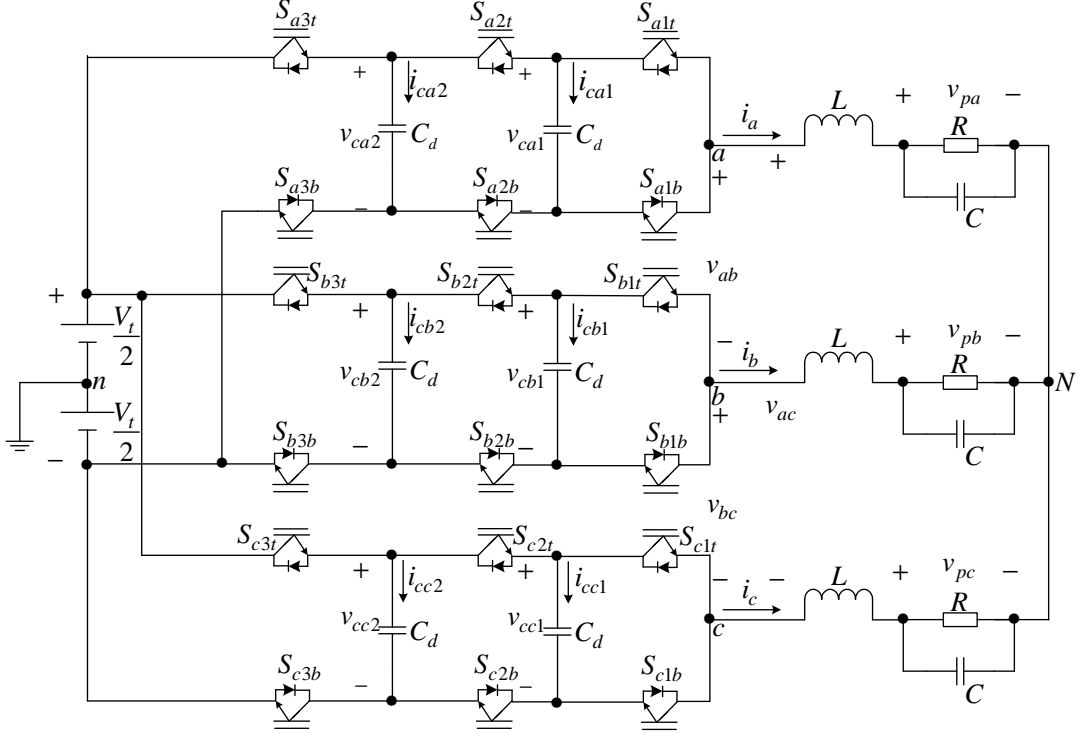


Figure 3.7: 3-cell 3-phase multicell converter

3.4.1 Circuit analysis

The switching functions s_{a1} and s_{a2} are defined the same way as in equations 3.3 and 3.4 whilst s_{a3} is defined as follows:

$$s_{a3}(t) = \begin{cases} 1 & \text{if } S_{a3t} \text{ is closed} \\ -1 & \text{if } S_{a3b} \text{ is closed} \end{cases} \quad (3.20)$$

The switching functions for phases B and C are defined in a similar way.

Expressing v_{an} , v_{bn} and v_{cn} in terms of the a, b and c switching functions results in

$$\begin{bmatrix} v_{an} \\ v_{bn} \\ v_{cn} \end{bmatrix} = \begin{bmatrix} s_{a3} \\ s_{b3} \\ s_{c3} \end{bmatrix} \frac{V_t}{2} + \frac{1}{2} \begin{bmatrix} s_{a2} - s_{a3} & 0 & 0 \\ 0 & s_{b2} - s_{b3} & 0 \\ 0 & 0 & s_{c2} - s_{c3} \end{bmatrix} \begin{bmatrix} v_{ca2} \\ v_{cb2} \\ v_{cc2} \end{bmatrix} \\ + \frac{1}{2} \begin{bmatrix} s_{a1} - s_{a2} & 0 & 0 \\ 0 & s_{b1} - s_{b2} & 0 \\ 0 & 0 & s_{c1} - s_{c2} \end{bmatrix} \begin{bmatrix} v_{ca1} \\ v_{cb1} \\ v_{cc1} \end{bmatrix} \quad (3.21)$$

while the cell capacitor currents are given by 3.22 and 3.23:

$$\begin{bmatrix} i_{ca1} \\ i_{cb1} \\ i_{cc1} \end{bmatrix} = \frac{1}{2} \begin{bmatrix} s_{a2} - s_{a1} & 0 & 0 \\ 0 & s_{b2} - s_{b1} & 0 \\ 0 & 0 & s_{c2} - s_{c1} \end{bmatrix} \begin{bmatrix} i_a \\ i_b \\ i_c \end{bmatrix} \quad (3.22)$$

$$\begin{bmatrix} i_{ca2} \\ i_{cb2} \\ i_{cc2} \end{bmatrix} = \frac{1}{2} \begin{bmatrix} s_{a3} - s_{a2} & 0 & 0 \\ 0 & s_{b3} - s_{b2} & 0 \\ 0 & 0 & s_{c3} - s_{c2} \end{bmatrix} \begin{bmatrix} i_a \\ i_b \\ i_c \end{bmatrix} \quad (3.23)$$

The differential equations describing the system are given by:

$$\begin{bmatrix} \frac{dv_{ca1}}{dt} \\ \frac{dv_{ca2}}{dt} \\ \frac{dv_{cb1}}{dt} \\ \frac{dv_{cb2}}{dt} \\ \frac{dv_{cc1}}{dt} \\ \frac{dv_{cc2}}{dt} \end{bmatrix} = \frac{1}{2C_d} \begin{bmatrix} s_{a2} - s_{a1} & 0 & 0 & 0 & 0 & 0 \\ 0 & s_{a3} - s_{a2} & 0 & 0 & 0 & 0 \\ 0 & 0 & s_{b2} - s_{b1} & 0 & 0 & 0 \\ 0 & 0 & 0 & s_{b3} - s_{b2} & 0 & 0 \\ 0 & 0 & 0 & 0 & s_{c2} - s_{c1} & 0 \\ 0 & 0 & 0 & 0 & 0 & s_{c3} - s_{c2} \end{bmatrix} \begin{bmatrix} i_a \\ i_a \\ i_b \\ i_b \\ i_c \\ i_c \end{bmatrix} \quad (3.24)$$

3.4.2 Equivalent circuit

The difference between the required voltage of the cell capacitor and the actual voltage across the cell capacitor is given by:

$$v_{\delta a1} = \frac{V_t}{3} - v_{ca1}$$

$$v_{\delta b1} = \frac{V_t}{3} - v_{cb1}$$

$$v_{\delta c1} = \frac{V_t}{3} - v_{cc1}$$

$$v_{\delta a2} = \frac{2V_t}{3} - v_{ca2}$$

$$v_{\delta b2} = \frac{2V_t}{3} - v_{cb2}$$

$$v_{\delta c2} = \frac{2V_t}{3} - v_{cc2}$$

The difference switching functions are given by:

$$s_{da1} = \frac{1}{2} \{s_{a2} - s_{a1}\}$$

$$s_{db1} = \frac{1}{2} \{s_{b2} - s_{b1}\}$$

$$s_{dc1} = \frac{1}{2} \{s_{c2} - s_{c1}\}$$

$$s_{da2} = \frac{1}{2} \{s_{a3} - s_{a2}\}$$

$$s_{db2} = \frac{1}{2} \{s_{b3} - s_{b2}\}$$

$$s_{dc2} = \frac{1}{2} \{s_{c3} - s_{c2}\}$$

The total switching functions are given by:

$$s_{ta} = \frac{1}{2} \{s_{a1} + s_{a2} + s_{a3}\}$$

$$s_{tb} = \frac{1}{2} \{s_{b1} + s_{b2} + s_{b3}\}$$

$$s_{tc} = \frac{1}{2} \{s_{c1} + s_{c2} + s_{c3}\}$$

Thus equation 3.21 can be written as follows:

$$\begin{bmatrix} v_{an} \\ v_{bn} \\ v_{cn} \end{bmatrix} = \begin{bmatrix} s_{ta} \frac{V_t}{3} + s_{da1} v_{\delta a1} + s_{da2} v_{\delta a2} \\ s_{tb} \frac{V_t}{3} + s_{db1} v_{\delta b1} + s_{db2} v_{\delta b2} \\ s_{tc} \frac{V_t}{3} + s_{dc1} v_{\delta c1} + s_{dc2} v_{\delta c2} \end{bmatrix} \quad (3.25)$$

and equations 3.22 and 3.23 as follows:

$$\begin{bmatrix} i_{ca1} \\ i_{cb1} \\ i_{cc1} \end{bmatrix} = \begin{bmatrix} s_{da1} & 0 & 0 \\ 0 & s_{db1} & 0 \\ 0 & 0 & s_{dc1} \end{bmatrix} \begin{bmatrix} i_a \\ i_b \\ i_c \end{bmatrix} \quad (3.26)$$

$$\begin{bmatrix} i_{ca2} \\ i_{cb2} \\ i_{cc2} \end{bmatrix} = \begin{bmatrix} s_{da2} & 0 & 0 \\ 0 & s_{db2} & 0 \\ 0 & 0 & s_{dc2} \end{bmatrix} \begin{bmatrix} i_a \\ i_b \\ i_c \end{bmatrix} \quad (3.27)$$

The differential equations in 3.24 are rewritten in terms of d and t parameters as follows:

$$\begin{bmatrix} \frac{dv_{\delta a1}}{dt} \\ \frac{dv_{\delta a2}}{dt} \\ \frac{dv_{\delta b1}}{dt} \\ \frac{dv_{\delta b2}}{dt} \\ \frac{dv_{\delta c1}}{dt} \\ \frac{dv_{\delta c2}}{dt} \end{bmatrix} = -\frac{1}{C_d} \begin{bmatrix} s_{da1}i_a \\ s_{da2}i_a \\ s_{db1}i_b \\ s_{db2}i_b \\ s_{dc1}i_c \\ s_{dc2}i_c \end{bmatrix} = -\frac{1}{C_d} \begin{bmatrix} i_{ca1} \\ i_{ca2} \\ i_{cb1} \\ i_{cb2} \\ i_{cc1} \\ i_{cc2} \end{bmatrix} \tag{3.28}$$

Using similar reasoning to that in section 3.3.2 we obtain the equivalent circuit to the 3-phase 3-cell multicell converter given by Figure 3.8.

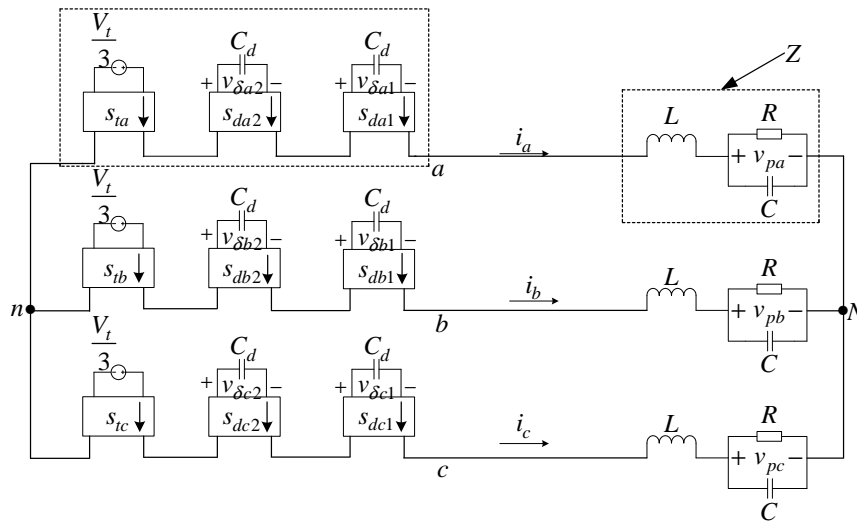


Figure 3.8: Equivalent circuit for 3-cell 3-phase multicell converter

3.5 Interleaved Switching

The main advantage of interleaved switching is that the switching frequency is effectively multiplied by the number of cells. That is, it is doubled for 2-cell and tripled for 3-cell. In order to analyze the behaviour of the three-phase multicell converter, it is important to study the harmonics of the PWM switching functions. We use the double Fourier series to study the harmonics of the switching functions. This approach was originally devised by W.R. Bennet and H.S. Black [2], [32] and then adapted for use with power converter systems by Bowes [60] and has been used in other application [25], [30], [33], [61], [72]. The harmonics of interleaved sinusoidal PWM were analyzed in [34] and the harmonic cancellation for non-sinusoidal reference signal was verified using simulation in [35]. However the detailed theoretical analysis of the harmonics of interleaved switching for non-sinusoidal reference signal was first applied in series-stacked converter [71]. In this study we use the approach that is similar to the one used in [71], [73]. We will derive the Fourier Coefficients using the switching functions of single-cell converter, followed by the study of the switching functions of the 2-cell and 3-cell 3-phase multicell converter.

Throughout this section we assume that the frequency modulation ratio(m_f) is given by

$$m_f = \frac{f_s}{f_0}$$

where

f_s is the switching frequency; and

f_0 is the frequency of the reference signal.

We also assume that m_f is an integer.

Also, the angular switching frequency and fundamental frequency are respectively given by $\omega_s = 2\pi f_s$ and $\omega_0 = 2\pi f_0$.

3.5.1 Switching functions of a single-cell converter

In this subsection we summarise the switching functions of a single-cell (half-bridge) converter since these were studied in [73]. The reason for this is that the sections which will follow are based on the calculations of the coefficients of the single-cell.

Figure 3.9 depicts the pulsewidth modulation applied to a single-cell converter. The reference signal $f_r(t)$ is periodic along the t-axis and can be written as follows:

$$f_r(t) = m_a \sin(\omega_0 t) \tag{3.29}$$

where m_a is the modulation index.

The carrier signal f_c as shown in Figure 3.9 (a) is written as follows:

$$f_c(t) = \frac{2}{\pi} \arcsin[\sin(\omega_s t)] \tag{3.30}$$

Figure 3.9 (b) shows the resulting switching function $s(t)$, defined by:

$$s(t) = \begin{cases} 1 & \text{if } f_r(t) > f_c(t) \\ -1 & \text{if } f_r(t) < f_c(t) \end{cases} \quad (3.31)$$

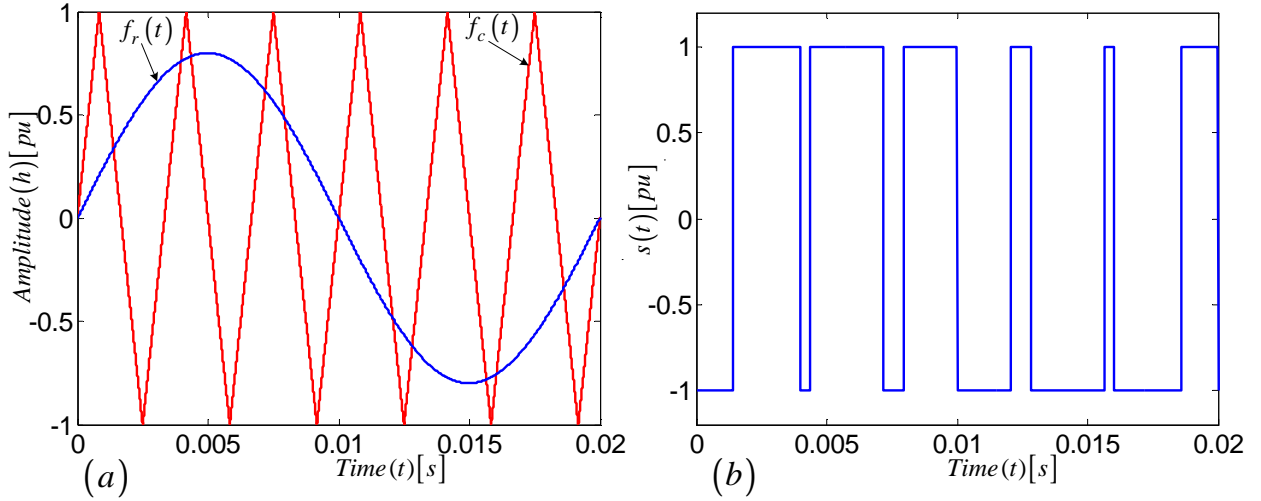


Figure 3.9: Generation of interleaved switching for cell 1 of phase A of 2-cell multicell converter

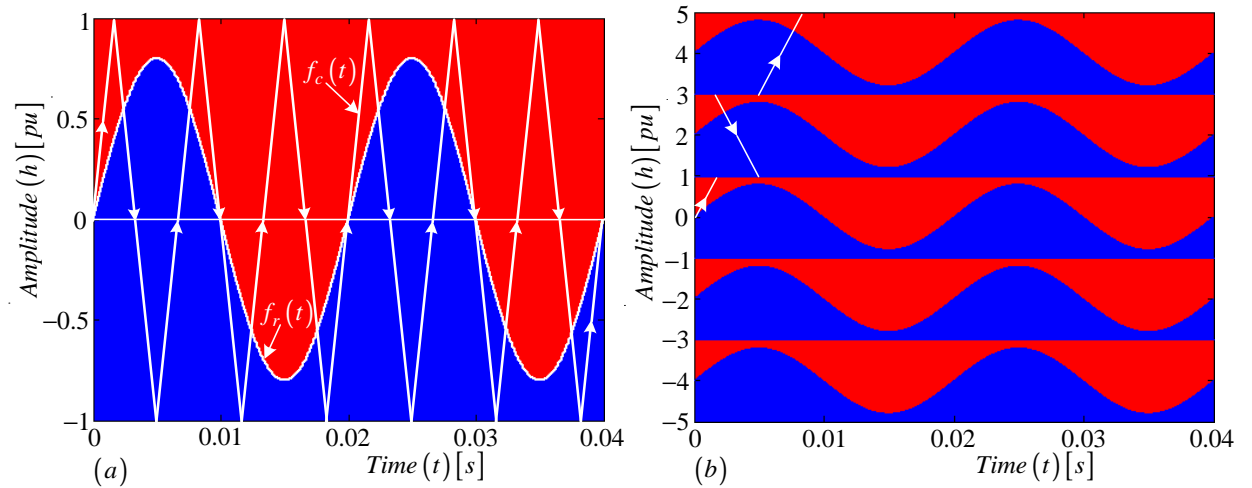


Figure 3.10: Construction of the background function $F(h, t)$

Now from Figure 3.10 (a), the area below $f_r(t)$ is coloured blue and is located where $s(t) = 1$ whereas the area above $f_r(t)$ is coloured red and is situated where $s(t) = -1$ when viewed in three dimensions. That is:

$$s(t) = \begin{cases} 1 & \text{for the blue region} \\ -1 & \text{for the red region} \end{cases} \quad (3.32)$$

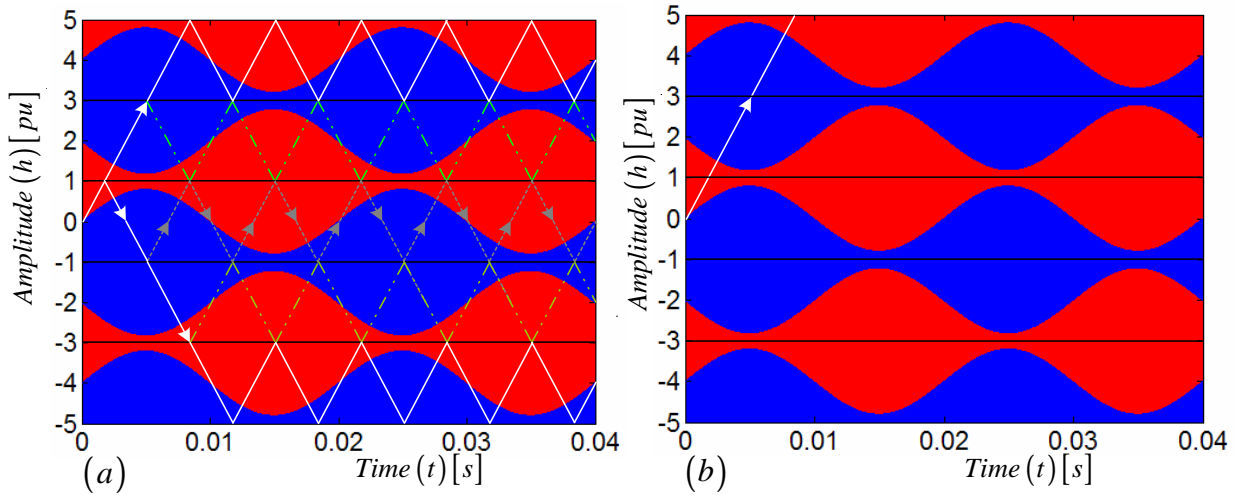


Figure 3.11: Construction of the background function $F(h, t)$

Figures 3.10 and 3.11 illustrate the construction of a background function $F(h, t)$. In Figure 3.10 (a) we have placed arrows on the carrier signal to indicate direction. In Figure 3.10 (b) we separate the carrier signal into quarters of a period and place them on top of each other. Then we place the arrows in one direction to form a straight line by choosing the 'up' direction as the correct direction. The resulting figure is shown in Figure 3.11 (b). The alternative method is that of Figure 3.11 (a). Here we stretch the carrier by turning it at the first corner from the origin. The resulting triangular carrier will occupy regions between 1 and 3 above the zero reference and -1 and -3 below the zero reference. We repeat the same procedure in such a way that the resulting triangular carrier will occupy regions between 3 and 5 above the zero reference and -3 and -5 below the zero reference as shown in the figure. Similarly this results in Figure 3.11 (b). Figure 3.11 (b) depicts the background function $F(h, t)$ that is periodic in both the h and t directions, which can therefore be represented in a double Fourier series.

Figure 3.12 illustrates the top view of the three-dimensional background function, that is a two dimensional function $F(h, t)$.

We define the two-dimensional function $F(h, t)$ as follows:

$$F(h, t) = \begin{cases} 1 & \text{if } -5 < f_c(t) \leq -4 + f_r(t) \\ -1 & \text{if } -4 + f_r(t) < f_c(t) \leq -2 - f_r(t) \\ 1 & \text{if } -2 - f_r(t) < f_c(t) \leq f_r(t) \\ -1 & \text{if } f_r(t) < f_c(t) \leq 2 - f_r(t) \\ 1 & \text{if } 2 - f_r(t) < f_c(t) \leq 4 + f_r(t) \\ -1 & \text{if } 4 + f_r(t) < f_c(t) \leq 5 \end{cases} \quad (3.33)$$

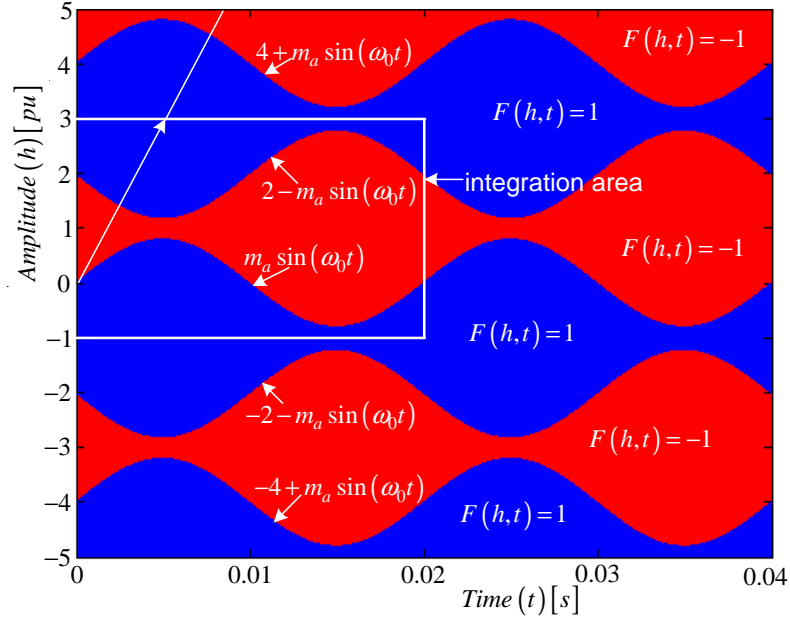


Figure 3.12: Top view of the three-dimensional background function

We give the switching function of the cell the value of $F(h, t)$ when following the line:

$$(h, t) = \left(\frac{2\omega_s}{\pi} t, t \right) \quad (3.34)$$

in the TOH-plane. This line is shown in Figure 3.12. The gradient of this line segment is given by $\frac{2\omega_s}{\pi}$. Thus the expression of the switching function is as follows:

$$s(t) = F\left(\frac{2\omega_s}{\pi} t, t\right) \quad (3.35)$$

From [2] the function $F(h, t)$ can be written as follows:

$$\begin{aligned} F(h, t) &= \frac{1}{2}A_{00} + \sum_{n=1}^{\infty} (A_{0n} \cos(n\omega_0 t) + B_{0n} \sin(n\omega_0 t)) \\ &+ \sum_{m=1}^{\infty} \left(A_{m0} \cos\left(\frac{m\pi h}{2}\right) + B_{m0} \sin\left(\frac{m\pi h}{2}\right) \right) \\ &+ \sum_{m=1}^{\infty} \sum_{n=\pm 1}^{\pm\infty} \left(A_{mn} \cos\left(\frac{m\pi h}{2} + n\omega_0 t\right) + B_{m0} \sin\left(\frac{m\pi h}{2} + n\omega_0 t\right) \right) \end{aligned} \quad (3.36)$$

where the Fourier coefficient is given by:

$$A_{mn} + jB_{mn} = \frac{\omega_0}{4\pi} \int_0^{\frac{2\pi}{\omega_0}} \int_{-1}^3 F(h, t) e^{j\left(\frac{m\pi h}{2} + n\omega_0 t\right)} dh dt \quad (3.37)$$

when using the area of integration as shown in Figure 3.12. The area of integration is given by:

$$\text{Area of integration} = 4T_0 = 4\left(\frac{2\pi}{\omega_0}\right) = \frac{8\pi}{\omega_0} \quad (3.38)$$

The term $\frac{\omega_0}{4\pi}$ is obtained by calculating $\frac{2}{\text{Area of integration}}$.

Substituting equation 3.35 into equation 3.36 we obtain the switching function of the single cell as follows:

$$\begin{aligned}
s(t) &= F\left(\frac{2\omega_s}{\pi}t, t\right) \\
&= \frac{1}{2}A_{00} + \sum_{n=1}^{\infty} (A_{0n} \cos(n\omega_0 t) + B_{0n} \sin(n\omega_0 t)) \\
&\quad + \sum_{m=1}^{\infty} (A_{m0} \cos(m\omega_s t) + B_{m0} \sin(m\omega_s t)) \\
&\quad + \sum_{m=1}^{\infty} \sum_{n=\pm 1}^{\pm\infty} (A_{mn} \cos(m\omega_s t + n\omega_0 t) + B_{mn} \sin(m\omega_s t + n\omega_0 t)) \quad (3.39)
\end{aligned}$$

The first term $\frac{1}{2}A_{00}$ is the DC-component of $s(t)$ which is zero. The second term $A_{0n} + jB_{0n}$ is the Fourier coefficient of the reference signal $f_r(t)$. The third term $A_{m0} + jB_{m0}$ represents components at the switching frequency ω_s . The last term $A_{mn} + jB_{mn}$ represents the harmonic side-bands around integer multiples of the switching frequency.

The coefficients for this switching function are calculated in appendix A.1 and are summarised below:

- $m \neq 0$ and n odd:

$$A_{mn} + jB_{mn} = \frac{2j}{m\pi} J_n\left(\frac{m\pi m_a}{2}\right) (1 + e^{jm\pi}) \quad (3.40)$$

- $m \neq 0$ and n even:

$$A_{mn} + jB_{mn} = \frac{2}{jm\pi} J_n\left(\frac{m\pi m_a}{2}\right) (1 - e^{jm\pi}) \quad (3.41)$$

- $m = 0$ and $n = 1$:

$$A_{mn} + jB_{mn} = jm_a \quad (3.42)$$

- $m = 0$ and $n \neq 1$:

$$A_{mn} + jB_{mn} = 0 \quad (3.43)$$

where J_n is the n 'th order Bessel function of the first kind given by:

$$J_n(m\pi m_a) = \frac{1}{2\pi} \int_{-\pi}^{\pi} e^{-j(m\pi m_a)} e^{jn\theta} d\theta \quad (3.44)$$

or

$$J_n(m\pi m_a) = \frac{1}{2\pi} \int_{-\pi}^{\pi} e^{j(m\pi m_a \sin\theta)} e^{-jn\theta} d\theta \quad (3.45)$$

with $J_{-n}(-m\pi m_a) = J_n(m\pi m_a)$ and $J_{-n}(m\pi m_a) = (-1)^n J_n(m\pi m_a)$

The properties of the above coefficients are shown in appendix A.2. They were initially derived in [25] and then modified for the case of the single-cell in [73].

3.5.2 Switching functions of 2-cell converter

Phase A

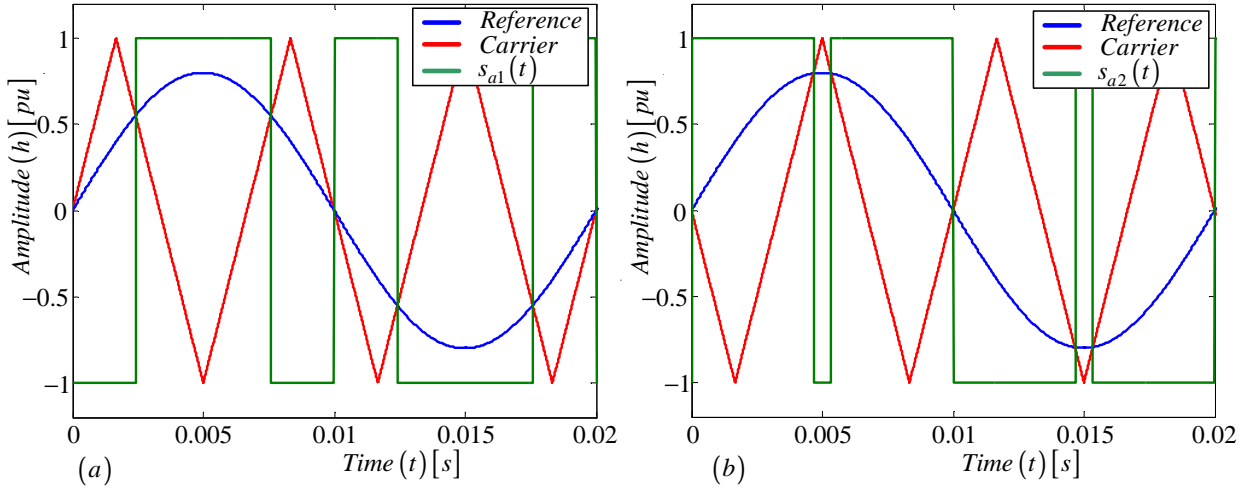


Figure 3.13: Generation of interleaved switching 2-cell multicell converter

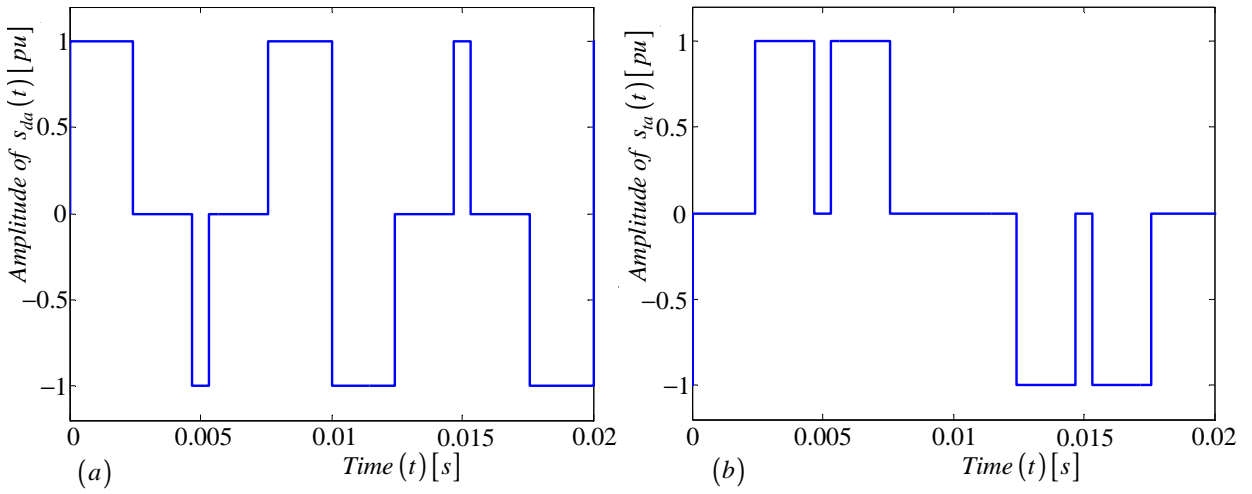


Figure 3.14: Generation of interleaved switching 2-cell multicell converter

From the previous subsection we established that the equation for the switching function of a single cell is given by equation 3.39. The background function given in Figure 3.13 for $s_{a1}(t)$ is similar to the background function given in Figure 3.9 for $f_s = 150\text{Hz}$. Thus the value of h and the switching function equation for $s(t)$ and $s_{a1}(t)$ will be the same. That is:

$$s_{a1}(t) = \frac{1}{2}A_{00} + \sum_{n=1}^{\infty} (A_{0n} \cos(n\omega_0 t) + B_{0n} \sin(n\omega_0 t))$$

$$\begin{aligned}
& + \sum_{m=1}^{\infty} (A_{m0} \cos(m\omega_s t) + B_{m0} \sin(m\omega_s t)) \\
& + \sum_{m=1}^{\infty} \sum_{n=\pm 1}^{\pm \infty} (A_{mn} \cos(m\omega_s t + n\omega_0 t) + B_{mn} \sin(m\omega_s t + n\omega_0 t)) \quad (3.46)
\end{aligned}$$

Now, to obtain the value for h for the switching function $s_{a2}(t)$ we follow the following procedure:

- We establish the nearest point to zero where the carrier signal cuts the t - axis.
- This point will be our t - intercept.
- We substitute our t - intercept into the line equation given by $h = \frac{2\omega_s}{\pi}t + c$ to obtain c where c is our h - intercept.
- We substitute the value of h into the term $\frac{m\pi h}{2}$.
- Then finally we substitute the value of $\frac{m\pi h}{2}$ into equation 3.36.

Following the above procedure for switching function $s_{a2}(t)$ we obtain $c = -2$ and h given by:

$$h = \frac{2\omega_s}{\pi}t - 2 \quad (3.47)$$

and

$$\frac{m\pi h}{2} = m\omega_s t - m\pi \quad (3.48)$$

Figure 3.15 illustrates the top view of the background function of $s_{a1}(t)$ and $s_{a2}(t)$.

Substituting equation 3.48 into equation 3.36 we obtain the switching function of the second cell as follows:

$$\begin{aligned}
s_{a2}(t) & = \frac{1}{2}A_{00} + \sum_{n=1}^{\infty} (A_{0n} \cos(n\omega_0 t) + B_{0n} \sin(n\omega_0 t)) \\
& + \sum_{m=1}^{\infty} (A_{m0} \cos(m\omega_s t - m\pi) + B_{m0} \sin(m\omega_s t - m\pi)) \\
& + \sum_{m=1}^{\infty} \sum_{n=\pm 1}^{\pm \infty} \{A_{mn} \cos((m\omega_s + n\omega_0)t - m\pi) \\
& + B_{mn} \sin((m\omega_s + n\omega_0)t - m\pi)\} \quad (3.49)
\end{aligned}$$

The trigonometric terms with $-m\pi$ can be simplified as follows:

$$\cos(m\omega_s - m\pi) = \begin{cases} \cos(m\omega_s t) & \text{if } m \text{ even} \\ -\cos(m\omega_s t) & \text{if } m \text{ odd} \end{cases} \quad (3.50)$$

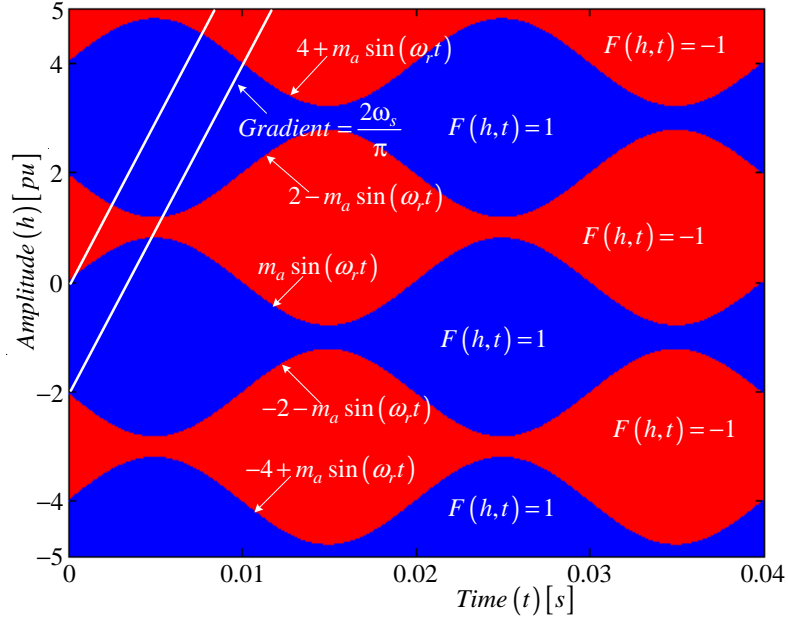


Figure 3.15: Top view of the background function of $s_{a1}(t)$ and $s_{a2}(t)$

$$\sin(m\omega_s - m\pi) = \begin{cases} \sin(m\omega_s t) & \text{if } m \text{ even} \\ -\sin(m\omega_s t) & \text{if } m \text{ odd} \end{cases} \quad (3.51)$$

$$\cos((m\omega_s + n\omega_0)t - m\pi) = \begin{cases} \cos(m\omega_s t + n\omega_0 t) & \text{if } m \text{ even} \\ -\cos(m\omega_s t + n\omega_0 t) & \text{if } m \text{ odd} \end{cases} \quad (3.52)$$

$$\sin((m\omega_s + n\omega_0)t - m\pi) = \begin{cases} \sin(m\omega_s t + n\omega_0 t) & \text{if } m \text{ even} \\ -\sin(m\omega_s t + n\omega_0 t) & \text{if } m \text{ odd} \end{cases} \quad (3.53)$$

Now using the above trigonometric identities we rewrite equation 3.49 as follows:

$$\begin{aligned} s_{a2}(t) = & \frac{1}{2}A_{00} + \sum_{n=1}^{\infty} (A_{0n} \cos(n\omega_0 t) + B_{0n} \sin(n\omega_0 t)) + \\ & \sum_{m=2,4,\dots}^{\infty} (A_{m0} \cos(m\omega_s t) + B_{m0} \sin(m\omega_s t)) - \\ & \sum_{m=1,3,\dots}^{\infty} (A_{m0} \cos(m\omega_s t - m\pi) + B_{m0} \sin(m\omega_s t)) + \\ & \sum_{m=2,4,\dots}^{\infty} \sum_{n=\pm 1}^{\pm\infty} \{A_{mn} \cos(m\omega_s t + n\omega_0 t) + B_{mn} \sin(m\omega_s t + n\omega_0 t)\} - \\ & \sum_{m=1,3,\dots}^{\infty} \sum_{n=\pm 1}^{\pm\infty} \{A_{mn} \cos(m\omega_s t + n\omega_0 t) + B_{mn} \sin(m\omega_s t + n\omega_0 t)\} \end{aligned} \quad (3.54)$$

Using equations 3.46 and 3.49 we obtain the phasor representation for phase A of a 2-cell converter shown in Figure 3.16.

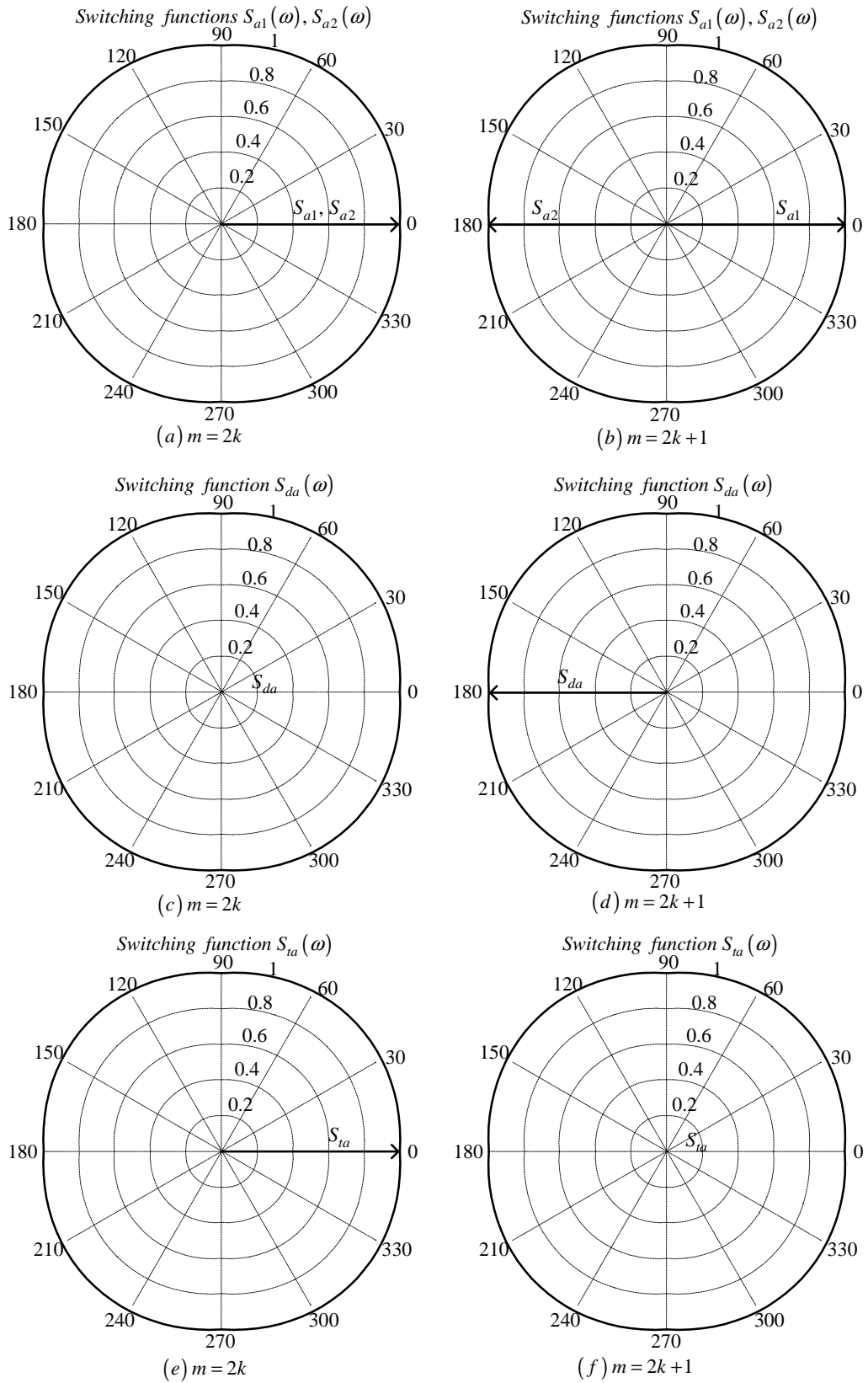


Figure 3.16: Phasor representation for phase A of 2-cell converter

Phase B

The equation for the reference signal for phase B is given by:

$$f_r(t) = m_a \sin \left(\omega_0 \left(t - \frac{T_0}{3} \right) \right) \quad (3.55)$$

We want to use the same background function as that used for the single-cell converter so that we can employ the Fourier coefficients calculated for the single-cell. For us to do this we use Figure 3.17 and follow the procedure below:

- Make substitution:

$$t_1 = t - \frac{T_0}{3}$$

This moves the zero-crossing of the reference waveform of phase B to the origin.

- Find the value of t_x after shifting the background function to the left by $\frac{T_0}{3}$.
- Substitute the value t_x in the line equation to find c and then h .
- Substitute the value of h into the term $\frac{m\pi h}{2}$.
- Substitute the value of $\frac{m\pi h}{2}$ into equation 3.36. This will give us the Fourier series expansion of the switching function in terms of t_1 .
- Finally substitute

$$t = t_1 + \frac{T_0}{3}$$

to rewrite the Fourier series in terms of t .

Figure 3.17 depicts the phase B background function after $\frac{T_0}{3}$ phase-shift.

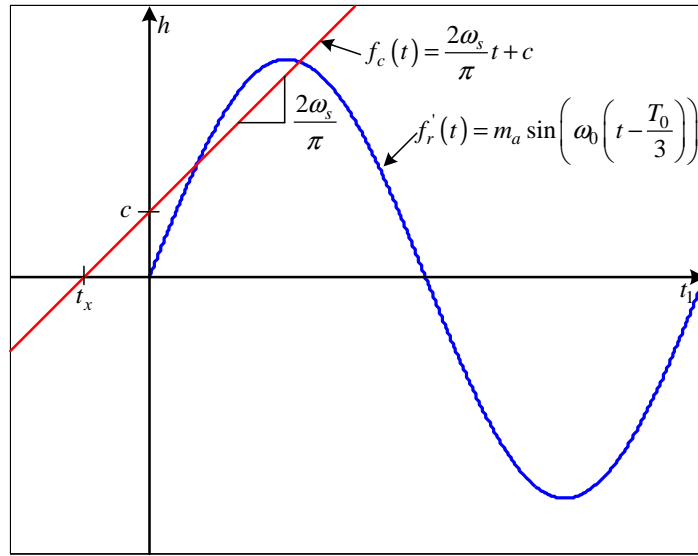


Figure 3.17: Phase B background function after $\frac{T_0}{3}$ phase-shift.

Example

To demonstrate the above procedure we employ the background function produced using $f_0 = 50\text{Hz}$, $f_s = 200\text{Hz}$ and $m_a = 0.8$ for $s_{b1}(t)$. This also demonstrates a situation where the frequency modulation index $m_f = 3k + 1$. Figures 3.18 (a) and (b) show the background function before and after phase shifting by $\frac{T_0}{3}$ respectively. From Figure 3.18

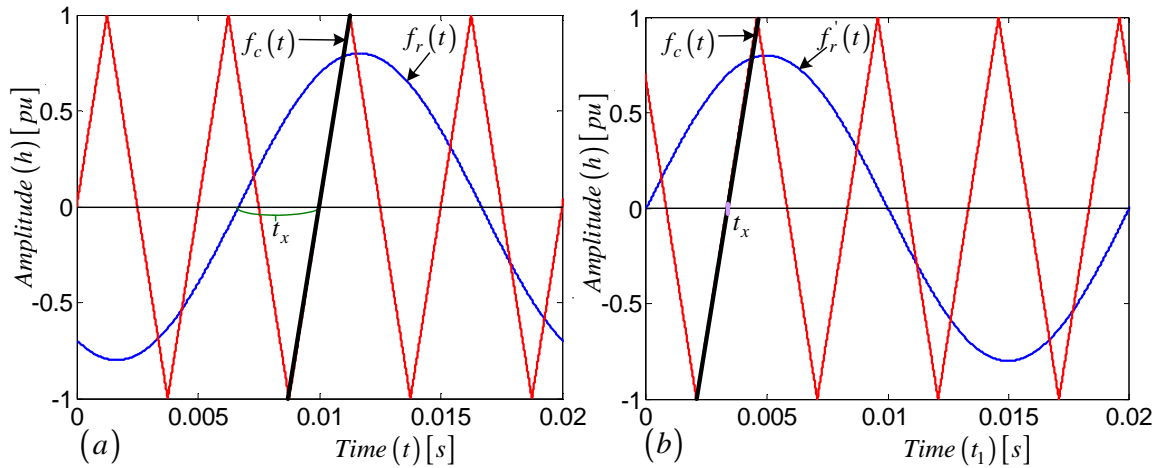


Figure 3.18: Generation of interleaved switching 2-cell multicell converter $m_f = 3k + 1$ for s_{b1}

(a) we can observe that

$$t_x = 2T_s - \frac{1}{3}T_0$$

$$\begin{aligned}
&= 2T_s - \frac{1}{3}m_f T_s \\
&= 2T_s - \frac{4}{3}T_s \\
&= \frac{2}{3}T_s
\end{aligned} \tag{3.56}$$

Now substituting the value of t_x into equation $f_c(t) = \frac{2\omega_s}{\pi}t + c$ we obtain the h -intercept which is given by $c = -\frac{8}{3}$. Thus h will be given by:

$$h = \frac{2\omega_s}{\pi}t_1 - \frac{8}{3} \tag{3.57}$$

and

$$\frac{m\pi h}{2} = m\omega_s t_1 - \frac{4}{3}m\pi \tag{3.58}$$

Now substituting equation 3.58 into equation 3.36 we obtain:

$$\begin{aligned}
s_{b1}(t_1) &= \frac{1}{2}A_{00} + \sum_{n=1}^{\infty} (A_{0n} \cos(n\omega_0 t_1) + B_{0n} \sin(n\omega_0 t_1)) \\
&+ \sum_{m=1}^{\infty} \left(A_{m0} \cos\left(m\omega_s t_1 - \frac{4}{3}m\pi\right) + B_{m0} \sin\left(m\omega_s t_1 - \frac{4}{3}m\pi\right) \right) \\
&+ \sum_{m=1}^{\infty} \sum_{n=\pm 1}^{\pm\infty} \left\{ A_{mn} \cos\left((m\omega_s + n\omega_0)t_1 - \frac{4}{3}m\pi\right) \right. \\
&\quad \left. + B_{mn} \sin\left((m\omega_s + n\omega_0)t_1 - \frac{4}{3}m\pi\right) \right\}
\end{aligned} \tag{3.59}$$

We now substitute $t = t_1 + \frac{T_0}{3}$ back into equation 3.59 and obtain:

$$\begin{aligned}
s_{b1}(t) &= \frac{1}{2}A_{00} + \sum_{n=1}^{\infty} \left(A_{0n} \cos\left(n\omega_0 \left(t - \frac{2\pi}{3\omega_0}\right)\right) + B_{0n} \sin\left(n\omega_0 \left(t - \frac{2\pi}{3\omega_0}\right)\right) \right) \\
&+ \sum_{m=1}^{\infty} \left(A_{m0} \cos\left(m\omega_s \left(t - \frac{2\pi}{3\omega_0}\right) - \frac{4}{3}m\pi\right) \right. \\
&\quad \left. + B_{m0} \sin\left(m\omega_s \left(t - \frac{2\pi}{3\omega_0}\right) - \frac{4}{3}m\pi\right) \right) \\
&+ \sum_{m=1}^{\infty} \sum_{n=\pm 1}^{\pm\infty} \left\{ A_{mn} \cos\left((m\omega_s + n\omega_0) \left(t - \frac{2\pi}{3\omega_0}\right) - \frac{4}{3}m\pi\right) \right. \\
&\quad \left. + B_{mn} \sin\left((m\omega_s + n\omega_0) \left(t - \frac{2\pi}{3\omega_0}\right) - \frac{4}{3}m\pi\right) \right\}
\end{aligned} \tag{3.60}$$

For the frequency modulation index $m_f = 3k + 1$ the phasor representations for phase B of a 2-cell converter are illustrated in Figures C.8, C.9 and C.10.

Phase C

The equation for the reference signal for phase C is given by:

$$f_r(t) = m_a \sin \left(\omega_0 \left(t - \frac{2T_0}{3} \right) \right) \quad (3.61)$$

We follow the same procedure as for phase B except that we use Figure 3.19 and the substitution for t is as follows:

$$t_2 = t - \frac{2T_0}{3} \quad (3.62)$$

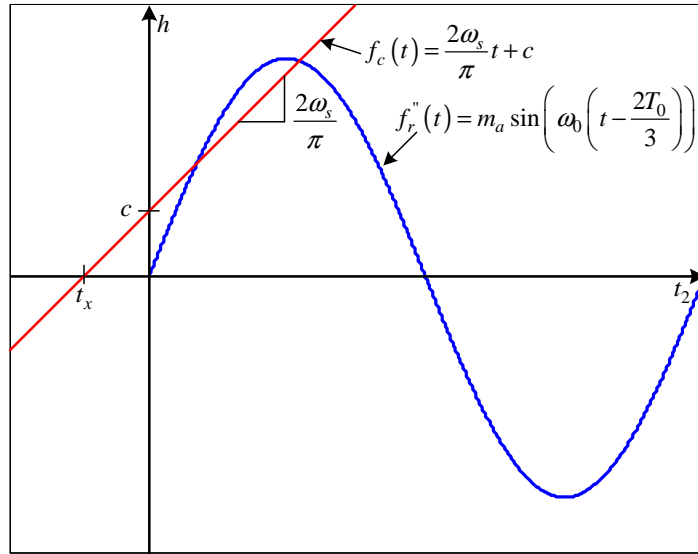


Figure 3.19: Phase C background function after $\frac{2T_0}{3}$ phase-shift

Example

Now we employ the background function produced using $f_0 = 50\text{Hz}$, $f_s = 250\text{Hz}$ and $m_a = 0.8$ for $s_{c2}(t)$. This also demonstrates a situation where the frequency modulation index $m_f = 3k + 2$. Figures 3.20 (a) and (b) show the background function before and after phase shifting by $\frac{2T_0}{3}$ respectively.

From Figure 3.20 (a) t_x is calculated as follows:

$$\begin{aligned} t_x &= \frac{7}{2}T_s - \frac{2}{3}T_0 \\ &= \frac{1}{6}T_s \end{aligned} \quad (3.63)$$

Thus $c = -\frac{2}{3}$ and h will be given by:

$$h = \frac{2\omega_s}{\pi}t_2 - \frac{2}{3} \quad (3.64)$$

and

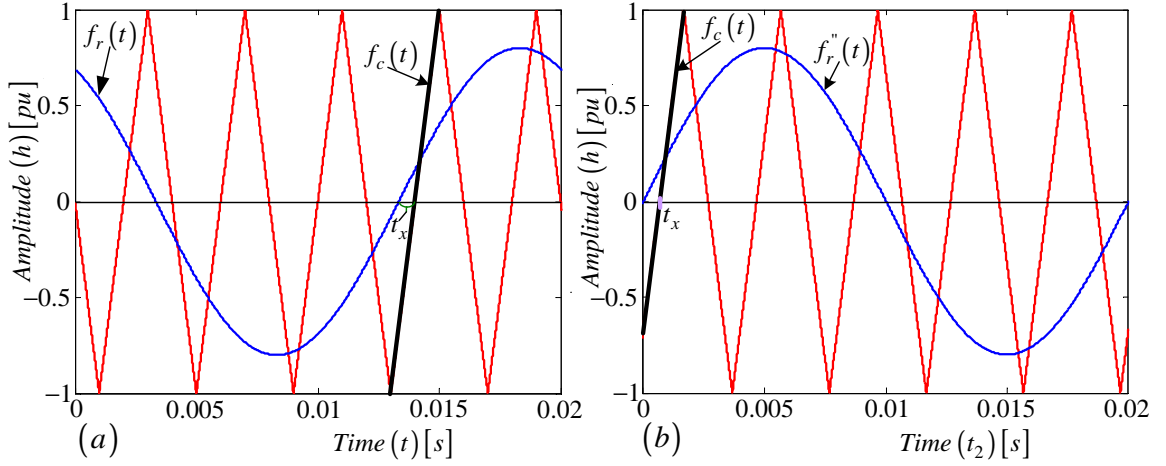


Figure 3.20: Generation of interleaved switching 2-cell multicell converter $m_f = 3k + 2$ for s_{c2}

$$\frac{m\pi h}{2} = m\omega_s t_2 - \frac{m\pi}{3} \quad (3.65)$$

Now substituting equation 3.58 into equation 3.36 we obtain:

$$\begin{aligned} s_{c2}(t_2) &= \frac{1}{2}A_{00} + \sum_{n=1}^{\infty} (A_{0n} \cos(n\omega_0 t_2) + B_{0n} \sin(n\omega_0 t_2)) \\ &+ \sum_{m=1}^{\infty} \left(A_{m0} \cos\left(m\omega_s t_2 - \frac{m\pi}{3}\right) + B_{m0} \sin\left(m\omega_s t_2 - \frac{m\pi}{3}\right) \right) \\ &+ \sum_{m=1}^{\infty} \sum_{n=\pm 1}^{\pm \infty} \left\{ A_{mn} \cos\left((m\omega_s + n\omega_0)t_2 - \frac{m\pi}{3}\right) \right. \\ &\quad \left. + B_{mn} \sin\left((m\omega_s + n\omega_0)t_2 - \frac{m\pi}{3}\right) \right\} \end{aligned} \quad (3.66)$$

We now substitute $t = t_2 + \frac{2T_0}{3}$ back into equation 3.59 and obtain:

$$\begin{aligned} s_{c2}(t) &= \frac{1}{2}A_{00} + \sum_{n=1}^{\infty} \left(A_{0n} \cos\left(n\omega_0 \left(t - \frac{4\pi}{3\omega_0}\right)\right) + B_{0n} \sin\left(n\omega_0 \left(t - \frac{4\pi}{3\omega_0}\right)\right) \right) \\ &+ \sum_{m=1}^{\infty} \left(A_{m0} \cos\left(m\omega_s \left(t - \frac{4\pi}{3\omega_0}\right) - \frac{m\pi}{3}\right) \right. \\ &\quad \left. + B_{m0} \sin\left(m\omega_s \left(t - \frac{4\pi}{3\omega_0}\right) - \frac{m\pi}{3}\right) \right) \\ &+ \sum_{m=1}^{\infty} \sum_{n=\pm 1}^{\pm \infty} \left\{ A_{mn} \cos\left((m\omega_s + n\omega_0) \left(t - \frac{4\pi}{3\omega_0}\right) - \frac{m\pi}{3}\right) \right. \\ &\quad \left. + B_{mn} \sin\left((m\omega_s + n\omega_0) \left(t - \frac{4\pi}{3\omega_0}\right) - \frac{m\pi}{3}\right) \right\} \end{aligned} \quad (3.67)$$

For a frequency modulation index $m_f = 3k + 2$ the phasor representations for phase C of the 2-cell converter are shown in Figures C.17, C.18 and C.19.

Table 3.1 indicates the values of t_x , c and h for the background function of different functions and for the case of $m_f \in \{3k : k = 1, 2, 3 \dots\}$, $m_f \in \{3k + 1 : k = 1, 2, 3 \dots\}$ and $m_f \in \{3k + 2 : k = 1, 2, 3 \dots\}$.

Table 3.1: Values for t_x , c and h of background function for 2-cell multicell converter

m_f		s_{a1}	s_{a2}	s_{b1}	s_{b2}	s_{c1}	s_{c2}
$3k$	t_x	0	$\frac{1}{2}T_s$	0	$\frac{1}{2}T_s$	0	$\frac{1}{2}T_s$
	c	0	-2	0	-2	0	-2
	h	$\frac{2\omega_s t}{\pi}$	$\frac{2\omega_s t}{\pi} - 2$	$\frac{2\omega_s t_1}{\pi}$	$\frac{2\omega_s t_1}{\pi} - 2$	$\frac{2\omega_s t_2}{\pi}$	$\frac{2\omega_s t_2}{\pi} - 2$
$3k + 1$	t_x	0	$\frac{1}{2}T_s$	$\frac{2}{3}T_s$	$\frac{1}{6}T_s$	$\frac{1}{3}T_s$	$-\frac{1}{6}T_s$
	c	0	-2	$-\frac{8}{3}$	$-\frac{2}{3}$	$-\frac{4}{3}$	$\frac{2}{3}$
	h	$\frac{2\omega_s t}{\pi}$	$\frac{2\omega_s t}{\pi} - 2$	$\frac{2\omega_s t_1}{\pi} - \frac{8}{3}$	$\frac{2\omega_s t_1}{\pi} - \frac{2}{3}$	$\frac{2\omega_s t_2}{\pi} - \frac{4}{3}$	$\frac{2\omega_s t_2}{\pi} + \frac{2}{3}$
$3k + 2$	t_x	0	$\frac{1}{2}T_s$	$\frac{1}{3}T_s$	$-\frac{1}{6}T_s$	$\frac{2}{3}T_s$	$\frac{1}{6}T_s$
	c	0	-2	$-\frac{4}{3}$	$\frac{2}{3}$	$-\frac{8}{3}$	$-\frac{2}{3}$
	h	$\frac{2\omega_s t}{\pi}$	$\frac{2\omega_s t}{\pi} - 2$	$\frac{2\omega_s t_1}{\pi} - \frac{4}{3}$	$\frac{2\omega_s t_1}{\pi} + \frac{2}{3}$	$\frac{2\omega_s t_2}{\pi} - \frac{8}{3}$	$\frac{2\omega_s t_2}{\pi} - \frac{2}{3}$

Figures 3.21 (a) and (b) depict the background functions for the cases of $m_f = 3k + 1$ and $m_f = 3k + 2$ respectively. The difference is in the values of the switching frequency f_s which affects the slope of h as can be seen in the two figures.

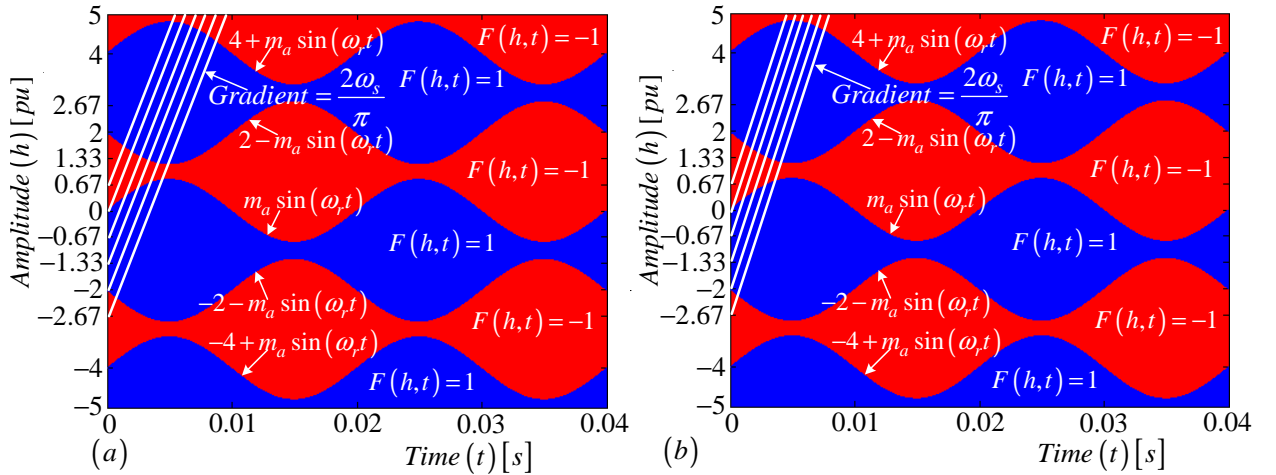


Figure 3.21: Top view of the background functions for the case of (a) $m_f = 3k + 1$ and (b) $m_f = 3k + 2$

The broad discussion of the switching functions for phases A, B and C with frequency modulation index of $m_f = 3k$, $m_f = 3k + 1$ and $m_f = 3k + 2$ is undertaken in the Appendix

chapter C section C.1 using Table 3.1. From the resulting phasor diagrams represented in Figures C.1 to C.19 we make the following observations, shown in Tables 3.2, 3.3 and 3.4.

Table 3.2: Observation from phasor diagrams for Phase A

$S_{da}(\omega)$	$S_{ta}(\omega)$	m	n	m_f
0	$ S_{ta}(\omega) $	$m = 2k$	$\forall n$	$\forall m_f$
$ S_{da}(\omega) e^{j\pi}$	0	$m = 2k + 1$	$\forall n$	$\forall m_f$

Table 3.3: Observation from phasor diagrams for Phase B

$S_{db}(\omega)$	$S_{tb}(\omega)$	m	n	m_f
0	$ S_{tb}(\omega) $	$m = 2k$	$n = 3p$ or $n = -3p$	$\forall m_f$
$ S_{db}(\omega) e^{j\pi}$	0	$m = 2k + 1$	$n = 3p$ or $n = -3p$	$\forall m_f$
0	$ S_{tb}(\omega) e^{-j\frac{2\pi}{3}}$	$m = 2k$	$n = 3p + 1$ or $n = -(3p + 2)$	$\forall m_f$
$ S_{db}(\omega) e^{j\frac{\pi}{3}}$	0	$m = 2k + 1$	$n = 3p + 1$ or $n = -(3p + 2)$	$\forall m_f$
0	$ S_{tb}(\omega) e^{j\frac{2\pi}{3}}$	$m = 2k$	$n = 3p + 2$ or $n = -(3p + 1)$	$\forall m_f$
$ S_{db}(\omega) e^{-j\frac{\pi}{3}}$	0	$m = 2k + 1$	$n = 3p + 2$ or $n = -(3p + 1)$	$\forall m_f$

Table 3.4: Observation from phasor diagrams for Phase C

$S_{dc}(\omega)$	$S_{tc}(\omega)$	m	n	m_f
0	$ S_{tc}(\omega) $	$m = 2k$	$n = 3p$ or $n = -3p$	$\forall m_f$
$ S_{dc}(\omega) e^{j\pi}$	0	$m = 2k + 1$	$n = 3p$ or $n = -3p$	$\forall m_f$
0	$ S_{tc}(\omega) e^{j\frac{2\pi}{3}}$	$m = 2k$	$n = 3p + 1$ or $n = -(3p + 2)$	$\forall m_f$
$ S_{dc}(\omega) e^{-j\frac{\pi}{3}}$	0	$m = 2k + 1$	$n = 3p + 1$ or $n = -(3p + 2)$	$\forall m_f$
0	$ S_{tc}(\omega) e^{-j\frac{2\pi}{3}}$	$m = 2k$	$n = 3p + 2$ or $n = -(3p + 1)$	$\forall m_f$
$ S_{dc}(\omega) e^{j\frac{\pi}{3}}$	0	$m = 2k + 1$	$n = 3p + 2$ or $n = -(3p + 1)$	$\forall m_f$

Simulations

In this section we depict the amplitude and phase spectra of the switching functions. These spectra are developed using theory and verified using Simplorer and Newton-Raphson simulations. Detailed derivation and plotting of spectra using Newton-Raphson simulation is performed in the section B.2 of the Appendix chapter B. The simulation parameters are given by Table 3.5.

Table 3.5: *Simulation parameters*

<i>DC – bus voltage</i>	V_t	100 V
<i>DC – bus capacitance</i>	C_d	40 μF
<i>Switching frequency</i>	f_s	6 kHz
<i>Modulation frequency</i>	f_1	50 Hz
<i>Filter inductance</i>	L	200 μH
<i>Filter capacitance</i>	C	50 μF
<i>Load resistance</i>	R	10 Ω

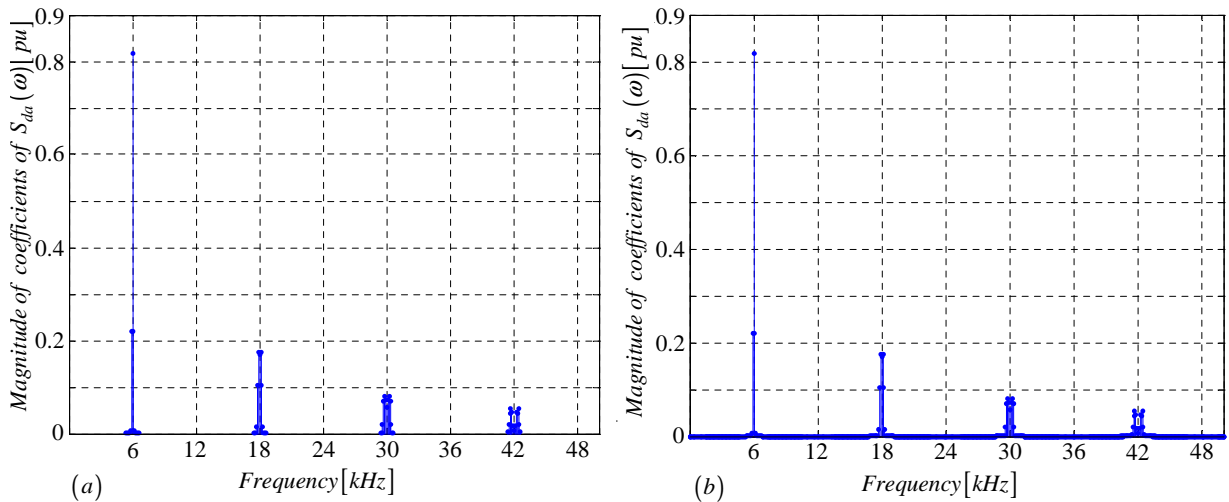


Figure 3.22: *Amplitude spectrum of $S_{da}(\omega)$ generated using (a) Newton-Raphson simulation and (b) Theory*

Figures 3.22 (a) and (b) illustrate the amplitude spectrum of the switching function $S_{da}(\omega)$ generated using Newton-Raphson simulation and theory respectively, whilst Figures 3.23 (a) and (b) show the phase spectrum of the switching function $S_{da}(\omega)$ generated employing Newton-Raphson simulation and theory respectively. Similarly Figures 3.24 (a) and (b) depict the amplitude spectrum of the switching function $S_{ta}(\omega)$ generated using

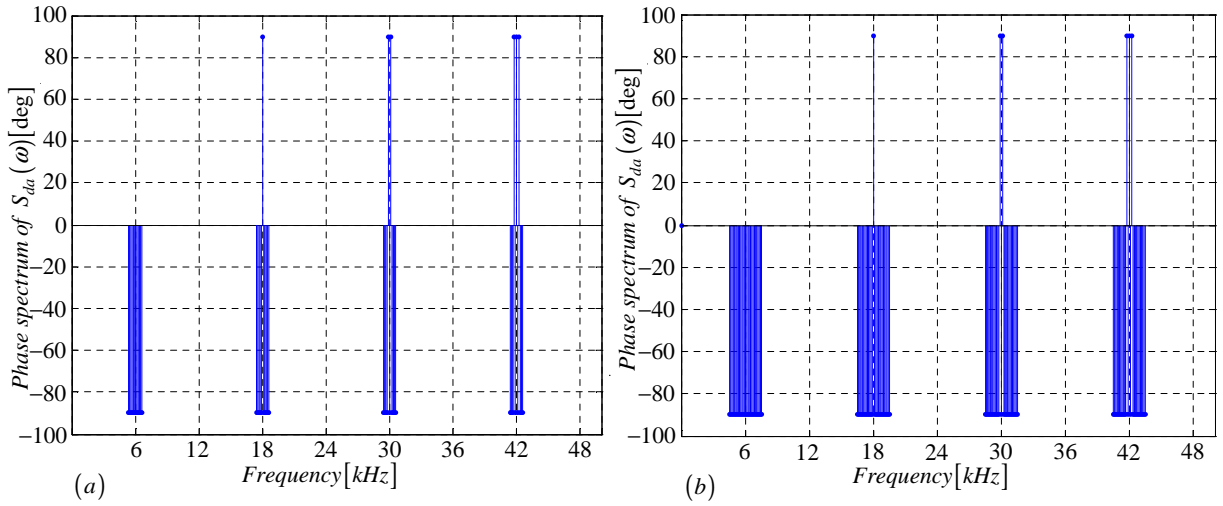


Figure 3.23: Phase spectrum of $S_{da}(\omega)$ generated using (a) Newton-Raphson simulation and (b) Theory

Newton-Raphson simulation and theory respectively, whilst Figures 3.25 (a) and (b) show the phase spectrum of the switching function $S_{ta}(\omega)$ generated using Newton-Raphson simulation and theory respectively.

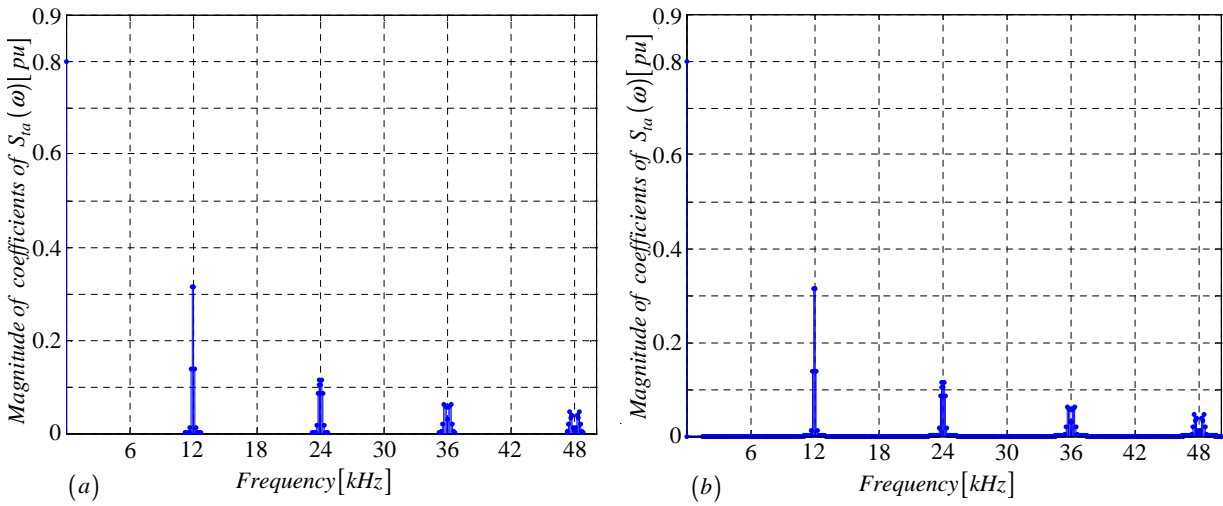


Figure 3.24: Amplitude spectrum of $S_{ta}(\omega)$ generated using (a) Newton-Raphson simulation and (b) Theory

The amplitude spectra for $S_{db}(\omega)$ and $S_{dc}(\omega)$ are the same as the amplitude spectrum for $S_{da}(\omega)$ while the amplitude spectra for $S_{tb}(\omega)$ and $S_{tc}(\omega)$ are the same as the amplitude spectrum for S_{ta} . The phase spectrum for $S_{db}(\omega)$ derived from simulation and theory are given by Figures 3.26 (a) and (b) respectively, whilst the phase spectrum for $S_{tb}(\omega)$ derived from simulation and theory are given by Figures 3.27 (a) and (b) respectively.

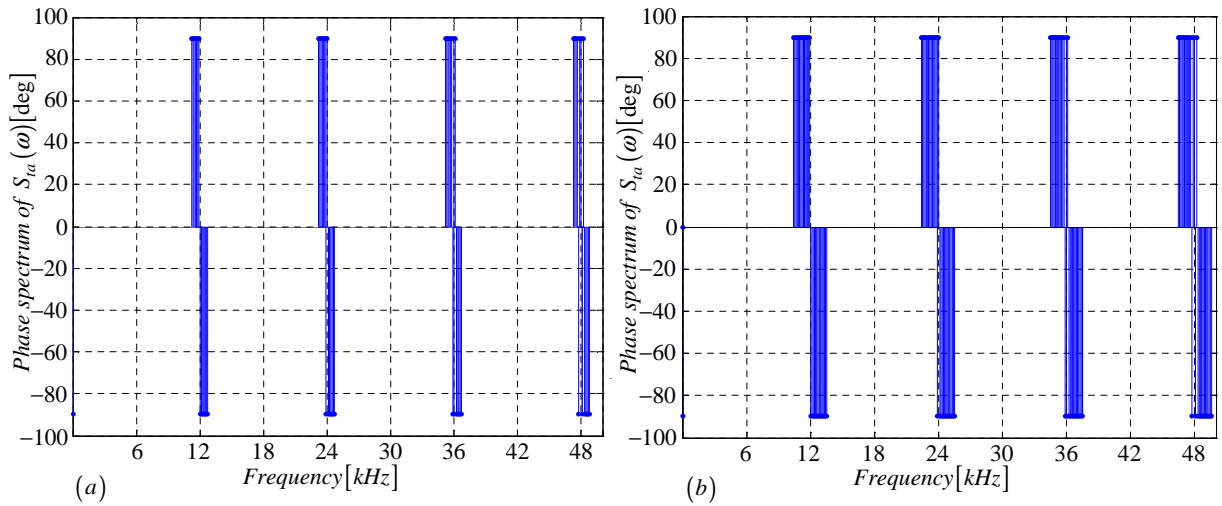


Figure 3.25: Phase spectrum of $S_{ta}(\omega)$ generated using (a) Newton-Raphson simulation and (b) Theory

Similarly the phase spectrum for $S_{dc}(\omega)$ derived from simulation and theory are given by Figures 3.28 (a) and (b) respectively, whilst the phase spectrum for $S_{tc}(\omega)$ derived from simulation and theory are given by Figures 3.29 (a) and (b) respectively.

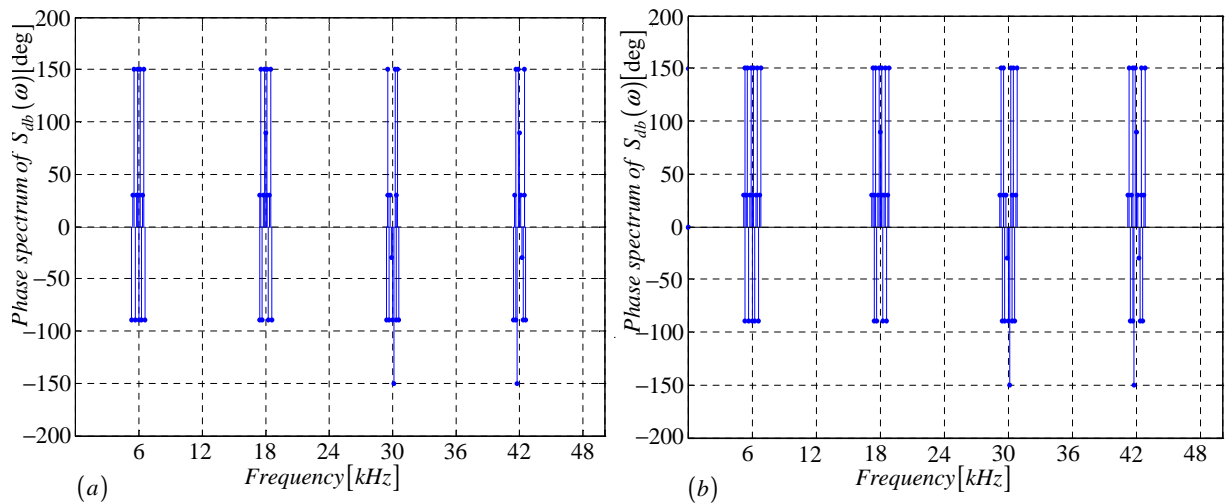


Figure 3.26: Phase spectrum of $S_{db}(\omega)$ generated using (a) Newton-Raphson simulation and (b) Theory

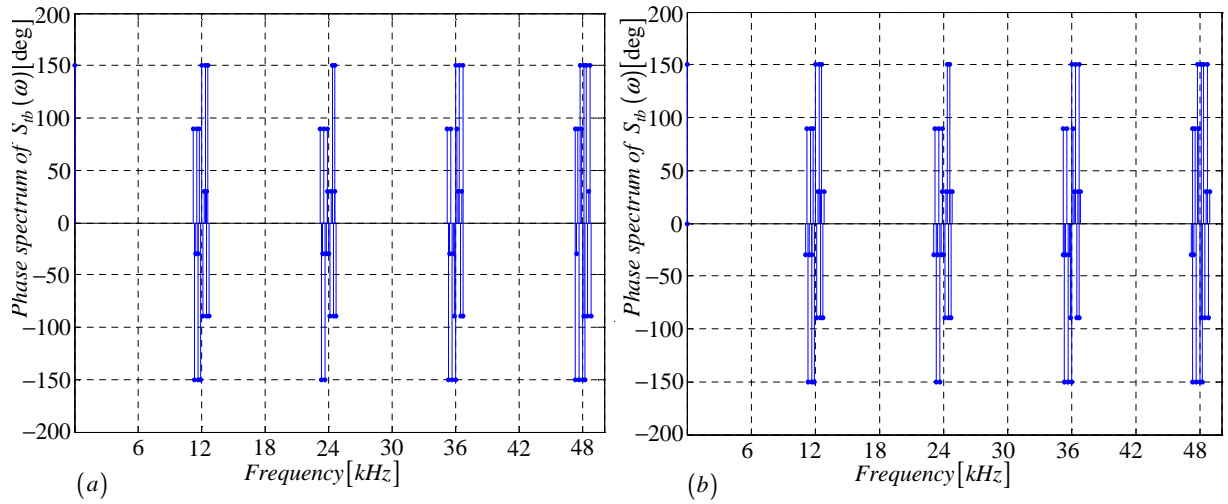


Figure 3.27: Phase spectrum of $S_{tb}(\omega)$ generated using (a) Newton-Raphson simulation and (b) Theory

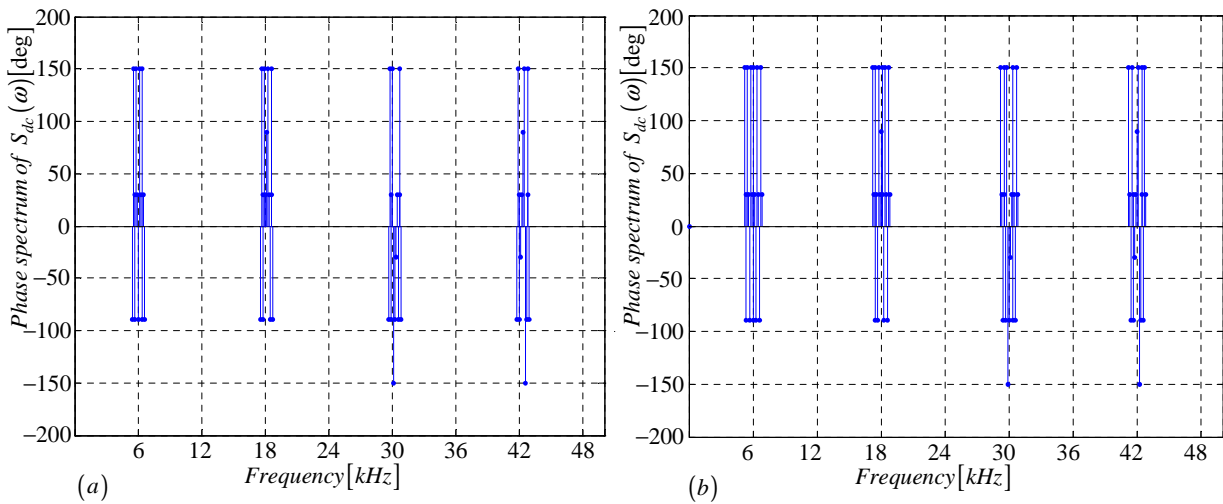


Figure 3.28: Phase spectrum of $S_{dc}(\omega)$ generated using (a) Newton-Raphson simulation and (b) Theory

From equations 3.40 to 3.43, and the spectra in Figures 3.22 to 3.29 and Tables 3.2, 3.3 and 3.4, we observe the following:

- The difference switching functions $S_{da}(\omega)$, $S_{db}(\omega)$ and $S_{dc}(\omega)$ contain harmonics around odd multiples of the switching frequency.
- The total switching functions $S_{ta}(\omega)$, $S_{tb}(\omega)$ and $S_{tc}(\omega)$ contain harmonics around even multiples of the switching frequency.

3.5.3 Switching functions of 3-cell converter

The difference switching functions $s_{da1}(t)$, $s_{da2}(t)$, $s_{db1}(t)$, $s_{db2}(t)$, $s_{dc1}(t)$ and $s_{dc2}(t)$ and the total switching functions $s_{ta}(t)$, $s_{tb}(t)$ and $s_{tc}(t)$ are defined in section 3.4. For convenience we define the switching functions $s_{a1}(t)$, $s_{a2}(t)$ and $s_{a3}(t)$ as follows:

$$s_{a1}(t) = \begin{cases} 1 & \text{if } f_{c1} < f_{r1} \\ -1 & \text{if } f_{c1} > f_{r1} \end{cases} \quad (3.71)$$

$$s_{a2}(t) = \begin{cases} 1 & \text{if } f_{c2} < f_{r1} \\ -1 & \text{if } f_{c2} > f_{r1} \end{cases} \quad (3.72)$$

$$s_{a3}(t) = \begin{cases} 1 & \text{if } f_{c3} < f_{r1} \\ -1 & \text{if } f_{c3} > f_{r1} \end{cases} \quad (3.73)$$

Switching functions for phases B and C are defined in a similar way. The PWM is generated by using three reference signals phase-shifted by $\frac{2\pi}{3}$, given by equations 3.74, 3.75 and 3.76 and three carrier signals phase-shifted by $\frac{2\pi}{3}$, given by equations 3.77, 3.78 and 3.79. For the reference signal we use a sinusoidal wave with an angular frequency of ω_0 and for the carrier signal we use a triangular wave with an angular frequency of ω_s . The PWM of each cell is generated by comparing one carrier signal with the corresponding reference signal.

$$f_{r1} = \sin\omega_0 t \quad (3.74)$$

$$f_{r2} = \sin\left(\omega_0 t - \frac{2\pi}{3}\right) \quad (3.75)$$

$$f_{r3} = \sin\left(\omega_0 t - \frac{4\pi}{3}\right) \quad (3.76)$$

$$f_{c1} = \frac{2}{\pi} \arcsin\omega_s t \quad (3.77)$$

$$f_{c2} = \frac{2}{\pi} \arcsin\left(\omega_s t - \frac{2\pi}{3}\right) \quad (3.78)$$

$$f_{c3} = \frac{2}{\pi} \arcsin\left(\omega_s t - \frac{4\pi}{3}\right) \quad (3.79)$$

Figure 3.30, 3.31 and 3.32 depict the generation of the switching functions of the 3-cell multicell converter using interleaved switching.

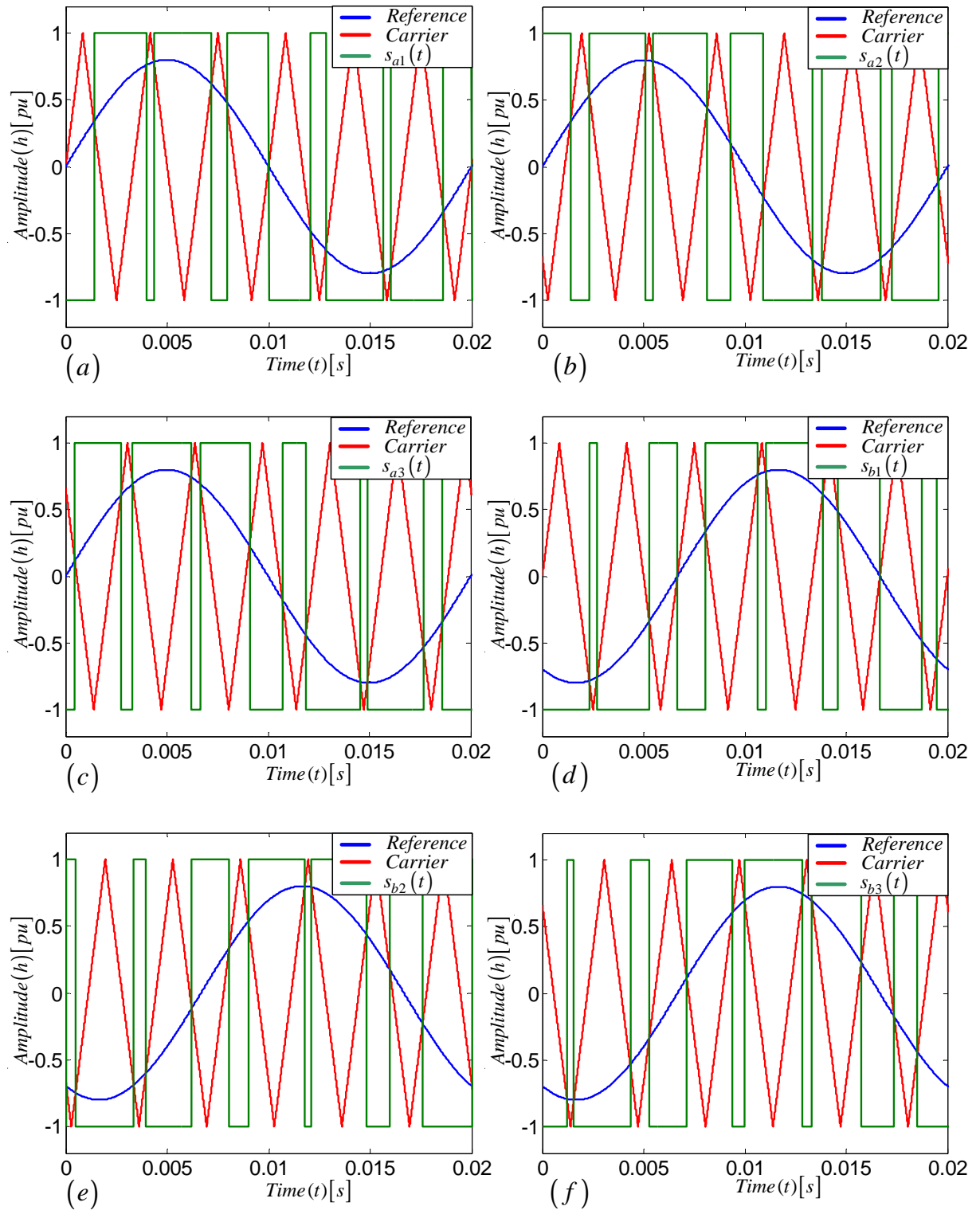


Figure 3.30: Generation of interleaved switching 3-cell multicell converter

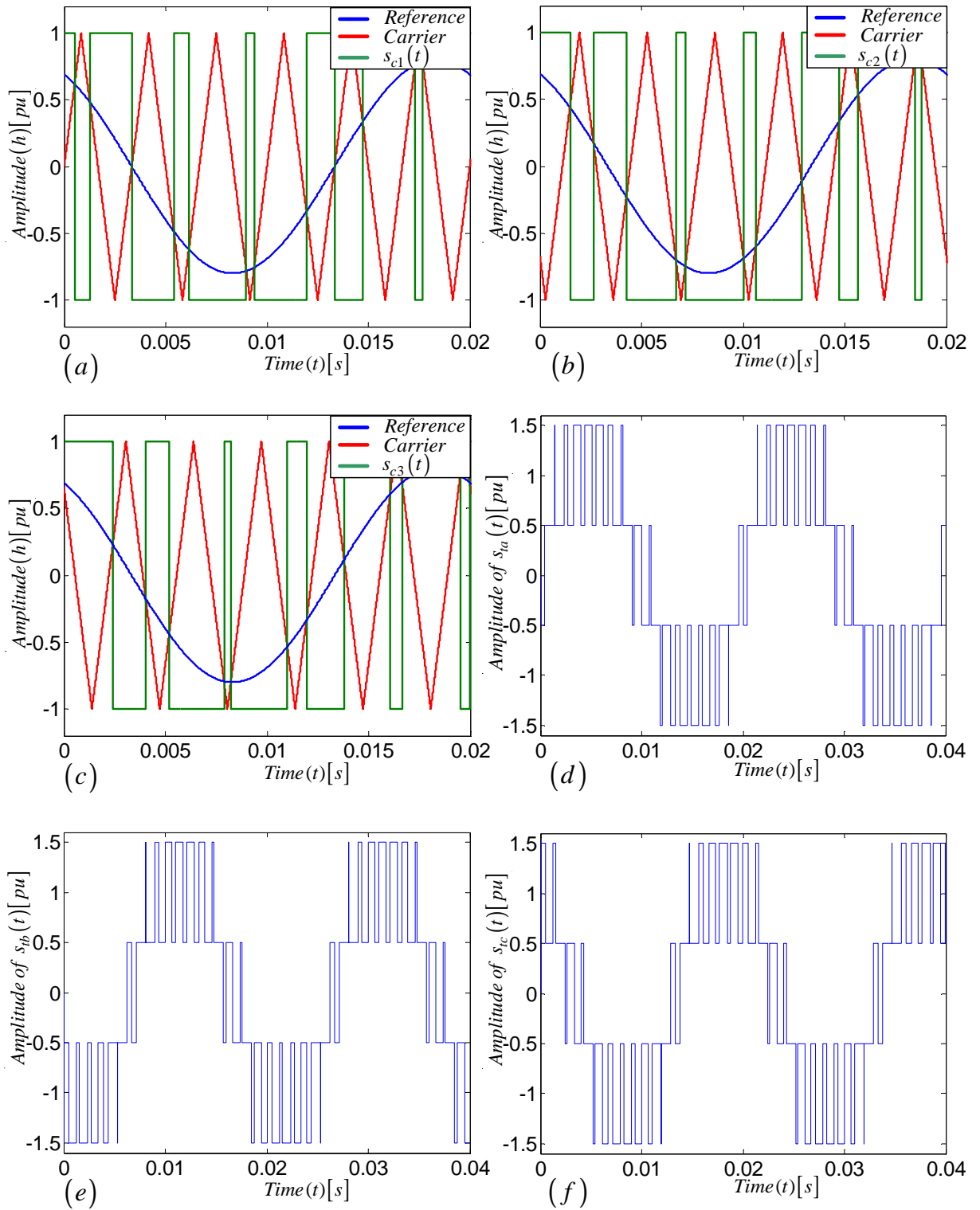


Figure 3.31: Generation of interleaved switching 3-cell multicell converter

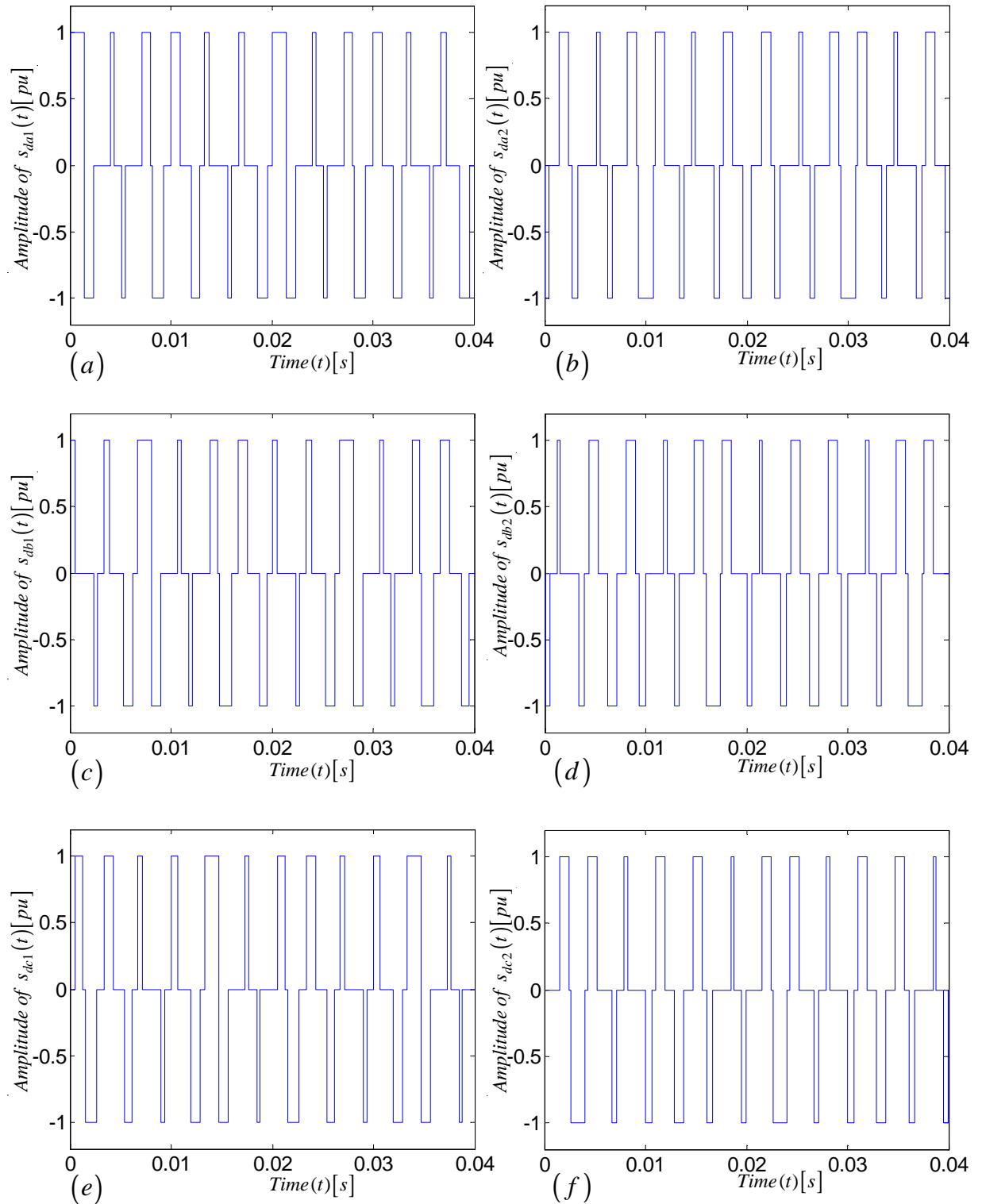


Figure 3.32: Generation of interleaved switching 3-cell multicell converter

Now using a similar approach to that in subsection 3.5.2 we obtain Tables 3.6 and 3.7 which show the values of t_x , c and h for the background function of different functions and for the case of $m_f \in \{3k : k = 1, 2, 3 \dots\}$, $m_f \in \{3k + 1 : k = 1, 2, 3 \dots\}$ and $m_f \in$

$$\{3k + 2 : k = 1, 2, 3 \dots\}.$$

Table 3.6: Values for t_x and c of background function for 3-cell multicell converter

m_f		s_{a1}	s_{a2}	s_{a3}	s_{b1}	s_{b2}	s_{b3}
$3k$	t_x	0	$\frac{1}{3}T_s$	$\frac{2}{3}T_s$	0	$\frac{1}{3}T_s$	$\frac{2}{3}T_s$
	c	0	$-\frac{4}{3}$	$-\frac{8}{3}$	0	$-\frac{4}{3}$	$-\frac{8}{3}$
	h	$\frac{2\omega_s t}{\pi}$	$\frac{2\omega_s t}{\pi} - \frac{4}{3}$	$\frac{2\omega_s t}{\pi} - \frac{8}{3}$	$\frac{2\omega_s t_1}{\pi}$	$\frac{2\omega_s t_1}{\pi} - \frac{4}{3}$	$\frac{2\omega_s t_1}{\pi} - \frac{8}{3}$
$3k + 1$	t_x	0	$\frac{1}{3}T_s$	$\frac{2}{3}T_s$	$\frac{2}{3}T_s$	0	$\frac{1}{3}T_s$
	c	0	$-\frac{4}{3}$	$-\frac{8}{3}$	$-\frac{8}{3}$	0	$-\frac{4}{3}$
	h	$\frac{2\omega_s t}{\pi}$	$\frac{2\omega_s t}{\pi} - \frac{4}{3}$	$\frac{2\omega_s t}{\pi} - \frac{8}{3}$	$\frac{2\omega_s t_1}{\pi} - \frac{8}{3}$	$\frac{2\omega_s t_1}{\pi}$	$\frac{2\omega_s t_1}{\pi} - \frac{4}{3}$
$3k + 2$	t_x	0	$\frac{1}{3}T_s$	$\frac{2}{3}T_s$	$\frac{1}{3}T_s$	$\frac{2}{3}T_s$	0
	c	0	$-\frac{4}{3}$	$-\frac{8}{3}$	$-\frac{4}{3}$	$-\frac{8}{3}$	0
	h	$\frac{2\omega_s t}{\pi}$	$\frac{2\omega_s t}{\pi} - \frac{4}{3}$	$\frac{2\omega_s t}{\pi} - \frac{8}{3}$	$\frac{2\omega_s t_1}{\pi} - \frac{4}{3}$	$\frac{2\omega_s t_1}{\pi} - \frac{8}{3}$	$\frac{2\omega_s t_1}{\pi}$

Table 3.7: Values for t_x and c of background function for 3-cell multicell converter

m_f		s_{c1}	s_{c2}	s_{c3}
$3k$	t_x	0	$\frac{1}{3}T_s$	$\frac{2}{3}T_s$
	c	0	$-\frac{4}{3}$	$-\frac{8}{3}$
	h	$\frac{2\omega_s t_2}{\pi}$	$\frac{2\omega_s t_2}{\pi} - \frac{4}{3}$	$\frac{2\omega_s t_2}{\pi} - \frac{8}{3}$
$3k + 1$	t_x	$\frac{1}{3}T_s$	$\frac{2}{3}T_s$	0
	c	$-\frac{4}{3}$	$-\frac{8}{3}$	0
	h	$\frac{2\omega_s t_2}{\pi} - \frac{4}{3}$	$\frac{2\omega_s t_2}{\pi} - \frac{8}{3}$	$\frac{2\omega_s t_2}{\pi}$
$3k + 2$	t_x	$\frac{2}{3}T_s$	0	$\frac{1}{3}T_s$
	c	$-\frac{8}{3}$	0	$-\frac{4}{3}$
	h	$\frac{2\omega_s t_2}{\pi} - \frac{8}{3}$	$\frac{2\omega_s t_2}{\pi}$	$\frac{2\omega_s t_2}{\pi} - \frac{4}{3}$

Figures 3.33 (a) and (b) illustrate the background functions for the case of $m_f = 3k$ ($f_s = 300$) and $m_f = 3k + 1$ ($f_s = 350$) respectively. The difference is in the values of the switching frequency f_s , which affects the slope of h as can be seen in the two figures.

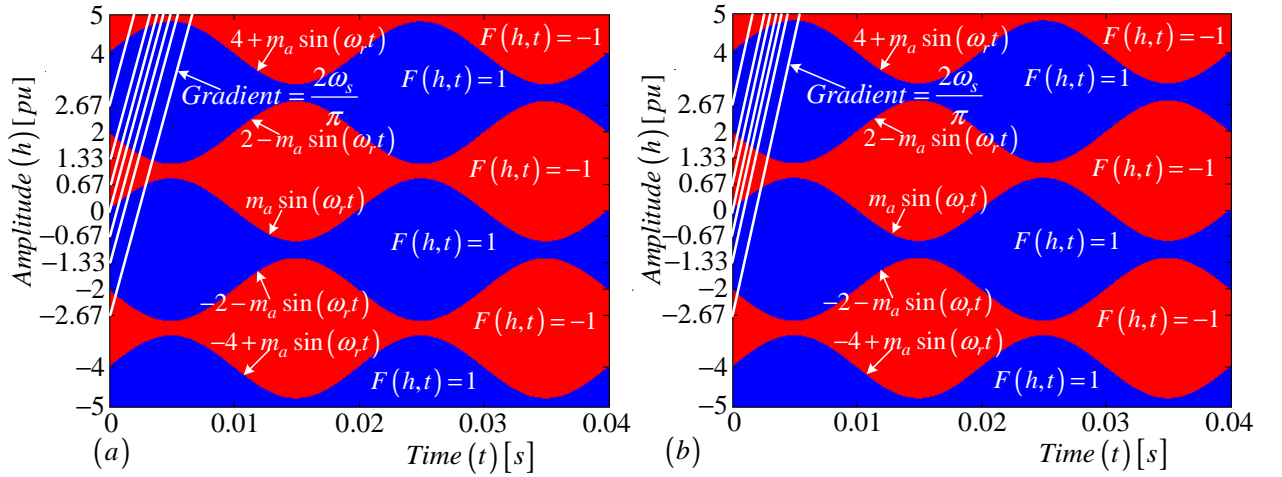


Figure 3.33: Top view of the background functions for the case of (a) $m_f = 3k$ and (b) $m_f = 3k + 1$.

The broad discussion on the switching functions for phases A, B and C with frequency modulation index of $m_f = 3k$, $m_f = 3k + 1$ and $m_f = 3k + 2$ is to be found in the Appendix, chapter C section C.2 using Tables 3.6 and 3.7. From the resulting phasor diagrams represented in Figures C.20 to C.38 we make the following observations shown in Tables 3.8, 3.9 and 3.10, 3.11 and 3.12, 3.13 and 3.14.

Table 3.8: Observation from phasor diagrams for Phase A

$S_{da2}(\omega)$	$S_{da1}(\omega)$	$S_{ta}(\omega)$	m	n	m_f
0	0	$ S_{ta}(\omega) $	$m = 3k$	$\forall n$	$\forall m_f$
$ S_{da2}(\omega) e^{j\frac{\pi}{2}}$	$ S_{da1}(\omega) e^{-j\frac{5\pi}{6}}$	0	$m = 3k + 1$	$\forall n$	$\forall m_f$
$ S_{da2}(\omega) e^{-j\frac{\pi}{2}}$	$ S_{da1}(\omega) e^{j\frac{5\pi}{6}}$	0	$m = 3k + 2$	$\forall n$	$\forall m_f$

Table 3.9: Observation from phasor diagrams for Phase B with $m_f = 3k$

$S_{db2}(\omega)$	$S_{db1}(\omega)$	$S_{tb}(\omega)$	m	n
0	0	$ S_{tb}(\omega) $	$m = 3k$	$n = 3p$ or $n = -3p$
0	0	$ S_{tb}(\omega) e^{-j\frac{2\pi}{3}}$	$m = 3k$	$n = 3p + 1$ or $n = -(3p + 2)$
0	0	$ S_{tb}(\omega) e^{j\frac{2\pi}{3}}$	$m = 3k$	$n = 3p + 2$ or $n = -(3p + 1)$
$ S_{db2}(\omega) e^{j\frac{\pi}{2}}$	$ S_{db1}(\omega) e^{-j\frac{5\pi}{6}}$	0	$m = 3k + 1$	$n = 3p$ or $n = -3p$
$ S_{db2}(\omega) e^{-j\frac{\pi}{6}}$	$ S_{db1}(\omega) e^{j\frac{\pi}{2}}$	0	$m = 3k + 1$	$n = 3p + 1$ or $n = -(3p + 2)$
$ S_{db2}(\omega) e^{-j\frac{5\pi}{6}}$	$ S_{db1}(\omega) e^{-j\frac{\pi}{6}}$	0	$m = 3k + 1$	$n = 3p + 2$ or $n = -(3p + 1)$
$ S_{db2}(\omega) e^{-j\frac{\pi}{2}}$	$ S_{db1}(\omega) e^{j\frac{5\pi}{6}}$	0	$m = 3k + 2$	$n = 3p$ or $n = -3p$
$ S_{db2}(\omega) e^{j\frac{5\pi}{6}}$	$ S_{db1}(\omega) e^{j\frac{\pi}{6}}$	0	$m = 3k + 2$	$n = 3p + 1$ or $n = -(3p + 2)$
$ S_{db2}(\omega) e^{j\frac{\pi}{6}}$	$ S_{db1}(\omega) e^{-j\frac{\pi}{2}}$	0	$m = 3k + 2$	$n = 3p + 2$ or $n = -(3p + 1)$

Table 3.10: Observation from phasor diagrams for Phase C with $m_f = 3k$

$S_{dc2}(\omega)$	$S_{dc1}(\omega)$	$S_{tc}(\omega)$	m	n
0	0	$ S_{tc}(\omega) $	$m = 3k$	$n = 3p$ or $n = -3p$
0	0	$ S_{tc}(\omega) e^{j\frac{2\pi}{3}}$	$m = 3k$	$n = 3p + 1$ or $n = -(3p + 2)$
0	0	$ S_{tc}(\omega) e^{-j\frac{2\pi}{3}}$	$m = 3k$	$n = 3p + 2$ or $n = -(3p + 1)$
$ S_{dc2}(\omega) e^{j\frac{\pi}{2}}$	$ S_{dc1}(\omega) e^{-j\frac{5\pi}{6}}$	0	$m = 3k + 1$	$n = 3p$ or $n = -3p$
$ S_{dc2}(\omega) e^{-j\frac{5\pi}{6}}$	$ S_{dc1}(\omega) e^{-j\frac{\pi}{6}}$	0	$m = 3k + 1$	$n = 3p + 1$ or $n = -(3p + 2)$
$ S_{dc2}(\omega) e^{-j\frac{\pi}{6}}$	$ S_{dc1}(\omega) e^{j\frac{\pi}{2}}$	0	$m = 3k + 1$	$n = 3p + 2$ or $n = -(3p + 1)$
$ S_{dc2}(\omega) e^{j\frac{\pi}{2}}$	$ S_{dc1}(\omega) e^{-j\frac{5\pi}{6}}$	0	$m = 3k + 2$	$n = 3p$ or $n = -3p$
$ S_{dc2}(\omega) e^{j\frac{\pi}{6}}$	$ S_{dc1}(\omega) e^{-j\frac{\pi}{2}}$	0	$m = 3k + 2$	$n = 3p + 1$ or $n = -(3p + 2)$
$ S_{dc2}(\omega) e^{j\frac{5\pi}{6}}$	$ S_{dc1}(\omega) e^{j\frac{\pi}{6}}$	0	$m = 3k + 2$	$n = 3p + 2$ or $n = -(3p + 1)$

Table 3.11: Observation from phasor diagrams for Phase B with $m_f = 3k + 1$

$S_{db2}(\omega)$	$S_{db1}(\omega)$	$S_{tb}(\omega)$	m	n
0	0	$ S_{tb}(\omega) $	$m = 3k$	$n = 3p$ or $n = -3p$
0	0	$ S_{tb}(\omega) e^{-j\frac{2\pi}{3}}$	$m = 3k$	$n = 3p + 1$ or $n = -(3p + 2)$
0	0	$ S_{tb}(\omega) e^{j\frac{2\pi}{3}}$	$m = 3k$	$n = 3p + 2$ or $n = -(3p + 1)$
$ S_{db2}(\omega) e^{-j\frac{5\pi}{6}}$	$ S_{db1}(\omega) e^{-j\frac{\pi}{6}}$	0	$m = 3k + 1$	$n = 3p$ or $n = -3p$
$ S_{db2}(\omega) e^{j\frac{\pi}{2}}$	$ S_{db1}(\omega) e^{-j\frac{5\pi}{6}}$	0	$m = 3k + 1$	$n = 3p + 1$ or $n = -(3p + 2)$
$ S_{db2}(\omega) e^{-j\frac{\pi}{6}}$	$ S_{db1}(\omega) e^{j\frac{\pi}{2}}$	0	$m = 3k + 1$	$n = 3p + 2$ or $n = -(3p + 1)$
$ S_{db2}(\omega) e^{j\frac{5\pi}{6}}$	$ S_{db1}(\omega) e^{j\frac{\pi}{6}}$	0	$m = 3k + 2$	$n = 3p$ or $n = -3p$
$ S_{db2}(\omega) e^{j\frac{\pi}{6}}$	$ S_{db1}(\omega) e^{-j\frac{\pi}{2}}$	0	$m = 3k + 2$	$n = 3p + 1$ or $n = -(3p + 2)$
$ S_{db2}(\omega) e^{-j\frac{\pi}{2}}$	$ S_{db1}(\omega) e^{j\frac{5\pi}{6}}$	0	$m = 3k + 2$	$n = 3p + 2$ or $n = -(3p + 1)$

Table 3.12: Observation from phasor diagrams for Phase C with $m_f = 3k + 1$

$S_{dc2}(\omega)$	$S_{dc1}(\omega)$	$S_{tc}(\omega)$	m	n
0	0	$ S_{tc}(\omega) $	$m = 3k$	$n = 3p$ or $n = -3p$
0	0	$ S_{tc}(\omega) e^{j\frac{2\pi}{3}}$	$m = 3k$	$n = 3p + 1$ or $n = -(3p + 2)$
0	0	$ S_{tc}(\omega) e^{-j\frac{2\pi}{3}}$	$m = 3k$	$n = 3p + 2$ or $n = -(3p + 1)$
$ S_{dc2}(\omega) e^{-j\frac{\pi}{6}}$	$ S_{dc1}(\omega) e^{j\frac{\pi}{2}}$	0	$m = 3k + 1$	$n = 3p$ or $n = -3p$
$ S_{dc2}(\omega) e^{j\frac{\pi}{2}}$	$ S_{dc1}(\omega) e^{-j\frac{5\pi}{6}}$	0	$m = 3k + 1$	$n = 3p + 1$ or $n = -(3p + 2)$
$ S_{dc2}(\omega) e^{-j\frac{5\pi}{6}}$	$ S_{dc1}(\omega) e^{-j\frac{\pi}{6}}$	0	$m = 3k + 1$	$n = 3p + 2$ or $n = -(3p + 1)$
$ S_{dc2}(\omega) e^{j\frac{\pi}{6}}$	$ S_{dc1}(\omega) e^{-j\frac{\pi}{2}}$	0	$m = 3k + 2$	$n = 3p$ or $n = -3p$
$ S_{dc2}(\omega) e^{j\frac{5\pi}{6}}$	$ S_{dc1}(\omega) e^{j\frac{\pi}{6}}$	0	$m = 3k + 2$	$n = 3p + 1$ or $n = -(3p + 2)$
$ S_{dc2}(\omega) e^{-j\frac{\pi}{2}}$	$ S_{dc1}(\omega) e^{j\frac{5\pi}{6}}$	0	$m = 3k + 2$	$n = 3p + 2$ or $n = -(3p + 1)$

Table 3.13: Observation from phasor diagrams for Phase B with $m_f = 3k + 2$

$S_{db2}(\omega)$	$S_{db1}(\omega)$	$S_{tb}(\omega)$	m	n
0	0	$ S_{tb}(\omega) $	$m = 3k$	$n = 3p$ or $n = -3p$
0	0	$ S_{tb}(\omega) e^{-j\frac{2\pi}{3}}$	$m = 3k$	$n = 3p + 1$ or $n = -(3p + 2)$
0	0	$ S_{tb}(\omega) e^{j\frac{2\pi}{3}}$	$m = 3k$	$n = 3p + 2$ or $n = -(3p + 1)$
$ S_{db2}(\omega) e^{-j\frac{\pi}{6}}$	$ S_{db1}(\omega) e^{j\frac{\pi}{2}}$	0	$m = 3k + 1$	$n = 3p$ or $n = -3p$
$ S_{db2}(\omega) e^{-j\frac{5\pi}{6}}$	$ S_{db1}(\omega) e^{-j\frac{\pi}{6}}$	0	$m = 3k + 1$	$n = 3p + 1$ or $n = -(3p + 2)$
$ S_{db2}(\omega) e^{j\frac{\pi}{2}}$	$ S_{db1}(\omega) e^{-j\frac{5\pi}{6}}$	0	$m = 3k + 1$	$n = 3p + 2$ or $n = -(3p + 1)$
$ S_{db2}(\omega) e^{j\frac{\pi}{6}}$	$ S_{db1}(\omega) e^{-j\frac{\pi}{2}}$	0	$m = 3k + 2$	$n = 3p$ or $n = -3p$
$ S_{db2}(\omega) e^{-j\frac{\pi}{2}}$	$ S_{db1}(\omega) e^{j\frac{5\pi}{6}}$	0	$m = 3k + 2$	$n = 3p + 1$ or $n = -(3p + 2)$
$ S_{db2}(\omega) e^{j\frac{5\pi}{6}}$	$ S_{db1}(\omega) e^{j\frac{\pi}{6}}$	0	$m = 3k + 2$	$n = 3p + 2$ or $n = -(3p + 1)$

Table 3.14: Observation from phasor diagrams for Phase C with $m_f = 3k + 2$

$S_{dc2}(\omega)$	$S_{dc1}(\omega)$	$S_{tc}(\omega)$	m	n
0	0	$ S_{tc}(\omega) $	$m = 3k$	$n = 3p$ or $n = -3p$
0	0	$ S_{tc}(\omega) e^{j\frac{2\pi}{3}}$	$m = 3k$	$n = 3p + 1$ or $n = -(3p + 2)$
0	0	$ S_{tc}(\omega) e^{-j\frac{2\pi}{3}}$	$m = 3k$	$n = 3p + 2$ or $n = -(3p + 1)$
$ S_{dc2}(\omega) e^{-j\frac{5\pi}{6}}$	$ S_{dc1}(\omega) e^{-j\frac{\pi}{6}}$	0	$m = 3k + 1$	$n = 3p$ or $n = -3p$
$ S_{dc2}(\omega) e^{-j\frac{\pi}{6}}$	$ S_{dc1}(\omega) e^{j\frac{\pi}{2}}$	0	$m = 3k + 1$	$n = 3p + 1$ or $n = -(3p + 2)$
$ S_{dc2}(\omega) e^{j\frac{\pi}{2}}$	$ S_{dc1}(\omega) e^{-j\frac{5\pi}{6}}$	0	$m = 3k + 1$	$n = 3p + 2$ or $n = -(3p + 1)$
$ S_{dc2}(\omega) e^{j\frac{5\pi}{6}}$	$ S_{dc1}(\omega) e^{j\frac{\pi}{6}}$	0	$m = 3k + 2$	$n = 3p$ or $n = -3p$
$ S_{dc2}(\omega) e^{-j\frac{\pi}{2}}$	$ S_{dc1}(\omega) e^{j\frac{5\pi}{6}}$	0	$m = 3k + 2$	$n = 3p + 1$ or $n = -(3p + 2)$
$ S_{dc2}(\omega) e^{j\frac{\pi}{6}}$	$ S_{dc1}(\omega) e^{-j\frac{\pi}{2}}$	0	$m = 3k + 2$	$n = 3p + 2$ or $n = -(3p + 1)$

Simulations

Figures 3.34 (a) and (b) illustrate the amplitude spectrum $S_{da1}(\omega)$ derived from simulation and theory respectively. The amplitude spectra of $S_{da2}(\omega)$, $S_{db1}(\omega)$, $S_{db2}(\omega)$, $S_{dc1}(\omega)$, $S_{dc2}(\omega)$ are the same as that of $S_{da1}(\omega)$.

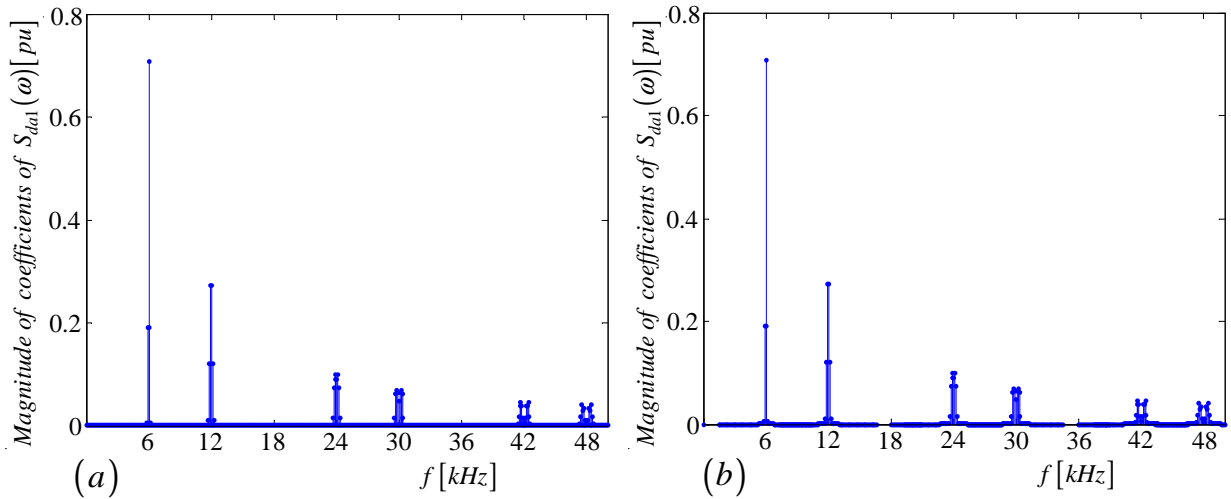


Figure 3.34: (a) Harmonics of $S_{da1}(\omega)$ derived from simulation (b) Harmonics of $S_{da1}(\omega)$ derived from theory

Figures 3.35 (a) and (b) depict the amplitude spectrum $S_{ta}(\omega)$ derived from simulation and theory respectively. The amplitude spectra of $S_{tb}(\omega)$ and $S_{tc}(\omega)$ are the same as that of $S_{ta}(\omega)$.

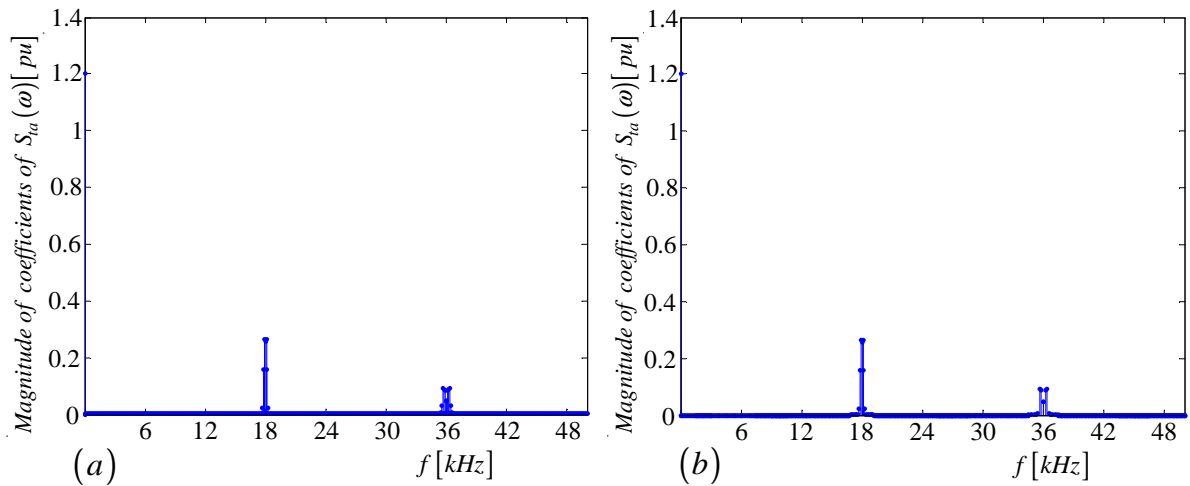


Figure 3.35: (a) Harmonics of $S_{ta}(\omega)$ derived from simulation (b) Harmonics of $S_{ta}(\omega)$ derived from theory

Figures 3.36 (a) and (b) show the amplitude spectra $|S_{da1}(\omega)|$ and $|S_{ta}(\omega)|$ derived from sim-

ulation and theory respectively. The amplitude spectra of $|S_{da2}(\omega)| |S_{ta}(\omega)|$, $|S_{db1}(\omega)| |S_{tb}(\omega)|$, $|S_{db2}(\omega)| |S_{tb}(\omega)|$, $|S_{dc1}(\omega)| |S_{tc}(\omega)|$ and $|S_{dc2}(\omega)| |S_{tc}(\omega)|$ are the same as that of $|S_{da1}(\omega)| |S_{ta}(\omega)|$.

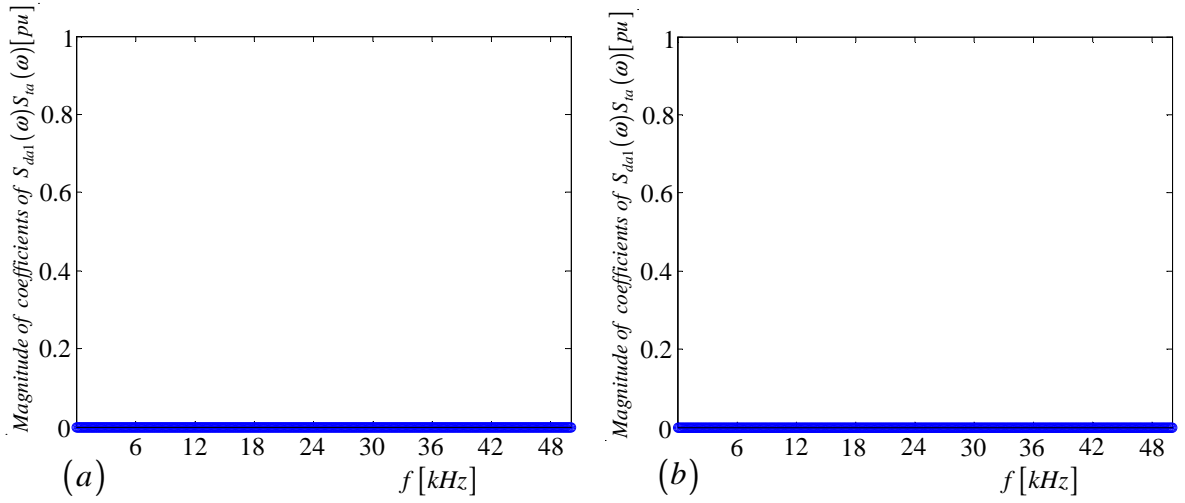


Figure 3.36: (a) Harmonics of $|S_{da1}(\omega)| |S_{ta}(\omega)|$ derived from simulation (b) Harmonics of $|S_{da1}(\omega)| |S_{ta}(\omega)|$ derived from theory

The phase spectra for all the switching functions of 3-cell multicell are derived in Appendix chapter B section B.3.

From equations 3.40 to 3.43, the spectra in Figures 3.34, 3.35 and 3.36 and Tables 3.8 to 3.14 we observe the following:

- The difference switching functions $S_{da1}(\omega)$, $S_{da2}(\omega)$, $S_{db1}(\omega)$, $S_{db2}(\omega)$, $S_{dc1}(\omega)$, and $S_{dc2}(\omega)$ contain harmonics around $3k + 1$ and $3k + 2$ multiples of the switching frequency for integer k .
- The total switching functions $S_{ta}(\omega)$, $S_{tb}(\omega)$ and $S_{tc}(\omega)$ contains harmonics around $3k$ multiples of the switching frequency for integer k .

From the above observations we reach the following conclusions:

$$|S_{da1}(\omega)| |S_{ta}(\omega)| \approx 0 \quad (3.80)$$

$$|S_{da2}(\omega)| |S_{ta}(\omega)| \approx 0 \quad (3.81)$$

$$|S_{db1}(\omega)| |S_{tb}(\omega)| \approx 0 \quad (3.82)$$

$$|S_{db2}(\omega)| |S_{tb}(\omega)| \approx 0 \quad (3.83)$$

$$|S_{dc1}(\omega)| |S_{tc}(\omega)| \approx 0 \quad (3.84)$$

$$|S_{dc2}(\omega)| |S_{tc}(\omega)| \approx 0 \quad (3.85)$$

3.6 Summary

In this chapter we studied the switching functions of 2-cell and 3-phase multicell converter under interleaved switching. The technique uses a geometric mathematical model and double Fourier series to calculate the magnitude and phase of the harmonics of the switched waveforms. The harmonics obtained were verified using both simplorer and Newton-Raphson simulations. For a 2-cell 3-phase multicell inverter we observed the following:

- The difference switching functions $S_{da}(\omega)$, $S_{db}(\omega)$ and $S_{dc}(\omega)$ contain harmonics around odd multiples of the switching frequency.
- The total switching functions $S_{ta}(\omega)$, $S_{tb}(\omega)$ and $S_{tc}(\omega)$ contain harmonics around even multiples of the switching frequency.

For a 3-cell multicell converter we observed the following:

- The difference switching functions $S_{da1}(\omega)$, $S_{da2}(\omega)$, $S_{db1}(\omega)$, $S_{db2}(\omega)$, $S_{dc1}(\omega)$, and $S_{dc2}(\omega)$ contain harmonics around $3k + 1$ and $3k + 2$ multiples of the switching frequency for integer k .
- The total switching functions $S_{ta}(\omega)$, $S_{tb}(\omega)$ and $S_{tc}(\omega)$ contain harmonics around $3k$ multiples of the switching frequency for integer k .

Chapter 4

Steady State Analysis

4.1 Introduction

In this chapter we study the 2-cell and 3-cell multicell converters under steady-state conditions. We do this by mathematically modelling the coefficients of the switching functions to obtain the steady-state behaviour of the 2-cell and 3-cell three-phase multicell converter. The derived steady-state equations are used to describe the balancing of the cell capacitor voltages. It will be found that as long as the switching frequency is chosen to be sufficiently higher than the highest frequency component of the reference signal and the impedance of the load is not purely inductive, then the cell capacitor voltages will naturally balance. Although it is possible to force the cell capacitor voltages to balance through active control, due to natural balancing this is not necessary in general. Furthermore we assume that the cell capacitor is very large and that the cell capacitor voltages change much slower compared to the rest of the system.

4.2 Steady State Balancing of 2-cell Converter

In this section we study the steady-state analysis of a 2-cell multicell converter. We derive the equations that are important for describing the balancing of the cell capacitor voltages under steady-state conditions.

The equivalent circuit of the 2-cell three-phase multicell converter was derived in section 3.3 in terms of d and t parameters. For convenience we represent Figure 3.6 as Figure 4.1 below:

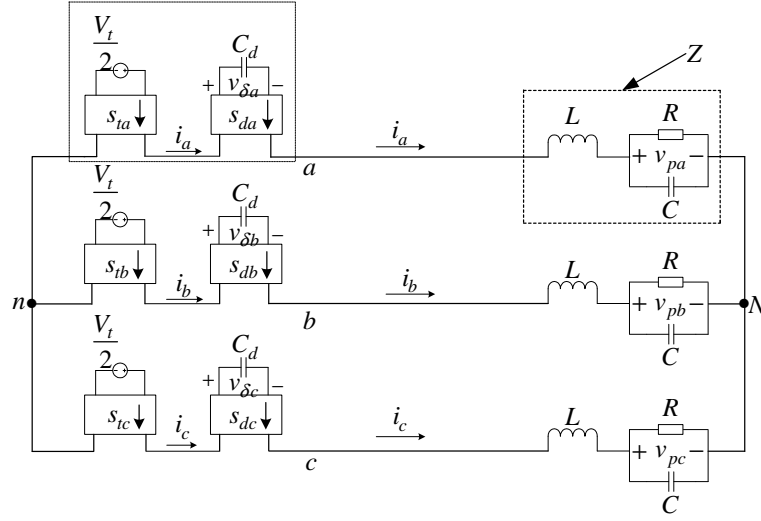


Figure 4.1: Equivalent circuit of 2-cell 3-phase multicell converter

The load in Figure 4.1 acts as an impedance divider and hence we have:

$$V_{Nn} = \frac{1}{3} \{V_{an} + V_{bn} + V_{cn}\} \quad (4.1)$$

Now applying the superposition principle and assuming that the cell capacitor voltages change much slower than the rest of the system in such a way that the rest of the system appears to be in a steady state. That is, the capacitor voltages can be viewed as constant or DC capacitor voltages. Hence we only need to calculate the DC current. Now using also equation 3.17 we write the DC current for phase A as follows:

$$\begin{aligned} I_a(\omega) &= \frac{V_{an} - V_{Nn}}{Z(\omega)} \\ &= \frac{1}{3} \left\{ \frac{V_t S_{ta}(\omega) + 2V_{\delta a} S_{da}(\omega)}{Z(\omega)} - \frac{\frac{V_t}{2} S_{tb}(\omega) + V_{\delta b} S_{db}(\omega)}{Z(\omega)} \right. \\ &\quad \left. - \frac{\frac{V_t}{2} S_{tc}(\omega) + V_{\delta c} S_{dc}(\omega)}{Z(\omega)} \right\} \end{aligned} \quad (4.2)$$

Similarly

$$\begin{aligned} I_b(\omega) &= \frac{V_{bn} - V_{Nn}}{Z(\omega)} \\ &= \frac{1}{3} \left\{ \frac{2S_{tb}(\omega)\frac{V_t}{2} + 2S_{db}(\omega)V_{\delta b} - S_{ta}(\omega)\frac{V_t}{2} - S_{da}(\omega)V_{\delta a}}{Z(\omega)} \right. \\ &\quad \left. - \frac{S_{tc}(\omega)\frac{V_t}{2} + S_{dc}(\omega)V_{\delta c}}{Z(\omega)} \right\} \end{aligned} \quad (4.3)$$

and

$$I_c(\omega) = \frac{V_{cn} - V_{Nn}}{Z(\omega)}$$

$$= \frac{1}{3} \left\{ \frac{2S_{tc}(\omega)\frac{V_t}{2} + 2S_{dc}(\omega)V_{\delta c} - S_{ta}(\omega)\frac{V_t}{2} - S_{da}(\omega)V_{\delta a}}{Z(\omega)} - \frac{S_{tb}(\omega)\frac{V_t}{2} + S_{db}(\omega)V_{\delta b}}{Z(\omega)} \right\} \quad (4.4)$$

The phase A cell capacitor current $I_{c_{da}}$ which is the DC-component of i_{ca} is given by

$$I_{c_{da}}(\omega) = -I_a(\omega) * S_{da}(\omega) \quad (4.5)$$

Now substituting equation 4.2 into 4.5 we obtain the following equation

$$\begin{aligned} I_{c_{da}}(\omega) = & -\frac{1}{3} \left\{ \left\{ \frac{V_t S_{ta}(\omega)}{Z(\omega)} \right\} * S_{da}(\omega) + \left\{ \frac{2V_{\delta a} S_{da}(\omega)}{Z(\omega)} \right\} * S_{da}(\omega) \right. \\ & - \left\{ \frac{\frac{V_t}{2} S_{tb}(\omega)}{Z(\omega)} \right\} * S_{da}(\omega) - \left\{ \frac{V_{\delta b} S_{db}(\omega)}{Z(\omega)} \right\} * S_{da}(\omega) \\ & \left. - \left\{ \frac{\frac{V_t}{2} S_{tc}(\omega)}{Z(\omega)} \right\} * S_{da}(\omega) - \left\{ \frac{V_{\delta c} S_{dc}(\omega)}{Z(\omega)} \right\} * S_{da}(\omega) \right\} \end{aligned} \quad (4.6)$$

Now applying the definition of the convolution integral; we have

$$\begin{aligned} I_{c_{da}}(\omega) = & -\frac{1}{3} \left\{ V_t \int_{-\infty}^{\infty} \frac{S_{ta}(u)}{Z(u)} S_{da}(\omega - u) du + 2V_{\delta a} \int_{-\infty}^{\infty} \frac{S_{da}(u)}{Z(u)} S_{da}(\omega - u) du \right. \\ & - \frac{V_t}{2} \int_{-\infty}^{\infty} \frac{S_{tb}(u)}{Z(u)} S_{da}(\omega - u) du - V_{\delta b} \int_{-\infty}^{\infty} \frac{S_{db}(u)}{Z(u)} S_{da}(\omega - u) \\ & \left. - \frac{V_t}{2} \int_{-\infty}^{\infty} \frac{S_{tc}(u)}{Z(u)} S_{da}(\omega - u) du - V_{\delta c} \int_{-\infty}^{\infty} \frac{S_{dc}(u)}{Z(u)} S_{da}(\omega - u) du \right\} \end{aligned} \quad (4.7)$$

Since the average value of i_{ca} is equal to zero amperes at steady state, we have $I_{c_{da}}(\omega)|_{\omega=0}$. Thus equation 4.7 can be written as follows

$$\begin{aligned} 0 = & -\frac{1}{3} \left\{ V_t \int_{-\infty}^{\infty} \frac{S_{ta}(u)}{Z(u)} \overline{S_{da}(u)} du + 2V_{\delta a} \int_{-\infty}^{\infty} \frac{|S_{da}(u)|^2}{Z(u)} du \right. \\ & - \frac{V_t}{2} \int_{-\infty}^{\infty} \frac{S_{tb}(u)}{Z(u)} \overline{S_{da}(u)} du - V_{\delta b} \int_{-\infty}^{\infty} \frac{S_{db}(u)}{Z(u)} \overline{S_{da}(u)} du \\ & \left. - \frac{V_t}{2} \int_{-\infty}^{\infty} \frac{S_{tc}(u)}{Z(u)} \overline{S_{da}(u)} du - V_{\delta c} \int_{-\infty}^{\infty} \frac{S_{dc}(u)}{Z(u)} \overline{S_{da}(u)} du \right\} \end{aligned} \quad (4.8)$$

Similarly for $I_{c_{ab}}(\omega)|_{\omega=0}$ we have

$$\begin{aligned} 0 = & -\frac{1}{3} \left\{ V_t \int_{-\infty}^{\infty} \frac{S_{tb}(u)}{Z(u)} \overline{S_{db}(u)} du + 2V_{\delta b} \int_{-\infty}^{\infty} \frac{|S_{db}(u)|^2}{Z(u)} du \right. \\ & - \frac{V_t}{2} \int_{-\infty}^{\infty} \frac{S_{ta}(u)}{Z(u)} \overline{S_{db}(u)} du - V_{\delta a} \int_{-\infty}^{\infty} \frac{S_{da}(u)}{Z(u)} \overline{S_{db}(u)} du \\ & \left. - \frac{V_t}{2} \int_{-\infty}^{\infty} \frac{S_{tc}(u)}{Z(u)} \overline{S_{db}(u)} du - V_{\delta c} \int_{-\infty}^{\infty} \frac{S_{dc}(u)}{Z(u)} \overline{S_{db}(u)} du \right\} \end{aligned} \quad (4.9)$$

and similarly for $I_{cdc}(\omega)|_{\omega=0}$ we have

$$\begin{aligned}
0 = & -\frac{1}{3} \left\{ V_t \int_{-\infty}^{\infty} \frac{S_{tc}(u)}{Z(u)} \overline{S_{dc}(u)} du + 2V_{\delta c} \int_{-\infty}^{\infty} \frac{|S_{dc}(u)|^2}{Z(u)} du \right. \\
& - \frac{V_t}{2} \int_{-\infty}^{\infty} \frac{S_{ta}(u)}{Z(u)} \overline{S_{dc}(u)} du - V_{\delta a} \int_{-\infty}^{\infty} \frac{S_{da}(u)}{Z(u)} \overline{S_{dc}(u)} du \\
& \left. - \frac{V_t}{2} \int_{-\infty}^{\infty} \frac{S_{tb}(u)}{Z(u)} \overline{S_{dc}(u)} du - V_{\delta b} \int_{-\infty}^{\infty} \frac{S_{db}(u)}{Z(u)} \overline{S_{dc}(u)} du \right\} \quad (4.10)
\end{aligned}$$

Writing equations 4.8, 4.9 and 5.5 in the matrix form we obtain

$$\begin{aligned}
& \begin{bmatrix} V_{\delta a} \\ V_{\delta b} \\ V_{\delta c} \end{bmatrix} = \\
& - \begin{bmatrix} 2 \int_{-\infty}^{\infty} \frac{|S_{da}|^2}{Z(u)} du & - \int_{-\infty}^{\infty} \frac{S_{db}(u)}{Z(u)} \overline{S_{da}(u)} du & - \int_{-\infty}^{\infty} \frac{S_{dc}(u)}{Z(u)} \overline{S_{da}(u)} du \\ - \int_{-\infty}^{\infty} \frac{S_{da}(u)}{Z(u)} \overline{S_{db}(u)} du & 2 \int_{-\infty}^{\infty} \frac{|S_{db}(u)|^2}{Z(u)} du & - \int_{-\infty}^{\infty} \frac{S_{dc}(u)}{Z(u)} \overline{S_{db}(u)} du \\ - \int_{-\infty}^{\infty} \frac{S_{da}(u)}{Z(u)} \overline{S_{dc}(u)} du & - \int_{-\infty}^{\infty} \frac{S_{db}(u)}{Z(u)} \overline{S_{dc}(u)} du & 2 \int_{-\infty}^{\infty} \frac{|S_{dc}(u)|^2}{Z(u)} du \end{bmatrix}^{-1} \\
& \times \begin{bmatrix} \int_{-\infty}^{\infty} \frac{S_{ta}}{Z(u)} \overline{S_{da}(u)} du - \frac{1}{2} \int_{-\infty}^{\infty} \frac{S_{tb}(u)}{Z(u)} \overline{S_{da}(u)} du - \frac{1}{2} \int_{-\infty}^{\infty} \frac{S_{tc}(u)}{Z(u)} \overline{S_{da}(u)} du \\ \int_{-\infty}^{\infty} \frac{S_{tb}(u)}{Z(u)} \overline{S_{db}(u)} du - \frac{1}{2} \int_{-\infty}^{\infty} \frac{S_{ta}(u)}{Z(u)} \overline{S_{db}(u)} du - \frac{1}{2} \int_{-\infty}^{\infty} \frac{S_{tc}(u)}{Z(u)} \overline{S_{db}(u)} du \\ \int_{-\infty}^{\infty} \frac{S_{tc}(u)}{Z(u)} \overline{S_{dc}(u)} du - \frac{1}{2} \int_{-\infty}^{\infty} \frac{S_{ta}(u)}{Z(u)} \overline{S_{dc}(u)} du - \frac{V_t}{2} \int_{-\infty}^{\infty} \frac{S_{tb}(u)}{Z(u)} \overline{S_{dc}(u)} du \end{bmatrix} V_t \quad (4.11)
\end{aligned}$$

Since the above functions are periodic and the analysis is in steady state (which implies $u = l\omega_0$ where l is the harmonic number) we have

$$\begin{aligned}
 & \begin{bmatrix} V_{\delta a} \\ V_{\delta b} \\ V_{\delta c} \end{bmatrix} = \\
 & - \begin{bmatrix} 2 \int_{-\infty}^{\infty} \frac{|S_{da}(l\omega_0)|^2}{Z(l\omega_0)} dl\omega_0 & - \int_{-\infty}^{\infty} \frac{S_{db}(l\omega_0)}{Z(l\omega_0)} \overline{S_{da}(l\omega_0)} dl\omega_0 & - \int_{-\infty}^{\infty} \frac{S_{dc}(l\omega_0)}{Z(l\omega_0)} \overline{S_{da}(l\omega_0)} dl\omega_0 \\ - \int_{-\infty}^{\infty} \frac{S_{da}(l\omega_0)}{Z(l\omega_0)} \overline{S_{db}(l\omega_0)} dl\omega_0 & 2 \int_{-\infty}^{\infty} \frac{|S_{db}(l\omega_0)|^2}{Z(l\omega_0)} dl\omega_0 & - \int_{-\infty}^{\infty} \frac{S_{dc}(l\omega_0)}{Z(l\omega_0)} \overline{S_{db}(l\omega_0)} dl\omega_0 \\ - \int_{-\infty}^{\infty} \frac{S_{da}(l\omega_0)}{Z(l\omega_0)} \overline{S_{dc}(l\omega_0)} dl\omega_0 & - \int_{-\infty}^{\infty} \frac{S_{db}(l\omega_0)}{Z(l\omega_0)} \overline{S_{dc}(l\omega_0)} dl\omega_0 & 2 \int_{-\infty}^{\infty} \frac{|S_{dc}(l\omega_0)|^2}{Z(l\omega_0)} dl\omega_0 \end{bmatrix}^{-1} \\
 & \times \begin{bmatrix} \int_{-\infty}^{\infty} \frac{S_{ta}(l\omega_0)}{Z(l\omega_0)} \overline{S_{da}(l\omega_0)} dl\omega_0 - \frac{1}{2} \int_{-\infty}^{\infty} \frac{S_{tb}(l\omega_0)}{Z(l\omega_0)} \overline{S_{da}(l\omega_0)} dl\omega_0 - \frac{1}{2} \int_{-\infty}^{\infty} \frac{S_{tc}(l\omega_0)}{Z(l\omega_0)} \overline{S_{da}(l\omega_0)} dl\omega_0 \\ \int_{-\infty}^{\infty} \frac{S_{tb}(l\omega_0)}{Z(l\omega_0)} \overline{S_{db}(l\omega_0)} dl\omega_0 - \frac{1}{2} \int_{-\infty}^{\infty} \frac{S_{ta}(l\omega_0)}{Z(l\omega_0)} \overline{S_{db}(l\omega_0)} dl\omega_0 - \frac{1}{2} \int_{-\infty}^{\infty} \frac{S_{tc}(l\omega_0)}{Z(l\omega_0)} \overline{S_{db}(l\omega_0)} dl\omega_0 \\ \int_{-\infty}^{\infty} \frac{S_{tc}(l\omega_0)}{Z(l\omega_0)} \overline{S_{dc}(l\omega_0)} dl\omega_0 - \frac{1}{2} \int_{-\infty}^{\infty} \frac{S_{ta}(l\omega_0)}{Z(l\omega_0)} \overline{S_{dc}(l\omega_0)} dl\omega_0 - \frac{V_t}{2} \int_{-\infty}^{\infty} \frac{S_{tb}(l\omega_0)}{Z(l\omega_0)} \overline{S_{dc}(l\omega_0)} dl\omega_0 \end{bmatrix} V_t
 \end{aligned} \tag{4.12}$$

From chapter 3 the phase-b switching functions are the same as those for phase-a but delayed by $\frac{T}{3}$ and that the phase-c switching functions are the same as those for phase-a but delayed by $\frac{2T}{3}$ where T is the period of the switching function. Since the functions in the matrix equation 4.12 are periodic we write it in terms of exponential fourier series as shown in matrix equation 4.13.

$$\begin{aligned}
 & \begin{bmatrix} V_{\delta a} \\ V_{\delta b} \\ V_{\delta c} \end{bmatrix} = \\
 & - \begin{bmatrix} 2 \sum_{l=-\infty}^{\infty} \frac{|D_{al}|^2}{Z(l\omega_0)} & - \sum_{l=-\infty}^{\infty} \frac{|D_{al}|^2}{Z(l\omega_0)} e^{-jl\frac{2\pi}{3}} & - \sum_{l=-\infty}^{\infty} \frac{|D_{al}|^2}{Z(l\omega_0)} e^{jl\frac{2\pi}{3}} \\ - \sum_{l=-\infty}^{\infty} \frac{|D_{al}|^2}{Z(l\omega_0)} e^{jl\frac{2\pi}{3}} & 2 \sum_{l=-\infty}^{\infty} \frac{|D_{al}|^2}{Z(l\omega_0)} & - \sum_{l=-\infty}^{\infty} \frac{|D_{al}|^2}{Z(l\omega_0)} e^{-jl\frac{2\pi}{3}} \\ - \sum_{l=-\infty}^{\infty} \frac{|D_{al}|^2}{Z(l\omega_0)} e^{-jl\frac{2\pi}{3}} & - \sum_{l=-\infty}^{\infty} \frac{|D_{al}|^2}{Z(l\omega_0)} e^{jl\frac{2\pi}{3}} & 2 \sum_{l=-\infty}^{\infty} \frac{|D_{al}|^2}{Z(l\omega_0)} \end{bmatrix}^{-1}
 \end{aligned}$$

$$\times \begin{bmatrix} \sum_{l=-\infty}^{\infty} \frac{B_{al}\overline{D_{al}}}{Z(l\omega_0)} \left\{ 1 - \frac{1}{2}e^{-jl\frac{2\pi}{3}} - \frac{1}{2}e^{jl\frac{2\pi}{3}} \right\} \\ \sum_{l=-\infty}^{\infty} \frac{B_{al}\overline{D_{al}}}{Z(l\omega_0)} \left\{ 1 - \frac{1}{2}e^{jl\frac{2\pi}{3}} - \frac{1}{2}e^{-jl\frac{2\pi}{3}} \right\} \\ \sum_{l=-\infty}^{\infty} \frac{B_{al}\overline{D_{al}}}{Z(l\omega_0)} \left\{ 1 - \frac{1}{2}e^{-jl\frac{2\pi}{3}} - \frac{1}{2}e^{jl\frac{2\pi}{3}} \right\} \end{bmatrix} V_t \quad (4.13)$$

To simplify analyses of matrix equation 4.13 we write $e^{jl\frac{2\pi}{3}}$ and $e^{-jl\frac{2\pi}{3}}$ in terms of three classes as shown in Table 4.1. The harmonic number l is written as follows:

$$l = m \frac{f_s}{f_0} + n = mm_f + n \quad (4.14)$$

where f_s is the switching frequency and f_0 is the fundamental frequency.

Table 4.1: *Different classes of harmonics*

m_f	m	n	<i>Class</i>
$3k$	$\forall m$	$n = 3p$ or $n = -3p$	<i>Class 1</i>
$3k$	$\forall m$	$n = 3p + 1$ or $n = -(3p + 2)$	<i>Class 2</i>
$3k$	$\forall m$	$n = 3p + 2$ or $n = -(3p + 1)$	<i>Class 3</i>
$3k + 1$	$m = 3k$	$n = 3p$ or $n = -3p$	<i>Class 1</i>
$3k + 1$	$m = 3k + 1$	$n = 3p + 2$ or $n = -(3p + 1)$	<i>Class 1</i>
$3k + 1$	$m = 3k + 2$	$n = 3p + 1$ or $n = -(3p + 2)$	<i>Class 1</i>
$3k + 1$	$m = 3k$	$n = 3p + 1$ or $n = -(3p + 2)$	<i>Class 2</i>
$3k + 1$	$m = 3k + 1$	$n = 3p$ or $n = -3p$	<i>Class 2</i>
$3k + 1$	$m = 3k + 2$	$n = 3p + 2$ or $n = -(3p + 1)$	<i>Class 2</i>
$3k + 1$	$m = 3k$	$n = 3p + 2$ or $n = -(3p + 1)$	<i>Class 3</i>
$3k + 1$	$m = 3k + 1$	$n = 3p + 1$ or $n = -(3p + 2)$	<i>Class 3</i>
$3k + 1$	$m = 3k + 2$	$n = 3p$ or $n = -3p$	<i>Class 3</i>
$3k + 2$	$m = 3k$	$n = 3p$ or $n = -3p$	<i>Class 1</i>
$3k + 2$	$m = 3k + 1$	$n = 3p + 1$ or $n = -(3p + 2)$	<i>Class 1</i>
$3k + 2$	$m = 3k + 2$	$n = 3p + 2$ or $n = -(3p + 1)$	<i>Class 1</i>
$3k + 2$	$m = 3k$	$n = 3p + 1$ or $n = -(3p + 2)$	<i>Class 2</i>
$3k + 2$	$m = 3k + 1$	$n = 3p + 2$ or $n = -(3p + 1)$	<i>Class 2</i>
$3k + 2$	$m = 3k + 2$	$n = 3p$ or $n = -3p$	<i>Class 2</i>
$3k + 2$	$m = 3k$	$n = 3p + 2$ or $n = -(3p + 1)$	<i>Class 3</i>
$3k + 2$	$m = 3k + 1$	$n = 3p$ or $n = -3p$	<i>Class 3</i>
$3k + 2$	$m = 3k + 2$	$n = 3p + 1$ or $n = -(3p + 2)$	<i>Class 3</i>

where for

Class 1

$$e^{jl\frac{2\pi}{3}} = e^{j2\pi} = 1$$

$$e^{-jl\frac{2\pi}{3}} = e^{j2\pi} = 1$$

Class 2

$$e^{jl\frac{2\pi}{3}} = e^{j\frac{2\pi}{3}}$$

$$e^{-jl\frac{2\pi}{3}} = e^{-j\frac{2\pi}{3}}$$

Class 3

$$e^{jl\frac{2\pi}{3}} = e^{-j\frac{2\pi}{3}}$$

$$e^{-jl\frac{2\pi}{3}} = e^{j\frac{2\pi}{3}}$$

for $k = 0 \dots \infty$ and $p = -\infty \dots \infty$

Since the switching functions are real valued, and knowing that $\overline{D_{al}} = D_{a(-l)}$ and $\overline{B_{al}} = B_{a(-l)}$, we write the following functions as follows:

$$\begin{aligned} \sum_{l=-\infty}^{\infty} \frac{|D_{al}|^2}{Z(l\omega_0)} &= \sum_{l=-\infty}^0 \frac{|D_{al}|^2}{Z(l\omega_0)} + \sum_{l=0}^{\infty} \frac{|D_{al}|^2}{Z(l\omega_0)} \\ &= \sum_{l=0}^{\infty} \frac{|D_{a(-l)}|^2}{Z(-l\omega_0)} + \sum_{l=0}^{\infty} \frac{|D_{a(-l)}|^2}{Z(-l\omega_0)} \\ &= \sum_{l=0}^{\infty} \frac{|\overline{D_{al}}|^2}{Z(l\omega_0)} + \sum_{l=0}^{\infty} \frac{|D_{al}|^2}{Z(l\omega_0)} \\ &= 2\Re e \sum_{l=0}^{\infty} \frac{|D_{al}|^2}{Z(l\omega_0)} \end{aligned} \tag{4.15}$$

and

$$\begin{aligned} \sum_{l=-\infty}^{\infty} \frac{B_{al}\overline{D_{al}}}{Z(l\omega_0)} &= \sum_{l=-\infty}^0 \frac{B_{al}\overline{D_{al}}}{Z(l\omega_0)} + \sum_{l=0}^{\infty} \frac{B_{al}\overline{D_{al}}}{Z(l\omega_0)} \\ &= \sum_{l=0}^{\infty} \frac{B_{a(-l)}\overline{D_{a(-l)}}}{Z(-l\omega_0)} + \sum_{l=0}^{\infty} \frac{B_{al}\overline{D_{al}}}{Z(l\omega_0)} \\ &= \sum_{l=0}^{\infty} \frac{\overline{B_{al}D_{al}}}{Z(l\omega_0)} + \sum_{l=0}^{\infty} \frac{B_{al}\overline{D_{al}}}{Z(l\omega_0)} \\ &= 2\Re e \sum_{l=0}^{\infty} \frac{B_{al}\overline{D_{al}}}{Z(l\omega_0)} \end{aligned} \tag{4.16}$$

Now for convenience we define the following variables:

$$\lambda_1 = 2\Re e \left\{ \sum_{class\ 1} \frac{|D_{al}|^2}{Z(l\omega_0)} \right\} \quad (4.17)$$

$$\lambda_2 = 2\Re e \left\{ \sum_{class\ 2} \frac{|D_{al}|^2}{Z(l\omega_0)} \right\} \quad (4.18)$$

$$\lambda_3 = 2\Re e \left\{ \sum_{class\ 3} \frac{|D_{al}|^2}{Z(l\omega_0)} \right\} \quad (4.19)$$

$$\phi_2 = 2\Re e \left\{ \sum_{class\ 2} \frac{B_{al}\overline{D_{al}}}{Z(l\omega_0)} \right\} \quad (4.20)$$

$$\phi_3 = 2\Re e \left\{ \sum_{class\ 3} \frac{B_{al}\overline{D_{al}}}{Z(l\omega_0)} \right\} \quad (4.21)$$

Substituting λ_1 , λ_2 , λ_3 , ϕ_2 and ϕ_3 into equation 4.13 we obtain:

$$\begin{aligned} \begin{bmatrix} V_{\delta a} \\ V_{\delta b} \\ V_{\delta c} \end{bmatrix} &= - \left\{ \begin{bmatrix} 2\lambda_1 & -\lambda_1 & -\lambda_1 \\ -\lambda_1 & 2\lambda_1 & -\lambda_1 \\ -\lambda_1 & -\lambda_1 & 2\lambda_1 \end{bmatrix} + \begin{bmatrix} 2\lambda_2 & -\lambda_2 e^{-j\frac{2\pi}{3}} & -\lambda_2 e^{j\frac{2\pi}{3}} \\ -\lambda_2 e^{j\frac{2\pi}{3}} & 2\lambda_2 & -\lambda_2 e^{-j\frac{2\pi}{3}} \\ -\lambda_2 e^{-j\frac{2\pi}{3}} & -\lambda_2 e^{j\frac{2\pi}{3}} & 2\lambda_2 \end{bmatrix} \right. \\ &\quad \left. + \begin{bmatrix} 2\lambda_3 & -\lambda_3 e^{j\frac{2\pi}{3}} & -\lambda_3 e^{-j\frac{2\pi}{3}} \\ -\lambda_3 e^{-j\frac{2\pi}{3}} & 2\lambda_3 & -\lambda_3 e^{j\frac{2\pi}{3}} \\ -\lambda_3 e^{j\frac{2\pi}{3}} & -\lambda_3 e^{-j\frac{2\pi}{3}} & 2\lambda_3 \end{bmatrix} \right\}^{-1} \\ &\quad \begin{bmatrix} \phi_2 + \phi_3 \\ \phi_2 + \phi_3 \\ \phi_2 + \phi_3 \end{bmatrix} \frac{3V_t}{2} \end{aligned} \quad (4.22)$$

We can write equation 4.22 as:

$$\mathbf{V}_\delta = -\{\Lambda\}^{-1} \Phi \frac{3V_t}{2} \quad (4.23)$$

where

$$\mathbf{V}_\delta = \begin{bmatrix} V_{\delta a} \\ V_{\delta b} \\ V_{\delta c} \end{bmatrix} \quad (4.24)$$

$$\Lambda = \begin{bmatrix} 2\lambda_1 & -\lambda_1 & -\lambda_1 \\ -\lambda_1 & 2\lambda_1 & -\lambda_1 \\ -\lambda_1 & -\lambda_1 & 2\lambda_1 \end{bmatrix} + \begin{bmatrix} 2\lambda_2 & -\lambda_2 e^{-j\frac{2\pi}{3}} & -\lambda_2 e^{j\frac{2\pi}{3}} \\ -\lambda_2 e^{j\frac{2\pi}{3}} & 2\lambda_2 & -\lambda_2 e^{-j\frac{2\pi}{3}} \\ -\lambda_2 e^{-j\frac{2\pi}{3}} & -\lambda_2 e^{j\frac{2\pi}{3}} & 2\lambda_2 \end{bmatrix} \\ + \begin{bmatrix} 2\lambda_3 & -\lambda_3 e^{j\frac{2\pi}{3}} & -\lambda_3 e^{-j\frac{2\pi}{3}} \\ -\lambda_3 e^{-j\frac{2\pi}{3}} & 2\lambda_3 & -\lambda_3 e^{j\frac{2\pi}{3}} \\ -\lambda_3 e^{j\frac{2\pi}{3}} & -\lambda_3 e^{-j\frac{2\pi}{3}} & 2\lambda_3 \end{bmatrix} \quad (4.25)$$

$$\Phi = \begin{bmatrix} \phi_2 + \phi_3 \\ \phi_2 + \phi_3 \\ \phi_2 + \phi_3 \end{bmatrix} \quad (4.26)$$

We rewrite equation 4.23 as follows:

$$\frac{\mathbf{V}_\delta}{V_t} = -\frac{3}{2} \{\Lambda\}^{-1} \Phi \quad (4.27)$$

The determinant of Λ is given by:

$$\det(\Lambda) = 27(\lambda_2 + \lambda_3)(\lambda_2 + \lambda_1)(\lambda_3 + \lambda_1) \quad (4.28)$$

which implies that the inverse of Λ exists and has a unique solution provided that $(\lambda_2 + \lambda_3) \neq 0$, $(\lambda_2 + \lambda_1) \neq 0$ and $(\lambda_3 + \lambda_1) \neq 0$.

By direct computation the inverse of Λ is given by:

$$\Lambda^{-1} = \begin{bmatrix} \Lambda_{11} & \lambda_2^2 e^{-j\frac{2\pi}{3}} + \lambda_3^2 e^{j\frac{2\pi}{3}} - \lambda_1^2 & \lambda_2^2 e^{j\frac{2\pi}{3}} + \lambda_3^2 e^{-j\frac{2\pi}{3}} + \lambda_1^2 \\ \lambda_2^2 e^{j\frac{2\pi}{3}} + \lambda_3^2 e^{-j\frac{2\pi}{3}} + \lambda_1^2 & \Lambda_{22} & \lambda_2^2 e^{-j\frac{2\pi}{3}} + \lambda_3^2 e^{j\frac{2\pi}{3}} - \lambda_1^2 \\ \lambda_2^2 e^{-j\frac{2\pi}{3}} + \lambda_3^2 e^{j\frac{2\pi}{3}} - \lambda_1^2 & \lambda_2^2 e^{j\frac{2\pi}{3}} + \lambda_3^2 e^{-j\frac{2\pi}{3}} + \lambda_1^2 & \Lambda_{33} \end{bmatrix} \left\{ \frac{1}{9(\lambda_1 + \lambda_2)(\lambda_1 + \lambda_3)(\lambda_2 + \lambda_3)} \right\} \quad (4.29)$$

where

$$\Lambda_{11} = \Lambda_{22} = \Lambda_{33} = \lambda_1^2 + \lambda_2^2 + \lambda_3^2 + 3\lambda_1\lambda_2 + 3\lambda_1\lambda_3 + 3\lambda_2\lambda_3 \quad (4.30)$$

Substituting equation 4.29 into equation 4.27 we obtain the equation that gives us insight into the balancing of cell capacitor voltages of a 2-cell three-phase multicell converter, shown below:

$$\begin{aligned} \frac{V_{\delta a}}{V_t} = \frac{V_{\delta b}}{V_t} = \frac{V_{\delta c}}{V_t} &= -\frac{1}{6} \left\{ \frac{(\phi_2 + \phi_3) (\Lambda_{11} + \lambda_2^2 e^{-j\frac{2\pi}{3}} + \lambda_3^2 e^{j\frac{2\pi}{3}} - \lambda_1^2)}{(\lambda_1 + \lambda_2)(\lambda_1 + \lambda_3)(\lambda_2 + \lambda_3)} \right\} \\ &= -\frac{1}{6} \left\{ \frac{(\phi_2 + \phi_3) (\lambda_1^2 + 3\lambda_1\lambda_2 + 3\lambda_1\lambda_3 + 3\lambda_2\lambda_3)}{(\lambda_1 + \lambda_2)(\lambda_1 + \lambda_3)(\lambda_2 + \lambda_3)} \right\} \end{aligned} \quad (4.31)$$

Now using the definitions of λ_1 , λ_2 , λ_3 , ϕ_2 and ϕ_3 in equations 4.17 to 4.21 we can conclude that equation 4.31 demonstrates that the steady state balancing of the cell capacitor voltage is influenced by the following two factors:

1. The impedance of the output filter and load $Z(l\omega)$.
2. The values of $B_{al}\overline{D_{al}}$ and $|D_{al}|^2$.

B_{al} and D_{al} are Fourier coefficients $A_{mn} + jB_{mn}$ of the switching functions $s_{ta}(t)$ and $s_{da}(t)$ respectively. These coefficients were calculated in [73] using a single-cell single-phase converter.

Example 3.1

For an interleaved switching with a switching frequency of $f_s = 6kHz$, reference frequency of $f_0 = 50Hz$ and modulation index $m_a = 0.8$, we plot the amplitude spectra of $|B_{al}|$ and $|D_{al}|$ as shown in Figures 4.2 (a) and (b) respectively. We let A_{al} be the Fourier coefficient of the switching function $s_{a1}(t)$. Figures 4.3 (a) and (b) show amplitude spectra of $|A_{al}|$ and $|B_{al}| |D_{al}|$ respectively.

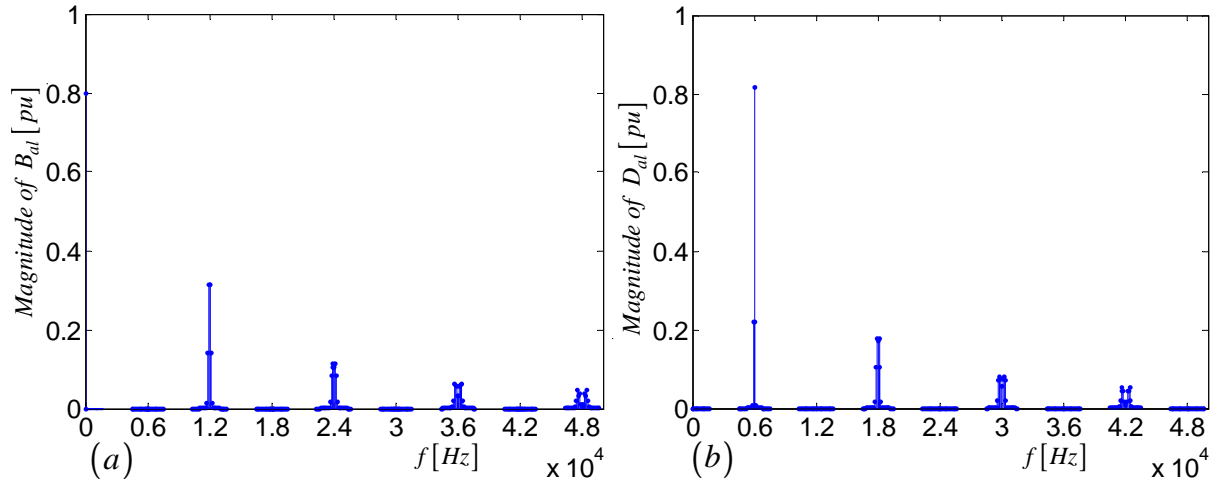


Figure 4.2: (a) Amplitude spectrum of $|B_{al}|$ and (b) Amplitude spectrum of $|D_{al}|$

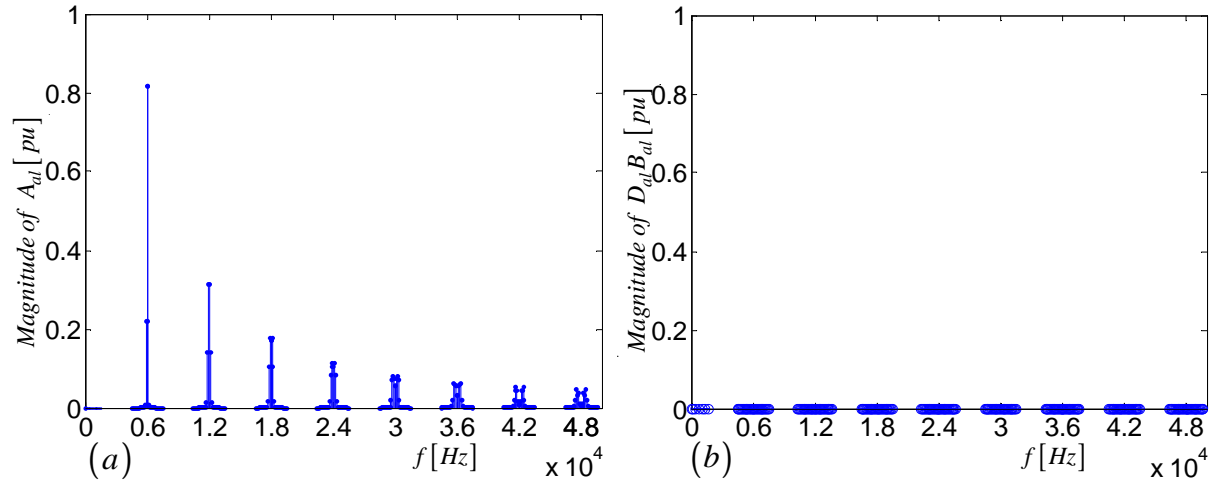


Figure 4.3: (a) Amplitude spectrum of $|A_{al}|$ and (b) Amplitude spectrum of $|D_{al}||B_{al}|$

Using the phasor diagrams in chapter 3 we observed that $s_{ta}(t)$ contains the frequency components of $s_{a1}(t)$ around the even multiples of the switching frequency whereas $s_{da}(t)$ contains the frequency components of $s_{a1}(t)$ around the odd multiples of the switching frequency. Similarly in Figure 4.2 we also observe that B_{al} contains frequency components around the even multiples of the switching frequency whereas D_{al} contains frequency components around the odd multiples of the switching frequency. That is, B_{al} and D_{al} do not overlap as confirmed in Figure 4.3 (b), hence:

$$|B_{al}||D_{al}| \approx 0 \quad (4.32)$$

This property is one of the necessary condition to prove natural balance.

Example 3.2

When the switching frequency is not sufficiently high it causes the sidebands of different multiples of the switching frequency groups to overlap. This will result in an overlap in the spectra of B_{al} and D_{al} . We demonstrate this property for interleaved switching with a switching frequency of $f_s = 350\text{Hz}$, a reference frequency of $f_0 = 50\text{Hz}$ and a modulation index $m_a = 0.8$.

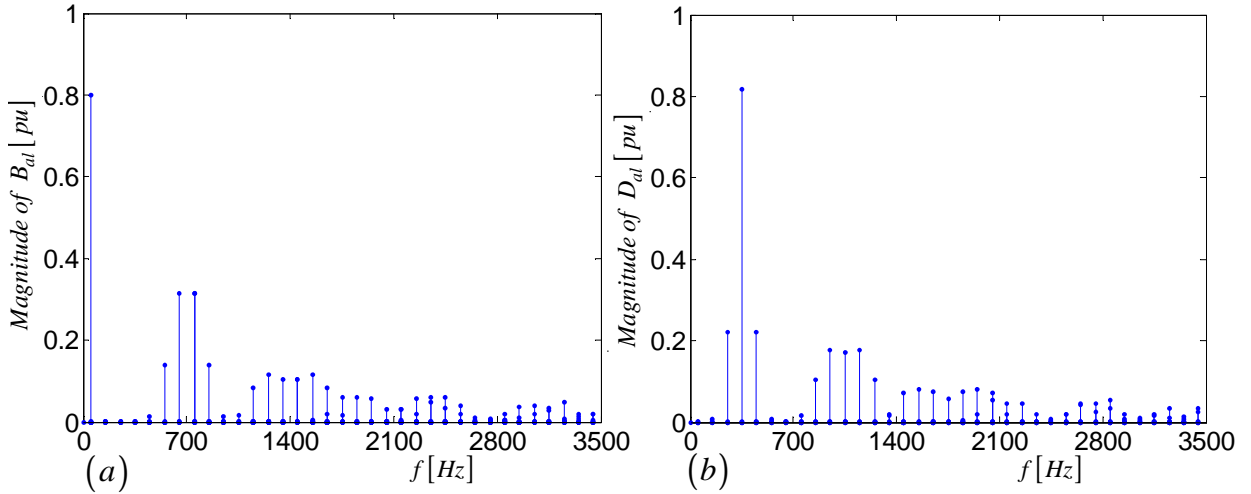


Figure 4.4: (a) Amplitude spectrum of $|B_{al}|$ and (b) Amplitude spectrum of $|D_{al}|$

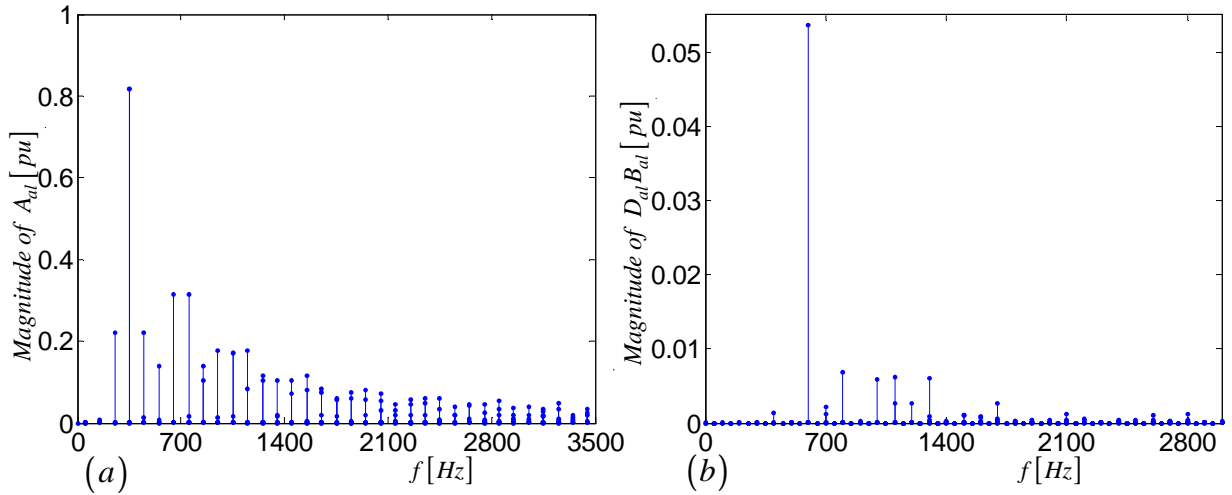


Figure 4.5: (a) Amplitude spectrum of $|A_{al}|$ and (b) Amplitude spectrum of $|D_{al}| |B_{al}|$

The amplitude spectrum of $|B_{al}|$ and $|D_{al}|$ is shown in Figures 4.4 (a) and (b) respectively. From these figures we observe the overlap of the sidebands of different switching frequency groups. Figures 4.5 (a) and (b) show the amplitude spectra of $|A_{al}|$ and $|B_{al}| |D_{al}|$ respectively. From Figure 4.5 (b) it is clear that $|D_{al}| |B_{al}| > 0$. This property

will imply that

$$\frac{V_{\delta a}}{V_t} = \frac{V_{\delta b}}{V_t} = \frac{V_{\delta c}}{V_t} > 0 \tag{4.33}$$

This in turn will cause imbalance in the cell capacitor voltage.

Example 3.3

When the reference signal contains high frequency components the sidebands of multiples of switching frequency groups overlap which results in the overlap of B_{al} and D_{al} . We establish this property for interleaved switching with switching frequency of $f_s = 6300Hz$, a reference frequency of $f_0 = 900Hz$ and modulation index $m_a = 0.8$.

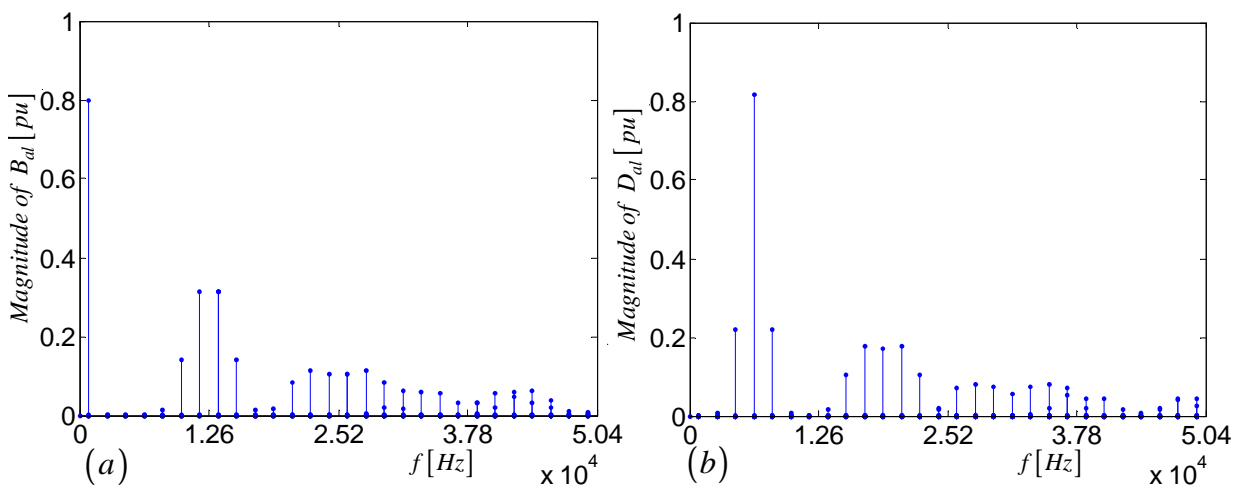


Figure 4.6: (a) Amplitude spectrum of $|B_{al}|$ and (b) Amplitude spectrum of $|D_{al}|$

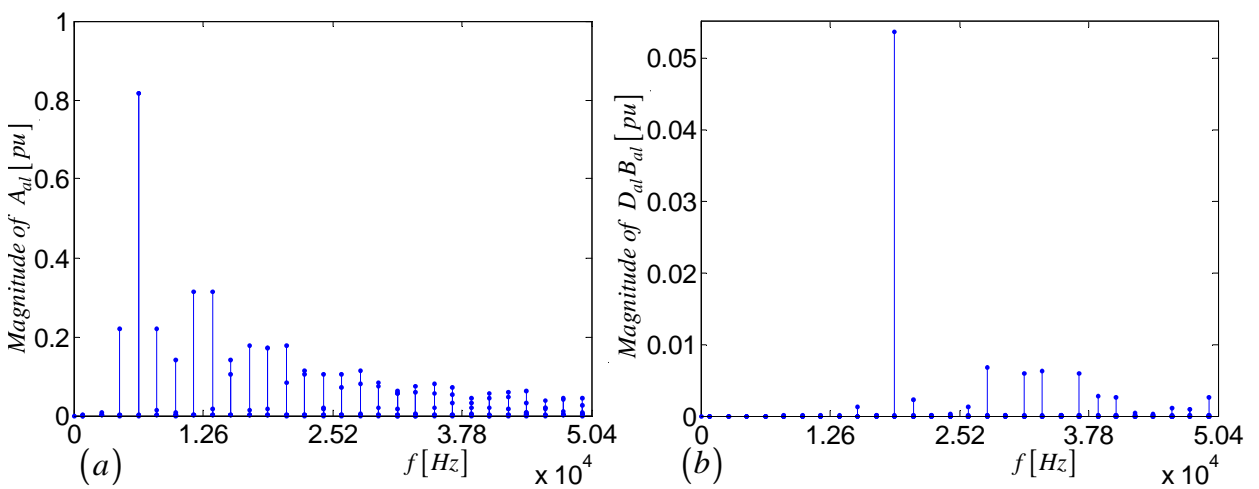


Figure 4.7: (a) Amplitude spectrum of $|A_{al}|$ and (b) Amplitude spectrum of $|D_{al}| |B_{al}|$

From Figures 4.6 and 4.7 we observe the overlap of the sidebands of different switching frequency groups. This leads to the overlap of sidebands of switching frequency groups of B_{al} and D_{al} as shown in Figure 4.7 (b). This result implies that there will be an imbalance in the cell capacitor voltages of a 2-cell three-phase converter.

In this section we derived the theory which establishes the factors that influence the balancing of the cell capacitor voltage of the 2-cell three-phase converter. We further furnished examples of factors that cause imbalance in the cell capacitor voltages.

4.3 Steady State Balancing of 3-Cell Multicell Converter

In this section we study the steady-state analysis of a 3-cell multicell converter. We derive the equations that are important for describing the balancing of the cell capacitor voltages under steady-state conditions.

For convenience we represent Figure 3.8 as Figure 4.8 below:

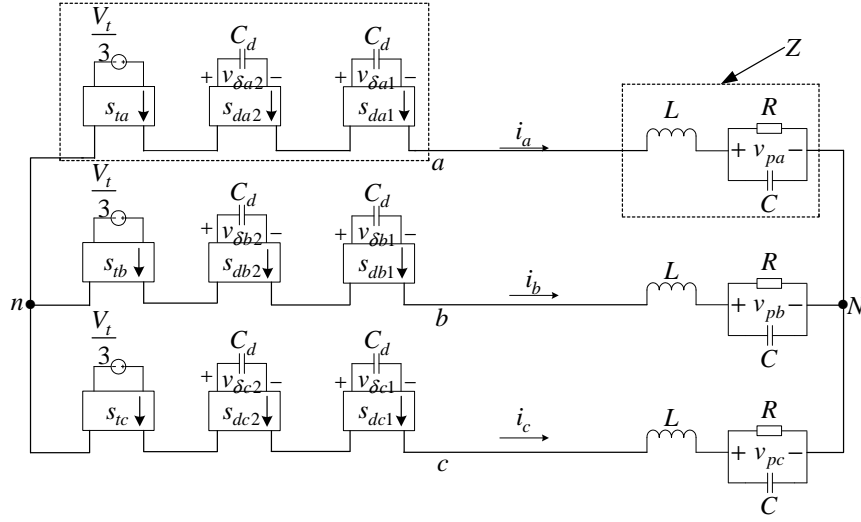


Figure 4.8: Equivalent circuit of 3-cell 3-phase multicell converter

The load in Figure 4.8 acts as an impedance divider and hence we have:

$$V_{Nn} = \frac{1}{3} \{V_{an} + V_{bn} + V_{cn}\} \quad (4.34)$$

Following the same procedure as in section 4.2 we find that the cell capacitor current for the first cell in phase A yield:

$$\begin{aligned} I_{c_{da1}}(\omega) = & -\frac{1}{3} \left\{ \frac{2V_t}{3} \int_{-\infty}^{\infty} \frac{S_{ta}(u)}{Z(u)} S_{da1}(\omega - u) du + 2V_{\delta a} \int_{-\infty}^{\infty} \frac{S_{da1}(u)}{Z(u)} S_{da1}(\omega - u) du \right. \\ & + 2V_{\delta a} \int_{-\infty}^{\infty} \frac{S_{da2}(u)}{Z(u)} S_{da1}(\omega - u) du - \frac{V_t}{3} \int_{-\infty}^{\infty} \frac{S_{tb}(u)}{Z(u)} S_{da1}(\omega - u) du \\ & - V_{\delta b1} \int_{-\infty}^{\infty} \frac{S_{db1}(u)}{Z(u)} S_{da1}(\omega - u) - V_{\delta b2} \int_{-\infty}^{\infty} \frac{S_{db2}(u)}{Z(u)} S_{da1}(\omega - u) \\ & \left. - \frac{V_t}{3} \int_{-\infty}^{\infty} \frac{S_{tc}(u)}{Z(u)} S_{da1}(\omega - u) du - V_{\delta c1} \int_{-\infty}^{\infty} \frac{S_{dc1}(u)}{Z(u)} S_{da1}(\omega - u) du \right\} \end{aligned}$$

$$\left. -V_{\delta c2} \int_{-\infty}^{\infty} \frac{S_{dc2}(u)}{Z(u)} S_{da1}(\omega - u) du \right\} \quad (4.35)$$

Since the average value of i_{ca1} is equal to zero amperes at steady state, we have $I_{c_{da1}}(\omega)|_{\omega=0}$. Thus equation 4.35 can be written as follows

$$\begin{aligned} 0 &= \frac{2V_t}{3} \int_{-\infty}^{\infty} \frac{S_{ta}(u)}{Z(u)} \overline{S_{da1}(u)} du + 2V_{\delta a1} \int_{-\infty}^{\infty} \frac{S_{da1}(u)}{Z(u)} \overline{S_{da1}(u)} du \\ &+ 2V_{\delta a2} \int_{-\infty}^{\infty} \frac{S_{da2}(u)}{Z(u)} \overline{S_{da1}(u)} du - \frac{V_t}{3} \int_{-\infty}^{\infty} \frac{S_{tb}(u)}{Z(u)} \overline{S_{da1}(u)} du \\ &- V_{\delta b1} \int_{-\infty}^{\infty} \frac{S_{db1}(u)}{Z(u)} \overline{S_{da1}(u)} du - V_{\delta b2} \int_{-\infty}^{\infty} \frac{S_{db2}(u)}{Z(u)} \overline{S_{da1}(u)} du \\ &- \frac{V_t}{3} \int_{-\infty}^{\infty} \frac{S_{tc}(u)}{Z(u)} \overline{S_{da1}(u)} du - V_{\delta c1} \int_{-\infty}^{\infty} \frac{S_{dc1}(u)}{Z(u)} \overline{S_{da1}(u)} du \\ &- V_{\delta c2} \int_{-\infty}^{\infty} \frac{S_{dc2}(u)}{Z(u)} \overline{S_{da1}(u)} du \end{aligned} \quad (4.36)$$

Similarly for $I_{c_{da2}}(\omega)|_{\omega=0}$ we have

$$\begin{aligned} 0 &= \frac{2V_t}{3} \int_{-\infty}^{\infty} \frac{S_{ta}(u)}{Z(u)} \overline{S_{da2}(u)} du + 2V_{\delta a1} \int_{-\infty}^{\infty} \frac{S_{da1}(u)}{Z(u)} \overline{S_{da2}(u)} du \\ &+ 2V_{\delta a2} \int_{-\infty}^{\infty} \frac{S_{da2}(u)}{Z(u)} \overline{S_{da2}(u)} du - \frac{V_t}{3} \int_{-\infty}^{\infty} \frac{S_{tb}(u)}{Z(u)} \overline{S_{da2}(u)} du \\ &- V_{\delta b1} \int_{-\infty}^{\infty} \frac{S_{db1}(u)}{Z(u)} \overline{S_{da2}(u)} du - V_{\delta b2} \int_{-\infty}^{\infty} \frac{S_{db2}(u)}{Z(u)} \overline{S_{da2}(u)} du \\ &- \frac{V_t}{3} \int_{-\infty}^{\infty} \frac{S_{tc}(u)}{Z(u)} \overline{S_{da2}(u)} du - V_{\delta c1} \int_{-\infty}^{\infty} \frac{S_{dc1}(u)}{Z(u)} \overline{S_{da2}(u)} du \\ &- V_{\delta c2} \int_{-\infty}^{\infty} \frac{S_{dc2}(u)}{Z(u)} \overline{S_{da2}(u)} du \end{aligned} \quad (4.37)$$

Similarly for $I_{c_{db1}}(\omega)|_{\omega=0}$ we have

$$\begin{aligned} 0 &= \frac{2V_t}{3} \int_{-\infty}^{\infty} \frac{S_{tb}(u)}{Z(u)} \overline{S_{db1}(u)} du + 2V_{\delta b1} \int_{-\infty}^{\infty} \frac{S_{db1}(u)}{Z(u)} \overline{S_{db1}(u)} du \\ &+ 2V_{\delta b2} \int_{-\infty}^{\infty} \frac{S_{db2}(u)}{Z(u)} \overline{S_{db1}(u)} du - \frac{V_t}{3} \int_{-\infty}^{\infty} \frac{S_{ta}(u)}{Z(u)} \overline{S_{db1}(u)} du \\ &- V_{\delta a1} \int_{-\infty}^{\infty} \frac{S_{da1}(u)}{Z(u)} \overline{S_{db1}(u)} du - V_{\delta a2} \int_{-\infty}^{\infty} \frac{S_{da2}(u)}{Z(u)} \overline{S_{db1}(u)} du \end{aligned}$$

$$\begin{aligned}
& -\frac{V_t}{3} \int_{-\infty}^{\infty} \frac{S_{tc}(u)}{Z(u)} \overline{S_{db1}(u)} du - V_{\delta c1} \int_{-\infty}^{\infty} \frac{S_{dc1}(u)}{Z(u)} \overline{S_{db1}(u)} du \\
& -V_{\delta c2} \int_{-\infty}^{\infty} \frac{S_{dc2}(u)}{Z(u)} \overline{S_{db1}(u)} du
\end{aligned} \tag{4.38}$$

Similarly for $I_{c_{ab2}}(\omega)|_{\omega=0}$ we have

$$\begin{aligned}
0 &= \frac{2V_t}{3} \int_{-\infty}^{\infty} \frac{S_{tb}(u)}{Z(u)} \overline{S_{ab2}(u)} du + 2V_{\delta b1} \int_{-\infty}^{\infty} \frac{S_{db1}(u)}{Z(u)} \overline{S_{ab2}(u)} du \\
& + 2V_{\delta b2} \int_{-\infty}^{\infty} \frac{S_{db2}(u)}{Z(u)} \overline{S_{ab2}(u)} du - \frac{V_t}{3} \int_{-\infty}^{\infty} \frac{S_{ta}(u)}{Z(u)} \overline{S_{ab2}(u)} du \\
& -V_{\delta a1} \int_{-\infty}^{\infty} \frac{S_{da1}(u)}{Z(u)} \overline{S_{ab2}(u)} du - V_{\delta a2} \int_{-\infty}^{\infty} \frac{S_{da2}(u)}{Z(u)} \overline{S_{ab2}(u)} du \\
& -\frac{V_t}{3} \int_{-\infty}^{\infty} \frac{S_{tc}(u)}{Z(u)} \overline{S_{ab2}(u)} du - V_{\delta c1} \int_{-\infty}^{\infty} \frac{S_{dc1}(u)}{Z(u)} \overline{S_{ab2}(u)} du \\
& -V_{\delta c2} \int_{-\infty}^{\infty} \frac{S_{dc2}(u)}{Z(u)} \overline{S_{ab2}(u)} du
\end{aligned} \tag{4.39}$$

Similarly for $I_{c_{dc1}}(\omega)|_{\omega=0}$ we have

$$\begin{aligned}
0 &= \frac{2V_t}{3} \int_{-\infty}^{\infty} \frac{S_{tc}(u)}{Z(u)} \overline{S_{dc1}(u)} du + 2V_{\delta c1} \int_{-\infty}^{\infty} \frac{S_{dc1}(u)}{Z(u)} \overline{S_{dc1}(u)} du \\
& + 2V_{\delta c2} \int_{-\infty}^{\infty} \frac{S_{dc2}(u)}{Z(u)} \overline{S_{dc1}(u)} du - \frac{V_t}{3} \int_{-\infty}^{\infty} \frac{S_{ta}(u)}{Z(u)} \overline{S_{dc1}(u)} du \\
& -V_{\delta a1} \int_{-\infty}^{\infty} \frac{S_{da1}(u)}{Z(u)} \overline{S_{dc1}(u)} du - V_{\delta a2} \int_{-\infty}^{\infty} \frac{S_{da2}(u)}{Z(u)} \overline{S_{dc1}(u)} du \\
& -\frac{V_t}{3} \int_{-\infty}^{\infty} \frac{S_{tb}(u)}{Z(u)} \overline{S_{dc1}(u)} du - V_{\delta b1} \int_{-\infty}^{\infty} \frac{S_{db1}(u)}{Z(u)} \overline{S_{dc1}(u)} du \\
& -V_{\delta b2} \int_{-\infty}^{\infty} \frac{S_{db2}(u)}{Z(u)} \overline{S_{dc1}(u)} du
\end{aligned} \tag{4.40}$$

Similarly for $I_{c_{dc2}}(\omega)|_{\omega=0}$ we have

$$\begin{aligned}
0 &= \frac{2V_t}{3} \int_{-\infty}^{\infty} \frac{S_{tc}(u)}{Z(u)} \overline{S_{dc2}(u)} du + 2V_{\delta c1} \int_{-\infty}^{\infty} \frac{S_{dc1}(u)}{Z(u)} \overline{S_{dc2}(u)} du \\
& + 2V_{\delta c2} \int_{-\infty}^{\infty} \frac{S_{dc2}(u)}{Z(u)} \overline{S_{dc2}(u)} du - \frac{V_t}{3} \int_{-\infty}^{\infty} \frac{S_{ta}(u)}{Z(u)} \overline{S_{dc2}(u)} du
\end{aligned}$$

$$\begin{aligned}
& -V_{\delta a1} \int_{-\infty}^{\infty} \frac{S_{da1}(u)}{Z(u)} \overline{S_{dc2}(u)} du - V_{\delta a2} \int_{-\infty}^{\infty} \frac{S_{da2}(u)}{Z(u)} \overline{S_{dc2}(u)} du \\
& -\frac{V_t}{3} \int_{-\infty}^{\infty} \frac{S_{tb}(u)}{Z(u)} \overline{S_{dc2}(u)} du - V_{\delta b1} \int_{-\infty}^{\infty} \frac{S_{db1}(u)}{Z(u)} \overline{S_{dc2}(u)} du \\
& -V_{\delta b2} \int_{-\infty}^{\infty} \frac{S_{db2}(u)}{Z(u)} \overline{S_{dc2}(u)} du
\end{aligned} \tag{4.41}$$

From chapter 3 the phase-b switching functions are the same as those for phase-a but delayed by $\frac{T}{3}$ and that the phase-c switching functions are the same as those for phase-a but delayed by $\frac{2T}{3}$ where T is the period of the switching function.

For $T = \frac{2\pi}{\omega_0}$ and since the above functions are periodic and the analysis is in steady state (which implies $u = l\omega_0$) and also since for a single phase the three cells are out of phase by $\frac{2\pi}{3}$ radians, that is

$$s_{da2} = s_{da1} e^{jl\frac{2\pi}{3}}$$

we then represent equations 4.36, 4.37, 4.38, 4.39, 4.40 and 4.41 by the matrix equation given by 4.42

$$\begin{bmatrix}
2 \int_{-\infty}^{\infty} \frac{|S_{da1}(l\omega_0)|^2}{Z(l\omega_0)} d\omega_0 \\
2 \int_{-\infty}^{\infty} \frac{|S_{da1}(l\omega_0)|^2}{Z(l\omega_0)} e^{-jl\frac{2\pi}{3}} d\omega_0 \\
- \int_{-\infty}^{\infty} \frac{|S_{da1}(l\omega_0)|^2}{Z(l\omega_0)} e^{-jl\frac{2\pi}{3}} d\omega_0 \\
- \int_{-\infty}^{\infty} \frac{|S_{da1}(l\omega_0)|^2}{Z(l\omega_0)} e^{jl\frac{2\pi}{3}} d\omega_0 \\
- \int_{-\infty}^{\infty} \frac{|S_{da1}(l\omega_0)|^2}{Z(l\omega_0)} e^{jl\frac{2\pi}{3}} d\omega_0 \\
- \int_{-\infty}^{\infty} \frac{|S_{da1}(l\omega_0)|^2}{Z(l\omega_0)} d\omega_0
\end{bmatrix} v_{\delta a1} + \begin{bmatrix}
2 \int_{-\infty}^{\infty} \frac{|S_{da1}(l\omega_0)|^2}{Z(l\omega_0)} e^{jl\frac{2\pi}{3}} d\omega_0 \\
2 \int_{-\infty}^{\infty} \frac{|S_{da1}(l\omega_0)|^2}{Z(l\omega_0)} d\omega_0 \\
- \int_{-\infty}^{\infty} \frac{|S_{da1}(l\omega_0)|^2}{Z(l\omega_0)} d\omega_0 \\
- \int_{-\infty}^{\infty} \frac{|S_{da1}(l\omega_0)|^2}{Z(l\omega_0)} e^{-jl\frac{2\pi}{3}} d\omega_0 \\
- \int_{-\infty}^{\infty} \frac{|S_{da1}(l\omega_0)|^2}{Z(l\omega_0)} e^{-jl\frac{2\pi}{3}} d\omega_0 \\
- \int_{-\infty}^{\infty} \frac{|S_{da1}(l\omega_0)|^2}{Z(l\omega_0)} e^{jl\frac{2\pi}{3}} d\omega_0
\end{bmatrix} v_{\delta a2}$$

$$\begin{aligned}
 & + \left[\begin{array}{c} -\int_{-\infty}^{\infty} \frac{|S_{da1}(l\omega_0)|^2}{Z(l\omega_0)} e^{jl\frac{2\pi}{3}} d\omega_0 \\ -\int_{-\infty}^{\infty} \frac{|S_{da1}(l\omega_0)|^2}{Z(l\omega_0)} d\omega_0 \\ 2\int_{-\infty}^{\infty} \frac{|S_{da1}(l\omega_0)|^2}{Z(l\omega_0)} d\omega_0 \\ 2\int_{-\infty}^{\infty} \frac{|S_{da1}(l\omega_0)|^2}{Z(l\omega_0)} e^{-jl\frac{2\pi}{3}} d\omega_0 \\ -\int_{-\infty}^{\infty} \frac{|S_{da1}(l\omega_0)|^2}{Z(l\omega_0)} e^{-jl\frac{2\pi}{3}} d\omega_0 \\ -\int_{-\infty}^{\infty} \frac{|S_{da1}(l\omega_0)|^2}{Z(l\omega_0)} e^{jl\frac{2\pi}{3}} d\omega_0 \end{array} \right] v_{\delta b1} + \left[\begin{array}{c} -\int_{-\infty}^{\infty} \frac{|S_{da1}(l\omega_0)|^2}{Z(l\omega_0)} e^{-jl\frac{2\pi}{3}} d\omega_0 \\ -\int_{-\infty}^{\infty} \frac{|S_{da1}(l\omega_0)|^2}{Z(l\omega_0)} e^{jl\frac{2\pi}{3}} d\omega_0 \\ 2\int_{-\infty}^{\infty} \frac{|S_{da1}(l\omega_0)|^2}{Z(l\omega_0)} e^{jl\frac{2\pi}{3}} d\omega_0 \\ 2\int_{-\infty}^{\infty} \frac{|S_{da1}(l\omega_0)|^2}{Z(l\omega_0)} d\omega_0 \\ -\int_{-\infty}^{\infty} \frac{|S_{da1}(l\omega_0)|^2}{Z(l\omega_0)} d\omega_0 \\ -\int_{-\infty}^{\infty} \frac{|S_{da1}(l\omega_0)|^2}{Z(l\omega_0)} e^{-jl\frac{2\pi}{3}} d\omega_0 \end{array} \right] v_{\delta b2} \\
 & + \left[\begin{array}{c} -\int_{-\infty}^{\infty} \frac{|S_{da1}|^2}{Z(l\omega_0)} e^{-jl\frac{2\pi}{3}} d\omega_0 \\ -\int_{-\infty}^{\infty} \frac{|S_{da1}(l\omega_0)|^2}{Z(l\omega_0)} e^{jl\frac{2\pi}{3}} d\omega_0 \\ -\int_{-\infty}^{\infty} \frac{|S_{da1}|^2}{Z(\omega_0)} e^{jl\frac{2\pi}{3}} d\omega_0 \\ -\int_{-\infty}^{\infty} \frac{|S_{da1}(l\omega_0)|^2}{Z(l\omega_0)} d\omega_0 \\ 2\int_{-\infty}^{\infty} \frac{|S_{da1}(l\omega_0)|^2}{Z(l\omega_0)} d\omega_0 \\ 2\int_{-\infty}^{\infty} \frac{|S_{da1}(l\omega_0)|^2}{Z(l\omega_0)} e^{-jl\frac{2\pi}{3}} d\omega_0 \end{array} \right] v_{\delta c1} + \left[\begin{array}{c} -\int_{-\infty}^{\infty} \frac{|S_{da1}(l\omega_0)|^2}{Z(l\omega_0)} d\omega_0 \\ -\int_{-\infty}^{\infty} \frac{|S_{da1}(l\omega_0)|^2}{Z(l\omega_0)} e^{-jl\frac{2\pi}{3}} d\omega_0 \\ -\int_{-\infty}^{\infty} \frac{|S_{da1}(l\omega_0)|^2}{Z(l\omega_0)} e^{-jl\frac{2\pi}{3}} d\omega_0 \\ -\int_{-\infty}^{\infty} \frac{|S_{da1}(l\omega_0)|^2}{Z(l\omega_0)} e^{jl\frac{2\pi}{3}} d\omega_0 \\ 2\int_{-\infty}^{\infty} \frac{|S_{da1}(l\omega_0)|^2}{Z(l\omega_0)} e^{jl\frac{2\pi}{3}} d\omega_0 \\ 2\int_{-\infty}^{\infty} \frac{|S_{da1}(l\omega_0)|^2}{Z(l\omega_0)} d\omega_0 \end{array} \right] v_{\delta c2} \\
 = & \left\{ \left[\begin{array}{c} -2\int_{-\infty}^{\infty} \frac{S_{ta}(l\omega_0)}{Z(l\omega_0)} \overline{S_{da1}(l\omega_0)} d\omega_0 \\ -2\int_{-\infty}^{\infty} \frac{S_{ta}}{Z(l\omega_0)} \overline{S_{da1}(l\omega_0)} e^{-jl\frac{2\pi}{3}} d\omega_0 \\ -2\int_{-\infty}^{\infty} \frac{S_{ta}(l\omega_0)}{Z(l\omega_0)} \overline{S_{da1}(l\omega_0)} d\omega_0 \\ -2\int_{-\infty}^{\infty} \frac{S_{ta}(l\omega_0)}{Z(l\omega_0)} \overline{S_{da1}(l\omega_0)} e^{-jl\frac{2\pi}{3}} d\omega_0 \\ -2\int_{-\infty}^{\infty} \frac{S_{ta}(l\omega_0)}{Z(l\omega_0)} \overline{S_{da1}(l\omega_0)} d\omega_0 \\ -2\int_{-\infty}^{\infty} \frac{S_{ta}(l\omega_0)}{Z(l\omega_0)} \overline{S_{da1}(l\omega_0)} e^{-jl\frac{2\pi}{3}} d\omega_0 \end{array} \right] + \left[\begin{array}{c} \int_{-\infty}^{\infty} \frac{S_{ta}(l\omega_0)}{Z(l\omega_0)} \overline{S_{da1}(l\omega_0)} e^{jl\frac{2\pi}{3}} d\omega_0 \\ \int_{-\infty}^{\infty} \frac{S_{ta}(l\omega_0)}{Z(l\omega_0)} \overline{S_{da1}(l\omega_0)} d\omega_0 \\ \int_{-\infty}^{\infty} \frac{S_{ta}(l\omega_0)}{Z(l\omega_0)} \overline{S_{da1}(l\omega_0)} e^{-jl\frac{2\pi}{3}} d\omega_0 \\ \int_{-\infty}^{\infty} \frac{S_{ta}(l\omega_0)}{Z(l\omega_0)} \overline{S_{da1}(l\omega_0)} e^{jl\frac{2\pi}{3}} d\omega_0 \\ \int_{-\infty}^{\infty} \frac{S_{ta}(l\omega_0)}{Z(l\omega_0)} \overline{S_{da1}(l\omega_0)} e^{jl\frac{2\pi}{3}} d\omega_0 \\ \int_{-\infty}^{\infty} \frac{S_{ta}(l\omega_0)}{Z(l\omega_0)} \overline{S_{da1}(u)} d\omega_0 \end{array} \right] \right\}
 \end{aligned}$$

$$\begin{aligned}
 & \left[\begin{array}{c} \int_{-\infty}^{\infty} \frac{S_{ta}(l\omega_0)}{Z(l\omega_0)} \overline{S_{da1}(l\omega_0)} e^{-jl\frac{2\pi}{3}} d\omega_0 \\ \int_{-\infty}^{\infty} \frac{S_{ta}(l\omega_0)}{Z(l\omega_0)} \overline{S_{da1}(l\omega_0)} e^{jl\frac{2\pi}{3}} d\omega_0 \\ \int_{-\infty}^{\infty} \frac{S_{ta}(l\omega_0)}{Z(l\omega_0)} \overline{S_{da1}(l\omega_0)} e^{jl\frac{2\pi}{3}} d\omega_0 \\ \int_{-\infty}^{\infty} \frac{S_{ta}(l\omega_0)}{Z(l\omega_0)} \overline{S_{da1}(l\omega_0)} d\omega_0 \\ \int_{-\infty}^{\infty} \frac{S_{ta}(l\omega_0)}{Z(l\omega_0)} \overline{S_{da1}(l\omega_0)} e^{-jl\frac{2\pi}{3}} d\omega_0 \\ \int_{-\infty}^{\infty} \frac{S_{ta}(l\omega_0)}{Z(l\omega_0)} \overline{S_{da1}(l\omega_0)} e^{jl\frac{2\pi}{3}} d\omega_0 \end{array} \right] \left. \vphantom{\int_{-\infty}^{\infty}} \right\} \frac{V_t}{3} \\
 & + \left[\begin{array}{c} \int_{-\infty}^{\infty} \frac{S_{ta}(l\omega_0)}{Z(l\omega_0)} \overline{S_{da1}(l\omega_0)} e^{-jl\frac{2\pi}{3}} d\omega_0 \\ \int_{-\infty}^{\infty} \frac{S_{ta}(l\omega_0)}{Z(l\omega_0)} \overline{S_{da1}(l\omega_0)} e^{jl\frac{2\pi}{3}} d\omega_0 \\ \int_{-\infty}^{\infty} \frac{S_{ta}(l\omega_0)}{Z(l\omega_0)} \overline{S_{da1}(l\omega_0)} e^{jl\frac{2\pi}{3}} d\omega_0 \\ \int_{-\infty}^{\infty} \frac{S_{ta}(l\omega_0)}{Z(l\omega_0)} \overline{S_{da1}(l\omega_0)} d\omega_0 \\ \int_{-\infty}^{\infty} \frac{S_{ta}(l\omega_0)}{Z(l\omega_0)} \overline{S_{da1}(l\omega_0)} e^{-jl\frac{2\pi}{3}} d\omega_0 \\ \int_{-\infty}^{\infty} \frac{S_{ta}(l\omega_0)}{Z(l\omega_0)} \overline{S_{da1}(l\omega_0)} e^{jl\frac{2\pi}{3}} d\omega_0 \end{array} \right]
 \end{aligned} \tag{4.42}$$

Since the functions in the matrix equation 4.42 are periodic we write them in terms of exponential fourier series as shown in matrix equation 4.43.

$$\begin{aligned}
 & \left[\begin{array}{c} 2 \sum_{l=-\infty}^{\infty} \frac{|D_{a1l}|^2}{Z(l\omega_0)} \\ 2 \sum_{l=-\infty}^{\infty} \frac{D_{a1l} \overline{D_{a2l}}}{Z(l\omega_0)} \\ - \sum_{l=-\infty}^{\infty} \frac{|D_{a1l}|^2 e^{jl\frac{2\pi}{3}}}{Z(l\omega_0)} \\ - \sum_{l=-\infty}^{\infty} \frac{D_{a1l} \overline{D_{a2l}} e^{jl\frac{2\pi}{3}}}{Z(l\omega_0)} \\ - \sum_{l=-\infty}^{\infty} \frac{|D_{a1l}|^2 e^{-jl\frac{2\pi}{3}}}{Z(l\omega_0)} \\ - \sum_{l=-\infty}^{\infty} \frac{D_{a1l} \overline{D_{a2l}} e^{-jl\frac{2\pi}{3}}}{Z(l\omega_0)} \end{array} \right] V_{\delta a1} + \\
 & \left[\begin{array}{c} 2 \sum_{l=-\infty}^{\infty} \frac{D_{a2l} \overline{D_{a1l}}}{Z(l\omega_0)} \\ 2 \sum_{l=-\infty}^{\infty} \frac{|D_{a2l}|^2}{Z(l\omega_0)} \\ - \sum_{l=-\infty}^{\infty} \frac{D_{a2l} \overline{D_{a1l}} e^{jl\frac{2\pi}{3}}}{Z(l\omega_0)} \\ - \sum_{l=-\infty}^{\infty} \frac{|D_{a2l}|^2 e^{jl\frac{2\pi}{3}}}{Z(l\omega_0)} \\ - \sum_{l=-\infty}^{\infty} \frac{D_{a2l} \overline{D_{a1l}} e^{-jl\frac{2\pi}{3}}}{Z(l\omega_0)} \\ - \sum_{l=-\infty}^{\infty} \frac{|D_{a2l}|^2 e^{-jl\frac{2\pi}{3}}}{Z(l\omega_0)} \end{array} \right] V_{\delta a2}
 \end{aligned}$$

$$\begin{aligned}
 & + \left[\begin{array}{l} -\sum_{l=-\infty}^{\infty} \frac{|D_{a1l}|^2 e^{-jl\frac{2\pi}{3}}}{Z(l\omega_0)} \\ -\sum_{l=-\infty}^{\infty} \frac{D_{a1l}\overline{D_{a2l}} e^{-jl\frac{2\pi}{3}}}{Z(l\omega_0)} \\ 2\sum_{l=-\infty}^{\infty} \frac{|D_{a1l}|^2}{Z(l\omega_0)} \\ 2\sum_{l=-\infty}^{\infty} \frac{D_{a1l}\overline{D_{a2l}}}{Z(l\omega_0)} \\ -\sum_{l=-\infty}^{\infty} \frac{|D_{a1l}|^2 e^{jl\frac{2\pi}{3}}}{Z(l\omega_0)} \\ -\sum_{l=-\infty}^{\infty} \frac{D_{a1l}\overline{D_{a2l}} e^{jl\frac{2\pi}{3}}}{Z(l\omega_0)} \end{array} \right] V_{\delta b1} + \left[\begin{array}{l} -\sum_{l=-\infty}^{\infty} \frac{D_{a2l}\overline{D_{a1l}} e^{-jl\frac{2\pi}{3}}}{Z(l\omega_0)} \\ -\sum_{l=-\infty}^{\infty} \frac{|D_{a2l}|^2 e^{-jl\frac{2\pi}{3}}}{Z(l\omega_0)} \\ 2\sum_{l=-\infty}^{\infty} \frac{D_{a2l}\overline{D_{a1l}}}{Z(l\omega_0)} \\ 2\sum_{l=-\infty}^{\infty} \frac{|D_{a2l}|^2}{Z(l\omega_0)} \\ -\sum_{l=-\infty}^{\infty} \frac{D_{a2l}\overline{D_{a1l}} e^{jl\frac{2\pi}{3}}}{Z(l\omega_0)} \\ -\sum_{l=-\infty}^{\infty} \frac{|D_{a2l}|^2 e^{jl\frac{2\pi}{3}}}{Z(l\omega_0)} \end{array} \right] V_{\delta b2} \\
 & + \left[\begin{array}{l} -\sum_{l=-\infty}^{\infty} \frac{|D_{a1l}|^2 e^{jl\frac{2\pi}{3}}}{Z(l\omega_0)} \\ -\sum_{l=-\infty}^{\infty} \frac{D_{a1l}\overline{D_{a2l}} e^{jl\frac{2\pi}{3}}}{Z(l\omega_0)} \\ -\sum_{l=-\infty}^{\infty} \frac{|D_{a1l}|^2 e^{-jl\frac{2\pi}{3}}}{Z(l\omega_0)} \\ -\sum_{l=-\infty}^{\infty} \frac{D_{a1l}\overline{D_{a2l}} e^{-jl\frac{2\pi}{3}}}{Z(l\omega_0)} \\ 2\sum_{l=-\infty}^{\infty} \frac{|D_{a1l}|^2}{Z(l\omega_0)} \\ 2\sum_{l=-\infty}^{\infty} \frac{D_{a1l}\overline{D_{a2l}}}{Z(l\omega_0)} \end{array} \right] V_{\delta c1} + \left[\begin{array}{l} -\sum_{l=-\infty}^{\infty} \frac{D_{a2l}\overline{D_{a1l}} e^{jl\frac{2\pi}{3}}}{Z(l\omega_0)} \\ -\sum_{l=-\infty}^{\infty} \frac{|D_{a2l}|^2 e^{jl\frac{2\pi}{3}}}{Z(l\omega_0)} \\ -\sum_{l=-\infty}^{\infty} \frac{D_{a2l}\overline{D_{a1l}} e^{-jl\frac{2\pi}{3}}}{Z(l\omega_0)} \\ -\sum_{l=-\infty}^{\infty} \frac{|D_{a2l}|^2 e^{-jl\frac{2\pi}{3}}}{Z(l\omega_0)} \\ 2\sum_{l=-\infty}^{\infty} \frac{D_{a2l}\overline{D_{a1l}}}{Z(l\omega_0)} \\ 2\sum_{l=-\infty}^{\infty} \frac{|D_{a2l}|^2}{Z(l\omega_0)} \end{array} \right] V_{\delta c2} \\
 & = \left\{ \left[\begin{array}{l} -2\sum_{l=-\infty}^{\infty} \frac{B_{al}\overline{D_{a1l}}}{Z(l\omega_0)} \\ -2\sum_{l=-\infty}^{\infty} \frac{B_{al}\overline{D_{a2l}}}{Z(l\omega_0)} \\ -2\sum_{l=-\infty}^{\infty} \frac{B_{al}\overline{D_{a1l}}}{Z(l\omega_0)} \\ -2\sum_{l=-\infty}^{\infty} \frac{B_{al}\overline{D_{a2l}}}{Z(l\omega_0)} \\ -2\sum_{l=-\infty}^{\infty} \frac{B_{al}\overline{D_{a1l}}}{Z(l\omega_0)} \\ -2\sum_{l=-\infty}^{\infty} \frac{B_{al}\overline{D_{a2l}}}{Z(l\omega_0)} \end{array} \right] + \left[\begin{array}{l} \sum_{l=-\infty}^{\infty} \frac{B_{al}\overline{D_{a1l}} e^{-jl\frac{2\pi}{3}}}{Z(l\omega_0)} \\ \sum_{l=-\infty}^{\infty} \frac{B_{al}\overline{D_{a2l}} e^{-jl\frac{2\pi}{3}}}{Z(l\omega_0)} \\ \sum_{l=-\infty}^{\infty} \frac{B_{al}\overline{D_{a1l}} e^{jl\frac{2\pi}{3}}}{Z(l\omega_0)} \\ \sum_{l=-\infty}^{\infty} \frac{B_{al}\overline{D_{a2l}} e^{jl\frac{2\pi}{3}}}{Z(l\omega_0)} \\ \sum_{l=-\infty}^{\infty} \frac{B_{al}\overline{D_{a1l}} e^{-jl\frac{2\pi}{3}}}{Z(l\omega_0)} \\ \sum_{l=-\infty}^{\infty} \frac{B_{al}\overline{D_{a2l}} e^{-jl\frac{2\pi}{3}}}{Z(l\omega_0)} \end{array} \right] \right.
 \end{aligned}$$

$$\begin{aligned}
& + \left[\begin{array}{c} \sum_{l=-\infty}^{\infty} \frac{B_{a1} \overline{D_{a1l}} e^{jl \frac{2\pi}{3}}}{Z(l\omega_0)} \\ \sum_{l=-\infty}^{\infty} \frac{B_{a1} \overline{D_{a2l}} e^{jl \frac{2\pi}{3}}}{Z(l\omega_0)} \\ \sum_{l=-\infty}^{\infty} \frac{B_{a1} \overline{D_{a1l}} e^{-jl \frac{2\pi}{3}}}{Z(l\omega_0)} \\ \sum_{l=-\infty}^{\infty} \frac{B_{a1} \overline{D_{a2l}} e^{-jl \frac{2\pi}{3}}}{Z(l\omega_0)} \\ \sum_{l=-\infty}^{\infty} \frac{B_{a1} \overline{D_{a1l}} e^{jl \frac{2\pi}{3}}}{Z(l\omega_0)} \\ \sum_{l=-\infty}^{\infty} \frac{B_{a1} \overline{D_{a2l}} e^{jl \frac{2\pi}{3}}}{Z(l\omega_0)} \end{array} \right] \left. \vphantom{\sum_{l=-\infty}^{\infty}} \right\} \frac{V_t}{3}
\end{aligned} \tag{4.43}$$

For the case where interleaved switching is used, we will have the cells being phase shifted by $\frac{2l\pi}{3}$ for each phase. Hence the matrix equation 4.43 yield:

$$\begin{aligned}
& \left[\begin{array}{c} 2 \sum_{l=-\infty}^{\infty} \frac{|D_{a1l}|^2}{Z(l\omega_0)} \\ 2 \sum_{l=-\infty}^{\infty} \frac{|D_{a1l}|^2 e^{-jl \frac{2\pi}{3}}}{Z(l\omega_0)} \\ - \sum_{l=-\infty}^{\infty} \frac{|D_{a1l}|^2 e^{jl \frac{2\pi}{3}}}{Z(l\omega_0)} \\ - \sum_{l=-\infty}^{\infty} \frac{|D_{a1l}|^2}{Z(l\omega_0)} \\ - \sum_{l=-\infty}^{\infty} \frac{|D_{a1l}|^2 e^{-jl \frac{2\pi}{3}}}{Z(l\omega_0)} \\ - \sum_{l=-\infty}^{\infty} \frac{|D_{a1l}|^2 e^{jl \frac{2\pi}{3}}}{Z(l\omega_0)} \end{array} \right] V_{\delta a1} + \left[\begin{array}{c} 2 \sum_{l=-\infty}^{\infty} \frac{|D_{a1l}|^2 e^{jl \frac{2\pi}{3}}}{Z(l\omega_0)} \\ 2 \sum_{l=-\infty}^{\infty} \frac{|D_{a1l}|^2}{Z(l\omega_0)} \\ - \sum_{l=-\infty}^{\infty} \frac{|D_{a1l}|^2 e^{-jl \frac{2\pi}{3}}}{Z(l\omega_0)} \\ - \sum_{l=-\infty}^{\infty} \frac{|D_{a1l}|^2 e^{jl \frac{2\pi}{3}}}{Z(l\omega_0)} \\ - \sum_{l=-\infty}^{\infty} \frac{|D_{a1l}|^2}{Z(l\omega_0)} \\ - \sum_{l=-\infty}^{\infty} \frac{|D_{a1l}|^2 e^{-jl \frac{2\pi}{3}}}{Z(l\omega_0)} \end{array} \right] V_{\delta a2}
\end{aligned}$$

$$\begin{aligned}
 & + \left[\begin{array}{c} -\sum_{l=-\infty}^{\infty} \frac{|D_{a1l}|^2 e^{-jl\frac{2\pi}{3}}}{Z(l\omega_0)} \\ -\sum_{l=-\infty}^{\infty} \frac{|D_{a1l}|^2 e^{jl\frac{2\pi}{3}}}{Z(l\omega_0)} \\ 2\sum_{l=-\infty}^{\infty} \frac{|D_{a1l}|^2}{Z(l\omega_0)} \\ 2\sum_{l=-\infty}^{\infty} \frac{|D_{a1l}|^2 e^{-jl\frac{2\pi}{3}}}{Z(l\omega_0)} \\ -\sum_{l=-\infty}^{\infty} \frac{|D_{a1l}|^2 e^{jl\frac{2\pi}{3}}}{Z(l\omega_0)} \\ -\sum_{l=-\infty}^{\infty} \frac{|D_{a1l}|^2}{Z(l\omega_0)} \end{array} \right] V_{\delta b1} + \left[\begin{array}{c} -\sum_{l=-\infty}^{\infty} \frac{|D_{a1l}|^2}{Z(l\omega_0)} \\ -\sum_{l=-\infty}^{\infty} \frac{|D_{a1l}|^2 e^{-jl\frac{2\pi}{3}}}{Z(l\omega_0)} \\ 2\sum_{l=-\infty}^{\infty} \frac{|D_{a1l}|^2 e^{jl\frac{2\pi}{3}}}{Z(l\omega_0)} \\ 2\sum_{l=-\infty}^{\infty} \frac{|D_{a1l}|^2}{Z(l\omega_0)} \\ -\sum_{l=-\infty}^{\infty} \frac{|D_{a1l}|^2 e^{-jl\frac{2\pi}{3}}}{Z(l\omega_0)} \\ -\sum_{l=-\infty}^{\infty} \frac{|D_{a1l}|^2 e^{jl\frac{2\pi}{3}}}{Z(l\omega_0)} \end{array} \right] V_{\delta b2} \\
 & + \left[\begin{array}{c} -\sum_{l=-\infty}^{\infty} \frac{|D_{a1l}|^2 e^{jl\frac{2\pi}{3}}}{Z(l\omega_0)} \\ -\sum_{l=-\infty}^{\infty} \frac{|D_{a1l}|^2}{Z(l\omega_0)} \\ -\sum_{l=-\infty}^{\infty} \frac{|D_{a1l}|^2 e^{-jl\frac{2\pi}{3}}}{Z(l\omega_0)} \\ -\sum_{l=-\infty}^{\infty} \frac{|D_{a1l}|^2 e^{jl\frac{2\pi}{3}}}{Z(l\omega_0)} \\ 2\sum_{l=-\infty}^{\infty} \frac{|D_{a1l}|^2}{Z(l\omega_0)} \\ 2\sum_{l=-\infty}^{\infty} \frac{|D_{a1l}|^2 e^{-jl\frac{2\pi}{3}}}{Z(l\omega_0)} \end{array} \right] V_{\delta c1} + \left[\begin{array}{c} -\sum_{l=-\infty}^{\infty} \frac{|D_{a1l}|^2 e^{-jl\frac{2\pi}{3}}}{Z(l\omega_0)} \\ -\sum_{l=-\infty}^{\infty} \frac{|D_{a1l}|^2 e^{jl\frac{2\pi}{3}}}{Z(l\omega_0)} \\ -\sum_{l=-\infty}^{\infty} \frac{|D_{a1l}|^2}{Z(l\omega_0)} \\ -\sum_{l=-\infty}^{\infty} \frac{|D_{a1l}|^2 e^{-jl\frac{2\pi}{3}}}{Z(l\omega_0)} \\ 2\sum_{l=-\infty}^{\infty} \frac{|D_{a1l}|^2 e^{jl\frac{2\pi}{3}}}{Z(l\omega_0)} \\ 2\sum_{l=-\infty}^{\infty} \frac{|D_{a1l}|^2}{Z(l\omega_0)} \end{array} \right] V_{\delta c2} \\
 = & \left\{ \left[\begin{array}{c} -2\sum_{l=-\infty}^{\infty} \frac{B_{a1}\overline{D_{a1l}}}{Z(l\omega_0)} \\ -2\sum_{l=-\infty}^{\infty} \frac{B_{a1}\overline{D_{a1l}}e^{-jl\frac{2\pi}{3}}}{Z(l\omega_0)} \\ -2\sum_{l=-\infty}^{\infty} \frac{B_{a1}\overline{D_{a1l}}}{Z(l\omega_0)} \\ -2\sum_{l=-\infty}^{\infty} \frac{B_{a1}\overline{D_{a1l}}e^{-jl\frac{2\pi}{3}}}{Z(l\omega_0)} \\ -2\sum_{l=-\infty}^{\infty} \frac{B_{a1}\overline{D_{a1l}}}{Z(l\omega_0)} \\ -2\sum_{l=-\infty}^{\infty} \frac{B_{a1}\overline{D_{a1l}}e^{-jl\frac{2\pi}{3}}}{Z(l\omega_0)} \end{array} \right] + \left[\begin{array}{c} \sum_{l=-\infty}^{\infty} \frac{B_{a1}\overline{D_{a1l}}e^{-jl\frac{2\pi}{3}}}{Z(l\omega_0)} \\ \sum_{l=-\infty}^{\infty} \frac{B_{a1}\overline{D_{a1l}}e^{jl\frac{2\pi}{3}}}{Z(l\omega_0)} \\ \sum_{l=-\infty}^{\infty} \frac{B_{a1}\overline{D_{a1l}}e^{jl\frac{2\pi}{3}}}{Z(l\omega_0)} \\ \sum_{l=-\infty}^{\infty} \frac{B_{a1}\overline{D_{a1l}}}{Z(l\omega_0)} \\ \sum_{l=-\infty}^{\infty} \frac{B_{a1}\overline{D_{a1l}}e^{-jl\frac{2\pi}{3}}}{Z(l\omega_0)} \\ \sum_{l=-\infty}^{\infty} \frac{B_{a1}\overline{D_{a1l}}e^{jl\frac{2\pi}{3}}}{Z(l\omega_0)} \end{array} \right] \right\}
 \end{aligned}$$

$$+ \left[\begin{array}{c} \sum_{l=-\infty}^{\infty} \frac{B_{al} \overline{D_{a1l}} e^{jl \frac{2\pi}{3}}}{Z(l\omega_0)} \\ \sum_{l=-\infty}^{\infty} \frac{B_{al} \overline{D_{a1l}}}{Z(l\omega_0)} \\ \sum_{l=-\infty}^{\infty} \frac{B_{al} \overline{D_{a1l}} e^{-jl \frac{2\pi}{3}}}{Z(l\omega_0)} \\ \sum_{l=-\infty}^{\infty} \frac{B_{al} \overline{D_{a1l}} e^{jl \frac{2\pi}{3}}}{Z(l\omega_0)} \\ \sum_{l=-\infty}^{\infty} \frac{B_{al} \overline{D_{a1l}} e^{jl \frac{2\pi}{3}}}{Z(l\omega_0)} \\ \sum_{l=-\infty}^{\infty} \frac{B_{al} \overline{D_{a1l}}}{Z(l\omega_0)} \end{array} \right] \left. \vphantom{\sum_{l=-\infty}^{\infty}} \right\} \frac{V_t}{3} \tag{4.44}$$

To simplify the analyses of matrix equation 4.44 we write $e^{jl \frac{2\pi}{3}}$ and $e^{-jl \frac{2\pi}{3}}$ in terms of three classes. This classes are shown in Table 4.1 of section 4.2. By substituting λ_1 , λ_2 , λ_3 , ϕ_2 and ϕ_3 into matrix equation 4.44 we obtain:

$$\mathbf{V}_\delta = -\frac{1}{3} \{\Lambda\}^{-1} \Phi V_t \tag{4.45}$$

where

$$\mathbf{V}_\delta = \left[\begin{array}{c} V_{\delta a1} \\ V_{\delta a2} \\ V_{\delta b1} \\ V_{\delta b2} \\ V_{\delta c1} \\ V_{\delta c2} \end{array} \right] \tag{4.46}$$

and

$$\begin{aligned}
\Lambda = & \begin{bmatrix} 2\lambda_1 & 2\lambda_1 & -\lambda_1 & -\lambda_1 & -\lambda_1 & -\lambda_1 \\ 2\lambda_1 & 2\lambda_1 & -\lambda_1 & -\lambda_1 & -\lambda_1 & -\lambda_1 \\ -\lambda_1 & -\lambda_1 & 2\lambda_1 & 2\lambda_1 & -\lambda_1 & -\lambda_1 \\ -\lambda_1 & -\lambda_1 & 2\lambda_1 & 2\lambda_1 & -\lambda_1 & -\lambda_1 \\ -\lambda_1 & -\lambda_1 & -\lambda_1 & -\lambda_1 & 2\lambda_1 & 2\lambda_1 \\ -\lambda_1 & -\lambda_1 & -\lambda_1 & -\lambda_1 & 2\lambda_1 & 2\lambda_1 \end{bmatrix} \\
+ & \begin{bmatrix} 2\lambda_2 & 2\lambda_2 e^{j\frac{2\pi}{3}} & -\lambda_2 e^{-j\frac{2\pi}{3}} & -\lambda_2 & -\lambda_2 e^{j\frac{2\pi}{3}} & -\lambda_2 e^{-j\frac{2\pi}{3}} \\ 2\lambda_2 e^{-j\frac{2\pi}{3}} & 2\lambda_2 & -\lambda_2 e^{j\frac{2\pi}{3}} & -\lambda_2 e^{-j\frac{2\pi}{3}} & -\lambda_2 & -\lambda_2 e^{j\frac{2\pi}{3}} \\ -\lambda_2 e^{j\frac{2\pi}{3}} & -\lambda_2 e^{-j\frac{2\pi}{3}} & 2\lambda_2 & 2\lambda_2 e^{j\frac{2\pi}{3}} & -\lambda_2 e^{-j\frac{2\pi}{3}} & -\lambda_2 \\ -\lambda_2 & -\lambda_2 e^{j\frac{2\pi}{3}} & 2\lambda_2 e^{-j\frac{2\pi}{3}} & 2\lambda_2 & -\lambda_2 e^{j\frac{2\pi}{3}} & -\lambda_2 e^{-j\frac{2\pi}{3}} \\ -\lambda_2 e^{-j\frac{2\pi}{3}} & -\lambda_2 & -\lambda_2 e^{j\frac{2\pi}{3}} & -\lambda_2 e^{-j\frac{2\pi}{3}} & 2\lambda_2 & 2\lambda_2 e^{j\frac{2\pi}{3}} \\ -\lambda_2 e^{j\frac{2\pi}{3}} & -\lambda_2 e^{-j\frac{2\pi}{3}} & -\lambda_2 & -\lambda_2 e^{j\frac{2\pi}{3}} & 2\lambda_2 e^{-j\frac{2\pi}{3}} & 2\lambda_2 \end{bmatrix} \\
+ & \begin{bmatrix} 2\lambda_3 & 2\lambda_3 e^{-j\frac{2\pi}{3}} & -\lambda_3 e^{j\frac{2\pi}{3}} & -\lambda_3 & -\lambda_3 e^{-j\frac{2\pi}{3}} & -\lambda_3 e^{j\frac{2\pi}{3}} \\ 2\lambda_3 e^{j\frac{2\pi}{3}} & 2\lambda_3 & -\lambda_3 e^{-j\frac{2\pi}{3}} & -\lambda_3 e^{j\frac{2\pi}{3}} & -\lambda_3 & -\lambda_3 e^{-j\frac{2\pi}{3}} \\ -\lambda_3 e^{-j\frac{2\pi}{3}} & -\lambda_3 e^{j\frac{2\pi}{3}} & 2\lambda_3 & 2\lambda_3 e^{-j\frac{2\pi}{3}} & -\lambda_3 e^{j\frac{2\pi}{3}} & -\lambda_3 \\ -\lambda_3 & -\lambda_3 e^{-j\frac{2\pi}{3}} & 2\lambda_3 e^{j\frac{2\pi}{3}} & 2\lambda_3 & -\lambda_3 e^{-j\frac{2\pi}{3}} & -\lambda_3 e^{j\frac{2\pi}{3}} \\ -\lambda_3 e^{j\frac{2\pi}{3}} & -\lambda_3 & -\lambda_3 e^{-j\frac{2\pi}{3}} & -\lambda_3 e^{j\frac{2\pi}{3}} & 2\lambda_3 & 2\lambda_3 e^{-j\frac{2\pi}{3}} \\ -\lambda_3 e^{-j\frac{2\pi}{3}} & -\lambda_3 e^{j\frac{2\pi}{3}} & -\lambda_3 & -\lambda_3 e^{-j\frac{2\pi}{3}} & 2\lambda_3 e^{j\frac{2\pi}{3}} & 2\lambda_3 \end{bmatrix} \quad (4.47)
\end{aligned}$$

and

$$\Phi = \begin{bmatrix} \phi_2 + \phi_3 \\ \phi_2 e^{-j\frac{2\pi}{3}} + \phi_3 e^{j\frac{2\pi}{3}} \\ \phi_2 + \phi_3 \\ \phi_2 e^{-j\frac{2\pi}{3}} + \phi_3 e^{j\frac{2\pi}{3}} \\ \phi_2 + \phi_3 \\ \phi_2 e^{-j\frac{2\pi}{3}} + \phi_3 e^{j\frac{2\pi}{3}} \end{bmatrix} \quad (4.48)$$

We rewrite equation 4.45 as follows:

$$\frac{\mathbf{V}_\delta}{V_t} = -\frac{1}{3} \{\Lambda\}^{-1} \Phi \quad (4.49)$$

The determinant of Λ is given by:

$$\det(\Lambda) = 19683\lambda_1^2\lambda_2^2\lambda_3^2 \quad (4.50)$$

which implies that the inverse of Λ exists provided λ_1 , λ_2 and λ_3 are nonzero.

By direct computation we found that the inverse of equation 4.47 is given by:

$$\Lambda^{-1} = \begin{bmatrix} \Lambda_{11} & \Lambda_{12} & \Lambda_{13} & \Lambda_{14} & \Lambda_{15} & \Lambda_{16} \\ \Lambda_{21} & \Lambda_{22} & \Lambda_{23} & \Lambda_{24} & \Lambda_{25} & \Lambda_{26} \\ \Lambda_{31} & \Lambda_{32} & \Lambda_{33} & \Lambda_{34} & \Lambda_{35} & \Lambda_{36} \\ \Lambda_{41} & \Lambda_{42} & \Lambda_{43} & \Lambda_{44} & \Lambda_{45} & \Lambda_{46} \\ \Lambda_{51} & \Lambda_{52} & \Lambda_{53} & \Lambda_{54} & \Lambda_{55} & \Lambda_{56} \\ \Lambda_{61} & \Lambda_{62} & \Lambda_{63} & \Lambda_{64} & \Lambda_{65} & \Lambda_{66} \end{bmatrix} \frac{1}{27\lambda_1^2\lambda_2^2\lambda_3^2} \quad (4.51)$$

where

$$\Lambda_{11} = \Lambda_{22} = \Lambda_{33} = \Lambda_{44} = \Lambda_{55} = \Lambda_{66} = 2\lambda_2\lambda_3 + 2\lambda_1\lambda_2 + 2\lambda_1\lambda_3 \quad (4.52)$$

$$\Lambda_{12} = \Lambda_{34} = \Lambda_{56} = \lambda_2\lambda_3 + \lambda_1\lambda_2 e^{-j\frac{2\pi}{3}} + \lambda_1\lambda_3 e^{j\frac{2\pi}{3}} \quad (4.53)$$

$$\Lambda_{13} = \Lambda_{24} = \Lambda_{35} = \Lambda_{46} = \Lambda_{51} = \Lambda_{62} = -\lambda_2\lambda_3 - \lambda_1\lambda_2e^{j\frac{2\pi}{3}} - \lambda_1\lambda_3e^{-j\frac{2\pi}{3}} \quad (4.54)$$

$$\Lambda_{14} = \Lambda_{25} = \Lambda_{36} = \Lambda_{41} = \Lambda_{52} = \Lambda_{63} = \lambda_2\lambda_3 + \lambda_1\lambda_2 + \lambda_1\lambda_3 \quad (4.55)$$

$$\Lambda_{15} = \Lambda_{26} = \Lambda_{31} = \Lambda_{42} = \Lambda_{53} = \Lambda_{64} = -\lambda_2\lambda_3 - \lambda_1\lambda_2e^{-j\frac{2\pi}{3}} - \lambda_1\lambda_3e^{j\frac{2\pi}{3}} \quad (4.56)$$

$$\Lambda_{16} = \Lambda_{32} = \Lambda_{54} = -2\lambda_2\lambda_3 - 2\lambda_1\lambda_2e^{j\frac{2\pi}{3}} - 2\lambda_1\lambda_3e^{-j\frac{2\pi}{3}} \quad (4.57)$$

$$\Lambda_{21} = \Lambda_{43} = \Lambda_{65} = \lambda_2\lambda_3 + \lambda_1\lambda_2e^{j\frac{2\pi}{3}} + \lambda_1\lambda_3e^{-j\frac{2\pi}{3}} \quad (4.58)$$

$$\Lambda_{23} = \Lambda_{45} = \Lambda_{61} = -2\lambda_2\lambda_3 - 2\lambda_1\lambda_2e^{-j\frac{2\pi}{3}} - 2\lambda_1\lambda_3e^{j\frac{2\pi}{3}} \quad (4.59)$$

Now we write the matrix equation that describes the balancing of cell capacitor voltage as shown in matrix equation 4.60.

$$\begin{bmatrix} \frac{V_{\delta a1}}{V_t} \\ \frac{V_{\delta a2}}{V_t} \\ \frac{V_{\delta b1}}{V_t} \\ \frac{V_{\delta b2}}{V_t} \\ \frac{V_{\delta c1}}{V_t} \\ \frac{V_{\delta c2}}{V_t} \end{bmatrix} = - \begin{bmatrix} \frac{(\phi_2 + \phi_3)(\Lambda_{11} + \Lambda_{13} + \Lambda_{15}) + (\phi_2 e^{-j\frac{2\pi}{3}} + \phi_3 e^{j\frac{2\pi}{3}})(\Lambda_{12} + \Lambda_{14} + \Lambda_{16})}{81\lambda_1^2\lambda_2^2\lambda_3^2} \\ \frac{(\phi_2 + \phi_3)(\Lambda_{21} + \Lambda_{23} + \Lambda_{25}) + (\phi_2 e^{-j\frac{2\pi}{3}} + \phi_3 e^{j\frac{2\pi}{3}})(\Lambda_{22} + \Lambda_{24} + \Lambda_{26})}{81\lambda_1^2\lambda_2^2\lambda_3^2} \\ \frac{(\phi_2 + \phi_3)(\Lambda_{31} + \Lambda_{33} + \Lambda_{35}) + (\phi_2 e^{-j\frac{2\pi}{3}} + \phi_3 e^{j\frac{2\pi}{3}})(\Lambda_{32} + \Lambda_{34} + \Lambda_{36})}{81\lambda_1^2\lambda_2^2\lambda_3^2} \\ \frac{(\phi_2 + \phi_3)(\Lambda_{41} + \Lambda_{43} + \Lambda_{45}) + (\phi_2 e^{-j\frac{2\pi}{3}} + \phi_3 e^{j\frac{2\pi}{3}})(\Lambda_{42} + \Lambda_{44} + \Lambda_{46})}{81\lambda_1^2\lambda_2^2\lambda_3^2} \\ \frac{(\phi_2 + \phi_3)(\Lambda_{51} + \Lambda_{53} + \Lambda_{55}) + (\phi_2 e^{-j\frac{2\pi}{3}} + \phi_3 e^{j\frac{2\pi}{3}})(\Lambda_{52} + \Lambda_{54} + \Lambda_{56})}{81\lambda_1^2\lambda_2^2\lambda_3^2} \\ \frac{(\phi_2 + \phi_3)(\Lambda_{61} + \Lambda_{63} + \Lambda_{65}) + (\phi_2 e^{-j\frac{2\pi}{3}} + \phi_3 e^{j\frac{2\pi}{3}})(\Lambda_{62} + \Lambda_{64} + \Lambda_{66})}{81\lambda_1^2\lambda_2^2\lambda_3^2} \end{bmatrix} \quad (4.60)$$

The denominator of the solution of matrix equation 4.60 is the same as the determinant of Λ but scaled to a constant. That is, if the determinant is non-zero under the set conditions, then the denominator is also non-zero.

Similarly using the definitions of λ_1 , λ_2 , λ_3 , ϕ_2 and ϕ_3 in equations 4.17 to 4.21 we can conclude that equation 4.60 shows that the steady state balancing of the cell capacitor voltage is influenced by the following two factors:

1. The impedance of the output filter and load $Z(l\omega)$; and.
2. The values of $B_{al}\overline{D_{al}}$, and $|D_{al}|^2$.

The following examples furnish examples of factors that cause imbalance in the cell capacitor voltages.

Example 3.4

When the switching frequency is not sufficiently high it causes the sidebands of different multiples of the switching frequency groups to overlap. This will result in an overlap in the spectra of B_{al} and D_{al} . We demonstrate this property for interleaved switching with a switching frequency of $f_s = 350\text{Hz}$, a reference frequency of $f_0 = 50\text{Hz}$ and a modulation index $m_a = 0.8$.

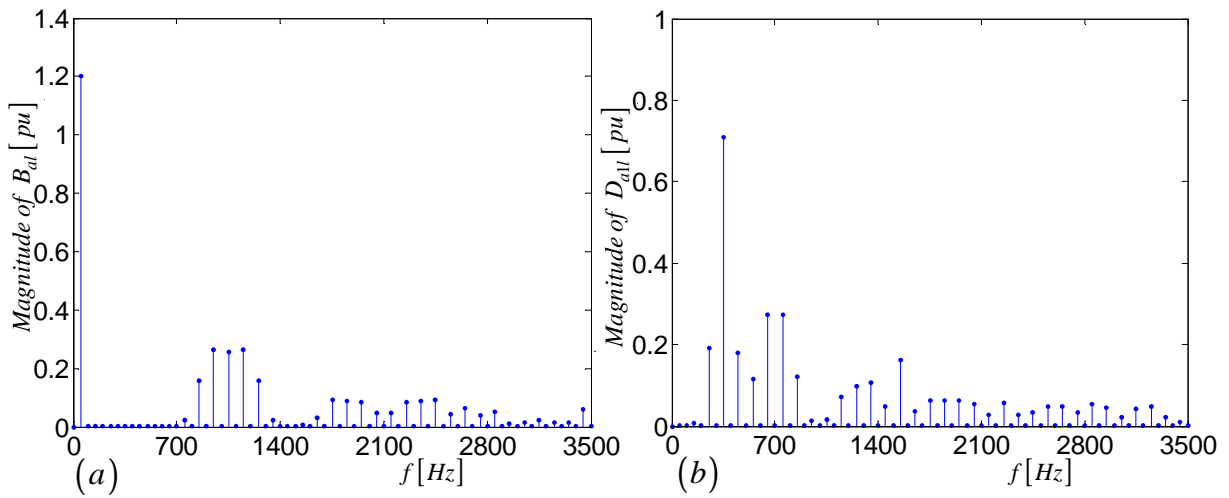


Figure 4.9: (a) Amplitude spectrum of $|B_{al}|$ and (b) Amplitude spectrum of $|D_{al}|$

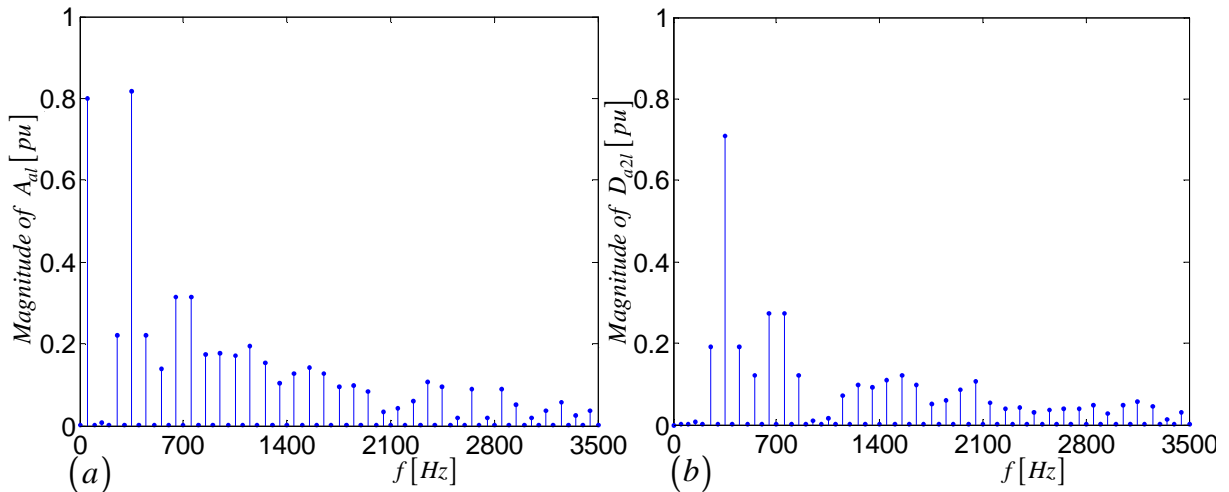


Figure 4.10: (a) Amplitude spectrum of $|A_{al}|$ and (b) Amplitude spectrum of $|D_{a2l}|$

The amplitude spectrum of $|B_{al}|$ and $|D_{al}|$ is shown in Figures 4.9 (a) and (b) respectively and those of $|A_{al}|$ and $|D_{a2l}|$ is shown in Figures 4.10 (a) and (b) respectively.

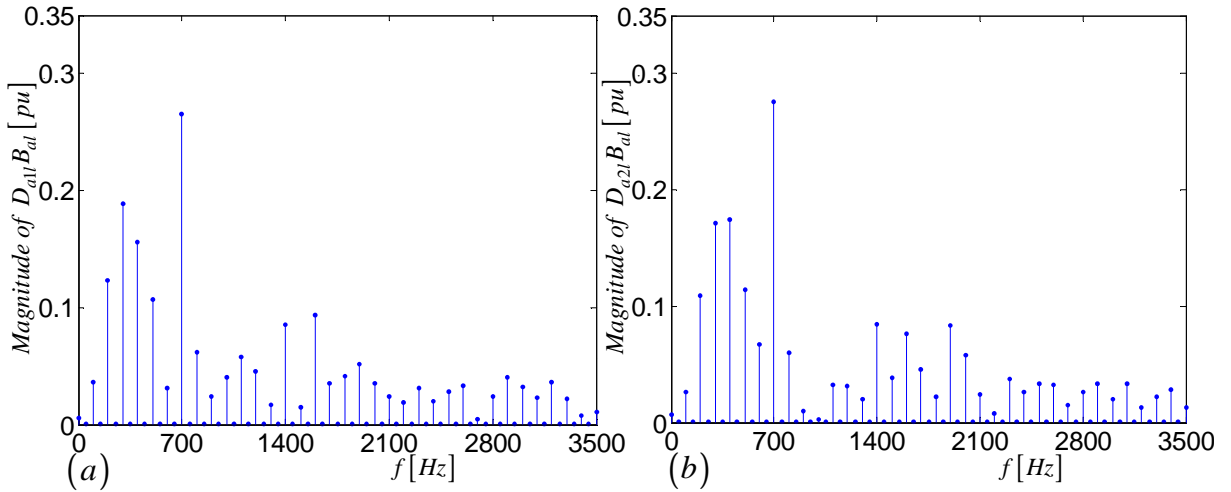


Figure 4.11: (a) Amplitude spectrum of $|D_{a1l}| |B_{al}|$ and (b) Amplitude spectrum of $|D_{a2l}| |B_{al}|$

Figures 4.11 (a) and (b) show the amplitude spectra of $|D_{a1l}| |B_{al}|$ and $|D_{a2l}| |B_{al}|$ respectively. From these figures it is clear that $|D_{a1l}| |B_{al}| > 0$ and $|D_{a2l}| |B_{al}| > 0$. This property will in turn cause imbalance in the cell capacitor voltage.

Example 3.5

When the reference signal contains high frequency components the sidebands of multiples of switching frequency groups overlap which results in the overlap of B_{al} and D_{al} . We establish this property for interleaved switching with switching frequency of $f_s = 6300 Hz$, a reference frequency of $f_0 = 900 Hz$ and modulation index $m_a = 0.8$.

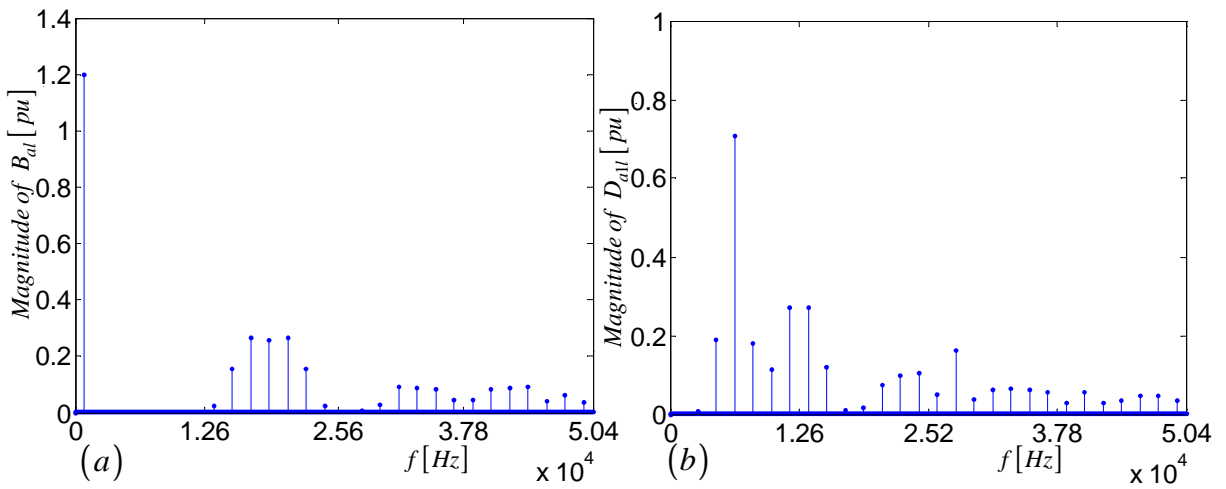


Figure 4.12: (a) Amplitude spectrum of $|B_{al}|$ and (b) Amplitude spectrum of $|D_{a1l}|$

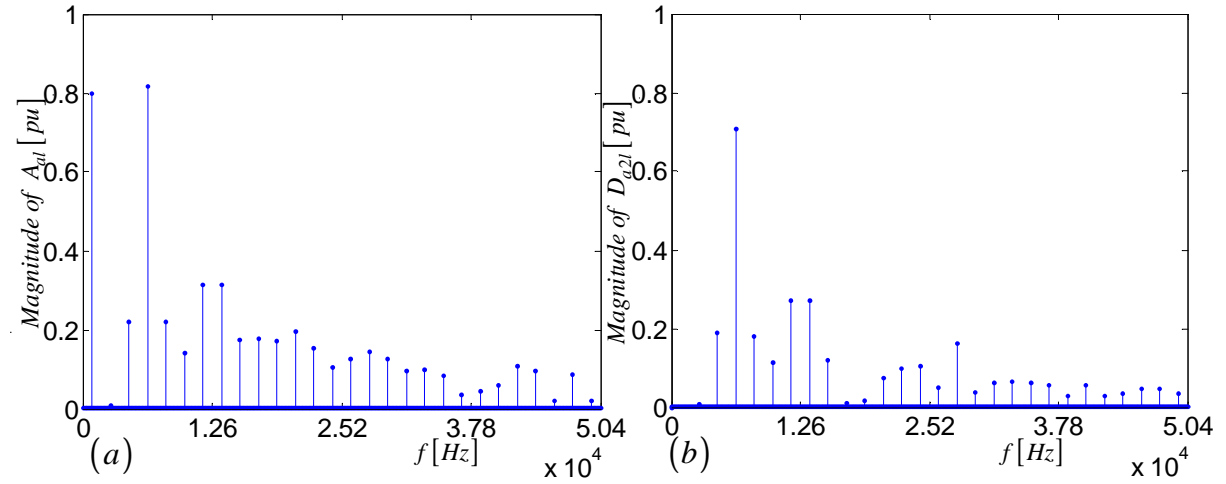


Figure 4.13: (a) Amplitude spectrum of $|A_{al}|$ and (b) Amplitude spectrum of $|D_{a2l}|$

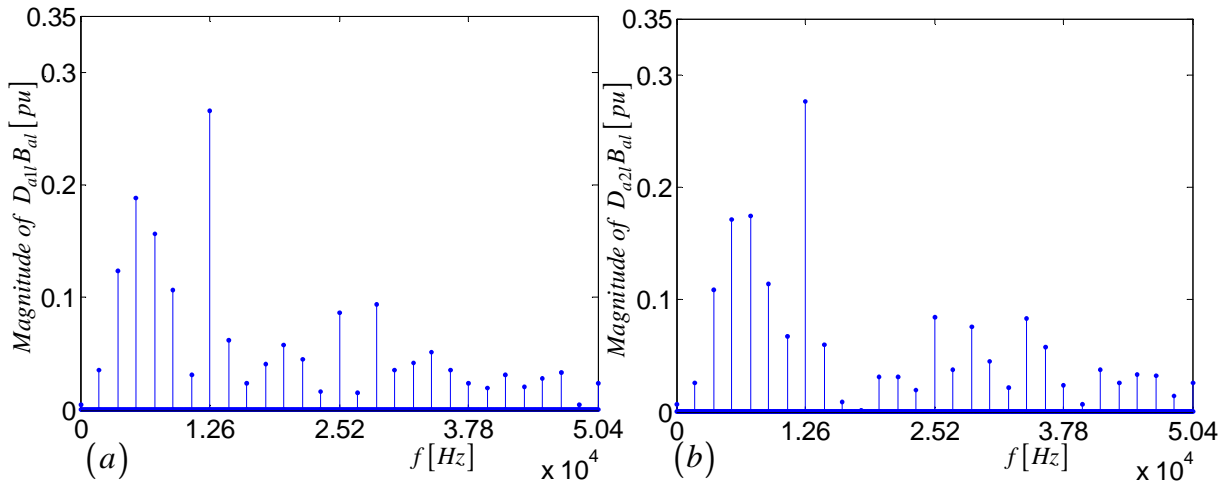


Figure 4.14: (a) Amplitude spectrum of $|D_{a1l}| |B_{al}|$ and (b) Amplitude spectrum of $|D_{a2l}| |B_{al}|$

The amplitude spectrum of $|B_{al}|$ and $|D_{a1l}|$ is shown in Figures 4.12 (a) and (b) respectively and those of $|A_{al}|$ and $|D_{a2l}|$ is shown in Figures 4.13 (a) and (b) respectively. Figures 4.14 (a) and (b) show the amplitude spectra of $|D_{a1l}| |B_{al}|$ and $|D_{a2l}| |B_{al}|$ respectively. Similarly from these figures it is observed that $|D_{a1l}| |B_{al}| > 0$ and $|D_{a2l}| |B_{al}| > 0$. This property will cause an imbalance in the cell capacitor.

4.4 Summary

The aim of this chapter was to derive the balancing theory for the cell capacitor voltages of the 2-cell and 3-cell multicell converter under steady state conditions. From the derived equations we found that factors affecting the natural balancing of 2-cell and 3-cell multicell converters are:

1. The impedance of the output filter and load $Z(l\omega)$; and
2. The values of $B_{al}\overline{D_{al}}$ and $|D_{al}|^2$ for the 2-cell converter and $B_{al}\overline{D_{a1l}}$ and $|D_{a1l}|^2$ for the 3-cell converter.

However it was found that the cell capacitor voltages may not balance if one or both of the following conditions are satisfied:

1. The switching frequency is not sufficiently higher than the frequency of the reference signal so that the spectrum of the d coefficients overlaps with the spectrum of the t coefficients. That is, when $|B_{al}||D_{al}| > 0$ for the 2-cell three-phase multicell converter and $|B_{al}||D_{a1l}| > 0$ and $|B_{al}||D_{a2l}| > 0$ for the 3-cell three-phase multicell converter.
2. The frequency component of the reference signal is high in such a way that the sidebands of the multiples of the switching frequency group for d coefficients overlap with the sidebands of the multiples of the switching frequency group for t coefficients.
3. The load impedance is purely inductive, that is if $Z(l\omega) = 0$.

Chapter 5

Time Constant Analysis

5.1 Introduction

In this chapter we calculate the time constant associated with the rebalancing of the DC-bus voltages following a perturbation. This time constant can be seen as a measure of the strength of the balancing mechanisms.

For calculating this constant we use the theory of linear systems of differential equations given below, with the aim of expressing the DC capacitor currents as a system of homogeneous linear differential equations:

The fundamental theorem for linear systems [3] of differential equations states that if \mathbf{A} is an $n \times n$ matrix, then for a given $\mathbf{x}_0 \in \mathfrak{R}^n$, the initial value problem

$$\dot{\mathbf{x}} = \mathbf{A}\mathbf{x}$$

$$\mathbf{x}(0) = \mathbf{x}_0$$

has a unique solution given by:

$$\mathbf{x}(t) = e^{\mathbf{A}t}\mathbf{x}_0$$

If \mathbf{A} is an $n \times n$ matrix with distinct eigenvalues $\lambda_1, \dots, \lambda_n$ [4][5], then the solution to the differential equation

$$\dot{\mathbf{x}} = \mathbf{A}\mathbf{x}$$

$$\mathbf{x}(0) = \mathbf{x}_0$$

is given by:

$$x_i(t) = y_1 e^{t\lambda_1} + \dots + y_n e^{t\lambda_n} \tag{5.1}$$

where y_i is the corresponding eigenvector for the eigenvalue x_i for $i = 1, \dots, n$.

The corresponding time constants [9] will be given by $\tau_i = -\frac{1}{\Re\{\lambda_i\}}$ for $i = 1, \dots, n$.

Now for us to calculate these time constants we make the following assumptions:

- The cell capacitors are very large;
- The cell capacitor voltages change much slower than the rest of the system; and
- The DC-bus voltage V_t is zero in order to calculate the homogeneous solutions of the differential equations characterising the cell capacitor currents.

5.2 2-Cell Multicell Converter

5.2.1 Time Constant

The exponential decay is associated with the DC currents I_{cda} , I_{cdb} and I_{cdc} . Referring to the equivalent circuit of the 2-cell 3-phase multicell converter given in Figure 3.6, the change in the capacitor voltage of C_{da} , C_{db} and C_{dc} is slow; hence the state of the circuit can be taken as steady. The assumption that $V_t = 0$, implies that we short-circuit voltage source $\frac{V_t}{2}$ in the equivalent circuit to obtain $V_t = 0$. The resulting circuit is depicted in Figure 5.1. Thus equation 4.7 is rewritten as follows:

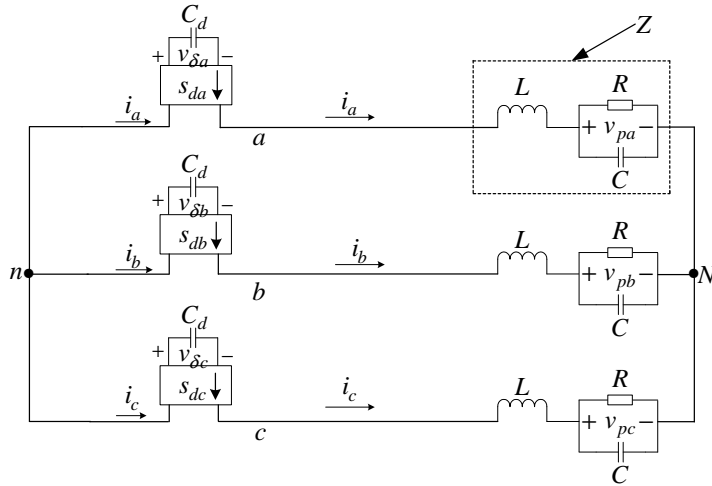


Figure 5.1: *Equivalent circuit of the 2-cell three-phase multicell converter with voltage source short-circuited*

$$\begin{aligned}
 I_{cda} = & -\frac{1}{3} \left\{ 2V_{\delta a} \int_{-\infty}^{\infty} \frac{|S_{da}(u)|^2}{Z(u)} du - V_{\delta b} \int_{-\infty}^{\infty} \frac{S_{db}(u)}{Z(u)} \overline{S_{da}(u)} du \right. \\
 & \left. - V_{\delta c} \int_{-\infty}^{\infty} \frac{S_{dc}(u)}{Z(u)} \overline{S_{da}(u)} du \right\} \quad (5.2)
 \end{aligned}$$

Since $I_{c_{da}}$ can be written as a first-order differential equation in the form $I_{c_{da}} = C_{da} \frac{dV_{\delta a}}{dt}$ we rewrite equation 5.2 as follows:

$$\begin{aligned} \frac{dV_{\delta a}}{dt} = & -\frac{1}{3C_{da}} \left\{ 2V_{\delta a} \int_{-\infty}^{\infty} \frac{|S_{da}(u)|^2}{Z(u)} du - V_{\delta b} \int_{-\infty}^{\infty} \frac{S_{db}(u)}{Z(u)} \overline{S_{da}(u)} du \right. \\ & \left. - V_{\delta c} \int_{-\infty}^{\infty} \frac{S_{dc}(u)}{Z(u)} \overline{S_{da}(u)} du \right\} \end{aligned} \quad (5.3)$$

Similarly for $I_{c_{db}} = C_{db} \frac{dV_{\delta b}}{dt}$ we have:

$$\begin{aligned} \frac{dV_{\delta b}}{dt} = & -\frac{1}{3C_{db}} \left\{ 2V_{\delta b} \int_{-\infty}^{\infty} \frac{|S_{db}(u)|^2}{Z(u)} du - V_{\delta a} \int_{-\infty}^{\infty} \frac{S_{da}(u)}{Z(u)} \overline{S_{db}(u)} du \right. \\ & \left. - V_{\delta c} \int_{-\infty}^{\infty} \frac{S_{dc}(u)}{Z(u)} \overline{S_{db}(u)} du \right\} \end{aligned} \quad (5.4)$$

and similarly for $I_{c_{dc}} = C_{dc} \frac{dV_{\delta c}}{dt}$ we have:

$$\begin{aligned} \frac{dV_{\delta c}}{dt} = & -\frac{1}{3C_{dc}} \left\{ 2V_{\delta c} \int_{-\infty}^{\infty} \frac{|S_{dc}(u)|^2}{Z(u)} du - V_{\delta a} \int_{-\infty}^{\infty} \frac{S_{da}(u)}{Z(u)} \overline{S_{dc}(u)} du \right. \\ & \left. - V_{\delta b} \int_{-\infty}^{\infty} \frac{S_{db}(u)}{Z(u)} \overline{S_{dc}(u)} du \right\} \end{aligned} \quad (5.5)$$

Since the functions in the equations 5.3, 5.4 and 5.5 are periodic we write it in terms of exponential fourier series as shown in matrix equation 5.6.

$$\begin{aligned} - \begin{bmatrix} 6C_{da} \frac{dV_{\delta a}}{dt} \\ 6C_{db} \frac{dV_{\delta b}}{dt} \\ 6C_{dc} \frac{dV_{\delta c}}{dt} \end{bmatrix} = & \begin{bmatrix} 2 \sum_{l=-\infty}^{\infty} \frac{|D_{al}|^2}{Z(l\omega_0)} \\ - \sum_{l=-\infty}^{\infty} \frac{|D_{al}|^2}{Z(l\omega_0)} e^{jl\frac{2\pi}{3}} \\ - \sum_{l=-\infty}^{\infty} \frac{|D_{al}|^2}{Z(l\omega_0)} e^{-jl\frac{2\pi}{3}} \end{bmatrix} V_{\delta a} + \begin{bmatrix} - \sum_{l=-\infty}^{\infty} \frac{|D_{al}|^2}{Z(l\omega_0)} e^{-jl\frac{2\pi}{3}} \\ 2 \sum_{l=-\infty}^{\infty} \frac{|D_{al}|^2}{Z(l\omega_0)} \\ - \sum_{l=-\infty}^{\infty} \frac{|D_{al}|^2}{Z(l\omega_0)} e^{jl\frac{2\pi}{3}} \end{bmatrix} V_{\delta b} \\ & + \begin{bmatrix} - \sum_{l=-\infty}^{\infty} \frac{|D_{al}|^2}{Z(l\omega_0)} e^{jl\frac{2\pi}{3}} \\ - \sum_{l=-\infty}^{\infty} \frac{|D_{al}|^2}{Z(l\omega_0)} e^{-jl\frac{2\pi}{3}} \\ 2 \sum_{l=-\infty}^{\infty} \frac{|D_{al}|^2}{Z(l\omega_0)} \end{bmatrix} V_{\delta c} \end{aligned} \quad (5.6)$$

Since $C_{da} = C_{db} = C_{dc} = C_d$ the above equation simplifies to:

$$-6C_d \begin{bmatrix} \frac{dV_{\delta a}}{dt} \\ \frac{dV_{\delta b}}{dt} \\ \frac{dV_{\delta c}}{dt} \end{bmatrix}$$

$$= \begin{bmatrix} 2 \sum_{l=-\infty}^{\infty} \frac{|D_{al}|^2}{Z(l\omega_0)} & - \sum_{l=-\infty}^{\infty} \frac{|D_{al}|^2}{Z(l\omega_0)} e^{-jl\frac{2\pi}{3}} & - \sum_{l=-\infty}^{\infty} \frac{|D_{al}|^2}{Z(l\omega_0)} e^{jl\frac{2\pi}{3}} \\ - \sum_{l=-\infty}^{\infty} \frac{|D_{al}|^2}{Z(l\omega_0)} e^{jl\frac{2\pi}{3}} & 2 \sum_{l=-\infty}^{\infty} \frac{|D_{al}|^2}{Z(l\omega_0)} & - \sum_{l=-\infty}^{\infty} \frac{|D_{al}|^2}{Z(l\omega_0)} e^{-jl\frac{2\pi}{3}} \\ - \sum_{l=-\infty}^{\infty} \frac{|D_{al}|^2}{Z(l\omega_0)} e^{-jl\frac{2\pi}{3}} & - \sum_{l=-\infty}^{\infty} \frac{|D_{al}|^2}{Z(l\omega_0)} e^{jl\frac{2\pi}{3}} & 2 \sum_{l=-\infty}^{\infty} \frac{|D_{al}|^2}{Z(l\omega_0)} \end{bmatrix} \quad (5.7)$$

Now writing $e^{-jl\frac{2\pi}{3}}$ and $e^{jl\frac{2\pi}{3}}$ into three classes as shown in Table 4.1 of section 4.2 and representing the matrices in terms of λ_1 , λ_2 and λ_3 which are defined in equations 4.17, 4.18 and 4.19 we obtain the following matrix:

$$-6C_d \begin{bmatrix} \frac{dV_{\delta a}}{dt} \\ \frac{dV_{\delta b}}{dt} \\ \frac{dV_{\delta c}}{dt} \end{bmatrix} = \begin{bmatrix} 2\lambda_1 + 2\lambda_2 + 2\lambda_3 & -\lambda_1 - \lambda_2 e^{-j\frac{2\pi}{3}} - \lambda_3 e^{j\frac{2\pi}{3}} & -\lambda_1 - \lambda_2 e^{j\frac{2\pi}{3}} - \lambda_3 e^{-j\frac{2\pi}{3}} \\ -\lambda_1 - \lambda_2 e^{j\frac{2\pi}{3}} - \lambda_3 e^{-j\frac{2\pi}{3}} & 2\lambda_1 + 2\lambda_2 + 2\lambda_3 & -\lambda_1 - \lambda_2 e^{-j\frac{2\pi}{3}} - \lambda_3 e^{j\frac{2\pi}{3}} \\ -\lambda_1 - \lambda_2 e^{-j\frac{2\pi}{3}} - \lambda_3 e^{j\frac{2\pi}{3}} & -\lambda_1 - \lambda_2 e^{j\frac{2\pi}{3}} - \lambda_3 e^{-j\frac{2\pi}{3}} & 2\lambda_1 + 2\lambda_2 + 2\lambda_3 \end{bmatrix} \begin{bmatrix} V_{\delta a} \\ V_{\delta b} \\ V_{\delta c} \end{bmatrix} \quad (5.8)$$

Which can be written as:

$$\dot{\mathbf{V}}_{\delta} = -\frac{1}{6C_d} \Lambda \mathbf{V}_{\delta} \quad (5.9)$$

where

$$\dot{\mathbf{V}}_{\delta} = \begin{bmatrix} \frac{dV_{\delta a}}{dt} \\ \frac{dV_{\delta b}}{dt} \\ \frac{dV_{\delta c}}{dt} \end{bmatrix}$$

$$\mathbf{V}_{\delta} = \begin{bmatrix} V_{\delta a} \\ V_{\delta b} \\ V_{\delta c} \end{bmatrix}$$

and

$$\Lambda = \begin{bmatrix} 2\lambda_1 + 2\lambda_2 + 2\lambda_3 & -\lambda_1 - \lambda_2 e^{-j\frac{2\pi}{3}} - \lambda_3 e^{j\frac{2\pi}{3}} & -\lambda_1 - \lambda_2 e^{j\frac{2\pi}{3}} - \lambda_3 e^{-j\frac{2\pi}{3}} \\ -\lambda_1 - \lambda_2 e^{j\frac{2\pi}{3}} - \lambda_3 e^{-j\frac{2\pi}{3}} & 2\lambda_1 + 2\lambda_2 + 2\lambda_3 & -\lambda_1 - \lambda_2 e^{-j\frac{2\pi}{3}} - \lambda_3 e^{j\frac{2\pi}{3}} \\ -\lambda_1 - \lambda_2 e^{-j\frac{2\pi}{3}} - \lambda_3 e^{j\frac{2\pi}{3}} & -\lambda_1 - \lambda_2 e^{j\frac{2\pi}{3}} - \lambda_3 e^{-j\frac{2\pi}{3}} & 2\lambda_1 + 2\lambda_2 + 2\lambda_3 \end{bmatrix}$$

The solution of equation 5.9 is given by:

$$\mathbf{V}_\delta = \mathbf{V}_{\delta 0} e^{-\frac{1}{6C_d}\Lambda t} \quad (5.10)$$

The eigenvalues of $-\frac{1}{6C_d}\Lambda$ were numerically calculated using the Maple package as follows:

$$\epsilon_1 = -\frac{\lambda_1 + \lambda_3}{2C_d} \quad (5.11)$$

$$\epsilon_2 = -\frac{\lambda_1 + \lambda_2}{2C_d} \quad (5.12)$$

$$\epsilon_3 = -\frac{\lambda_2 + \lambda_3}{2C_d} \quad (5.13)$$

From equation 5.1 the solution of equation 5.9 is yielded:

$$V_\delta = y_1 e^{\epsilon_1 t} + y_2 e^{\epsilon_2 t} + y_3 e^{\epsilon_3 t} \quad (5.14)$$

where y_1 , y_2 and y_3 are corresponding eigenvectors of ϵ_1 , ϵ_2 and ϵ_3 respectively.

Using the values λ_1 , λ_2 and λ_3 which are defined in equations 4.17, 4.18 and 4.19 the time constants are given by the following equations:

$$\begin{aligned} \tau_1 &= \frac{2C_d}{\lambda_1 + \lambda_3} \\ &= \frac{C_d}{\Re \left\{ \sum_{class 1} \frac{|D_{ai}|^2}{Z(l\omega_0)} \right\} + \Re \left\{ \sum_{class 3} \frac{|D_{ai}|^2}{Z(l\omega_0)} \right\}} \end{aligned} \quad (5.15)$$

$$\begin{aligned} \tau_2 &= \frac{2C_d}{\lambda_1 + \lambda_2} \\ &= \frac{C_d}{\Re \left\{ \sum_{class 1} \frac{|D_{ai}|^2}{Z(l\omega_0)} \right\} + \Re \left\{ \sum_{class 2} \frac{|D_{ai}|^2}{Z(l\omega_0)} \right\}} \end{aligned} \quad (5.16)$$

$$\begin{aligned} \tau_3 &= \frac{2C_d}{\lambda_2 + \lambda_3} \\ &= \frac{C_d}{\Re \left\{ \sum_{class 2} \frac{|D_{ai}|^2}{Z(l\omega_0)} \right\} + \Re \left\{ \sum_{class 3} \frac{|D_{ai}|^2}{Z(l\omega_0)} \right\}} \end{aligned} \quad (5.17)$$

From equations 5.15, 5.16 and 5.17 we observe that factors influencing the value of the time constants associated with the rebalancing of the capacitor voltages are:

1. The impedance of the output filter and load; and
2. The value of $|s_{da}(l\omega_0)|^2$, that is, the overlap of the spectra $s_{da}(l\omega_0)$ and $\overline{s_{da}(l\omega_0)}$.

Furthermore, the properties of these time constants as regards the balancing of the cell capacitor voltage are similar to those found for the single phase 2-cell multicell converter, that is:

- If $\lambda_1 + \lambda_3 = 0$, $\lambda_1 + \lambda_2 = 0$ and $\lambda_2 + \lambda_3 = 0$ then the time constants $\tau_1 \rightarrow \infty$, $\tau_2 \rightarrow \infty$ and $\tau_3 \rightarrow \infty$ which implies $-\frac{\Lambda t}{6C_d} \rightarrow 0$ and the cell capacitor imbalance $\mathbf{V}_\delta \rightarrow \mathbf{V}_{\delta 0}$, which implies that the cell capacitor voltage will not balance. This can only happen if the load impedance is purely imaginary, that is $\Re Z(l\omega_0) = 0$ or when $s_{da}(l\omega_0) = 0$.
- If $\lambda_1 + \lambda_3 = \infty$, $\lambda_1 + \lambda_2 = \infty$ and $\lambda_2 + \lambda_3 = \infty$ then the time constants $\tau_1 \rightarrow 0$, $\tau_2 \rightarrow 0$ and $\tau_3 \rightarrow 0$ which implies $-\frac{\Lambda t}{6C_d} \rightarrow -\infty$ and the cell capacitor imbalance $\mathbf{V}_\delta \rightarrow 0$. This implies that the cell capacitor will balance. Time constant $-\frac{6C_d}{\Lambda} \rightarrow 0$ implies an infinite cell capacitor current, which is impossible.
- If $0 < \lambda_1 + \lambda_3 < \infty$, $0 < \lambda_1 + \lambda_2 < \infty$ and $0 < \lambda_2 + \lambda_3 < \infty$ then the time constants τ_1 , τ_2 and τ_3 will be as defined in equations 5.15, 5.16 and 5.17 which implies that the cell capacitor will exponentially decay according to $\mathbf{V}_\delta = \mathbf{V}_{\delta 0} e^{-\frac{1}{6C_d}\Lambda t}$.

5.2.2 Simulations

To ensure the validity of the theory developed, this section compares the theoretical results obtained using equation 5.10 and the Matlab package with the simulated results of the practical converter using Ansoft Corporation, Simplorer package and FFT analysis. The simulation parameters for both 2-cell and 3-cell multicell converter are as follows:

Table 5.1: *Simulation parameters*

<i>DC – bus voltage</i>	V_t	100 V
<i>DC – bus capacitance</i>	C_d	40 μF
<i>Switching frequency</i>	f_s	6 kHz
<i>Modulation frequency</i>	f_1	50 Hz
<i>Filter inductance</i>	L	200 μH
<i>Filter capacitance</i>	C	50 μF
<i>Load resistance</i>	R	10 Ω

Taking the initial values of $V_{\delta a}$, $V_{\delta b}$ and $V_{\delta c}$ to be 25 V, -25 V and 0 V respectively we obtain the natural balancing of the cell capacitor voltages shown in Figures 5.2, 5.3 and 5.4 for the modulation index of 0.6, 0.8 and 1 respectively. The red curve indicates the exponential decay obtained using theory whilst the blue curve indicates the exponential decay obtained using simulation.

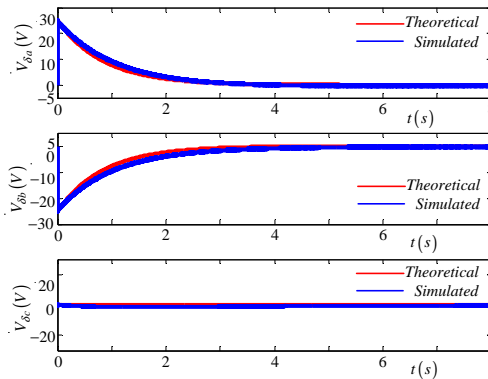


Figure 5.2: *Exponential decay of $V_{\delta a}$, $V_{\delta b}$ and $V_{\delta c}$ for modulation index of 0.6 without balancing circuit. The blue curve is obtained using Simplorer simulation and the red curve is obtained from theoretical results.*

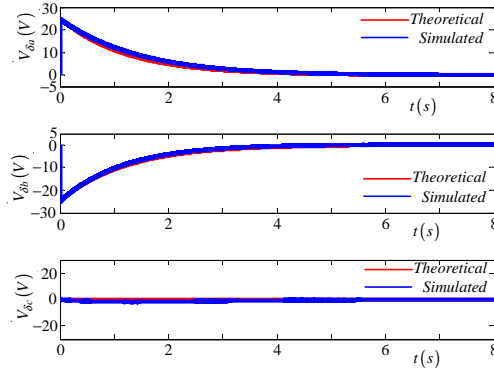


Figure 5.3: Exponential decay of $V_{\delta a}$, $V_{\delta b}$ and $V_{\delta c}$ for modulation index of 0.8 without balancing circuit. The blue curve is obtained using Simplorer simulation and the red curve is obtained from theoretical results.

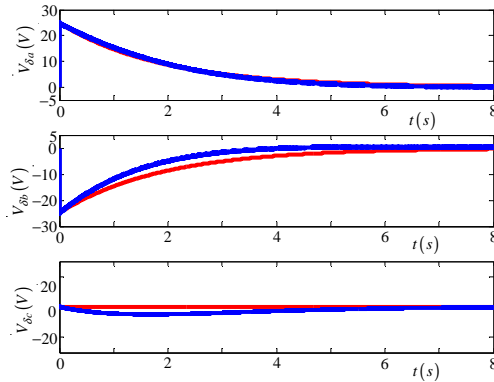
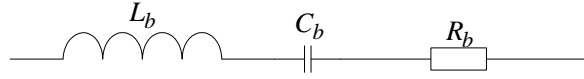
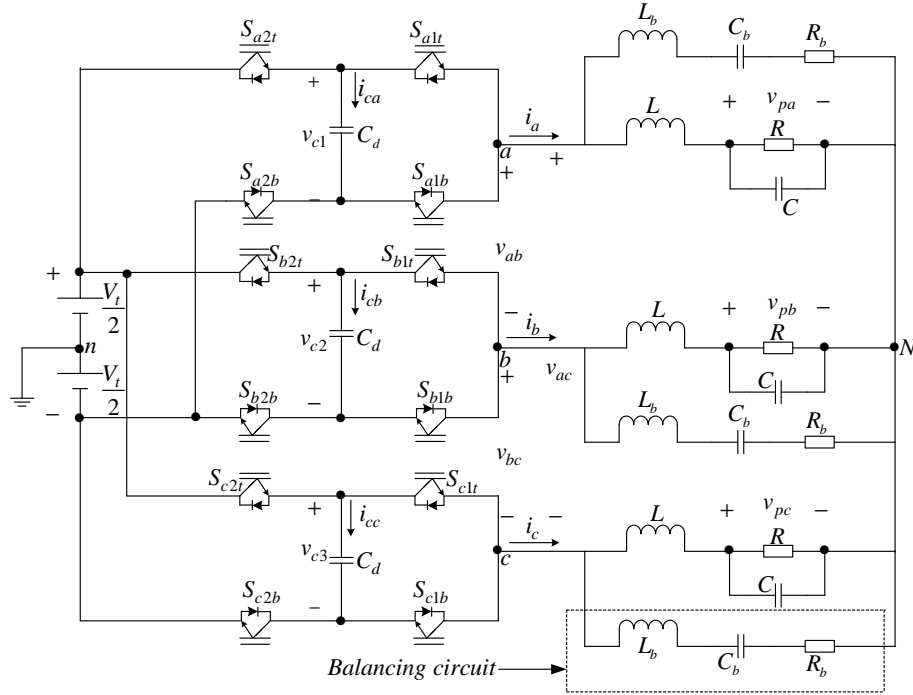


Figure 5.4: Exponential decay of $V_{\delta a}$, $V_{\delta b}$ and $V_{\delta c}$ for modulation index of 1 without balancing circuit. The blue curve is obtained using Simplorer simulation and the red curve is obtained from theoretical results

From equations 5.10, 5.15, 5.16 and 5.17 one of the factors that affect the balancing of the capacitor voltages is the impedance of the output filter and load. Decreasing the load impedance is done by connecting the balancing circuit at the frequency where the largest component of harmonics of S_{da} occurs, that is, in this case at the switching frequency. Figure 5.5 illustrates the balancing circuit that acts as a band-pass filter providing a low impedance at the switching frequency whilst Figure 5.6 shows the balancing circuit connected to the 2-cell multicell converter.


Figure 5.5: *Balancing circuit*

Figure 5.6: *2-cell multicell converter with a balancing circuit connected*

The impedance $Z(s)$ is given by

$$Z(s) = Ls + \frac{1}{sC} + R$$

and

$$\begin{aligned} Z(j\omega) &= j\omega L + \frac{1}{j\omega C} + R \\ &= j\omega L - \frac{j}{\omega C} + R \end{aligned}$$

Hence

$$|Z(j\omega)| = \sqrt{\left(L\omega - \frac{1}{\omega C}\right)^2 + R^2}$$

The minimum magnitude of $|Z(j\omega)|$ is given by

$$\begin{aligned} Z_{min} &= |Z(j\omega_0)| \\ &= \sqrt{\left(L\omega_0 - \frac{1}{\omega_0 C}\right)^2 + R^2} \end{aligned}$$

Since $\omega_0 = \frac{1}{\sqrt{LC}}$

$$\begin{aligned} Z_{min} &= \sqrt{R^2} \\ &= R \end{aligned}$$

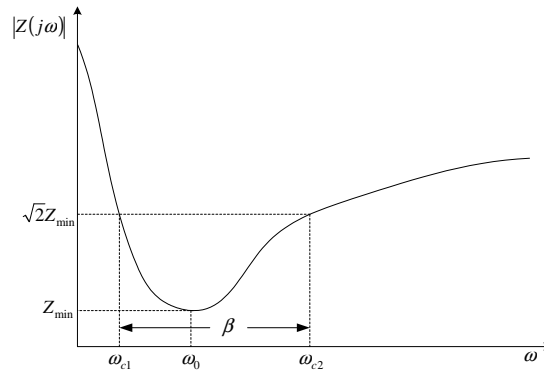


Figure 5.7: *The frequency response plot for the RLC balance booster circuit*

Figure 5.7 shows the frequency response plot for the RLC balance booster circuit. At the cut-off frequencies, the magnitude of the transfer function is $\sqrt{2}H_{min} = \sqrt{2}R$.

Solving for ω_c yields

$$\sqrt{2}R = \sqrt{\left(L\omega_c - \frac{1}{\omega_c C}\right)^2 + R^2}$$

$$\omega_c = -\frac{R}{2L} \pm \sqrt{\left(\frac{R}{2L}\right)^2 + \frac{1}{LC}}$$

or

$$\omega_c = \frac{R}{2L} \pm \sqrt{\left(\frac{R}{2L}\right)^2 + \frac{1}{LC}}$$

Taking only the positive values we have

$$\omega_{c1} = -\frac{R}{2L} + \sqrt{\left(\frac{R}{2L}\right)^2 + \frac{1}{LC}}$$

$$\omega_{c2} = \frac{R}{2L} + \sqrt{\left(\frac{R}{2L}\right)^2 + \frac{1}{LC}}$$

Bandwidth(β), which is the width of the passband, is given by

$$\begin{aligned}\beta &= \omega_{c1} - \omega_{c2} \\ &= \left(\frac{R}{2L} + \sqrt{\left(\frac{R}{2L}\right)^2 + \frac{1}{LC}} \right) - \left(-\frac{R}{2L} + \sqrt{\left(\frac{R}{2L}\right)^2 + \frac{1}{LC}} \right) \\ &= \frac{R}{L}\end{aligned}$$

Quality factor(Q), which is the ratio of the centre frequency to the bandwidth, is given by

$$\begin{aligned}Q &= \frac{\omega_0}{\beta} \\ &= \frac{1}{\frac{R}{L}} \\ &= \sqrt{\frac{L}{R^2C}}\end{aligned}$$

Let Q_1, Q_2, Q_3, Q_4 and Q_5 be quality factors such that

$$Q_1 > Q_2 > Q_3 > Q_4 > Q_5$$

Then Figure 5.8 shows the effect of the quality factor. This shows that the smaller quality factor corresponds to the larger bandwidth and conversely.

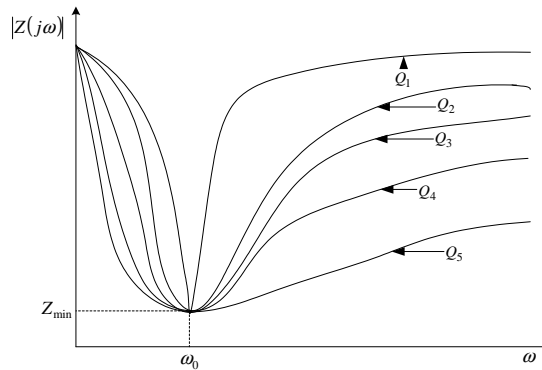


Figure 5.8: *Effect of the quality factor*

For the parameters of this balancing circuit, we assume that its resistance R_b is 2.2Ω and its capacitance C_b is $4.3 \mu F$. Thus we will have

$$\begin{aligned}\omega_0 &= \frac{1}{\sqrt{L_b C_b}} \\ 2\pi \times (6 \text{ kHz}) &= \frac{1}{\sqrt{L_b C_b}}\end{aligned}\tag{5.18}$$

Hence the balancing circuit inductance is given by:

$$\begin{aligned} L_b &= \left(\frac{1}{2\pi \times (6 \text{ kHz})} \right) \times \left(\frac{1}{4.3 \mu\text{F}} \right) \\ &= 163.632 \mu\text{H} \end{aligned} \quad (5.19)$$

The natural balancing of the cell capacitor voltages of the 2-cell multicell converter with a balancing circuit connected is shown in Figures 5.9, 5.10 and 5.11 for modulation indices of 0.6, 0.8 and 1 respectively. The red curve indicates the exponential decay obtained using theory whilst the blue curve indicates the exponential decay obtained using simulation. From these figures it can be observed that when the balancing booster is connected the capacitor voltages balance faster.

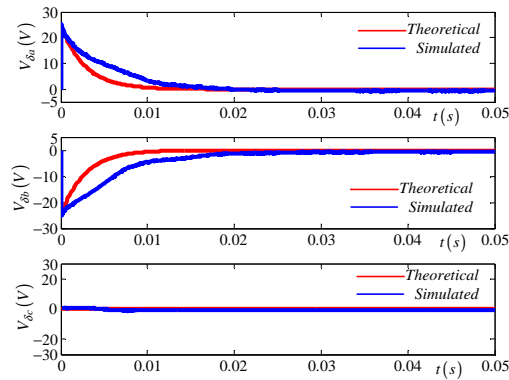


Figure 5.9: Exponential decay of $V_{\delta a}$, $V_{\delta b}$ and $V_{\delta c}$ for modulation index of 0.6 with balancing circuit. The blue curve is obtained using Simplorer simulation and the red curve is obtained from theoretical results

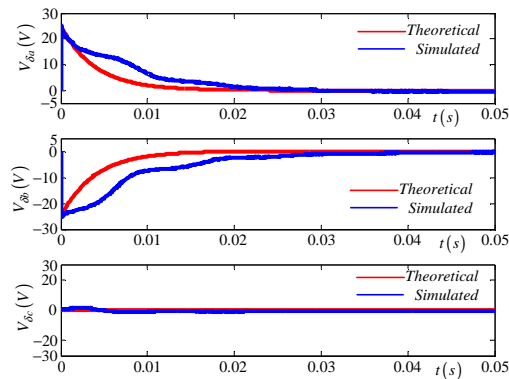


Figure 5.10: Exponential decay of $V_{\delta a}$, $V_{\delta b}$ and $V_{\delta c}$ for modulation index of 0.8 with balancing circuit. The blue curve is obtained using Simplorer simulation and the red curve is obtained from theoretical results

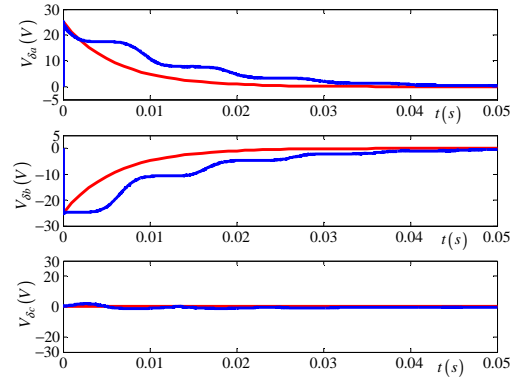


Figure 5.11: Exponential decay of $V_{\delta a}$, $V_{\delta b}$ and $V_{\delta c}$ for modulation index of 1 with balancing circuit. The blue curve is obtained using Simpler simulation and the red curve is obtained from theoretical results

5.3 3-Cell Multicell Converter

5.3.1 Time constant

Exponential decay is associated with the DC currents I_{cda1} , I_{cda2} , I_{cdb1} , I_{cdb2} , I_{cdc1} and I_{cdc2} . Referring to the equivalent circuit of the 3-cell 3-phase multicell converter given in Figure 3.8, the change in the capacitor voltage of C_{da1} , C_{da2} , C_{db1} , C_{db2} , C_{dc1} and C_{dc2} is slow; hence the state of the circuit can be taken as steady. Using the assumption that $V_t = 0$, implies that we short-circuit voltage source $\frac{V_t}{3}$ in the equivalent circuit to obtain $V_t = 0$. The resulting circuit is depicted in Figure 5.12.

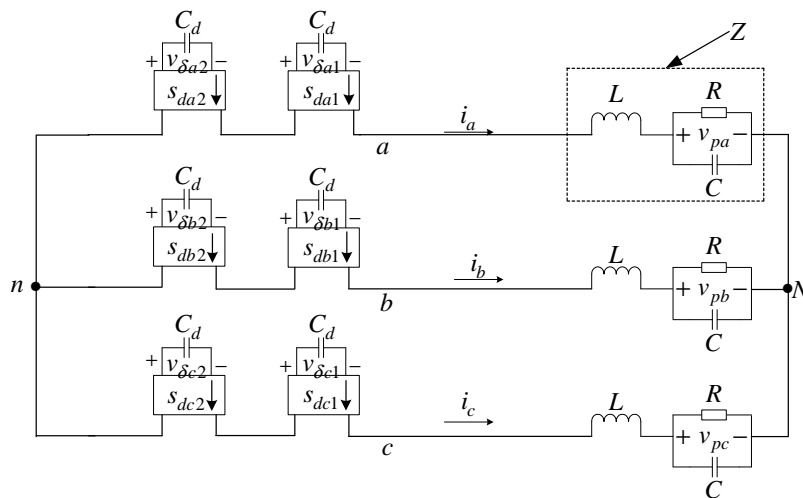


Figure 5.12: Equivalent circuit of 3-cell three-phase multicell converter with voltage source short-circuited

We now use the same reasoning as in subsection 5.2.1.

We thus rewrite equation 4.35 as follows:

$$\begin{aligned} \frac{dV_{\delta a1}}{dt} = & -\frac{1}{3C_{da1}} \left\{ 2V_{\delta a1} \int_{-\infty}^{\infty} \frac{S_{da1}(u)}{Z(u)} \overline{S_{da1}(u)} du + 2V_{\delta a2} \int_{-\infty}^{\infty} \frac{S_{da2}(u)}{Z(u)} \overline{S_{da1}(u)} du \right. \\ & - V_{\delta b1} \int_{-\infty}^{\infty} \frac{S_{db1}(u)}{Z(u)} \overline{S_{da1}(u)} du - V_{\delta b2} \int_{-\infty}^{\infty} \frac{S_{db2}(u)}{Z(u)} \overline{S_{da1}(u)} du \\ & \left. - V_{\delta c1} \int_{-\infty}^{\infty} \frac{S_{dc1}(u)}{Z(u)} \overline{S_{da1}(u)} du - V_{\delta c2} \int_{-\infty}^{\infty} \frac{S_{dc2}(u)}{Z(u)} \overline{S_{da1}(u)} du \right\} \end{aligned} \quad (5.20)$$

Similarly for $I_{c_{da2}} = C_{da2} \frac{dV_{\delta a2}}{dt}$ we have:

$$\begin{aligned} \frac{dV_{\delta a2}}{dt} = & -\frac{1}{3C_{da2}} \left\{ 2V_{\delta a1} \int_{-\infty}^{\infty} \frac{S_{da1}(u)}{Z(u)} \overline{S_{da2}(u)} du + 2V_{\delta a2} \int_{-\infty}^{\infty} \frac{S_{da2}(u)}{Z(u)} \overline{S_{da2}(u)} du \right. \\ & - V_{\delta b1} \int_{-\infty}^{\infty} \frac{S_{db1}(u)}{Z(u)} \overline{S_{da2}(u)} du - V_{\delta b2} \int_{-\infty}^{\infty} \frac{S_{db2}(u)}{Z(u)} \overline{S_{da2}(u)} du \\ & \left. - V_{\delta c1} \int_{-\infty}^{\infty} \frac{S_{dc1}(u)}{Z(u)} \overline{S_{da2}(u)} du - V_{\delta c2} \int_{-\infty}^{\infty} \frac{S_{dc2}(u)}{Z(u)} \overline{S_{da2}(u)} du \right\} \end{aligned} \quad (5.21)$$

Similarly for $I_{c_{ab1}} = C_{db1} \frac{dV_{\delta b1}}{dt}$ we have:

$$\begin{aligned} \frac{dV_{\delta b1}}{dt} = & -\frac{1}{3C_{db1}} \left\{ 2V_{\delta b1} \int_{-\infty}^{\infty} \frac{S_{db1}(u)}{Z(u)} \overline{S_{db1}(u)} du + 2V_{\delta b2} \int_{-\infty}^{\infty} \frac{S_{db2}(u)}{Z(u)} \overline{S_{db1}(u)} du \right. \\ & - V_{\delta a1} \int_{-\infty}^{\infty} \frac{S_{da1}(u)}{Z(u)} \overline{S_{db1}(u)} du - V_{\delta a2} \int_{-\infty}^{\infty} \frac{S_{da2}(u)}{Z(u)} \overline{S_{db1}(u)} du \\ & \left. - V_{\delta c1} \int_{-\infty}^{\infty} \frac{S_{dc1}(u)}{Z(u)} \overline{S_{db1}(u)} du - V_{\delta c2} \int_{-\infty}^{\infty} \frac{S_{dc2}(u)}{Z(u)} \overline{S_{db1}(u)} du \right\} \end{aligned} \quad (5.22)$$

Similarly for $I_{c_{ab2}} = C_{db2} \frac{dV_{\delta b2}}{dt}$ we have:

$$\begin{aligned} \frac{dV_{\delta b2}}{dt} = & -\frac{1}{3C_{db2}} \left\{ 2V_{\delta b1} \int_{-\infty}^{\infty} \frac{S_{db1}(u)}{Z(u)} \overline{S_{db2}(u)} du + 2V_{\delta b2} \int_{-\infty}^{\infty} \frac{S_{db2}(u)}{Z(u)} \overline{S_{db2}(u)} du \right. \\ & - V_{\delta a1} \int_{-\infty}^{\infty} \frac{S_{da1}(u)}{Z(u)} \overline{S_{db2}(u)} du - V_{\delta a2} \int_{-\infty}^{\infty} \frac{S_{da2}(u)}{Z(u)} \overline{S_{db2}(u)} du \\ & \left. - V_{\delta c1} \int_{-\infty}^{\infty} \frac{S_{dc1}(u)}{Z(u)} \overline{S_{db2}(u)} du - V_{\delta c2} \int_{-\infty}^{\infty} \frac{S_{dc2}(u)}{Z(u)} \overline{S_{db2}(u)} du \right\} \end{aligned} \quad (5.23)$$

Similarly for $I_{c_{dc1}} = C_{dc1} \frac{dV_{\delta c1}}{dt}$ we have:

$$\frac{dV_{\delta c1}}{dt} = -\frac{1}{3C_{dc1}} \left\{ 2V_{\delta c1} \int_{-\infty}^{\infty} \frac{S_{dc1}(u)}{Z(u)} \overline{S_{dc1}(u)} du + 2V_{\delta c2} \int_{-\infty}^{\infty} \frac{S_{dc2}(u)}{Z(u)} \overline{S_{dc1}(u)} du \right.$$

$$\begin{aligned}
& -V_{\delta a1} \int_{-\infty}^{\infty} \frac{S_{da1}(u)}{Z(u)} \overline{S_{dc1}(u)} du - V_{\delta a2} \int_{-\infty}^{\infty} \frac{S_{da2}(u)}{Z(u)} \overline{S_{dc1}(u)} du \\
& -V_{\delta b1} \int_{-\infty}^{\infty} \frac{S_{db1}(u)}{Z(u)} \overline{S_{dc1}(u)} du - V_{\delta b2} \int_{-\infty}^{\infty} \frac{S_{db2}(u)}{Z(u)} \overline{S_{dc1}(u)} du \} \quad (5.24)
\end{aligned}$$

Similarly for $I_{c_{dc2}} = C_{dc2} \frac{dV_{\delta c2}}{dt}$ we have:

$$\begin{aligned}
\frac{dV_{\delta c2}}{dt} &= -\frac{1}{3C_{dc2}} \left\{ 2V_{\delta c1} \int_{-\infty}^{\infty} \frac{S_{dc1}(u)}{Z(u)} \overline{S_{dc2}(u)} du + 2V_{\delta c2} \int_{-\infty}^{\infty} \frac{S_{dc2}(u)}{Z(u)} \overline{S_{dc2}(u)} du \right. \\
& -V_{\delta a1} \int_{-\infty}^{\infty} \frac{S_{da1}(u)}{Z(u)} \overline{S_{dc2}(u)} du - V_{\delta a2} \int_{-\infty}^{\infty} \frac{S_{da2}(u)}{Z(u)} \overline{S_{dc2}(u)} du \\
& \left. -V_{\delta b1} \int_{-\infty}^{\infty} \frac{S_{db1}(u)}{Z(u)} \overline{S_{dc2}(u)} du - V_{\delta b2} \int_{-\infty}^{\infty} \frac{S_{db2}(u)}{Z(u)} \overline{S_{dc2}(u)} du \right\} \quad (5.25)
\end{aligned}$$

Since the functions in the equations 5.20, 5.21, 5.22, 5.23, 5.24 and 5.25 are periodic we write it in terms of exponential fourier series as shown in matrix equation 5.26.

$$\begin{aligned}
& - \begin{bmatrix} 6C_{da1} \frac{dV_{\delta a1}}{dt} \\ 6C_{da2} \frac{dV_{\delta a2}}{dt} \\ 6C_{db1} \frac{dV_{\delta b1}}{dt} \\ 6C_{db2} \frac{dV_{\delta b2}}{dt} \\ 6C_{dc1} \frac{dV_{\delta c1}}{dt} \\ 6C_{dc2} \frac{dV_{\delta c2}}{dt} \end{bmatrix} \\
& = \begin{bmatrix} 2 \sum_{l=-\infty}^{\infty} \frac{|D_{a1l}|^2}{Z(l\omega_0)} \\ 2 \sum_{l=-\infty}^{\infty} \frac{|D_{a1l}|^2 e^{-jl \frac{2\pi}{3}}}{Z(l\omega_0)} \\ - \sum_{l=-\infty}^{\infty} \frac{|D_{a1l}|^2 e^{jl \frac{2\pi}{3}}}{Z(l\omega_0)} \\ - \sum_{l=-\infty}^{\infty} \frac{|D_{a1l}|^2}{Z(l\omega_0)} \\ - \sum_{l=-\infty}^{\infty} \frac{|D_{a1l}|^2 e^{-jl \frac{2\pi}{3}}}{Z(l\omega_0)} \\ - \sum_{l=-\infty}^{\infty} \frac{|D_{a1l}|^2 e^{jl \frac{2\pi}{3}}}{Z(l\omega_0)} \end{bmatrix} V_{\delta a1} + \begin{bmatrix} 2 \sum_{l=-\infty}^{\infty} \frac{|D_{a1l}|^2 e^{jl \frac{2\pi}{3}}}{Z(l\omega_0)} \\ 2 \sum_{l=-\infty}^{\infty} \frac{|D_{a1l}|^2}{Z(l\omega_0)} \\ - \sum_{l=-\infty}^{\infty} \frac{|D_{a1l}|^2 e^{-jl \frac{2\pi}{3}}}{Z(l\omega_0)} \\ - \sum_{l=-\infty}^{\infty} \frac{|D_{a1l}|^2 e^{jl \frac{2\pi}{3}}}{Z(l\omega_0)} \\ - \sum_{l=-\infty}^{\infty} \frac{|D_{a1l}|^2}{Z(l\omega_0)} \\ - \sum_{l=-\infty}^{\infty} \frac{|D_{a1l}|^2 e^{-jl \frac{2\pi}{3}}}{Z(l\omega_0)} \end{bmatrix} V_{\delta a2}
\end{aligned}$$

$$\begin{aligned}
 & + \left[\begin{array}{c} -\sum_{l=-\infty}^{\infty} \frac{|D_{a1l}|^2 e^{-jl\frac{2\pi}{3}}}{Z(l\omega_0)} \\ -\sum_{l=-\infty}^{\infty} \frac{|D_{a1l}|^2 e^{jl\frac{2\pi}{3}}}{Z(l\omega_0)} \\ 2\sum_{l=-\infty}^{\infty} \frac{|D_{a1l}|^2}{Z(l\omega_0)} \\ 2\sum_{l=-\infty}^{\infty} \frac{|D_{a1l}|^2 e^{-jl\frac{2\pi}{3}}}{Z(l\omega_0)} \\ -\sum_{l=-\infty}^{\infty} \frac{|D_{a1l}|^2 e^{jl\frac{2\pi}{3}}}{Z(l\omega_0)} \\ -\sum_{l=-\infty}^{\infty} \frac{|D_{a1l}|^2}{Z(l\omega_0)} \end{array} \right] V_{\delta b1} + \left[\begin{array}{c} -\sum_{l=-\infty}^{\infty} \frac{|D_{a1l}|^2}{Z(l\omega_0)} \\ -\sum_{l=-\infty}^{\infty} \frac{|D_{a1l}|^2 e^{-jl\frac{2\pi}{3}}}{Z(l\omega_0)} \\ 2\sum_{l=-\infty}^{\infty} \frac{|D_{a1l}|^2 e^{jl\frac{2\pi}{3}}}{Z(l\omega_0)} \\ 2\sum_{l=-\infty}^{\infty} \frac{|D_{a1l}|^2}{Z(l\omega_0)} \\ -\sum_{l=-\infty}^{\infty} \frac{|D_{a1l}|^2 e^{-jl\frac{2\pi}{3}}}{Z(l\omega_0)} \\ -\sum_{l=-\infty}^{\infty} \frac{|D_{a1l}|^2 e^{jl\frac{2\pi}{3}}}{Z(l\omega_0)} \end{array} \right] V_{\delta b2} \\
 & + \left[\begin{array}{c} -\sum_{l=-\infty}^{\infty} \frac{|D_{a1l}|^2 e^{jl\frac{2\pi}{3}}}{Z(l\omega_0)} \\ -\sum_{l=-\infty}^{\infty} \frac{|D_{a1l}|^2}{Z(l\omega_0)} \\ -\sum_{l=-\infty}^{\infty} \frac{|D_{a1l}|^2 e^{-jl\frac{2\pi}{3}}}{Z(l\omega_0)} \\ -\sum_{l=-\infty}^{\infty} \frac{|D_{a1l}|^2 e^{jl\frac{2\pi}{3}}}{Z(l\omega_0)} \\ 2\sum_{l=-\infty}^{\infty} \frac{|D_{a1l}|^2}{Z(l\omega_0)} \\ 2\sum_{l=-\infty}^{\infty} \frac{|D_{a1l}|^2 e^{-jl\frac{2\pi}{3}}}{Z(l\omega_0)} \end{array} \right] V_{\delta c1} + \left[\begin{array}{c} -\sum_{l=-\infty}^{\infty} \frac{|D_{a1l}|^2 e^{-jl\frac{2\pi}{3}}}{Z(l\omega_0)} \\ -\sum_{l=-\infty}^{\infty} \frac{|D_{a1l}|^2 e^{jl\frac{2\pi}{3}}}{Z(l\omega_0)} \\ -\sum_{l=-\infty}^{\infty} \frac{|D_{a1l}|^2}{Z(l\omega_0)} \\ -\sum_{l=-\infty}^{\infty} \frac{|D_{a1l}|^2 e^{-jl\frac{2\pi}{3}}}{Z(l\omega_0)} \\ 2\sum_{l=-\infty}^{\infty} \frac{|D_{a1l}|^2 e^{jl\frac{2\pi}{3}}}{Z(l\omega_0)} \\ 2\sum_{l=-\infty}^{\infty} \frac{|D_{a1l}|^2}{Z(l\omega_0)} \end{array} \right] V_{\delta c2}
 \end{aligned} \tag{5.26}$$

Now substituting λ_1 and λ_2, λ_3 into matrix equation 5.26 we obtain matrix equation 5.27:

$$\begin{aligned}
& - \begin{bmatrix} 6C_{da1} \frac{dV_{\delta a1}}{dt} \\ 6C_{da2} \frac{dV_{\delta a2}}{dt} \\ 6C_{db1} \frac{dV_{\delta b1}}{dt} \\ 6C_{db2} \frac{dV_{\delta b2}}{dt} \\ 6C_{dc1} \frac{dV_{\delta c1}}{dt} \\ 6C_{dc2} \frac{dV_{\delta c2}}{dt} \end{bmatrix} \\
= & \left\{ \begin{bmatrix} 2\lambda_1 & 2\lambda_1 & -\lambda_1 & -\lambda_1 & -\lambda_1 & -\lambda_1 \\ 2\lambda_1 & 2\lambda_1 & -\lambda_1 & -\lambda_1 & -\lambda_1 & -\lambda_1 \\ -\lambda_1 & -\lambda_1 & 2\lambda_1 & 2\lambda_1 & -\lambda_1 & -\lambda_1 \\ -\lambda_1 & -\lambda_1 & 2\lambda_1 & 2\lambda_1 & -\lambda_1 & -\lambda_1 \\ -\lambda_1 & -\lambda_1 & -\lambda_1 & -\lambda_1 & 2\lambda_1 & 2\lambda_1 \\ -\lambda_1 & -\lambda_1 & -\lambda_1 & -\lambda_1 & 2\lambda_1 & 2\lambda_1 \end{bmatrix} \right. \\
& + \begin{bmatrix} 2\lambda_2 & 2\lambda_2 e^{j\frac{2\pi}{3}} & -\lambda_2 e^{-j\frac{2\pi}{3}} & -\lambda_2 & -\lambda_2 e^{j\frac{2\pi}{3}} & -\lambda_2 e^{-j\frac{2\pi}{3}} \\ 2\lambda_2 e^{-j\frac{2\pi}{3}} & 2\lambda_2 & -\lambda_2 e^{j\frac{2\pi}{3}} & -\lambda_2 e^{-j\frac{2\pi}{3}} & -\lambda_2 & -\lambda_2 e^{j\frac{2\pi}{3}} \\ -\lambda_2 e^{j\frac{2\pi}{3}} & -\lambda_2 e^{-j\frac{2\pi}{3}} & 2\lambda_2 & 2\lambda_2 e^{j\frac{2\pi}{3}} & -\lambda_2 e^{-j\frac{2\pi}{3}} & -\lambda_2 \\ -\lambda_2 & -\lambda_2 e^{j\frac{2\pi}{3}} & 2\lambda_2 e^{-j\frac{2\pi}{3}} & 2\lambda_2 & -\lambda_2 e^{j\frac{2\pi}{3}} & -\lambda_2 e^{-j\frac{2\pi}{3}} \\ -\lambda_2 e^{-j\frac{2\pi}{3}} & -\lambda_2 & -\lambda_2 e^{j\frac{2\pi}{3}} & -\lambda_2 e^{-j\frac{2\pi}{3}} & 2\lambda_2 & 2\lambda_2 e^{j\frac{2\pi}{3}} \\ -\lambda_2 e^{j\frac{2\pi}{3}} & -\lambda_2 e^{-j\frac{2\pi}{3}} & -\lambda_2 & -\lambda_2 e^{j\frac{2\pi}{3}} & 2\lambda_2 e^{-j\frac{2\pi}{3}} & 2\lambda_2 \end{bmatrix}
\end{aligned}$$

$$+ \begin{bmatrix} 2\lambda_3 & 2\lambda_3 e^{-j\frac{2\pi}{3}} & -\lambda_3 e^{j\frac{2\pi}{3}} & -\lambda_3 & -\lambda_3 e^{-j\frac{2\pi}{3}} & -\lambda_3 e^{j\frac{2\pi}{3}} \\ 2\lambda_3 e^{j\frac{2\pi}{3}} & 2\lambda_3 & -\lambda_3 e^{-j\frac{2\pi}{3}} & -\lambda_3 e^{j\frac{2\pi}{3}} & -\lambda_3 & -\lambda_3 e^{-j\frac{2\pi}{3}} \\ -\lambda_3 e^{-j\frac{2\pi}{3}} & -\lambda_3 e^{j\frac{2\pi}{3}} & 2\lambda_3 & 2\lambda_3 e^{-j\frac{2\pi}{3}} & -\lambda_3 e^{j\frac{2\pi}{3}} & -\lambda_3 \\ -\lambda_3 & -\lambda_3 e^{-j\frac{2\pi}{3}} & 2\lambda_3 e^{j\frac{2\pi}{3}} & 2\lambda_3 & -\lambda_3 e^{-j\frac{2\pi}{3}} & -\lambda_3 e^{j\frac{2\pi}{3}} \\ -\lambda_3 e^{j\frac{2\pi}{3}} & -\lambda_3 & -\lambda_3 e^{-j\frac{2\pi}{3}} & -\lambda_3 e^{j\frac{2\pi}{3}} & 2\lambda_3 & 2\lambda_3 e^{-j\frac{2\pi}{3}} \\ -\lambda_3 e^{-j\frac{2\pi}{3}} & -\lambda_3 e^{j\frac{2\pi}{3}} & -\lambda_3 & -\lambda_3 e^{-j\frac{2\pi}{3}} & 2\lambda_3 e^{j\frac{2\pi}{3}} & 2\lambda_3 \end{bmatrix} \begin{bmatrix} V_{\delta a1} \\ V_{\delta a2} \\ V_{\delta b1} \\ V_{\delta b2} \\ V_{\delta c1} \\ V_{\delta c2} \end{bmatrix} \quad (5.27)$$

which can be written as equation 5.28 since $C_{da1} = C_{da2} = C_{db1} = C_{db2} = C_{dc1} = C_{dc2} = C_d$:

$$\dot{\mathbf{V}}_{\delta} = -\frac{1}{6C_d} \Lambda \mathbf{V}_{\delta} \quad (5.28)$$

where

$$\dot{\mathbf{V}}_{\delta} = \begin{bmatrix} \frac{dV_{\delta a1}}{dt} \\ \frac{dV_{\delta a2}}{dt} \\ \frac{dV_{\delta b1}}{dt} \\ \frac{dV_{\delta b2}}{dt} \\ \frac{dV_{\delta c1}}{dt} \\ \frac{dV_{\delta c2}}{dt} \end{bmatrix}$$

$$\mathbf{V}_\delta = \begin{bmatrix} V_{\delta a1} \\ V_{\delta a2} \\ V_{\delta b1} \\ V_{\delta b2} \\ V_{\delta c1} \\ V_{\delta c2} \end{bmatrix}$$

and

$$\Lambda = \begin{bmatrix} 2\lambda_1 & 2\lambda_1 & -\lambda_1 & -\lambda_1 & -\lambda_1 & -\lambda_1 \\ 2\lambda_1 & 2\lambda_1 & -\lambda_1 & -\lambda_1 & -\lambda_1 & -\lambda_1 \\ -\lambda_1 & -\lambda_1 & 2\lambda_1 & 2\lambda_1 & -\lambda_1 & -\lambda_1 \\ -\lambda_1 & -\lambda_1 & 2\lambda_1 & 2\lambda_1 & -\lambda_1 & -\lambda_1 \\ -\lambda_1 & -\lambda_1 & -\lambda_1 & -\lambda_1 & 2\lambda_1 & 2\lambda_1 \\ -\lambda_1 & -\lambda_1 & -\lambda_1 & -\lambda_1 & 2\lambda_1 & 2\lambda_1 \end{bmatrix}$$

$$+ \begin{bmatrix} 2\lambda_2 & 2\lambda_2 e^{j\frac{2\pi}{3}} & -\lambda_2 e^{-j\frac{2\pi}{3}} & -\lambda_2 & -\lambda_2 e^{j\frac{2\pi}{3}} & -\lambda_2 e^{-j\frac{2\pi}{3}} \\ 2\lambda_2 e^{-j\frac{2\pi}{3}} & 2\lambda_2 & -\lambda_2 e^{j\frac{2\pi}{3}} & -\lambda_2 e^{-j\frac{2\pi}{3}} & -\lambda_2 & -\lambda_2 e^{j\frac{2\pi}{3}} \\ -\lambda_2 e^{j\frac{2\pi}{3}} & -\lambda_2 e^{-j\frac{2\pi}{3}} & 2\lambda_2 & 2\lambda_2 e^{j\frac{2\pi}{3}} & -\lambda_2 e^{-j\frac{2\pi}{3}} & -\lambda_2 \\ -\lambda_2 & -\lambda_2 e^{j\frac{2\pi}{3}} & 2\lambda_2 e^{-j\frac{2\pi}{3}} & 2\lambda_2 & -\lambda_2 e^{j\frac{2\pi}{3}} & -\lambda_2 e^{-j\frac{2\pi}{3}} \\ -\lambda_2 e^{-j\frac{2\pi}{3}} & -\lambda_2 & -\lambda_2 e^{j\frac{2\pi}{3}} & -\lambda_2 e^{-j\frac{2\pi}{3}} & 2\lambda_2 & 2\lambda_2 e^{j\frac{2\pi}{3}} \\ -\lambda_2 e^{j\frac{2\pi}{3}} & -\lambda_2 e^{-j\frac{2\pi}{3}} & -\lambda_2 & -\lambda_2 e^{j\frac{2\pi}{3}} & 2\lambda_2 e^{-j\frac{2\pi}{3}} & 2\lambda_2 \end{bmatrix}$$

$$+ \left[\begin{array}{cccccc}
2\lambda_3 & 2\lambda_3 e^{-j\frac{2\pi}{3}} & -\lambda_3 e^{j\frac{2\pi}{3}} & -\lambda_3 & -\lambda_3 e^{-j\frac{2\pi}{3}} & -\lambda_3 e^{j\frac{2\pi}{3}} \\
2\lambda_3 e^{j\frac{2\pi}{3}} & 2\lambda_3 & -\lambda_3 e^{-j\frac{2\pi}{3}} & -\lambda_3 e^{j\frac{2\pi}{3}} & -\lambda_3 & -\lambda_3 e^{-j\frac{2\pi}{3}} \\
-\lambda_3 e^{-j\frac{2\pi}{3}} & -\lambda_3 e^{j\frac{2\pi}{3}} & 2\lambda_3 & 2\lambda_3 e^{-j\frac{2\pi}{3}} & -\lambda_3 e^{j\frac{2\pi}{3}} & -\lambda_3 \\
-\lambda_3 & -\lambda_3 e^{-j\frac{2\pi}{3}} & 2\lambda_3 e^{j\frac{2\pi}{3}} & 2\lambda_3 & -\lambda_3 e^{-j\frac{2\pi}{3}} & -\lambda_3 e^{j\frac{2\pi}{3}} \\
-\lambda_3 e^{j\frac{2\pi}{3}} & -\lambda_3 & -\lambda_3 e^{-j\frac{2\pi}{3}} & -\lambda_3 e^{j\frac{2\pi}{3}} & 2\lambda_3 & 2\lambda_3 e^{-j\frac{2\pi}{3}} \\
-\lambda_3 e^{-j\frac{2\pi}{3}} & -\lambda_3 e^{j\frac{2\pi}{3}} & -\lambda_3 & -\lambda_3 e^{-j\frac{2\pi}{3}} & 2\lambda_3 e^{j\frac{2\pi}{3}} & 2\lambda_3
\end{array} \right] \quad (5.29)$$

The solution of equation 5.28 is given by:

$$V_\delta = V_{\delta 0} e^{-\frac{1}{6C_d} \Lambda t} \quad (5.30)$$

The eigenvalues of $-\frac{1}{6C_d} \Lambda$ are given by $\epsilon_1 = -\frac{\lambda_1 + \lambda_3 + \sqrt{\lambda_1^2 - \lambda_1 \lambda_2 + \lambda_3^2}}{2C_d}$, $\epsilon_2 = -\frac{\lambda_1 + \lambda_3 - \sqrt{\lambda_1^2 - \lambda_1 \lambda_2 + \lambda_3^2}}{2C_d}$, $\epsilon_3 = -\frac{\lambda_2 + \lambda_3 + \sqrt{\lambda_2^2 - \lambda_2 \lambda_3 + \lambda_3^2}}{2C_d}$, $\epsilon_4 = -\frac{\lambda_2 + \lambda_3 - \sqrt{\lambda_2^2 - \lambda_2 \lambda_3 + \lambda_3^2}}{2C_d}$, $\epsilon_5 = -\frac{\lambda_2 + \lambda_1 + \sqrt{\lambda_2^2 - \lambda_1 \lambda_2 + \lambda_1^2}}{2C_d}$ and $\epsilon_6 = -\frac{\lambda_2 + \lambda_1 - \sqrt{\lambda_2^2 - \lambda_1 \lambda_2 + \lambda_1^2}}{2C_d}$

From equation 5.1 the solution of equation 5.28 is yielded by:

$$V_\delta = y_1 e^{\epsilon_1 t} + y_2 e^{\epsilon_2 t} + y_3 e^{\epsilon_3 t} + y_4 e^{\epsilon_4 t} + y_5 e^{\epsilon_5 t} + y_6 e^{\epsilon_6 t}$$

where y_1 , y_2 and y_3 are corresponding eigenvectors of ϵ_1 , ϵ_2 and ϵ_3 respectively.

The time constants are given by:

$$\begin{aligned}
\tau_1 &= \frac{2C_d}{\lambda_1 + \lambda_3 + \sqrt{\lambda_1^2 - \lambda_1 \lambda_2 + \lambda_3^2}} \\
\tau_2 &= \frac{2C_d}{\lambda_1 + \lambda_3 - \sqrt{\lambda_1^2 - \lambda_1 \lambda_2 + \lambda_3^2}} \\
\tau_3 &= \frac{2C_d}{\lambda_2 + \lambda_3 + \sqrt{\lambda_2^2 - \lambda_2 \lambda_3 + \lambda_3^2}} \\
\tau_4 &= \frac{2C_d}{\lambda_2 + \lambda_3 - \sqrt{\lambda_2^2 - \lambda_2 \lambda_3 + \lambda_3^2}} \\
\tau_5 &= \frac{2C_d}{\lambda_2 + \lambda_1 + \sqrt{\lambda_2^2 - \lambda_1 \lambda_2 + \lambda_1^2}}
\end{aligned}$$

$$\tau_6 = \frac{2C_d}{\lambda_2 + \lambda_1 - \sqrt{\lambda_2^2 - \lambda_1\lambda_2 + \lambda_1^2}} \quad (5.31)$$

From the equations given in 5.31 we observe that the factors influencing the value of the time constants associated with the rebalancing of the cell capacitor voltages are:

1. The impedance of the output filter and load; and
2. The value of $|S_{da}(l\omega_0)|^2$, that is, the overlap of the spectra $S_{da}(l\omega_0)$ and $\overline{S_{da}(l\omega_0)}$.

To ensure the validity of the theory developed, we compare theoretical results obtained using equation 5.30 and the Matlab package with simulated results of the practical converter using Ansoft Corporation, Simplorer package and FFT analysis. We take the initial values of $V_{\delta a1}$, $V_{\delta a2}$, $V_{\delta b1}$, $V_{\delta b2}$, $V_{\delta c1}$ and $V_{\delta c2}$ to be 25 V, 0 V, 0 V, 0 V, 0 V and 0 V respectively.

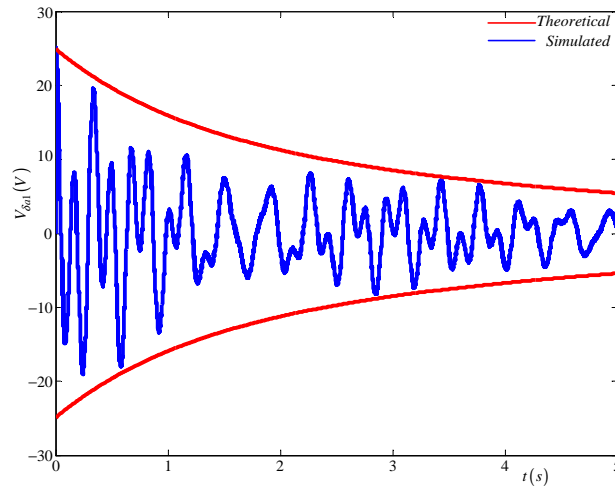


Figure 5.13: $V_{\delta a1}$ for modulation index of 1 without balancing circuit. The blue line=Simplorer simulation and the red line= theoretical simulation

Figures 5.13, 5.14, 5.15 and 5.16 depict the natural balancing of the cell capacitor voltages for modulation index of 1, 0.8, 0.6 and 0.4 respectively when the balancing circuit is not connected. The red curve indicates the exponential decay obtained using theory whilst the blue curve indicates the exponential decay obtained using simulation.

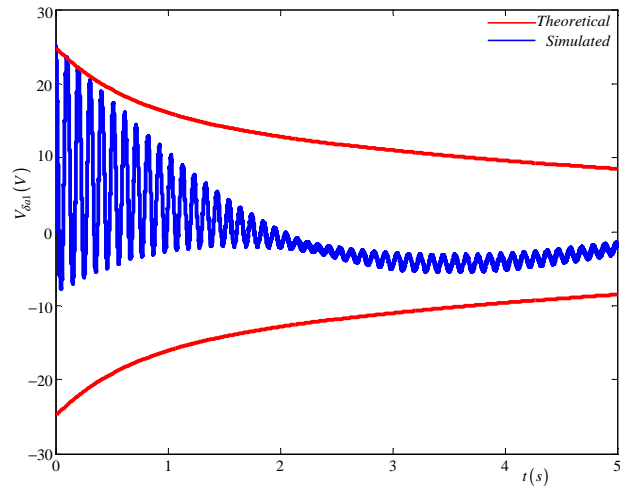


Figure 5.14: $V_{\delta a1}$ for modulation index of 0.8 without balancing circuit. The blue line=Simpler simulation and the red line= theoretical simulation

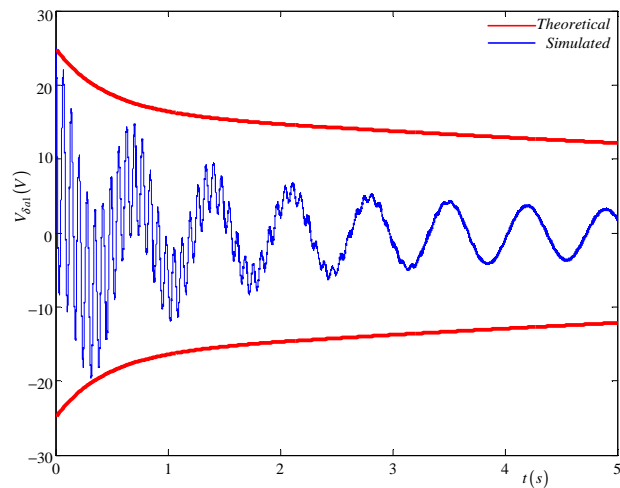


Figure 5.15: $V_{\delta a1}$ for modulation index of 0.6 without balancing circuit. The blue line=Simpler simulation and the red line= theoretical simulation

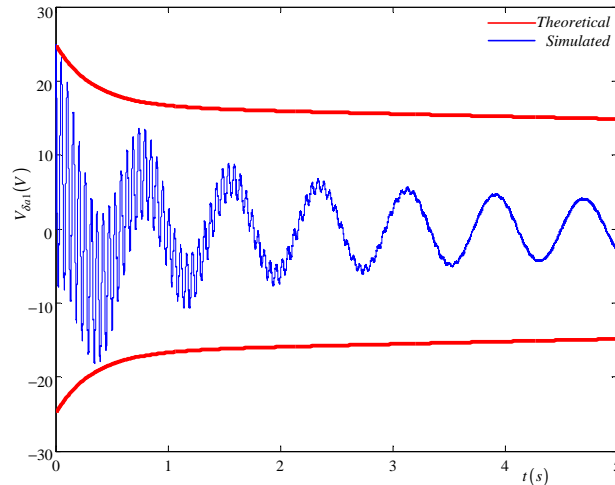


Figure 5.16: $V_{\delta a1}$ for modulation index of 0.4 without balancing circuit. The blue line=Simpler simulation and the red line= theoretical simulation

Similar to the 2-cell case, we connect a balancing circuit to enhance the capacitor voltage balance. Figures 5.17, 5.18, 5.19 and 5.20 show the natural balancing of the cell capacitor voltages for modulation index of 1, 0.8 and 0.6 respectively with the balancing circuit connected. It is observed from these figures that the balancing circuit causes the natural balancing to be achieved faster.

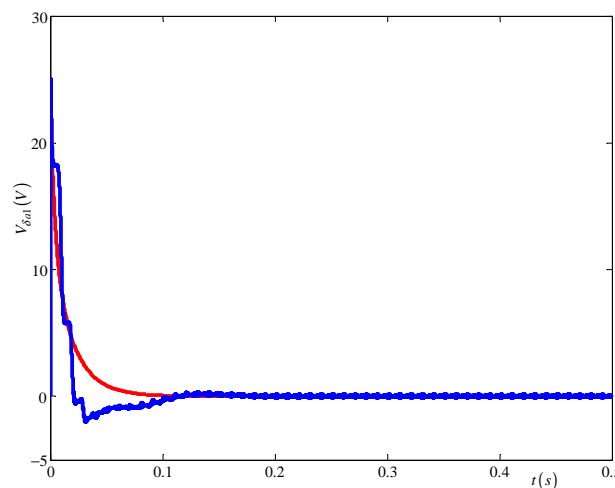


Figure 5.17: $V_{\delta a1}$ for modulation index of 1 with balancing circuit. The blue line=Simpler simulation and the red line= theoretical simulation

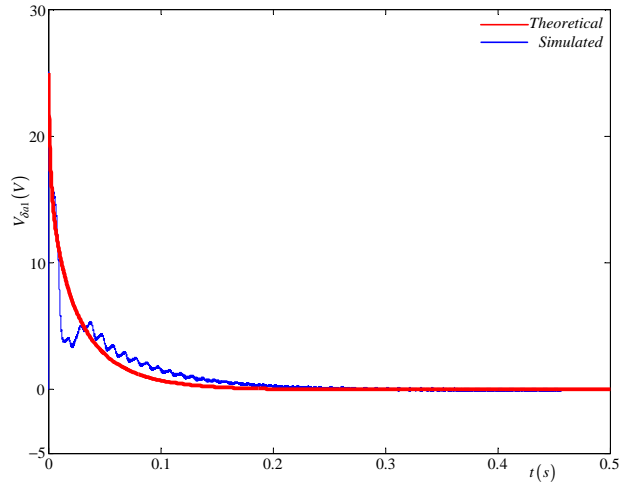


Figure 5.18: $V_{\delta a1}$ for modulation index of 0.8 with balancing circuit. The blue line=Simplorer simulation and the red line= theoretical simulation

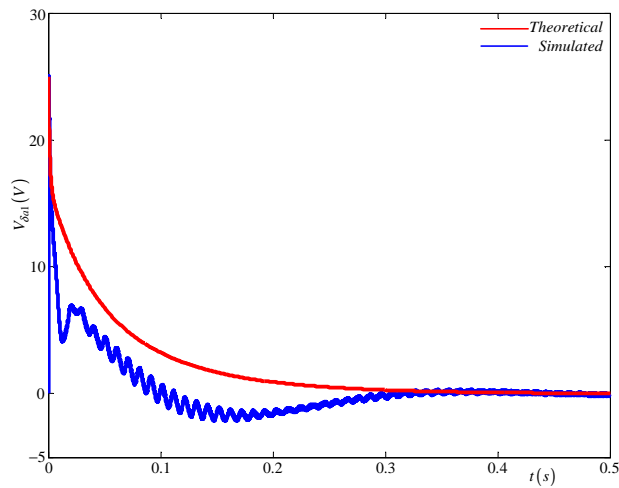


Figure 5.19: $V_{\delta a1}$ for modulation index of 0.6 with balancing circuit. The blue line=Simplorer simulation and the red line= theoretical simulation

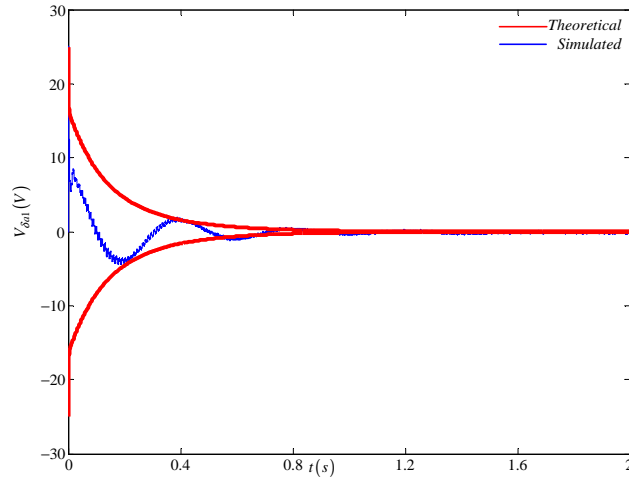


Figure 5.20: $V_{\delta a1}$ for modulation index of 0.4 with balancing circuit. The blue line=Simplorer simulation and the red line= theoretical simulation

5.4 Summary

This chapter calculated the time constants for the 2-cell and the 3-cell multicell converter. It further demonstrated the rebalancing of the capacitor voltages using the derived theory and simulations using the Simplorer package. It was observed that for both the 2-cell and 3-cell cases natural balancing was achieved. When the balancing circuit is added the rebalance of the capacitor voltages occurred faster. The theoretical results compared very well with the simulation results.

Chapter 6

Space Vector Analysis

6.1 Introduction

In this chapter we study the natural balancing of the 2-cell multicell converter under space vector modulation. In [48] Celanovic et al. studied the space-vector modulation of n-level three-phase converters using duty-cycle computation and the nearest three vectors. In [36] McGrath et al. identified how to sequence the three nearest space vectors in the switching period in order to minimise the total number of switching transitions and optimise the harmonic profile of the output voltage. In this chapter we compute the switch combination sequences of the 2-cell multicell converter which have more redundant vector states than other 3-level converters. For convenience the computations of the duty cycles of other five sectors and the switching combinations are carried out in Appendixes D and E. Furthermore we plot the waveforms of the reference vector when in different regions of the six sectors. We then prove, using simulations, that 2-cell multicell converters naturally balance under space-vector modulation.

6.2 Switching Vectors

In this section we furnish the switching vectors of the three-level voltage source converter. There are 27 different voltage levels for these converters. These switching states are then arranged into 19 different switching vectors as shown in Figure 6.1 due to similarities of coordinates in the α - β parameter. X_0 is the zero vector, while $(X_1 - X_6)$ are small vectors, $(X_7 - X_{12})$ are medium vectors and $(X_{13} - X_{18})$ are large vectors.

These vectors in Figure 6.1 represent converter output line voltages in a two-dimensional (V_{ab} , V_{bc} and V_{ca}) plane and are produced by switching different states of the converter as shown in Tables 6.1, 6.4, 6.5, 6.2 and 6.3. The said represent the 19 switching vectors grouped into zero vectors, small vectors, medium vectors and large vectors respectively. These groups are composed of switching vectors for s_a , s_b , s_c where s_a , s_b and s_c represent

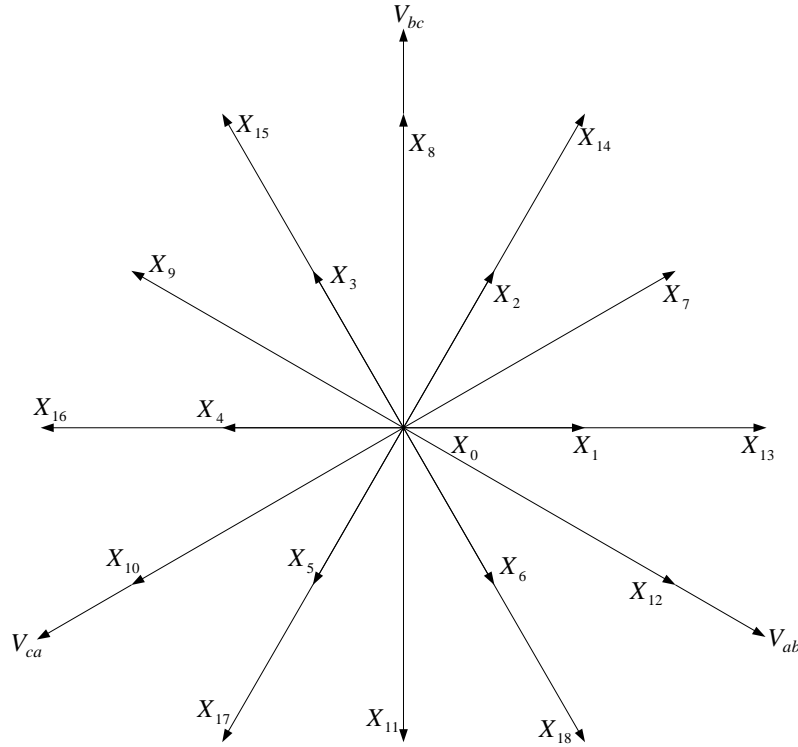


Figure 6.1: *Switching vectors of a three-level Multicell converter*

switching states of phases A, B and C as shown in subsection 3.3.1 for the general case of a 3-level converter. Now the switching states are further simplified for a multicell converter to include switching states for each cell represented by $[s_{a1}, s_{a2}]$, $[s_{b1}, s_{b2}]$, $[s_{c1}, s_{c2}]$ where $[s_{a1}, s_{a2}]$ represent switching states for the first and second cells of phase A, $[s_{b1}, s_{b2}]$ represent switching states for first and second cells of phase B and $[s_{c1}, s_{c2}]$ represent switching states for first and second cells of phase C. For a 2-cell multicell converter with four different switching states for each phase we will have 64 possible switching states. Thus we will have many redundant switching states producing the same vector as shown in Tables 6.1, 6.4, 6.5, 6.2 and 6.3. θ indicates the angle position of the vector.

Switching vectors for s_α and s_β are given by:

$$\begin{bmatrix} s_\alpha \\ s_\beta \end{bmatrix} = A \begin{bmatrix} s_a \\ s_b \\ s_c \end{bmatrix} \tag{6.1}$$

where

$$A = \sqrt{\frac{2}{3}} \begin{bmatrix} 1 & -\frac{1}{2} & -\frac{1}{2} \\ 0 & \frac{\sqrt{3}}{2} & -\frac{\sqrt{3}}{2} \end{bmatrix} \tag{6.2}$$

Table 6.1: *Zero switching vectors*

<i>Vectors</i>	$[s_{a1}, s_{a2}], [s_{b1}, s_{b2}], [s_{c1}, s_{c2}]$	$s_a s_b s_c$	s_α	s_β	θ
X_0	$[1, 1], [1, 1], [1, 1]$	111	0	0	0
	$[1, -1], [1, -1], [1, -1]$				
	$[-1, 1], [1, -1], [1, -1]$				
	$[1, -1], [-1, 1], [-1, 1]$				
	$[-1, 1], [-1, 1], [-1, 1]$				
	$[1, -1], [-1, 1], [1, -1]$				
	$[-1, 1], [-1, 1], [1, -1]$				
	$[1, -1], [1, -1], [-1, 1]$				
	$[-1, 1], [1, -1], [-1, 1]$				
		000	0	0	0
	$[-1, -1], [-1, -1], [-1, -1]$	-1-1-1	0	0	0

Table 6.2: *Medium switching vectors*

<i>Vectors</i>	$[s_{a1}, s_{a2}], [s_{b1}, s_{b2}], [s_{c1}, s_{c2}]$	$s_a s_b s_c$	s_α	s_β	θ
X_7	$[1, 1], [1, -1], [-1, -1]$	10-1	$\sqrt{\frac{3}{2}}$	$\frac{1}{\sqrt{2}}$	$\frac{\pi}{6}$
	$[1, 1], [-1, 1], [-1, -1]$				
X_8	$[1, -1], [1, 1], [-1, -1]$	01-1	0	$\sqrt{2}$	$\frac{\pi}{2}$
	$[-1, 1], [1, 1], [-1, -1]$				
X_9	$[-1, -1], [1, 1], [1, -1]$	-110	$-\sqrt{\frac{3}{2}}$	$\frac{1}{\sqrt{2}}$	$\frac{5\pi}{6}$
	$[-1, -1], [1, 1], [-1, 1]$				
X_{10}	$[-1, -1], [1, -1], [1, 1]$	-101	$-\sqrt{\frac{3}{2}}$	$-\frac{1}{\sqrt{2}}$	$-\frac{5\pi}{6}$
	$[-1, -1], [-1, 1], [1, 1]$				
X_{11}	$[1, -1], [-1, -1], [1, 1]$	0-11	0	$-\sqrt{2}$	$-\frac{\pi}{2}$
	$[-1, 1], [-1, -1], [1, 1]$				
X_{12}	$[1, 1], [-1, -1], [1, -1]$	1-10	$\sqrt{\frac{3}{2}}$	$-\frac{1}{\sqrt{2}}$	$-\frac{\pi}{6}$
	$[1, 1], [-1, -1], [-1, 1]$				

Table 6.3: *Large switching vectors*

<i>Vectors</i>	$[s_{a1}, s_{a2}], [s_{b1}, s_{b2}], [s_{c1}, s_{c2}]$	$s_a s_b s_c$	s_α	s_β	θ
X_{13}	$[1, 1], [-1, -1], [-1, -1]$	1-1-1	$2\sqrt{\frac{2}{3}}$	0	0
X_{14}	$[1, 1], [1, 1], [-1, -1]$	11-1	$\sqrt{\frac{2}{3}}$	$\sqrt{2}$	$\frac{\pi}{3}$
X_{15}	$[-1, -1], [1, 1], [-1, -1]$	-11-1	$-\sqrt{\frac{2}{3}}$	$\sqrt{2}$	$\frac{2\pi}{3}$
X_{16}	$[-1, -1], [1, 1], [1, 1]$	-111	$-2\sqrt{\frac{2}{3}}$	0	π
X_{17}	$[-1, -1], [-1, -1], [1, 1]$	-1-11	$-\sqrt{\frac{2}{3}}$	$-\sqrt{2}$	$-\frac{2\pi}{3}$
X_{18}	$[1, 1], [-1, -1], [1, 1]$	1-11	$\sqrt{\frac{2}{3}}$	$-\sqrt{2}$	$-\frac{\pi}{3}$

Table 6.4: *Small switching vectors*

<i>Vectors</i>	$[s_{a1}, s_{a2}], [s_{b1}, s_{b2}], [s_{c1}, s_{c2}]$	$s_a s_b s_c$	s_α	s_β	θ
X_1	$[1, 1], [1, -1], [1, -1]$	100	$\sqrt{\frac{2}{3}}$	0	0
	$[1, 1], [-1, 1], [-1, 1]$				
	$[1, 1], [-1, 1], [1, -1]$				
	$[1, 1], [1, -1], [-1, 1]$				
	$[1, -1], [-1, -1], [-1, -1]$	0-1-1	$\sqrt{\frac{2}{3}}$	0	0
	$[-1, 1], [-1, -1], [-1, -1]$				
X_2	$[1, 1], [1, 1], [1, -1]$	110	$\frac{1}{\sqrt{6}}$	$\frac{1}{\sqrt{2}}$	$\frac{\pi}{3}$
	$[1, 1], [1, 1], [-1, 1]$				
	$[1, -1], [1, -1], [-1, -1]$	00-1	$\frac{1}{\sqrt{6}}$	$\frac{1}{\sqrt{2}}$	$\frac{\pi}{3}$
	$[-1, 1], [1, -1], [-1, -1]$				
	$[1, -1], [-1, 1], [-1, -1]$				
	$[-1, 1], [-1, 1], [-1, -1]$				
X_3	$[1, -1], [1, 1], [1, -1]$	010	$-\frac{1}{\sqrt{6}}$	$\frac{1}{\sqrt{2}}$	$\frac{2\pi}{3}$
	$[-1, 1], [1, 1], [1, -1]$				
	$[1, -1], [1, 1], [-1, 1]$				
	$[-1, 1], [1, 1], [-1, 1]$				
	$[-1, -1], [1, -1], [-1, -1]$	-10-1	$-\frac{1}{\sqrt{6}}$	$\frac{1}{\sqrt{2}}$	$\frac{2\pi}{3}$
	$[-1, -1], [-1, 1], [-1, -1]$				

Table 6.5: *Small switching vectors*

<i>Vectors</i>	$[s_{a1}, s_{a2}], [s_{b1}, s_{b2}], [s_{c1}, s_{c2}]$	$s_a s_b s_c$	s_α	s_β	θ
X_4	$[1, -1], [1, 1], [1, 1]$	011	$-\sqrt{\frac{2}{3}}$	0	π
	$[-1, 1], [1, 1], [1, 1]$				
	$[-1, -1], [1, -1], [1, -1]$	-100	$-\sqrt{\frac{2}{3}}$	0	π
	$[-1, -1], [-1, 1], [-1, 1]$				
	$[-1, -1], [-1, 1], [1, -1]$				
	$[-1, -1], [1, -1], [-1, 1]$				
X_5	$[1, -1], [1, -1], [1, 1]$	001	$-\frac{1}{\sqrt{6}}$	$-\frac{1}{\sqrt{2}}$	$-\frac{2\pi}{3}$
	$[-1, 1], [1, -1], [1, 1]$				
	$[1, -1], [-1, 1], [1, 1]$				
	$[-1, 1], [-1, 1], [1, 1]$	-1-10	$-\frac{1}{\sqrt{6}}$	$-\frac{1}{\sqrt{2}}$	$-\frac{2\pi}{3}$
	$[-1, -1], [-1, -1], [1, -1]$				
	$[-1, -1], [-1, -1], [-1, 1]$				
X_6	$[1, 1], [1, -1], [1, 1]$	101	$\frac{1}{\sqrt{6}}$	$-\frac{1}{\sqrt{2}}$	$-\frac{\pi}{3}$
	$[1, 1], [-1, 1], [1, 1]$				
	$[1, -1], [-1, -1], [1, -1]$	0-10	$\frac{1}{\sqrt{6}}$	$-\frac{1}{\sqrt{2}}$	$-\frac{\pi}{3}$
	$[-1, 1], [-1, -1], [1, -1]$				
	$[1, -1], [-1, -1], [-1, 1]$				
	$[-1, 1], [-1, -1], [-1, 1]$				

6.3 Duty Cycles

We divide Figure 6.1 into six sectors spaced anticlockwise by $\frac{\pi}{3}$ radians from each other. Each sector consists of four regions. We now study the duty cycles of each region. These duty cycles are obtained by synthesising the reference vector using the space vector modulation of the three switching state vectors nearest to the reference vector at every sampling instant. The duty cycles of other sectors have the same magnitude but are shifted in phase. Duty cycle(D_T) is the ratio of the period, that the particular vector is selected, to the total period of the signal and is given by:

$$D_T = \frac{\Delta t}{T_s}$$

where T_s is the switching period and Δt is the period that the particular vector is selected.

Figure 6.2 illustrates the first sector of the switching state vectors of the 2-cell multicell converter and the four regions within this sector. The reference vector V_r is synthesised

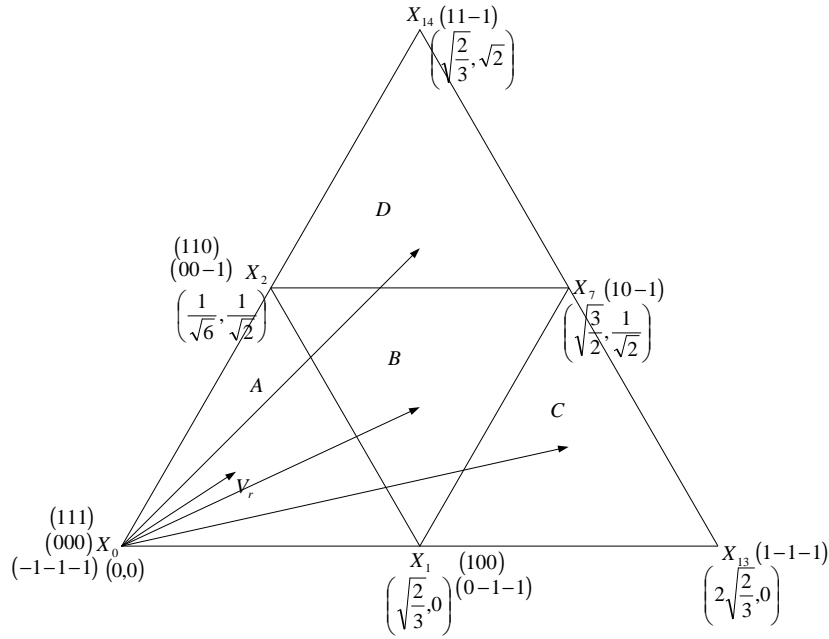


Figure 6.2: Regions of vector modulation of the 2-cell multicell converter in the first sector

using the space vector modulation of the three switching state vectors nearest to the reference vector at every sampling instant. The nearest three switching state vectors are selected by locating the reference vector in one of the four regions as shown in Figure 6.2. The reference vector is given by the general formula:

$$V_r = d_p X_e + d_q X_f + d_r X_g$$

where d_p , d_q and d_r are the duty cycles/durations for the switching vectors X_e , X_f and X_g respectively.

In this section we will only study the duty cycles for sector I, since the duty cycles for other five sectors are considered in Appendix D. In addition, the detailed switching combinations are done in Appendix E

6.3.1 Duty cycles for Sector I

In this subsection we study the sequences and combinations of duty cycles of regions A, B, C and D of sector I. Figure 6.2 shows the first sector of six sectors with its regions. From Figure 6.2 we observe that region A has one vector with a redundancy of 3 and two vectors with a redundancy of 2; region B contains one vector with a redundancy of 1 and two vectors with a redundancy of 2; regions C and D have one vector with a redundancy of 2 and two vectors with a redundancy of 1. The choice of combination is influenced by the movement of the reference vector from one region to the next. We

choose the three nearest space vectors and then add the fourth space vector so that either the first or fourth vector is redundant; then the sequence is reversed [36]. The duty cycles of the first and fourth vector are split into equal halves for optimal harmonic performance [36]. However for a 2-cell multicell converter using Tables 6.1, 6.2, 6.3, 6.4 and 6.5 we note that region A has one vector with a redundancy of 10 and two vectors with a redundancy of 6; region B has one vector with a redundancy of 2 and two vectors with a redundancy of 6; regions C and D contain one vector with a redundancy of 6, one vector with a redundancy of 2 and one vector with a redundancy of 1. We show the switch combinations using all redundancy in the Appendix E section E.1.

Region A:

For $\theta \leq \frac{\pi}{6}$

Now we consider the switch combination sequence for the nearest three vectors moving from region *VIA* to *IA* where *VIA* denotes the region *A* of the sixth sector and *IA* denotes the region *A* of the first sector. The combination starts with the vector (100) which is the redundant vector of the first vector in region *VIA*2. Looking at the combination it can be noted that we change the switching state of one phase at a time. The combination is given by:

$d_1(100)$ to $d_0(000)$ to $d_2(00-1)$ to $d_1(0-1-1)$ to $d_1(0-1-1)$ to $d_2(00-1)$ to $d_0(000)$ to $d_1(100)$

The PWM of this duty cycle is shown in Figure 6.3.

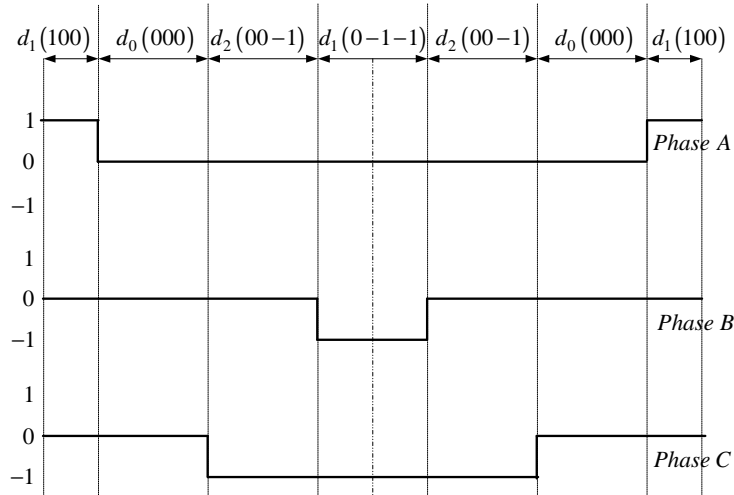


Figure 6.3: PWM for duty cycles of region *IA1*

The corresponding reference voltage vector waveform equations for phase A, B and C are yielded by equations 6.3, 6.4 and 6.5 respectively:

$$V_{ref_{IA1}} = \frac{1}{4}d_1$$

$$= \frac{1}{2\sqrt{2}}m_a \cos\left(\omega t + \frac{\pi}{6}\right) \quad (6.3)$$

$$\begin{aligned} V_{ref_{IA1}} &= -\frac{1}{4}d_1 \\ &= -\frac{1}{2\sqrt{2}}m_a \cos\left(\omega t + \frac{\pi}{6}\right) \end{aligned} \quad (6.4)$$

$$\begin{aligned} V_{ref_{IA1}} &= -\frac{1}{2}d_2 - \frac{1}{4}d_1 \\ &= -\frac{\sqrt{3}}{2\sqrt{2}}m_a \sin\left(\omega t + \frac{\pi}{6}\right) \end{aligned} \quad (6.5)$$

For $\theta \geq \frac{\pi}{6}$

The switch combination sequence for the nearest three vectors moving from region *IA* to *IIA* starts with vector (110) which only differs from the first vector combination of region *IA1* by the switching states of phase B. The combination is given by:

$d_2(110)$ to $d_1(100)$ to $d_0(000)$ to $d_2(00-1)$ to $d_2(00-1)$ to $d_0(000)$ to $d_1(100)$ to $d_2(110)$

The PWM of this duty cycle is illustrated in Figure 6.4 and the corresponding reference

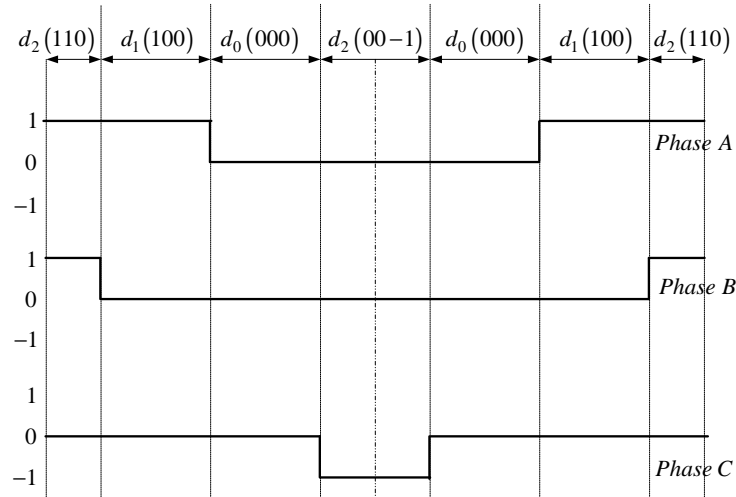


Figure 6.4: PWM for Duty cycles of Region *IA2*

voltage vector waveform equations for phase A, B and C are given by equations 6.6, 6.7 and 6.8 respectively:

$$\begin{aligned} V_{ref_{IA2}} &= \frac{1}{4}d_2 + \frac{1}{2}d_1 \\ &= \frac{\sqrt{3}}{2\sqrt{2}}m_a \cos \omega t \end{aligned} \quad (6.6)$$

$$\begin{aligned} V_{ref_{IA2}} &= \frac{1}{4}d_2 \\ &= \frac{1}{2\sqrt{2}}m_a \sin \omega t \end{aligned} \quad (6.7)$$

$$\begin{aligned}
V_{refc_{IA2}} &= -\frac{1}{4}d_2 \\
&= -\frac{1}{2\sqrt{2}}m_a \sin \omega t
\end{aligned} \tag{6.8}$$

Region IB:

For $\theta \leq \frac{\pi}{6}$

The switch combination sequence for the nearest three vectors moving from region *IC* to *IB1* starts with vector (100) which is the same as the redundant vector of the first vector of region *IC*. The combination yields:

$d_1(100)$ to $d_7(10-1)$ to $d_2(00-1)$ to $d_1(0-1-1)$ to $d_1(0-1-1)$ to $d_2(00-1)$ to $d_7(10-1)$ to $d_1(100)$.

The PWM of this duty cycle is shown in Figure 6.5 and the corresponding reference

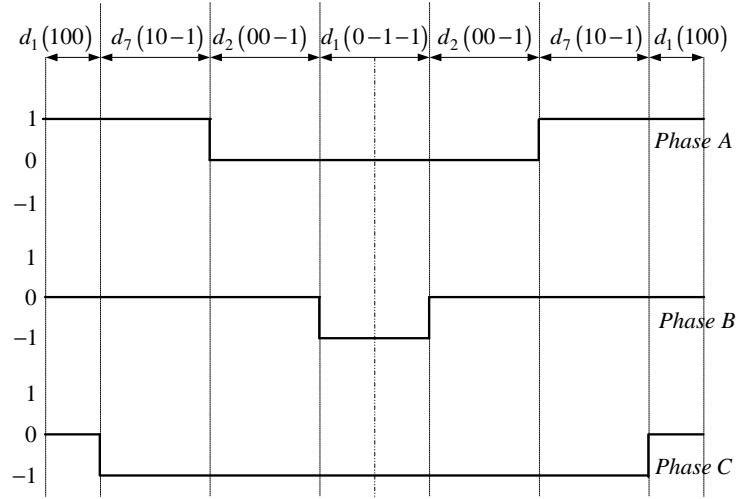


Figure 6.5: PWM for Duty cycles of Region *IB1*

voltage vector waveform equations for phases A, B and C are yielded by equations 6.9, 6.10 and 6.11 respectively:

$$\begin{aligned}
V_{refa_{IB1}} &= \frac{1}{4}d_1 + \frac{1}{2}d_7 \\
&= \frac{\sqrt{3}}{2\sqrt{2}}m_a \cos \omega t - \frac{1}{4}
\end{aligned} \tag{6.9}$$

$$\begin{aligned}
V_{refb_{IB1}} &= -\frac{1}{4}d_1 \\
&= \frac{1}{2\sqrt{2}}m_a \sin \omega t - \frac{1}{4}
\end{aligned} \tag{6.10}$$

$$\begin{aligned}
V_{refc_{IB1}} &= -\frac{1}{2}d_7 - \frac{1}{2}d_2 - \frac{1}{4}d_1 \\
&= -\frac{1}{2\sqrt{2}}m_a \sin \omega t - \frac{1}{4}
\end{aligned} \tag{6.11}$$

For $\theta \geq \frac{\pi}{6}$

The switch combination sequence for the nearest three vectors moving from region $IB2$ to ID starts with the vector (110) which differs from the first vector of region $IB1$ by the switching states of phase B. The combination is given by:

$d_2(110)$ to $d_1(100)$ to $d_7(10-1)$ to $d_2(00-1)$ to $d_2(00-1)$ to $d_7(10-1)$ to $d_1(100)$ to $d_2(110)$.

The PWM of this duty cycle is depicted in Figure 6.6 and the corresponding reference

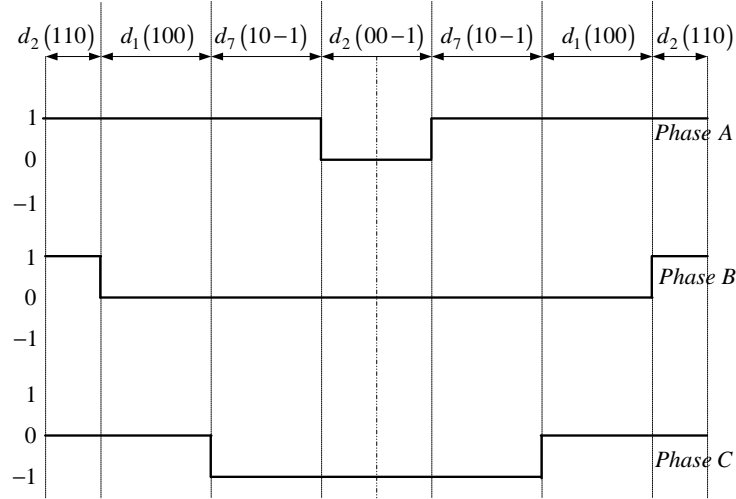


Figure 6.6: PWM for Duty cycles of region $IB2$

voltage vector waveform equations for phases A, B and C are yielded by equations 6.12, 6.13 and 6.14 respectively.

$$\begin{aligned} V_{refa_{IB2}} &= \frac{1}{4}d_2 + \frac{1}{2}d_1 + \frac{1}{2}d_7 \\ &= \frac{1}{2\sqrt{2}}m_a \cos\left(\omega t + \frac{\pi}{6}\right) + \frac{1}{4} \end{aligned} \quad (6.12)$$

$$\begin{aligned} V_{refb_{IB2}} &= \frac{1}{4}d_2 \\ &= -\frac{1}{2\sqrt{2}}m_a \cos\left(\omega t + \frac{\pi}{6}\right) + \frac{1}{4} \end{aligned} \quad (6.13)$$

$$\begin{aligned} V_{refc_{IB2}} &= -\frac{1}{2}d_7 + \frac{1}{4}d_2 \\ &= -\frac{\sqrt{3}}{2\sqrt{2}}m_a \sin\left(\omega t + \frac{\pi}{6}\right) + \frac{1}{4} \end{aligned} \quad (6.14)$$

Region IC:

The switch combination sequence for the nearest three vectors moving from region *VID* to *IC* starts with vector (100) which is the redundant vector of the first vector in region *VID*. The combination is yielded by:

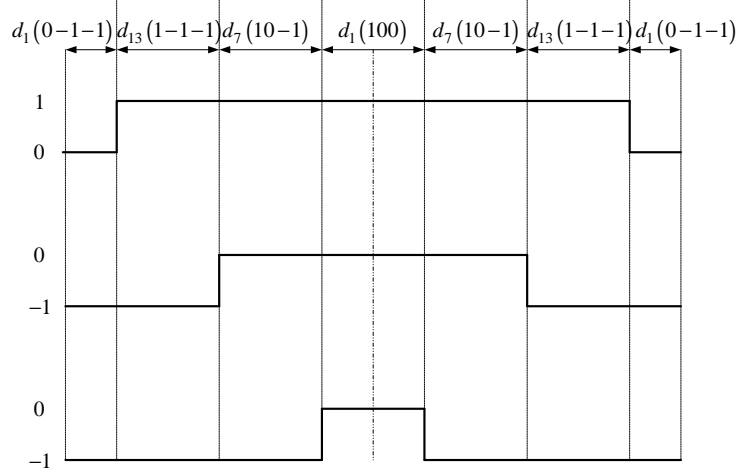


Figure 6.7: PWM for duty cycles of Region IC

and the corresponding reference voltage vector waveform equations for phase A, B and C are given by equations 6.15, 6.16 and 6.17 respectively.

$$\begin{aligned}
 V_{refa_{IC}} &= \frac{1}{4}d_1 + \frac{1}{2}d_{13} + \frac{1}{2}d_7 \\
 &= \frac{1}{2\sqrt{2}}m_a \cos(\omega t - \frac{\pi}{6})
 \end{aligned} \tag{6.15}$$

$$\begin{aligned}
 V_{refb_{IC}} &= -\frac{1}{4}d_1 - \frac{1}{2}d_{13} \\
 &= \frac{\sqrt{3}}{2\sqrt{2}}m_a \sin(\omega t - \frac{\pi}{6})
 \end{aligned} \tag{6.16}$$

$$\begin{aligned}
 V_{refc_{IC}} &= -\frac{1}{4}d_1 - \frac{1}{2}d_{13} - \frac{1}{2}d_7 \\
 &= -\frac{1}{2\sqrt{2}}m_a \cos(\omega t - \frac{\pi}{6})
 \end{aligned} \tag{6.17}$$

Region ID:

The switch combination sequence for the nearest three vector moving from region *IB2* to *ID* starts with the vector (00 - 1) which is the same as the redundant vector of the

first vector in region $IB2$. The combination is given by:

$d_2(00-1)$ to $d_7(10-1)$ to $d_{14}(11-1)$ to $d_2(110)$ to $d_2(110)$ to $d_{14}(11-1)$ to $d_7(10-1)$ to $d_2(00-1)$.

The PWM of this duty cycle is shown in Figure 6.8 and the corresponding reference

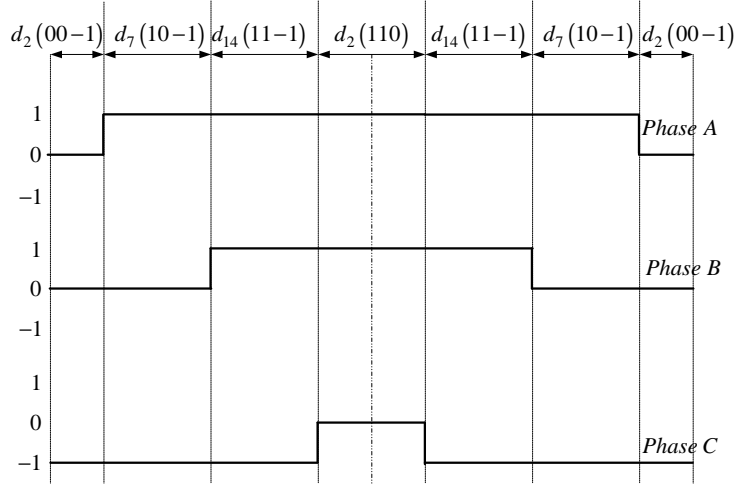


Figure 6.8: PWM for Duty cycles of Region ID

voltage vector waveform equations for phase A, B and C are given by equations 6.18, 6.19 and 6.20 respectively.

$$\begin{aligned} V_{refa_{ID}} &= \frac{1}{4}d_2 + \frac{1}{2}d_7 + \frac{1}{2}d_{14} \\ &= \frac{1}{2\sqrt{2}}m_a \cos\left(\omega t - \frac{\pi}{6}\right) \end{aligned} \quad (6.18)$$

$$\begin{aligned} V_{refb_{ID}} &= \frac{1}{4}d_2 + \frac{1}{2}d_7 + \frac{1}{2}d_{14} \\ &= \frac{\sqrt{3}}{2\sqrt{2}}m_a \sin\left(\omega t - \frac{\pi}{6}\right) \end{aligned} \quad (6.19)$$

$$\begin{aligned} V_{refc_{ID}} &= -\frac{1}{4}d_2 - \frac{1}{2}d_7 - \frac{1}{2}d_{14} \\ &= -\frac{1}{2\sqrt{2}}m_a \cos\left(\omega t - \frac{\pi}{6}\right) \end{aligned} \quad (6.20)$$

6.3.2 Waveforms of V_{refa} , V_{refb} and V_{refc}

Now for the modulation index given by $m_a = \sqrt{2}$ we use the reference voltage vector waveform equations V_{refa} , V_{refb} and V_{refc} , passing only through regions C and D of the six sectors, to draw the waveform of reference vector V_{refa} for phase A as shown in blue in Figure 6.9, V_{refb} for phase B as shown in red in Figure 6.9 and V_{refc} for phase C as shown in green in Figure 6.9.

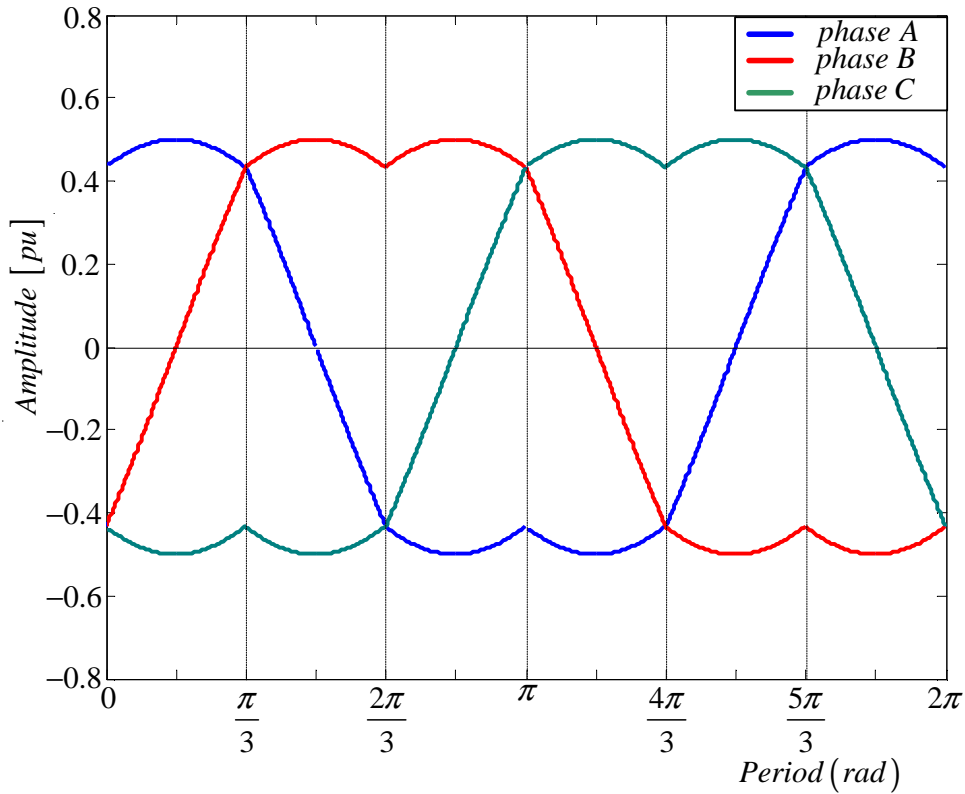


Figure 6.9: *Waveform of reference vectors V_{refa} , V_{refb} and V_{refc} for the six sectors of the 2-cell multicell converter passing through regions C and D for $m_a = \sqrt{2}$*

Now for the modulation index given by $m_a = \frac{2}{\sqrt{3}}$ with the reference vector passing only through regions C, B and D of the six sectors we draw the waveform of reference vector V_{refa} for phase A as shown in blue in Figure 6.10, V_{refb} for phase B as shown in red in Figure 6.10 and V_{refc} for phase C as shown in green in Figure 6.10

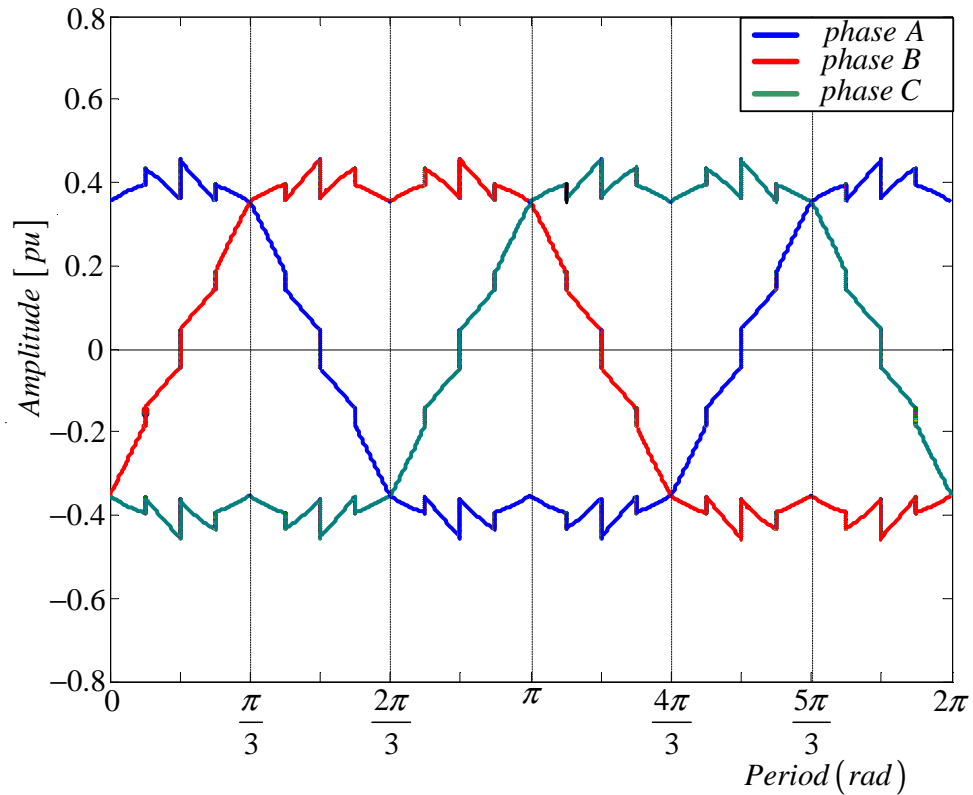


Figure 6.10: Waveform of reference vectors V_{refa} , V_{refb} and V_{refc} for the six sectors of the 2-cell multicell converter passing through regions C, B and D for $m_a = \frac{2}{\sqrt{3}}$

For the modulation index given by $m_a = \frac{1}{\sqrt{6}}$ with the reference vector passing only through region A of the six sectors we draw the waveform of reference vector V_{refa} for phase A as shown in Figure 6.11, V_{refb} for phase B as shown in Figure 6.11 and V_{refc} for phase C as shown in Figure 6.11.

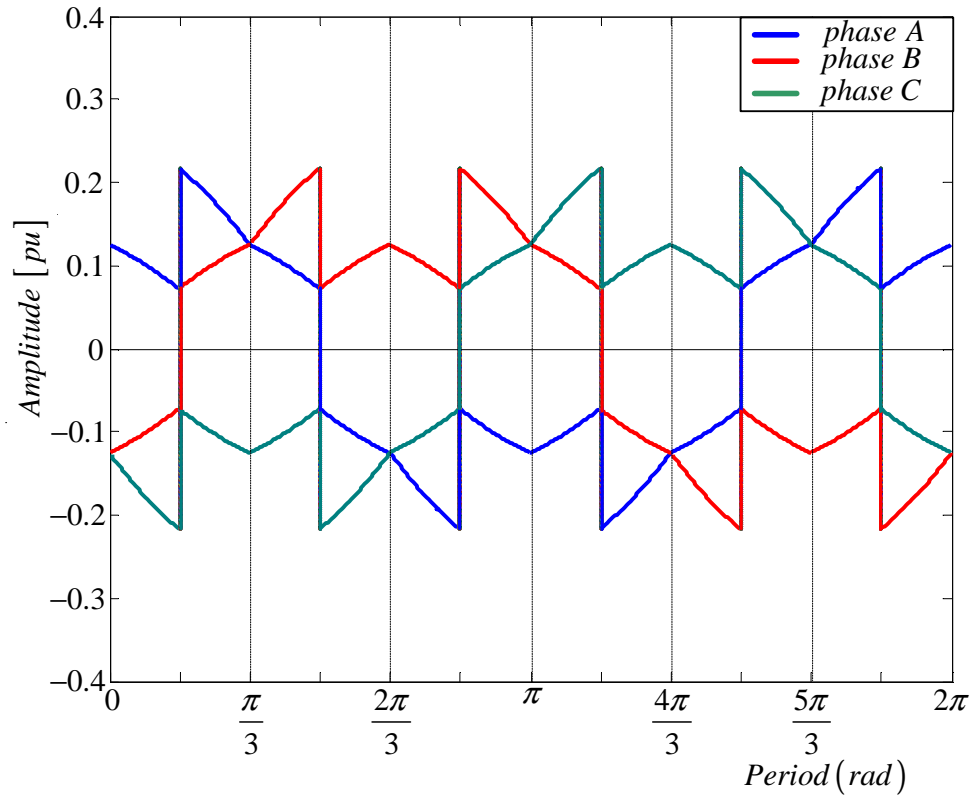


Figure 6.11: Waveform of reference vectors V_{refa} , V_{refb} and V_{refc} for the six sectors of the 2-cell multicell converter passing through region A for $m_a = \frac{1}{\sqrt{6}}$

Now for the modulation index given by $m_a = \sqrt{\frac{2}{3}}$ with the reference vector passing only through region B of the six sectors we draw the waveform of reference vector V_{refa} for phase A as shown in Figure 6.12, V_{refb} for phase B as shown in Figure 6.12 and V_{refc} for phase C as shown in Figure 6.12.

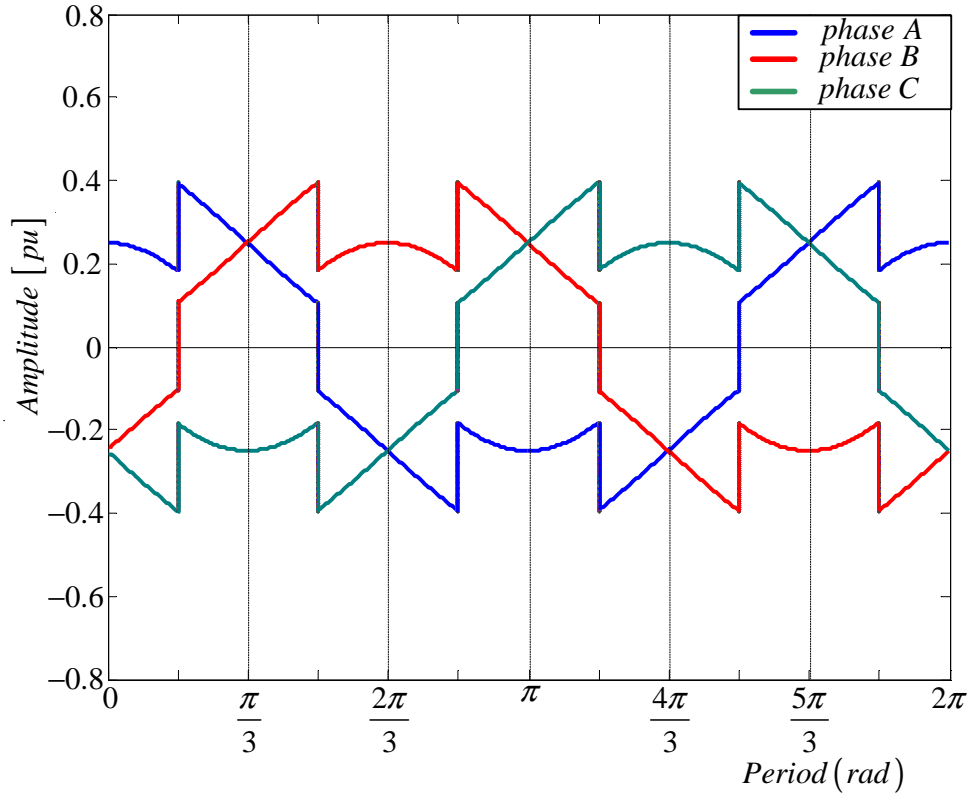


Figure 6.12: Waveform of reference vectors V_{refa} , V_{refb} and V_{refc} for the six sectors of the 2-cell multicell converter passing through region B for $m_a = \sqrt{\frac{2}{3}}$

6.4 Simulations

6.4.1 Boundary for Regions A, B, C and D

In this subsection we use Figure 6.13 to calculate boundary equations for Regions A, B, C and D. It is important to be able to determine the boundaries in order to decide in which sector we are.

Equations for the line and gradient are yielded by:

$$y - y_1 = m(x - x_1)$$

and

$$m = \frac{y_2 - y_1}{x_2 - x_1}$$

Region A1:

$$m = \frac{\frac{1}{\sqrt{2}} - 0}{\frac{1}{\sqrt{6}} - \sqrt{\frac{2}{3}}} = -\sqrt{3}$$

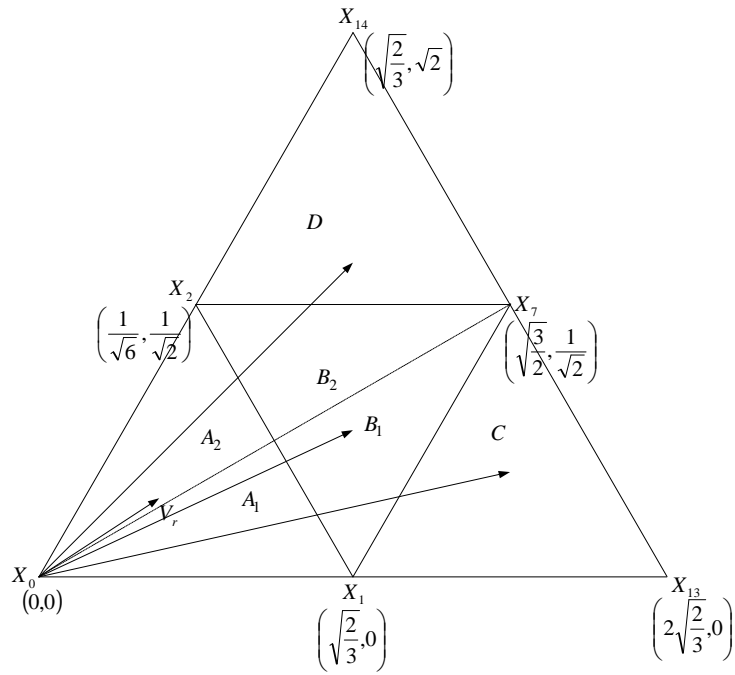


Figure 6.13: Sector I with coordinates for each region

$$\begin{aligned}
 y - 0 &\leq -\sqrt{3} \left(x - \sqrt{\frac{2}{3}} \right) \\
 &\leq -\sqrt{3}x + \sqrt{2}
 \end{aligned}$$

$$y + \sqrt{3}x \leq \sqrt{2}$$

$$y \leq \frac{1}{\sqrt{3}}x$$

Region A2:

$$y + \sqrt{3}x \leq \sqrt{2}$$

$$y \geq \frac{1}{\sqrt{3}}x$$

Region B1:

$$\begin{aligned}
 y - 0 &\geq \sqrt{3} \left(x - \sqrt{\frac{2}{3}} \right) \\
 &\geq \sqrt{3}x - \sqrt{2}
 \end{aligned}$$

$$\sqrt{3}x - y \leq \sqrt{2}$$

$$y + \sqrt{3}x \geq \sqrt{2}$$

$$y \leq \frac{1}{\sqrt{3}}x$$

Region B2:

$$y \leq \frac{1}{\sqrt{2}}$$

$$y + \sqrt{3}x \geq \sqrt{2}$$

$$y \geq \frac{1}{\sqrt{3}}x$$

Region C:

$$\sqrt{3}x - y \geq \sqrt{2}$$

Region D:

$$y \geq \frac{1}{\sqrt{2}}$$

6.4.2 Combination of switching states

Now for us to undertake a simulation setup in Simplorer we need the switching states combination for the 2-cell multicell converter. There are only four combinations of the switching states that balance the charges that pass through the cell capacitor. In the first combination we switch the top switch of the first cell, then the bottom switch of the second cell (that is $[1, -1]$) for the first three sectors of the three phases, then we switch the bottom switch of the first cell, then the top switch of the second cell (that is $[-1, 1]$) for the last three sectors of the three phases. In the second combination we do the reverse of the first combination. In the third combination we switch the top switch of the first cell, then the bottom switch of the second cell (that is $[1, -1]$) for sectors I, III and V, then switch the bottom switch of the first cell, then the top switch of the second cell (that is $[-1, 1]$) for sectors II, IV and VI. The fourth combination reverses the third combination. We show the first and third combinations in section E.7 of Appendix E.

6.4.3 Simulation results

In this section we provide the simulation results of natural balancing under space vector modulation. The simulation parameters for this section are as follows:

Table 6.6: *Simulation parameters*

<i>DC – bus voltage</i>	V_t	100 V
<i>DC – bus capacitance</i>	C_d	2 500 μF
<i>Switching frequency</i>	f_s	6 kHz
<i>Modulation frequency</i>	f_1	50 Hz
<i>Filter inductance</i>	L	200 μH
<i>Filter capacitance</i>	C	50 μF
<i>Load resistance</i>	R	10 Ω

Figures 6.14, 6.17, 6.20 and 6.23 illustrate the unfiltered phase and line output voltage waveform of the 2-cell multicell converter under vector control modulation for reference vector in different regions. Figures 6.15, 6.18, 6.21 and 6.24 show in part (a) and (b) the switching functions $s_{da}(t)$ and $s_{ta}(t)$ respectively in the time domain. Figures 6.16, 6.19, 6.22 and 6.25 show in part (a) and (b) the harmonic spectra of $S_{da}(\omega)$ and $S_{ta}(\omega)$ respectively. As can be observed from the harmonics it is difficult to establish where the highest harmonic occur to be able to apply balancing circuit.

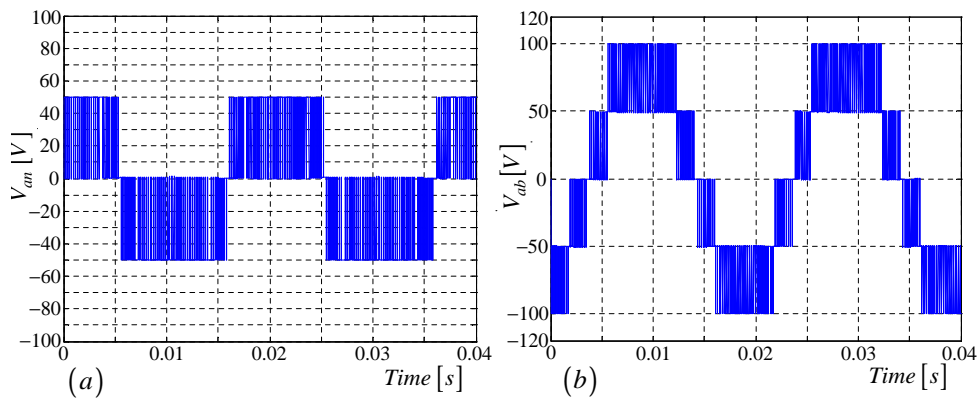


Figure 6.14: (a) Phase voltage and (b) Line voltage for reference voltage vector in regions C, B and D

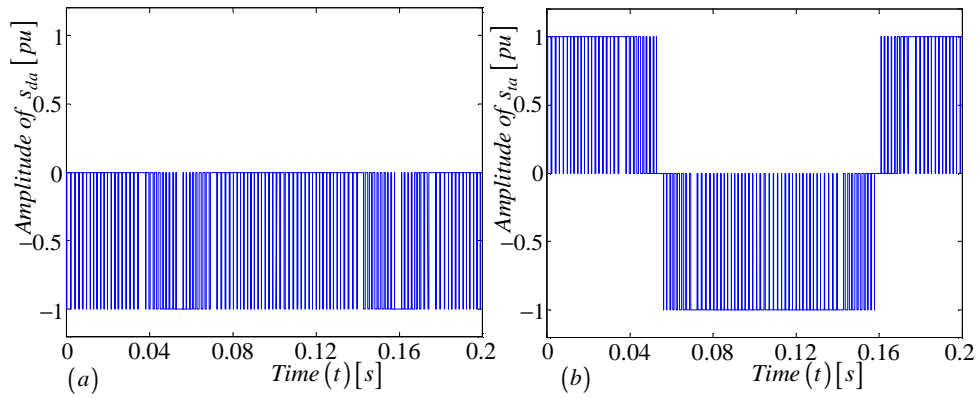


Figure 6.15: (a) Switching functions of $s_{da}(t)$ and (b) $s_{ta}(t)$ in time domain for reference voltage vector in regions C, B and D

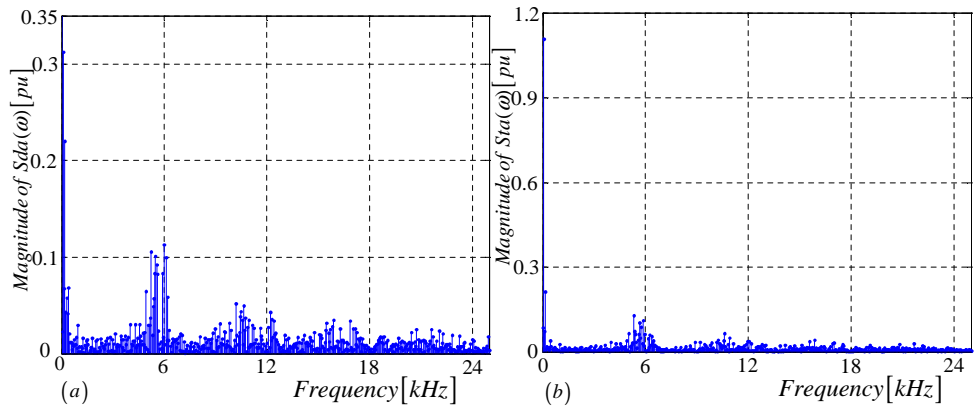


Figure 6.16: (a) Harmonics of $S_{da}(\omega)$ and (b) $S_{ta}(\omega)$ for reference voltage vector in regions C, B and D

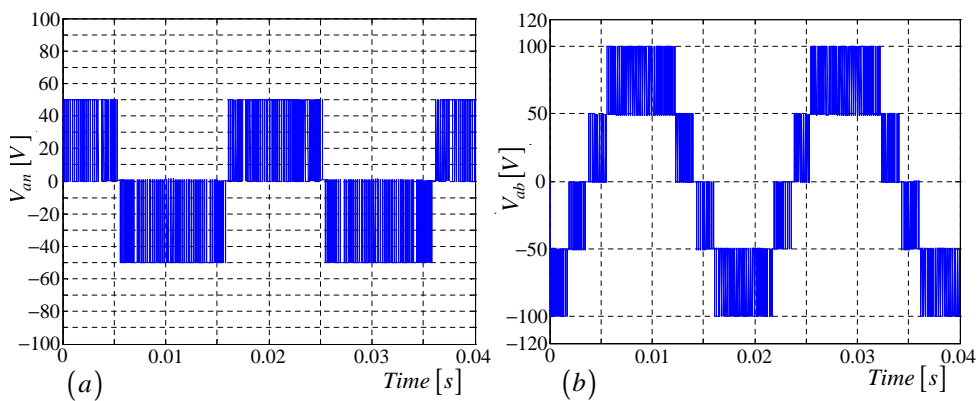


Figure 6.17: (a) Phase voltage and (b) Line voltage for reference voltage vector in regions C and D

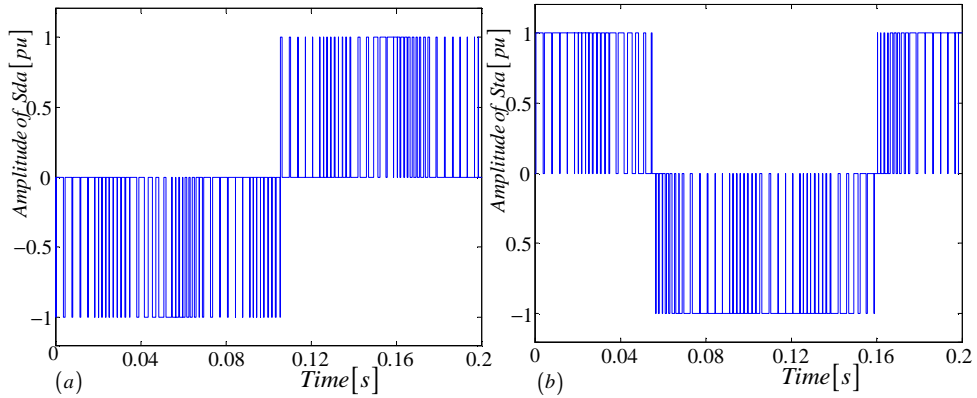


Figure 6.18: (a) Switching functions of $s_{da}(t)$, $s_{da}(t)$ and (b) $s_{da}(t) \cdot s_{da}(t)$ in time domain for reference voltage vector in regions C and D

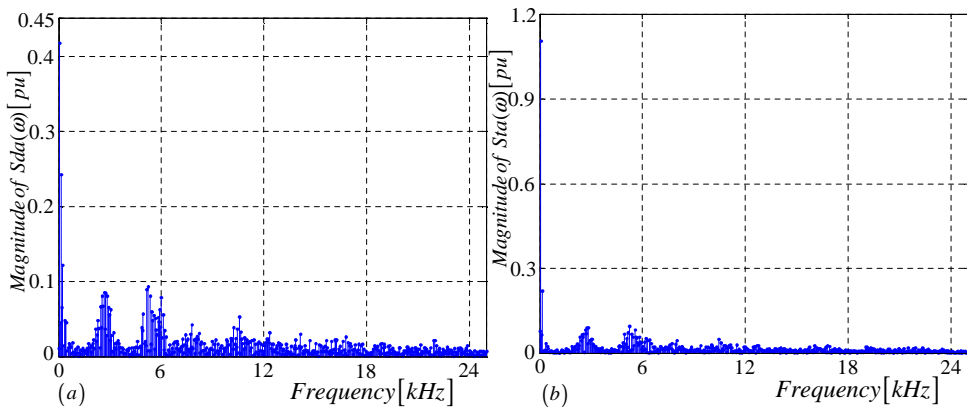


Figure 6.19: (a) Harmonics of $s_{da}(t)$, $S_{da}(\omega)$ and (b) $S_{da}(t) \cdot s_{da}(\omega)$ for reference voltage vector in regions C and D

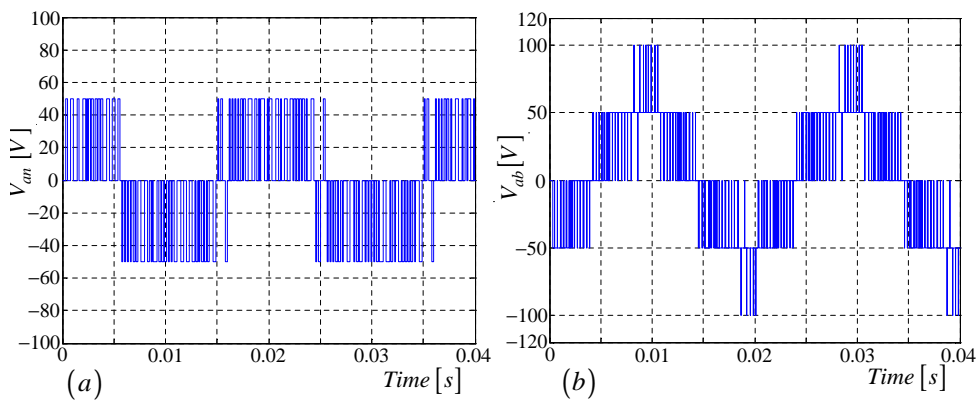


Figure 6.20: (a) Phase voltage and (b) Line voltage for reference voltage vector in regions A and B

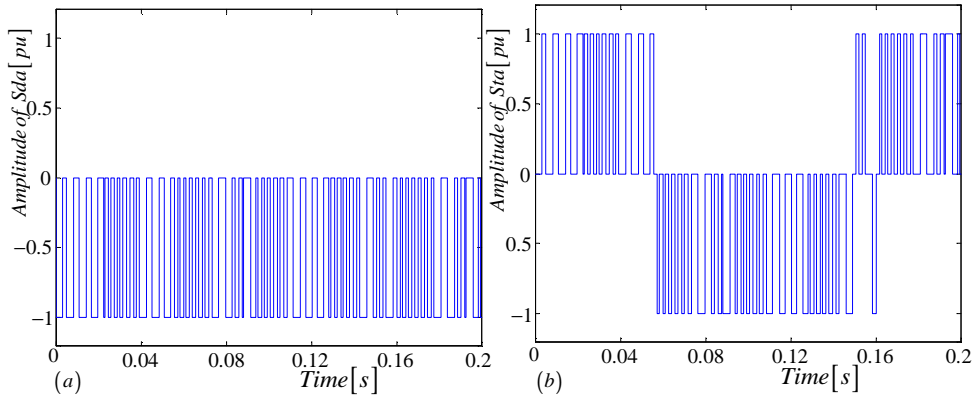


Figure 6.21: (a) Switching functions of $s_{da}(t)$ and (b) $s_{ta}(t)$ in time domain for reference voltage vector in regions A and B

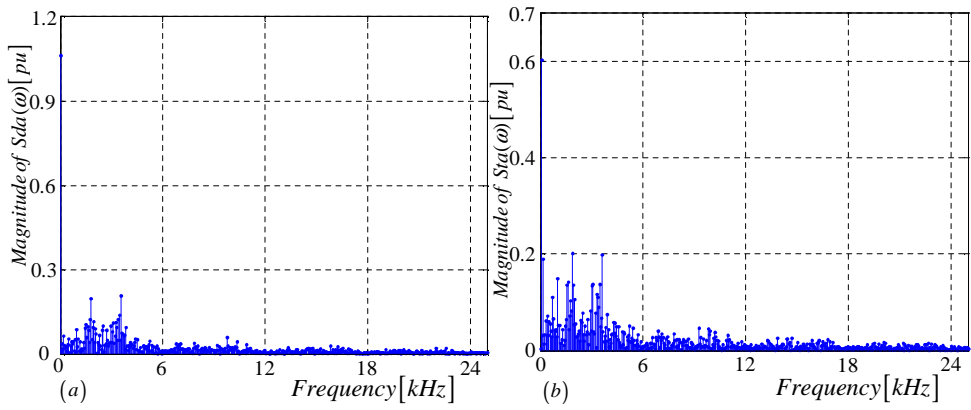


Figure 6.22: (a) Harmonics of $S_{da}(\omega)$ and (b) $S_{ta}(\omega)$ for reference voltage vector in regions A and B

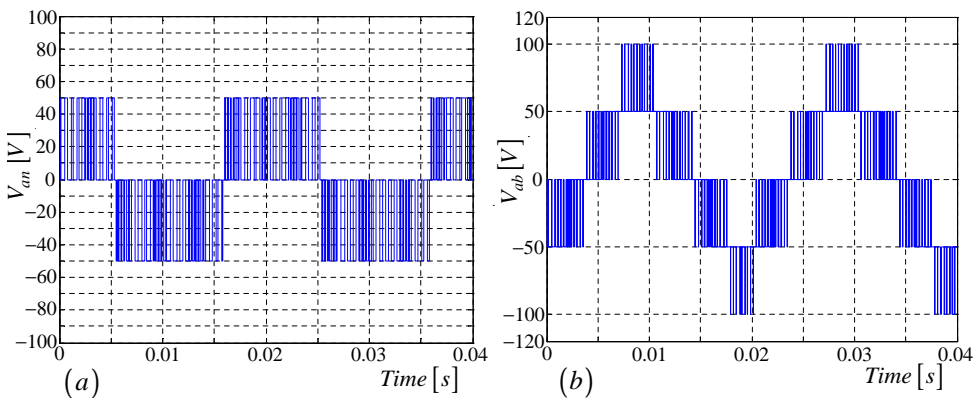


Figure 6.23: (a) Phase voltage and (b) Line voltage for reference voltage vector in region B

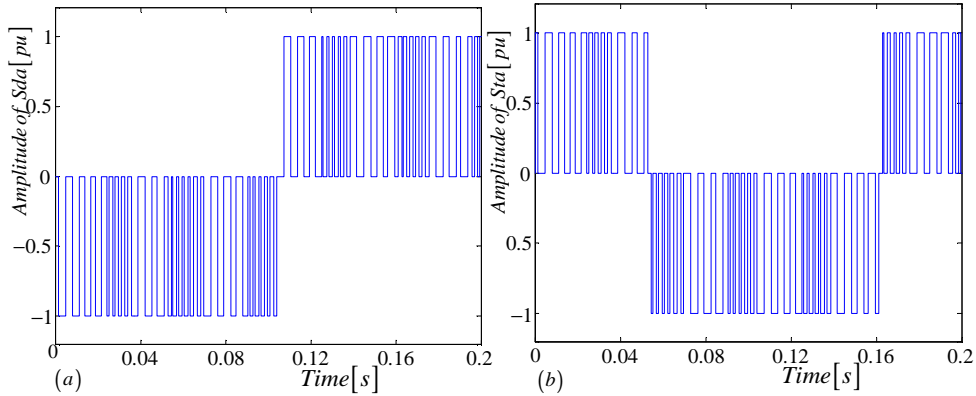


Figure 6.24: (a) Switching functions of $s_{da}(t)$ and (b) $s_{ta}(t)$ in time domain for reference voltage vector in regions B

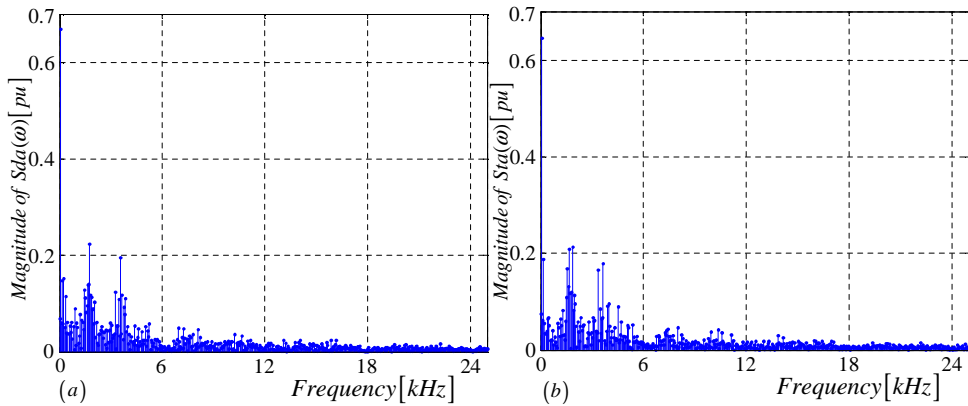


Figure 6.25: (a) Harmonics of $S_{da}(\omega)$ and (b) $S_{ta}(\omega)$ for reference voltage vector in regions B

Figures 6.26 and 6.27 depict the natural balancing of capacitor voltages of the 2-cell multicell converter for voltage vectors in region A, region B, region A and B, region C, B and D and region C and D respectively. The red curves signify results obtained using the exponential decay equation $\mathbf{V}_\delta = \mathbf{V}_{\delta 0} e^{-\frac{1}{6C_d} \Lambda t}$, derived and given by equation 5.10 in chapter 5 with the Matlab package. The blue curves represent the exponential decay of the difference capacitor voltages \mathbf{V}_δ , obtained using the Simplorer package.

The above results demonstrate that cell capacitor voltages of the 2-cell three-phase multicell converter balance naturally under space vector modulation. However the addition of a balancing circuit did not make a significant difference to the exponential decay of \mathbf{V}_δ . When the reference voltage vector is in regions C and D, the capacitor voltage difference \mathbf{V}_δ did not exponentially decay to zero when using Simplorer simulation.

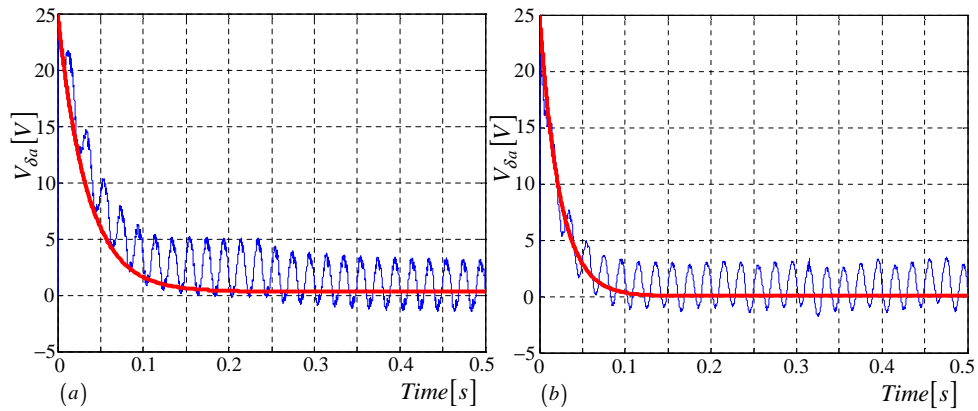


Figure 6.26: Natural balancing for reference voltage vector (a) in region A and (b) in region B.

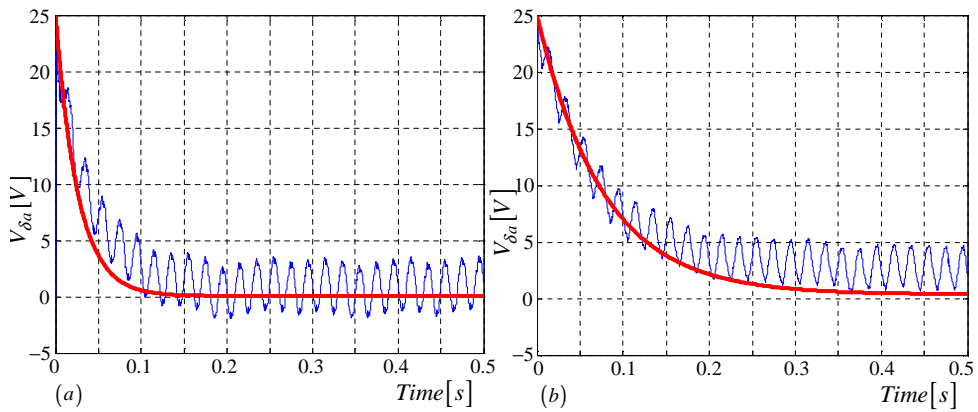


Figure 6.27: Natural balancing for reference voltage vector (a) in regions A and B and (b) in in regions C, B and D

6.5 Summary

In this chapter we studied simulations of a 2-cell multicell converter under space-vector modulation. We derived the duty cycles of each region for the six sectors and then derived the switch combination sequence for the nearest three vectors in each region. Furthermore we plotted graphs for the reference voltage vector in different regions. The phase and line voltage were shown using Simplorer simulation. Furthermore we observed that the behaviour of the switching functions is in agreement with the theory developed in chapter 3. Then we proved using Simplorer and Matlab simulations that the 2-cell multicell converter naturally balances under space vector modulation.

Chapter 7

Summary and Conclusions

This chapter furnishes a summary of contributions made in this dissertation. It also identifies possible future work to be done.

7.1 Contributions and conclusions from this study

- In Chapter 3, the 2-cell and 3-cell multicell topologies were modelled. These multicell converters were modelled using two-port circuit to obtain their equivalent topology in the d and t parameters. The resulting model forms the basis for the analysis done in Chapters 4 and 5.
- The switching functions were analysed using interleaved switching. The technique uses geometric mathematical model and double Fourier series to calculate the magnitude and phase of the harmonics of the switched waveforms. Different examples were used to demonstrate the generation of this switching for all frequency modulation ratio $m_f \in \mathbf{Z}$. A procedure was developed, that helped to represent the background functions for phase B and C after the $\frac{T_0}{3}$ and $\frac{2T_0}{3}$ phase-shift respectively. This helped in employing the Fourier coefficients calculated for the single-cell converter as shown in Appendix A.
- The phasor representation for the three-phases were done for all frequency modulation ratio $m_f \in \mathbf{Z}$. The derivation of these phasor diagrams is illustrated in detail in Appendix C. Observations from the phasor diagrams are shown in Tables 3.2, 3.3, 3.4, 3.8, 3.9, 3.10, 3.11, 3.12, 3.13 and 3.14. They demonstrate that the product of the magnitude of the difference function and the total function will be zero for all $m_f \in \mathbf{Z}$.
- To validate the theory developed in Chapter 3, the harmonics of the switching functions obtained using the theoretical results were compared with the harmonics when using simulations. The first simulation was done using Simplorer package

and the second simulation using Newton-Raphson theory which is studied in detail in Appendix B. The amplitude and phase spectrum from the three sources were found to be in agreement. The different classes of harmonics are further applied in Chapter 4.

- The coefficients of the switching functions were modelled to obtain the steady-state behaviour of the 2-cell and 3-cell three-phase multicell converters. From the derived equations the factors affecting the natural balancing of 2-cell and 3-cell converter were obtained. Also it was demonstrated using examples, the factors that cause imbalance in the cell capacitor voltages.
- Using the theory of linear systems of differential equations and the DC-component of the cell capacitor current calculated in Chapter 4, the voltage difference in terms of the eigenvalues and time constants is obtained. The exponential decay of this voltage difference is generated using both theory and simulations. It is observed that when the balancing circuit is connected, the capacitor voltage difference decays faster.
- Natural balancing of the 2-cell multicell converter is also studied under space vector modulation. The switch combination sequences of the 2-cell multicell converter is computed using duty cycles of different sectors and waveforms of the reference vector when in different regions of the six sectors is plotted.
- For the simulation setup, the switching state combination that balance the charges that pass through the cell capacitor is used. The four combinations are shown in Appendix D. The exponential decay of the capacitor voltage difference is shown for different positions of the reference voltage vector.

7.2 Conclusion

This work has established that 2-cell and 3-cell multicell converters balance naturally under interleaved switching. The factors influencing this balance and conditions under which the converter does not balance are stated in Chapter 4. Furthermore it was established that the 2-cell multicell converter balances under space vector modulation.

7.3 Future Work

Natural balancing has been developed for 2-cell and 3-cell multicell converters under interleaved switching. Simulations have been carried out for 2-cell multicell converters under space vector modulation. Future work to be done include the theoretical and

experimental analysis of the p-cell multicell converter under space vector modulation. Though much research has been done as regards the natural balancing of p-cell single and three phase converters, there is still the opportunity to extend this theory to cover p-cell three-phase multicell converters.

Bibliography

Textbooks

- [1] J Arrillaga, Y. H. Liu and N. R. Watson, *Flexible Power Transmission* John Wiley and sons,Inc., 2007.
- [2] H. S. Black, *Modulation theory*, New York: Van Nostrand, pp. 263-281, 1953.
- [3] L. Perko, *Differential Equations and Dynamical Systems*, Springer-Verlag Inc, New York, pp.16,17, 1991.
- [4] P. Hartman, *Ordinary Differential Equations*, Birkhäuser, Boston, pp.57-61, 1982.
- [5] M. W. Hirsch and S. Smale, *Differential Equations, Dynamic Systems and Linear Algebra*, Academic Press, New York, pp.51,89,90, 1974.
- [6] R. J. Beerends, H. G. ter Morsche, J. C. van den Berg and E. M. van de Vrie, *Fourier and Laplace Transforms*, Cambridge University Press, pp. 78, 2003.
- [7] D. G. Holmes and T. A. Lipo, *Pulse width modulation for power converters*, IEEE Press, 2003.
- [8] N. Mohan, T. M. Undeland and W. P. Robbins, *Power Electronics*, John Wiley and sons,Inc., Second Edition, pp. 200-245, 1995.
- [9] J. W. Nilsson and S. A. Riedel, *Electric Circuits*, Prentice Hall, Sixth Edition, pp. 719-722, 2000.
- [10] I. S. Gradshteyn and I. M. Ryzhik, *Tables of Integrals, Series, and Products*, Alan Jeffrey, Fifth Edition, pp. 942-1003, 1994.
- [11] F. Oberhettinger, *Tables of Bessel Transforms*, Springer, pp. 279-281, 1972.
- [12] J. Stewart, *Calculus*, Thomson Brooks/Cole, Fifth Edition, pp. 294-295, 2003.

Journal articles

- [13] A. Nabae, I. Takahashi, and H. Akagi, "A new neutral-point-clamped PWM inverter," *IEEE Trans. Ind. App.*, vol. IA-17, no. 5, pp. 518-523, Sept./Oct. 1981.
- [14] J. S. Lai and F. Z. Peng, "Multilevel converters - A new breed of power converters," *IEEE Trans. Ind. App.*, vol. 32, no. 3, pp. 509-517, May/June 1996.
- [15] J. Rodriguez, J-S. Lai and F. Z. Peng, "Multilevel inverters: A survey of topologies, controls, and applications," *IEEE Trans. Ind. Applications*, vol. 49, no. 4, pp. 724-738, August 2002.
- [16] L. M. Tolbert, F. Z. Peng, T. Cunnyngham and J. N. Chiasson, "Charge balance control schemes for cascade multilevel converter in hybrid electric vehicles," *IEEE Trans. Ind. Electron.*, vol. 49, no. 5, pp. 1058-1064, Oct. 2002.
- [17] L. Gyuyai, "Dynamic compensation of AC transmission lines by solid-state synchronous voltage sources," *IEEE Trans. on Power Delivery*, vol. 9, no. 2, April 1994, pp. 904-911.
- [18] A. van Zyl, J. H. R. Enslin, R. Spee, "A new unified approach to power quality management," *IEEE Trans. on Power Electron.*, vol. 11, no. 5, Sept. 1996, pp. 691-697.
- [19] R. Rojas, T. Ohnishi, and T. Suzuki, "An improved voltage vector control method for neutral-point-clamped inverters," *IEEE Trans. Power Electron.*, vol. 10, no. 6, pp. 666-672, Nov. 1995.
- [20] R. Rojas, T. Ohnishi, and T. Suzuki, "Neutral-point-clamped inverter with improved voltage waveform and control range," *IEEE Trans. Power Electron.*, vol. 42, no. 6, pp. 587-594, Dec. 1995.
- [21] G. Carrara, S. Gardella, M. Marchesoni, R. Salutari and G. Sciutto, "A new multilevel PWM method: A Theoretical Analysis," *IEEE Trans. Power Electron.*, vol. 7, no. 3, pp. 497-505, July 1992.
- [22] G. C. Cho, G. H. Jung, N. S. Choi, and G. H. Cho, "Analysis and controller design of static var compensator using three-level GTO inverter," *IEEE Trans. Power Electron.*, vol. 11, no. 1, pp. 57-65, Jan. 1996.
- [23] N. Celanovic and D. Boroyevich, "A comprehensive study of neutral-point voltage balancing problem in three-level neutral-point-clamped voltage source PWM inverters," *IEEE Trans. Power Electron.*, vol. 15, no. 2, pp. 242-249, March 2000.
- [24] T. A. Meynard, M. Fadel and N. Aouda, "Modeling of multilevel converters," *IEEE Trans. Ind. Elec.*, vol. 44, no. 3, pp. 356-364, June 1997.

- [25] H. du T. Mouton, "Natural balancing of three-level neutral-point-clamped PWM inverters," *IEEE Trans. Ind. Electron.*, vol. 49, no. 5, pp. 1017-1025, Oct. 2002.
- [26] X. Yuan, H. Stemmler and I. Barbi, "Self-balancing of the clamping-capacitor-voltages in the multilevel capacitor-clamping-inverter under sub-harmonic PWM modulation," *IEEE Trans. on Power Electron.*, vol. 16, No. 2, pp. 256-263.
- [27] B. P. McGrath, D. G. Holmes, "Analytical modelling of voltage balance dynamics for a flying capacitor multilevel converter," *IEEE Trans. on Power Electron.*, vol. 23, no. 2, March 2008, pp. 543-550.
- [28] B. P. McGrath, D. G. Holmes, "Natural current balancing of multicell current source converters," *IEEE Trans. on Power Electron.*, vol. 23, no. 3, May 2008, pp. 1239-1246.
- [29] B. P. McGrath, D. G. Holmes, "Natural capacitor voltage balancing for a flying capacitor converter induction motor drive," *IEEE Trans. on Power Electron.*, vol. 24, no. 6, June 2009, pp. 1554-1561.
- [30] R. Wilkinson, H. du T. Mouton and T. Meynard, "Natural balance of multicell converters: The two-cell case," *IEEE Trans. Power Electron.*, vol. 21, no. 6, pp. 1649-1657, Nov. 2006.
- [31] R. Wilkinson, H. du T. Mouton and T. Meynard, "Natural balance of multicell converters: The general case," *IEEE Trans. Power Electron.*, vol. 21, no. 6, pp. 1658-1666, Nov. 2006.
- [32] W. R. Bennet, "New results in the calculation of modulation products," *Bell Sytems Technical Journal*, vol. 12, pp. 228-243, 1933.
- [33] B.P. McGrath, D.G. Holmes, An analytical technique for the determination of spectral components of multilevel carrier-based PWM methods, *IEEE Trans. on Ind. Electronics*, vol. 49, no. 4, pp. 847-857, August 2002.
- [34] J. Kuang, B. T. Ooi, "Series connected voltage-source converter modules for force commuted SVC and DC-transmission," *IEEE Trans. Power Deliv.*, vol. 9, no. 2, pp. 977-983, April 1994.
- [35] B. Mwinyiwiwa, Z. Wolanski, and B. T. Ooi, "Microprocessor-implemented SPWM for multiconverters with phase-shifted triangle carriers," *IEEE Trans. Ind. App.*, vol. 34, no. 3, pp. 487-494, May/June 1998.
- [36] B. P. McGrath and D. G. Holmes, "Optimised space vector switching sequence for multilevel inverters," *IEEE Trans. Power Electron.*, vol.18, no. 6, pp. 1293-1301, Nov. 2003.

- [37] C. A. Martins, X. Roboam, T. A. Meynard and A. S. Carvalho, "Switching frequency imposition and ripple reduction in DTC drives by using a multilevel converter," *IEEE Trans. Power Electron.*, vol. 17, no. 2, March 2002.
- [38] H. L. Liu and G. H. Cho, "Three-level space vector PWM in low index modulation region avoiding narrow pulse problem," *IEEE Trans. Power Electron.*, vol. 9, no. 5, pp. 481-487, Sept. 1994.
- [39] Y. H. Lee, B. S. Suh and D. S. Hyun, "A novel PWM scheme for a three-level voltage source inverter with GTO thyristors," *IEEE Trans. Ind. App.*, vol. 32, no. 2, pp. 260-268, March/April 1996.
- [40] J. Steinke, "Switching frequency optimal PWM control of a three-level inverter," *IEEE Trans. Power Electron.*, vol. 7, no. 3, pp. 487-496, July 1992.
- [41] J. Hamman and F. S. Van der Merwe, "Voltage harmonics generated by voltage-fed inverters using PWM natural sampling," *IEEE Trans. Power Electron.*, vol. 3, no. 3, pp. 297-302 July 1988.
- [42] H. W. Van der Broeck, H. C. Skudelny and G. V. Stanke, "Analysis and realization of a pulsewidth modulator based on voltage space vectors," *IEEE Trans. on Industrial Applications*, vol. 24, no. 1, pp. 142-150, Jan./Feb. 1988.
- [43] W. R. Bennett, "New results in the calculation of modulation products," *Bell syst. Tech.J.*, vol. 12, pp. 228-243, 1933.
- [44] D. Zhou, "A self-balancing space vector switching modulator for three-level motor drives," *IEEE Trans. Power Electron.*, vol. 17, no. 6, pp. 1024-1031, Nov.2002.
- [45] S. Fukuda, "Optimal-regulator-based control of NPC boost rectifiers for unity power factor and reduced neutral-point-potential variations," *IEEE Trans. Ind. Electron.*, vol. 46, no. 3, pp. 527-534, June 1999.
- [46] K. Zhou and D. Wang, "Relationship between space-vector modulation and three-phase carrier-based PWM: A comprehensive analysis," *IEEE Trans. Ind. Electron.*, vol. 49, no. 1, pp. 186-196, Feb. 2002.
- [47] H. Akagi, Y. Kanazawa and A. Nabae, "Instantaneous reactive power compensators comprising switching devices without energy storage components," *IEEE Trans. Ind. App.*, vol. 20, no. 3, pp. 625-630, May/June 1984.
- [48] N. Celanovic and D. Boroyevich, "A fast space-vector modulation algorithm for multilevel three-phase converters," *IEEE Trans. Ind. App.*, vol. 37, no. 2, March/April 2001.

- [49] F. Wang, "Sine-triangle vs space vector modulation for three-level pwm voltage source inverters," *IEEE Trans. Ind. App.*, vol. 38, no. 2, March/April 2002, pp. 500-506.

Conference papers

- [50] T. A. Meynard and H. Foch, "Multi-level conversion: high voltage choppers and voltage-source inverters," *IEEE PESC'92 Conf. Proc.*, Toledo, Spain, pp. 397-403, June 1992.
- [51] L. M. Tolbert, F. Z. Peng, "Multilevel Converters as a Utility Interface for Renewable Energy System," *IEEE Power Engineering society Summer Meeting*, vol. 2, pp. 1271-1274, 2000.
- [52] C. Hochgraf, R. Lasseter, D. Divan, and T. A. Lipo, "Comparison of multilevel inverters for static var compensation," in *Conf. Rec. IEEE-IAS Annu. Meeting*, pp. 921-928, Oct. 1994.
- [53] C. Hochgraf and R. H. Lasseter, "A transformer-less static synchronous compensator employing a multi-level inverter," *IEEE PES Meeting*, pp. 1-7, July28-Aug.1 1996.
- [54] L. Gyuayi, "Application characteristics of converter-based Facts controllers," *Proc. IEEE*, vol. 76, no. 4, pp. 483-493.
- [55] B. P. McGrath and D. G. Holmes, "A Comparison of Multicarrier PWM Strategies for Cascaded and Neutral Point Clamped Multilevel Inverters," *IEEE PESC'2000 Conf. Proc.*, pp. 674-679, 2000.
- [56] I. M. Salagae and H. du T. Mouton, "Natural balancing of the neutral-point-clamped converters under POD modulation," *IEEE PESC'03 Conf. Proc.*, Acapulco, Mexico, pp.47-52, June 2003.
- [57] B. P. McGrath, D. G. Holmes, "Analytical determination of the capacitor voltage balancing dynamics for three phase flying capacitor converters," *Proc. IEEE Industry Applications Society(IAS) Annual Meeting*, pp. 1974-1981, 2007.
- [58] A. Ruderman, B. Reznikov and M. Margaliot, "Analysis of a flying capacitor converter: A switched systems approach," *13th International Power Electronics and Motion Control Conference*, vol. 49, no. 4, pp. 260-267, September 2008.
- [59] B. P. McGrath, D. G. Holmes, "Natural capacitor voltage balancing for a flying capacitor converter induction motor drive," *Proc. IEEE PESC*, pp. 1681-1687, June 2008.

- [60] S. R. Bowes and B. M. Bird, "Novel approach to the analysis and synthesis of modulation processes in power converters," *Proc. IEE*, vol. 122, no. 5, pp. 507-513, May 1975.
- [61] S. R. Bowes, "New sinusoidal pulsewidth-modulated inverter," *Proc. IEE*, vol. 122, no. 11, pp. 1279-1285, Nov. 1975.
- [62] D. G. Holmes, "A General Analytical Method for Determining the Theoretical Harmonic Components of Carrier Based PWM Strategies," in *Conf. Rec. IEEE-IAS Annu. Meeting*, pp. 1207-1214, 1998.
- [63] J. F. Moynihan, M. G. Egan and J. M. D. Murphy, "Theoretical spectra of space-vector-modulated waveforms," *IEE Proc.-Electr. Power Appl.*, vol. 145, no. 1, pp. 17-24, Jan. 1998.
- [64] J. T. Boys and P. G. Handley, "Harmonic analysis of space vector modulated PWM waveform," *IEE Proc.*, vol. 137, no. 4, pp. 197-204, July 1990.
- [65] A. von Jouanne, S. Dai and H. Zhang, "A simple method for balancing the DC-link voltage of three-level inverters," *IEEE PESC'2001 Conf. Proc.*, pp. 1341-1345, June 2001.
- [66] H. Akagi, Y. Kanazawa and A. Nabae, "Generalized theory of the instantaneous reactive power in three-phase circuits," *IPEC'83-Int. Power Electronics Conf.*, Tokyo, Japan, pp. 1375-1386, 1983.
- [67] M. A. S. Mendes, Z. M. A. Peixoto, P. Donoso-Garcia and A. M. N. Lima, "A space vector pwm method for three-level flying-capacitor inverters," *Proc. IEEE PESC*, pp. 182-187, June 2001.
- [68] J. Holtz, "Pulsewidth modulation for electronic power conversion," *Proc. of the IEEE*, vol. 82, no. 8, pp. 1194-1214, Aug. 1994.
- [69] S. J. Watkins and L. Zhang, "Multilevel space vector pwm control schemes for a flying-capacitor inverter," *Proc. PEMD 2nd Int. Conf.*, Edinburg, UK, vol. 1, pp. 12-17, March/April 2004.

Dissertations

- [70] S. Sirisukprasert, "The Modeling and control of a Cascaded-Multilevel Converter-Based STATCOM," PhD thesis, Virginia Polytechnic Institute and State University, Virginia, February 2004.

- [71] H. du T. Mouton, "Analysis and synthesis of a 2 MVA series-stacked power-quality conditioner," PhD thesis , University of Stellenbosch, Stellenbosch, December 1999.
- [72] I. M. Salagae, "Natural balancing of the neutral-point-clamped converter," MSc thesis, University of Stellenbosch, Stellenbosch, December 2003.
- [73] R.W. Wilkinson, "Natural Balancing of Multicell Converters," PhD thesis, University of Stellenbosch, Stellenbosch, April 2004.

Appendix A

Fourier Coefficients

A.1 Fourier Coefficients Calculations

The calculation of Fourier Coefficients for single-cell converter was done in [73]. We summarise the derivation here since we will be using it in chapter 3.

Equation A.1 is used in calculating the double Fourier series coefficients:

$$A_{mn} + jB_{mn} = \frac{\omega_0}{4\pi} \int_0^{\frac{2\pi}{\omega_0}} \int_{-1}^3 F(h, t) e^{j(\frac{m\pi h}{2} + n\omega_0 t)} dh dt \quad (\text{A.1})$$

Figure A.1 is used in aiding the calculation of the double Fourier series coefficients of interleaved switching for sinusoidal modulation.

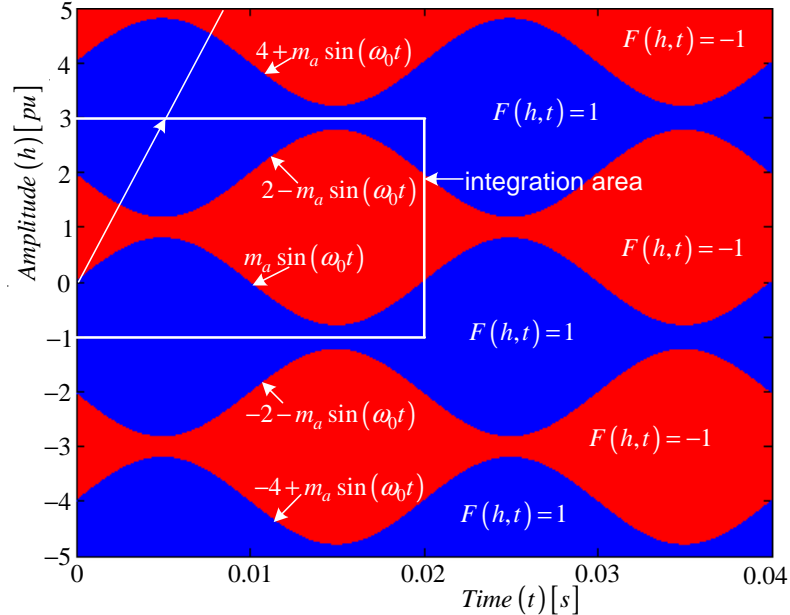


Figure A.1: Generation of interleaved switching single-cell multicell converter

Using the area of integration shown in Figure A.1, a sinusoidal reference of the

following form:

$$f_r = m_a \sin \omega_0 t \quad (\text{A.2})$$

with modulation index of m_a and frequency of ω_0 , equation A.1 can be written as follows:

$$\begin{aligned} A_{mn} + jB_{mn} &= \frac{\omega_r}{4\pi} \int_0^{\frac{2\pi}{\omega_0}} \int_{-1}^3 F(h, t) e^{j(\frac{m\pi h}{2} + n\omega_0 t)} dh dt \\ &= \frac{\omega_r}{4\pi} \int_0^{\frac{2\pi}{\omega_0}} \left\{ \int_{-1}^{m_a} (1) e^{j\frac{m\pi h}{2}} dh + \int_{m_a \sin \omega_0 t}^{2-m_a \sin \omega_0 t} (-1) e^{j\frac{m\pi h}{2}} dh \right. \\ &\quad \left. + \int_{2-m_a \sin \omega_0 t}^3 (1) e^{j\frac{m\pi h}{2}} dh \right\} e^{jn\omega_0 t} dt \end{aligned} \quad (\text{A.3})$$

This equation is calculated for two cases:

- Case 1: $m \neq 0$

$$\begin{aligned} A_{mn} + jB_{mn} &= \frac{2\omega_0}{4jm\pi^2} \int_0^{\frac{2\pi}{\omega_0}} \left\{ e^{j\frac{m\pi}{2}(m_a \sin \omega_0 t)} - e^{j\frac{m\pi}{2}} - e^{j\frac{m\pi}{2}(2-m_a \sin \omega_0 t)} + e^{j\frac{m\pi}{2}(m_a \sin \omega_0 t)} \right. \\ &\quad \left. + e^{j\frac{3m\pi}{2}} - e^{j\frac{m\pi}{2}(2-m_a \sin \omega_0 t)} \right\} e^{jn\omega_0 t} dt \\ &= \frac{\omega_0}{jm\pi^2} \int_0^{\frac{2\pi}{\omega_0}} \left\{ e^{j\frac{m\pi}{2}m_a \sin \omega_0 t + jn\omega_0 t} - e^{j\frac{m\pi}{2}(2-m_a \sin \omega_0 t) + jn\omega_0 t} \right\} \end{aligned} \quad (\text{A.4})$$

Let $\theta = \omega_0 t$, thus $d\theta = \omega_0 dt$, $dt = \frac{1}{\omega_0} d\theta$. At $t = \frac{2\pi}{\omega_0}$, $\theta = 2\pi$. Changing the variables in A.4 we obtain the following:

$$A_{mn} + jB_{mn} = \frac{1}{jm\pi^2} \int_0^{2\pi} \left(e^{j\frac{m\pi}{2}m_a \sin \theta + jn\theta} - e^{j\frac{m\pi}{2}(2-m_a \sin \theta) + jn\theta} \right) d\theta \quad (\text{A.5})$$

To change the boundaries of the integrals, we make this substitution: $\phi = \theta - \pi$ and $d\phi = d\theta$. The integration boundaries change as follows:

$$\phi = \begin{cases} -\pi & \text{if } \theta = 0 \\ \pi & \text{if } \theta = 2\pi \end{cases} \quad (\text{A.6})$$

Substituting the above variable into equation A.5 results in the following:

$$\begin{aligned} A_{mn} + jB_{mn} &= \frac{1}{jm\pi^2} \int_{-\pi}^{\pi} \left(e^{j\frac{m\pi}{2}m_a \sin(\phi+\pi) + jn(\phi+\pi)} - e^{j\frac{m\pi}{2}(2-m_a \sin(\phi+\pi)) + jn(\phi+\pi)} \right) d\phi \\ &= \frac{1}{jm\pi^2} \int_{-\pi}^{\pi} \left(e^{j\frac{m\pi}{2}(-m_a \sin \phi) + jn(\phi+\pi)} - e^{-j\frac{m\pi}{2}(2+m_a \sin \phi) + jn(\phi+\pi)} \right) d\phi \\ &= \frac{1}{jm\pi^2} \int_{-\pi}^{\pi} \left(e^{jn\pi} e^{-j\frac{m\pi}{2}m_a \sin \phi + jn\phi} - e^{j(m+n)\pi} e^{j\frac{m\pi}{2}m_a \sin \phi + jn\phi} \right) d\phi \end{aligned} \quad (\text{A.7})$$

Equation A.7 can be written in terms of Bessel functions of the first kind using the following properties:

$$J_n(x) = \frac{1}{2\pi} \int_{-\pi}^{\pi} e^{j(x \sin y - ny)} dy \quad (\text{A.8})$$

$$J_n(-x) = (-1)^n J_n(x) \quad (\text{A.9})$$

$$J_{-n}(x) = (-1)^n J_n(x) \quad (\text{A.10})$$

Using the Bessel functions properties listed in A.8 to A.10, equation A.7 can be written as follows:

$$\begin{aligned} A_{mn} + jB_{mn} &= \frac{2}{jm\pi} \left(e^{jn\pi} J_{-n} \left(-\frac{m\pi m_a}{2} \right) - e^{j(m+n)\pi} J_{-n} \left(\frac{m\pi m_a}{2} \right) \right) \\ &= \frac{2}{jm\pi} \left(e^{jn\pi} (-1)^n J_n \left(-\frac{m\pi m_a}{2} \right) - e^{j(m+n)\pi} (-1)^n J_n \left(\frac{m\pi m_a}{2} \right) \right) \\ &= \frac{2}{jm\pi} \left(e^{jn\pi} (-1)^n (-1)^n J_n \left(\frac{m\pi m_a}{2} \right) - e^{j(m+n)\pi} (-1)^n J_n \left(\frac{m\pi m_a}{2} \right) \right) \\ &= \frac{2}{jm\pi} J_n \left(\frac{m\pi m_a}{2} \right) (e^{jn\pi} - e^{jm\pi + jn\pi} (-1)^n) \end{aligned} \quad (\text{A.11})$$

If n is odd, equation A.11 can be simplified as follows:

$$\begin{aligned} A_{mn} + jB_{mn} &= \frac{2}{jm\pi} J_n \left(\frac{m\pi m_a}{2} \right) (e^{jn\pi} - e^{jm\pi + jn\pi} (-1)^n) \\ &= \frac{2}{jm\pi} J_n \left(\frac{m\pi m_a}{2} \right) (-1 + e^{jm\pi} (-1)) \\ &= \frac{2j}{m\pi} J_n \left(\frac{m\pi m_a}{2} \right) (1 + e^{jm\pi}) \end{aligned} \quad (\text{A.12})$$

If n is even, equation A.11 can be simplified as follows:

$$\begin{aligned} A_{mn} + jB_{mn} &= \frac{2}{jm\pi} J_n \left(\frac{m\pi m_a}{2} \right) (e^{jn\pi} - e^{jm\pi + jn\pi} (-1)^n) \\ &= \frac{2}{jm\pi} J_n \left(\frac{m\pi m_a}{2} \right) (1 - e^{jm\pi} (1)) \\ &= \frac{2}{jm\pi} J_n \left(\frac{m\pi m_a}{2} \right) (1 - e^{jm\pi}) \end{aligned} \quad (\text{A.13})$$

- Case 2: $m = 0$

$$A_{0n} + jB_{0n} = \frac{\omega_0}{4\pi} \int_0^{\frac{2\pi}{\omega_0}} \int_{-1}^3 F(h, t) e^{j\left(\frac{m\pi h}{2}\right) + n\omega_0 t} dh dt$$

$$\begin{aligned}
&= \frac{\omega_0}{4\pi} \int_0^{\frac{2\pi}{\omega_0}} \left\{ \int_{-1}^{m_a \sin \omega_0 t} (1) dh + \int_{m_a \sin \omega_0 t}^{2-m_a \sin \omega_0 t} (-1) dh \right. \\
&\quad \left. + \int_{2-m_a \sin \omega_0 t}^3 (-1) dh \right\} e^{jn\omega_0 t} dt \\
&= \frac{\omega_0}{4\pi} \int_0^{\frac{2\pi}{\omega_0}} m_a \sin(\omega_0 t) e^{jn\omega_0 t} dt
\end{aligned} \tag{A.14}$$

Let $\theta = \omega_0 t$, thus $d\theta = \omega_0 dt$. The boundary values change as follows:

$$\phi = \begin{cases} -\pi & \text{if } \theta = 0 \\ \pi & \text{if } \theta = 2\pi \end{cases} \tag{A.15}$$

Substituting the above boundary values into equation A.14 results in the following:

$$A_{0n} + jB_{0n} = \frac{1}{\pi} \int_0^{2\pi} m_a \sin \theta e^{jn\theta} d\theta \tag{A.16}$$

If $n = 1$:

$$\begin{aligned}
A_{01} + jB_{01} &= \frac{1}{\pi} \int_0^{2\pi} m_a \sin \theta e^{j\theta} d\theta \\
&= \frac{m_a}{\pi} \int_0^{2\pi} \frac{1}{2j} (e^{j\theta} - e^{-j\theta}) e^{j\theta} d\theta \\
&= \frac{m_a}{\pi} \left[\int_0^{2\pi} \frac{1}{2j} e^{j\theta} d\theta - \int_0^{2\pi} \frac{1}{2j} d\theta \right] \\
&= jm_a
\end{aligned} \tag{A.17}$$

- For odd values of both n and m :

$$A_{mn} + jB_{mn} = \frac{2j}{m\pi} J_n \left(\frac{m\pi m_a}{2} \right) (1 + e^{jm\pi}) = 0 \tag{A.18}$$

- For even values of both n and m :

$$A_{mn} + jB_{mn} = \frac{2}{jm\pi} J_n \left(\frac{m\pi m_a}{2} \right) (1 - e^{jm\pi}) = 0 \tag{A.19}$$

The coefficients are summarised as follows:

- $m \neq 0$ and n odd:

$$A_{mn} + jB_{mn} = \frac{2j}{m\pi} J_n \left(\frac{m\pi m_a}{2} \right) (1 + e^{jm\pi}) \tag{A.20}$$

- $m \neq 0$ and n even:

$$A_{mn} + jB_{mn} = \frac{2}{jm\pi} J_n \left(\frac{m\pi m_a}{2} \right) (1 - e^{jm\pi}) \tag{A.21}$$

- $m = 0$ and $n = 1$:

$$A_{01} + jB_{01} = jm_a \quad (\text{A.22})$$

- $m = 0$ and $n \neq 0$:

$$A_{0n} + jB_{0n} = 0 \quad (\text{A.23})$$

A.2 Properties of Fourier Coefficients

- When $m \neq 0$ equation A.1 can be rewritten as follows:

$$\begin{aligned} A_{mn} + jB_{mn} &= \frac{\omega_0}{2\pi} \int_0^{\frac{2\pi}{\omega_0}} \int_{-f_r}^{f_r} e^{j(m\pi h + jn\omega_0 t)} dh dt \\ &= \frac{\omega_0}{2\pi} \int_0^{\frac{2\pi}{\omega_0}} \left(\int_{-f_r(t)}^{f_r(t)} e^{jm\pi h} \right) e^{jn\omega_0 t} dh dt \\ &= \frac{\omega_0}{2jm\pi^2} \int_0^{\frac{2\pi}{\omega_0}} \left(e^{jm\pi f_r(t)} - e^{-jm\pi f_r(t)} \right) e^{jn\omega_0 t} dt \\ &= \frac{\omega_0}{m\pi^2} \int_0^{\frac{2\pi}{\omega_0}} \sin(m\pi f_r(t)) e^{jn\omega_0 t} dt \end{aligned} \quad (\text{A.24})$$

- When $m = 0$ equation A.1 is written as follows:

$$\begin{aligned} A_{mn} + jB_{mn} &= \frac{\omega_0}{2\pi} \int_0^{\frac{2\pi}{\omega_0}} \int_{-f_r}^{f_r} e^{jn\omega_0 t} dh dt \\ &= \frac{\omega_0}{2\pi} \int_0^{\frac{2\pi}{\omega_0}} (f_r(t) + f_r(t)) e^{jn\omega_0 t} dh dt \\ &= \frac{\omega_0}{\pi} \int_0^{\frac{2\pi}{\omega_0}} f_r(t) e^{jn\omega_0 t} dt \end{aligned} \quad (\text{A.25})$$

Equations A.24 and A.25 play an important role in the following analysis:

1. If $m \neq 0$, then

$$\begin{aligned} |A_{mn} + jB_{mn}| &= \left| \frac{\omega_0}{m\pi^2} \int_0^{\frac{2\pi}{\omega_0}} \sin(m\pi f_r(t)) e^{jn\omega_0 t} dt \right| \\ &\leq \frac{\omega_0}{m\pi^2} \int_0^{\frac{2\pi}{\omega_0}} |\sin(m\pi f_r(t)) e^{jn\omega_0 t}| dt \\ &= \frac{\omega_0}{m\pi^2} \int_0^{\frac{2\pi}{\omega_0}} |\sin(m\pi f_r(t))| dt \\ &\leq \frac{\omega_0}{m\pi^2} \cdot \frac{2\pi}{\omega_0} \\ &= \frac{2}{m\pi} \end{aligned} \quad (\text{A.26})$$

Equation A.26 shows that $A_{mn} + jB_{mn} \rightarrow 0$ as $m \rightarrow \infty$.

2. If $m \neq 0$ and $n \neq 0$, then equation A.24 is integrated by parts as follows:

$$\begin{aligned}
 A_{mn} + jB_{mn} &= \frac{\omega_0}{m\pi^2} \int_0^{\frac{2\pi}{\omega_0}} \sin(m\pi f_r(t)) e^{jn\omega_0 t} dt \\
 &= \frac{\omega_0}{m\pi^2} \left(\left[\sin(m\pi f_r(t)) \frac{1}{jn\omega_0} e^{jn\omega_0 t} \right]_0^{\frac{2\pi}{\omega_0}} dt \right. \\
 &\quad \left. - \frac{1}{jn\omega_0} \int_0^{\frac{2\pi}{\omega_0}} e^{jn\omega_0 t} \cos(m\pi f_r(t)) m\pi \frac{df_r(t)}{dt} dt \right) \quad (\text{A.27})
 \end{aligned}$$

Since $f_r(t)$ is periodic with frequency ω_0 , the first term in equation A.27 is zero. Hence,

$$\begin{aligned}
 A_{mn} + jB_{mn} &= \left| \frac{1}{jmn\pi^2} \int_0^{\frac{2\pi}{\omega_0}} e^{jn\omega_0 t} \cos(m\pi f_r(t)) m\pi \frac{df_r(t)}{dt} dt \right| \\
 &= \left| \frac{-j}{n\pi} \int_0^{\frac{2\pi}{\omega_0}} e^{jn\omega_0 t} \cos(m\pi f_r(t)) \frac{df_r(t)}{dt} dt \right| \\
 &\leq \frac{1}{|n|\pi} \int_0^{\frac{2\pi}{\omega_0}} \left| e^{jn\omega_0 t} \cos(m\pi f_r(t)) \frac{df_r(t)}{dt} \right| dt \\
 &= \frac{1}{|n|\pi} \int_0^{\frac{2\pi}{\omega_0}} \left| \frac{df_r(t)}{dt} \right| dt \quad (\text{A.28})
 \end{aligned}$$

Since $\int_0^{\frac{2\pi}{\omega_0}} \left| \frac{df_r(t)}{dt} \right| dt$ is a constant, this shows that $|A_{mn} + jB_{mn}| \rightarrow 0$ as $n \rightarrow \infty$

3. Combining the above results gives the following expression:

$$|A_{mn} + jB_{mn}| \leq \min \left(\frac{2}{m\pi}, \frac{1}{|n|\pi} \int_0^{\frac{2\pi}{\omega_0}} \left| \frac{df_r(t)}{dt} \right| dt \right) \quad (\text{A.29})$$

Property 2 essentially means if the switching frequency is chosen significantly higher than the highest frequency harmonic of the reference function $f_r(t)$, then the harmonics of $s(t)$ appear in clusters around integer multiples of $m\omega_s$. For values of $m > 0$, the clusters consists of harmonics at frequencies of $m\omega_s + n\omega_0$, where $n = \pm 1, \pm 2, \dots$. The magnitude of the clusters of harmonics decreases as $|n|$ increases. The magnitude of the harmonics found in these clusters can be determined by $\int_0^{\frac{2\pi}{\omega_0}} \left| \frac{df_r(t)}{dt} \right| dt$. If the value of this integral is small, then the magnitude of the side-band harmonics attenuates quickly as n increases and these side bands do not overlap with neighbouring clusters.

Appendix B

Newton-Raphson Simulation

B.1 Theoretical Background

B.1.1 Newton Raphson Theory

In this subsection we show the Newton Raphson method for finding the root of a function [12]. Figure B.1 show the geometry behind the Newton Raphson method.

Our first approximation for the root r is x_1 which is obtained by guessing. The tangent

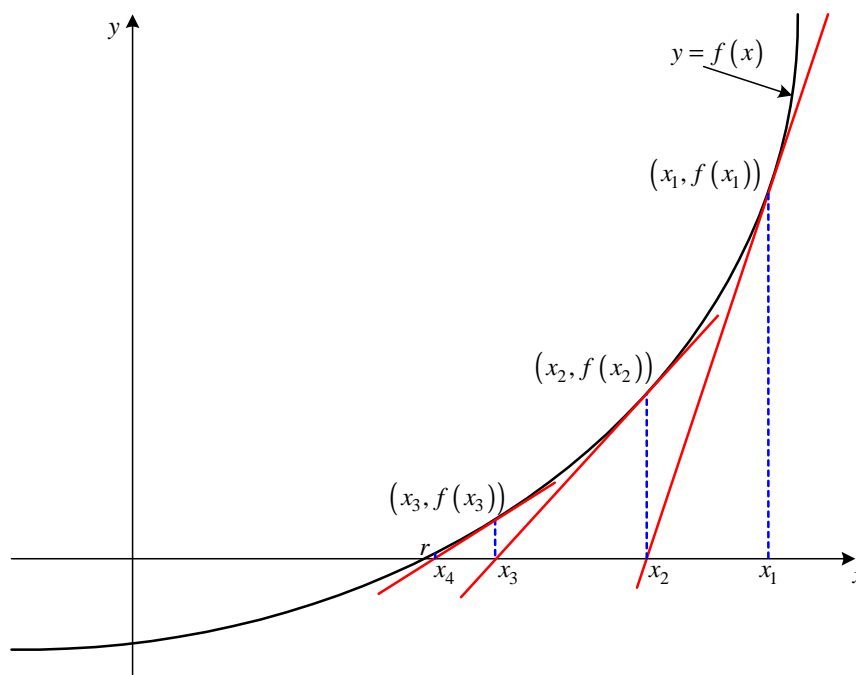


Figure B.1: *Geometry behind Newton Raphson method*

line of $y = f(x)$ in Figure B.1 at $(x_1, f(x_1))$ has x_2 as its x-intercept. The idea is that the tangent line is close to the curve and thus its x-intercept, x_2 is close to the x-intercept of

the curve, that the root of the function. From Figure B.1 we have:

$$x_2 = x_1 - \frac{f(x_1)}{f'(x_1)} \quad (\text{B.1})$$

Continuing with this process we obtain the third approximation x_3 given by:

$$x_3 = x_2 - \frac{f(x_2)}{f'(x_2)} \quad (\text{B.2})$$

This process when repeated will generate a sequence of numbers $\{x_n\}$ which approximates r . In general if x_n is the n th approximation and $f'(x_n) \neq 0$, then the next approximation is given by:

$$x_{n+1} = x_n - \frac{f(x_n)}{f'(x_n)} \quad (\text{B.3})$$

B.1.2 Shift in time

The following theorem can be found in [6] and we use it in sections B.2 and B.3 for calculating Fourier transform of the pwm over multiple of cycles of the switching period.

Theorem Shift in time

When c_n are the Fourier coefficients of $f(t)$, then

$$f(t - t_0) \leftrightarrow e^{-jn\omega_0 t_0} c_n$$

Proof

The coefficients of $f(t - t_0)$ can be calculated using the definition. In this calculation we introduce the variable $\tau = t - t_0$ and we integrate over $(-\frac{T}{2}, \frac{T}{2})$ instead of $(-\frac{T}{2} + t_0, \frac{T}{2} + t_0)$, since this gives the same result:

$$\begin{aligned} \frac{1}{T} \int_{-\frac{T}{2}}^{\frac{T}{2}} f(t - t_0) e^{-jn\omega_0 t} dt &= e^{-jn\omega_0 t_0} \frac{1}{T} \int_{-\frac{T}{2} + t_0}^{\frac{T}{2} + t_0} f(t - t_0) e^{-jn\omega_0(t - t_0)} d(t - t_0) \\ &= e^{-jn\omega_0 t_0} \frac{1}{T} \int_{-\frac{T}{2}}^{\frac{T}{2}} f(\tau) e^{-jn\omega_0 \tau} d\tau \\ &= e^{-jn\omega_0 t_0} c_n \end{aligned}$$

B.2 Newton-Raphson Method for Simulation of a 2-cell Converter

The main purpose of this section is to use Newton-Raphson simulation method for plotting the spectrum of the switching functions of 2-cell multicell converter. This will then be compared with the spectrum obtained using double-Fourier analysis. The Newton-Raphson theory is discussed in Appendix for convenience.

B.2.1 Derivation of the spectrum for the switching function

$$s_{a1}(t)$$

This subsection deals with the derivation of the intersection points of the reference signal with the carrier signal using Newton-Raphson method. The resulting pwm is used to obtain the amplitude and phase spectrum using the Matlab program. Figure B.2 show the reference and carrier signal that produce the switching function $s_{a1}(t)$ For the general

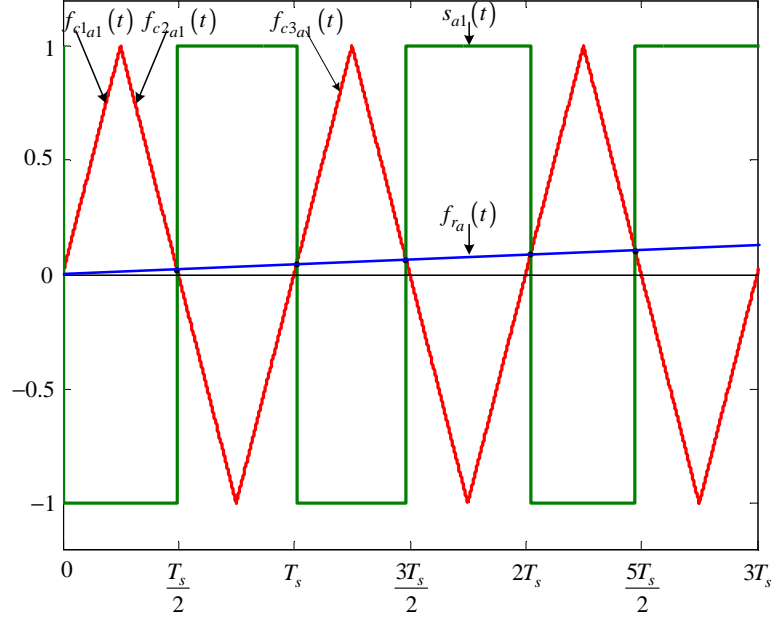


Figure B.2: *Newton-Raphson method of switching function $s_{a1}(t)$*

case over one cycle of the modulating signal for $n = 1 \dots m_f$.

Modulation signal $f_{ra}(t)$ is given by:

$$f_{ra}(t) = m_a \sin(\omega_0 t) \quad (\text{B.4})$$

The rising side of the carrier signal $f_{c1a1}(t)$ is given by:

$$f_{c1a1}(t) = \frac{4}{T_s} t - 4(n - 1) \quad (\text{B.5})$$

The falling side of the carrier signal $f_{c2a1}(t)$ is given by:

$$f_{c2a1}(t) = -\frac{4}{T_s} t + 4n - 2 \quad (\text{B.6})$$

The next rising side of the carrier signal $f_{c3a1}(t)$ is given by:

$$f_{c3a1}(t) = \frac{4}{T_s} t - 4n \quad (\text{B.7})$$

Where the rising side of the carrier signal $f_{c1a1}(t)$ intersect the modulating signal $f_{ra}(t)$ we define the function $f_{1a1}(t)$ as:

$$f_{1a1}(t) = m_a \sin(\omega_0 t) - \frac{4}{T_s} t + 4(n-1) \quad (\text{B.8})$$

and where the falling side of the carrier signal $f_{1a1}(t)$ intersect the modulating signal $f_{ra}(t)$ we define the function $f_{2a1}(t)$ as:

$$f_{2a1}(t) = m_a \sin(\omega_0 t) + \frac{4}{T_s} t - 4n + 2 \quad (\text{B.9})$$

and similarly where the rising side of the carrier signal $f_{c3a1}(t)$ intersect the modulating signal $f_{ra}(t)$ we define the function $f_{3a1}(t)$ as:

$$f_{3a1}(t) = m_a \sin(\omega_0 t) - \frac{4}{T_s} t + 4n \quad (\text{B.10})$$

Now using the Newton-Raphson method discussed in appendix section B.1.2 we approximate the root of equation B.8 as:

$$t_{12a1} = t_{11a1} - \frac{f_{1a1}(t_{11a1})}{f'_{1a1}(t_{11a1})} = t_{11a1} - \frac{m_a \sin(\omega_0 t_{11a1}) - \frac{4}{T_s} t_{11a1} + 4(n-1)}{\omega_0 m_a \cos(\omega_0 t_{11a1}) - \frac{4}{T_s}} \quad (\text{B.11})$$

where the initial guess t_{11a1} is given by:

$$t_{11a1} = \frac{1}{4} T_s \cdot 4(n-1) \quad \text{for } 0 < t_{11a1} < m_f T_s \quad (\text{B.12})$$

After i successive approximations we will have equation B.11 written as:

$$t_{1(i+1)a1} = t_{1i a1} - \frac{f_{1a1}(t_{1i a1})}{f'_{1a1}(t_{1i a1})} \quad (\text{B.13})$$

Similarly using the Newton-Raphson method we approximate the root of equation B.9 as:

$$t_{22a1} = t_{21a1} - \frac{f_{2a1}(t_{21a1})}{f'_{2a1}(t_{21a1})} = t_{21a1} - \frac{m_a \sin(\omega_0 t_{21a1}) + \frac{4}{T_s} t_{21a1} - 4n + 2}{\omega_0 m_a \cos(\omega_0 t_{21a1}) + \frac{4}{T_s}} \quad (\text{B.14})$$

where the initial guess t_{21a1} is given by:

$$t_{21a1} = \frac{1}{4} T_s \cdot (4n-2) \quad \text{for } 0 < t_{21a1} < m_f T_s \quad (\text{B.15})$$

After i successive approximations we will have equation B.14 written as:

$$t_{2(i+1)a1} = t_{2i a1} - \frac{f_{2a1}(t_{2i a1})}{f'_{2a1}(t_{2i a1})} \quad (\text{B.16})$$

And similarly using the Newton-Raphson method we approximate the root of equation B.10 as:

$$t_{32a1} = t_{31a1} - \frac{f_{1a1}(t_{31a1})}{f'_{1a1}(t_{31a1})} = t_{31a1} - \frac{m_a \sin(\omega_0 t_{31a1}) - \frac{4}{T_s} t_{31a1} + 4n}{\omega_0 m_a \cos(\omega_0 t_{31a1}) - \frac{4}{T_s}} \quad (\text{B.17})$$

where the initial guess $t_{31_{a1}}$ is given by:

$$t_{31_{a1}} = \frac{1}{4}T_s \cdot 4n \quad \text{for } 0 < t_{31_{a1}} < m_f T_s \quad (\text{B.18})$$

After i successive approximations we will have equation B.17 written as:

$$t_{3(i+1)_{a1}} = t_{3i_{a1}} - \frac{f_{3_{a1}}(t_{3i_{a1}})}{f'_{3_{a1}}(t_{3i_{a1}})} \quad (\text{B.19})$$

Now we consider the pwm resulting from the intersection of $f_{c1_{a1}}$, $f_{c2_{a1}}$ and $f_{c3_{a1}}$ with f_{r_a} . First we look at the pulse formed between $t_{1(i+1)_{a1}}$ and $t_{2(i+1)_{a1}}$. The width of this pulse is given by:

$$W_{1_{a1}} = t_{2(i+1)_{a1}} - t_{1(i+1)_{a1}}$$

We now place this pulse so that it is centred around the origin as shown in Figure B.3 and then calculate its Fourier transform. Taking the Fourier transform of the pulse in

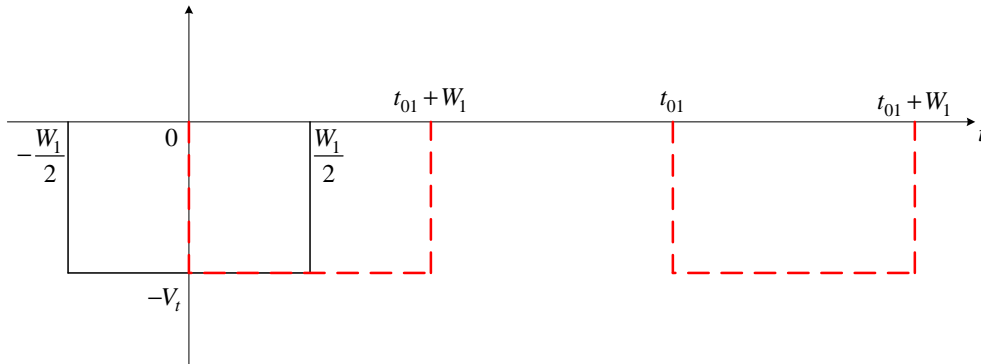


Figure B.3: *Negative Pulse shift process by $t_{01} + \frac{W_1}{2}$*

Figure B.3 results in:

$$\begin{aligned} F(\omega) &= \int_{-\frac{W_{1_{a1}}}{2}}^{\frac{W_{1_{a1}}}{2}} (-V_t) e^{-j\omega_0 t} dt \\ &= \frac{V_t}{j\omega_0} \left(e^{-j\omega_0(t_{2(i+1)_{a1}} - t_{1(i+1)_{a1}})} \right) \end{aligned} \quad (\text{B.20})$$

From Appendix B.1.1 we can find the Fourier transform of the negative pulses generated in Figure B.2 by shifting the pulse between $t_{1(i+1)_{a1}}$ and $t_{2(i+1)_{a1}}$ by $t_{01_{a1}}$ as shown in Figure B.3 where $t_{01_{a1}}$ is given by:

$$t_{01_{a1}} = t_{1(i+1)_{a1}} + \frac{W_{1_{a1}}}{2} \quad (\text{B.21})$$

Thus the resulting Fourier transform of the shifted negative pulse is given by:

$$\begin{aligned}
 F(\omega) &= \int_{-\frac{W_{1a1}}{2}}^{\frac{W_{1a1}}{2}} (-V_t) e^{-j\omega_0 t} e^{-j\omega_0 t_{01a1}} dt \\
 &= \frac{V_t}{j\omega_0} \left(e^{-j\omega_0(t_{2(i+1)a1} - t_{1(i+1)a1})} e^{-j\omega_0 t_{01a1}} \right)
 \end{aligned}
 \tag{B.22}$$

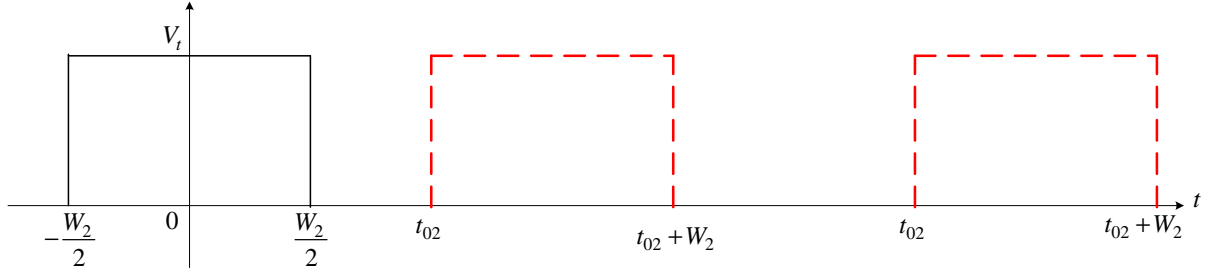


Figure B.4: Positive Pulse shift process by $t_{02a1} + \frac{W_{2a1}}{2}$

Similarly we consider the pulse formed between $t_{2(i+1)a1}$ and $t_{3(i+1)a1}$ in Figure B.2. The width of this pulse is given by:

$$W_{2a1} = t_{3(i+1)a1} - t_{2(i+1)a1}$$

and its Fourier transform using the positive pulse in Figure B.4 results in:

$$\begin{aligned}
 F(\omega) &= \int_{-\frac{W_{2a1}}{2}}^{\frac{W_{2a1}}{2}} (V_t) e^{-j\omega_0 t} dt \\
 &= -\frac{V_t}{j\omega_0} \left(e^{-j\omega_0(t_{3(i+1)a1} - t_{2(i+1)a1})} \right)
 \end{aligned}
 \tag{B.23}$$

The shifting of this positive pulse by t_{02a1} is shown in Figure B.4 where t_{02a1} is given by:

$$t_{02a1} = t_{2(i+1)a1} + \frac{W_{2a1}}{2} \tag{B.24}$$

The resulting Fourier transform of the shifted positive pulse is given by:

$$\begin{aligned}
 F(\omega) &= \int_{-\frac{W_{2a1}}{2}}^{\frac{W_{2a1}}{2}} (V_t) e^{-j\omega_0 t} e^{-j\omega_0 t_{02a1}} dt \\
 &= -\frac{V_t}{j\omega_0} \left(e^{-j\omega_0(t_{3(i+1)a1} - t_{2(i+1)a1})} e^{-j\omega_0 t_{02a1}} \right)
 \end{aligned}
 \tag{B.25}$$

To obtain the spectrum of $S_{a1}(\omega)$ we sum up all the Fourier transform for the negative and positive pulses over any number of cycles of the switching period.

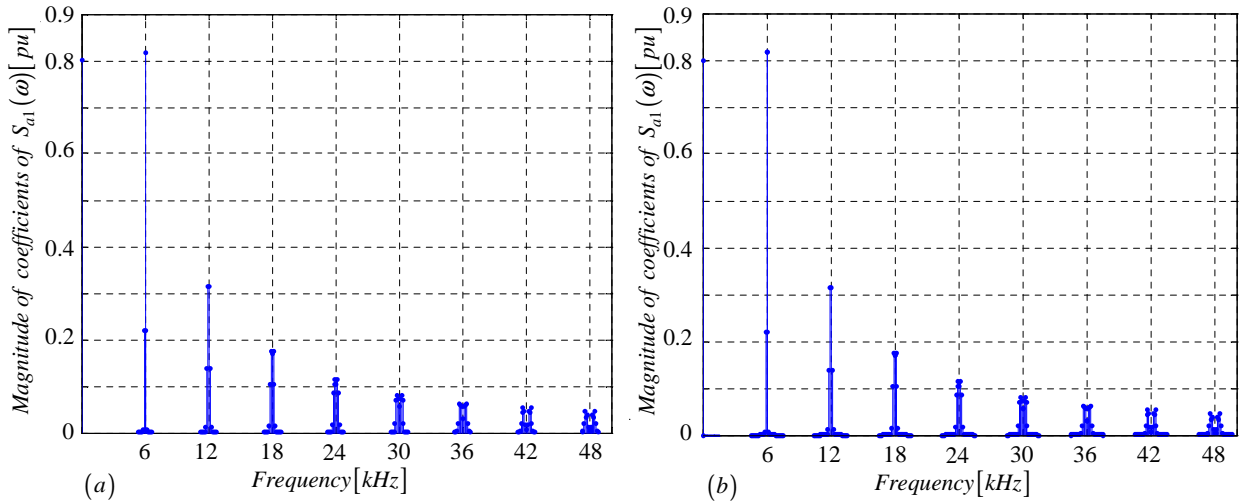


Figure B.5: Amplitude spectrum of $S_{a1}(\omega)$ generated using (a) Newton-Raphson simulation and (b) Theory

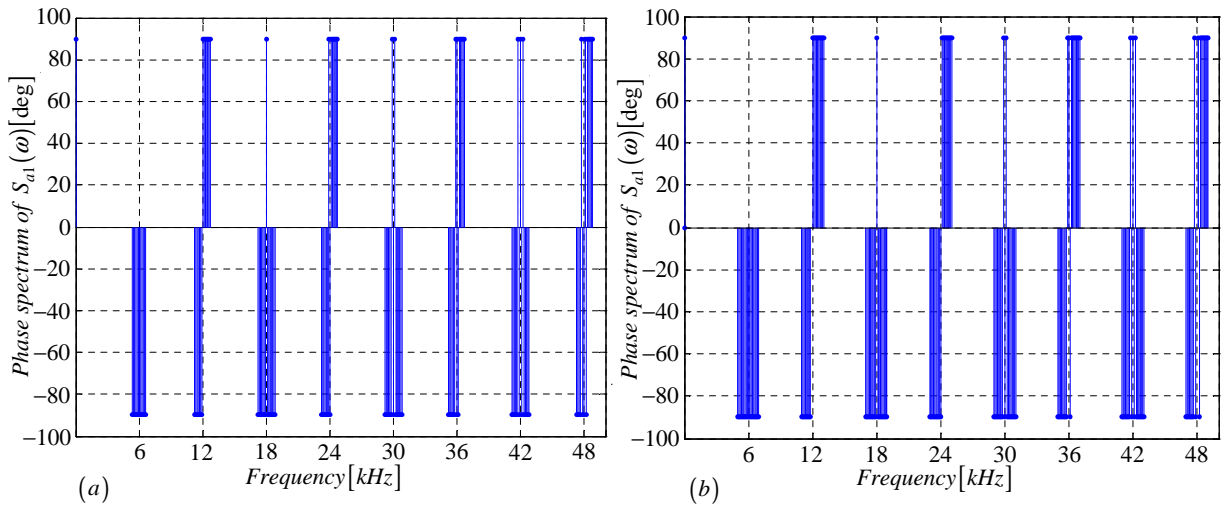


Figure B.6: Phase spectrum of $S_{a1}(\omega)$ generated using (a) Newton-Raphson simulation and (b) Theory

B.2.2 Derivation of the spectrum for the switching function

$$s_{a2}(t)$$

In this subsection we derive equations that are necessary for the plotting of $S_{a2}(\omega)$ spectrum. The procedure is the same as in subsection B.2.1 except that the carrier signal in Figure B.7 is out of phase by 180 degrees with the one in Figure B.2.

Modulation signal $f_{ra}(t)$ is given by:

$$f_{ra}(t) = m_a \sin(\omega_0 t) \tag{B.26}$$

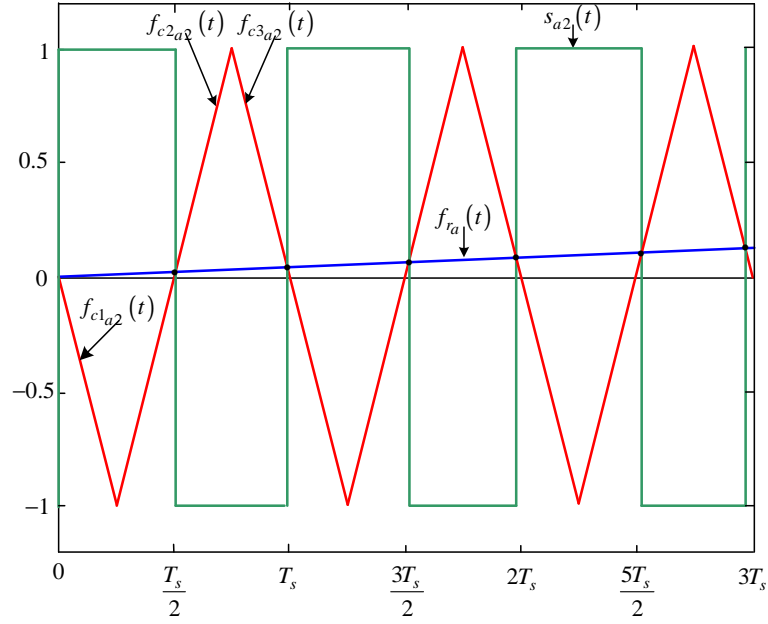


Figure B.7: *Newton-Raphson method of switching function $s_{a2}(t)$*

The falling side of the carrier signal $f_{c1a2}(t)$ is given by:

$$f_{c1a2}(t) = -\frac{4}{T_s}t + 4(n-1) \quad (\text{B.27})$$

The rising side of the carrier signal $f_{c2a2}(t)$ is given by:

$$f_{c2a2}(t) = \frac{4}{T_s}t - 4n + 2 \quad (\text{B.28})$$

The next falling side of the carrier signal $f_{c3a2}(t)$ is given by:

$$f_{c3a2}(t) = -\frac{4}{T_s}t + 4n \quad (\text{B.29})$$

Where the falling side of the carrier signal $f_{c1a2}(t)$ intersect the modulating signal $f_{ra}(t)$ we define the function $f_{1a2}(t)$ as:

$$f_{1a2}(t) = m_a \sin(\omega_0 t) + \frac{4}{T_s}t - 4(n-1) \quad (\text{B.30})$$

and where the falling side of the carrier signal $f_{c1a2}(t)$ intersect the modulating signal $f_{ra}(t)$ we define the function $f_{2a2}(t)$ as:

$$f_{2a2}(t) = m_a \sin(\omega_0 t) - \frac{4}{T_s}t + 4n - 2 \quad (\text{B.31})$$

and similarly where the rising side of the carrier signal $f_{c3a2}(t)$ intersect the modulating signal $f_{ra}(t)$ we define the function $f_{3a2}(t)$ as:

$$f_{3a2}(t) = m_a \sin(\omega_0 t) + \frac{4}{T_s}t - 4n \quad (\text{B.32})$$

Now using the Newton-Raphson method discussed in appendix B.1.2 we approximate the root of equation B.30 as:

$$t_{12_{a2}} = t_{11_{a2}} - \frac{f_{1_{a2}}(t_{11_{a2}})}{f'_{1_{a2}}(t_{11_{a2}})} = t_{11_{a2}} - \frac{m_a \sin(\omega_0 t_{11_{a2}}) + \frac{4}{T_s} t_{11_{a2}} - 4(n-1)}{\omega_0 m_a \cos(\omega_0 t_{11_{a2}}) + \frac{4}{T_s}} \quad (\text{B.33})$$

where the initial guess $t_{11_{a2}}$ is given by:

$$t_{11_{a2}} = \frac{1}{4} T_s \cdot 4(n-1) \quad \text{for } 0 < t_{11_{a2}} < m_f T_s \quad (\text{B.34})$$

After i successive approximations we will have equation B.33 written as:

$$t_{1(i+1)_{a2}} = t_{1i_{a2}} - \frac{f_{1_{a2}}(t_{1i_{a2}})}{f'_{1_{a2}}(t_{1i_{a2}})} \quad (\text{B.35})$$

Similarly using the Newton-Raphson method we approximate the root of equation B.31 as:

$$t_{22_{a2}} = t_{21_{a2}} - \frac{f_{2_{a2}}(t_{21_{a2}})}{f'_{2_{a2}}(t_{21_{a2}})} = t_{21_{a2}} - \frac{m_a \sin(\omega_0 t_{21_{a2}}) - \frac{4}{T_s} t_{21_{a2}} + 4n - 2}{\omega_0 m_a \cos(\omega_0 t_{21_{a2}}) - \frac{4}{T_s}} \quad (\text{B.36})$$

where the initial guess $t_{21_{a2}}$ is given by:

$$t_{21_{a2}} = \frac{1}{4} T_s \cdot (4n - 2) \quad \text{for } 0 < t_{21_{a2}} < m_f T_s \quad (\text{B.37})$$

After i successive approximations we will have equation B.36 written as:

$$t_{2(i+1)_{a2}} = t_{2i_{a2}} - \frac{f_{2_{a2}}(t_{2i_{a2}})}{f'_{2_{a2}}(t_{2i_{a2}})} \quad (\text{B.38})$$

And similarly using the Newton-Raphson method we approximate the root of equation B.32 as:

$$t_{32_{a2}} = t_{31_{a2}} - \frac{f_{1_{a2}}(t_{31_{a2}})}{f'_{1_{a2}}(t_{31_{a2}})} = t_{31_{a2}} - \frac{m_a \sin(\omega_0 t_{31_{a2}}) + \frac{4}{T_s} t_{31_{a2}} - 4n}{\omega_0 m_a \cos(\omega_0 t_{31_{a2}}) + \frac{4}{T_s}} \quad (\text{B.39})$$

where the initial guess $t_{31_{a2}}$ is given by:

$$t_{31_{a2}} = \frac{1}{4} T_s \cdot 4n \quad \text{for } 0 < t_{31_{a2}} < m_f T_s \quad (\text{B.40})$$

After i successive approximations we will have equation B.39 written as:

$$t_{3(i+1)_{a2}} = t_{3i_{a2}} - \frac{f_{3_{a2}}(t_{3i_{a2}})}{f'_{3_{a2}}(t_{3i_{a2}})} \quad (\text{B.41})$$

Now we consider the pwm resulting from the intersection of $f_{c1_{a2}}$, $f_{c2_{a2}}$ and $f_{c3_{a2}}$ with f_{r_a} . First we look at the pulse formed between $t_{1(i+1)_{a2}}$ and $t_{2(i+1)_{a2}}$. The width of this pulse is given by

$$W_{1_{a2}} = t_{2(i+1)_{a2}} - t_{1(i+1)_{a2}}$$

Now following the same method as in section B.2.1 the Fourier transform of the positive pulse is given by:

$$\begin{aligned}
F(\omega) &= \int_{-\frac{W_{1a2}}{2}}^{\frac{W_{1a2}}{2}} (V_t) e^{-j\omega_0 t} dt \\
&= -\frac{V_t}{j\omega_0} \left(e^{-j\omega_0(t_{2(i+1)a2} - t_{1(i+1)a2})} \right)
\end{aligned} \tag{B.42}$$

and the Fourier transform of the positive pulses generated by shifting the pulse between $t_{1(i+1)a2}$ and $t_{2(i+1)a2}$ by t_{01a2} where t_{01a2} is given by:

$$t_{01a2} = t_{1(i+1)a2} + \frac{W_{1a2}}{2} \tag{B.43}$$

can be represented as follows:

$$\begin{aligned}
F(\omega) &= \int_{-\frac{W_{1a2}}{2}}^{\frac{W_{1a2}}{2}} (V_t) e^{-j\omega_0 t} e^{-j\omega_0 t_{01a2}} dt \\
&= -\frac{V_t}{j\omega_0} \left(e^{-j\omega_0(t_{2(i+1)a2} - t_{1(i+1)a2})} e^{-j\omega_0 t_{01a2}} \right)
\end{aligned} \tag{B.44}$$

Similarly we consider the pulse formed between $t_{2(i+1)a2}$ and $t_{3(i+1)a2}$ in Figure B.7. The width of this pulse is given by:

$$W_{2a2} = t_{3(i+1)a2} - t_{2(i+1)a2}$$

and its Fourier transform using the negative pulse results in:

$$\begin{aligned}
F(\omega) &= \int_{-\frac{W_{2a2}}{2}}^{\frac{W_{2a2}}{2}} (-V_t) e^{-j\omega_0 t} dt \\
&= \frac{V_t}{j\omega_0} \left(e^{-j\omega_0(t_{3(i+1)a2} - t_{2(i+1)a2})} \right)
\end{aligned} \tag{B.45}$$

The shifting of this negative pulse by t_{02a2} is shown in Figure B.4 where t_{02a2} is given by:

$$t_{02a2} = t_{2(i+1)a2} + \frac{W_{2a2}}{2} \tag{B.46}$$

The resulting Fourier transform of the shifted negative pulse is given by:

$$\begin{aligned}
F(\omega) &= \int_{-\frac{W_{2a2}}{2}}^{\frac{W_{2a2}}{2}} (-V_t) e^{-j\omega_0 t} e^{-j\omega_0 t_{02a2}} dt \\
&= \frac{V_t}{j\omega_0} \left(e^{-j\omega_0(t_{3(i+1)a2} - t_{2(i+1)a2})} e^{-j\omega_0 t_{02a2}} \right)
\end{aligned} \tag{B.47}$$

To obtain the spectrum of $S_{a2}(\omega)$ we sum up all the Fourier transform for the negative and positive pulses over any number of cycles of the switching period. The amplitude spectrum is the same as the one shown in Figure B.5 for $S_{a1}(\omega)$.

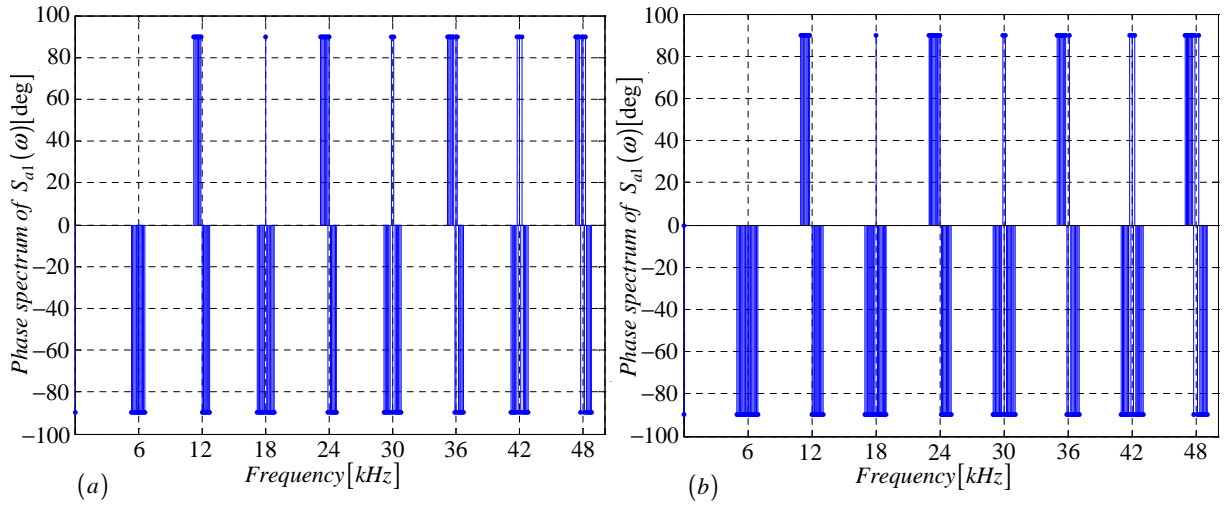


Figure B.8: Phase spectrum of $S_{a2}(\omega)$ generated using (a) Newton-Rapson simulation and (b) Theory

B.2.3 Derivation of the spectrum for the switching function

$$s_{da}(t)$$

In this subsection we derive equations that are necessary for the plotting of $S_{da}(\omega)$ spectrum. We use the definition of $s_{da}(t)$ to obtain Figure B.9 from Figures B.2 and B.7.

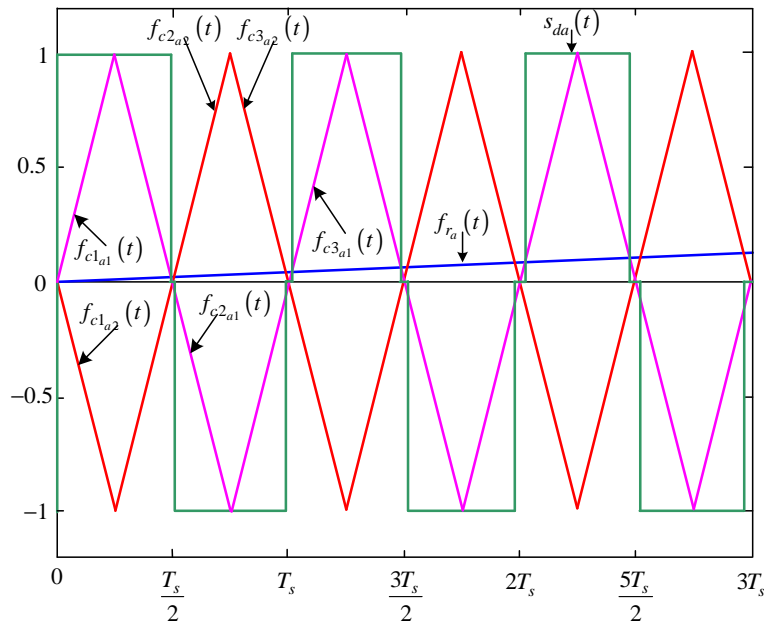


Figure B.9: Newton-Raphson method of switching function $s_{da}(t)$

The width of the positive pulse is given by:

$$W_{1_{sda}} = t_{2(i+1)_{a1}} - t_{1(i+1)_{a1}} \quad (\text{B.48})$$

The Fourier transform of the positive pulses generated by shifting the pulse between $t_{1(i+1)_{a1}}$ and $t_{2(i+1)_{a1}}$ by $t_{01_{sda}}$ where $t_{01_{sda}}$ is given by:

$$t_{01_{sda}} = t_{1(i+1)_{a1}} + \frac{W_{1_{sda}}}{2} \quad (\text{B.49})$$

is given by:

$$\begin{aligned} F(\omega) &= \int_{-\frac{W_{1_{sda}}}{2}}^{\frac{W_{1_{sda}}}{2}} (V_t) e^{-j\omega_0 t} e^{-j\omega_0 t_{01_{sda}}} dt \\ &= -\frac{V_t}{j\omega_0} \left(e^{-j\omega_0(t_{2(i+1)_{a1}} - t_{1(i+1)_{a1}})} e^{-j\omega_0 t_{01_{sda}}} \right) \end{aligned} \quad (\text{B.50})$$

The width of the negative pulse is given by:

$$W_{2_{sda}} = t_{3(i+1)_{a2}} - t_{2(i+1)_{a2}} \quad (\text{B.51})$$

The Fourier transform of the negative pulses generated by shifting the pulse between $t_{2(i+1)_{a2}}$ and $t_{3(i+1)_{a2}}$ by $t_{02_{sda}}$ where $t_{02_{sda}}$ is given by:

$$t_{02_{sda}} = t_{2(i+1)_{a2}} + \frac{W_{2_{sda}}}{2} \quad (\text{B.52})$$

is given by:

$$\begin{aligned} F(\omega) &= \int_{-\frac{W_{2_{sda}}}{2}}^{\frac{W_{2_{sda}}}{2}} (-V_t) e^{-j\omega_0 t} e^{-j\omega_0 t_{02_{sda}}} dt \\ &= \frac{V_t}{j\omega_0} \left(e^{-j\omega_0(t_{3(i+1)_{a2}} - t_{2(i+1)_{a2}})} e^{-j\omega_0 t_{02_{sda}}} \right) \end{aligned} \quad (\text{B.53})$$

To obtain the spectrum of $S_{da}(\omega)$ we sum up all the Fourier transform for the negative and positive pulses over any number of cycles of the switching period.

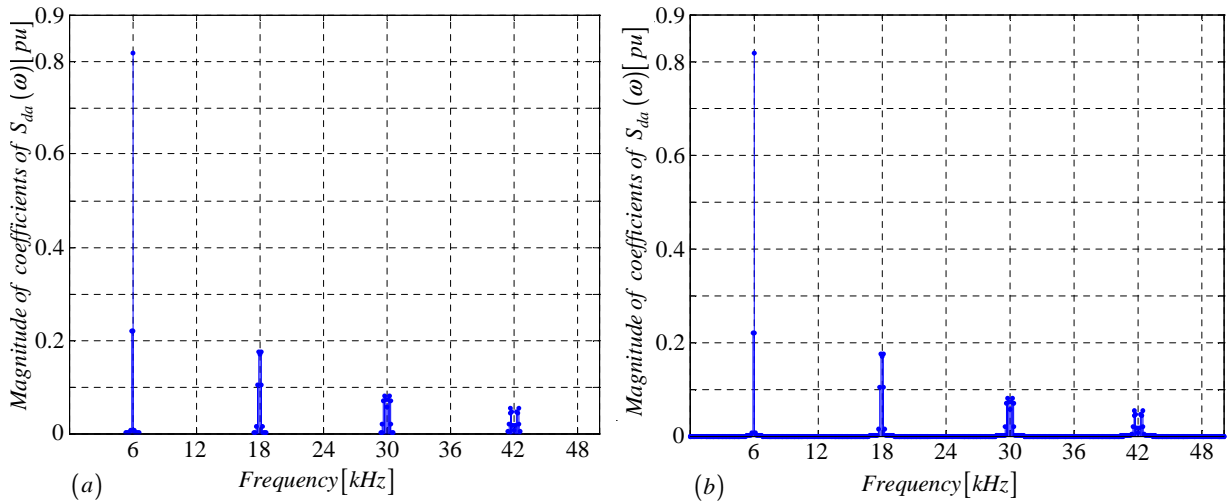


Figure B.10: Amplitude spectrum of $S_{da}(\omega)$ generated using (a) Newton-Raphson simulation and (b) Theory

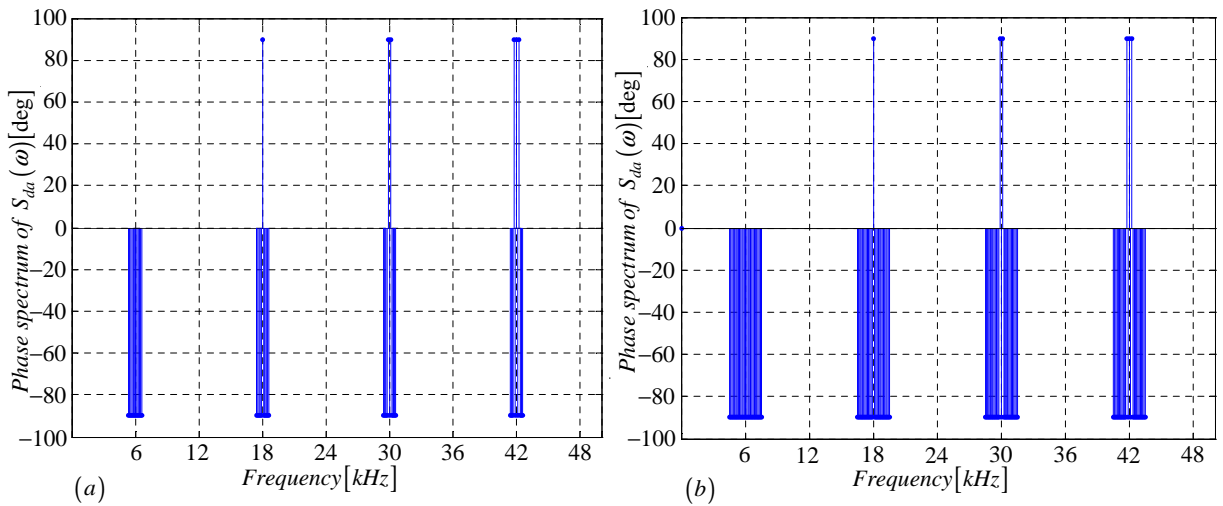


Figure B.11: Phase spectrum of $S_{da}(\omega)$ generated using (a) Newton-Raphson simulation and (b) Theory

B.2.4 Derivation of the spectrum for the switching function

$$s_{ta}(t)$$

In this subsection we derive equations that are necessary for the plotting of $S_{ta}(\omega)$ spectrum. We use the definition of $s_{ta}(t)$ to obtain Figure B.12 from Figures B.2 and B.7.

The width of the positive pulse between $t_{2(i+1)a1}$ and $t_{2(i+1)a2}$ is given by:

$$W_{1sda} = t_{2(i+1)a2} - t_{2(i+1)a1} \quad (\text{B.54})$$

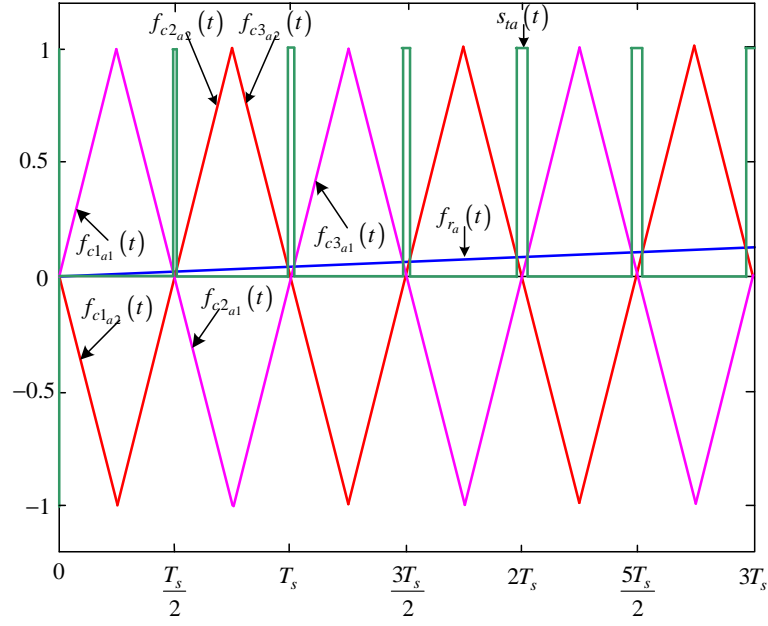


Figure B.12: Newton-Raphson method of switching function $s_{ta}(t)$

The Fourier transform of the positive pulses generated by shifting the pulse between $t_{2(i+1)a1}$ and $t_{2(i+1)a2}$ by t_{01sta} where t_{01sta} is given by:

$$t_{01sta} = t_{2(i+1)a1} + \frac{W_{1sta}}{2} \quad (\text{B.55})$$

is given by:

$$\begin{aligned} F(\omega) &= \int_{-\frac{W_{1sta}}{2}}^{\frac{W_{1sta}}{2}} (V_t) e^{-j\omega_0 t} e^{-j\omega_0 t_{01sta}} dt \\ &= -\frac{V_t}{j\omega_0} \left(e^{-j\omega_0(t_{2(i+1)a2} - t_{2(i+1)a1})} e^{-j\omega_0 t_{01sta}} \right) \end{aligned} \quad (\text{B.56})$$

The width of the positive pulse between $t_{3(i+1)a2}$ and $t_{3(i+1)a1}$ by t_{02sta} is given by:

$$W_{2sta} = t_{3(i+1)a1} - t_{3(i+1)a2} \quad (\text{B.57})$$

The Fourier transform of the negative pulses generated by shifting the pulse between $t_{3(i+1)a2}$ and $t_{3(i+1)a1}$ by t_{02sta} where t_{02sta} is given by:

$$t_{02sta} = t_{3(i+1)a2} + \frac{W_{2sta}}{2} \quad (\text{B.58})$$

is given by:

$$\begin{aligned} F(\omega) &= \int_{-\frac{W_{2sta}}{2}}^{\frac{W_{2sta}}{2}} (V_t) e^{-j\omega_0 t} e^{-j\omega_0 t_{02sta}} dt \\ &= -\frac{V_t}{j\omega_0} \left(e^{-j\omega_0(t_{3(i+1)a1} - t_{3(i+1)a2})} e^{-j\omega_0 t_{02sta}} \right) \end{aligned} \quad (\text{B.59})$$

To obtain the spectrum of $S_{ta}(\omega)$ we sum up all the Fourier transform for the positive pulses over any number of cycles of the switching period.

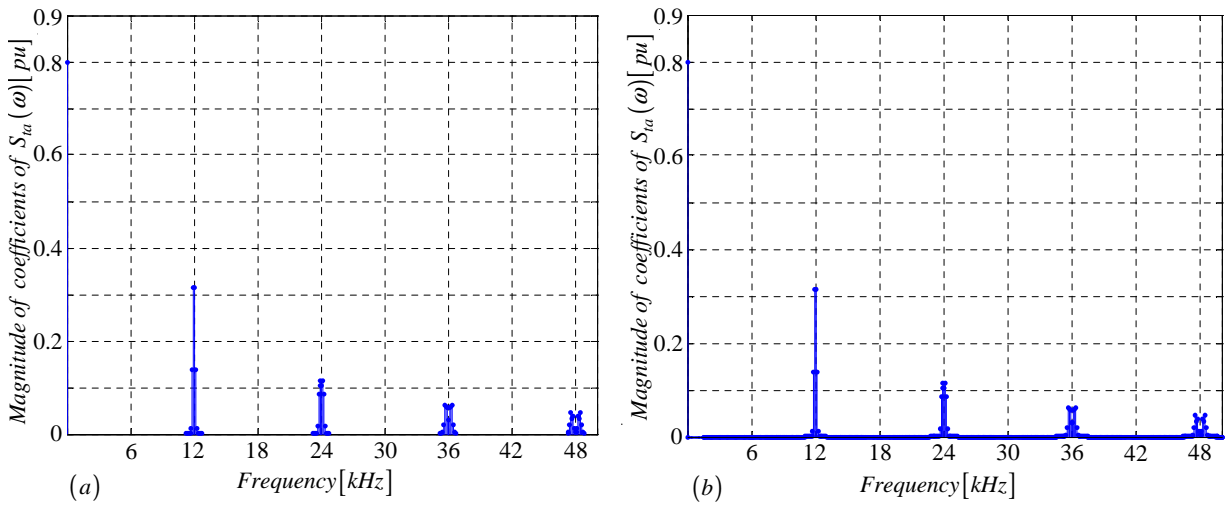


Figure B.13: Amplitude spectrum of $S_{ta}(\omega)$ generated using (a) Newton-Raphson simulation and (b) Theory

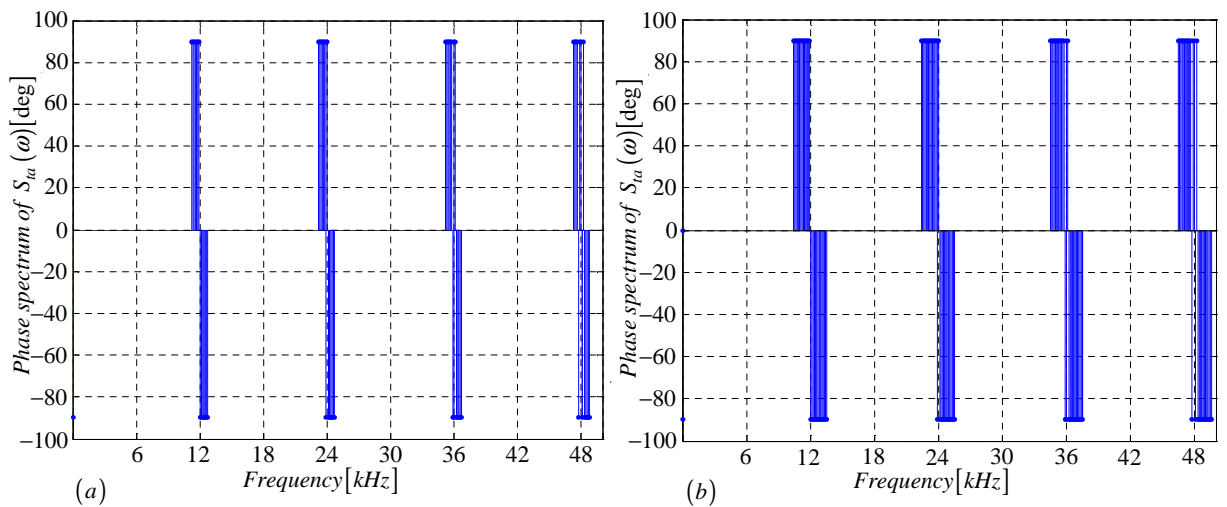


Figure B.14: Phase spectrum of $S_{ta}(\omega)$ generated using (a) Newton-Raphson simulation and (b) Theory

B.2.5 Derivation of the spectrum for the switching function

$$s_{b1}(t)$$

In this subsection we derive equations that are necessary for the plotting of $S_{b1}(\omega)$ spectrum. The procedure is the same as in subsection B.2.1 except that the reference signal in Figure B.15 is out of phase by 120 degrees with the one in Figure B.2.

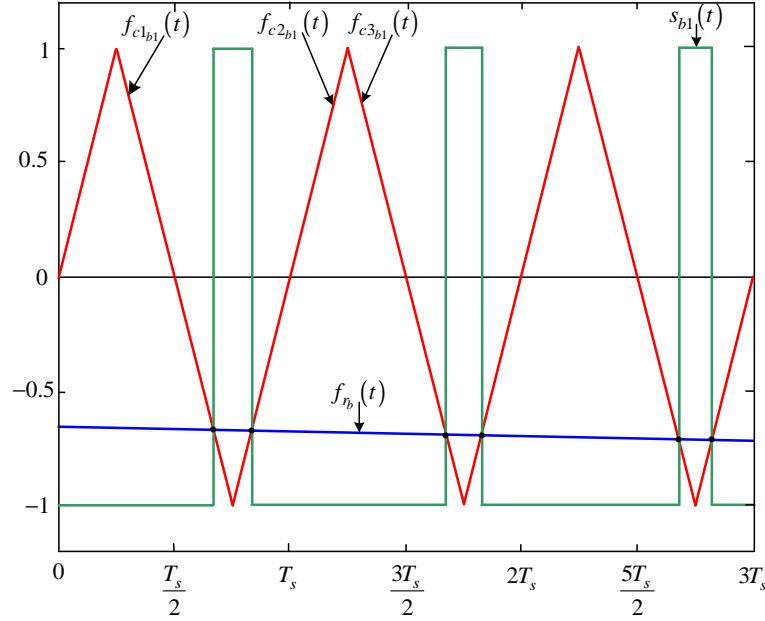


Figure B.15: *Newton-Raphson method of switching function $s_{b1}(t)$*

Modulation signal $f_{r_b}(t)$ is given by:

$$f_{r_b}(t) = m_a \sin\left(\omega_0 t - \frac{2\pi}{3}\right) \quad (\text{B.60})$$

The falling side of the carrier signal $f_{c1_{b1}}(t)$ is given by:

$$f_{c1_{b1}}(t) = -\frac{4}{T_s}t + 4n - 2 \quad (\text{B.61})$$

The rising side of the carrier signal $f_{c2_{b1}}(t)$ is given by:

$$f_{c2_{b1}}(t) = \frac{4}{T_s}t - 4(n) \quad (\text{B.62})$$

The next falling side of the carrier signal $f_{c3_{b1}}(t)$ is given by:

$$f_{c3_{b1}}(t) = -\frac{4}{T_s}t + 4n + 2 \quad (\text{B.63})$$

Where the falling side of the carrier signal $f_{c1_{b1}}(t)$ intersect the modulating signal $f_{r_b}(t)$ we define the function $f_{1_{b1}}(t)$ as:

$$f_{1_{b1}}(t) = m_a \sin(\omega_0 t) + \frac{4}{T_s}t - 4n + 2 \quad (\text{B.64})$$

and where the falling side of the carrier signal $f_{1b1}(t)$ intersect the modulating signal $f_{r_b}(t)$ we define the function $f_{2b1}(t)$ as:

$$f_{2b1}(t) = m_a \sin(\omega_0 t) - \frac{4}{T_s} t + 4(n) \quad (\text{B.65})$$

and similarly where the rising side of the carrier signal $f_{c3b1}(t)$ intersect the modulating signal $f_{r_b}(t)$ we define the function $f_{3b1}(t)$ as:

$$f_{3b1}(t) = m_a \sin(\omega_0 t) + \frac{4}{T_s} t - 4n - 2 \quad (\text{B.66})$$

Now using the Newton-Raphson method discussed in appendix section B.1.2 we approximate the root of equation B.64 as:

$$t_{12b1} = t_{11b1} - \frac{f_{1b1}(t_{11b1})}{f'_{1b1}(t_{11b1})} = t_{11b1} - \frac{m_a \sin(\omega_0 t_{11b1}) + \frac{4}{T_s} t_{11} - 4n + 2}{\omega_0 m_a \cos(\omega_0 t_{11b1}) + \frac{4}{T_s}} \quad (\text{B.67})$$

where the initial guess t_{11b1} is given by:

$$t_{11b1} = \frac{1}{4} T_s \cdot (4n - 2) \quad \text{for } 0 < t_{11b1} < m_f T_s \quad (\text{B.68})$$

After i successive approximations we will have equation B.67 written as:

$$t_{1(i+1)b1} = t_{1ib1} - \frac{f_{1b1}(t_{1ib1})}{f'_{1b1}(t_{1ib1})} \quad (\text{B.69})$$

Similarly using the Newton-Raphson method we approximate the root of equation B.65 as:

$$t_{22b1} = t_{21b1} - \frac{f_{2b1}(t_{21b1})}{f'_{2b1}(t_{21b1})} = t_{21b1} - \frac{m_a \sin(\omega_0 t_{21b1}) - \frac{4}{T_s} t_{21b1} + 4n}{\omega_0 m_a \cos(\omega_0 t_{21b1}) - \frac{4}{T_s}} \quad (\text{B.70})$$

where the initial guess t_{21b1} is given by:

$$t_{21b1} = \frac{1}{4} T_s \cdot (4n) \quad \text{for } 0 < t_{21b1} < m_f T_s \quad (\text{B.71})$$

After i successive approximations we will have equation B.70 written as:

$$t_{2(i+1)b1} = t_{2ib1} - \frac{f_{2b1}(t_{2ib1})}{f'_{2b1}(t_{2ib1})} \quad (\text{B.72})$$

And similarly using the Newton-Raphson method we approximate the root of equation B.66 as:

$$t_{32b1} = t_{31b1} - \frac{f_{1b1}(t_{31b1})}{f'_{1b1}(t_{31b1})} = t_{31b1} - \frac{m_a \sin(\omega_0 t_{31b1}) + \frac{4}{T_s} t_{31b1} - 4n - 2}{\omega_0 m_a \cos(\omega_0 t_{31b1}) + \frac{4}{T_s}} \quad (\text{B.73})$$

where the initial guess t_{31b1} is given by:

$$t_{31b1} = \frac{1}{4} T_s \cdot (4n + 2) \quad \text{for } 0 < t_{31b1} < m_f T_s \quad (\text{B.74})$$

After i successive approximations we will have equation B.73 written as:

$$t_{3(i+1)b_1} = t_{3ib_1} - \frac{f_{3b_1}(t_{3ib_1})}{f'_{3b_1}(t_{3ib_1})} \quad (\text{B.75})$$

Now we consider the pwm resulting from the intersection of f_{c1b_1} , f_{c2b_1} and f_{c3b_1} with f_{rb} . First we look at the pulse formed between $t_{1(i+1)b_1}$ and $t_{2(i+1)b_1}$. The width of this pulse is given by

$$W_{1b_1} = t_{2(i+1)b_1} - t_{1(i+1)b_1}$$

Now following the same method as in section B.2.1 the Fourier transform of the positive pulse is given by:

$$\begin{aligned} F(\omega) &= \int_{-\frac{W_{1b_1}}{2}}^{\frac{W_{1b_1}}{2}} (V_t) e^{-j\omega_0 t} dt \\ &= -\frac{V_t}{j\omega_0} \left(e^{-j\omega_0(t_{2(i+1)b_1} - t_{1(i+1)b_1})} \right) \end{aligned} \quad (\text{B.76})$$

and the Fourier transform of the positive pulses generated by shifting the pulse between $t_{1(i+1)b_1}$ and $t_{2(i+1)b_1}$ by t_{01b_1} where t_{01b_1} is given by:

$$t_{01b_1} = t_{1(i+1)b_1} + \frac{W_{1b_1}}{2} \quad (\text{B.77})$$

can be represented as follows:

$$\begin{aligned} F(\omega) &= \int_{-\frac{W_{1b_1}}{2}}^{\frac{W_{1b_1}}{2}} (V_t) e^{-j\omega_0 t} e^{-j\omega_0 t_{01b_1}} dt \\ &= -\frac{V_t}{j\omega_0} \left(e^{-j\omega_0(t_{2(i+1)b_1} - t_{1(i+1)b_1})} e^{-j\omega_0 t_{01b_1}} \right) \end{aligned} \quad (\text{B.78})$$

Similarly we consider the pulse formed between $t_{2(i+1)b_1}$ and $t_{3(i+1)b_1}$ in Figure B.7. The width of this pulse is given by:

$$W_{2b_1} = t_{3(i+1)b_1} - t_{2(i+1)b_1}$$

and its Fourier transform using the negative pulse results in:

$$\begin{aligned} F(\omega) &= \int_{-\frac{W_{2b_1}}{2}}^{\frac{W_{2b_1}}{2}} (-V_t) e^{-j\omega_0 t} dt \\ &= \frac{V_t}{j\omega_0} \left(e^{-j\omega_0(t_{3(i+1)b_1} - t_{2(i+1)b_1})} \right) \end{aligned} \quad (\text{B.79})$$

B.2.6 Derivation of the spectrum for the switching function

$$s_{b2}(t)$$

In this subsection we derive equations that are necessary for the plotting of $S_{b2}(\omega)$ spectrum. The procedure is the same as in subsection B.2.5 except that the carrier signal in Figure B.17 is out of phase by 180 degrees with the one in Figure B.15.

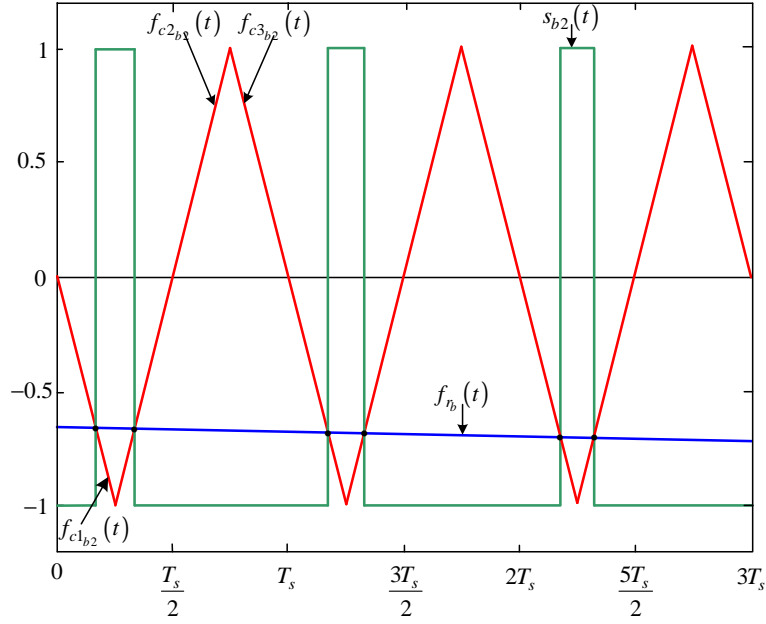


Figure B.17: *Newton-Raphson method of switching function $s_{b2}(t)$*

Modulation signal $f_{r_b}(t)$ is given by:

$$f_{r_b}(t) = m_a \sin(\omega_0 t - \frac{2\pi}{3}) \quad (\text{B.82})$$

The falling side of the carrier signal $f_{c1_{b2}}(t)$ is given by:

$$f_{c1_{b2}}(t) = -\frac{4}{T_s}t + 4(n-1) \quad (\text{B.83})$$

The rising side of the carrier signal $f_{c2_{b2}}(t)$ is given by:

$$f_{c2_{b2}}(t) = \frac{4}{T_s}t - 4n + 2 \quad (\text{B.84})$$

The next falling side of the carrier signal $f_{c3_{b2}}(t)$ is given by:

$$f_{c3_{b2}}(t) = -\frac{4}{T_s}t + 4n \quad (\text{B.85})$$

Where the falling side of the carrier signal $f_{c1_{b2}}(t)$ intersect the modulating signal $f_{r_b}(t)$ we define the function $f_{1_{b2}}(t)$ as:

$$f_{1_{b2}}(t) = m_a \sin(\omega_0 t) + \frac{4}{T_s}t - 4(n-1) \quad (\text{B.86})$$

and where the falling side of the carrier signal $f_{1b_2}(t)$ intersect the modulating signal $f_{r_b}(t)$ we define the function $f_{2b_2}(t)$ as:

$$f_{2b_2}(t) = m_a \sin(\omega_0 t) - \frac{4}{T_s} t + 4n - 2 \quad (\text{B.87})$$

and similarly where the rising side of the carrier signal $f_{c3b_2}(t)$ intersect the modulating signal $f_{r_b}(t)$ we define the function $f_{3b_2}(t)$ as:

$$f_{3b_2}(t) = m_a \sin(\omega_0 t) + \frac{4}{T_s} t - 4n \quad (\text{B.88})$$

Now using the Newton-Raphson method discussed in appendix section B.1.2 we approximate the root of equation B.86 as:

$$t_{12b_2} = t_{11b_2} - \frac{f_{1b_2}(t_{11b_2})}{f'_{1b_2}(t_{11b_2})} = t_{11b_2} - \frac{m_a \sin(\omega_0 t_{11b_2}) + \frac{4}{T_s} t_{11} - 4(n-1)}{\omega_0 m_a \cos(\omega_0 t_{11b_2}) + \frac{4}{T_s}} \quad (\text{B.89})$$

where the initial guess t_{11b_2} is given by:

$$t_{11b_2} = \frac{1}{4} T_s \cdot 4(n-1) \quad \text{for } 0 < t_{11b_2} < m_f T_s \quad (\text{B.90})$$

After i successive approximations we will have equation B.89 written as:

$$t_{1(i+1)b_2} = t_{1i b_2} - \frac{f_{1b_2}(t_{1i b_2})}{f'_{1b_2}(t_{1i b_2})} \quad (\text{B.91})$$

Similarly using the Newton-Raphson method we approximate the root of equation B.87 as:

$$t_{22b_2} = t_{21b_2} - \frac{f_{2b_2}(t_{21b_2})}{f'_{2b_2}(t_{21b_2})} = t_{21b_2} - \frac{m_a \sin(\omega_0 t_{21b_2}) - \frac{4}{T_s} t_{21b_2} + 4n - 2}{\omega_0 m_a \cos(\omega_0 t_{21b_2}) - \frac{4}{T_s}} \quad (\text{B.92})$$

where the initial guess t_{21b_2} is given by:

$$t_{21b_2} = \frac{1}{4} T_s \cdot (4n - 2) \quad \text{for } 0 < t_{21b_2} < m_f T_s \quad (\text{B.93})$$

After i successive approximations we will have equation B.92 written as:

$$t_{2(i+1)b_2} = t_{2i b_2} - \frac{f_{2b_2}(t_{2i b_2})}{f'_{2b_2}(t_{2i b_2})} \quad (\text{B.94})$$

And similarly using the Newton-Raphson method we approximate the root of equation B.88 as:

$$t_{32b_2} = t_{31b_2} - \frac{f_{1b_2}(t_{31b_2})}{f'_{1b_2}(t_{31b_2})} = t_{31b_2} - \frac{m_a \sin(\omega_0 t_{31b_2}) + \frac{4}{T_s} t_{31b_2} - 4n}{\omega_0 m_a \cos(\omega_0 t_{31b_2}) + \frac{4}{T_s}} \quad (\text{B.95})$$

where the initial guess t_{31b_2} is given by:

$$t_{31b_2} = \frac{1}{4} T_s \cdot 4n \quad \text{for } 0 < t_{31b_2} < m_f T_s \quad (\text{B.96})$$

After i successive approximations we will have equation B.95 written as:

$$t_{3(i+1)b_2} = t_{3ib_2} - \frac{f_{3b_2}(t_{3ib_2})}{f'_{3b_2}(t_{3ib_2})} \quad (\text{B.97})$$

Now we consider the pwm resulting from the intersection of f_{c1b_2} , f_{c2b_2} and f_{c3b_2} with f_{r_b} . First we look at the pulse formed between $t_{1(i+1)b_2}$ and $t_{2(i+1)b_2}$. The width of this pulse is given by

$$W_{1b_2} = t_{2(i+1)b_2} - t_{1(i+1)b_2}$$

Now following the same method as in section B.2.1 the Fourier transform of the positive pulse is given by:

$$\begin{aligned} F(\omega) &= \int_{-\frac{W_{1b_2}}{2}}^{\frac{W_{1b_2}}{2}} (V_t) e^{-j\omega_0 t} dt \\ &= -\frac{V_t}{j\omega_0} \left(e^{-j\omega_0(t_{2(i+1)b_2} - t_{1(i+1)b_2})} \right) \end{aligned} \quad (\text{B.98})$$

and the Fourier transform of the positive pulses generated by shifting the pulse between $t_{1(i+1)b_2}$ and $t_{2(i+1)b_2}$ by t_{01b_2} where t_{01b_2} is given by:

$$t_{01b_2} = t_{1(i+1)b_2} + \frac{W_{1b_2}}{2} \quad (\text{B.99})$$

can be represented as follows:

$$\begin{aligned} F(\omega) &= \int_{-\frac{W_{1b_2}}{2}}^{\frac{W_{1b_2}}{2}} (V_t) e^{-j\omega_0 t} e^{-j\omega_0 t_{01b_2}} dt \\ &= -\frac{V_t}{j\omega_0} \left(e^{-j\omega_0(t_{2(i+1)b_2} - t_{1(i+1)b_2})} e^{-j\omega_0 t_{01b_2}} \right) \end{aligned} \quad (\text{B.100})$$

Similarly we consider the pulse formed between $t_{2(i+1)b_2}$ and $t_{3(i+1)b_2}$ in Figure B.7. The width of this pulse is given by:

$$W_{2b_2} = t_{3(i+1)b_2} - t_{2(i+1)b_2}$$

and its Fourier transform using the negative pulse results in:

$$\begin{aligned} F(\omega) &= \int_{-\frac{W_{2b_2}}{2}}^{\frac{W_{2b_2}}{2}} (-V_t) e^{-j\omega_0 t} dt \\ &= \frac{V_t}{j\omega_0} \left(e^{-j\omega_0(t_{3(i+1)b_2} - t_{2(i+1)b_2})} \right) \end{aligned} \quad (\text{B.101})$$

The shifting of this negative pulse by t_{02b_2} is done similar to the one shown in Figure B.4 where t_{02b_2} is given by:

$$t_{02b_2} = t_{2(i+1)b_2} + \frac{W_{2b_2}}{2} \quad (\text{B.102})$$

The resulting Fourier transform of the shifted negative pulse is given by:

$$\begin{aligned} F(\omega) &= \int_{-\frac{W_{2b_2}}{2}}^{\frac{W_{2b_2}}{2}} (-V_t) e^{-j\omega_0 t} e^{-j\omega_0 t_{02b_2}} dt \\ &= \frac{V_t}{j\omega_0} \left(e^{-j\omega_0(t_{3(i+1)b_2} - t_{2(i+1)b_2})} e^{-j\omega_0 t_{02b_2}} \right) \end{aligned} \quad (\text{B.103})$$

To obtain the spectrum of $S_{b_2}(\omega)$ we sum up all the Fourier transform for the negative and positive pulses over any number of cycles of the switching period. The amplitude spectrum is the same as the one shown in Figure B.5 for $S_{a_1}(\omega)$.

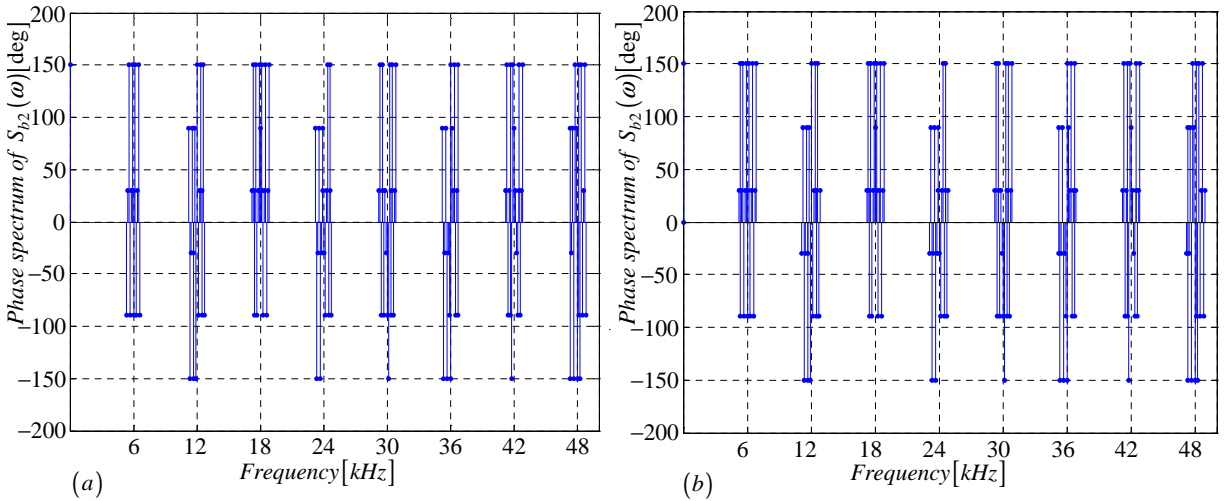


Figure B.18: Phase spectrum of $S_{b_2}(\omega)$ generated using (a) Newton-Raphson simulation and (b) Theory

B.2.7 Derivation of the spectrum for the switching function

$$s_{db}(t)$$

In this subsection we derive equations that are necessary for the plotting of $S_{db}(\omega)$ spectrum. We use the definition of $s_{db}(t)$ to obtain Figure B.19 from Figures B.15 and B.17.

The width of the positive pulse is given by:

$$W_{1s_{db}} = t_{2(i+1)b_2} - t_{1(i+1)b_2} \quad (\text{B.104})$$

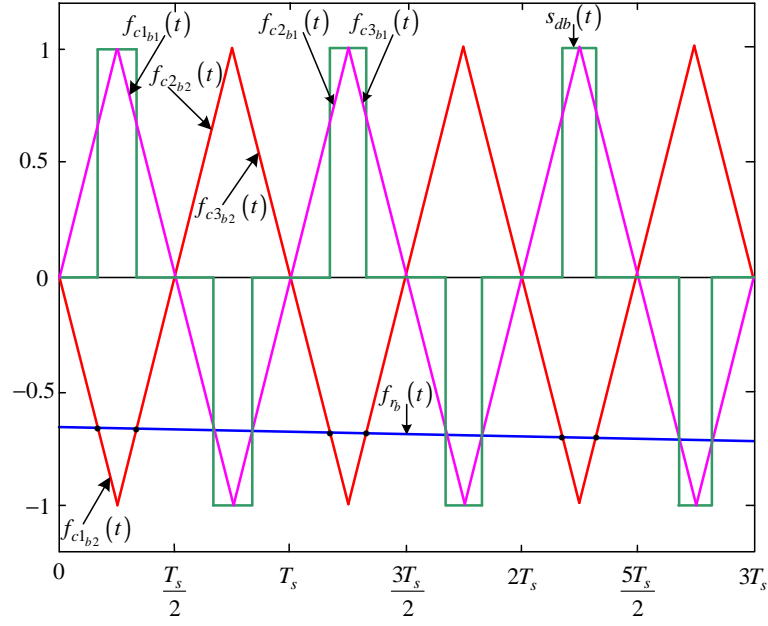


Figure B.19: Newton-Raphson method of switching function $s_{db}(t)$

The Fourier transform of the positive pulses generated by shifting the pulse between $t_{1(i+1)b2}$ and $t_{2(i+1)b2}$ by t_{01_sdb} where t_{01_sdb} is given by:

$$t_{01_sdb} = t_{1(i+1)b2} + \frac{W_{1_sdb}}{2} \quad (\text{B.105})$$

is given by:

$$\begin{aligned} F(\omega) &= \int_{-\frac{W_{1_sdb}}{2}}^{\frac{W_{1_sdb}}{2}} (V_t) e^{-j\omega_0 t} e^{-j\omega_0 t_{01_sdb}} dt \\ &= -\frac{V_t}{j\omega_0} \left(e^{-j\omega_0(t_{2(i+1)b2} - t_{1(i+1)b2})} e^{-j\omega_0 t_{01_sdb}} \right) \end{aligned} \quad (\text{B.106})$$

The width of the negative pulse is given by:

$$W_{2_sdb} = t_{2(i+1)b1} - t_{1(i+1)b1} \quad (\text{B.107})$$

The Fourier transform of the negative pulses generated by shifting the pulse between $t_{1(i+1)b1}$ and $t_{2(i+1)b1}$ by t_{02_sdb} where t_{02_sdb} is given by:

$$t_{02_sdb} = t_{1(i+1)b1} + \frac{W_{2_sdb}}{2} \quad (\text{B.108})$$

is given by:

$$\begin{aligned} F(\omega) &= \int_{-\frac{W_{2_sdb}}{2}}^{\frac{W_{2_sdb}}{2}} (-V_t) e^{-j\omega_0 t} e^{-j\omega_0 t_{02_sdb}} dt \\ &= \frac{V_t}{j\omega_0} \left(e^{-j\omega_0(t_{2(i+1)b1} - t_{1(i+1)b1})} e^{-j\omega_0 t_{02_sdb}} \right) \end{aligned} \quad (\text{B.109})$$

To obtain the spectrum of $S_{db}(\omega)$ we sum up all the Fourier transform for the negative and positive pulses over any number of cycles of the switching period. The amplitude spectrum is the same as the one shown in Figure B.10 for $S_{da}(\omega)$.

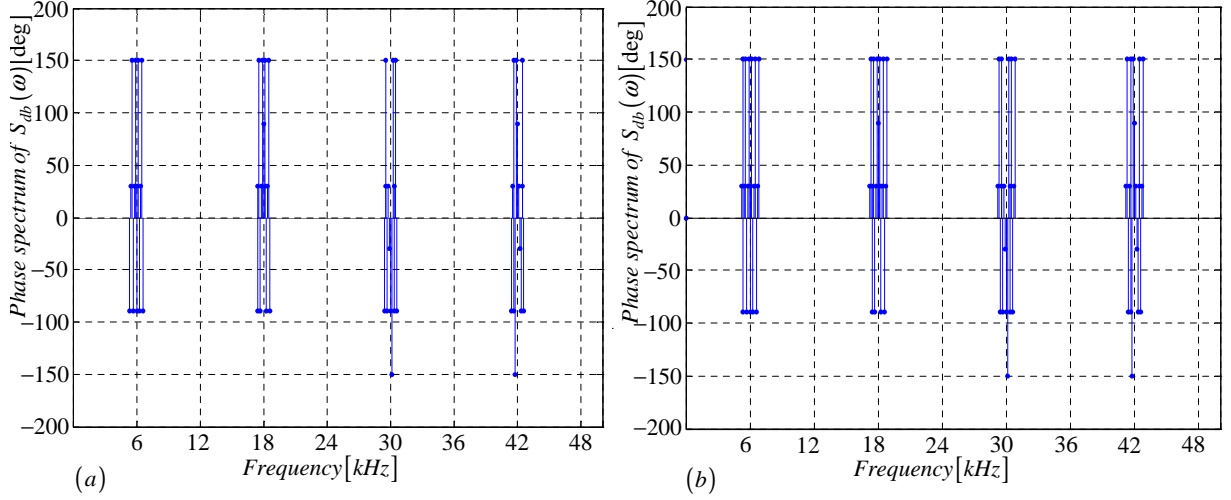


Figure B.20: Phase spectrum of $S_{db}(\omega)$ generated using (a) Newton-Raphson simulation and (b) Theory

B.2.8 Derivation of the spectrum for the switching function

$$s_{tb}(t)$$

In this subsection we derive equations that are necessary for the plotting of $S_{tb}(\omega)$ spectrum. We use the definition of $s_{tb}(t)$ to obtain Figure B.21 from Figures B.15 and B.17.

The width of the negative pulse between $t_{2(i+1)b2}$ and $t_{1(i+1)b1}$ is given by:

$$W_{1_{sdb}} = t_{1(i+1)b1} - t_{2(i+1)b2} \quad (\text{B.110})$$

The Fourier transform of the negative pulses generated by shifting the pulse between $t_{2(i+1)b2}$ and $t_{1(i+1)b1}$ by $t_{01_{stb}}$ where $t_{01_{stb}}$ is given by:

$$t_{01_{stb}} = t_{2(i+1)b2} + \frac{W_{1_{stb}}}{2} \quad (\text{B.111})$$

is given by:

$$\begin{aligned} F(\omega) &= \int_{-\frac{W_{1_{stb}}}{2}}^{\frac{W_{1_{stb}}}{2}} (-V_t) e^{-j\omega t} e^{-j\omega_0 t_{01_{stb}}} dt \\ &= \frac{V_t}{j\omega_0} \left(e^{-j\omega_0(t_{1(i+1)b1} - t_{2(i+1)b2})} e^{-j\omega_0 t_{01_{stb}}} \right) \end{aligned} \quad (\text{B.112})$$

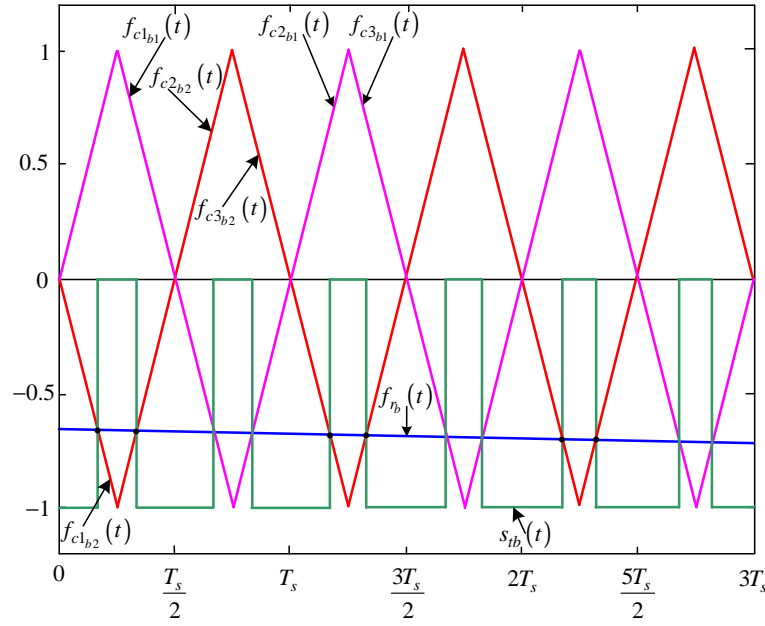


Figure B.21: Newton-Raphson method of switching function $s_{tb}(t)$

The width of the negative pulse between $t_{2(i+1)b_1}$ and $t_{3(i+1)b_2}$ by $t_{02_{stb}}$ is given by:

$$W_{2_{stb}} = t_{3(i+1)b_2} - t_{2(i+1)b_1} \quad (\text{B.113})$$

The Fourier transform of the negative pulses generated by shifting the pulse between $t_{2(i+1)b_1}$ and $t_{3(i+1)b_2}$ by $t_{02_{stb}}$ where $t_{02_{stb}}$ is given by:

$$t_{02_{stb}} = t_{2(i+1)b_1} + \frac{W_{2_{stb}}}{2} \quad (\text{B.114})$$

is given by:

$$\begin{aligned} F(\omega) &= \int_{-\frac{W_{2_{stb}}}{2}}^{\frac{W_{2_{stb}}}{2}} (-V_t) e^{-j\omega_0 t} e^{-j\omega_0 t_{02_{stb}}} dt \\ &= \frac{V_t}{j\omega_0} \left(e^{-j\omega_0(t_{3(i+1)b_2} - t_{2(i+1)b_1})} e^{-j\omega_0 t_{02_{stb}}} \right) \end{aligned} \quad (\text{B.115})$$

To obtain the spectrum of $S_{tb}(\omega)$ we sum up all the Fourier transform for the positive pulses over any number of cycles of the switching period. The amplitude spectrum is the same as the one shown in Figure B.13 for $S_{ta}(\omega)$.

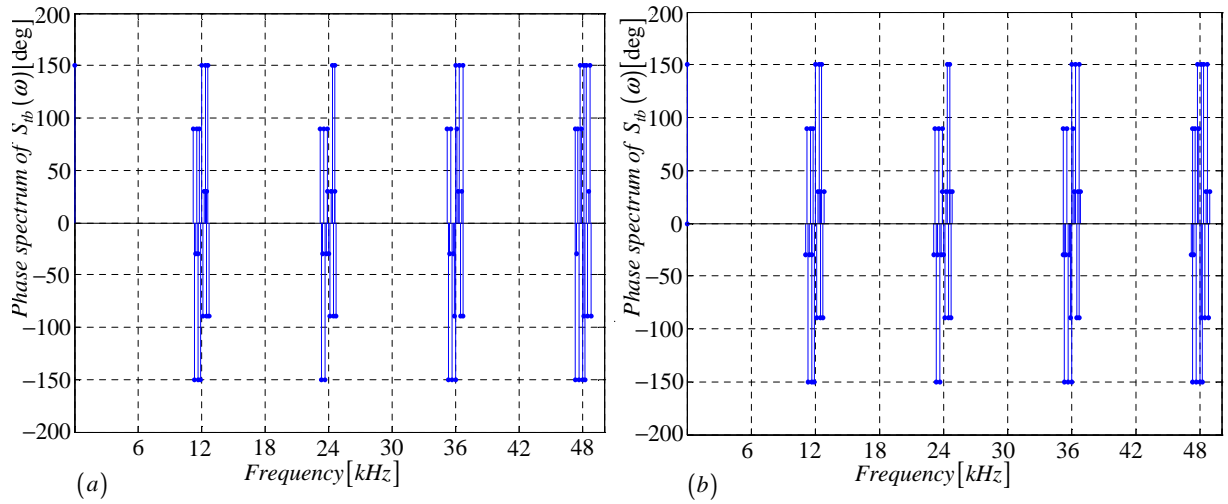


Figure B.22: Phase spectrum of $S_{ib}(\omega)$ generated using (a) Newton-Raphson simulation and (b) Theory

B.2.9 Derivation of the spectrum for the switching function

$$s_{c1}(t)$$

In this subsection we derive equations that are necessary for the plotting of $S_{c1}(\omega)$ spectrum. The procedure is the same as in subsection B.2.1 except that the reference signal in Figure B.23 is out of phase by 240 degrees with the one in Figure B.2.

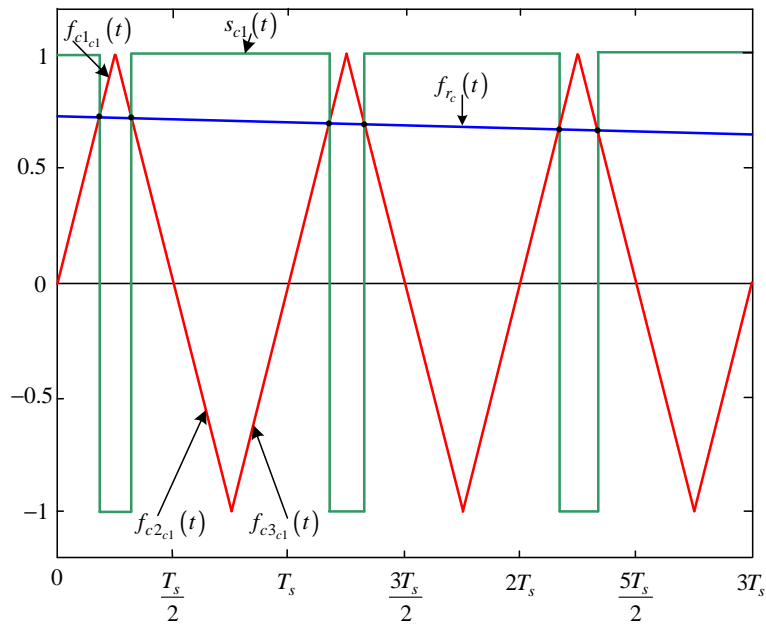


Figure B.23: Newton-Raphson method of switching function $s_{c1}(t)$

Modulation signal $f_{r_c}(t)$ is given by:

$$f_{r_c}(t) = m_a \sin\left(\omega_0 t + \frac{2\pi}{3}\right) \quad (\text{B.116})$$

The rising side of the carrier signal $f_{c1_{c1}}(t)$ is given by:

$$f_{c1_{c1}}(t) = \frac{4}{T_s}t - 4(n-1) \quad (\text{B.117})$$

The falling side of the carrier signal $f_{c2_{c1}}(t)$ is given by:

$$f_{c2_{c1}}(t) = -\frac{4}{T_s}t + 4n - 2 \quad (\text{B.118})$$

The next rising side of the carrier signal $f_{c3_{c1}}(t)$ is given by:

$$f_{c3_{c1}}(t) = \frac{4}{T_s}t - 4n \quad (\text{B.119})$$

Where the rising side of the carrier signal $f_{c1_{c1}}(t)$ intersect the modulating signal $f_{r_c}(t)$ we define the function $f_{1_{c1}}(t)$ as:

$$f_{1_{c1}}(t) = m_a \sin(\omega_0 t) - \frac{4}{T_s}t + 4(n-1) \quad (\text{B.120})$$

and where the falling side of the carrier signal $f_{c2_{c1}}(t)$ intersect the modulating signal $f_{r_c}(t)$ we define the function $f_{2_{c1}}(t)$ as:

$$f_{2_{c1}}(t) = m_a \sin(\omega_0 t) + \frac{4}{T_s}t - 4n + 2 \quad (\text{B.121})$$

and similarly where the rising side of the carrier signal $f_{c3_{c1}}(t)$ intersect the modulating signal $f_{r_c}(t)$ we define the function $f_{3_{c1}}(t)$ as:

$$f_{3_{c1}}(t) = m_a \sin(\omega_0 t) - \frac{4}{T_s}t + 4n \quad (\text{B.122})$$

Now using the Newton-Raphson method discussed in appendix section B.1.2 we approximate the root of equation B.120 as:

$$t_{12_{c1}} = t_{11_{c1}} - \frac{f_{1_{c1}}(t_{11_{c1}})}{f'_{1_{c1}}(t_{11_{c1}})} = t_{11_{c1}} - \frac{m_a \sin(\omega_0 t_{11_{c1}}) - \frac{4}{T_s}t_{11_{c1}} + 4(n-1)}{\omega_0 m_a \cos(\omega_0 t_{11_{c1}}) - \frac{4}{T_s}} \quad (\text{B.123})$$

where the initial guess $t_{11_{c1}}$ is given by:

$$t_{11_{c1}} = \frac{1}{4}T_s \cdot 4(n-1) \quad \text{for } 0 < t_{11_{c1}} < m_f T_s \quad (\text{B.124})$$

After i successive approximations we will have equation B.123 written as:

$$t_{1(i+1)_{c1}} = t_{1i_{c1}} - \frac{f_{1_{c1}}(t_{1i_{c1}})}{f'_{1_{c1}}(t_{1i_{c1}})} \quad (\text{B.125})$$

Similarly using the Newton-Raphson method we approximate the root of equation B.121 as:

$$t_{22_{c1}} = t_{21_{c1}} - \frac{f_{2_{c1}}(t_2)}{f'_{2_{c1}}(t_{21_{c1}})} = t_{21_{c1}} - \frac{m_a \sin(\omega_0 t_{21_{c1}}) + \frac{4}{T_s} t_{21_{c1}} - 4n + 2}{\omega_0 m_a \cos(\omega_0 t_{21_{c1}}) + \frac{4}{T_s}} \quad (\text{B.126})$$

where the initial guess $t_{21_{c1}}$ is given by:

$$t_{21_{c1}} = \frac{1}{4} T_s \cdot (4n - 2) \quad \text{for } 0 < t_{21_{c1}} < m_f T_s \quad (\text{B.127})$$

After i successive approximations we will have equation B.126 written as:

$$t_{2(i+1)_{c1}} = t_{2i_{c1}} - \frac{f_{2_{c1}}(t_{2i_{c1}})}{f'_{2_{c1}}(t_{2i_{c1}})} \quad (\text{B.128})$$

And similarly using the Newton-Raphson method we approximate the root of equation B.122 as:

$$t_{32_{c1}} = t_{31_{c1}} - \frac{f_{3_{c1}}(t_{31_{c1}})}{f'_{3_{c1}}(t_{31_{c1}})} = t_{31_{c1}} - \frac{m_a \sin(\omega_0 t_{31_{c1}}) - \frac{4}{T_s} t_{31_{c1}} + 4n}{\omega_0 m_a \cos(\omega_0 t_{31_{c1}}) - \frac{4}{T_s}} \quad (\text{B.129})$$

where the initial guess $t_{31_{c1}}$ is given by:

$$t_{31_{c1}} = \frac{1}{4} T_s \cdot 4n \quad \text{for } 0 < t_{31_{c1}} < m_f T_s \quad (\text{B.130})$$

After i successive approximations we will have equation B.129 written as:

$$t_{3(i+1)_{c1}} = t_{3i_{c1}} - \frac{f_{3_{c1}}(t_{3i_{c1}})}{f'_{3_{c1}}(t_{3i_{c1}})} \quad (\text{B.131})$$

Now we consider the pwm resulting from the intersection of $f_{c1_{c1}}$, $f_{c2_{c1}}$ and $f_{c3_{c1}}$ with f_{rc} . First we look at the pulse formed between $t_{1(i+1)_{c1}}$ and $t_{2(i+1)_{c1}}$. The width of this pulse is given by:

$$W_{1_{c1}} = t_{2(i+1)_{c1}} - t_{1(i+1)_{c1}}$$

Now following the same method as in section B.2.1 the Fourier transform of the negative pulse is given by:

$$\begin{aligned} F(\omega) &= \int_{-\frac{W_{1_{c1}}}{2}}^{\frac{W_{1_{c1}}}{2}} (V_t) e^{-j\omega_0 t} dt \\ &= -\frac{V_t}{j\omega_0} \left(e^{-j\omega_0(t_{2(i+1)_{c1}} - t_{1(i+1)_{c1}})} \right) \end{aligned} \quad (\text{B.132})$$

and the Fourier transform of the negative pulses generated by shifting the pulse between $t_{1(i+1)_{c1}}$ and $t_{2(i+1)_{c1}}$ by $t_{01_{c1}}$ where $t_{01_{c1}}$ is given by:

$$t_{01_{c1}} = t_{1(i+1)_{c1}} + \frac{W_{1_{c1}}}{2} \quad (\text{B.133})$$

can be represented as follows:

$$\begin{aligned}
 F(\omega) &= \int_{-\frac{w_{1c1}}{2}}^{\frac{w_{1c1}}{2}} (-V_t) e^{-j\omega_0 t} e^{-j\omega_0 t_{01c1}} dt \\
 &= \frac{V_t}{j\omega_0} \left(e^{-j\omega_0(t_{2(i+1)c1} - t_{1(i+1)c1})} e^{-j\omega_0 t_{01c1}} \right)
 \end{aligned} \tag{B.134}$$

Similarly we consider the pulse formed between $t_{2(i+1)c1}$ and $t_{3(i+1)c1}$ in Figure B.23. The width of this pulse is given by:

$$W_{2c1} = t_{3(i+1)c1} - t_{2(i+1)c1}$$

and its Fourier transform using the positive pulse results in:

$$\begin{aligned}
 F(\omega) &= \int_{-\frac{w_{2c1}}{2}}^{\frac{w_{2c1}}{2}} (V_t) e^{-j\omega_0 t} dt \\
 &= -\frac{V_t}{j\omega_0} \left(e^{-j\omega_0(t_{3(i+1)c1} - t_{2(i+1)c1})} \right)
 \end{aligned} \tag{B.135}$$

The shifting of this positive pulse by t_{02c1} is done similar to the one shown in Figure B.4 where t_{02c1} is given by:

$$t_{02c1} = t_{2(i+1)c1} + \frac{W_{2c1}}{2} \tag{B.136}$$

The resulting Fourier transform of the shifted positive pulse is given by:

$$\begin{aligned}
 F(\omega) &= \int_{-\frac{w_{2c1}}{2}}^{\frac{w_{2c1}}{2}} (V_t) e^{-j\omega_0 t} e^{-j\omega_0 t_{02c1}} dt \\
 &= -\frac{V_t}{j\omega_0} \left(e^{-j\omega_0(t_{3(i+1)c1} - t_{2(i+1)c1})} e^{-j\omega_0 t_{02c1}} \right)
 \end{aligned} \tag{B.137}$$

To obtain the spectrum of $S_{c1}(\omega)$ we sum up all the Fourier transform for the negative and positive pulses over any number of cycles of the switching period. The amplitude spectrum is the same as the one shown in Figure B.5 for $S_{a1}(\omega)$.

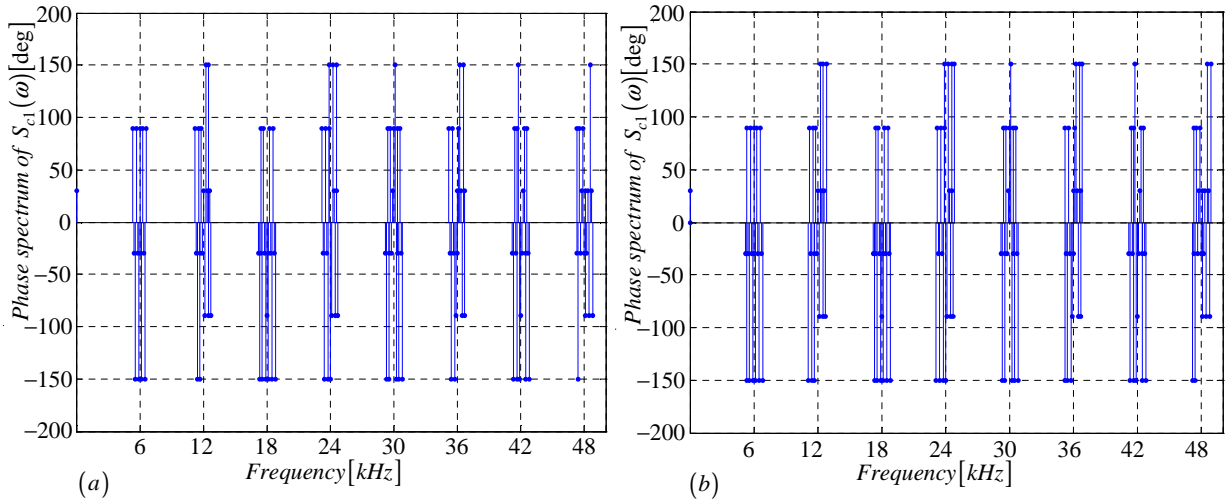


Figure B.24: Phase spectrum of $S_{c1}(\omega)$ generated using (a) Newton-Raphson simulation and (b) Theory

B.2.10 Derivation of the spectrum for the switching function $s_{c2}(t)$

In this subsection we derive equations that are necessary for the plotting of $S_{c2}(\omega)$ spectrum. The procedure is the same as in subsection B.2.9 except that the carrier signal in Figure B.25 is out of phase by 180 degrees with the one in Figure B.23.

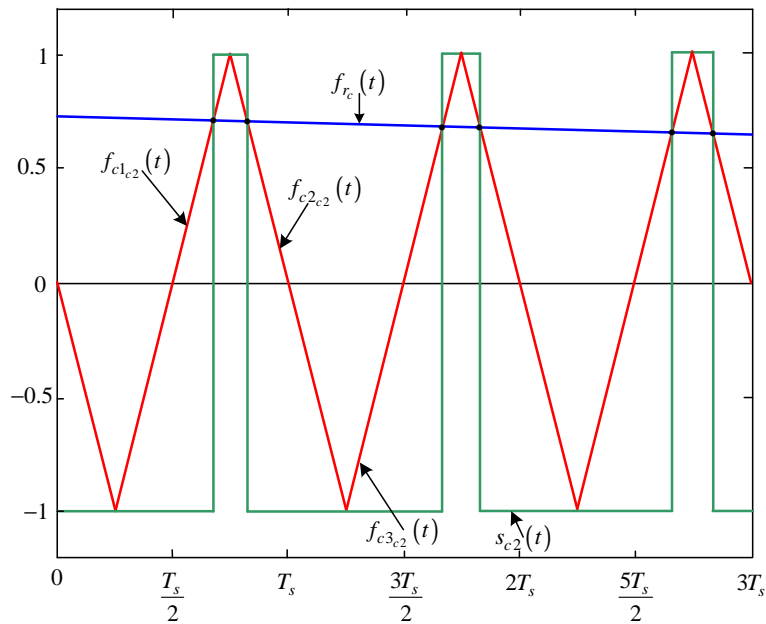


Figure B.25: Newton-Raphson method of switching function $s_{c2}(t)$

Modulation signal $f_{r_c}(t)$ is given by:

$$f_{r_c}(t) = m_a \sin\left(\omega_0 t + \frac{2\pi}{3}\right) \quad (\text{B.138})$$

The rising side of the carrier signal $f_{c1_{c2}}(t)$ is given by:

$$f_{c1_{c2}}(t) = \frac{4}{T_s}t - 4n + 2 \quad (\text{B.139})$$

The falling side of the carrier signal $f_{c2_{c2}}(t)$ is given by:

$$f_{c2_{c2}}(t) = -\frac{4}{T_s}t + 4n \quad (\text{B.140})$$

The next rising side of the carrier signal $f_{c3_{c2}}(t)$ is given by:

$$f_{c3_{c2}}(t) = \frac{4}{T_s}t - 4n - 2 \quad (\text{B.141})$$

Where the rising side of the carrier signal $f_{c1_{c2}}(t)$ intersect the modulating signal $f_{r_c}(t)$ we define the function $f_{1_{c2}}(t)$ as:

$$f_{1_{c2}}(t) = m_a \sin(\omega_0 t) - \frac{4}{T_s}t + 4n - 2 \quad (\text{B.142})$$

and where the falling side of the carrier signal $f_{c2_{c2}}(t)$ intersect the modulating signal $f_{r_c}(t)$ we define the function $f_{2_{c2}}(t)$ as:

$$f_{2_{c2}}(t) = m_a \sin(\omega_0 t) + \frac{4}{T_s}t - 4n \quad (\text{B.143})$$

and similarly where the rising side of the carrier signal $f_{c3_{c2}}(t)$ intersect the modulating signal $f_{r_c}(t)$ we define the function $f_{3_{c2}}(t)$ as:

$$f_{3_{c2}}(t) = m_a \sin(\omega_0 t) - \frac{4}{T_s}t + 4n + 2 \quad (\text{B.144})$$

Now using the Newton-Raphson method discussed in appendix section B.1.2 we approximate the root of equation B.142 as:

$$t_{12_{c2}} = t_{11_{c2}} - \frac{f_{1_{c2}}(t_{11_{c2}})}{f'_{1_{c2}}(t_{11_{c2}})} = t_{11_{c2}} - \frac{m_a \sin(\omega_0 t_{11_{c2}}) - \frac{4}{T_s}t_{11_{c2}} + 4n - 2}{\omega_0 m_a \cos(\omega_0 t_{11_{c2}}) - \frac{4}{T_s}} \quad (\text{B.145})$$

where the initial guess $t_{11_{c2}}$ is given by:

$$t_{11_{c2}} = \frac{1}{4}T_s \cdot (4n - 2) \quad \text{for } 0 < t_{11_{c2}} < m_f T_s \quad (\text{B.146})$$

After i successive approximations we will have equation B.145 written as:

$$t_{1(i+1)_{c2}} = t_{1i_{c2}} - \frac{f_{1_{c2}}(t_{1i_{c2}})}{f'_{1_{c2}}(t_{1i_{c2}})} \quad (\text{B.147})$$

Similarly using the Newton-Raphson method we approximate the root of equation B.143 as:

$$t_{22c2} = t_{21c2} - \frac{f_{2c2}(t_2)}{f'_{2c2}(t_{21c2})} = t_{21c2} - \frac{m_a \sin(\omega_0 t_{2c2}) + \frac{4}{T_s} t_{21c2} - 4n}{\omega_0 m_a \cos(\omega_0 t_{21c2}) + \frac{4}{T_s}} \quad (\text{B.148})$$

where the initial guess t_{21c2} is given by:

$$t_{21c2} = \frac{1}{4} T_s \cdot (4n) \quad \text{for } 0 < t_{21c2} < m_f T_s \quad (\text{B.149})$$

After i successive approximations we will have equation B.148 written as:

$$t_{2(i+1)c2} = t_{2ic2} - \frac{f_{2c2}(t_{2ic2})}{f'_{2c2}(t_{2ic2})} \quad (\text{B.150})$$

And similarly using the Newton-Raphson method we approximate the root of equation B.144 as:

$$t_{32c2} = t_{31c2} - \frac{f_{1c2}(t_{31c2})}{f'_{1c2}(t_{31c2})} = t_{31c2} - \frac{m_a \sin(\omega_0 t_{31c2}) - \frac{4}{T_s} t_{31c2} + 4n + 2}{\omega_0 m_a \cos(\omega_0 t_{31c2}) - \frac{4}{T_s}} \quad (\text{B.151})$$

where the initial guess t_{31c2} is given by:

$$t_{31c2} = \frac{1}{4} T_s \cdot (4n + 2) \quad \text{for } 0 < t_{31c2} < m_f T_s \quad (\text{B.152})$$

After i successive approximations we will have equation B.151 written as:

$$t_{3(i+1)c2} = t_{3ic2} - \frac{f_{3c2}(t_{3ic2})}{f'_{3c2}(t_{3ic2})} \quad (\text{B.153})$$

Now we consider the pwm resulting from the intersection of f_{c1c2} , f_{c2c2} and f_{c3c2} with f_{rc} . First we look at the pulse formed between $t_{1(i+1)c2}$ and $t_{2(i+1)c2}$. The width of this pulse is given by:

$$W_{1c2} = t_{2(i+1)c2} - t_{1(i+1)c2}$$

Now following the same method as in section B.2.1 the Fourier transform of the positive pulse is given by:

$$\begin{aligned} F(\omega) &= \int_{-\frac{W_{1c2}}{2}}^{\frac{W_{1c2}}{2}} (-V_t) e^{-j\omega_0 t} dt \\ &= \frac{V_t}{j\omega_0} \left(e^{-j\omega_0(t_{2(i+1)c2} - t_{1(i+1)c2})} \right) \end{aligned} \quad (\text{B.154})$$

and the Fourier transform of the positive pulses generated by shifting the pulse between $t_{1(i+1)c2}$ and $t_{2(i+1)c2}$ by t_{01c2} where t_{01c2} is given by:

$$t_{01c2} = t_{1(i+1)c2} + \frac{W_{1c2}}{2} \quad (\text{B.155})$$

can be represented as follows:

$$\begin{aligned}
 F(\omega) &= \int_{-\frac{w_{1c2}}{2}}^{\frac{w_{1c2}}{2}} (V_t) e^{-j\omega_0 t} e^{-j\omega_0 t_{01c2}} dt \\
 &= -\frac{V_t}{j\omega_0} \left(e^{-j\omega_0(t_{2(i+1)c2} - t_{1(i+1)c2})} e^{-j\omega_0 t_{01c2}} \right)
 \end{aligned}
 \tag{B.156}$$

Similarly we consider the pulse formed between $t_{2(i+1)c2}$ and $t_{3(i+1)c2}$ in Figure B.25. The width of this pulse is given by:

$$W_{2c2} = t_{3(i+1)c2} - t_{2(i+1)c2}$$

and its Fourier transform using the negative pulse results in:

$$\begin{aligned}
 F(\omega) &= \int_{-\frac{w_{2c2}}{2}}^{\frac{w_{2c2}}{2}} (-V_t) e^{-j\omega_0 t} dt \\
 &= \frac{V_t}{j\omega_0} \left(e^{-j\omega_0(t_{3(i+1)c2} - t_{2(i+1)c2})} \right)
 \end{aligned}
 \tag{B.157}$$

The shifting of this negative pulse by t_{02c2} is done similar to the one shown in Figure B.4 where t_{02c2} is given by:

$$t_{02c2} = t_{2(i+1)c2} + \frac{W_{2c2}}{2} \tag{B.158}$$

The resulting Fourier transform of the shifted negative pulse is given by:

$$\begin{aligned}
 F(\omega) &= \int_{-\frac{w_{2c2}}{2}}^{\frac{w_{2c2}}{2}} (-V_t) e^{-j\omega_0 t} e^{-j\omega_0 t_{02c2}} dt \\
 &= \frac{V_t}{j\omega_0} \left(e^{-j\omega_0(t_{3(i+1)c2} - t_{2(i+1)c2})} e^{-j\omega_0 t_{02c2}} \right)
 \end{aligned}
 \tag{B.159}$$

To obtain the spectrum of $S_{c2}(\omega)$ we sum up all the Fourier transform for the negative and positive pulses over any number of cycles of the switching period. The amplitude spectrum is the same as the one shown in Figure B.5 for $S_{a1}(\omega)$.

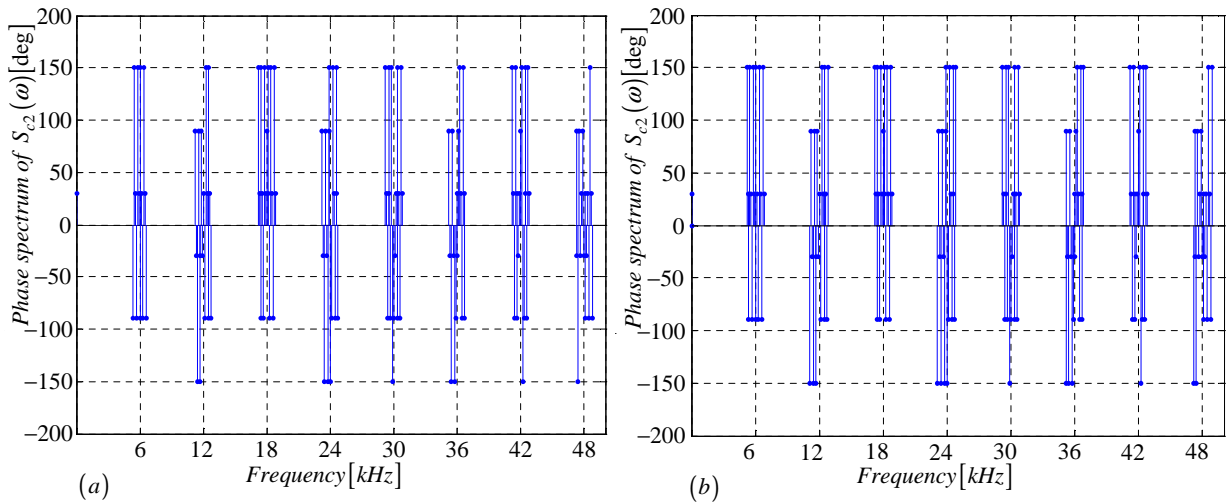


Figure B.26: Phase spectrum of $S_{c2}(\omega)$ generated using (a) Newton-Raphson simulation and (b) Theory

B.2.11 Derivation of the spectrum for the switching function $s_{dc}(t)$

$$s_{dc}(t)$$

In this subsection we derive equations that are necessary for the plotting of $S_{dc}(\omega)$ spectrum. We use the definition of $s_{dc}(t)$ to obtain Figure B.27 from Figures B.23 and B.25.

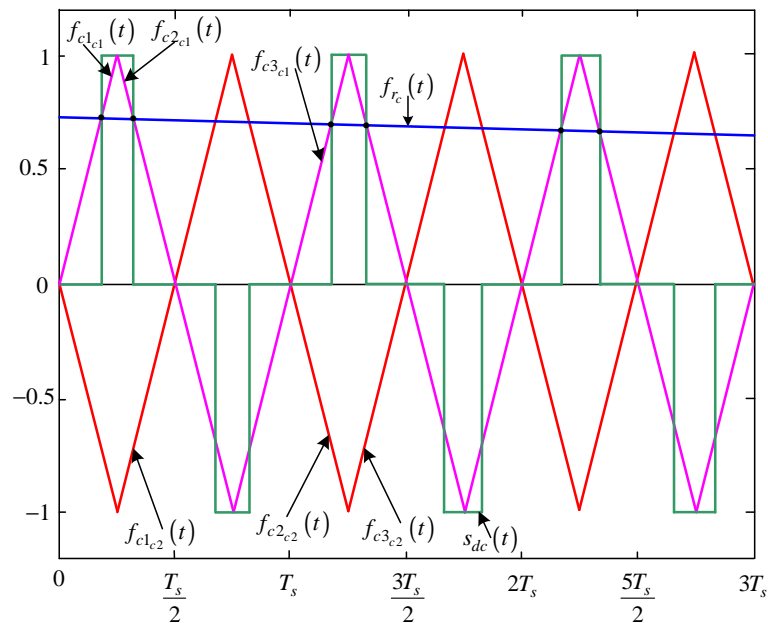


Figure B.27: Newton-Raphson method of switching function $s_{dc}(t)$

The width of the positive pulse is given by:

$$W_{1_{sdc}} = t_{2(i+1)c1} - t_{1(i+1)c1} \quad (\text{B.160})$$

The Fourier transform of the positive pulses generated by shifting the pulse between $t_{1(i+1)c1}$ and $t_{2(i+1)c1}$ by $t_{01_{sdc}}$ where $t_{01_{sdc}}$ is given by:

$$t_{01_{sdb}} = t_{1(i+1)c1} + \frac{W_{1_{sdc}}}{2} \quad (\text{B.161})$$

is given by:

$$\begin{aligned} F(\omega) &= \int_{-\frac{W_{1_{sdc}}}{2}}^{\frac{W_{1_{sdc}}}{2}} (V_t) e^{-j\omega_0 t} e^{-j\omega_0 t_{01_{sdc}}} dt \\ &= -\frac{V_t}{j\omega_0} \left(e^{-j\omega_0(t_{2(i+1)c1} - t_{1(i+1)c1})} e^{-j\omega_0 t_{01_{sdc}}} \right) \end{aligned} \quad (\text{B.162})$$

The width of the negative pulse is given by:

$$W_{2_{sdc}} = t_{2(i+1)c2} - t_{1(i+1)c2} \quad (\text{B.163})$$

The Fourier transform of the negative pulses generated by shifting the pulse between $t_{1(i+1)c2}$ and $t_{2(i+1)c2}$ by $t_{02_{sdc}}$ where $t_{02_{sdc}}$ is given by:

$$t_{02_{sdc}} = t_{1(i+1)c2} + \frac{W_{2_{sdc}}}{2} \quad (\text{B.164})$$

is given by:

$$\begin{aligned} F(\omega) &= \int_{-\frac{W_{2_{sdc}}}{2}}^{\frac{W_{2_{sdc}}}{2}} (-V_t) e^{-j\omega_0 t} e^{-j\omega_0 t_{02_{sdc}}} dt \\ &= \frac{V_t}{j\omega_0} \left(e^{-j\omega_0(t_{2(i+1)c2} - t_{1(i+1)c2})} e^{-j\omega_0 t_{02_{sdc}}} \right) \end{aligned} \quad (\text{B.165})$$

To obtain the spectrum of $S_{dc}(\omega)$ we sum up all the Fourier transform for the negative and positive pulses over any number of cycles of the switching period. The amplitude spectrum is the same as the one shown in Figure B.10 for $S_{da}(\omega)$.

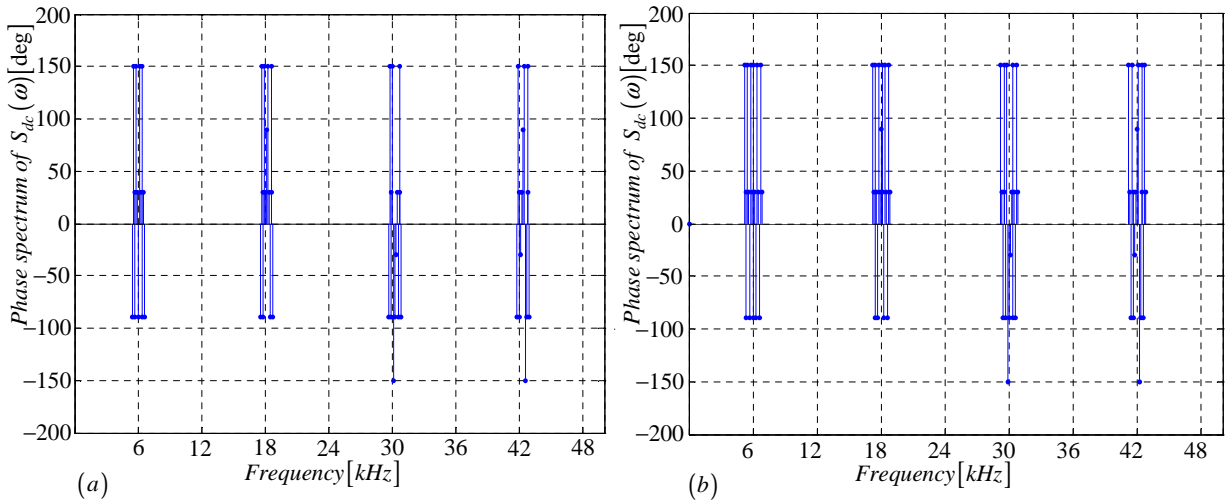


Figure B.28: Phase spectrum of $S_{dc}(\omega)$ generated using (a) Newton-Raphson simulation and (b) Theory

B.2.12 Derivation of the spectrum for the switching function $s_{tc}(t)$

In this subsection we derive equations that are necessary for the plotting of $S_{tc}(\omega)$ spectrum. We use the definition of $s_{tc}(t)$ to obtain Figure B.29 from Figures B.23 and B.25.

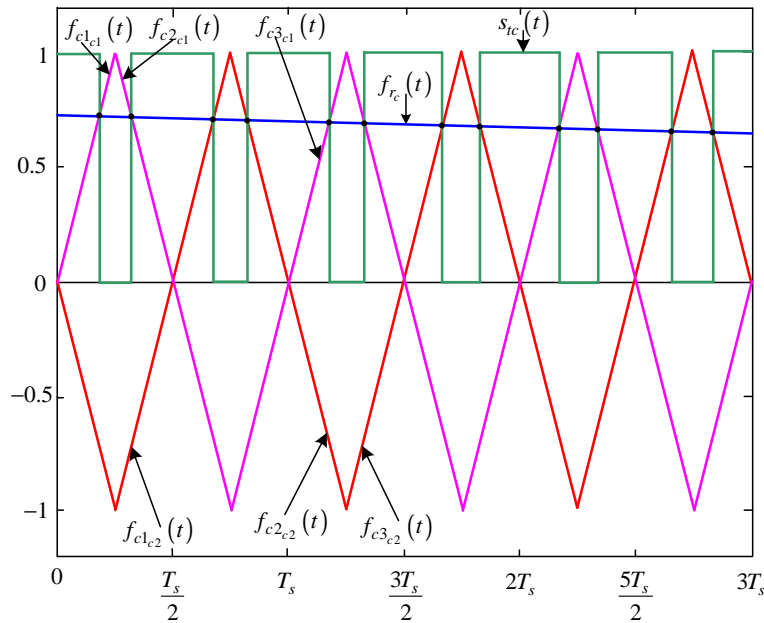


Figure B.29: Newton-Raphson method of switching function $s_{tc}(t)$

The width of the positive pulse between $t_{2(i+1)c1}$ and $t_{1(i+1)c2}$ is given by:

$$W_{1_{sdc}} = t_{1(i+1)c2} - t_{2(i+1)c1} \quad (\text{B.166})$$

The Fourier transform of the positive pulses generated by shifting the pulse between $t_{2(i+1)c1}$ and $t_{1(i+1)c2}$ by $t_{01_{stc}}$ where $t_{01_{stc}}$ is given by:

$$t_{01_{stc}} = t_{2(i+1)c1} + \frac{W_{1_{stc}}}{2} \quad (\text{B.167})$$

is given by:

$$\begin{aligned} F(\omega) &= \int_{-\frac{W_{1_{stc}}}{2}}^{\frac{W_{1_{stc}}}{2}} (V_t) e^{-j\omega_0 t} e^{-j\omega_0 t_{01_{stc}}} dt \\ &= -\frac{V_t}{j\omega_0} \left(e^{-j\omega_0(t_{1(i+1)c2} - t_{2(i+1)c1})} e^{-j\omega_0 t_{01_{stc}}} \right) \end{aligned} \quad (\text{B.168})$$

The width of the positive pulse between $t_{2(i+1)c2}$ and $t_{3(i+1)c1}$ by $t_{02_{stc}}$ is given by:

$$W_{2_{stc}} = t_{3(i+1)c1} - t_{2(i+1)c2} \quad (\text{B.169})$$

The Fourier transform of the positive pulses generated by shifting the pulse between $t_{2(i+1)c2}$ and $t_{3(i+1)c1}$ by $t_{02_{stc}}$ where $t_{02_{stc}}$ is given by:

$$t_{02_{stc}} = t_{2(i+1)c2} + \frac{W_{2_{stc}}}{2} \quad (\text{B.170})$$

is given by:

$$\begin{aligned} F(\omega) &= \int_{-\frac{W_{2_{stc}}}{2}}^{\frac{W_{2_{stc}}}{2}} (V_t) e^{-j\omega_0 t} e^{-j\omega_0 t_{02_{stc}}} dt \\ &= -\frac{V_t}{j\omega_0} \left(e^{-j\omega_0(t_{3(i+1)c1} - t_{2(i+1)c2})} e^{-j\omega_0 t_{02_{stc}}} \right) \end{aligned} \quad (\text{B.171})$$

To obtain the spectrum of $S_{tc}(\omega)$ we sum up all the Fourier transform for the positive pulses over any number of cycles of the switching period. The amplitude spectrum is the same as the one shown in Figure B.13 for $S_{ta}(\omega)$.

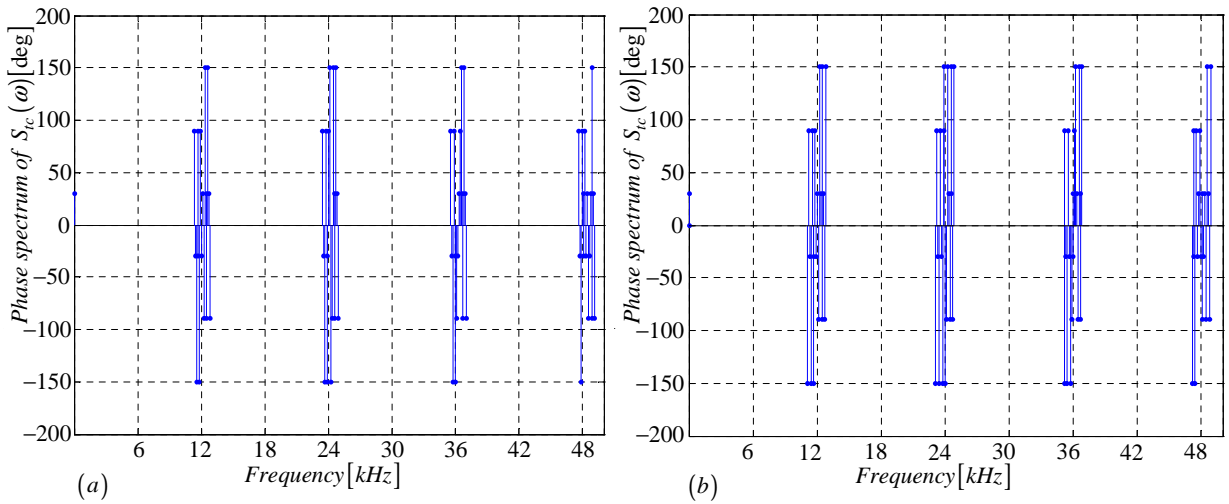


Figure B.30: Phase spectrum of $S_{tc}(\omega)$ generated using (a) Newton-Raphson simulation and (b) Theory

B.3 Newton-Raphson Method for Simulation of a 3-cell converter

The main purpose of this section is to use Newton-Raphson simulation method for plotting the spectrum of the switching functions of 3-cell multicell converter. This will then be compared with the spectrum obtained using double-Fourier analysis. The spectrum for the switching functions $s_{a1}(t)$, $s_{b1}(t)$ and $s_{c1}(t)$ are the same as those derived for 2-cell converter.

B.3.1 Derivation of the spectrum for the switching function

$$s_{a2}(t)$$

In this subsection we derive equations that are necessary for the plotting of $S_{a2}(\omega)$ spectrum. The procedure is the same as in subsection B.2.1 except that the carrier signal in Figure B.31 is out of phase by 120 degrees with the one in Figure B.2.

Modulation signal $f_{ra}(t)$ is given by:

$$f_{ra}(t) = m_a \sin(\omega_0 t) \quad (\text{B.172})$$

The rising side of the carrier signal $f_{c1a2}(t)$ is given by:

$$f_{c1a2}(t) = \frac{4}{T_s} t - \left(4n - \frac{8}{3}\right) \quad (\text{B.173})$$

The falling side of the carrier signal $f_{c2a2}(t)$ is given by:

$$f_{c2a2}(t) = -\frac{4}{T_s} t + \left(4n - \frac{2}{3}\right) \quad (\text{B.174})$$

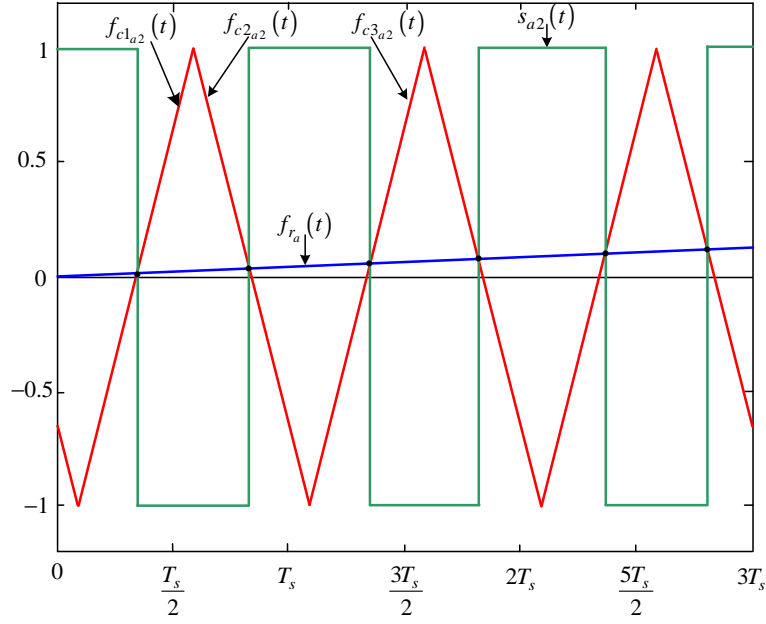


Figure B.31: Newton-Raphson method of switching function $s_{a2}(t)$

The next rising side of the carrier signal $f_{c_{3a2}}(t)$ is given by:

$$f_{c_{3a2}}(t) = \frac{4}{T_s}t - \left(4n + \frac{10}{3}\right) \quad (\text{B.175})$$

Where the rising side of the carrier signal $f_{c_{1a2}}(t)$ intersect the modulating signal $f_{r_a}(t)$ we define the function $f_{1a2}(t)$ as:

$$f_{1a2}(t) = m_a \sin(\omega_0 t) - \frac{4}{T_s}t + \left(4n - \frac{8}{3}\right) \quad (\text{B.176})$$

and where the falling side of the carrier signal $f_{1a2}(t)$ intersect the modulating signal $f_{r_a}(t)$ we define the function $f_{2a2}(t)$ as:

$$f_{2a2}(t) = m_a \sin(\omega_0 t) + \frac{4}{T_s}t - \left(4n - \frac{2}{3}\right) \quad (\text{B.177})$$

and similarly where the rising side of the carrier signal $f_{c_{3a2}}(t)$ intersect the modulating signal $f_{r_a}(t)$ we define the function $f_{3a2}(t)$ as:

$$f_{3a2}(t) = m_a \sin(\omega_0 t) - \frac{4}{T_s}t + \left(4n + \frac{10}{3}\right) \quad (\text{B.178})$$

Now using the Newton-Raphson method discussed in appendix section B.1.2 we approximate the root of equation B.176 as:

$$t_{12a2} = t_{11a2} - \frac{f_{1a2}(t_{11a2})}{f'_{1a2}(t_{11a2})} = t_{11a2} - \frac{m_a \sin(\omega_0 t_{11a2}) - \frac{4}{T_s}t_{11a2} + \left(4n - \frac{8}{3}\right)}{\omega_0 m_a \cos(\omega_0 t_{11a2}) + \frac{4}{T_s}} \quad (\text{B.179})$$

where the initial guess t_{11a2} is given by:

$$t_{11a2} = \frac{1}{4}T_s \cdot \left(4n - \frac{8}{3}\right) \quad \text{for } 0 < t_{11a2} < m_f T_s \quad (\text{B.180})$$

After i successive approximations we will have equation B.179 written as:

$$t_{1(i+1)a_2} = t_{1ia_2} - \frac{f_{1a_2}(t_{1ia_2})}{f'_{1a_2}(t_{1ia_2})} \quad (\text{B.181})$$

Similarly using the Newton-Raphson method we approximate the root of equation B.177 as:

$$t_{2a_2} = t_{21a_2} - \frac{f_{2a_2}(t_{21a_2})}{f'_{2a_2}(t_{21a_2})} = t_{21a_2} - \frac{m_a \sin(\omega_0 t_{2a_2}) + \frac{4}{T_s} t_{21a_2} - (4n - \frac{2}{3})}{\omega_0 m_a \cos(\omega_0 t_{21a_2}) - \frac{4}{T_s}} \quad (\text{B.182})$$

where the initial guess t_{21a_2} is given by:

$$t_{21a_2} = \frac{1}{4} T_s \cdot (4n - \frac{2}{3}) \quad \text{for } 0 < t_{21a_2} < m_f T_s \quad (\text{B.183})$$

After i successive approximations we will have equation B.182 written as:

$$t_{2(i+1)a_2} = t_{2ia_2} - \frac{f_{2a_2}(t_{2ia_2})}{f'_{2a_2}(t_{2ia_2})} \quad (\text{B.184})$$

And similarly using the Newton-Raphson method we approximate the root of equation B.178 as:

$$t_{3a_2} = t_{31a_2} - \frac{f_{1a_2}(t_{31a_2})}{f'_{1a_2}(t_{31a_2})} = t_{31a_2} - \frac{m_a \sin(\omega_0 t_{31a_2}) - \frac{4}{T_s} t_{3a_2} + (4n + \frac{10}{3})}{\omega_0 m_a \cos(\omega_0 t_{31a_2}) + \frac{4}{T_s}} \quad (\text{B.185})$$

where the initial guess t_{31a_2} is given by:

$$t_{31a_2} = \frac{1}{4} T_s \cdot (4n + \frac{10}{3})n \quad \text{for } 0 < t_{31a_2} < m_f T_s \quad (\text{B.186})$$

After i successive approximations we will have equation B.185 written as:

$$t_{3(i+1)a_2} = t_{3ia_2} - \frac{f_{3a_2}(t_{3ia_2})}{f'_{3a_2}(t_{3ia_2})} \quad (\text{B.187})$$

Now we consider the pwm resulting from the intersection of f_{c1a_2} , f_{c2a_2} and f_{c3a_2} with f_{ra} . First we look at the pulse formed between $t_{1(i+1)a_2}$ and $t_{2(i+1)a_2}$. The width of this pulse is given by:

$$W_{1a_2} = t_{2(i+1)a_2} - t_{1(i+1)a_2}$$

Now following the same method as in section B.2.1 the Fourier transform of the negative pulse is given by:

$$\begin{aligned} F(\omega) &= \int_{-\frac{W_{1a_2}}{2}}^{\frac{W_{1a_2}}{2}} (-V_t) e^{-j\omega_0 t} dt \\ &= \frac{V_t}{j\omega_0} \left(e^{-j\omega_0(t_{2(i+1)a_2} - t_{1(i+1)a_2})} \right) \end{aligned} \quad (\text{B.188})$$

and the Fourier transform of the negative pulses generated by shifting the pulse between $t_{1(i+1)a_2}$ and $t_{2(i+1)a_2}$ by t_{01a_2} where t_{01a_2} is given by:

$$t_{01a_2} = t_{1(i+1)a_2} + \frac{W_{1a_2}}{2} \quad (\text{B.189})$$

can be represented as follows:

$$\begin{aligned} F(\omega) &= \int_{-\frac{W_{1a_2}}{2}}^{\frac{W_{1a_2}}{2}} (-V_t) e^{-j\omega_0 t} e^{-j\omega_0 t_{01a_2}} dt \\ &= \frac{V_t}{j\omega_0} \left(e^{-j\omega_0(t_{2(i+1)a_2} - t_{1(i+1)a_2})} e^{-j\omega_0 t_{01a_2}} \right) \end{aligned} \quad (\text{B.190})$$

Similarly we consider the pulse formed between $t_{2(i+1)a_2}$ and $t_{3(i+1)a_2}$ in Figure B.31. The width of this pulse is given by:

$$W_{2a_2} = t_{3(i+1)a_2} - t_{2(i+1)a_2}$$

and its Fourier transform using the positive pulse results in:

$$\begin{aligned} F(\omega) &= \int_{-\frac{W_{2a_2}}{2}}^{\frac{W_{2a_2}}{2}} (V_t) e^{-j\omega_0 t} dt \\ &= -\frac{V_t}{j\omega_0} \left(e^{-j\omega_0(t_{3(i+1)a_2} - t_{2(i+1)a_2})} \right) \end{aligned} \quad (\text{B.191})$$

The shifting of this positive pulse by t_{02a_2} where t_{02a_2} is given by:

$$t_{02a_2} = t_{2(i+1)a_2} + \frac{W_{2a_2}}{2} \quad (\text{B.192})$$

The resulting Fourier transform of the shifted positive pulse is given by:

$$\begin{aligned} F(\omega) &= \int_{-\frac{W_{2a_2}}{2}}^{\frac{W_{2a_2}}{2}} (V_t) e^{-j\omega_0 t} e^{-j\omega_0 t_{02a_2}} dt \\ &= -\frac{V_t}{j\omega_0} \left(e^{-j\omega_0(t_{3(i+1)a_2} - t_{2(i+1)a_2})} e^{-j\omega_0 t_{02a_2}} \right) \end{aligned} \quad (\text{B.193})$$

To obtain the spectrum of $S_{a_2}(\omega)$ we sum up all the Fourier transform for the negative and positive pulses over any number of cycles of the switching period. The amplitude spectrum is the same as the one for $S_{a_2}(\omega)$ in the 2-cell multicell converter shown in Figure B.5.

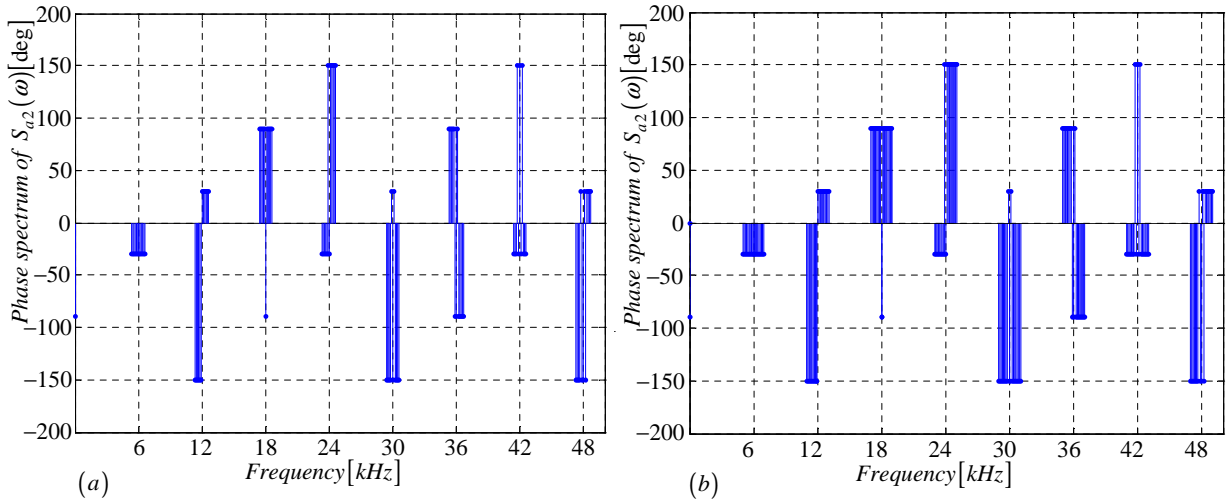


Figure B.32: Phase spectrum of $S_{a2}(\omega)$ generated using (a) Newton-Raphson simulation and (b) Theory

B.3.2 Derivation of the spectrum for the switching function $s_{a3}(t)$

In this subsection we derive equations that are necessary for the plotting of $S_{a3}(\omega)$ spectrum. The procedure is the same as in subsection B.2.1 except that the carrier signal in Figure B.33 is out of phase by 240 degrees with the one in Figure B.2.

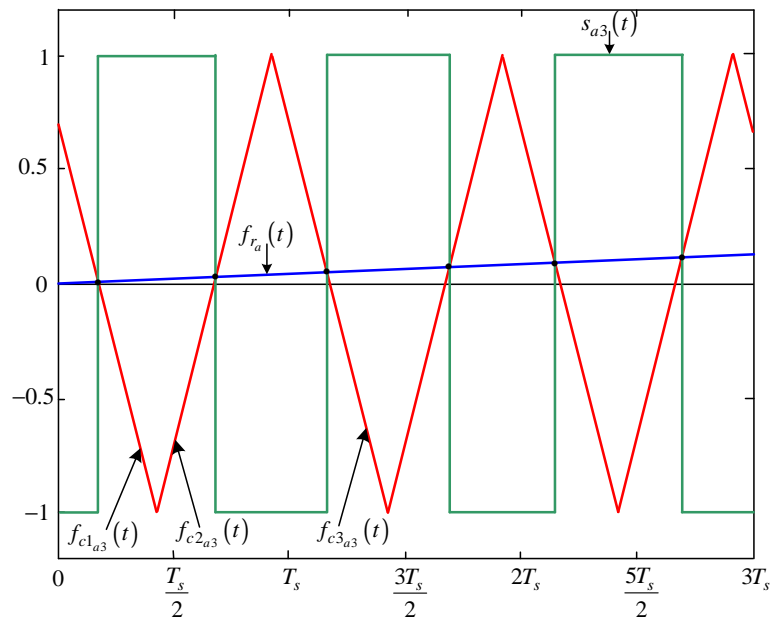


Figure B.33: Newton-Raphson method of switching function $s_{a3}(t)$

Modulation signal $f_{r_a}(t)$ is given by:

$$f_{r_a}(t) = m_a \sin(\omega_0 t) \quad (\text{B.194})$$

The falling side of the carrier signal $f_{c1_{a3}}(t)$ is given by:

$$f_{c1_{a3}}(t) = -\frac{4}{T_s}t + (4n - \frac{10}{3}) \quad (\text{B.195})$$

The rising side of the carrier signal $f_{c2_{a3}}(t)$ is given by:

$$f_{c2_{a3}}(t) = \frac{4}{T_s}t - (4n - \frac{4}{3}) \quad (\text{B.196})$$

The next falling side of the carrier signal $f_{c3_{a3}}(t)$ is given by:

$$f_{c3_{a3}}(t) = -\frac{4}{T_s}t + (4n + \frac{2}{3}) \quad (\text{B.197})$$

Where the falling side of the carrier signal $f_{c1_{a3}}(t)$ intersect the modulating signal $f_{r_a}(t)$ we define the function $f_{1_{a3}}(t)$ as:

$$f_{1_{a3}}(t) = m_a \sin(\omega_0 t) + \frac{4}{T_s}t - (4n - \frac{10}{3}) \quad (\text{B.198})$$

and where the falling side of the carrier signal $f_{1_{a3}}(t)$ intersect the modulating signal $f_{r_a}(t)$ we define the function $f_{2_{a3}}(t)$ as:

$$f_{2_{a3}}(t) = m_a \sin(\omega_0 t) - \frac{4}{T_s}t + (4n - \frac{4}{3}) \quad (\text{B.199})$$

and similarly where the rising side of the carrier signal $f_{c3_{a3}}(t)$ intersect the modulating signal $f_{r_a}(t)$ we define the function $f_{3_{a3}}(t)$ as:

$$f_{3_{a3}}(t) = m_a \sin(\omega_0 t) + \frac{4}{T_s}t - (4n + \frac{2}{3}) \quad (\text{B.200})$$

Now using the Newton-Raphson method discussed in appendix section B.1.2 we approximate the root of equation B.198 as:

$$t_{12_{a3}} = t_{11_{a3}} - \frac{f_{1_{a3}}(t_{11_{a3}})}{f'_{1_{a3}}(t_{11_{a3}})} = t_{11_{a3}} - \frac{m_a \sin(\omega_0 t_{11_{a3}}) + \frac{4}{T_s}t_{11_{a3}} - (4n - \frac{10}{3})}{\omega_0 m_a \cos(\omega_0 t_{11_{a3}}) + \frac{4}{T_s}} \quad (\text{B.201})$$

where the initial guess $t_{11_{a3}}$ is given by:

$$t_{11_{a3}} = \frac{1}{4}T_s \cdot (4n - \frac{10}{3}) \quad \text{for } 0 < t_{11_{a3}} < m_f T_s \quad (\text{B.202})$$

After i successive approximations we will have equation B.201 written as:

$$t_{1(i+1)_{a3}} = t_{1i_{a3}} - \frac{f_{1_{a3}}(t_{1i_{a3}})}{f'_{1_{a3}}(t_{1i_{a3}})} \quad (\text{B.203})$$

Similarly using the Newton-Raphson method we approximate the root of equation B.199 as:

$$t_{22_{a3}} = t_{21_{a3}} - \frac{f_{2_{a3}}(t_2)}{f'_{2_{a3}}(t_{21_{a3}})} = t_{21_{a3}} - \frac{m_a \sin(\omega_0 t_{21_{a3}}) - \frac{4}{T_s}t_{21_{a3}} + (4n - \frac{4}{3})}{\omega_0 m_a \cos(\omega_0 t_{21_{a3}}) - \frac{4}{T_s}} \quad (\text{B.204})$$

where the initial guess $t_{21_{a3}}$ is given by:

$$t_{21_{a3}} = \frac{1}{4}T_s \cdot (4n - \frac{4}{3}) \quad \text{for } 0 < t_{21_{a3}} < m_f T_s \quad (\text{B.205})$$

After i successive approximations we will have equation B.204 written as:

$$t_{2(i+1)_{a3}} = t_{2i_{a3}} - \frac{f_{2_{a3}}(t_{2i_{a3}})}{f'_{2_{a3}}(t_{2i_{a3}})} \quad (\text{B.206})$$

And similarly using the Newton-Raphson method we approximate the root of equation B.200 as:

$$t_{32_{a3}} = t_{31_{a3}} - \frac{f_{1_{a3}}(t_{31_{a3}})}{f'_{1_{a2}}(t_{31_{a3}})} = t_{31_{a3}} - \frac{m_a \sin(\omega_0 t_{31_{a3}}) + \frac{4}{T_s} t_{3_{a3}} - (4n + \frac{2}{3})}{\omega_0 m_a \cos(\omega_0 t_{31_{a3}}) + \frac{4}{T_s}} \quad (\text{B.207})$$

where the initial guess $t_{31_{a3}}$ is given by:

$$t_{31_{a3}} = \frac{1}{4}T_s \cdot (4n + \frac{2}{3})n \quad \text{for } 0 < t_{31_{a3}} < m_f T_s \quad (\text{B.208})$$

After i successive approximations we will have equation B.207 written as:

$$t_{3(i+1)_{a3}} = t_{3i_{a3}} - \frac{f_{3_{a3}}(t_{3i_{a3}})}{f'_{3_{a3}}(t_{3i_{a3}})} \quad (\text{B.209})$$

Now we consider the pwm resulting from the intersection of $f_{c1_{a3}}$, $f_{c2_{a3}}$ and $f_{c3_{a3}}$ with f_{r_a} . First we look at the pulse formed between $t_{1(i+1)_{a3}}$ and $t_{2(i+1)_{a3}}$. The width of this pulse is given by:

$$W_{1_{a3}} = t_{2(i+1)_{a3}} - t_{1(i+1)_{a3}}$$

Now following the same method as in section B.2.1 the Fourier transform of the positive pulse is given by:

$$\begin{aligned} F(\omega) &= \int_{-\frac{W_{1_{a3}}}{2}}^{\frac{W_{1_{a3}}}{2}} (V_t) e^{-j\omega_0 t} dt \\ &= -\frac{V_t}{j\omega_0} \left(e^{-j\omega_0(t_{2(i+1)_{a3}} - t_{1(i+1)_{a3}})} \right) \end{aligned} \quad (\text{B.210})$$

and the Fourier transform of the positive pulses generated by shifting the pulse between $t_{1(i+1)_{a3}}$ and $t_{2(i+1)_{a3}}$ by $t_{01_{a3}}$ where $t_{01_{a3}}$ is given by:

$$t_{01_{a3}} = t_{1(i+1)_{a3}} + \frac{W_{1_{a3}}}{2} \quad (\text{B.211})$$

can be represented as follows:

$$\begin{aligned} F(\omega) &= \int_{-\frac{W_{1_{a3}}}{2}}^{\frac{W_{1_{a3}}}{2}} (V_t) e^{-j\omega_0 t} e^{-j\omega_0 t_{01_{a3}}} dt \\ &= -\frac{V_t}{j\omega_0} \left(e^{-j\omega_0(t_{2(i+1)_{a3}} - t_{1(i+1)_{a3}})} e^{-j\omega_0 t_{01_{a3}}} \right) \end{aligned} \quad (\text{B.212})$$

Similarly we consider the pulse formed between $t_{2(i+1)a_3}$ and $t_{3(i+1)a_3}$ in Figure B.33. The width of this pulse is given by:

$$W_{2a_3} = t_{3(i+1)a_3} - t_{2(i+1)a_3}$$

and its Fourier transform using the negative pulse results in:

$$\begin{aligned} F(\omega) &= \int_{-\frac{W_{2a_3}}{2}}^{\frac{W_{2a_3}}{2}} (-V_t) e^{-j\omega_0 t} dt \\ &= \frac{V_t}{j\omega_0} \left(e^{-j\omega_0(t_{3(i+1)a_3} - t_{2(i+1)a_3})} \right) \end{aligned} \quad (\text{B.213})$$

The shifting of this negative pulse by t_{02a_3} where t_{02a_3} is given by:

$$t_{02a_3} = t_{2(i+1)a_3} + \frac{W_{2a_3}}{2} \quad (\text{B.214})$$

The resulting Fourier transform of the shifted negative pulse is given by:

$$\begin{aligned} F(\omega) &= \int_{-\frac{W_{2a_3}}{2}}^{\frac{W_{2a_3}}{2}} (-V_t) e^{-j\omega_0 t} e^{-j\omega_0 t_{02a_3}} dt \\ &= \frac{V_t}{j\omega_0} \left(e^{-j\omega_0(t_{3(i+1)a_3} - t_{2(i+1)a_3})} e^{-j\omega_0 t_{02a_3}} \right) \end{aligned} \quad (\text{B.215})$$

To obtain the spectrum of $S_{a_3}(\omega)$ we sum up all the Fourier transform for the negative and positive pulses over any number of cycles of the switching period. The amplitude spectrum is the same as the one for $S_{a_1}(\omega)$ in the 2-cell multicell converter shown in Figure B.5 $S_{a_1}(\omega)$.

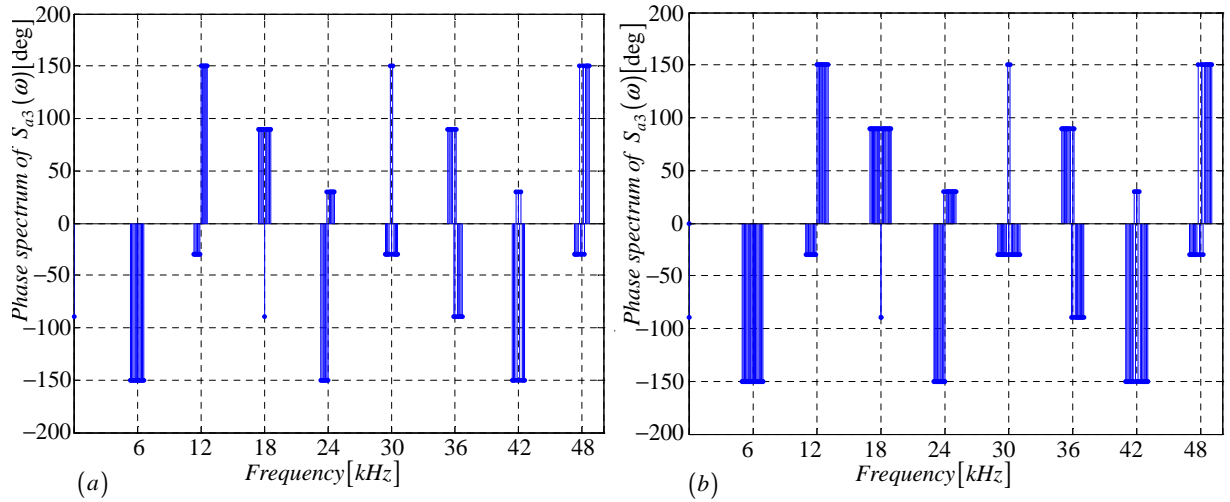


Figure B.34: Phase spectrum of $S_{a3}(\omega)$ generated using (a) Newton-Raphson simulation and (b) Theory

B.3.3 Derivation of the spectrum for the switching function $s_{b2}(t)$

In this subsection we derive equations that are necessary for the plotting of $S_{b2}(\omega)$ spectrum. The procedure is the same as in subsection B.2.1 except that the carrier and reference signals in Figure B.35 are out of phase by 120 degrees with those in Figure B.2.

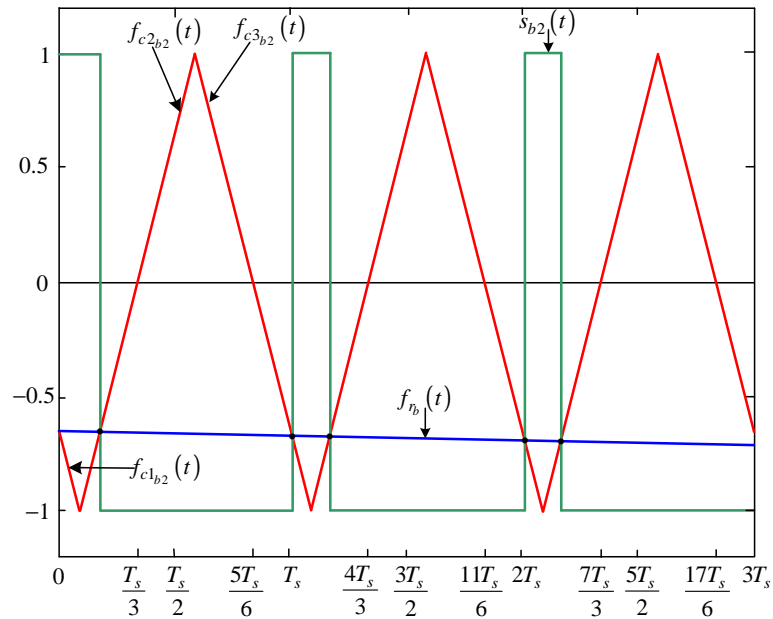


Figure B.35: Newton-Raphson method of switching function $s_{b2}(t)$

Modulation signal $f_{r_b}(t)$ is given by:

$$f_{r_b}(t) = m_a \sin(\omega_0 t - \frac{2\pi}{3}) \quad (\text{B.216})$$

The falling side of the carrier signal $f_{c1b2}(t)$ is given by:

$$f_{c2b2}(t) = -\frac{4}{T_s}t + (4(n-1) - \frac{2}{3}) \quad (\text{B.217})$$

The rising side of the carrier signal $f_{c2b2}(t)$ is given by:

$$f_{c1b2}(t) = \frac{4}{T_s}t - (4n - \frac{8}{3}) \quad (\text{B.218})$$

The next falling side of the carrier signal $f_{c3b2}(t)$ is given by:

$$f_{c2b2}(t) = -\frac{4}{T_s}t + (4n - \frac{2}{3}) \quad (\text{B.219})$$

Where the falling side of the carrier signal $f_{c1b2}(t)$ intersect the modulating signal $f_{r_b}(t)$ we define the function $f_{1b2}(t)$ as:

$$f_{1b2}(t) = m_a \sin(\omega_0 t) + \frac{4}{T_s}t - (4(n-1) - \frac{2}{3}) \quad (\text{B.220})$$

and where the rising side of the carrier signal $f_{2b2}(t)$ intersect the modulating signal $f_{r_b}(t)$ we define the function $f_{2b2}(t)$ as:

$$f_{1b2}(t) = m_a \sin(\omega_0 t) - \frac{4}{T_s}t + (4n - \frac{8}{3}) \quad (\text{B.221})$$

and similarly where the falling side of the carrier signal $f_{c3b2}(t)$ intersect the modulating signal $f_{r_b}(t)$ we define the function $f_{3b2}(t)$ as:

$$f_{2b2}(t) = m_a \sin(\omega_0 t) + \frac{4}{T_s}t - (4n - \frac{2}{3}) \quad (\text{B.222})$$

Now using the Newton-Raphson method discussed in appendix section B.1.2 we approximate the root of equation B.220 as:

$$t_{12b2} = t_{11b2} - \frac{f_{1b2}(t_{11b2})}{f'_{1b2}(t_{11b2})} = t_{11b2} - \frac{m_a \sin(\omega_0 t_{11b2}) + \frac{4}{T_s}t_{11b2} - (4(n-1) - \frac{2}{3})}{\omega_0 m_a \cos(\omega_0 t_{11b2}) - \frac{4}{T_s}} \quad (\text{B.223})$$

where the initial guess t_{11b2} is given by:

$$t_{11b2} = \frac{1}{4}T_s \cdot (4(n-1) - \frac{2}{3}) \quad \text{for } 0 < t_{11b2} < m_f T_s \quad (\text{B.224})$$

After i successive approximations we will have equation B.223 written as:

$$t_{1(i+1)b2} = t_{1ib2} - \frac{f_{1b2}(t_{1ib2})}{f'_{1b2}(t_{1ib2})} \quad (\text{B.225})$$

Similarly using the Newton-Raphson method we approximate the root of equation B.221 as:

$$t_{22_{b2}} = t_{21_{b2}} - \frac{f_{2_{b2}}(t_{21_{b2}})}{f'_{2_{b2}}(t_{21_{b2}})} = t_{21_{b2}} - \frac{m_a \sin(\omega_0 t_{21_{b2}}) - \frac{4}{T_s} t_{21_{b2}} + (4n - \frac{8}{3})}{\omega_0 m_a \cos(\omega_0 t_{21_{b2}}) + \frac{4}{T_s}} \quad (\text{B.226})$$

where the initial guess $t_{21_{b2}}$ is given by:

$$t_{21_{b2}} = \frac{1}{4} T_s \cdot (4n - \frac{8}{3}) \quad \text{for } 0 < t_{21_{b2}} < m_f T_s \quad (\text{B.227})$$

After i successive approximations we will have equation B.226 written as:

$$t_{2(i+1)_{b2}} = t_{2i_{b2}} - \frac{f_{2_{b2}}(t_{2i_{b2}})}{f'_{2_{b2}}(t_{2i_{b2}})} \quad (\text{B.228})$$

And similarly using the Newton-Raphson method we approximate the root of equation B.222 as:

$$t_{32_{b2}} = t_{31_{b2}} - \frac{f_{3_{b2}}(t_{31_{b2}})}{f'_{3_{b2}}(t_{31_{b2}})} = t_{31_{b2}} - \frac{m_a \sin(\omega_0 t_{31_{b2}}) + \frac{4}{T_s} t_{31_{b2}} - (4n - \frac{2}{3})}{\omega_0 m_a \cos(\omega_0 t_{31_{b2}}) - \frac{4}{T_s}} \quad (\text{B.229})$$

where the initial guess $t_{31_{b2}}$ is given by:

$$t_{31_{b2}} = \frac{1}{4} T_s \cdot (4n - \frac{2}{3}) \quad \text{for } 0 < t_{31_{b2}} < m_f T_s \quad (\text{B.230})$$

After i successive approximations we will have equation B.229 written as:

$$t_{3(i+1)_{b2}} = t_{3i_{b2}} - \frac{f_{3_{b2}}(t_{3i_{b2}})}{f'_{3_{b2}}(t_{3i_{b2}})} \quad (\text{B.231})$$

Now we consider the pwm resulting from the intersection of $f_{c1_{b2}}$, $f_{c2_{b2}}$ and $f_{c3_{b2}}$ with f_{r_b} . First we look at the pulse formed between $t_{1(i+1)_{b2}}$ and $t_{2(i+1)_{b2}}$. The width of this pulse is given by:

$$W_{1_{b2}} = t_{2(i+1)_{b2}} - t_{1(i+1)_{b2}}$$

Now following the same method as in section B.2.1 the Fourier transform of the positive pulse is given by:

$$\begin{aligned} F(\omega) &= \int_{\frac{W_{1_{b2}}}{2}}^{\frac{W_{1_{b2}}}{2}} (-V_t) e^{-j\omega_0 t} dt \\ &= -\frac{V_t}{j\omega_0} \left(e^{-j\omega_0(t_{2(i+1)_{b2}} - t_{1(i+1)_{b2}})} \right) \end{aligned} \quad (\text{B.232})$$

and the Fourier transform of the positive pulses generated by shifting the pulse between $t_{1(i+1)_{b2}}$ and $t_{2(i+1)_{b2}}$ by $t_{01_{b2}}$ where $t_{01_{b2}}$ is given by:

$$t_{01_{b2}} = t_{1(i+1)_{b2}} + \frac{W_{1_{b2}}}{2} \quad (\text{B.233})$$

can be represented as follows:

$$\begin{aligned}
 F(\omega) &= \int_{-\frac{w_{1b2}}{2}}^{\frac{w_{1b2}}{2}} (V_t) e^{-j\omega_0 t} e^{-j\omega_0 t_{01b2}} dt \\
 &= -\frac{V_t}{j\omega_0} \left(e^{-j\omega_0(t_{2(i+1)b2} - t_{1(i+1)b2})} e^{-j\omega_0 t_{01b2}} \right)
 \end{aligned} \tag{B.234}$$

Similarly we consider the pulse formed between $t_{2(i+1)b2}$ and $t_{3(i+1)b2}$ in Figure B.35. The width of this pulse is given by:

$$W_{2b2} = t_{3(i+1)b2} - t_{2(i+1)b2}$$

and its Fourier transform using the negative pulse results in:

$$\begin{aligned}
 F(\omega) &= \int_{-\frac{w_{2b2}}{2}}^{\frac{w_{2b2}}{2}} (-V_t) e^{-j\omega_0 t} dt \\
 &= \frac{V_t}{j\omega_0} \left(e^{-j\omega_0(t_{3(i+1)b2} - t_{2(i+1)b2})} \right)
 \end{aligned} \tag{B.235}$$

The shifting of this negative pulse by t_{02b2} where t_{02b2} is given by:

$$t_{02b2} = t_{2(i+1)b2} + \frac{W_{2b2}}{2} \tag{B.236}$$

The resulting Fourier transform of the shifted positive pulse is given by:

$$\begin{aligned}
 F(\omega) &= \int_{-\frac{w_{2b2}}{2}}^{\frac{w_{2b2}}{2}} (-V_t) e^{-j\omega_0 t} e^{-j\omega_0 t_{02b2}} dt \\
 &= \frac{V_t}{j\omega_0} \left(e^{-j\omega_0(t_{3(i+1)b2} - t_{2(i+1)b2})} e^{-j\omega_0 t_{02b2}} \right)
 \end{aligned} \tag{B.237}$$

To obtain the spectrum of $S_{b2}(\omega)$ we sum up all the Fourier transform for the negative and positive pulses over any number of cycles of the switching period. The amplitude spectrum is the same as the one for $S_{a1}(\omega)$ in the 2-cell multicell converter.

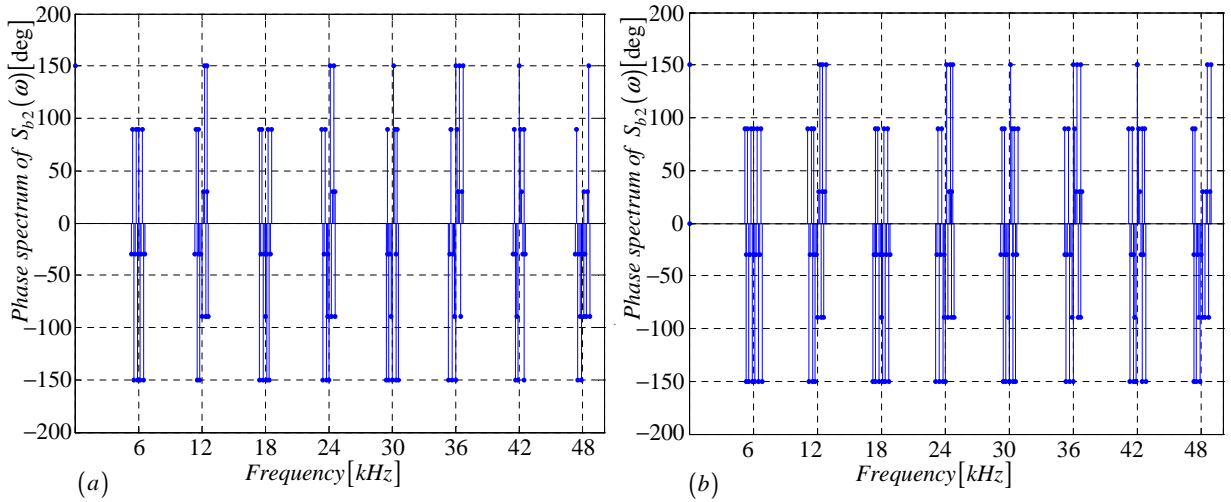


Figure B.36: Phase spectrum of $S_{b2}(\omega)$ generated using (a) Newton-Raphson simulation and (b) Theory

B.3.4 Derivation of the spectrum for the switching function $s_{b3}(t)$

In this subsection we derive equations that are necessary for the plotting of $S_{b3}(\omega)$ spectrum. The procedure is the same as in subsection B.2.1 except that the carrier and reference signals in Figure B.37 are out of phase by 120 and 240 degrees respectively with those in Figure B.2.

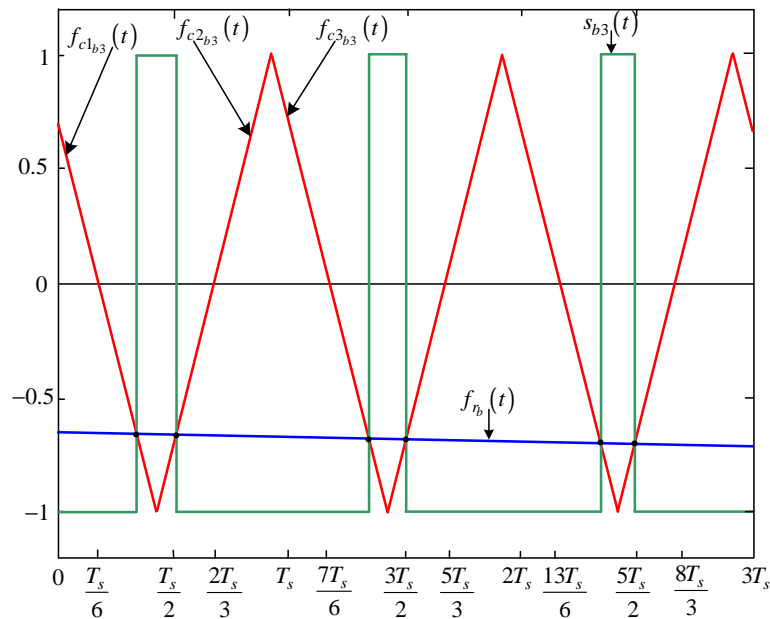


Figure B.37: Newton-Raphson method of switching function $s_{b3}(t)$

Modulation signal $f_{r_b}(t)$ is given by:

$$f_{r_b}(t) = m_a \sin(\omega_0 t - \frac{2\pi}{3}) \quad (\text{B.238})$$

The falling side of the carrier signal $f_{c1_{b3}}(t)$ is given by:

$$f_{c1_{b3}}(t) = -\frac{4}{T_s}t + (4n - \frac{10}{3}) \quad (\text{B.239})$$

The rising side of the carrier signal $f_{c2_{b3}}(t)$ is given by:

$$f_{c2_{b3}}(t) = \frac{4}{T_s}t - (4n - \frac{4}{3}) \quad (\text{B.240})$$

The next falling side of the carrier signal $f_{c3_{b3}}(t)$ is given by:

$$f_{c3_{b3}}(t) = -\frac{4}{T_s}t + (4n + \frac{2}{3}) \quad (\text{B.241})$$

Where the falling side of the carrier signal $f_{c1_{b3}}(t)$ intersect the modulating signal $f_{r_b}(t)$ we define the function $f_{1_{b3}}(t)$ as:

$$f_{1_{b3}}(t) = m_a \sin(\omega_0 t - \frac{2\pi}{3}) + \frac{4}{T_s}t - (4n - \frac{10}{3}) \quad (\text{B.242})$$

and where the falling side of the carrier signal $f_{1_{b3}}(t)$ intersect the modulating signal $f_{r_b}(t)$ we define the function $f_{2_{b3}}(t)$ as:

$$f_{2_{b3}}(t) = m_a \sin(\omega_0 t - \frac{2\pi}{3}) - \frac{4}{T_s}t + (4n - \frac{4}{3}) \quad (\text{B.243})$$

and similarly where the rising side of the carrier signal $f_{c3_{b3}}(t)$ intersect the modulating signal $f_{r_b}(t)$ we define the function $f_{3_{b3}}(t)$ as:

$$f_{3_{b3}}(t) = m_a \sin(\omega_0 t - \frac{2\pi}{3}) + \frac{4}{T_s}t - (4n + \frac{2}{3}) \quad (\text{B.244})$$

Now using the Newton-Raphson method discussed in appendix section B.1.2 we approximate the root of equation B.242 as:

$$t_{12_{b3}} = t_{11_{b3}} - \frac{f_{1_{b3}}(t_{11_{b3}})}{f'_{1_{b3}}(t_{11_{b3}})} = t_{11_{b3}} - \frac{m_a \sin(\omega_0 t_{11_{b3}} - \frac{2\pi}{3}) + \frac{4}{T_s}t_{11_{b3}} - (4n - \frac{10}{3})}{\omega_0 m_a \cos(\omega_0 t_{11_{b3}} - \frac{2\pi}{3}) + \frac{4}{T_s}} \quad (\text{B.245})$$

where the initial guess $t_{11_{b3}}$ is given by:

$$t_{11_{b3}} = \frac{1}{4}T_s \cdot (4n - \frac{10}{3}) \quad \text{for } 0 < t_{11_{b3}} < m_f T_s \quad (\text{B.246})$$

After i successive approximations we will have equation B.245 written as:

$$t_{1(i+1)_{b3}} = t_{1i_{b3}} - \frac{f_{1_{b3}}(t_{1i_{b3}})}{f'_{1_{b3}}(t_{1i_{b3}})} \quad (\text{B.247})$$

Similarly using the Newton-Raphson method we approximate the root of equation B.243 as:

$$t_{22_{b3}} = t_{21_{b3}} - \frac{f_{2_{b3}}(t_{21_{b3}})}{f'_{2_{b3}}(t_{21_{b3}})} = t_{21_{b3}} - \frac{m_a \sin(\omega_0 t_{21_{b3}} - \frac{2\pi}{3}) - \frac{4}{T_s} t_{21_{b3}} + (4n - \frac{4}{3})}{\omega_0 m_a \cos(\omega_0 t_{21_{b3}} - \frac{2\pi}{3}) - \frac{4}{T_s}} \quad (\text{B.248})$$

where the initial guess $t_{21_{b3}}$ is given by:

$$t_{21_{b3}} = \frac{1}{4} T_s \cdot (4n - \frac{4}{3}) \quad \text{for } 0 < t_{21_{b3}} < m_f T_s \quad (\text{B.249})$$

After i successive approximations we will have equation B.248 written as:

$$t_{2(i+1)_{b3}} = t_{2i_{b3}} - \frac{f_{2_{b3}}(t_{2i_{b3}})}{f'_{2_{b3}}(t_{2i_{b3}})} \quad (\text{B.250})$$

And similarly using the Newton-Raphson method we approximate the root of equation B.244 as:

$$t_{32_{b3}} = t_{31_{b3}} - \frac{f_{3_{b3}}(t_{31_{b3}})}{f'_{3_{b3}}(t_{31_{b3}})} = t_{31_{b3}} - \frac{m_a \sin(\omega_0 t_{31_{b3}}) + \frac{4}{T_s} t_{31_{b3}} - (4n + \frac{2}{3})}{\omega_0 m_a \cos(\omega_0 t_{31_{b3}} - \frac{2\pi}{3}) + \frac{4}{T_s}} \quad (\text{B.251})$$

where the initial guess $t_{31_{b3}}$ is given by:

$$t_{31_{b3}} = \frac{1}{4} T_s \cdot (4n + \frac{2}{3})n \quad \text{for } 0 < t_{31_{b3}} < m_f T_s \quad (\text{B.252})$$

After i successive approximations we will have equation B.251 written as:

$$t_{3(i+1)_{b3}} = t_{3i_{b3}} - \frac{f_{3_{b3}}(t_{3i_{b3}})}{f'_{3_{b3}}(t_{3i_{b3}})} \quad (\text{B.253})$$

Now we consider the pwm resulting from the intersection of $f_{c1_{b3}}$, $f_{c2_{b3}}$ and $f_{c3_{b3}}$ with f_{r_b} . First we look at the pulse formed between $t_{1(i+1)_{b3}}$ and $t_{2(i+1)_{b3}}$. The width of this pulse is given by:

$$W_{1_{b3}} = t_{2(i+1)_{b3}} - t_{1(i+1)_{b3}}$$

Now following the same method as in section B.2.1 the Fourier transform of the positive pulse is given by:

$$\begin{aligned} F(\omega) &= \int_{-\frac{W_{1_{b3}}}{2}}^{\frac{W_{1_{b3}}}{2}} (V_t) e^{-j\omega_0 t} dt \\ &= -\frac{V_t}{j\omega_0} \left(e^{-j\omega_0(t_{2(i+1)_{b3}} - t_{1(i+1)_{b3}})} \right) \end{aligned} \quad (\text{B.254})$$

and the Fourier transform of the positive pulses generated by shifting the pulse between $t_{1(i+1)_{b3}}$ and $t_{2(i+1)_{b3}}$ by $t_{01_{b3}}$ where $t_{01_{b3}}$ is given by:

$$t_{01_{b3}} = t_{1(i+1)_{b3}} + \frac{W_{1_{b3}}}{2} \quad (\text{B.255})$$

can be represented as follows:

$$\begin{aligned}
 F(\omega) &= \int_{-\frac{w_{1b3}}{2}}^{\frac{w_{1b3}}{2}} (V_t) e^{-j\omega_0 t} e^{-j\omega_0 t_{01b3}} dt \\
 &= -\frac{V_t}{j\omega_0} \left(e^{-j\omega_0(t_{2(i+1)b3} - t_{1(i+1)b3})} e^{-j\omega_0 t_{01b3}} \right)
 \end{aligned} \tag{B.256}$$

Similarly we consider the pulse formed between $t_{2(i+1)b3}$ and $t_{3(i+1)b3}$ in Figure B.33. The width of this pulse is given by:

$$W_{2b3} = t_{3(i+1)b3} - t_{2(i+1)b3}$$

and its Fourier transform using the negative pulse results in:

$$\begin{aligned}
 F(\omega) &= \int_{-\frac{w_{2b3}}{2}}^{\frac{w_{2b3}}{2}} (-V_t) e^{-j\omega_0 t} dt \\
 &= \frac{V_t}{j\omega_0} \left(e^{-j\omega_0(t_{3(i+1)b3} - t_{2(i+1)b3})} \right)
 \end{aligned} \tag{B.257}$$

The shifting of this negative pulse by t_{02b3} where t_{02b3} is given by:

$$t_{02b3} = t_{2(i+1)a3} + \frac{W_{2b3}}{2} \tag{B.258}$$

The resulting Fourier transform of the shifted negative pulse is given by:

$$\begin{aligned}
 F(\omega) &= \int_{-\frac{w_{2b3}}{2}}^{\frac{w_{2b3}}{2}} (-V_t) e^{-j\omega_0 t} e^{-j\omega_0 t_{02b3}} dt \\
 &= \frac{V_t}{j\omega_0} \left(e^{-j\omega_0(t_{3(i+1)b3} - t_{2(i+1)b3})} e^{-j\omega_0 t_{02b3}} \right)
 \end{aligned} \tag{B.259}$$

To obtain the spectrum of $S_{b3}(\omega)$ we sum up all the Fourier transform for the negative and positive pulses over any number of cycles of the switching period. The amplitude spectrum is the same as the one for $S_{a1}(\omega)$ in the 2-cell multicell converter.

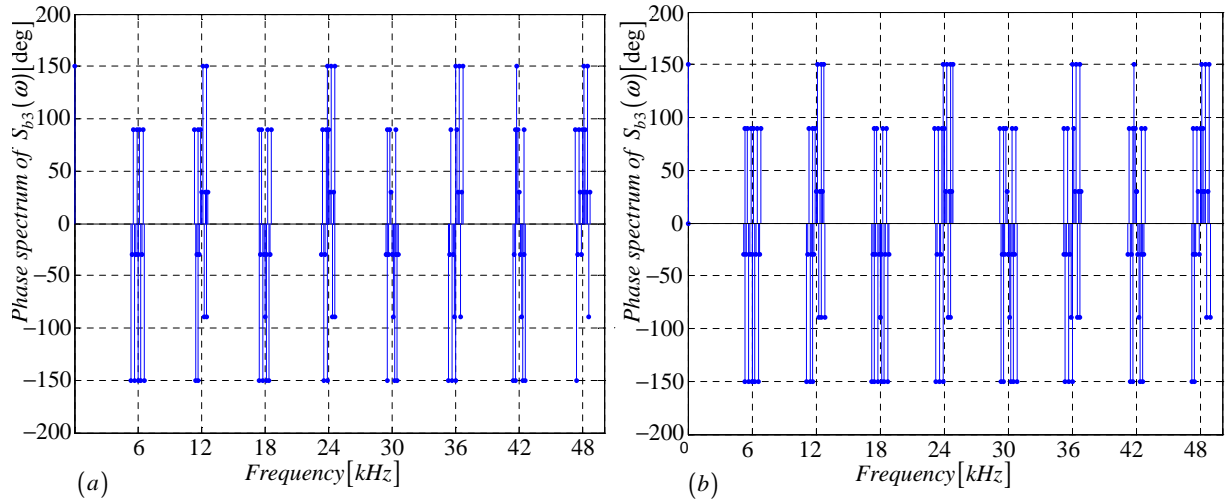


Figure B.38: Phase spectrum of $S_{b3}(\omega)$ generated using (a) Newton-Raphson simulation and (b) Theory

B.3.5 Derivation of the spectrum for the switching function $s_{c2}(t)$

In this subsection we derive equations that are necessary for the plotting of $S_{c2}(\omega)$ spectrum. The procedure is the same as in subsection B.2.1 except that the carrier and reference signals in Figure B.35 are out of phase by 120 and 240 degrees respectively with those in Figure B.2.

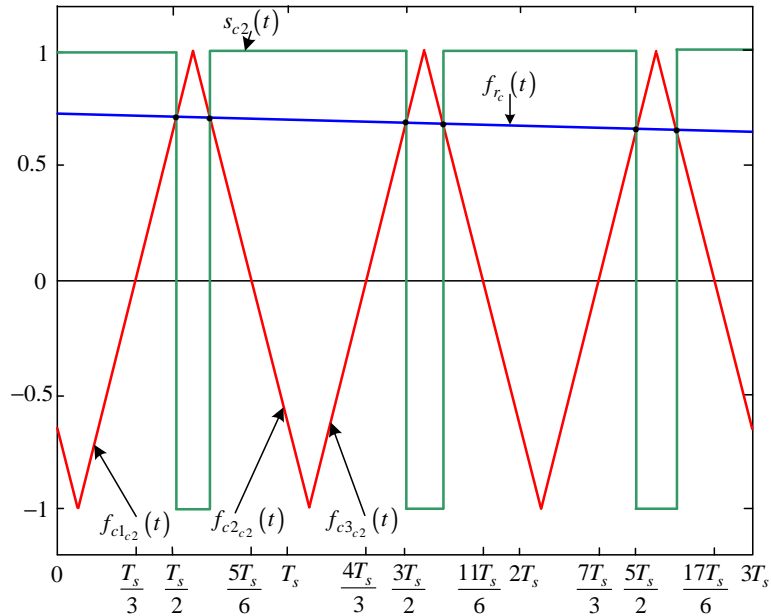


Figure B.39: Newton-Raphson method of switching function $s_{c2}(t)$

Modulation signal $f_{r_c}(t)$ is given by:

$$f_{r_c}(t) = m_a \sin\left(\omega_0 t + \frac{2\pi}{3}\right) \quad (\text{B.260})$$

The rising side of the carrier signal $f_{c1c2}(t)$ is given by:

$$f_{c1c2}(t) = \frac{4}{T_s}t - \left(4n - \frac{8}{3}\right) \quad (\text{B.261})$$

The falling side of the carrier signal $f_{c2c2}(t)$ is given by:

$$f_{c2c2}(t) = -\frac{4}{T_s}t + \left(4n - \frac{2}{3}\right) \quad (\text{B.262})$$

The next rising side of the carrier signal $f_{c3c2}(t)$ is given by:

$$f_{c3c2}(t) = \frac{4}{T_s}t - \left(4n + \frac{4}{3}\right) \quad (\text{B.263})$$

Where the rising side of the carrier signal $f_{c1c2}(t)$ intersect the modulating signal $f_{r_c}(t)$ we define the function $f_{1c2}(t)$ as:

$$f_{1c2}(t) = m_a \sin\left(\omega_0 t + \frac{2\pi}{3}\right) - \frac{4}{T_s}t + \left(4n - \frac{8}{3}\right) \quad (\text{B.264})$$

and where the rising side of the carrier signal $f_{2c2}(t)$ intersect the modulating signal $f_{r_c}(t)$ we define the function $f_{2c2}(t)$ as:

$$f_{2c2}(t) = m_a \sin\left(\omega_0 t + \frac{2\pi}{3}\right) + \frac{4}{T_s}t - \left(4n - \frac{2}{3}\right) \quad (\text{B.265})$$

and similarly where the falling side of the carrier signal $f_{c3c2}(t)$ intersect the modulating signal $f_{r_c}(t)$ we define the function $f_{3c2}(t)$ as:

$$f_{3c2}(t) = m_a \sin\left(\omega_0 t + \frac{2\pi}{3}\right) - \frac{4}{T_s}t + \left(4n + \frac{4}{3}\right) \quad (\text{B.266})$$

Now using the Newton-Raphson method discussed in appendix section B.1.2 we approximate the root of equation B.264 as:

$$t_{12c2} = t_{11c2} - \frac{f_{1c2}(t_{11c2})}{f'_{1c2}(t_{11c2})} = t_{11c2} - \frac{m_a \sin\left(\omega_0 t_{11c2} + \frac{2\pi}{3}\right) - \frac{4}{T_s}t_{11c2} + \left(4n - \frac{8}{3}\right)}{\omega_0 m_a \cos\left(\omega_0 t_{11c2} + \frac{2\pi}{3}\right) - \frac{4}{T_s}} \quad (\text{B.267})$$

where the initial guess t_{11c2} is given by:

$$t_{11c2} = \frac{1}{4}T_s \cdot \left(4n - \frac{8}{3}\right) \quad \text{for } 0 < t_{11c2} < m_f T_s \quad (\text{B.268})$$

After i successive approximations we will have equation B.267 written as:

$$t_{1(i+1)c2} = t_{1ic2} - \frac{f_{1c2}(t_{1ic2})}{f'_{1c2}(t_{1ic2})} \quad (\text{B.269})$$

Similarly using the Newton-Raphson method we approximate the root of equation B.265 as:

$$t_{22c2} = t_{21c2} - \frac{f_{2c2}(t_{21c2})}{f'_{2c2}(t_{21c2})} = t_{21c2} - \frac{m_a \sin(\omega_0 t_{21c2} + \frac{2\pi}{3}) + \frac{4}{T_s} t_{21c2} - (4n - \frac{2}{3})}{\omega_0 m_a \cos(\omega_0 t_{21c2} + \frac{2\pi}{3}) + \frac{4}{T_s}} \quad (\text{B.270})$$

where the initial guess t_{21c2} is given by:

$$t_{21c2} = \frac{1}{4} T_s \cdot (4n - \frac{2}{3}) \quad \text{for } 0 < t_{21c2} < m_f T_s \quad (\text{B.271})$$

After i successive approximations we will have equation B.270 written as:

$$t_{2(i+1)c2} = t_{2ic2} - \frac{f_{2c2}(t_{2ic2})}{f'_{2c2}(t_{2ic2})} \quad (\text{B.272})$$

And similarly using the Newton-Raphson method we approximate the root of equation B.266 as:

$$t_{32c2} = t_{31c2} - \frac{f_{3c2}(t_{31c2})}{f'_{3c2}(t_{31c2})} = t_{31c2} - \frac{m_a \sin(\omega_0 t_{31c2} + \frac{2\pi}{3}) - \frac{4}{T_s} t_{31c2} + (4n + \frac{4}{3})}{\omega_0 m_a \cos(\omega_0 t_{31c2} + \frac{2\pi}{3}) - \frac{4}{T_s}} \quad (\text{B.273})$$

where the initial guess t_{31c2} is given by:

$$t_{31c2} = \frac{1}{4} T_s \cdot (4n + \frac{4}{3}) \quad \text{for } 0 < t_{31c2} < m_f T_s \quad (\text{B.274})$$

After i successive approximations we will have equation B.273 written as:

$$t_{3(i+1)c2} = t_{3ic2} - \frac{f_{3c2}(t_{3ic2})}{f'_{3c2}(t_{3ic2})} \quad (\text{B.275})$$

Now we consider the pwm resulting from the intersection of f_{c1c2} , f_{c2c2} and f_{c3c2} with f_{rc} . First we look at the pulse formed between $t_{1(i+1)c2}$ and $t_{2(i+1)c2}$. The width of this pulse is given by:

$$W_{1c2} = t_{2(i+1)c2} - t_{1(i+1)c2}$$

Now following the same method as in section B.2.1 the Fourier transform of the negative pulse is given by:

$$\begin{aligned} F(\omega) &= \int_{\frac{W_{1c2}}{2}}^{\frac{W_{1c2}}{2}} (-V_t) e^{-j\omega_0 t} dt \\ &= \frac{V_t}{j\omega_0} \left(e^{-j\omega_0(t_{2(i+1)c2} - t_{1(i+1)c2})} \right) \end{aligned} \quad (\text{B.276})$$

and the Fourier transform of the negative pulses generated by shifting the pulse between $t_{1(i+1)c2}$ and $t_{2(i+1)c2}$ by t_{01c2} where t_{01c2} is given by:

$$t_{01c2} = t_{1(i+1)c2} + \frac{W_{1c2}}{2} \quad (\text{B.277})$$

can be represented as follows:

$$\begin{aligned}
 F(\omega) &= \int_{-\frac{w_{1c2}}{2}}^{\frac{w_{1c2}}{2}} (-V_t) e^{-j\omega_0 t} e^{-j\omega_0 t_{01c2}} dt \\
 &= \frac{V_t}{j\omega_0} \left(e^{-j\omega_0(t_{2(i+1)c2} - t_{1(i+1)c2})} e^{-j\omega_0 t_{01c2}} \right)
 \end{aligned} \tag{B.278}$$

Similarly we consider the pulse formed between $t_{2(i+1)c2}$ and $t_{3(i+1)c2}$ in Figure B.39. The width of this pulse is given by:

$$W_{2c2} = t_{3(i+1)c2} - t_{2(i+1)c2}$$

and its Fourier transform using the positive pulse results in:

$$\begin{aligned}
 F(\omega) &= \int_{-\frac{w_{2c2}}{2}}^{\frac{w_{2c2}}{2}} (V_t) e^{-j\omega_0 t} dt \\
 &= -\frac{V_t}{j\omega_0} \left(e^{-j\omega_0(t_{3(i+1)c2} - t_{2(i+1)c2})} \right)
 \end{aligned} \tag{B.279}$$

The shifting of this positive pulse by t_{02c2} where t_{02c2} is given by:

$$t_{02c2} = t_{2(i+1)c2} + \frac{W_{2c2}}{2} \tag{B.280}$$

The resulting Fourier transform of the shifted positive pulse is given by:

$$\begin{aligned}
 F(\omega) &= \int_{-\frac{w_{2c2}}{2}}^{\frac{w_{2c2}}{2}} (V_t) e^{-j\omega_0 t} e^{-j\omega_0 t_{02c2}} dt \\
 &= -\frac{V_t}{j\omega_0} \left(e^{-j\omega_0(t_{3(i+1)c2} - t_{2(i+1)c2})} e^{-j\omega_0 t_{02c2}} \right)
 \end{aligned} \tag{B.281}$$

To obtain the spectrum of $S_{c2}(\omega)$ we sum up all the Fourier transform for the negative and positive pulses over any number of cycles of the switching period. The amplitude spectrum is the same as the one for $S_{a1}(\omega)$ in the 2-cell multicell converter.

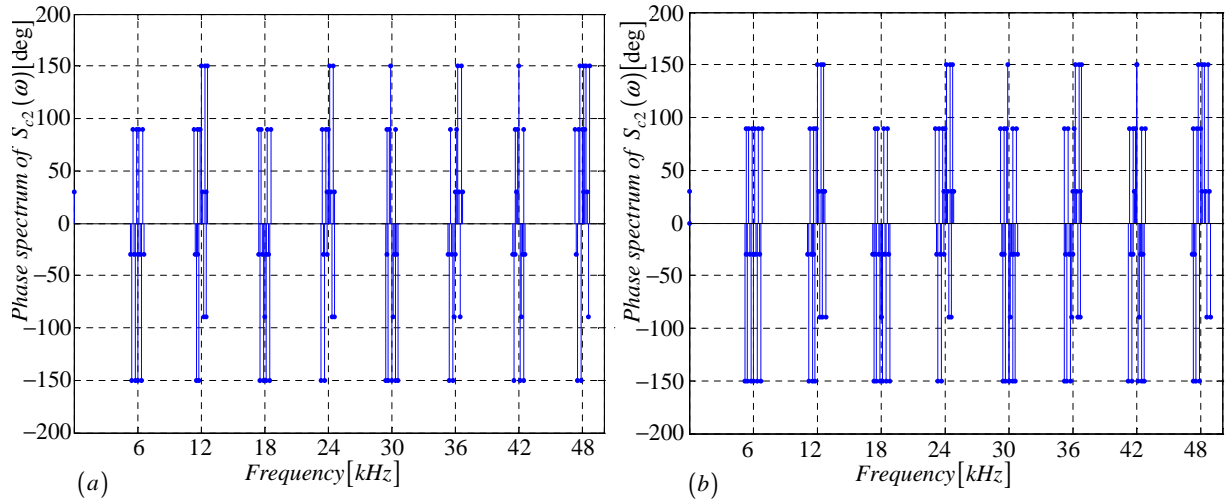


Figure B.40: Phase spectrum of $S_{c2}(\omega)$ generated using (a) Newton-Raphson simulation and (b) Theory

B.3.6 Derivation of the spectrum for the switching function $s_{c3}(t)$

In this subsection we derive equations that are necessary for the plotting of $S_{c3}(\omega)$ spectrum. The procedure is the same as in subsection B.2.1 except that the carrier and reference signals in Figure B.41 are out of phase by 240 degrees with those in Figure B.2.

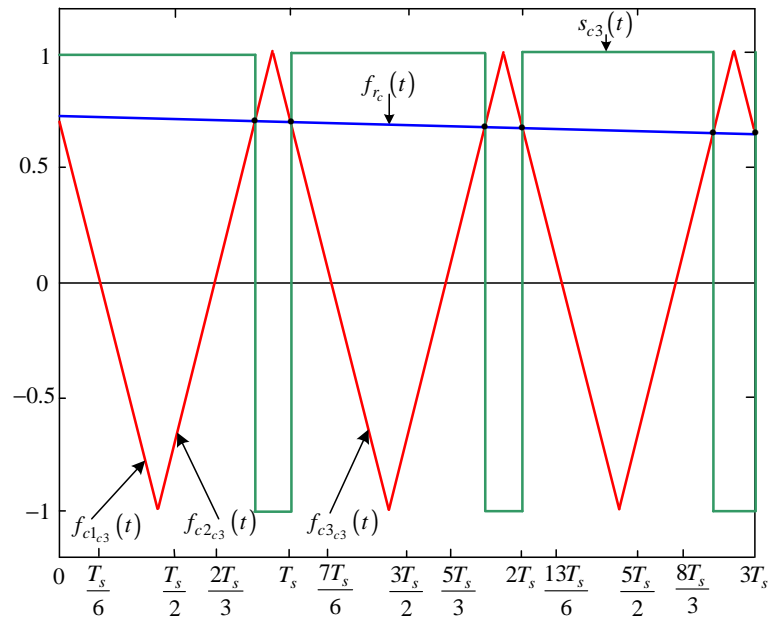


Figure B.41: Newton-Raphson method of switching function $s_{c3}(t)$

Modulation signal $f_{r_c}(t)$ is given by:

$$f_{r_c}(t) = m_a \sin\left(\omega_0 t + \frac{2\pi}{3}\right) \quad (\text{B.282})$$

The falling side of the carrier signal $f_{c1_{e3}}(t)$ is given by:

$$f_{c1_{e3}}(t) = -\frac{4}{T_s}t + \left(4n - \frac{10}{3}\right) \quad (\text{B.283})$$

The rising side of the carrier signal $f_{c2_{e3}}(t)$ is given by:

$$f_{c2_{e3}}(t) = \frac{4}{T_s}t - \left(4n - \frac{4}{3}\right) \quad (\text{B.284})$$

The next falling side of the carrier signal $f_{c3_{e3}}(t)$ is given by:

$$f_{c3_{e3}}(t) = -\frac{4}{T_s}t + \left(4n + \frac{2}{3}\right) \quad (\text{B.285})$$

Where the falling side of the carrier signal $f_{c1_{e3}}(t)$ intersect the modulating signal $f_{r_c}(t)$ we define the function $f_{1_{e3}}(t)$ as:

$$f_{1_{e3}}(t) = m_a \sin\left(\omega_0 t + \frac{2\pi}{3}\right) + \frac{4}{T_s}t - \left(4n - \frac{10}{3}\right) \quad (\text{B.286})$$

and where the falling side of the carrier signal $f_{1_{e3}}(t)$ intersect the modulating signal $f_{r_c}(t)$ we define the function $f_{2_{e3}}(t)$ as:

$$f_{2_{e3}}(t) = m_a \sin\left(\omega_0 t + \frac{2\pi}{3}\right) - \frac{4}{T_s}t + \left(4n - \frac{4}{3}\right) \quad (\text{B.287})$$

and similarly where the rising side of the carrier signal $f_{c3_{e3}}(t)$ intersect the modulating signal $f_{r_c}(t)$ we define the function $f_{3_{e3}}(t)$ as:

$$f_{3_{e3}}(t) = m_a \sin\left(\omega_0 t + \frac{2\pi}{3}\right) + \frac{4}{T_s}t - \left(4n + \frac{2}{3}\right) \quad (\text{B.288})$$

Now using the Newton-Raphson method discussed in appendix we approximate the root of equation B.286 as:

$$t_{12_{e3}} = t_{11_{e3}} - \frac{f_{1_{e3}}(t_{11_{e3}})}{f'_{1_{e3}}(t_{11_{e3}})} = t_{11_{e3}} - \frac{m_a \sin\left(\omega_0 t_{11_{e3}} + \frac{2\pi}{3}\right) + \frac{4}{T_s}t_{11_{e3}} - \left(4n - \frac{10}{3}\right)}{\omega_0 m_a \cos\left(\omega_0 t_{11_{e3}} + \frac{2\pi}{3}\right) + \frac{4}{T_s}} \quad (\text{B.289})$$

where the initial guess $t_{11_{e3}}$ is given by:

$$t_{11_{e3}} = \frac{1}{4}T_s \cdot \left(4n - \frac{10}{3}\right) \quad \text{for } 0 < t_{11_{e3}} < m_f T_s \quad (\text{B.290})$$

After i successive approximations we will have equation B.289 written as:

$$t_{1(i+1)_{e3}} = t_{1i_{e3}} - \frac{f_{1_{e3}}(t_{1i_{e3}})}{f'_{1_{e3}}(t_{1i_{e3}})} \quad (\text{B.291})$$

Similarly using the Newton-Raphson method we approximate the root of equation B.287 as:

$$t_{22c3} = t_{21c3} - \frac{f_{2c3}(t_2)}{f'_{2c3}(t_{21c3})} = t_{21c3} - \frac{m_a \sin(\omega_0 t_{21c3} - \frac{2\pi}{3}) - \frac{4}{T_s} t_{21c3} + (4n - \frac{4}{3})}{\omega_0 m_a \cos(\omega_0 t_{21c3} - \frac{2\pi}{3}) - \frac{4}{T_s}} \quad (\text{B.292})$$

where the initial guess t_{21c3} is given by:

$$t_{21c3} = \frac{1}{4} T_s \cdot (4n - \frac{4}{3}) \quad \text{for } 0 < t_{21c3} < m_f T_s \quad (\text{B.293})$$

After i successive approximations we will have equation B.292 written as:

$$t_{2(i+1)c3} = t_{2ic3} - \frac{f_{2c3}(t_{2ic3})}{f'_{2c3}(t_{2ic3})} \quad (\text{B.294})$$

And similarly using the Newton-Raphson method we approximate the root of equation B.288 as:

$$t_{32c3} = t_{31c3} - \frac{f_{1c3}(t_{31c3})}{f'_{1c3}(t_{31c3})} = t_{31c3} - \frac{m_a \sin(\omega_0 t_{31c3}) + \frac{4}{T_s} t_{31c3} - (4n + \frac{2}{3})}{\omega_0 m_a \cos(\omega_0 t_{31c3} - \frac{2\pi}{3}) + \frac{4}{T_s}} \quad (\text{B.295})$$

where the initial guess t_{31c3} is given by:

$$t_{31c3} = \frac{1}{4} T_s \cdot (4n + \frac{2}{3})n \quad \text{for } 0 < t_{31c3} < m_f T_s \quad (\text{B.296})$$

After i successive approximations we will have equation B.295 written as:

$$t_{3(i+1)c3} = t_{3ic3} - \frac{f_{3c3}(t_{3ic3})}{f'_{3c3}(t_{3ic3})} \quad (\text{B.297})$$

Now we consider the pwm resulting from the intersection of f_{c1c3} , f_{c2c3} and f_{c3c3} with f_{rc} . First we look at the pulse formed between $t_{1(i+1)c3}$ and $t_{2(i+1)c3}$. The width of this pulse is given by:

$$W_{1c3} = t_{2(i+1)c3} - t_{1(i+1)c3}$$

Now following the same method as in section B.2.1 the Fourier transform of the positive pulse is given by:

$$\begin{aligned} F(\omega) &= \int_{-\frac{W_{1c3}}{2}}^{\frac{W_{1c3}}{2}} (V_t) e^{-j\omega_0 t} dt \\ &= -\frac{V_t}{j\omega_0} \left(e^{-j\omega_0(t_{2(i+1)c3} - t_{1(i+1)c3})} \right) \end{aligned} \quad (\text{B.298})$$

and the Fourier transform of the positive pulses generated by shifting the pulse between $t_{1(i+1)c3}$ and $t_{2(i+1)c3}$ by t_{01c3} where t_{01c3} is given by:

$$t_{01c3} = t_{1(i+1)c3} + \frac{W_{1c3}}{2} \quad (\text{B.299})$$

can be represented as follows:

$$\begin{aligned}
 F(\omega) &= \int_{-\frac{w_{1c3}}{2}}^{\frac{w_{1c3}}{2}} (V_t) e^{-j\omega_0 t} e^{-j\omega_0 t_{01c3}} dt \\
 &= -\frac{V_t}{j\omega_0} \left(e^{-j\omega_0(t_{2(i+1)c3} - t_{1(i+1)c3})} e^{-j\omega_0 t_{01c3}} \right)
 \end{aligned} \tag{B.300}$$

Similarly we consider the pulse formed between $t_{2(i+1)c3}$ and $t_{3(i+1)c3}$ in Figure B.41. The width of this pulse is given by:

$$W_{2c3} = t_{3(i+1)c3} - t_{2(i+1)c3}$$

and its Fourier transform using the negative pulse results in:

$$\begin{aligned}
 F(\omega) &= \int_{-\frac{w_{2c3}}{2}}^{\frac{w_{2c3}}{2}} (-V_t) e^{-j\omega_0 t} dt \\
 &= \frac{V_t}{j\omega_0} \left(e^{-j\omega_0(t_{3(i+1)c3} - t_{2(i+1)c3})} \right)
 \end{aligned} \tag{B.301}$$

The shifting of this negative pulse by t_{02c3} where t_{02c3} is given by:

$$t_{02c3} = t_{2(i+1)c3} + \frac{W_{2c3}}{2} \tag{B.302}$$

The resulting Fourier transform of the shifted negative pulse is given by:

$$\begin{aligned}
 F(\omega) &= \int_{-\frac{w_{2c3}}{2}}^{\frac{w_{2c3}}{2}} (-V_t) e^{-j\omega_0 t} e^{-j\omega_0 t_{02c3}} dt \\
 &= \frac{V_t}{j\omega_0} \left(e^{-j\omega_0(t_{3(i+1)c3} - t_{2(i+1)c3})} e^{-j\omega_0 t_{02c3}} \right)
 \end{aligned} \tag{B.303}$$

To obtain the spectrum of $S_{c3}(\omega)$ we sum up all the Fourier transform for the negative and positive pulses over any number of cycles of the switching period. The amplitude spectrum is the same as the one for $S_{a1}(\omega)$ in the 2-cell multicell converter.

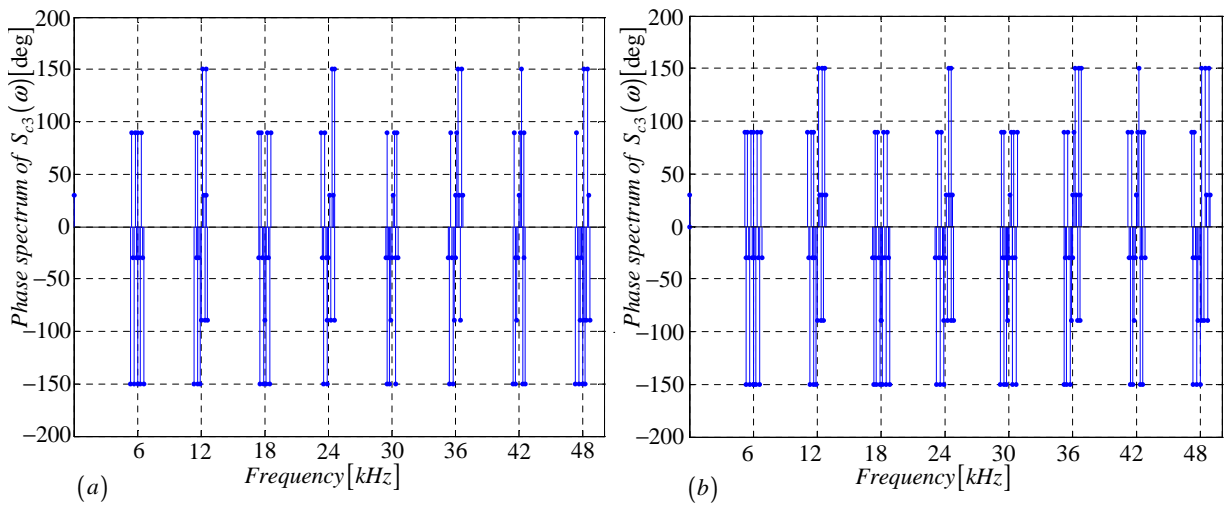


Figure B.42: Phase spectrum of $S_{c3}(\omega)$ generated using (a) Newton-Raphson simulation and (b) Theory

Appendix C

Phasor Diagrams

C.1 2-cell Multicell

For convenience we rewrite table 3.1 which was derived in chapter 2 as follows: Table C.1

Table C.1: Values for t_x , c and h of background function for 2-cell multicell converter

m_f		s_{a1}	s_{a2}	s_{b1}	s_{b2}	s_{c1}	s_{c2}
$3k$	t_x	0	$\frac{1}{2}T_s$	0	$\frac{1}{2}T_s$	0	$\frac{1}{2}T_s$
	c	0	-2	0	-2	0	-2
	h	$\frac{2\omega_s t}{\pi}$	$\frac{2\omega_s t}{\pi} - 2$	$\frac{2\omega_s t_1}{\pi}$	$\frac{2\omega_s t_1}{\pi} - 2$	$\frac{2\omega_s t_2}{\pi}$	$\frac{2\omega_s t_2}{\pi} - 2$
$3k + 1$	t_x	0	$\frac{1}{2}T_s$	$\frac{2}{3}T_s$	$\frac{1}{6}T_s$	$\frac{1}{3}T_s$	$-\frac{1}{6}T_s$
	c	0	-2	$-\frac{8}{3}$	$-\frac{2}{3}$	$-\frac{4}{3}$	$\frac{2}{3}$
	h	$\frac{2\omega_s t}{\pi}$	$\frac{2\omega_s t}{\pi} - 2$	$\frac{2\omega_s t_1}{\pi} - \frac{8}{3}$	$\frac{2\omega_s t_1}{\pi} - \frac{2}{3}$	$\frac{2\omega_s t_2}{\pi} - \frac{4}{3}$	$\frac{2\omega_s t_2}{\pi} + \frac{2}{3}$
$3k + 2$	t_x	0	$\frac{1}{2}T_s$	$\frac{1}{3}T_s$	$-\frac{1}{6}T_s$	$\frac{2}{3}T_s$	$\frac{1}{6}T_s$
	c	0	-2	$-\frac{4}{3}$	$\frac{2}{3}$	$-\frac{8}{3}$	$-\frac{2}{3}$
	h	$\frac{2\omega_s t}{\pi}$	$\frac{2\omega_s t}{\pi} - 2$	$\frac{2\omega_s t_1}{\pi} - \frac{4}{3}$	$\frac{2\omega_s t_1}{\pi} + \frac{2}{3}$	$\frac{2\omega_s t_2}{\pi} - \frac{8}{3}$	$\frac{2\omega_s t_2}{\pi} - \frac{2}{3}$

is used in evaluating the switching functions for different values of frequency modulation index m_f as will be shown below for $m_f = 3k$, $m_f = 3k + 1$ and $m_f = 3k + 2$. Also included in this section is the phasor representation for different cases of $S_{a1}(\omega)$, $S_{a2}(\omega)$, $S_{da}(\omega)$, $S_{ta}(\omega)$, $S_{b1}(\omega)$, $S_{b2}(\omega)$, $S_{db}(\omega)$, $S_{tb}(\omega)$, $S_{c1}(\omega)$, $S_{c2}(\omega)$, $S_{dc}(\omega)$, $S_{tc}(\omega)$.

C.1.1 For frequency modulation index $m_f = 3k$

Phase A

From table C.1 the value of h for the background function of $s_{a1}(t)$ is given by:

$$h = \frac{2\omega_s t}{\pi} \tag{C.1}$$

Substituting equation C.1 into the term $\frac{m\pi h}{2}$ of equation 3.36 we obtain:

$$\frac{m\pi h}{2} = m\omega_s t \quad (\text{C.2})$$

Now substituting equation C.2 into equation 3.36 we obtain:

$$\begin{aligned} s_{a1}(t) &= \frac{1}{2}A_{00} + \sum_{n=1}^{\infty} (A_{0n} \cos(n\omega_0 t) + B_{0n} \sin(n\omega_0 t)) \\ &\quad + \sum_{m=1}^{\infty} (A_{m0} \cos(m\omega_s t) + B_{m0} \sin(m\omega_s t)) \\ &\quad + \sum_{m=1}^{\infty} \sum_{n=\pm 1}^{\pm\infty} \{A_{mn} \cos((m\omega_s + n\omega_0)t) \\ &\quad + B_{mn} \sin((m\omega_s + n\omega_0)t)\} \end{aligned} \quad (\text{C.3})$$

From table C.1 for the background function of $s_{a2}(t)$ the value of h is given by:

$$h = \frac{2\omega_s}{\pi}t - 2 \quad (\text{C.4})$$

Substituting equation C.4 into the term $\frac{m\pi h}{2}$ of equation 3.36 we obtain:

$$\frac{m\pi h}{2} = m\omega_s t - m\pi \quad (\text{C.5})$$

Now substituting equation C.5 into equation 3.36 we obtain:

$$\begin{aligned} s_{a2}(t) &= \frac{1}{2}A_{00} + \sum_{n=1}^{\infty} (A_{0n} \cos(n\omega_0 t) + B_{0n} \sin(n\omega_0 t)) \\ &\quad + \sum_{m=1}^{\infty} (A_{m0} \cos(m\omega_s t - m\pi) + B_{m0} \sin(m\omega_s t - m\pi)) \\ &\quad + \sum_{m=1}^{\infty} \sum_{n=\pm 1}^{\pm\infty} \{A_{mn} \cos((m\omega_s + n\omega_0)t - m\pi) \\ &\quad + B_{mn} \sin((m\omega_s + n\omega_0)t - m\pi)\} \end{aligned} \quad (\text{C.6})$$

Now considering trigonometric terms in equation C.3 and C.6 we have:

$$\cos(m\omega_s t - m\pi) = \begin{cases} \cos(m\omega_s t) & \text{if } m = 2k \\ -\cos(m\omega_s t) & \text{if } m = 2k + 1 \end{cases} \quad (\text{C.7})$$

$$\sin(m\omega_s t - m\pi) = \begin{cases} \sin(m\omega_s t) & \text{if } m = 2k \\ -\sin(m\omega_s t) & \text{if } m = 2k + 1 \end{cases} \quad (\text{C.8})$$

$$\cos((m\omega_s + n\omega_0)t - m\pi) = \begin{cases} \cos(m\omega_s t + n\omega_0 t) & \text{if } m = 2k \\ -\cos(m\omega_s t + n\omega_0 t) & \text{if } m = 2k + 1 \end{cases} \quad (\text{C.9})$$

$$\sin((m\omega_s + n\omega_0)t - m\pi) = \begin{cases} \sin(m\omega_s t + n\omega_0 t) & \text{if } m = 2k \\ -\sin(m\omega_s t + n\omega_0 t) & \text{if } m = 2k + 1 \end{cases} \quad (\text{C.10})$$

Thus the phasor representation for phase A of 2-cell converter when $m_f = 3k$ is given by Figure C.1.

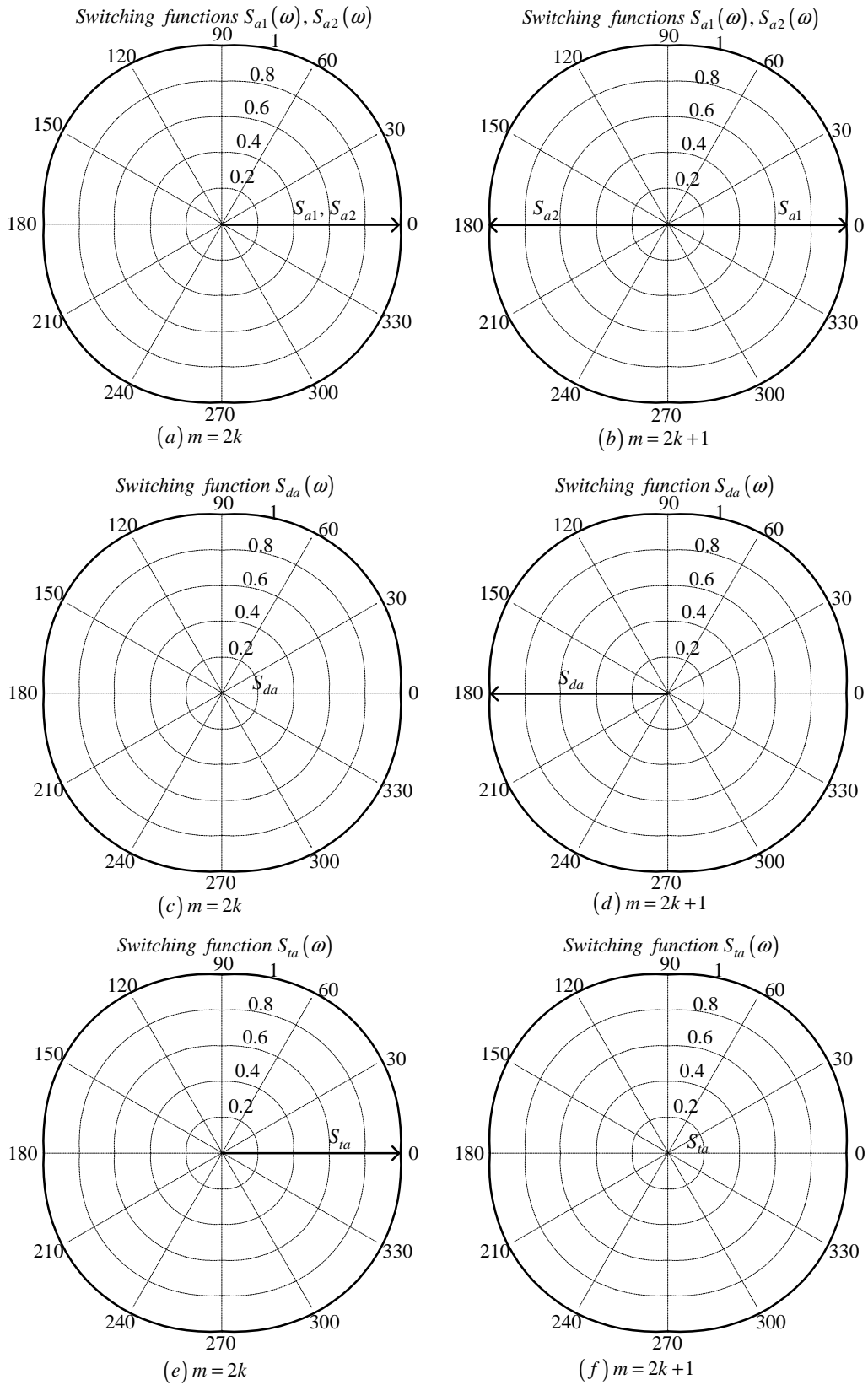


Figure C.1: Phasor representation for phase A of 2-cell converter

Phase B

From table C.1 the value of h for the background function of $s_{b1}(t)$ is given by:

$$h = \frac{2\omega_s}{\pi} t_1 \quad (\text{C.11})$$

Substituting equation C.11 into the term $\frac{m\pi h}{2}$ of equation 3.36 we obtain:

$$\frac{m\pi h}{2} = m\omega_s t_1 \quad (\text{C.12})$$

Now substituting equation C.12 into equation 3.36 we obtain:

$$\begin{aligned} s_{b1}(t_1) &= \frac{1}{2}A_{00} + \sum_{n=1}^{\infty} (A_{0n} \cos(n\omega_0 t_1) + B_{0n} \sin(n\omega_0 t_1)) \\ &+ \sum_{m=1}^{\infty} (A_{m0} \cos(m\omega_s t_1) + B_{m0} \sin(m\omega_s t_1)) \\ &+ \sum_{m=1}^{\infty} \sum_{n=\pm 1}^{\pm\infty} \{A_{mn} \cos((m\omega_s + n\omega_0) t_1) \\ &+ B_{mn} \sin((m\omega_s + n\omega_0) t_1)\} \end{aligned} \quad (\text{C.13})$$

We now substitute back $t = t_1 + \frac{T_0}{3}$ into equation C.13 and obtain:

$$\begin{aligned} s_{b1}(t) &= \frac{1}{2}A_{00} + \sum_{n=1}^{\infty} \left(A_{0n} \cos\left(n\omega_0 \left(t - \frac{2\pi}{3\omega_0}\right)\right) + B_{0n} \sin\left(n\omega_0 \left(t - \frac{2\pi}{3\omega_0}\right)\right) \right) \\ &+ \sum_{m=1}^{\infty} \left(A_{m0} \cos\left(m\omega_s \left(t - \frac{2\pi}{3\omega_0}\right)\right) \right. \\ &+ B_{m0} \sin\left(m\omega_s \left(t - \frac{2\pi}{3\omega_0}\right)\right) \left. \right) \\ &+ \sum_{m=1}^{\infty} \sum_{n=\pm 1}^{\pm\infty} \left\{ A_{mn} \cos\left((m\omega_s + n\omega_0) \left(t - \frac{2\pi}{3\omega_0}\right)\right) \right. \\ &+ B_{mn} \sin\left((m\omega_s + n\omega_0) \left(t - \frac{2\pi}{3\omega_0}\right)\right) \left. \right\} \end{aligned} \quad (\text{C.14})$$

From table C.1 for the background function of $s_{b2}(t)$ the value of h is given by:

$$h = \frac{2\omega_s}{\pi} t_1 - 2 \quad (\text{C.15})$$

Substituting equation C.15 into the term $\frac{m\pi h}{2}$ of equation 3.36 we obtain:

$$\frac{m\pi h}{2} = m\omega_s t_1 - m\pi \quad (\text{C.16})$$

Now substituting equation C.16 into equation 3.36 we obtain:

$$\begin{aligned}
s_{b2}(t_1) &= \frac{1}{2}A_{00} + \sum_{n=1}^{\infty} (A_{0n} \cos(n\omega_0 t_1) + B_{0n} \sin(n\omega_0 t_1)) \\
&+ \sum_{m=1}^{\infty} (A_{m0} \cos(m\omega_s t_1 - m\pi) + B_{m0} \sin(m\omega_s t_1 - m\pi)) \\
&+ \sum_{m=1}^{\infty} \sum_{n=\pm 1}^{\pm\infty} \{A_{mn} \cos((m\omega_s + n\omega_0)t_1 - m\pi) \\
&+ B_{mn} \sin((m\omega_s + n\omega_0)t_1 - m\pi)\}
\end{aligned} \tag{C.17}$$

We now substitute back $t = t_1 + \frac{T_0}{3}$ into equation C.13 and obtain:

$$\begin{aligned}
s_{b2}(t) &= \frac{1}{2}A_{00} + \sum_{n=1}^{\infty} \left(A_{0n} \cos\left(n\omega_0 \left(t - \frac{2\pi}{3\omega_0}\right)\right) + B_{0n} \sin\left(n\omega_0 \left(t - \frac{2\pi}{3\omega_0}\right)\right) \right) \\
&+ \sum_{m=1}^{\infty} \left(A_{m0} \cos\left(m\omega_s \left(t - \frac{2\pi}{3\omega_0}\right) - m\pi\right) \right. \\
&+ B_{m0} \sin\left(m\omega_s \left(t - \frac{2\pi}{3\omega_0}\right) - m\pi\right) \\
&+ \sum_{m=1}^{\infty} \sum_{n=\pm 1}^{\pm\infty} \left\{ A_{mn} \cos\left((m\omega_s + n\omega_0) \left(t - \frac{2\pi}{3\omega_0}\right) - m\pi\right) \right. \\
&+ B_{mn} \sin\left((m\omega_s + n\omega_0) \left(t - \frac{2\pi}{3\omega_0}\right) - m\pi\right) \left. \right\}
\end{aligned} \tag{C.18}$$

Now considering trigonometric terms in equation C.14 and C.18 we have:

$$\begin{aligned}
\cos\left(n\omega_0 \left(t - \frac{2\pi}{3\omega_0}\right)\right) &= \cos\left(n\omega_0 t - \frac{2n\pi}{3}\right) \\
&= \begin{cases} \cos(n\omega_0 t) & \text{if } n = 3p \\ \cos\left(n\omega_0 t - \frac{2\pi}{3}\right) & \text{if } n = 3p + 1 \\ \cos\left(n\omega_0 t + \frac{2\pi}{3}\right) & \text{if } n = 3p + 2 \end{cases}
\end{aligned} \tag{C.19}$$

$$\begin{aligned}
\sin\left(n\omega_0 \left(t - \frac{2\pi}{3\omega_0}\right)\right) &= \sin\left(n\omega_0 t - \frac{2n\pi}{3}\right) \\
&= \begin{cases} \sin(n\omega_0 t) & \text{if } n = 3p \\ \sin\left(n\omega_0 t - \frac{2\pi}{3}\right) & \text{if } n = 3p + 1 \\ \sin\left(n\omega_0 t + \frac{2\pi}{3}\right) & \text{if } n = 3p + 2 \end{cases}
\end{aligned} \tag{C.20}$$

$$\begin{aligned}
\cos\left(m\omega_s \left(t - \frac{2\pi}{3\omega_0}\right)\right) &= \cos\left(m\omega_s t - \frac{2m\pi}{3}m_f\right) \\
&= \cos(m\omega_s t)
\end{aligned} \tag{C.21}$$

$$\begin{aligned}\sin\left(m\omega_s\left(t - \frac{2\pi}{3\omega_0}\right)\right) &= \sin\left(m\omega_s t - \frac{2m\pi}{3}m_f\right) \\ &= \sin(m\omega_s t)\end{aligned}\tag{C.22}$$

$$\begin{aligned}\cos\left(m\omega_s\left(t - \frac{2\pi}{3\omega_0}\right) - m\pi\right) &= \cos\left(m\omega_s t - \frac{2m\pi}{3}m_f - m\pi\right) \\ &= \begin{cases} \cos(m\omega_s t) & \text{if } m = 2k \\ -\cos(m\omega_s t) & \text{if } m = 2k + 1 \end{cases}\end{aligned}\tag{C.23}$$

$$\begin{aligned}\sin\left(m\omega_s\left(t - \frac{2\pi}{3\omega_0}\right) - m\pi\right) &= \sin\left(m\omega_s t - \frac{2m\pi}{3}m_f - m\pi\right) \\ &= \begin{cases} \sin(m\omega_s t) & \text{if } m = 2k \\ -\sin(m\omega_s t) & \text{if } m = 2k + 1 \end{cases}\end{aligned}\tag{C.24}$$

$$\begin{aligned}\cos\left((m\omega_s + n\omega_0)\left(t - \frac{2\pi}{3\omega_0}\right)\right) &= \cos\left(m\omega_s t + n\omega_0 t - \frac{2m\pi}{3}m_f - \frac{2n\pi}{3}\right) \\ &= \begin{cases} \cos(m\omega_s t + n\omega_0 t) & \text{if } m = k \text{ and } n = 3p \\ \cos\left((m\omega_s + n\omega_0)t - \frac{2\pi}{3}\right) & \text{if } m = k \text{ and } n = 3p + 1 \\ \cos\left((m\omega_s + n\omega_0)t + \frac{2\pi}{3}\right) & \text{if } m = k \text{ and } n = 3p + 2 \\ \cos(m\omega_s t + n\omega_0 t) & \text{if } m = k \text{ and } n = -3p \\ \cos\left((m\omega_s + n\omega_0)t - \frac{2\pi}{3}\right) & \text{if } m = k \text{ and } n = -(3p + 2) \\ \cos\left((m\omega_s + n\omega_0)t + \frac{2\pi}{3}\right) & \text{if } m = k \text{ and } n = -(3p + 1) \end{cases}\end{aligned}\tag{C.25}$$

$$\begin{aligned}\sin\left((m\omega_s + n\omega_0)\left(t - \frac{2\pi}{3\omega_0}\right)\right) &= \sin\left(m\omega_s t + n\omega_0 t - \frac{2m\pi}{3}m_f - \frac{2n\pi}{3}\right) \\ &= \begin{cases} \cos(m\omega_s t + n\omega_0 t) & \text{if } m = k \text{ and } n = 3p \\ \sin\left((m\omega_s + n\omega_0)t - \frac{2\pi}{3}\right) & \text{if } m = k \text{ and } n = 3p + 1 \\ \sin\left((m\omega_s + n\omega_0)t + \frac{2\pi}{3}\right) & \text{if } m = k \text{ and } n = 3p + 2 \\ \sin(m\omega_s t + n\omega_0 t) & \text{if } m = k \text{ and } n = -3p \\ \sin\left((m\omega_s + n\omega_0)t - \frac{2\pi}{3}\right) & \text{if } m = k \text{ and } n = -(3p + 2) \\ \sin\left((m\omega_s + n\omega_0)t + \frac{2\pi}{3}\right) & \text{if } m = k \text{ and } n = -(3p + 1) \end{cases}\end{aligned}\tag{C.26}$$

$$\begin{aligned}
& \cos \left((m\omega_s + n\omega_0) \left(t - \frac{2\pi}{3\omega_0} \right) - m\pi \right) = \cos \left(m\omega_s t + n\omega_0 t - \frac{2m\pi}{3} m_f - \frac{2n\pi}{3} - m\pi \right) \\
= & \left\{ \begin{array}{ll} \cos(m\omega_s t + n\omega_0 t) & \text{if } m = 2k \text{ and } n = 3p \\ \cos \left((m\omega_s + n\omega_0) t - \frac{2\pi}{3} \right) & \text{if } m = 2k \text{ and } n = 3p + 1 \\ \cos \left((m\omega_s + n\omega_0) t + \frac{2\pi}{3} \right) & \text{if } m = 2k \text{ and } n = 3p + 2 \\ \cos(m\omega_s t + n\omega_0 t) & \text{if } m = 2k \text{ and } n = -3p \\ \cos \left((m\omega_s + n\omega_0) t - \frac{2\pi}{3} \right) & \text{if } m = 2k \text{ and } n = -(3p + 2) \\ \cos \left((m\omega_s + n\omega_0) t + \frac{2\pi}{3} \right) & \text{if } m = 2k \text{ and } n = -(3p + 1) \\ -\cos(m\omega_s t + n\omega_0 t) & \text{if } m = 2k + 1 \text{ and } n = 3p \\ -\cos \left((m\omega_s + n\omega_0) t - \frac{2\pi}{3} \right) & \text{if } m = 2k + 1 \text{ and } n = 3p + 1 \\ -\cos \left((m\omega_s + n\omega_0) t + \frac{2\pi}{3} \right) & \text{if } m = 2k + 1 \text{ and } n = 3p + 2 \\ -\cos(m\omega_s t + n\omega_0 t) & \text{if } m = 2k + 1 \text{ and } n = -3p \\ -\cos \left((m\omega_s + n\omega_0) t - \frac{2\pi}{3} \right) & \text{if } m = 2k + 1 \text{ and } n = -(3p + 2) \\ -\cos \left((m\omega_s + n\omega_0) t + \frac{2\pi}{3} \right) & \text{if } m = 2k + 1 \text{ and } n = -(3p + 1) \end{array} \right. \quad (\text{C.27})
\end{aligned}$$

$$\begin{aligned}
& \sin \left((m\omega_s + n\omega_0) \left(t - \frac{2\pi}{3\omega_0} \right) - m\pi \right) = \sin \left(m\omega_s t + n\omega_0 t - \frac{2m\pi}{3} m_f - \frac{2n\pi}{3} - m\pi \right) \\
= & \left\{ \begin{array}{ll} \sin(m\omega_s t + n\omega_0 t) & \text{if } m = 2k \text{ and } n = 3p \\ \sin \left((m\omega_s + n\omega_0) t - \frac{2\pi}{3} \right) & \text{if } m = 2k \text{ and } n = 3p + 1 \\ \sin \left((m\omega_s + n\omega_0) t + \frac{2\pi}{3} \right) & \text{if } m = 2k \text{ and } n = 3p + 2 \\ \sin(m\omega_s t + n\omega_0 t) & \text{if } m = 2k \text{ and } n = -3p \\ \sin \left((m\omega_s + n\omega_0) t - \frac{2\pi}{3} \right) & \text{if } m = 2k \text{ and } n = -(3p + 2) \\ \sin \left((m\omega_s + n\omega_0) t + \frac{2\pi}{3} \right) & \text{if } m = 2k \text{ and } n = -(3p + 1) \\ -\sin(m\omega_s t + n\omega_0 t) & \text{if } m = 2k + 1 \text{ and } n = 3p \\ -\sin \left((m\omega_s + n\omega_0) t - \frac{2\pi}{3} \right) & \text{if } m = 2k + 1 \text{ and } n = 3p + 1 \\ -\sin \left((m\omega_s + n\omega_0) t + \frac{2\pi}{3} \right) & \text{if } m = 2k + 1 \text{ and } n = 3p + 2 \\ -\sin(m\omega_s t + n\omega_0 t) & \text{if } m = 2k + 1 \text{ and } n = -3p \\ -\sin \left((m\omega_s + n\omega_0) t - \frac{2\pi}{3} \right) & \text{if } m = 2k + 1 \text{ and } n = -(3p + 2) \\ -\sin \left((m\omega_s + n\omega_0) t + \frac{2\pi}{3} \right) & \text{if } m = 2k + 1 \text{ and } n = -(3p + 1) \end{array} \right. \quad (\text{C.28})
\end{aligned}$$

Thus the phasor representation for phase B of 2-cell converter when $m_f = 3k$ is given by Figures C.2, C.3 and C.4.

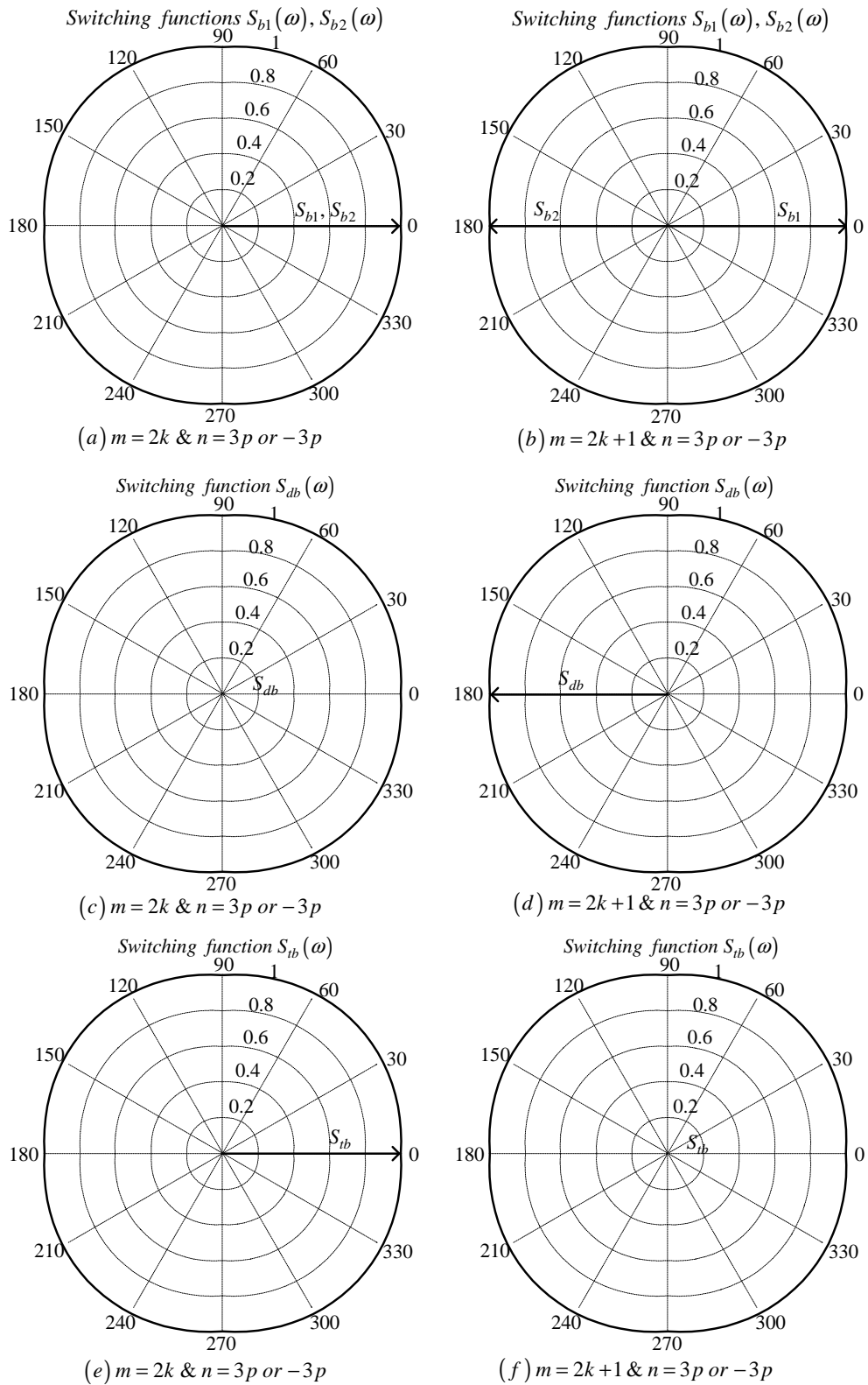


Figure C.2: Phasor representation for phase B of 2-cell converter for $n = 3p$ or $n = -3p$

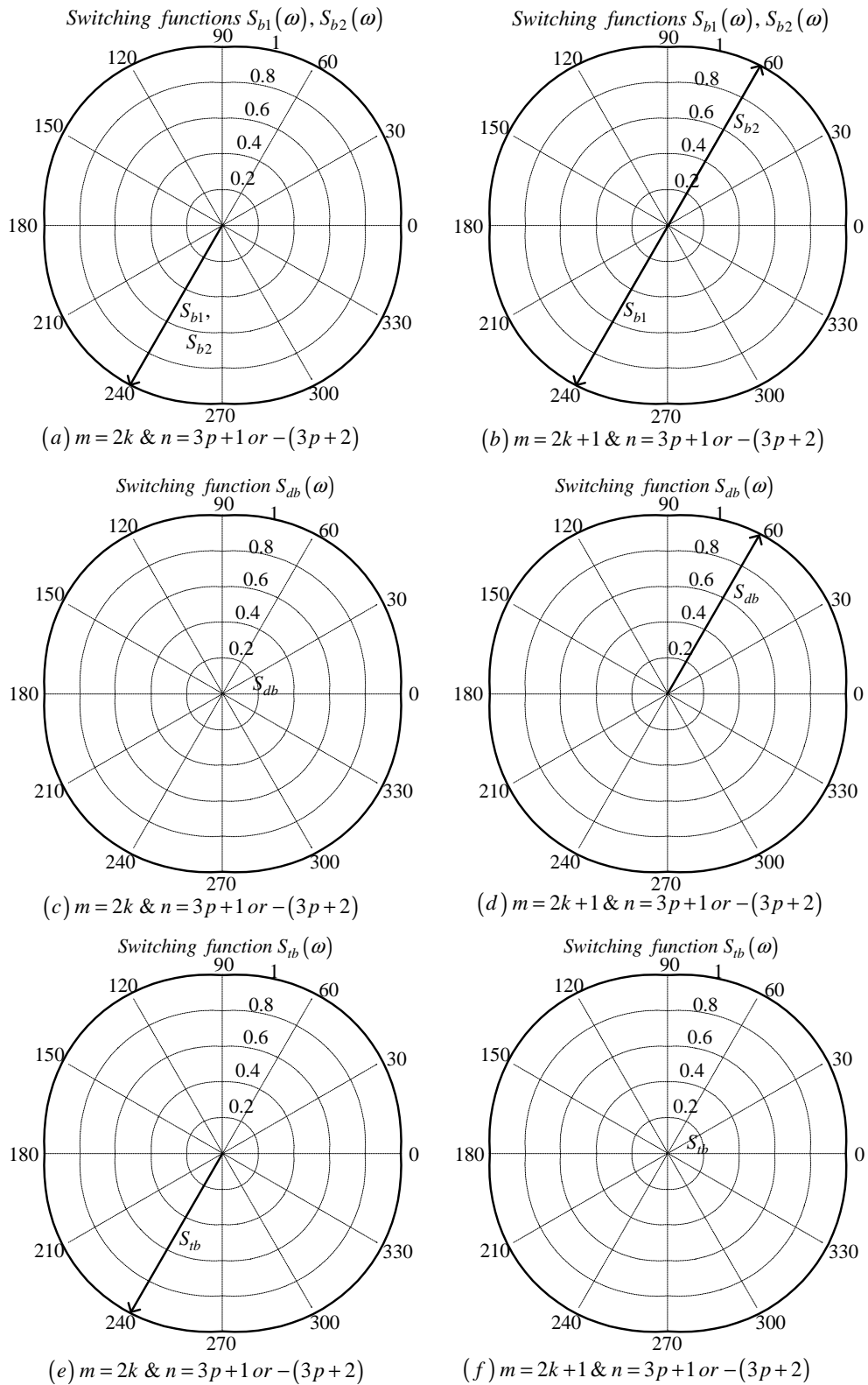


Figure C.3: Phasor representation for phase B of 2-cell converter for $n = 3p + 1$ or $n = -(3p + 2)$

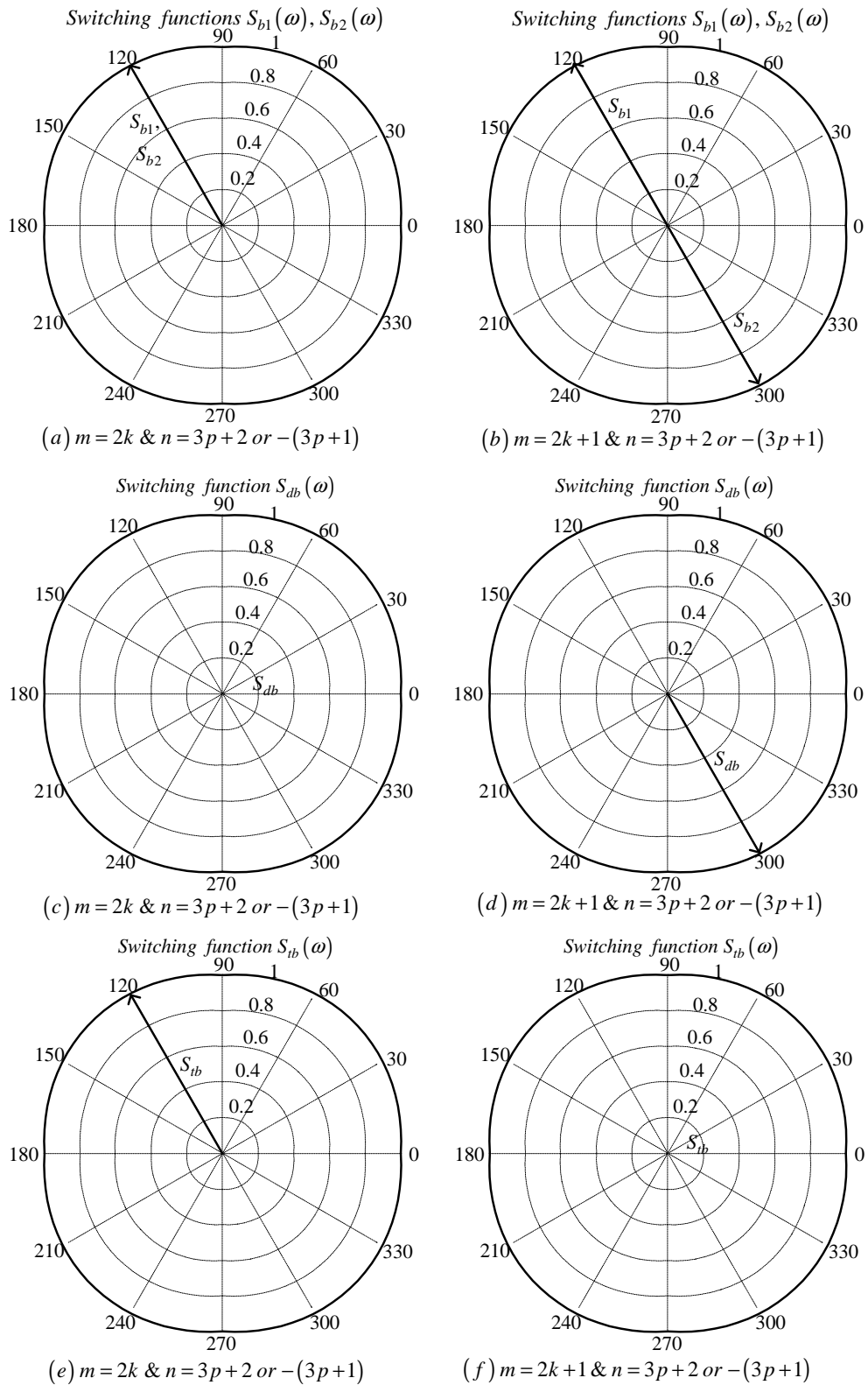


Figure C.4: Phasor representation for phase B of 2-cell converter for $n = 3p + 2$ or $n = -(3p + 1)$

Phase C

From table C.1 for the background function of $s_{c1}(t)$ the value of h is given by:

$$h = \frac{2\omega_s}{\pi}t_2 \quad (\text{C.29})$$

Substituting equation C.29 into the term $\frac{m\pi h}{2}$ of equation 3.36 we obtain:

$$\frac{m\pi h}{2} = m\omega_s t_2 \quad (\text{C.30})$$

Now substituting equation C.30 into equation 3.36 we obtain:

$$\begin{aligned} s_{c1}(t_2) &= \frac{1}{2}A_{00} + \sum_{n=1}^{\infty} (A_{0n} \cos(n\omega_0 t_2) + B_{0n} \sin(n\omega_0 t_2)) \\ &\quad + \sum_{m=1}^{\infty} (A_{m0} \cos(m\omega_s t_2) + B_{m0} \sin(m\omega_s t_2)) \\ &\quad + \sum_{m=1}^{\infty} \sum_{n=\pm 1}^{\pm\infty} \{A_{mn} \cos((m\omega_s + n\omega_0)t_2) \\ &\quad + B_{mn} \sin((m\omega_s + n\omega_0)t_2)\} \end{aligned} \quad (\text{C.31})$$

We now substitute back $t = t_2 + \frac{2T_0}{3}$ into equation C.31 and obtain:

$$\begin{aligned} s_{c1}(t) &= \frac{1}{2}A_{00} + \sum_{n=1}^{\infty} \left(A_{0n} \cos\left(n\omega_0 \left(t - \frac{4\pi}{3\omega_0}\right)\right) + B_{0n} \sin\left(n\omega_0 \left(t - \frac{4\pi}{3\omega_0}\right)\right) \right) \\ &\quad + \sum_{m=1}^{\infty} \left(A_{m0} \cos\left(m\omega_s \left(t - \frac{4\pi}{3\omega_0}\right)\right) + B_{m0} \sin\left(m\omega_s \left(t - \frac{4\pi}{3\omega_0}\right)\right) \right) \\ &\quad + \sum_{m=1}^{\infty} \sum_{n=\pm 1}^{\pm\infty} \left\{ A_{mn} \cos\left((m\omega_s + n\omega_0) \left(t - \frac{4\pi}{3\omega_0}\right)\right) \right. \\ &\quad \left. + B_{mn} \sin\left((m\omega_s + n\omega_0) \left(t - \frac{4\pi}{3\omega_0}\right)\right) \right\} \end{aligned} \quad (\text{C.32})$$

From table C.1 for the background function of $s_{c2}(t)$ the value of h is given by:

$$h = \frac{2\omega_s}{\pi}t_2 - 2 \quad (\text{C.33})$$

Substituting equation C.33 into the term $\frac{m\pi h}{2}$ of equation 3.36 we obtain:

$$\frac{m\pi h}{2} = m\omega_s t_2 - m\pi \quad (\text{C.34})$$

Now substituting equation C.34 into equation 3.36 we obtain:

$$\begin{aligned}
s_{c2}(t_2) &= \frac{1}{2}A_{00} + \sum_{n=1}^{\infty} (A_{0n} \cos(n\omega_0 t_2) + B_{0n} \sin(n\omega_0 t_2)) \\
&+ \sum_{m=1}^{\infty} (A_{m0} \cos(m\omega_s t_2 - m\pi) + B_{m0} \sin(m\omega_s t_2 - m\pi)) \\
&+ \sum_{m=1}^{\infty} \sum_{n=\pm 1}^{\pm\infty} \{A_{mn} \cos((m\omega_s + n\omega_0)t_2 - m\pi) \\
&+ B_{mn} \sin((m\omega_s + n\omega_0)t_2 - m\pi)\}
\end{aligned} \tag{C.35}$$

We now substitute back $t = t_2 + \frac{2T_0}{3}$ into equation C.35 and obtain:

$$\begin{aligned}
s_{c2}(t) &= \frac{1}{2}A_{00} + \sum_{n=1}^{\infty} \left(A_{0n} \cos\left(n\omega_0 \left(t - \frac{4\pi}{3\omega_0}\right)\right) + B_{0n} \sin\left(n\omega_0 \left(t - \frac{4\pi}{3\omega_0}\right)\right) \right) \\
&+ \sum_{m=1}^{\infty} \left(A_{m0} \cos\left(m\omega_s \left(t - \frac{4\pi}{3\omega_0}\right) - m\pi\right) \right. \\
&+ B_{m0} \sin\left(m\omega_s \left(t - \frac{4\pi}{3\omega_0}\right) - m\pi\right) \\
&+ \sum_{m=1}^{\infty} \sum_{n=\pm 1}^{\pm\infty} \left\{ A_{mn} \cos\left((m\omega_s + n\omega_0) \left(t - \frac{4\pi}{3\omega_0}\right) - m\pi\right) \right. \\
&+ B_{mn} \sin\left((m\omega_s + n\omega_0) \left(t - \frac{4\pi}{3\omega_0}\right) - m\pi\right) \left. \right\}
\end{aligned} \tag{C.36}$$

Now considering trigonometric terms in equations C.32 and C.36 we have:

$$\begin{aligned}
\cos\left(n\omega_0 \left(t - \frac{4\pi}{3\omega_0}\right)\right) &= \cos\left(n\omega_0 t - \frac{4n\pi}{3}\right) \\
&= \begin{cases} \cos(n\omega_0 t) & \text{if } n = 3p \\ \cos\left(n\omega_0 t + \frac{2\pi}{3}\right) & \text{if } n = 3p + 1 \\ \cos\left(n\omega_0 t - \frac{2\pi}{3}\right) & \text{if } n = 3p + 2 \end{cases}
\end{aligned} \tag{C.37}$$

$$\begin{aligned}
\sin\left(n\omega_0 \left(t - \frac{4\pi}{3\omega_0}\right)\right) &= \sin\left(n\omega_0 t - \frac{4n\pi}{3}\right) \\
&= \begin{cases} \sin(n\omega_0 t) & \text{if } n = 3p \\ \sin\left(n\omega_0 t + \frac{2\pi}{3}\right) & \text{if } n = 3p + 1 \\ \sin\left(n\omega_0 t - \frac{2\pi}{3}\right) & \text{if } n = 3p + 2 \end{cases}
\end{aligned} \tag{C.38}$$

$$\begin{aligned}
\cos\left(m\omega_s \left(t - \frac{4\pi}{3\omega_0}\right)\right) &= \cos\left(m\omega_s t - \frac{4m\pi}{3}m_f\right) \\
&= \cos(m\omega_s t)
\end{aligned} \tag{C.39}$$

$$\begin{aligned}\sin\left(m\omega_s\left(t - \frac{4\pi}{3\omega_0}\right)\right) &= \sin\left(m\omega_s t - \frac{4m\pi}{3}m_f\right) \\ &= \sin(m\omega_s t)\end{aligned}\tag{C.40}$$

$$\begin{aligned}\cos\left(m\omega_s\left(t - \frac{4\pi}{3\omega_0}\right) - m\pi\right) &= \cos\left(m\omega_s t - \frac{4m\pi}{3}m_f - m\pi\right) \\ &= \begin{cases} \cos(m\omega_s t) & \text{if } m = 2k \\ -\cos(m\omega_s t) & \text{if } m = 2k + 1 \end{cases}\end{aligned}\tag{C.41}$$

$$\begin{aligned}\sin\left(m\omega_s\left(t - \frac{4\pi}{3\omega_0}\right) - m\pi\right) &= \sin\left(m\omega_s t - \frac{4m\pi}{3}m_f - m\pi\right) \\ &= \begin{cases} \sin(m\omega_s t) & \text{if } m = 2k \\ -\sin(m\omega_s t) & \text{if } m = 2k + 1 \end{cases}\end{aligned}\tag{C.42}$$

$$\begin{aligned}\cos\left((m\omega_s + n\omega_0)\left(t - \frac{4\pi}{3\omega_0}\right)\right) &= \cos\left(m\omega_s t + n\omega_0 t - \frac{4m\pi}{3}m_f - \frac{4n\pi}{3}\right) \\ &= \begin{cases} \cos(m\omega_s t + n\omega_0 t) & \text{if } m = k \text{ and } n = 3p \\ \cos\left((m\omega_s + n\omega_0)t + \frac{2\pi}{3}\right) & \text{if } m = k \text{ and } n = 3p + 1 \\ \cos\left((m\omega_s + n\omega_0)t - \frac{2\pi}{3}\right) & \text{if } m = k \text{ and } n = 3p + 2 \\ \cos(m\omega_s t + n\omega_0 t) & \text{if } m = k \text{ and } n = -3p \\ \cos\left((m\omega_s + n\omega_0)t + \frac{2\pi}{3}\right) & \text{if } m = k \text{ and } n = -(3p + 2) \\ \cos\left((m\omega_s + n\omega_0)t - \frac{2\pi}{3}\right) & \text{if } m = k \text{ and } n = -(3p + 1) \end{cases}\end{aligned}\tag{C.43}$$

$$\begin{aligned}\sin\left((m\omega_s + n\omega_0)\left(t - \frac{4\pi}{3\omega_0}\right)\right) &= \cos\left(m\omega_s t + n\omega_0 t - \frac{4m\pi}{3}m_f - \frac{4n\pi}{3}\right) \\ &= \begin{cases} \sin(m\omega_s t + n\omega_0 t) & \text{if } m = k \text{ and } n = 3p \\ \sin\left((m\omega_s + n\omega_0)t + \frac{2\pi}{3}\right) & \text{if } m = k \text{ and } n = 3p + 1 \\ \sin\left((m\omega_s + n\omega_0)t - \frac{2\pi}{3}\right) & \text{if } m = k \text{ and } n = 3p + 2 \\ \sin(m\omega_s t + n\omega_0 t) & \text{if } m = k \text{ and } n = -3p \\ \sin\left((m\omega_s + n\omega_0)t + \frac{2\pi}{3}\right) & \text{if } m = k \text{ and } n = -(3p + 2) \\ \sin\left((m\omega_s + n\omega_0)t - \frac{2\pi}{3}\right) & \text{if } m = k \text{ and } n = -(3p + 1) \end{cases}\end{aligned}\tag{C.44}$$

$$\begin{aligned}
& \cos \left((m\omega_s + n\omega_0) \left(t - \frac{4\pi}{3\omega_0} \right) - m\pi \right) = \cos \left(m\omega_s t + n\omega_0 t - \frac{4m\pi}{3} m_f - \frac{4n\pi}{3} - m\pi \right) \\
= & \left\{ \begin{array}{ll} \cos(m\omega_s t + n\omega_0 t) & \text{if } m = 2k \text{ and } n = 3p \\ \cos \left((m\omega_s + n\omega_0) t + \frac{2\pi}{3} \right) & \text{if } m = 2k \text{ and } n = 3p + 1 \\ \cos \left((m\omega_s + n\omega_0) t - \frac{2\pi}{3} \right) & \text{if } m = 2k \text{ and } n = 3p + 2 \\ \cos(m\omega_s t + n\omega_0 t) & \text{if } m = 2k \text{ and } n = -3p \\ \cos \left((m\omega_s + n\omega_0) t + \frac{2\pi}{3} \right) & \text{if } m = 2k \text{ and } n = -(3p + 2) \\ \cos \left((m\omega_s + n\omega_0) t - \frac{2\pi}{3} \right) & \text{if } m = 2k \text{ and } n = -(3p + 1) \\ -\cos(m\omega_s t + n\omega_0 t) & \text{if } m = 2k + 1 \text{ and } n = 3p \\ -\cos \left((m\omega_s + n\omega_0) t + \frac{2\pi}{3} \right) & \text{if } m = 2k + 1 \text{ and } n = 3p + 1 \\ -\cos \left((m\omega_s + n\omega_0) t - \frac{2\pi}{3} \right) & \text{if } m = 2k + 1 \text{ and } n = 3p + 2 \\ -\cos(m\omega_s t + n\omega_0 t) & \text{if } m = 2k + 1 \text{ and } n = -3p \\ -\cos \left((m\omega_s + n\omega_0) t + \frac{2\pi}{3} \right) & \text{if } m = 2k + 1 \text{ and } n = -(3p + 2) \\ -\cos \left((m\omega_s + n\omega_0) t - \frac{2\pi}{3} \right) & \text{if } m = 2k + 1 \text{ and } n = -(3p + 1) \end{array} \right. \quad (\text{C.45})
\end{aligned}$$

$$\begin{aligned}
& \sin \left((m\omega_s + n\omega_0) \left(t - \frac{4\pi}{3\omega_0} \right) - m\pi \right) = \sin \left(m\omega_s t - \frac{4m\pi}{3} m_f - \frac{4n\pi}{3} - m\pi \right) \\
= & \left\{ \begin{array}{ll} \sin(m\omega_s t + n\omega_0 t) & \text{if } m = 2k \text{ and } n = 3p \\ \sin \left((m\omega_s + n\omega_0) t + \frac{2\pi}{3} \right) & \text{if } m = 2k \text{ and } n = 3p + 1 \\ \sin \left((m\omega_s + n\omega_0) t - \frac{2\pi}{3} \right) & \text{if } m = 2k \text{ and } n = 3p + 2 \\ \sin(m\omega_s t + n\omega_0 t) & \text{if } m = 2k \text{ and } n = -3p \\ \sin \left((m\omega_s + n\omega_0) t + \frac{2\pi}{3} \right) & \text{if } m = 2k \text{ and } n = -(3p + 2) \\ \sin \left((m\omega_s + n\omega_0) t - \frac{2\pi}{3} \right) & \text{if } m = 2k \text{ and } n = -(3p + 1) \\ -\sin(m\omega_s t + n\omega_0 t) & \text{if } m = 2k + 1 \text{ and } n = 3p \\ -\sin \left((m\omega_s + n\omega_0) t + \frac{2\pi}{3} \right) & \text{if } m = 2k + 1 \text{ and } n = 3p + 1 \\ -\sin \left((m\omega_s + n\omega_0) t - \frac{2\pi}{3} \right) & \text{if } m = 2k + 1 \text{ and } n = 3p + 2 \\ -\sin(m\omega_s t + n\omega_0 t) & \text{if } m = 2k + 1 \text{ and } n = -3p \\ -\sin \left((m\omega_s + n\omega_0) t + \frac{2\pi}{3} \right) & \text{if } m = 2k + 1 \text{ and } n = -(3p + 2) \\ -\sin \left((m\omega_s + n\omega_0) t - \frac{2\pi}{3} \right) & \text{if } m = 2k + 1 \text{ and } n = -(3p + 1) \end{array} \right. \quad (\text{C.46})
\end{aligned}$$

Thus the phasor representation for phase C of 2-cell converter when $m_f = 3k$ is given by Figures C.5, C.6 and C.7.

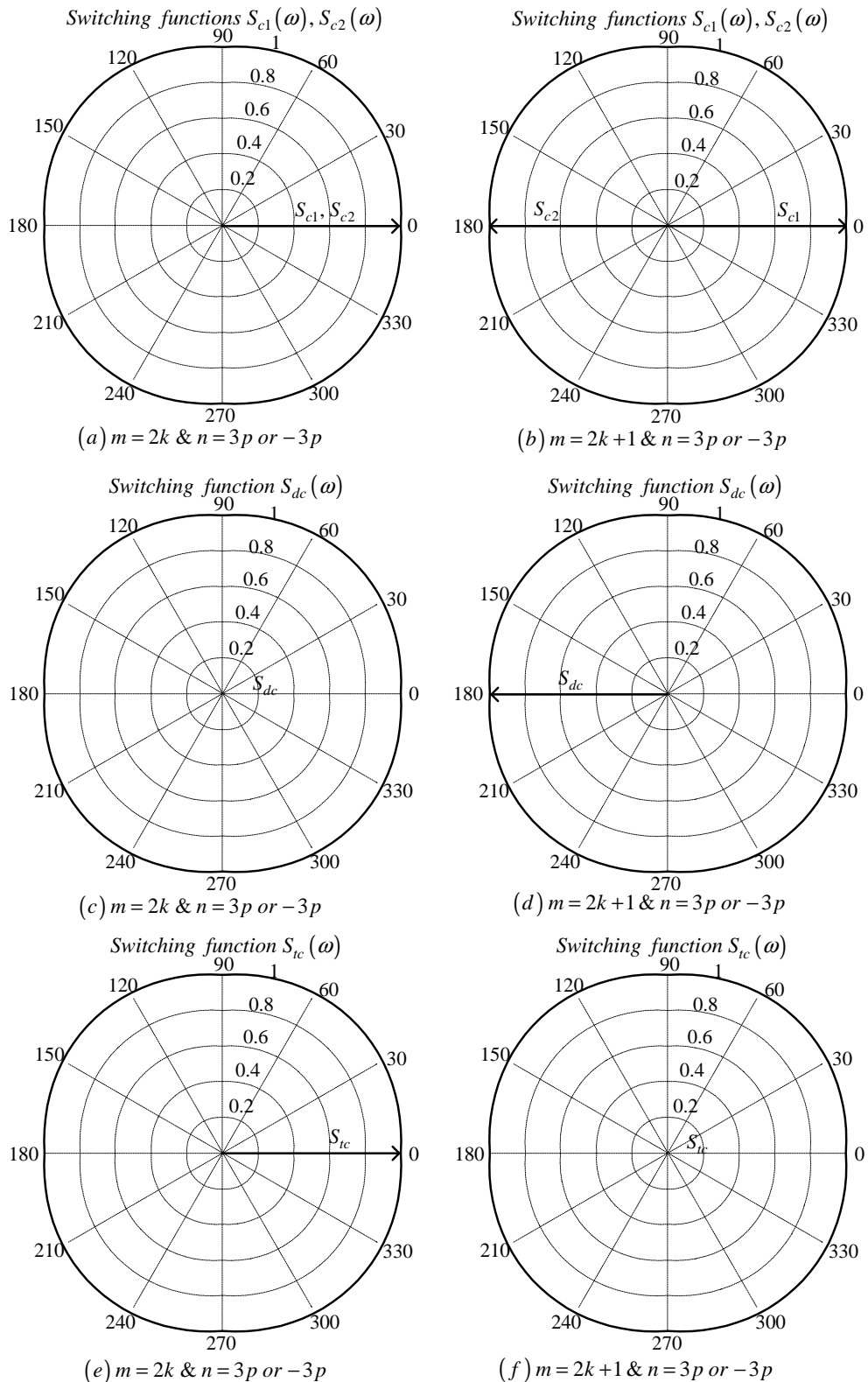


Figure C.5: Phasor representation for phase C of 2-cell converter for $n = 3p$ or $n = -3p$

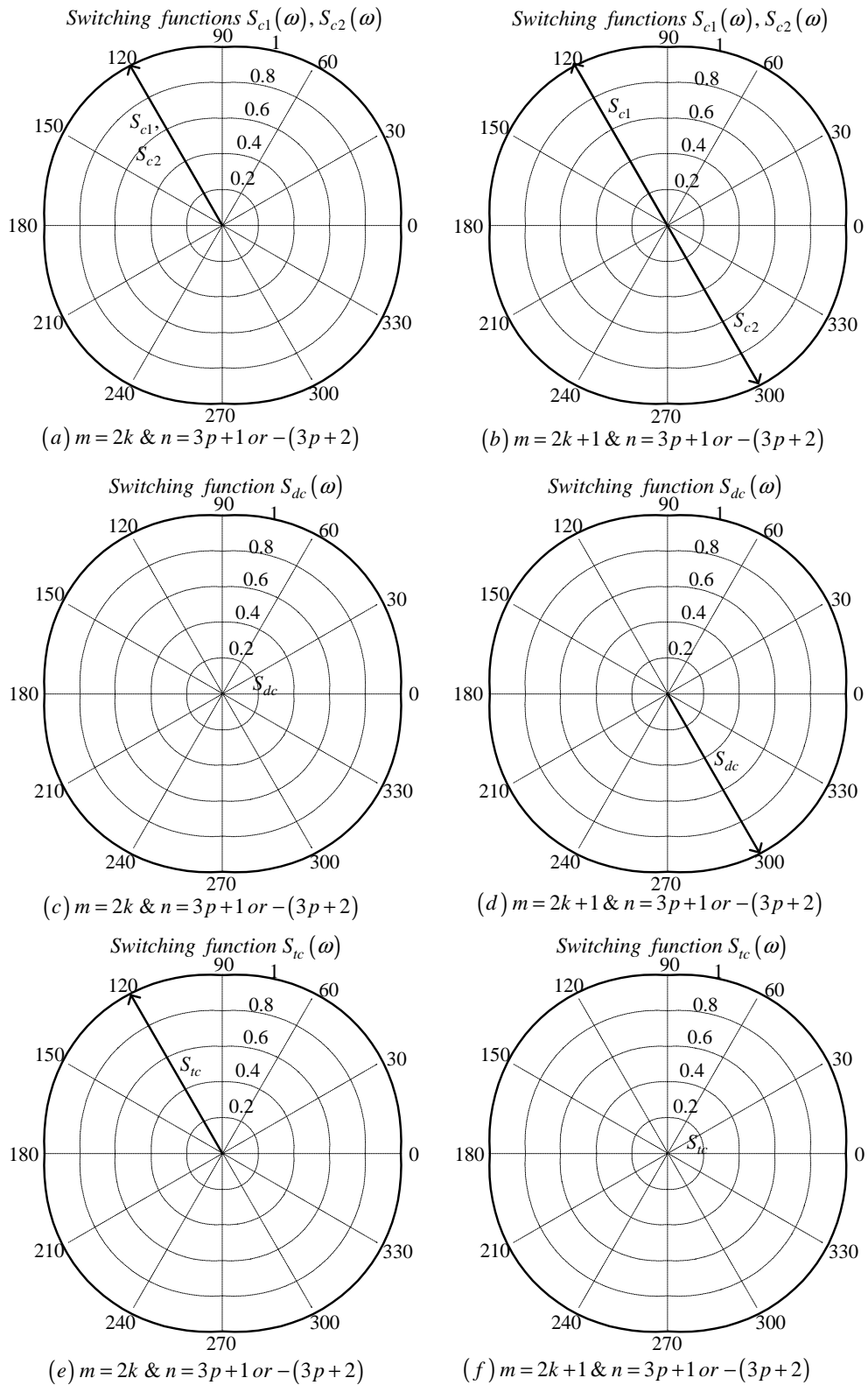


Figure C.6: Phasor representation for phase C of 2-cell converter for $n = 3p + 1$ or $n = -(3p + 2)$

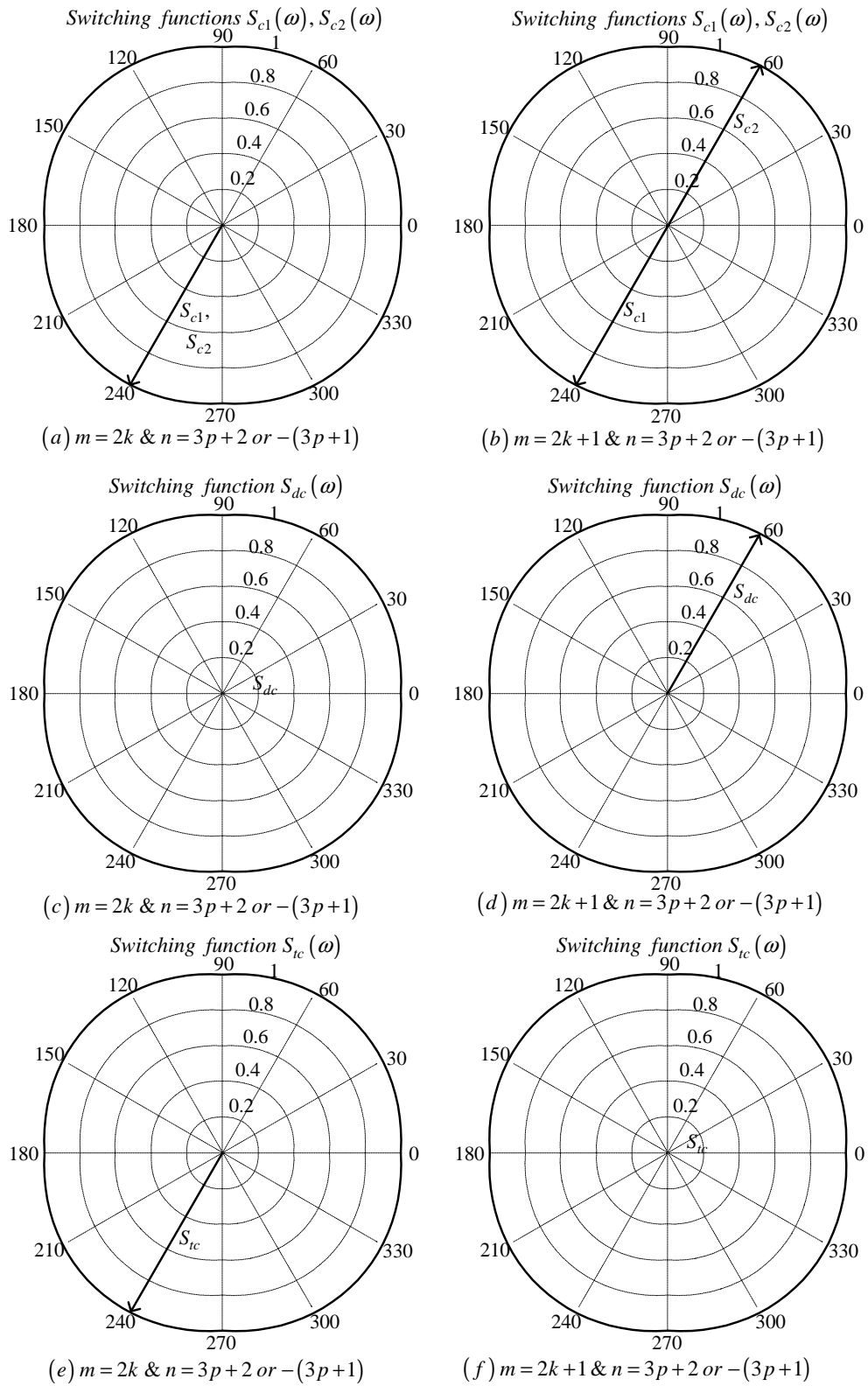


Figure C.7: Phasor representation for phase C of 2-cell converter for $n = 3p + 2$ or $n = -(3p + 1)$

C.1.2 For frequency modulation index $m_f = 3k + 1$

The case of phase A is the same as the one done in subsection C.1.1.

Phase B

From table C.1 the value of h for the background function of $s_{b1}(t)$ is given by:

$$h = \frac{2\omega_s}{\pi}t_1 - \frac{8}{3} \quad (\text{C.47})$$

Substituting equation C.47 into the term $\frac{m\pi h}{2}$ of equation 3.36 we obtain:

$$\frac{m\pi h}{2} = m\omega_s t_1 - \frac{4}{3}m\pi \quad (\text{C.48})$$

Now substituting equation C.48 into equation 3.36 we obtain:

$$\begin{aligned} s_{b1}(t_1) &= \frac{1}{2}A_{00} + \sum_{n=1}^{\infty} (A_{0n} \cos(n\omega_0 t_1) + B_{0n} \sin(n\omega_0 t_1)) \\ &+ \sum_{m=1}^{\infty} \left(A_{m0} \cos\left(m\omega_s t_1 - \frac{4}{3}m\pi\right) + B_{m0} \sin\left(m\omega_s t_1 - \frac{4}{3}m\pi\right) \right) \\ &+ \sum_{m=1}^{\infty} \sum_{n=\pm 1}^{\pm\infty} \left\{ A_{mn} \cos\left((m\omega_s + n\omega_0)t_1 - \frac{4}{3}m\pi\right) \right. \\ &\quad \left. + B_{mn} \sin\left((m\omega_s + n\omega_0)t_1 - \frac{4}{3}m\pi\right) \right\} \end{aligned} \quad (\text{C.49})$$

We now substitute back $t = t_1 + \frac{T_0}{3}$ into equation C.49 and obtain:

$$\begin{aligned} s_{b1}(t) &= \frac{1}{2}A_{00} + \sum_{n=1}^{\infty} \left(A_{0n} \cos\left(n\omega_0 \left(t - \frac{2\pi}{3\omega_0}\right)\right) + B_{0n} \sin\left(n\omega_0 \left(t - \frac{2\pi}{3\omega_0}\right)\right) \right) \\ &+ \sum_{m=1}^{\infty} \left(A_{m0} \cos\left(m\omega_s \left(t - \frac{2\pi}{3\omega_0}\right) - \frac{4}{3}m\pi\right) \right. \\ &\quad \left. + B_{m0} \sin\left(m\omega_s \left(t - \frac{2\pi}{3\omega_0}\right) - \frac{4}{3}m\pi\right) \right) \\ &+ \sum_{m=1}^{\infty} \sum_{n=\pm 1}^{\pm\infty} \left\{ A_{mn} \cos\left((m\omega_s + n\omega_0) \left(t - \frac{2\pi}{3\omega_0}\right) - \frac{4}{3}m\pi\right) \right. \\ &\quad \left. + B_{mn} \sin\left((m\omega_s + n\omega_0) \left(t - \frac{2\pi}{3\omega_0}\right) - \frac{4}{3}m\pi\right) \right\} \end{aligned} \quad (\text{C.50})$$

From table C.1 for the background function of $s_{b2}(t)$ the value of h is given by:

$$h = \frac{2\omega_s}{\pi}t_1 - \frac{2}{3} \quad (\text{C.51})$$

Substituting equation C.47 into the term $\frac{m\pi h}{2}$ of equation 3.36 we obtain:

$$\frac{m\pi h}{2} = m\omega_s t_1 - \frac{m\pi}{3} \quad (\text{C.52})$$

Now substituting equation C.52 into equation 3.36 we obtain:

$$\begin{aligned} s_{b2}(t_1) &= \frac{1}{2}A_{00} + \sum_{n=1}^{\infty} (A_{0n} \cos(n\omega_0 t_1) + B_{0n} \sin(n\omega_0 t_1)) \\ &+ \sum_{m=1}^{\infty} \left(A_{m0} \cos\left(m\omega_s t_1 - \frac{m\pi}{3}\right) + B_{m0} \sin\left(m\omega_s t_1 - \frac{m\pi}{3}\right) \right) \\ &+ \sum_{m=1}^{\infty} \sum_{n=\pm 1}^{\pm\infty} \left\{ A_{mn} \cos\left((m\omega_s + n\omega_0) t_1 - \frac{m\pi}{3}\right) \right. \\ &\quad \left. + B_{mn} \sin\left((m\omega_s + n\omega_0) t_1 - \frac{m\pi}{3}\right) \right\} \end{aligned} \quad (\text{C.53})$$

We now substitute back $t = t_1 + \frac{T_0}{3}$ into equation C.49 and obtain:

$$\begin{aligned} s_{b2}(t) &= \frac{1}{2}A_{00} + \sum_{n=1}^{\infty} \left(A_{0n} \cos\left(n\omega_0 \left(t - \frac{2\pi}{3\omega_0}\right)\right) + B_{0n} \sin\left(n\omega_0 \left(t - \frac{2\pi}{3\omega_0}\right)\right) \right) \\ &+ \sum_{m=1}^{\infty} \left(A_{m0} \cos\left(m\omega_s \left(t - \frac{2\pi}{3\omega_0}\right) - \frac{m\pi}{3}\right) \right. \\ &\quad \left. + B_{m0} \sin\left(m\omega_s \left(t - \frac{2\pi}{3\omega_0}\right) - \frac{m\pi}{3}\right) \right) \\ &+ \sum_{m=1}^{\infty} \sum_{n=\pm 1}^{\pm\infty} \left\{ A_{mn} \cos\left((m\omega_s + n\omega_0) \left(t - \frac{2\pi}{3\omega_0}\right) - \frac{m\pi}{3}\right) \right. \\ &\quad \left. + B_{mn} \sin\left((m\omega_s + n\omega_0) \left(t - \frac{2\pi}{3\omega_0}\right) - \frac{m\pi}{3}\right) \right\} \end{aligned} \quad (\text{C.54})$$

Now the difference and the total switching functions will be given by:

$$\begin{aligned} s_{db}(t) &= \sum_{m=1}^{\infty} \left(A_{m0} \cos\left(m\omega_s \left(t - \frac{2\pi}{3\omega_0}\right) - \frac{m\pi}{3}\right) \right. \\ &\quad \left. + B_{m0} \sin\left(m\omega_s \left(t - \frac{2\pi}{3\omega_0}\right) - \frac{m\pi}{3}\right) \right) \\ &- \sum_{m=1}^{\infty} \left(A_{m0} \cos\left(m\omega_s \left(t - \frac{2\pi}{3\omega_0}\right) - \frac{4}{3}m\pi\right) \right. \\ &\quad \left. + B_{m0} \sin\left(m\omega_s \left(t - \frac{2\pi}{3\omega_0}\right) - \frac{4}{3}m\pi\right) \right) \\ &+ \sum_{m=1}^{\infty} \sum_{n=\pm 1}^{\pm\infty} \left\{ A_{mn} \cos\left((m\omega_s + n\omega_0) \left(t - \frac{2\pi}{3\omega_0}\right) - \frac{m\pi}{3}\right) \right. \\ &\quad \left. + B_{mn} \sin\left((m\omega_s + n\omega_0) \left(t - \frac{2\pi}{3\omega_0}\right) - \frac{m\pi}{3}\right) \right\} \\ &- \sum_{m=1}^{\infty} \sum_{n=\pm 1}^{\pm\infty} \left\{ A_{mn} \cos\left((m\omega_s + n\omega_0) \left(t - \frac{2\pi}{3\omega_0}\right) - \frac{4}{3}m\pi\right) \right. \\ &\quad \left. + B_{mn} \sin\left((m\omega_s + n\omega_0) \left(t - \frac{2\pi}{3\omega_0}\right) - \frac{4}{3}m\pi\right) \right\} \end{aligned} \quad (\text{C.55})$$

Now considering trigonometric terms in equation C.50 and C.54 we have:

$$\begin{aligned} \cos\left(n\omega_0\left(t - \frac{2\pi}{3\omega_0}\right)\right) &= \cos\left(n\omega_0 t - \frac{2n\pi}{3}\right) \\ &= \begin{cases} \cos(n\omega_0 t) & \text{if } n = 3p \\ \cos\left(n\omega_0 t - \frac{2\pi}{3}\right) & \text{if } n = 3p + 1 \\ \cos\left(n\omega_0 t + \frac{2\pi}{3}\right) & \text{if } n = 3p + 2 \end{cases} \end{aligned} \quad (\text{C.56})$$

$$\begin{aligned} \sin\left(n\omega_0\left(t - \frac{2\pi}{3\omega_0}\right)\right) &= \sin\left(n\omega_0 t - \frac{2n\pi}{3}\right) \\ &= \begin{cases} \sin(n\omega_0 t) & \text{if } n = 3p \\ \sin\left(n\omega_0 t - \frac{2\pi}{3}\right) & \text{if } n = 3p + 1 \\ \sin\left(n\omega_0 t + \frac{2\pi}{3}\right) & \text{if } n = 3p + 2 \end{cases} \end{aligned} \quad (\text{C.57})$$

$$\begin{aligned} \cos\left(m\omega_s\left(t - \frac{2\pi}{3\omega_0}\right) - \frac{4m\pi}{3}\right) &= \cos\left(m\omega_s t - \frac{2m\pi}{3}m_f - \frac{4m\pi}{3}\right) \\ &= \cos(m\omega_s t) \end{aligned} \quad (\text{C.58})$$

$$\begin{aligned} \sin\left(m\omega_s\left(t - \frac{2\pi}{3\omega_0}\right) - \frac{4m\pi}{3}\right) &= \sin\left(m\omega_s t - \frac{2m\pi}{3}m_f - \frac{4m\pi}{3}\right) \\ &= \sin(m\omega_s t) \end{aligned} \quad (\text{C.59})$$

$$\begin{aligned} \cos\left(m\omega_s\left(t - \frac{2\pi}{3\omega_0}\right) - \frac{m\pi}{3}\right) &= \cos\left(m\omega_s t - \frac{2m\pi}{3}m_f - \frac{m\pi}{3}\right) \\ &= \begin{cases} \cos(m\omega_s t) & \text{if } m = 2k \\ -\cos(m\omega_s t) & \text{if } m = 2k + 1 \end{cases} \end{aligned} \quad (\text{C.60})$$

$$\begin{aligned} \sin\left(m\omega_s\left(t - \frac{2\pi}{3\omega_0}\right) - \frac{m\pi}{3}\right) &= \sin\left(m\omega_s t - \frac{2m\pi}{3}m_f - \frac{m\pi}{3}\right) \\ &= \begin{cases} \sin(m\omega_s t) & \text{if } m = 2k \\ -\sin(m\omega_s t) & \text{if } m = 2k + 1 \end{cases} \end{aligned} \quad (\text{C.61})$$

$$\begin{aligned} &\cos\left((m\omega_s + n\omega_0)\left(t - \frac{2\pi}{3\omega_0}\right) - \frac{4m\pi}{3}\right) = \cos\left(m\omega_s t + n\omega_0 t - \frac{2m\pi}{3}m_f - \frac{2n\pi}{3} - \frac{4m\pi}{3}\right) \\ &= \begin{cases} \cos(m\omega_s t + n\omega_0 t) & \text{if } m = k \text{ and } n = 3p \\ \cos\left((m\omega_s + n\omega_0)t - \frac{2\pi}{3}\right) & \text{if } m = k \text{ and } n = 3p + 1 \\ \cos\left((m\omega_s + n\omega_0)t + \frac{2\pi}{3}\right) & \text{if } m = k \text{ and } n = 3p + 2 \\ \cos(m\omega_s t + n\omega_0 t) & \text{if } m = k \text{ and } n = -3p \\ \cos\left((m\omega_s + n\omega_0)t - \frac{2\pi}{3}\right) & \text{if } m = k \text{ and } n = -(3p + 2) \\ \cos\left((m\omega_s + n\omega_0)t + \frac{2\pi}{3}\right) & \text{if } m = k \text{ and } n = -(3p + 1) \end{cases} \end{aligned} \quad (\text{C.62})$$

$$\begin{aligned}
& \sin \left((m\omega_s + n\omega_0) \left(t - \frac{2\pi}{3\omega_0} \right) - \frac{4m\pi}{3} \right) = \cos \left(m\omega_s t + n\omega_0 t - \frac{2m\pi}{3} m_f - \frac{2n\pi}{3} - \frac{4m\pi}{3} \right) \\
= & \left\{ \begin{array}{ll} \sin(m\omega_s t + n\omega_0 t) & \text{if } m = k \text{ and } n = 3p \\ \sin \left((m\omega_s + n\omega_0) t - \frac{2\pi}{3} \right) & \text{if } m = k \text{ and } n = 3p + 1 \\ \sin \left((m\omega_s + n\omega_0) t + \frac{2\pi}{3} \right) & \text{if } m = k \text{ and } n = 3p + 2 \\ \sin(m\omega_s t + n\omega_0 t) & \text{if } m = k \text{ and } n = -3p \\ \sin \left((m\omega_s + n\omega_0) t - \frac{2\pi}{3} \right) & \text{if } m = k \text{ and } n = -(3p + 2) \\ \sin \left((m\omega_s + n\omega_0) t + \frac{2\pi}{3} \right) & \text{if } m = k \text{ and } n = -(3p + 1) \end{array} \right. \quad (\text{C.63})
\end{aligned}$$

$$\begin{aligned}
& \cos \left((m\omega_s + n\omega_0) \left(t - \frac{2\pi}{3\omega_0} \right) - \frac{m\pi}{3} \right) = \cos \left(m\omega_s t + n\omega_0 t - \frac{2m\pi}{3} m_f - \frac{2n\pi}{3} - \frac{m\pi}{3} \right) \\
= & \left\{ \begin{array}{ll} \cos(m\omega_s t + n\omega_0 t) & \text{if } m = 2k \text{ and } n = 3p \\ \cos \left((m\omega_s + n\omega_0) t - \frac{2\pi}{3} \right) & \text{if } m = 2k \text{ and } n = 3p + 1 \\ \cos \left((m\omega_s + n\omega_0) t + \frac{2\pi}{3} \right) & \text{if } m = 2k \text{ and } n = 3p + 2 \\ \cos(m\omega_s t + n\omega_0 t) & \text{if } m = 2k \text{ and } n = -3p \\ \cos \left((m\omega_s + n\omega_0) t - \frac{2\pi}{3} \right) & \text{if } m = 2k \text{ and } n = -(3p + 2) \\ \cos \left((m\omega_s + n\omega_0) t + \frac{2\pi}{3} \right) & \text{if } m = 2k \text{ and } n = -(3p + 1) \\ -\cos(m\omega_s t + n\omega_0 t) & \text{if } m = 2k + 1 \text{ and } n = 3p \\ -\cos \left((m\omega_s + n\omega_0) t - \frac{2\pi}{3} \right) & \text{if } m = 2k + 1 \text{ and } n = 3p + 1 \\ -\cos \left((m\omega_s + n\omega_0) t + \frac{2\pi}{3} \right) & \text{if } m = 2k + 1 \text{ and } n = 3p + 2 \\ -\cos(m\omega_s t + n\omega_0 t) & \text{if } m = 2k + 1 \text{ and } n = -3p \\ -\cos \left((m\omega_s + n\omega_0) t - \frac{2\pi}{3} \right) & \text{if } m = 2k + 1 \text{ and } n = -(3p + 2) \\ -\cos \left((m\omega_s + n\omega_0) t + \frac{2\pi}{3} \right) & \text{if } m = 2k + 1 \text{ and } n = -(3p + 1) \end{array} \right. \quad (\text{C.64})
\end{aligned}$$

$$\begin{aligned}
& \sin \left((m\omega_s + n\omega_0) \left(t - \frac{2\pi}{3\omega_0} \right) - \frac{m\pi}{3} \right) = \sin \left(m\omega_s t + n\omega_0 t - \frac{2m\pi}{3} m_f - \frac{2n\pi}{3} - \frac{m\pi}{3} \right) \\
= & \left\{ \begin{array}{ll} \sin(m\omega_s t + n\omega_0 t) & \text{if } m = 2k \text{ and } n = 3p \\ \sin \left((m\omega_s + n\omega_0) t - \frac{2\pi}{3} \right) & \text{if } m = 2k \text{ and } n = 3p + 1 \\ \sin \left((m\omega_s + n\omega_0) t + \frac{2\pi}{3} \right) & \text{if } m = 2k \text{ and } n = 3p + 2 \\ \sin(m\omega_s t + n\omega_0 t) & \text{if } m = 2k \text{ and } n = -3p \\ \sin \left((m\omega_s + n\omega_0) t - \frac{2\pi}{3} \right) & \text{if } m = 2k \text{ and } n = -(3p + 2) \\ \sin \left((m\omega_s + n\omega_0) t + \frac{2\pi}{3} \right) & \text{if } m = 2k \text{ and } n = -(3p + 1) \\ -\sin(m\omega_s t + n\omega_0 t) & \text{if } m = 2k + 1 \text{ and } n = 3p \\ -\sin \left((m\omega_s + n\omega_0) t - \frac{2\pi}{3} \right) & \text{if } m = 2k + 1 \text{ and } n = 3p + 1 \\ -\sin \left((m\omega_s + n\omega_0) t + \frac{2\pi}{3} \right) & \text{if } m = 2k + 1 \text{ and } n = 3p + 2 \\ -\sin(m\omega_s t + n\omega_0 t) & \text{if } m = 2k + 1 \text{ and } n = -3p \\ -\sin \left((m\omega_s + n\omega_0) t - \frac{2\pi}{3} \right) & \text{if } m = 2k + 1 \text{ and } n = -(3p + 2) \\ -\sin \left((m\omega_s + n\omega_0) t + \frac{2\pi}{3} \right) & \text{if } m = 2k + 1 \text{ and } n = -(3p + 1) \end{array} \right. \quad (\text{C.65})
\end{aligned}$$

Thus the phasor representation for phase B of 2-cell converter when $m_f = 3k + 1$ is given by Figures C.8, C.9 and C.10.

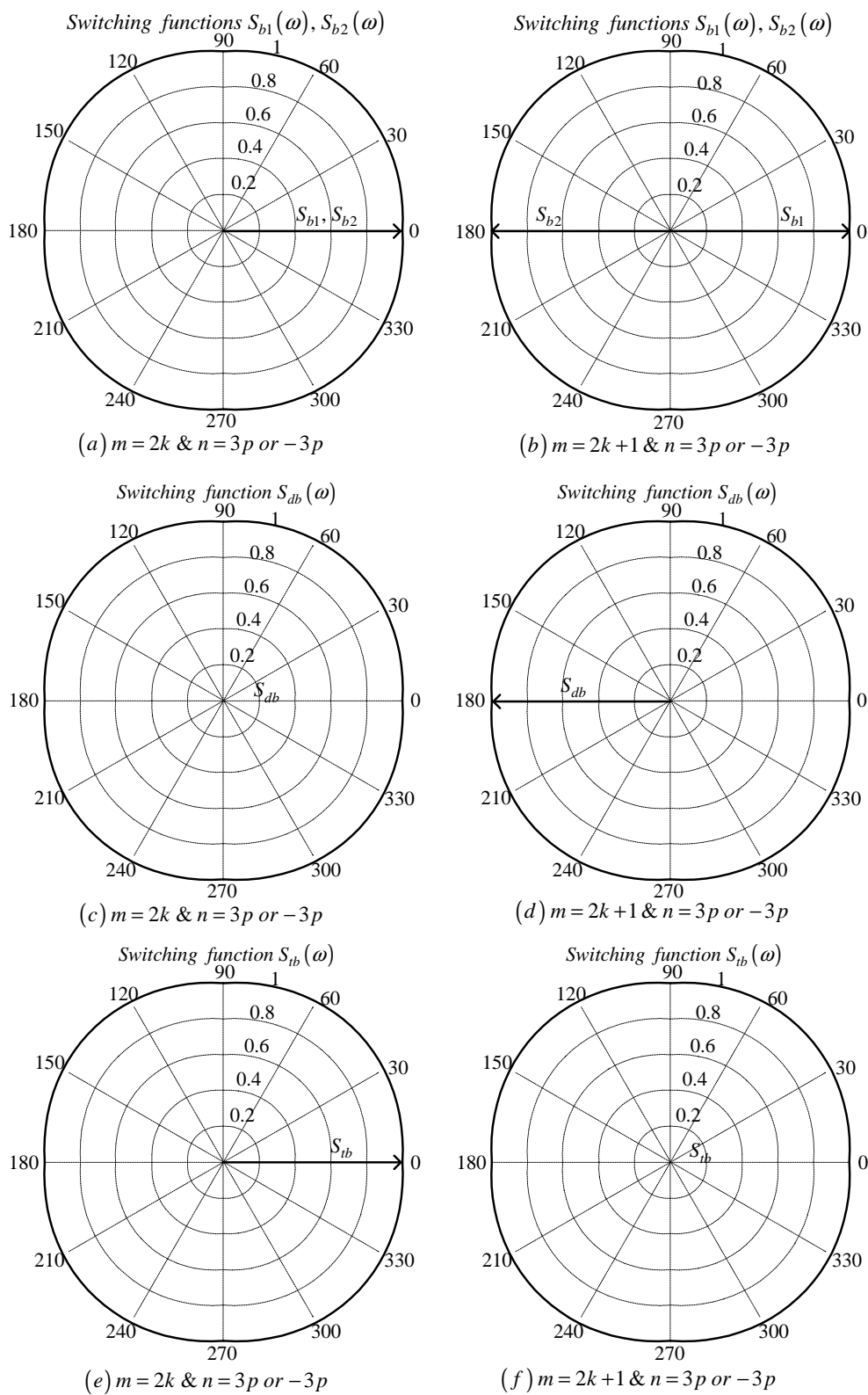


Figure C.8: Phase B phasor representation of 2-cell converter for $n = 3p$ or $n = -3p$

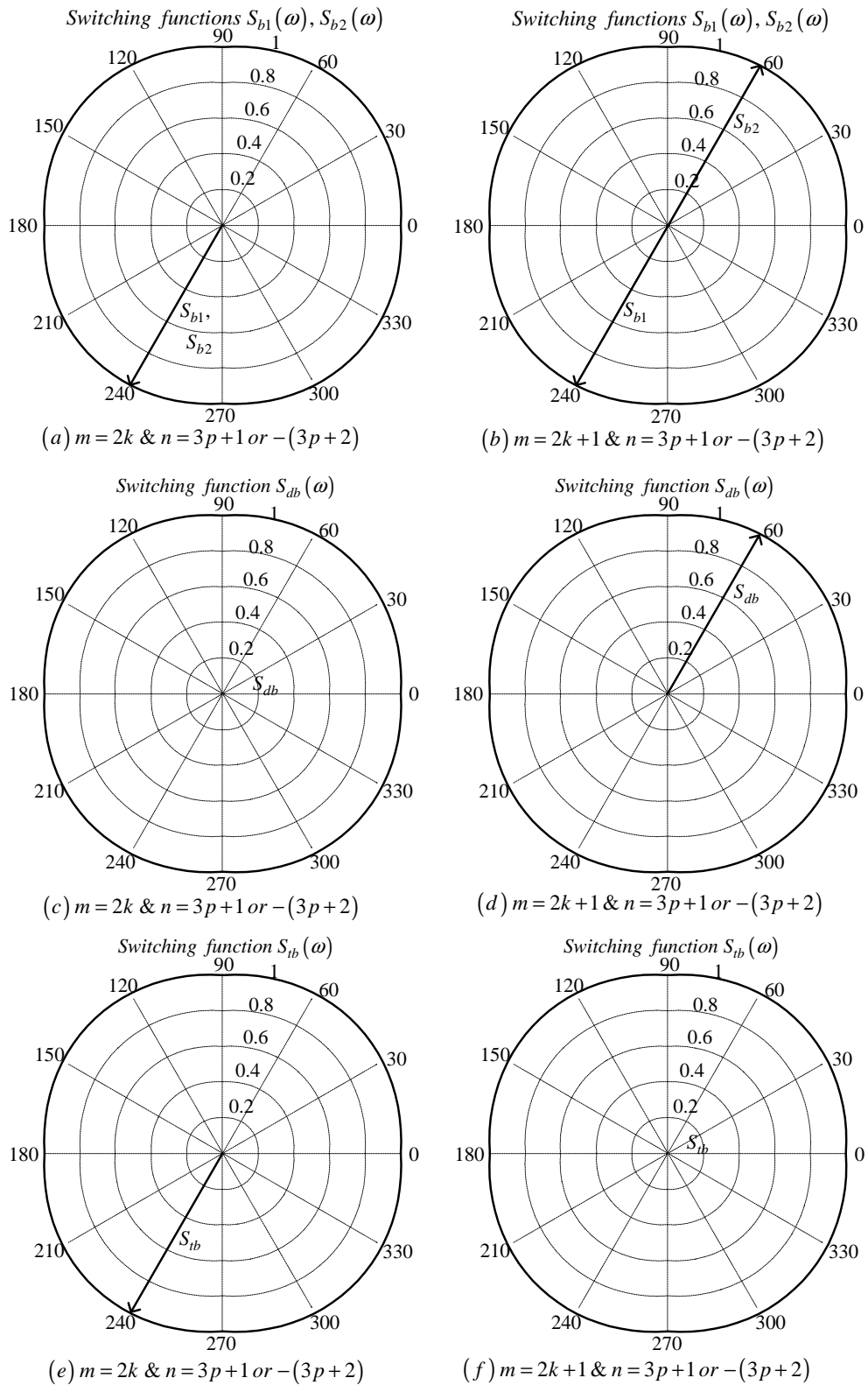


Figure C.9: Phasor representation for phase B of 2-cell converter for $n = 3p + 1$ or $n = -(3p + 2)$

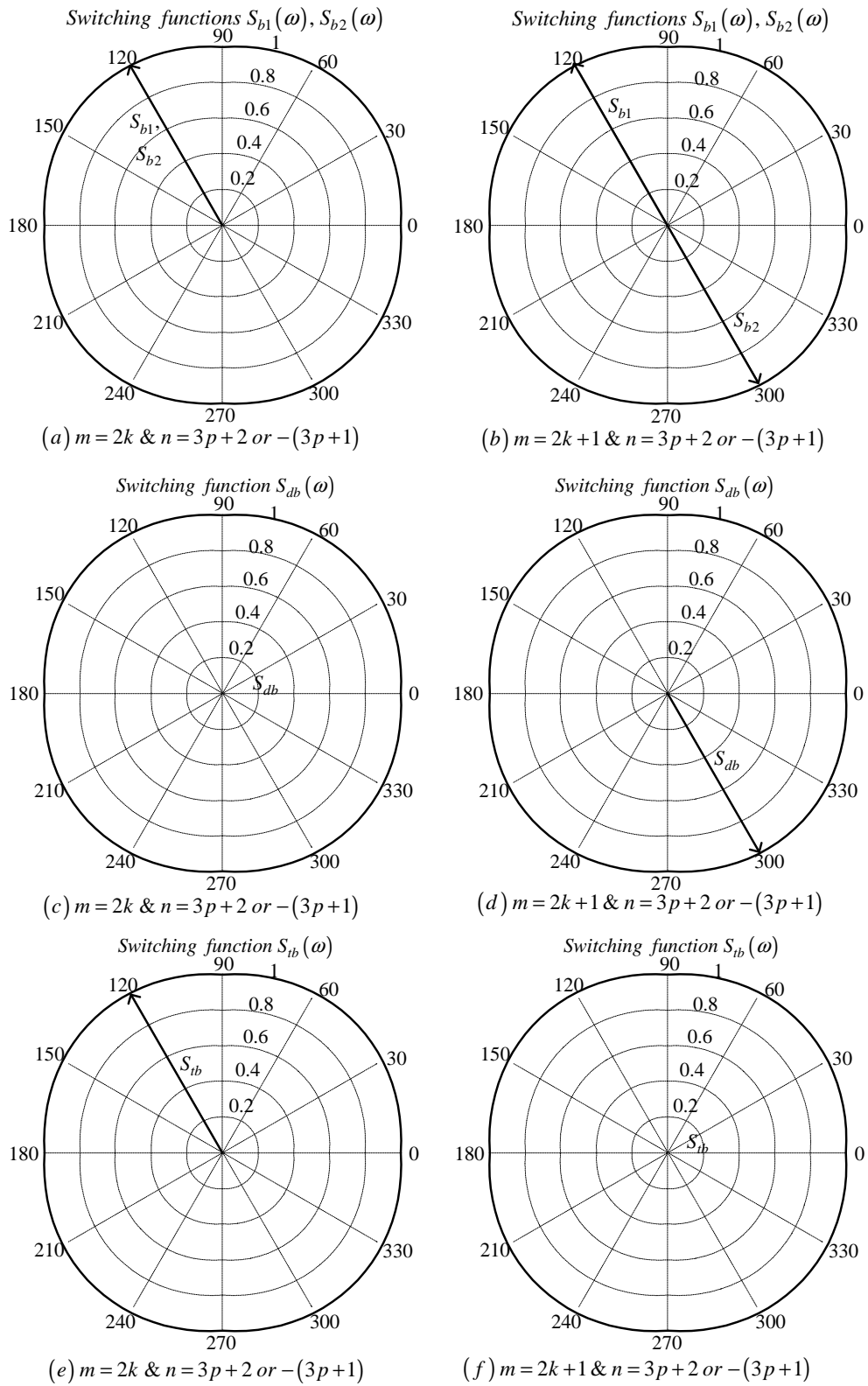


Figure C.10: Phasor representation for phase B of 2-cell converter for $n = 3p + 2$ or $n = -(3p + 1)$

Phase C

From table C.1 for the background function of $s_{c1}(t)$ the value of h is given by:

$$h = \frac{2\omega_s}{\pi}t_2 - \frac{4}{3} \quad (\text{C.66})$$

Substituting equation C.66 into the term $\frac{m\pi h}{2}$ of equation 3.36 we obtain:

$$\frac{m\pi h}{2} = m\omega_s t_2 - \frac{2}{3}m\pi \quad (\text{C.67})$$

Now substituting equation C.67 into equation 3.36 we obtain:

$$\begin{aligned} s_{c1}(t_2) &= \frac{1}{2}A_{00} + \sum_{n=1}^{\infty} (A_{0n} \cos(n\omega_0 t_2) + B_{0n} \sin(n\omega_0 t_2)) \\ &+ \sum_{m=1}^{\infty} \left(A_{m0} \cos\left(m\omega_s t_2 - \frac{2}{3}m\pi\right) + B_{m0} \sin\left(m\omega_s t_2 - \frac{2}{3}m\pi\right) \right) \\ &+ \sum_{m=1}^{\infty} \sum_{n=\pm 1}^{\pm\infty} \left\{ A_{mn} \cos\left((m\omega_s + n\omega_0) t_2 - \frac{2}{3}m\pi\right) \right. \\ &\left. + B_{mn} \sin\left((m\omega_s + n\omega_0) t_2 - \frac{2}{3}m\pi\right) \right\} \end{aligned} \quad (\text{C.68})$$

We now substitute back $t = t_2 + \frac{2T_0}{3}$ into equation C.68 and obtain:

$$\begin{aligned} s_{c1}(t) &= \frac{1}{2}A_{00} + \sum_{n=1}^{\infty} \left(A_{0n} \cos\left(n\omega_0 \left(t - \frac{4\pi}{3\omega_0}\right)\right) + B_{0n} \sin\left(n\omega_0 \left(t - \frac{4\pi}{3\omega_0}\right)\right) \right) \\ &+ \sum_{m=1}^{\infty} \left(A_{m0} \cos\left(m\omega_s \left(t - \frac{4\pi}{3\omega_0}\right) - \frac{2}{3}m\pi\right) \right. \\ &\left. + B_{m0} \sin\left(m\omega_s \left(t - \frac{4\pi}{3\omega_0}\right) - \frac{2}{3}m\pi\right) \right) \\ &+ \sum_{m=1}^{\infty} \sum_{n=\pm 1}^{\pm\infty} \left\{ A_{mn} \cos\left((m\omega_s + n\omega_0) \left(t - \frac{4\pi}{3\omega_0}\right) - \frac{2}{3}m\pi\right) \right. \\ &\left. + B_{mn} \sin\left((m\omega_s + n\omega_0) \left(t - \frac{4\pi}{3\omega_0}\right) - \frac{2}{3}m\pi\right) \right\} \end{aligned} \quad (\text{C.69})$$

From table C.1 for the background function of $s_{c2}(t)$ the value of h is given by:

$$h = \frac{2\omega_s}{\pi}t_2 + \frac{2}{3} \quad (\text{C.70})$$

Substituting equation C.70 into the term $\frac{m\pi h}{2}$ of equation 3.36 we obtain:

$$\frac{m\pi h}{2} = m\omega_s t_2 + \frac{m\pi}{3} \quad (\text{C.71})$$

Now substituting equation C.71 into equation 3.36 we obtain:

$$\begin{aligned}
s_{c2}(t_2) &= \frac{1}{2}A_{00} + \sum_{n=1}^{\infty} (A_{0n} \cos(n\omega_0 t_2) + B_{0n} \sin(n\omega_0 t_2)) \\
&+ \sum_{m=1}^{\infty} \left(A_{m0} \cos\left(m\omega_s t_2 + \frac{m\pi}{3}\right) + B_{m0} \sin\left(m\omega_s t_2 + \frac{m\pi}{3}\right) \right) \\
&+ \sum_{m=1}^{\infty} \sum_{n=\pm 1}^{\pm\infty} \left\{ A_{mn} \cos\left((m\omega_s + n\omega_0)t_2 + \frac{m\pi}{3}\right) \right. \\
&\quad \left. + B_{mn} \sin\left((m\omega_s + n\omega_0)t_2 + \frac{m\pi}{3}\right) \right\}
\end{aligned} \tag{C.72}$$

We now substitute back $t = t_2 + \frac{2T_0}{3}$ into equation C.72 and obtain:

$$\begin{aligned}
s_{c2}(t) &= \frac{1}{2}A_{00} + \sum_{n=1}^{\infty} \left(A_{0n} \cos\left(n\omega_0 \left(t - \frac{4\pi}{3\omega_0}\right)\right) + B_{0n} \sin\left(n\omega_0 \left(t - \frac{4\pi}{3\omega_0}\right)\right) \right) \\
&+ \sum_{m=1}^{\infty} \left(A_{m0} \cos\left(m\omega_s \left(t - \frac{4\pi}{3\omega_0}\right) + \frac{m\pi}{3}\right) \right. \\
&\quad \left. + B_{m0} \sin\left(m\omega_s \left(t - \frac{4\pi}{3\omega_0}\right) + \frac{m\pi}{3}\right) \right) \\
&+ \sum_{m=1}^{\infty} \sum_{n=\pm 1}^{\pm\infty} \left\{ A_{mn} \cos\left((m\omega_s + n\omega_0) \left(t - \frac{4\pi}{3\omega_0}\right) + \frac{m\pi}{3}\right) \right. \\
&\quad \left. + B_{mn} \sin\left((m\omega_s + n\omega_0) \left(t - \frac{4\pi}{3\omega_0}\right) + \frac{m\pi}{3}\right) \right\}
\end{aligned} \tag{C.73}$$

Now considering trigonometric terms in equations C.69 and C.73 we have:

$$\begin{aligned}
\cos\left(n\omega_0 \left(t - \frac{4\pi}{3\omega_0}\right)\right) &= \cos\left(n\omega_0 t - \frac{4n\pi}{3}\right) \\
&= \begin{cases} \cos(n\omega_0 t) & \text{if } n = 3p \\ \cos\left(n\omega_0 t + \frac{2\pi}{3}\right) & \text{if } n = 3p + 1 \\ \cos\left(n\omega_0 t - \frac{2\pi}{3}\right) & \text{if } n = 3p + 2 \end{cases}
\end{aligned} \tag{C.74}$$

$$\begin{aligned}
\sin\left(n\omega_0 \left(t - \frac{4\pi}{3\omega_0}\right)\right) &= \sin\left(n\omega_0 t - \frac{4n\pi}{3}\right) \\
&= \begin{cases} \sin(n\omega_0 t) & \text{if } n = 3p \\ \sin\left(n\omega_0 t + \frac{2\pi}{3}\right) & \text{if } n = 3p + 1 \\ \sin\left(n\omega_0 t - \frac{2\pi}{3}\right) & \text{if } n = 3p + 2 \end{cases}
\end{aligned} \tag{C.75}$$

$$\begin{aligned}
\cos\left(m\omega_s \left(t - \frac{4\pi}{3\omega_0}\right) - \frac{2m\pi}{3}\right) &= \cos\left(m\omega_s t - \frac{4m\pi}{3}m_f - \frac{2m\pi}{3}\right) \\
&= \cos(m\omega_s t)
\end{aligned} \tag{C.76}$$

$$\begin{aligned}\sin\left(m\omega_s\left(t - \frac{4\pi}{3\omega_0}\right) - \frac{2m\pi}{3}\right) &= \sin\left(m\omega_s t - \frac{4m\pi}{3}m_f - \frac{2m\pi}{3}\right) \\ &= \sin(m\omega_s t)\end{aligned}\tag{C.77}$$

$$\begin{aligned}\cos\left(m\omega_s\left(t - \frac{4\pi}{3\omega_0}\right) + \frac{m\pi}{3}\right) &= \cos\left(m\omega_s t - \frac{4m\pi}{3}m_f + \frac{m\pi}{3}\right) \\ &= \begin{cases} \cos(m\omega_s t) & \text{if } m = 2k \\ -\cos(m\omega_s t) & \text{if } m = 2k + 1 \end{cases}\end{aligned}\tag{C.78}$$

$$\begin{aligned}\sin\left(m\omega_s\left(t - \frac{4\pi}{3\omega_0}\right) + \frac{m\pi}{3}\right) &= \sin\left(m\omega_s t - \frac{4m\pi}{3}m_f + \frac{m\pi}{3}\right) \\ &= \begin{cases} \sin(m\omega_s t) & \text{if } m = 2k \\ -\sin(m\omega_s t) & \text{if } m = 2k + 1 \end{cases}\end{aligned}\tag{C.79}$$

$$\begin{aligned}\cos\left((m\omega_s + n\omega_0)\left(t - \frac{4\pi}{3\omega_0}\right) - \frac{2m\pi}{3}\right) &= \cos\left(m\omega_s t + n\omega_0 t - \frac{4m\pi}{3}m_f - \frac{4n\pi}{3} - \frac{2m\pi}{3}\right) \\ &= \begin{cases} \cos(m\omega_s t + n\omega_0 t) & \text{if } m = k \text{ and } n = 3p \\ \cos\left((m\omega_s + n\omega_0)t + \frac{2\pi}{3}\right) & \text{if } m = k \text{ and } n = 3p + 1 \\ \cos\left((m\omega_s + n\omega_0)t - \frac{2\pi}{3}\right) & \text{if } m = k \text{ and } n = 3p + 2 \\ \cos(m\omega_s t + n\omega_0 t) & \text{if } m = k \text{ and } n = -3p \\ \cos\left((m\omega_s + n\omega_0)t + \frac{2\pi}{3}\right) & \text{if } m = k \text{ and } n = -(3p + 2) \\ \cos\left((m\omega_s + n\omega_0)t - \frac{2\pi}{3}\right) & \text{if } m = k \text{ and } n = -(3p + 1) \end{cases}\end{aligned}\tag{C.80}$$

$$\begin{aligned}\sin\left((m\omega_s + n\omega_0)\left(t - \frac{4\pi}{3\omega_0}\right) - \frac{2m\pi}{3}\right) &= \cos\left(m\omega_s t + n\omega_0 t - \frac{4m\pi}{3}m_f - \frac{4n\pi}{3} - \frac{2m\pi}{3}\right) \\ &= \begin{cases} \sin(m\omega_s t + n\omega_0 t) & \text{if } m = k \text{ and } n = 3p \\ \sin\left((m\omega_s + n\omega_0)t - \frac{2\pi}{3}\right) & \text{if } m = k \text{ and } n = 3p + 1 \\ \sin\left((m\omega_s + n\omega_0)t + \frac{2\pi}{3}\right) & \text{if } m = k \text{ and } n = 3p + 2 \\ \sin(m\omega_s t + n\omega_0 t) & \text{if } m = k \text{ and } n = -3p \\ \sin\left((m\omega_s + n\omega_0)t + \frac{2\pi}{3}\right) & \text{if } m = k \text{ and } n = -(3p + 2) \\ \sin\left((m\omega_s + n\omega_0)t - \frac{2\pi}{3}\right) & \text{if } m = k \text{ and } n = -(3p + 1) \end{cases}\end{aligned}\tag{C.81}$$

$$\begin{aligned}
& \cos \left((m\omega_s + n\omega_0) \left(t - \frac{4\pi}{3\omega_0} \right) + \frac{m\pi}{3} \right) = \cos \left(m\omega_s t + n\omega_0 t - \frac{4m\pi}{3} m_f - \frac{4n\pi}{3} + \frac{m\pi}{3} \right) \\
= & \left\{ \begin{array}{ll} \cos (m\omega_s t + n\omega_0 t) & \text{if } m = 2k \text{ and } n = 3p \\ \cos \left((m\omega_s + n\omega_0) t + \frac{2\pi}{3} \right) & \text{if } m = 2k \text{ and } n = 3p + 1 \\ \cos \left((m\omega_s + n\omega_0) t - \frac{2\pi}{3} \right) & \text{if } m = 2k \text{ and } n = 3p + 2 \\ \cos (m\omega_s t + n\omega_0 t) & \text{if } m = 2k \text{ and } n = -3p \\ \cos \left((m\omega_s + n\omega_0) t + \frac{2\pi}{3} \right) & \text{if } m = 2k \text{ and } n = -(3p + 2) \\ \cos \left((m\omega_s + n\omega_0) t - \frac{2\pi}{3} \right) & \text{if } m = 2k \text{ and } n = -(3p + 1) \\ -\cos (m\omega_s t + n\omega_0 t) & \text{if } m = 2k + 1 \text{ and } n = 3p \\ -\cos \left((m\omega_s + n\omega_0) t + \frac{2\pi}{3} \right) & \text{if } m = 2k + 1 \text{ and } n = 3p + 1 \\ -\cos \left((m\omega_s + n\omega_0) t - \frac{2\pi}{3} \right) & \text{if } m = 2k + 1 \text{ and } n = 3p + 2 \\ -\cos (m\omega_s t + n\omega_0 t) & \text{if } m = 2k + 1 \text{ and } n = -3p \\ -\cos \left((m\omega_s + n\omega_0) t + \frac{2\pi}{3} \right) & \text{if } m = 2k + 1 \text{ and } n = -(3p + 2) \\ -\cos \left((m\omega_s + n\omega_0) t - \frac{2\pi}{3} \right) & \text{if } m = 2k + 1 \text{ and } n = -(3p + 1) \end{array} \right. \quad (\text{C.82})
\end{aligned}$$

$$\begin{aligned}
& \sin \left((m\omega_s + n\omega_0) \left(t - \frac{4\pi}{3\omega_0} \right) + \frac{m\pi}{3} \right) = \sin \left(m\omega_s t + n\omega_0 t - \frac{4m\pi}{3} m_f - \frac{4n\pi}{3} + \frac{m\pi}{3} \right) \\
= & \left\{ \begin{array}{ll} \sin (m\omega_s t + n\omega_0 t) & \text{if } m = 2k \text{ and } n = 3p \\ \sin \left((m\omega_s + n\omega_0) t + \frac{2\pi}{3} \right) & \text{if } m = 2k \text{ and } n = 3p + 1 \\ \sin \left((m\omega_s + n\omega_0) t - \frac{2\pi}{3} \right) & \text{if } m = 2k \text{ and } n = 3p + 2 \\ \sin (m\omega_s t + n\omega_0 t) & \text{if } m = 2k \text{ and } n = -3p \\ \sin \left((m\omega_s + n\omega_0) t + \frac{2\pi}{3} \right) & \text{if } m = 2k \text{ and } n = -(3p + 2) \\ \sin \left((m\omega_s + n\omega_0) t - \frac{2\pi}{3} \right) & \text{if } m = 2k \text{ and } n = -(3p + 1) \\ -\sin (m\omega_s t + n\omega_0 t) & \text{if } m = 2k + 1 \text{ and } n = 3p \\ -\sin \left((m\omega_s + n\omega_0) t + \frac{2\pi}{3} \right) & \text{if } m = 2k + 1 \text{ and } n = 3p + 1 \\ -\sin \left((m\omega_s + n\omega_0) t - \frac{2\pi}{3} \right) & \text{if } m = 2k + 1 \text{ and } n = 3p + 2 \\ -\sin (m\omega_s t + n\omega_0 t) & \text{if } m = 2k + 1 \text{ and } n = -3p \\ -\sin \left((m\omega_s + n\omega_0) t + \frac{2\pi}{3} \right) & \text{if } m = 2k + 1 \text{ and } n = -(3p + 2) \\ -\sin \left((m\omega_s + n\omega_0) t - \frac{2\pi}{3} \right) & \text{if } m = 2k + 1 \text{ and } n = -(3p + 1) \end{array} \right. \quad (\text{C.83})
\end{aligned}$$

Thus the phasor representation for phase C of 2-cell converter when $m_f = 3k + 1$ is given by Figures C.11, C.12 and C.13.

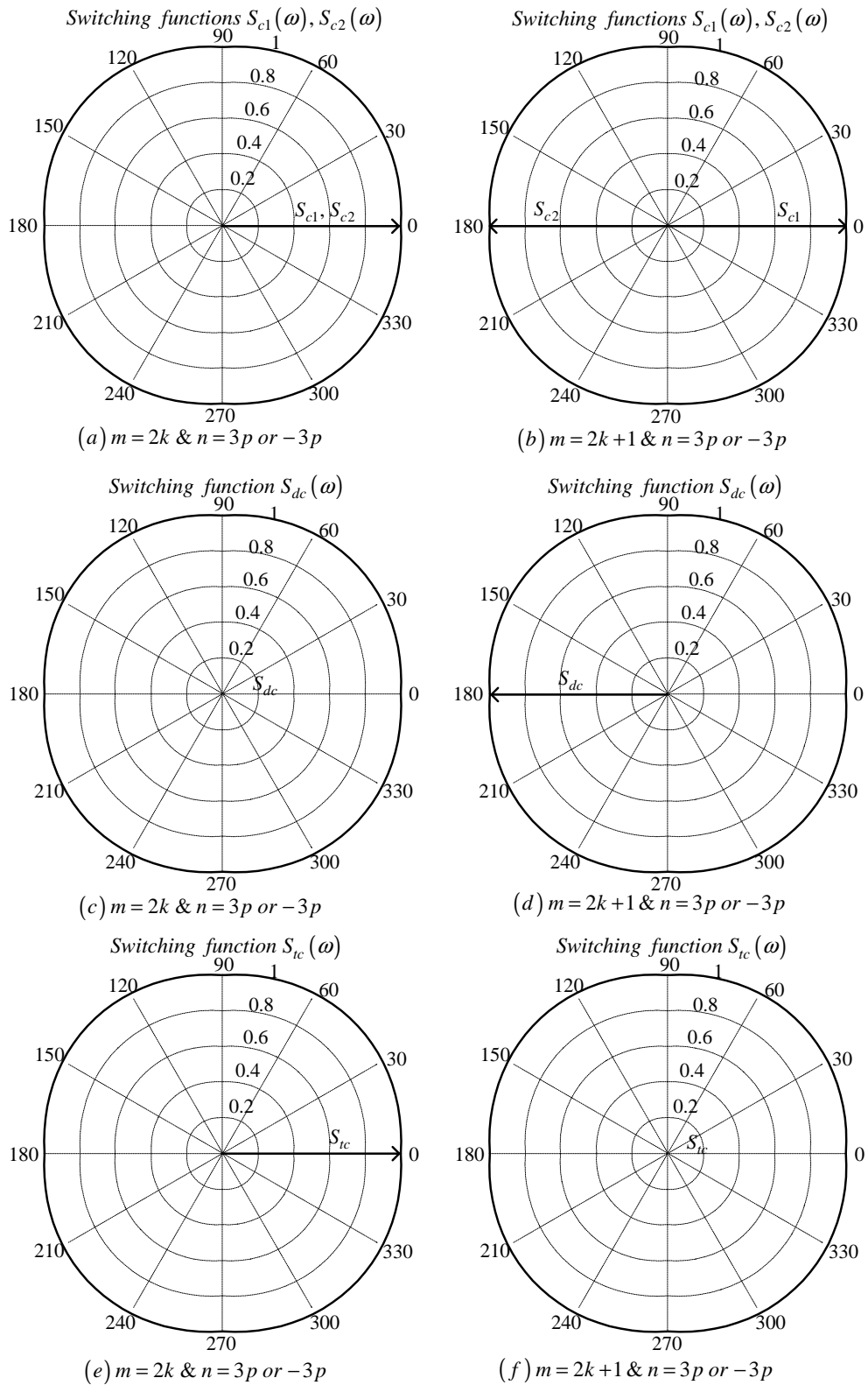


Figure C.11: Phasor representation for phase C of 2-cell converter for $n = 3p$ or $n = -3p$

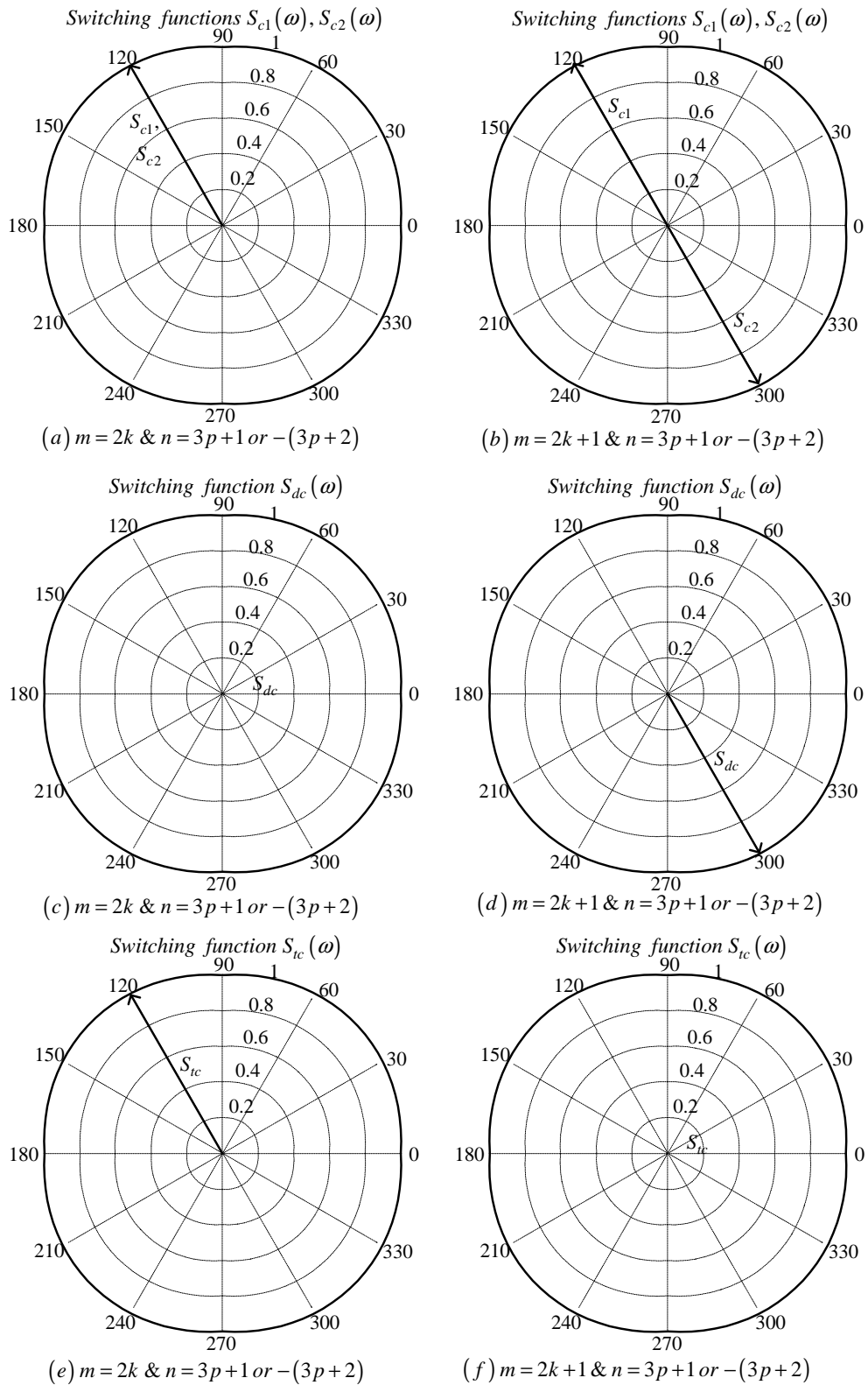


Figure C.12: Phasor representation for phase C of 2-cell converter for $n = 3p + 1$ or $n = -(3p + 2)$

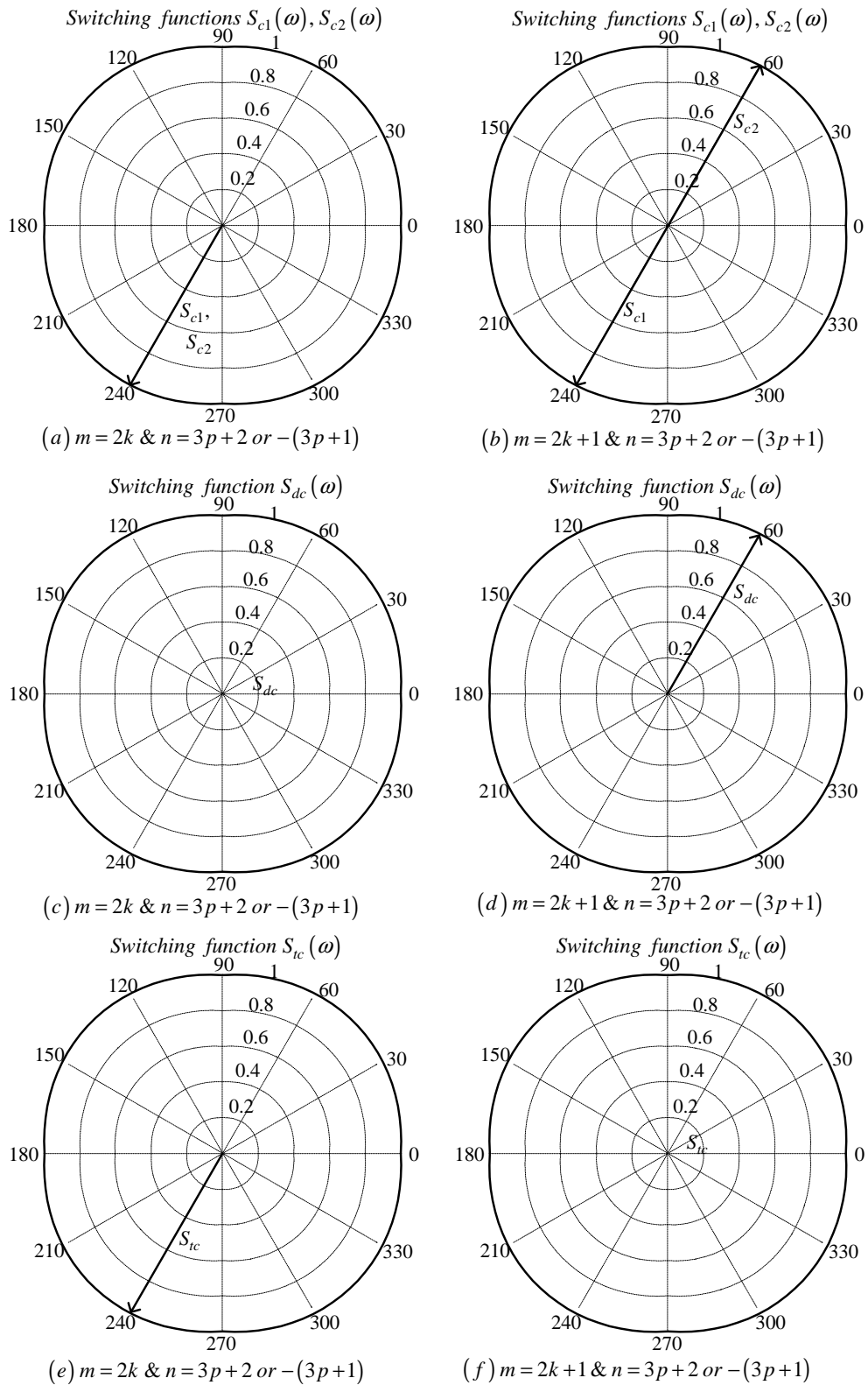


Figure C.13: Phasor representation for phase C of 2-cell converter for $n = 3p + 2$ or $n = -(3p + 1)$

C.1.3 For frequency modulation index $m_f = 3k + 2$

The case of phase A is the same as the one done in subsection C.1.1.

Phase B

From table C.1 for the background function of $s_{b1}(t)$ the value of h is given by:

$$h = \frac{2\omega_s}{\pi}t_1 - \frac{4}{3} \quad (\text{C.84})$$

Substituting equation C.84 into the term $\frac{m\pi h}{2}$ of equation 3.36 we obtain:

$$\frac{m\pi h}{2} = m\omega_s t_1 - \frac{2}{3}m\pi \quad (\text{C.85})$$

Now substituting equation C.85 into equation 3.36 we obtain:

$$\begin{aligned} s_{b1}(t_1) &= \frac{1}{2}A_{00} + \sum_{n=1}^{\infty} (A_{0n} \cos(n\omega_0 t_1) + B_{0n} \sin(n\omega_0 t_1)) \\ &+ \sum_{m=1}^{\infty} \left(A_{m0} \cos\left(m\omega_s t_1 - \frac{2}{3}m\pi\right) + B_{m0} \sin\left(m\omega_s t_1 - \frac{2}{3}m\pi\right) \right) \\ &+ \sum_{m=1}^{\infty} \sum_{n=\pm 1}^{\pm\infty} \left\{ A_{mn} \cos\left((m\omega_s + n\omega_0)t_1 - \frac{2}{3}m\pi\right) \right. \\ &\left. + B_{mn} \sin\left((m\omega_s + n\omega_0)t_1 - \frac{2}{3}m\pi\right) \right\} \end{aligned} \quad (\text{C.86})$$

We now substitute back $t = t_1 + \frac{T_0}{3}$ into equation C.86 and obtain:

$$\begin{aligned} s_{b1}(t) &= \frac{1}{2}A_{00} + \sum_{n=1}^{\infty} \left(A_{0n} \cos\left(n\omega_0 \left(t - \frac{2\pi}{3\omega_0}\right)\right) + B_{0n} \sin\left(n\omega_0 \left(t - \frac{2\pi}{3\omega_0}\right)\right) \right) \\ &+ \sum_{m=1}^{\infty} \left(A_{m0} \cos\left(m\omega_s \left(t - \frac{2\pi}{3\omega_0}\right) - \frac{2}{3}m\pi\right) \right. \\ &\left. + B_{m0} \sin\left(m\omega_s \left(t - \frac{2\pi}{3\omega_0}\right) - \frac{2}{3}m\pi\right) \right) \\ &+ \sum_{m=1}^{\infty} \sum_{n=\pm 1}^{\pm\infty} \left\{ A_{mn} \cos\left((m\omega_s + n\omega_0) \left(t - \frac{2\pi}{3\omega_0}\right) - \frac{2}{3}m\pi\right) \right. \\ &\left. + B_{mn} \sin\left((m\omega_s + n\omega_0) \left(t - \frac{2\pi}{3\omega_0}\right) - \frac{2}{3}m\pi\right) \right\} \end{aligned} \quad (\text{C.87})$$

From table C.1 for the background function of $s_{b2}(t)$ the value of h is given by:

$$h = \frac{2\omega_s}{\pi}t_1 + \frac{2}{3} \quad (\text{C.88})$$

Substituting equation C.84 into the term $\frac{m\pi h}{2}$ of equation 3.36 we obtain:

$$\frac{m\pi h}{2} = m\omega_s t_1 + \frac{m\pi}{3} \quad (\text{C.89})$$

Now substituting equation C.89 into equation 3.36 we obtain:

$$\begin{aligned} s_{b2}(t_1) &= \frac{1}{2}A_{00} + \sum_{n=1}^{\infty} (A_{0n} \cos(n\omega_0 t_1) + B_{0n} \sin(n\omega_0 t_1)) \\ &+ \sum_{m=1}^{\infty} \left(A_{m0} \cos\left(m\omega_s t_1 - \frac{m\pi}{3}\right) + B_{m0} \sin\left(m\omega_s t_1 + \frac{m\pi}{3}\right) \right) \\ &+ \sum_{m=1}^{\infty} \sum_{n=\pm 1}^{\pm\infty} \left\{ A_{mn} \cos\left((m\omega_s + n\omega_0) t_1 + \frac{m\pi}{3}\right) \right. \\ &\quad \left. + B_{mn} \sin\left((m\omega_s + n\omega_0) t_1 - \frac{m\pi}{3}\right) \right\} \end{aligned} \quad (\text{C.90})$$

We now substitute back $t = t_1 + \frac{T_0}{3}$ into equation C.86 and obtain:

$$\begin{aligned} s_{b2}(t) &= \frac{1}{2}A_{00} + \sum_{n=1}^{\infty} \left(A_{0n} \cos\left(n\omega_0 \left(t - \frac{2\pi}{3\omega_0}\right)\right) + B_{0n} \sin\left(n\omega_0 \left(t - \frac{2\pi}{3\omega_0}\right)\right) \right) \\ &+ \sum_{m=1}^{\infty} \left(A_{m0} \cos\left(m\omega_s \left(t - \frac{2\pi}{3\omega_0}\right) + \frac{m\pi}{3}\right) \right. \\ &\quad \left. + B_{m0} \sin\left(m\omega_s \left(t - \frac{2\pi}{3\omega_0}\right) + \frac{m\pi}{3}\right) \right) \\ &+ \sum_{m=1}^{\infty} \sum_{n=\pm 1}^{\pm\infty} \left\{ A_{mn} \cos\left((m\omega_s + n\omega_0) \left(t - \frac{2\pi}{3\omega_0}\right) + \frac{m\pi}{3}\right) \right. \\ &\quad \left. + B_{mn} \sin\left((m\omega_s + n\omega_0) \left(t - \frac{2\pi}{3\omega_0}\right) + \frac{m\pi}{3}\right) \right\} \end{aligned} \quad (\text{C.91})$$

Now considering trigonometric terms in equation C.91 we have:

$$\begin{aligned} \cos\left(n\omega_0 \left(t - \frac{2\pi}{3\omega_0}\right)\right) &= \cos\left(n\omega_0 t - \frac{2n\pi}{3}\right) \\ &= \begin{cases} \cos(n\omega_0 t) & \text{if } n = 3p \\ \cos\left(n\omega_0 t - \frac{2\pi}{3}\right) & \text{if } n = 3p + 1 \\ \cos\left(n\omega_0 t + \frac{2\pi}{3}\right) & \text{if } n = 3p + 2 \end{cases} \end{aligned} \quad (\text{C.92})$$

$$\begin{aligned} \sin\left(n\omega_0 \left(t - \frac{2\pi}{3\omega_0}\right)\right) &= \sin\left(n\omega_0 t - \frac{2n\pi}{3}\right) \\ &= \begin{cases} \sin(n\omega_0 t) & \text{if } n = 3p \\ \sin\left(n\omega_0 t - \frac{2\pi}{3}\right) & \text{if } n = 3p + 1 \\ \sin\left(n\omega_0 t + \frac{2\pi}{3}\right) & \text{if } n = 3p + 2 \end{cases} \end{aligned} \quad (\text{C.93})$$

$$\begin{aligned}\cos\left(m\omega_s\left(t - \frac{2\pi}{3\omega_0}\right) - \frac{2m\pi}{3}\right) &= \cos\left(m\omega_s t - \frac{2m\pi}{3}m_f - \frac{2m\pi}{3}\right) \\ &= \cos(m\omega_s t)\end{aligned}\tag{C.94}$$

$$\begin{aligned}\sin\left(m\omega_s\left(t - \frac{2\pi}{3\omega_0}\right) - \frac{2m\pi}{3}\right) &= \sin\left(m\omega_s t - \frac{2m\pi}{3}m_f - \frac{2m\pi}{3}\right) \\ &= \sin(m\omega_s t)\end{aligned}\tag{C.95}$$

$$\begin{aligned}\cos\left(m\omega_s\left(t - \frac{2\pi}{3\omega_0}\right) + \frac{m\pi}{3}\right) &= \cos\left(m\omega_s t - \frac{2m\pi}{3}m_f + \frac{m\pi}{3}\right) \\ &= \begin{cases} \cos(m\omega_s t) & \text{if } m = 2k \\ -\cos(m\omega_s t) & \text{if } m = 2k + 1 \end{cases}\end{aligned}\tag{C.96}$$

$$\begin{aligned}\sin\left(m\omega_s\left(t - \frac{2\pi}{3\omega_0}\right) + \frac{m\pi}{3}\right) &= \sin\left(m\omega_s t - \frac{2m\pi}{3}m_f + \frac{m\pi}{3}\right) \\ &= \begin{cases} \sin(m\omega_s t) & \text{if } m = 2k \\ -\sin(m\omega_s t) & \text{if } m = 2k + 1 \end{cases}\end{aligned}\tag{C.97}$$

$$\begin{aligned}\cos\left((m\omega_s + n\omega_0)\left(t - \frac{2\pi}{3\omega_0}\right) - \frac{2m\pi}{3}\right) &= \cos\left(m\omega_s t + n\omega_0 t - \frac{2m\pi}{3}m_f - \frac{2n\pi}{3} - \frac{2m\pi}{3}\right) \\ &= \begin{cases} \cos(m\omega_s t + n\omega_0 t) & \text{if } m = k \text{ and } n = 3p \\ \cos\left((m\omega_s + n\omega_0)t - \frac{2\pi}{3}\right) & \text{if } m = k \text{ and } n = 3p + 1 \\ \cos\left((m\omega_s + n\omega_0)t + \frac{2\pi}{3}\right) & \text{if } m = k \text{ and } n = 3p + 2 \\ \cos(m\omega_s t + n\omega_0 t) & \text{if } m = k \text{ and } n = -3p \\ \cos\left((m\omega_s + n\omega_0)t - \frac{2\pi}{3}\right) & \text{if } m = k \text{ and } n = -(3p + 2) \\ \cos\left((m\omega_s + n\omega_0)t + \frac{2\pi}{3}\right) & \text{if } m = k \text{ and } n = -(3p + 1) \end{cases}\end{aligned}\tag{C.98}$$

$$\begin{aligned}\sin\left((m\omega_s + n\omega_0)\left(t - \frac{2\pi}{3\omega_0}\right) - \frac{2m\pi}{3}\right) &= \cos\left(m\omega_s t + n\omega_0 t - \frac{2m\pi}{3}m_f - \frac{2n\pi}{3} - \frac{2m\pi}{3}\right) \\ &= \begin{cases} \sin(m\omega_s t + n\omega_0 t) & \text{if } m = k \text{ and } n = 3p \\ \sin\left((m\omega_s + n\omega_0)t - \frac{2\pi}{3}\right) & \text{if } m = k \text{ and } n = 3p + 1 \\ \sin\left((m\omega_s + n\omega_0)t + \frac{2\pi}{3}\right) & \text{if } m = k \text{ and } n = 3p + 2 \\ \sin(m\omega_s t + n\omega_0 t) & \text{if } m = k \text{ and } n = -3p \\ \sin\left((m\omega_s + n\omega_0)t - \frac{2\pi}{3}\right) & \text{if } m = k \text{ and } n = -(3p + 2) \\ \sin\left((m\omega_s + n\omega_0)t + \frac{2\pi}{3}\right) & \text{if } m = k \text{ and } n = -(3p + 1) \end{cases}\end{aligned}\tag{C.99}$$

$$\begin{aligned}
& \cos \left((m\omega_s + n\omega_0) \left(t - \frac{2\pi}{3\omega_0} \right) + \frac{m\pi}{3} \right) = \cos \left(m\omega_s t + n\omega_0 t - \frac{2m\pi}{3} m_f - \frac{2n\pi}{3} + \frac{m\pi}{3} \right) \\
= & \left\{ \begin{array}{ll} \cos(m\omega_s t + n\omega_0 t) & \text{if } m = 2k \text{ and } n = 3p \\ \cos \left((m\omega_s + n\omega_0) t - \frac{2\pi}{3} \right) & \text{if } m = 2k \text{ and } n = 3p + 1 \\ \cos \left((m\omega_s + n\omega_0) t + \frac{2\pi}{3} \right) & \text{if } m = 2k \text{ and } n = 3p + 2 \\ \cos(m\omega_s t + n\omega_0 t) & \text{if } m = 2k \text{ and } n = -3p \\ \cos \left((m\omega_s + n\omega_0) t - \frac{2\pi}{3} \right) & \text{if } m = 2k \text{ and } n = -(3p + 2) \\ \cos \left((m\omega_s + n\omega_0) t + \frac{2\pi}{3} \right) & \text{if } m = 2k \text{ and } n = -(3p + 1) \\ -\cos(m\omega_s t + n\omega_0 t) & \text{if } m = 2k + 1 \text{ and } n = 3p \\ -\cos \left((m\omega_s + n\omega_0) t - \frac{2\pi}{3} \right) & \text{if } m = 2k + 1 \text{ and } n = 3p + 1 \\ -\cos \left((m\omega_s + n\omega_0) t + \frac{2\pi}{3} \right) & \text{if } m = 2k + 1 \text{ and } n = 3p + 2 \\ -\cos(m\omega_s t + n\omega_0 t) & \text{if } m = 2k + 1 \text{ and } n = -3p \\ -\cos \left((m\omega_s + n\omega_0) t - \frac{2\pi}{3} \right) & \text{if } m = 2k + 1 \text{ and } n = -(3p + 2) \\ -\cos \left((m\omega_s + n\omega_0) t + \frac{2\pi}{3} \right) & \text{if } m = 2k + 1 \text{ and } n = -(3p + 1) \end{array} \right. \quad (\text{C.100})
\end{aligned}$$

$$\begin{aligned}
& \sin \left((m\omega_s + n\omega_0) \left(t - \frac{2\pi}{3\omega_0} \right) + \frac{m\pi}{3} \right) = \sin \left(m\omega_s t + n\omega_0 t - \frac{2m\pi}{3} m_f - \frac{2n\pi}{3} + \frac{m\pi}{3} \right) \\
= & \left\{ \begin{array}{ll} \sin(m\omega_s t + n\omega_0 t) & \text{if } m = 2k \text{ and } n = 3p \\ \sin \left((m\omega_s + n\omega_0) t - \frac{2\pi}{3} \right) & \text{if } m = 2k \text{ and } n = 3p + 1 \\ \sin \left((m\omega_s + n\omega_0) t + \frac{2\pi}{3} \right) & \text{if } m = 2k \text{ and } n = 3p + 2 \\ \sin(m\omega_s t + n\omega_0 t) & \text{if } m = 2k \text{ and } n = -3p \\ \sin \left((m\omega_s + n\omega_0) t - \frac{2\pi}{3} \right) & \text{if } m = 2k \text{ and } n = -(3p + 2) \\ \sin \left((m\omega_s + n\omega_0) t + \frac{2\pi}{3} \right) & \text{if } m = 2k \text{ and } n = -(3p + 1) \\ -\sin(m\omega_s t + n\omega_0 t) & \text{if } m = 2k + 1 \text{ and } n = 3p \\ -\sin \left((m\omega_s + n\omega_0) t - \frac{2\pi}{3} \right) & \text{if } m = 2k + 1 \text{ and } n = 3p + 1 \\ -\sin \left((m\omega_s + n\omega_0) t + \frac{2\pi}{3} \right) & \text{if } m = 2k + 1 \text{ and } n = 3p + 2 \\ -\sin(m\omega_s t + n\omega_0 t) & \text{if } m = 2k + 1 \text{ and } n = -3p \\ -\sin \left((m\omega_s + n\omega_0) t - \frac{2\pi}{3} \right) & \text{if } m = 2k + 1 \text{ and } n = -(3p + 2) \\ -\sin \left((m\omega_s + n\omega_0) t + \frac{2\pi}{3} \right) & \text{if } m = 2k + 1 \text{ and } n = -(3p + 1) \end{array} \right. \quad (\text{C.101})
\end{aligned}$$

Thus the phasor representation for phase B of 2-cell converter when $m_f = 3k + 2$ is given by Figures C.14, C.15 and C.16.

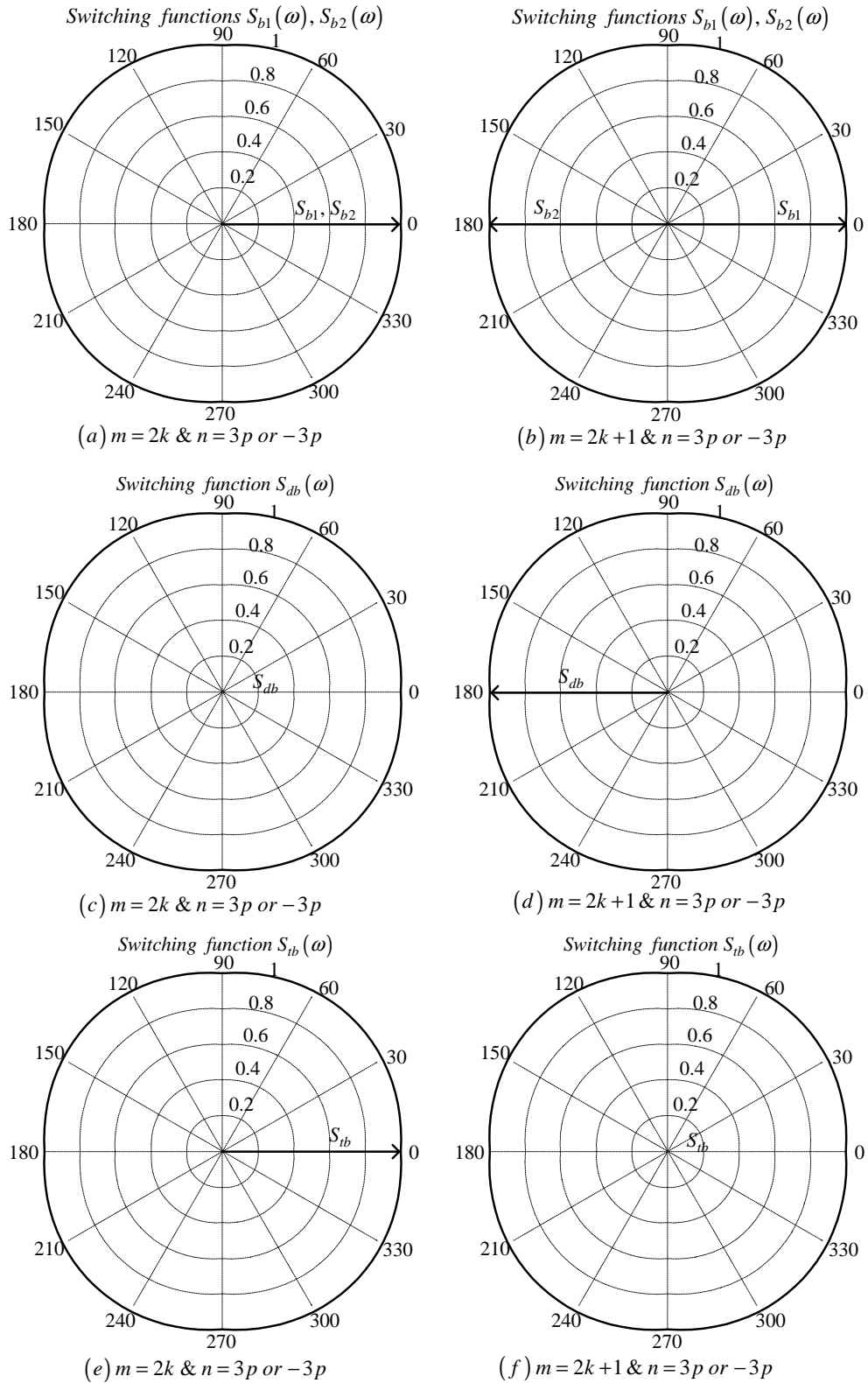


Figure C.14: Phasor representation for phase B of 2-cell converter for $n = 3p$ or $n = -3p$

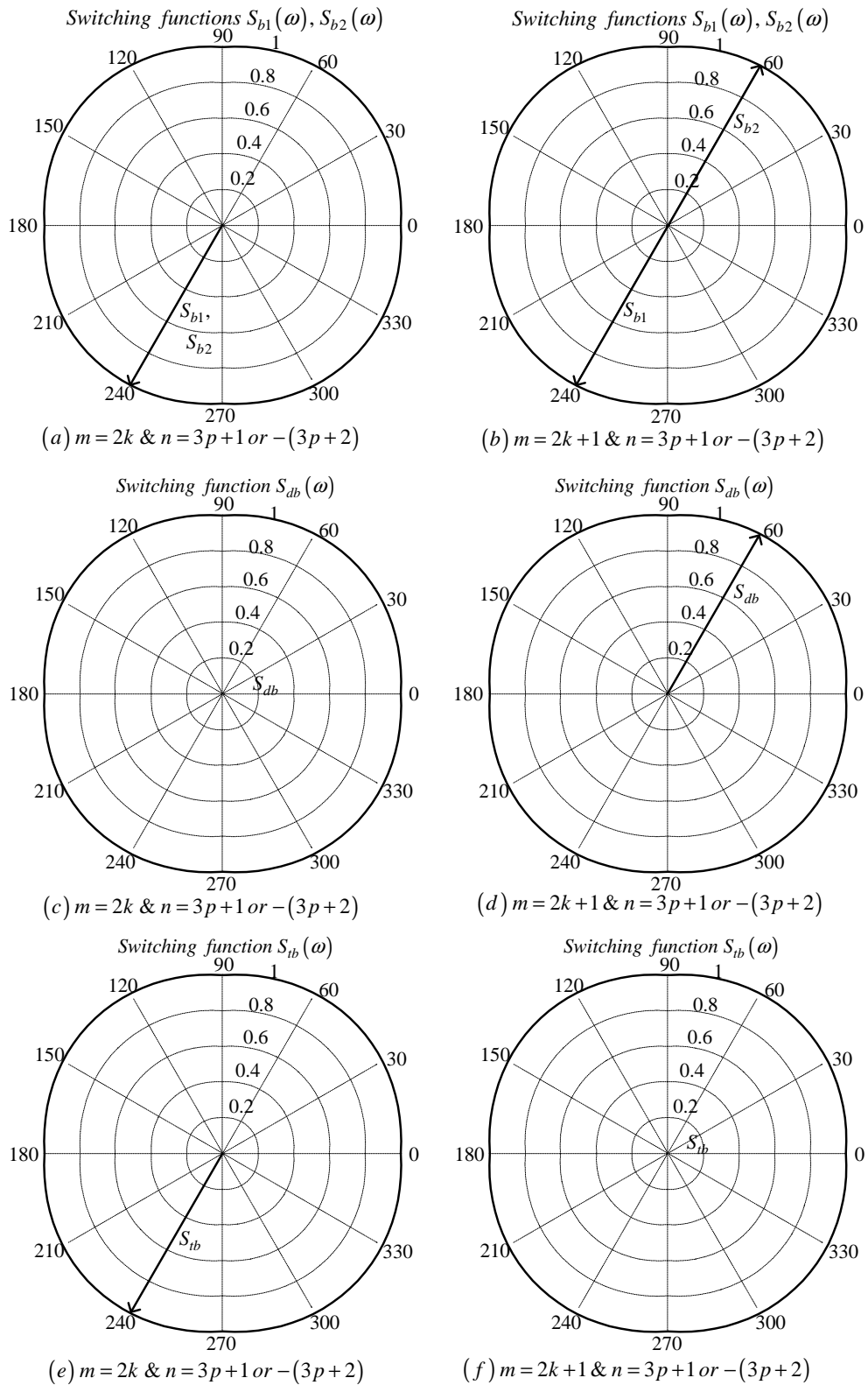


Figure C.15: Phasor representation for phase B of 2-cell converter for $n = 3p + 1$ or $n = -(3p + 2)$

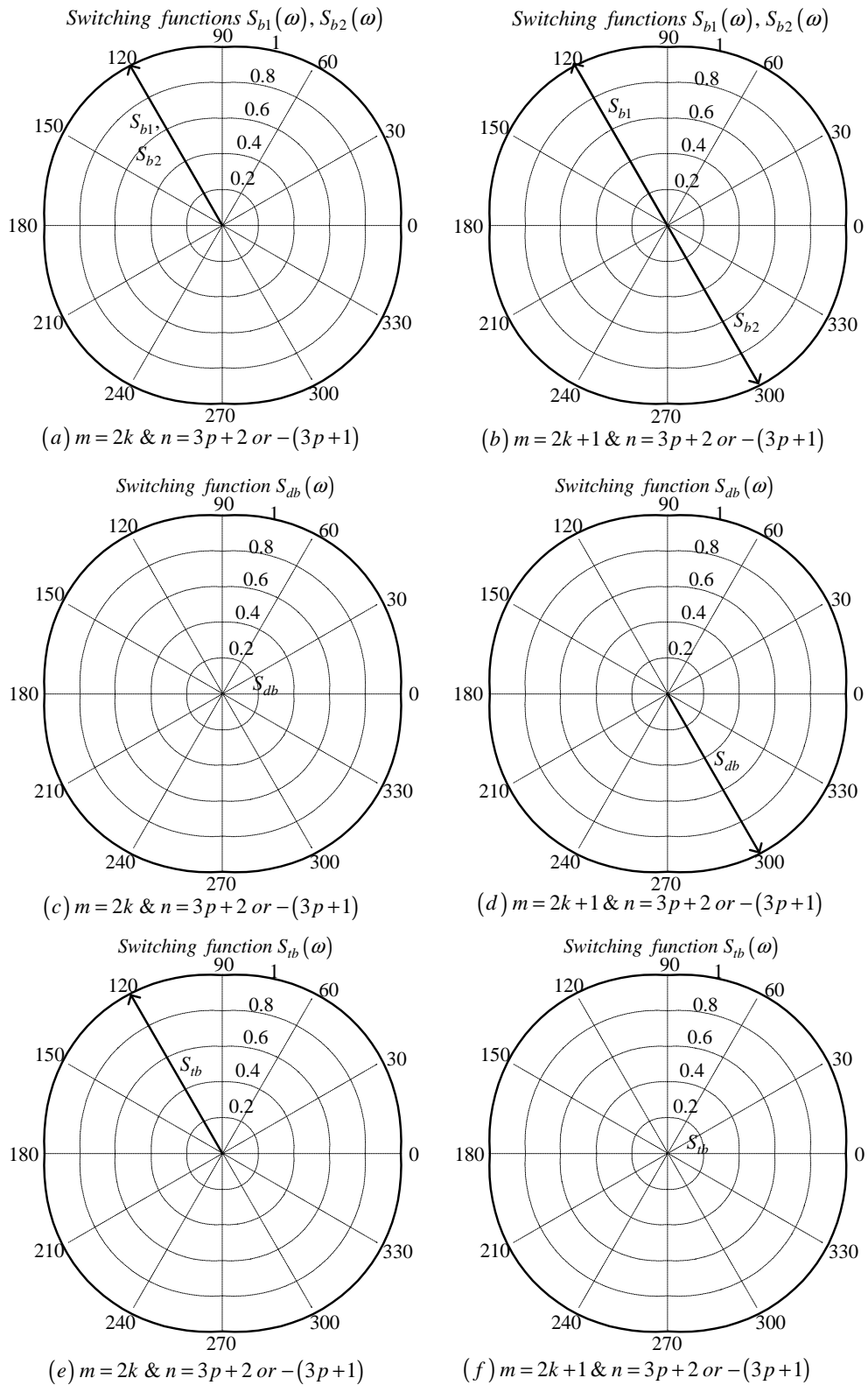


Figure C.16: Phasor representation for phase B of 2-cell converter for $n = 3p + 2$ or $n = -(3p + 1)$

Phase C

From table C.1 the value of h for background function of $s_{c1}(t)$ is given by:

$$h = \frac{2\omega_s}{\pi}t_2 - \frac{8}{3} \quad (\text{C.102})$$

Substituting equation C.102 into the term $\frac{m\pi h}{2}$ of equation 3.36 we obtain:

$$\frac{m\pi h}{2} = m\omega_s t_2 - \frac{4}{3}m\pi \quad (\text{C.103})$$

Now substituting equation C.103 into equation 3.36 we obtain:

$$\begin{aligned} s_{c1}(t_2) &= \frac{1}{2}A_{00} + \sum_{n=1}^{\infty} (A_{0n} \cos(n\omega_0 t_2) + B_{0n} \sin(n\omega_0 t_2)) \\ &+ \sum_{m=1}^{\infty} \left(A_{m0} \cos\left(m\omega_s t_2 - \frac{4}{3}m\pi\right) + B_{m0} \sin\left(m\omega_s t_2 - \frac{4}{3}m\pi\right) \right) \\ &+ \sum_{m=1}^{\infty} \sum_{n=\pm 1}^{\pm\infty} \left\{ A_{mn} \cos\left((m\omega_s + n\omega_0) t_2 - \frac{4}{3}m\pi\right) \right. \\ &\quad \left. + B_{mn} \sin\left((m\omega_s + n\omega_0) t_2 - \frac{4}{3}m\pi\right) \right\} \end{aligned} \quad (\text{C.104})$$

We now substitute back $t = t_2 + \frac{2T_0}{3}$ into equation C.104 and obtain:

$$\begin{aligned} s_{c1}(t) &= \frac{1}{2}A_{00} + \sum_{n=1}^{\infty} \left(A_{0n} \cos\left(n\omega_0 \left(t - \frac{4\pi}{3\omega_0}\right)\right) + B_{0n} \sin\left(n\omega_0 \left(t - \frac{4\pi}{3\omega_0}\right)\right) \right) \\ &+ \sum_{m=1}^{\infty} \left(A_{m0} \cos\left(m\omega_s \left(t - \frac{4\pi}{3\omega_0}\right) - \frac{4}{3}m\pi\right) \right. \\ &\quad \left. + B_{m0} \sin\left(m\omega_s \left(t - \frac{4\pi}{3\omega_0}\right) - \frac{4}{3}m\pi\right) \right) \\ &+ \sum_{m=1}^{\infty} \sum_{n=\pm 1}^{\pm\infty} \left\{ A_{mn} \cos\left((m\omega_s + n\omega_0) \left(t - \frac{4\pi}{3\omega_0}\right) - \frac{4}{3}m\pi\right) \right. \\ &\quad \left. + B_{mn} \sin\left((m\omega_s + n\omega_0) \left(t - \frac{4\pi}{3\omega_0}\right) - \frac{4}{3}m\pi\right) \right\} \end{aligned} \quad (\text{C.105})$$

From table C.1 the value of h for background function of $s_{c2}(t)$ is given by:

$$h = \frac{2\omega_s}{\pi}t_2 - \frac{2}{3} \quad (\text{C.106})$$

Substituting equation C.106 into the term $\frac{m\pi h}{2}$ of equation 3.36 we obtain:

$$\frac{m\pi h}{2} = m\omega_s t_2 - \frac{m\pi}{3} \quad (\text{C.107})$$

Now substituting equation C.107 into equation 3.36 we obtain:

$$\begin{aligned}
s_{c2}(t_2) &= \frac{1}{2}A_{00} + \sum_{n=1}^{\infty} (A_{0n} \cos(n\omega_0 t_2) + B_{0n} \sin(n\omega_0 t_2)) \\
&+ \sum_{m=1}^{\infty} \left(A_{m0} \cos\left(m\omega_s t_2 - \frac{m\pi}{3}\right) + B_{m0} \sin\left(m\omega_s t_2 - \frac{m\pi}{3}\right) \right) \\
&+ \sum_{m=1}^{\infty} \sum_{n=\pm 1}^{\pm\infty} \left\{ A_{mn} \cos\left((m\omega_s + n\omega_0)t_2 - \frac{m\pi}{3}\right) \right. \\
&\quad \left. + B_{mn} \sin\left((m\omega_s + n\omega_0)t_2 - \frac{m\pi}{3}\right) \right\}
\end{aligned} \tag{C.108}$$

We now substitute back $t = t_2 + \frac{2T_0}{3}$ into equation C.108 and obtain:

$$\begin{aligned}
s_{c2}(t) &= \frac{1}{2}A_{00} + \sum_{n=1}^{\infty} \left(A_{0n} \cos\left(n\omega_0 \left(t - \frac{4\pi}{3\omega_0}\right)\right) + B_{0n} \sin\left(n\omega_0 \left(t - \frac{4\pi}{3\omega_0}\right)\right) \right) \\
&+ \sum_{m=1}^{\infty} \left(A_{m0} \cos\left(m\omega_s \left(t - \frac{4\pi}{3\omega_0}\right) - \frac{m\pi}{3}\right) \right. \\
&\quad \left. + B_{m0} \sin\left(m\omega_s \left(t - \frac{4\pi}{3\omega_0}\right) - \frac{m\pi}{3}\right) \right) \\
&+ \sum_{m=1}^{\infty} \sum_{n=\pm 1}^{\pm\infty} \left\{ A_{mn} \cos\left((m\omega_s + n\omega_0) \left(t - \frac{4\pi}{3\omega_0}\right) - \frac{m\pi}{3}\right) \right. \\
&\quad \left. + B_{mn} \sin\left((m\omega_s + n\omega_0) \left(t - \frac{4\pi}{3\omega_0}\right) - \frac{m\pi}{3}\right) \right\}
\end{aligned} \tag{C.109}$$

Now considering trigonometric terms in equations C.69 and C.109 we have:

$$\begin{aligned}
\cos\left(n\omega_0 \left(t - \frac{4\pi}{3\omega_0}\right)\right) &= \cos\left(n\omega_0 t - \frac{4n\pi}{3}\right) \\
&= \begin{cases} \cos(n\omega_0 t) & \text{if } n = 3p \\ \cos\left(n\omega_0 t + \frac{2\pi}{3}\right) & \text{if } n = 3p + 1 \\ \cos\left(n\omega_0 t - \frac{2\pi}{3}\right) & \text{if } n = 3p + 2 \end{cases}
\end{aligned} \tag{C.110}$$

$$\begin{aligned}
\sin\left(n\omega_0 \left(t - \frac{4\pi}{3\omega_0}\right)\right) &= \sin\left(n\omega_0 t - \frac{4n\pi}{3}\right) \\
&= \begin{cases} \sin(n\omega_0 t) & \text{if } n = 3p \\ \sin\left(n\omega_0 t + \frac{2\pi}{3}\right) & \text{if } n = 3p + 1 \\ \sin\left(n\omega_0 t - \frac{2\pi}{3}\right) & \text{if } n = 3p + 2 \end{cases}
\end{aligned} \tag{C.111}$$

$$\begin{aligned}
\cos\left(m\omega_s \left(t - \frac{4\pi}{3\omega_0}\right) - \frac{4m\pi}{3}\right) &= \cos\left(m\omega_s t - \frac{4m\pi}{3}m_f - \frac{4m\pi}{3}\right) \\
&= \cos(m\omega_s t)
\end{aligned} \tag{C.112}$$

$$\begin{aligned}\sin\left(m\omega_s\left(t - \frac{4\pi}{3\omega_0}\right) - \frac{4m\pi}{3}\right) &= \sin\left(m\omega_s t - \frac{4m\pi}{3}m_f - \frac{4m\pi}{3}\right) \\ &= \sin(m\omega_s t)\end{aligned}\tag{C.113}$$

$$\begin{aligned}\cos\left(m\omega_s\left(t - \frac{4\pi}{3\omega_0}\right) - \frac{m\pi}{3}\right) &= \cos\left(m\omega_s t - \frac{4m\pi}{3}m_f - \frac{m\pi}{3}\right) \\ &= \begin{cases} \cos(m\omega_s t) & \text{if } m = 2k \\ -\cos(m\omega_s t) & \text{if } m = 2k + 1 \end{cases}\end{aligned}\tag{C.114}$$

$$\begin{aligned}\sin\left(m\omega_s\left(t - \frac{4\pi}{3\omega_0}\right) - \frac{m\pi}{3}\right) &= \sin\left(m\omega_s t - \frac{4m\pi}{3}m_f - \frac{m\pi}{3}\right) \\ &= \begin{cases} \sin(m\omega_s t) & \text{if } m = 2k \\ -\sin(m\omega_s t) & \text{if } m = 2k + 1 \end{cases}\end{aligned}\tag{C.115}$$

$$\begin{aligned}\cos\left((m\omega_s + n\omega_0)\left(t - \frac{4\pi}{3\omega_0}\right) - \frac{4m\pi}{3}\right) &= \cos\left(m\omega_s t + n\omega_0 t - \frac{4m\pi}{3}m_f - \frac{4n\pi}{3} - \frac{4m\pi}{3}\right) \\ &= \begin{cases} \cos(m\omega_s t + n\omega_0 t) & \text{if } m = k \text{ and } n = 3p \\ \cos\left((m\omega_s + n\omega_0)t + \frac{2\pi}{3}\right) & \text{if } m = k \text{ and } n = 3p + 1 \\ \cos\left((m\omega_s + n\omega_0)t - \frac{2\pi}{3}\right) & \text{if } m = k \text{ and } n = 3p + 2 \\ \cos(m\omega_s t + n\omega_0 t) & \text{if } m = k \text{ and } n = -3p \\ \cos\left((m\omega_s + n\omega_0)t + \frac{2\pi}{3}\right) & \text{if } m = k \text{ and } n = -(3p + 2) \\ \cos\left((m\omega_s + n\omega_0)t - \frac{2\pi}{3}\right) & \text{if } m = k \text{ and } n = -(3p + 1) \end{cases}\end{aligned}\tag{C.116}$$

$$\begin{aligned}\sin\left((m\omega_s + n\omega_0)\left(t - \frac{4\pi}{3\omega_0}\right) - \frac{4m\pi}{3}\right) &= \cos\left(m\omega_s t + n\omega_0 t - \frac{4m\pi}{3}m_f - \frac{4n\pi}{3} - \frac{4m\pi}{3}\right) \\ &= \begin{cases} \sin(m\omega_s t + n\omega_0 t) & \text{if } m = k \text{ and } n = 3p \\ \sin\left((m\omega_s + n\omega_0)t - \frac{2\pi}{3}\right) & \text{if } m = k \text{ and } n = 3p + 1 \\ \sin\left((m\omega_s + n\omega_0)t + \frac{2\pi}{3}\right) & \text{if } m = k \text{ and } n = 3p + 2 \\ \sin(m\omega_s t + n\omega_0 t) & \text{if } m = k \text{ and } n = -3p \\ \sin\left((m\omega_s + n\omega_0)t + \frac{2\pi}{3}\right) & \text{if } m = k \text{ and } n = -(3p + 2) \\ \sin\left((m\omega_s + n\omega_0)t - \frac{2\pi}{3}\right) & \text{if } m = k \text{ and } n = -(3p + 1) \end{cases}\end{aligned}\tag{C.117}$$

$$\begin{aligned}
& \cos \left((m\omega_s + n\omega_0) \left(t - \frac{4\pi}{3\omega_0} \right) - \frac{m\pi}{3} \right) = \cos \left(m\omega_s t + n\omega_0 t - \frac{4m\pi}{3} m_f - \frac{4n\pi}{3} - \frac{m\pi}{3} \right) \\
= & \left\{ \begin{array}{ll} \cos(m\omega_s t + n\omega_0 t) & \text{if } m = 2k \text{ and } n = 3p \\ \cos \left((m\omega_s + n\omega_0) t + \frac{2\pi}{3} \right) & \text{if } m = 2k \text{ and } n = 3p + 1 \\ \cos \left((m\omega_s + n\omega_0) t - \frac{2\pi}{3} \right) & \text{if } m = 2k \text{ and } n = 3p + 2 \\ \cos(m\omega_s t + n\omega_0 t) & \text{if } m = 2k \text{ and } n = -3p \\ \cos \left((m\omega_s + n\omega_0) t + \frac{2\pi}{3} \right) & \text{if } m = 2k \text{ and } n = -(3p + 2) \\ \cos \left((m\omega_s + n\omega_0) t - \frac{2\pi}{3} \right) & \text{if } m = 2k \text{ and } n = -(3p + 1) \\ -\cos(m\omega_s t + n\omega_0 t) & \text{if } m = 2k + 1 \text{ and } n = 3p \\ -\cos \left((m\omega_s + n\omega_0) t + \frac{2\pi}{3} \right) & \text{if } m = 2k + 1 \text{ and } n = 3p + 1 \\ -\cos \left((m\omega_s + n\omega_0) t - \frac{2\pi}{3} \right) & \text{if } m = 2k + 1 \text{ and } n = 3p + 2 \\ -\cos(m\omega_s t + n\omega_0 t) & \text{if } m = 2k + 1 \text{ and } n = -3p \\ -\cos \left((m\omega_s + n\omega_0) t + \frac{2\pi}{3} \right) & \text{if } m = 2k + 1 \text{ and } n = -(3p + 2) \\ -\cos \left((m\omega_s + n\omega_0) t - \frac{2\pi}{3} \right) & \text{if } m = 2k + 1 \text{ and } n = -(3p + 1) \end{array} \right. \quad (\text{C.118})
\end{aligned}$$

$$\begin{aligned}
& \sin \left((m\omega_s + n\omega_0) \left(t - \frac{4\pi}{3\omega_0} \right) - \frac{m\pi}{3} \right) = \sin \left(m\omega_s t + n\omega_0 t - \frac{4m\pi}{3} m_f - \frac{4n\pi}{3} - \frac{m\pi}{3} \right) \\
= & \left\{ \begin{array}{ll} \sin(m\omega_s t + n\omega_0 t) & \text{if } m = 2k \text{ and } n = 3p \\ \sin \left((m\omega_s + n\omega_0) t + \frac{2\pi}{3} \right) & \text{if } m = 2k \text{ and } n = 3p + 1 \\ \sin \left((m\omega_s + n\omega_0) t - \frac{2\pi}{3} \right) & \text{if } m = 2k \text{ and } n = 3p + 2 \\ \sin(m\omega_s t + n\omega_0 t) & \text{if } m = 2k \text{ and } n = -3p \\ \sin \left((m\omega_s + n\omega_0) t + \frac{2\pi}{3} \right) & \text{if } m = 2k \text{ and } n = -(3p + 2) \\ \sin \left((m\omega_s + n\omega_0) t - \frac{2\pi}{3} \right) & \text{if } m = 2k \text{ and } n = -(3p + 1) \\ -\sin(m\omega_s t + n\omega_0 t) & \text{if } m = 2k + 1 \text{ and } n = 3p \\ -\sin \left((m\omega_s + n\omega_0) t + \frac{2\pi}{3} \right) & \text{if } m = 2k + 1 \text{ and } n = 3p + 1 \\ -\sin \left((m\omega_s + n\omega_0) t - \frac{2\pi}{3} \right) & \text{if } m = 2k + 1 \text{ and } n = 3p + 2 \\ -\sin(m\omega_s t + n\omega_0 t) & \text{if } m = 2k + 1 \text{ and } n = -3p \\ -\sin \left((m\omega_s + n\omega_0) t + \frac{2\pi}{3} \right) & \text{if } m = 2k + 1 \text{ and } n = -(3p + 2) \\ -\sin \left((m\omega_s + n\omega_0) t - \frac{2\pi}{3} \right) & \text{if } m = 2k + 1 \text{ and } n = -(3p + 1) \end{array} \right. \quad (\text{C.119})
\end{aligned}$$

Thus the phasor representation for phase C of 2-cell converter when $m_f = 3k + 2$ is given by Figures C.17, C.18 and C.19.

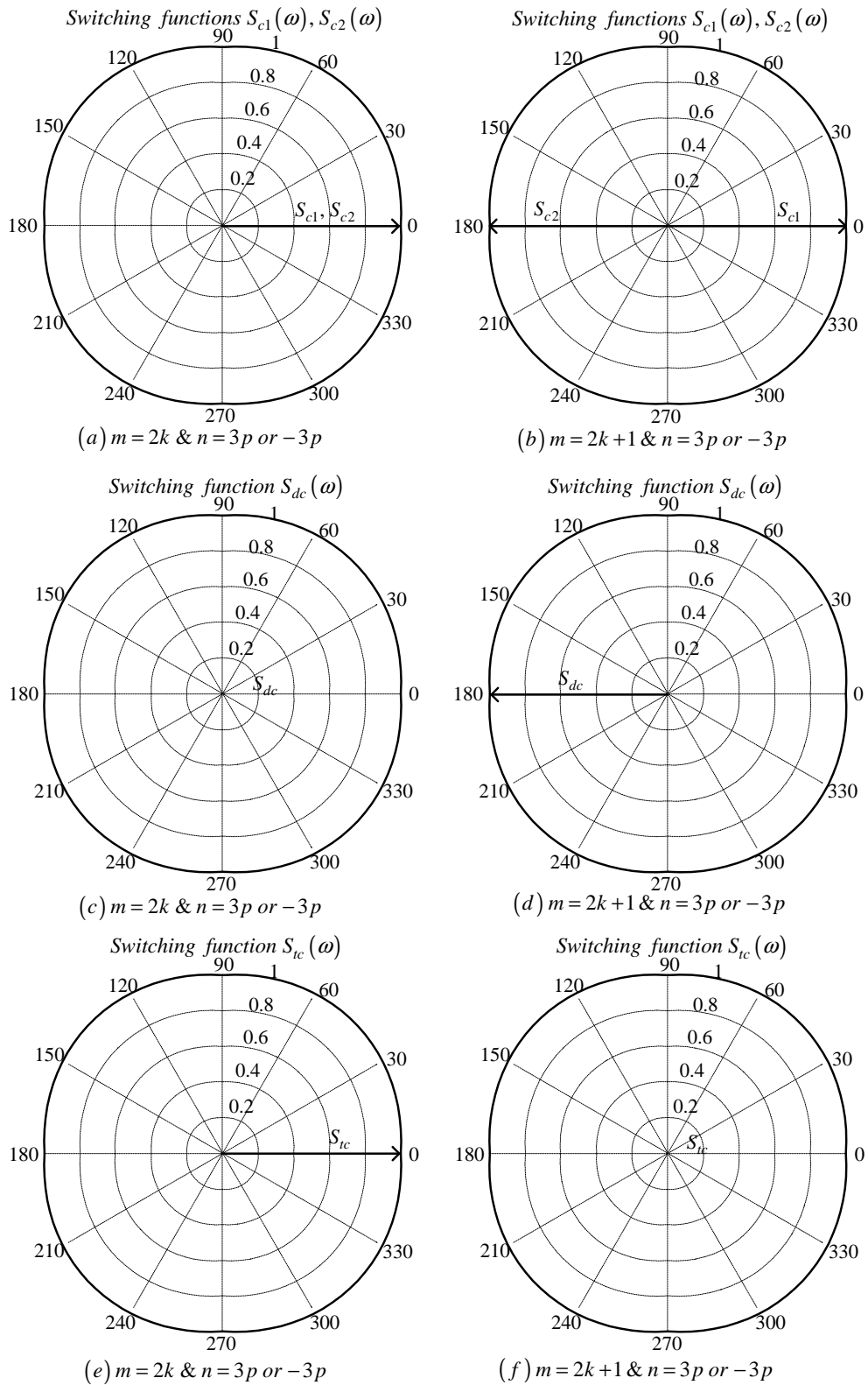


Figure C.17: Phasor representation for phase C of 2-cell converter for $n = 3p$ or $n = -3p$

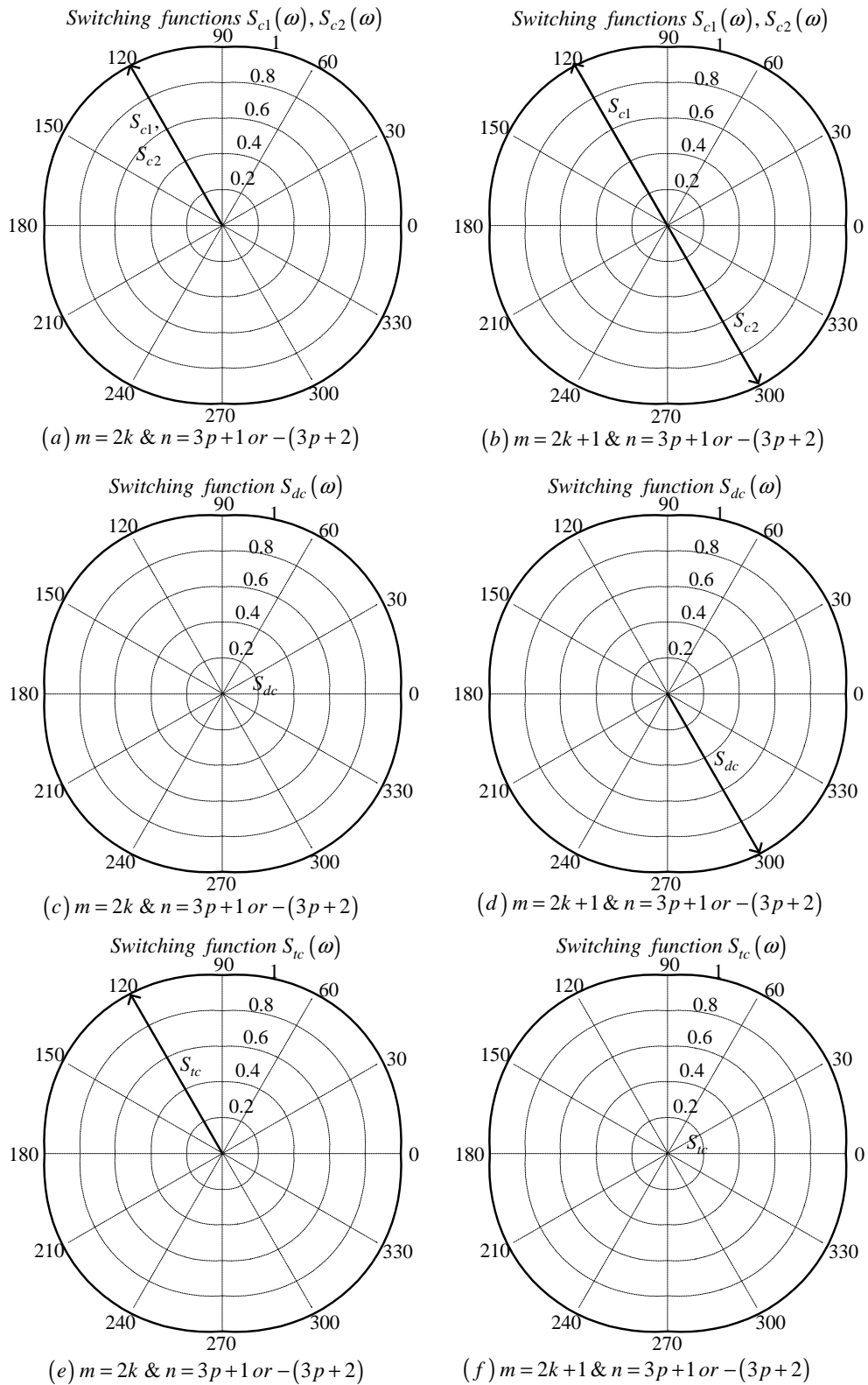


Figure C.18: Phasor representation for phase C of 2-cell converter for $n = 3p + 1$ or $n = -(3p + 2)$

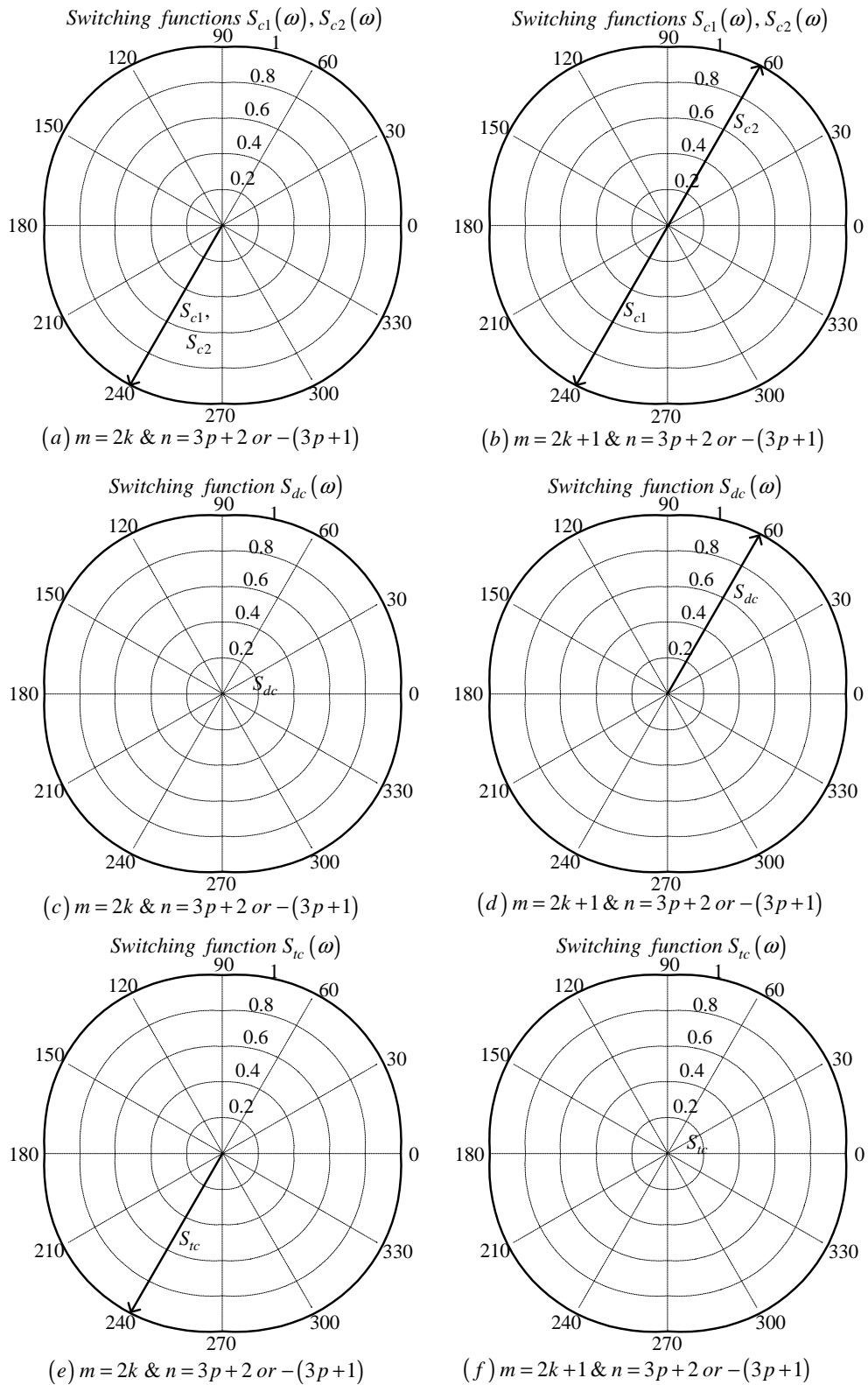


Figure C.19: Phasor representation for phase C of 2-cell converter for $n = 3p + 2$ or $n = -(3p + 1)$

C.2 3-cell Multicell

Table C.2: Values for t_x and c of background function for 3-cell multicell converter

m_f		s_{a1}	s_{a2}	s_{a3}	s_{b1}	s_{b2}	s_{b3}
$3k$	t_x	0	$\frac{1}{3}T_s$	$\frac{2}{3}T_s$	0	$\frac{1}{3}T_s$	$\frac{2}{3}T_s$
	c	0	$-\frac{4}{3}$	$-\frac{8}{3}$	0	$-\frac{4}{3}$	$-\frac{8}{3}$
	h	$\frac{2\omega_s t}{\pi}$	$\frac{2\omega_s t}{\pi} - \frac{4}{3}$	$\frac{2\omega_s t}{\pi} - \frac{8}{3}$	$\frac{2\omega_s t_1}{\pi}$	$\frac{2\omega_s t_1}{\pi} - \frac{4}{3}$	$\frac{2\omega_s t_1}{\pi} - \frac{8}{3}$
$3k + 1$	t_x	0	$\frac{1}{3}T_s$	$\frac{2}{3}T_s$	$\frac{2}{3}T_s$	0	$\frac{1}{3}T_s$
	c	0	$-\frac{4}{3}$	$-\frac{8}{3}$	$-\frac{8}{3}$	0	$-\frac{4}{3}$
	h	$\frac{2\omega_s t}{\pi}$	$\frac{2\omega_s t}{\pi} - \frac{4}{3}$	$\frac{2\omega_s t}{\pi} - \frac{8}{3}$	$\frac{2\omega_s t_1}{\pi} - \frac{8}{3}$	$\frac{2\omega_s t_1}{\pi}$	$\frac{2\omega_s t_1}{\pi} - \frac{4}{3}$
$3k + 2$	t_x	0	$\frac{1}{3}T_s$	$\frac{2}{3}T_s$	$\frac{1}{3}T_s$	$\frac{2}{3}T_s$	0
	c	0	$-\frac{4}{3}$	$-\frac{8}{3}$	$-\frac{4}{3}$	$-\frac{8}{3}$	0
	h	$\frac{2\omega_s t}{\pi}$	$\frac{2\omega_s t}{\pi} - \frac{4}{3}$	$\frac{2\omega_s t}{\pi} - \frac{8}{3}$	$\frac{2\omega_s t_1}{\pi} - \frac{4}{3}$	$\frac{2\omega_s t_1}{\pi} - \frac{8}{3}$	$\frac{2\omega_s t_1}{\pi}$

Table C.3: Values for t_x and c of background function for 3-cell multicell converter

m_f		s_{c1}	s_{c2}	s_{c3}
$3k$	t_x	0	$\frac{1}{3}T_s$	$\frac{2}{3}T_s$
	c	0	$-\frac{4}{3}$	$-\frac{8}{3}$
	h	$\frac{2\omega_s t_2}{\pi}$	$\frac{2\omega_s t_2}{\pi} - \frac{4}{3}$	$\frac{2\omega_s t_2}{\pi} - \frac{8}{3}$
$3k + 1$	t_x	$\frac{1}{3}T_s$	$\frac{2}{3}T_s$	0
	c	$-\frac{4}{3}$	$-\frac{8}{3}$	0
	h	$\frac{2\omega_s t_2}{\pi} - \frac{4}{3}$	$\frac{2\omega_s t_2}{\pi} - \frac{8}{3}$	$\frac{2\omega_s t_2}{\pi}$
$3k + 2$	t_x	$\frac{2}{3}T_s$	0	$\frac{1}{3}T_s$
	c	$-\frac{8}{3}$	0	$-\frac{4}{3}$
	h	$\frac{2\omega_s t_2}{\pi} - \frac{8}{3}$	$\frac{2\omega_s t_2}{\pi}$	$\frac{2\omega_s t_2}{\pi} - \frac{4}{3}$

Table C.2 and C.3 is used in evaluating the switching functions for different values of frequency modulation index m_f as will be shown in subsection for $m_f = 3k$, $m_f = 3k + 1$ and $m_f = 3k + 2$. Also included in this section is the phasor representation for different cases of $S_{a1}(\omega)$, $S_{a2}(\omega)$, $S_{a3}(\omega)$, $S_{da1}(\omega)$, $S_{da2}(\omega)$, $S_{ta}(\omega)$, $S_{b1}(\omega)$, $S_{b2}(\omega)$, $S_{b3}(\omega)$, $S_{db1}(\omega)$, $S_{db2}(\omega)$, $S_{tb}(\omega)$, $S_{c1}(\omega)$, $S_{c2}(\omega)$, $S_{c3}(\omega)$, $S_{dc1}(\omega)$, $S_{dc2}(\omega)$, $S_{tc}(\omega)$.

C.2.1 For frequency modulation index $m_f = 3k$

Phase A

From table C.2 the value of h for the background function of $s_{a1}(t)$ is given by:

$$h = \frac{2\omega_s t}{\pi} \quad (\text{C.120})$$

Substituting equation C.120 into the term $\frac{m\pi h}{2}$ of equation 3.36 we obtain:

$$\frac{m\pi h}{2} = m\omega_s t \quad (\text{C.121})$$

Now substituting equation C.121 into equation 3.36 we obtain:

$$\begin{aligned} s_{a1}(t) &= \frac{1}{2}A_{00} + \sum_{n=1}^{\infty} (A_{0n} \cos(n\omega_0 t) + B_{0n} \sin(n\omega_0 t)) \\ &\quad + \sum_{m=1}^{\infty} (A_{m0} \cos(m\omega_s t) + B_{m0} \sin(m\omega_s t)) \\ &\quad + \sum_{m=1}^{\infty} \sum_{n=\pm 1}^{\pm\infty} \{A_{mn} \cos((m\omega_s + n\omega_0) t) \\ &\quad + B_{mn} \sin((m\omega_s + n\omega_0) t)\} \end{aligned} \quad (\text{C.122})$$

From table C.2 for the background function of $s_{a2}(t)$ the value of h is given by:

$$h = \frac{2\omega_s t}{\pi} - \frac{4}{3} \quad (\text{C.123})$$

Substituting equation C.123 into the term $\frac{m\pi h}{2}$ of equation 3.36 we obtain:

$$\frac{m\pi h}{2} = m\omega_s t - \frac{2m\pi}{3} \quad (\text{C.124})$$

Now substituting equation C.124 into equation 3.36 we obtain:

$$\begin{aligned} s_{a2}(t) &= \frac{1}{2}A_{00} + \sum_{n=1}^{\infty} (A_{0n} \cos(n\omega_0 t) + B_{0n} \sin(n\omega_0 t)) \\ &\quad + \sum_{m=1}^{\infty} \left(A_{m0} \cos\left(m\omega_s t - \frac{2m\pi}{3}\right) + B_{m0} \sin\left(m\omega_s t - \frac{2m\pi}{3}\right) \right) \\ &\quad + \sum_{m=1}^{\infty} \sum_{n=\pm 1}^{\pm\infty} \left\{ A_{mn} \cos\left((m\omega_s + n\omega_0) t - \frac{2m\pi}{3}\right) \right. \\ &\quad \left. + B_{mn} \sin\left((m\omega_s + n\omega_0) t - \frac{2m\pi}{3}\right) \right\} \end{aligned} \quad (\text{C.125})$$

From table C.2 for the background function of $s_{a3}(t)$ the value of h is given by:

$$h = \frac{2\omega_s t}{\pi} - \frac{8}{3} \quad (\text{C.126})$$

Substituting equation C.126 into the term $\frac{m\pi h}{2}$ of equation 3.36 we obtain:

$$\frac{m\pi h}{2} = m\omega_s t - \frac{4m\pi}{3} \quad (\text{C.127})$$

Now substituting equation C.127 into equation 3.36 we obtain:

$$\begin{aligned} s_{a3}(t) &= \frac{1}{2}A_{00} + \sum_{n=1}^{\infty} (A_{0n} \cos(n\omega_0 t) + B_{0n} \sin(n\omega_0 t)) \\ &+ \sum_{m=1}^{\infty} \left(A_{m0} \cos\left(m\omega_s t - \frac{4m\pi}{3}\right) + B_{m0} \sin\left(m\omega_s t - \frac{4m\pi}{3}\right) \right) \\ &+ \sum_{m=1}^{\infty} \sum_{n=\pm 1}^{\pm\infty} \left\{ A_{mn} \cos\left((m\omega_s + n\omega_0)t - \frac{4m\pi}{3}\right) \right. \\ &\left. + B_{mn} \sin\left((m\omega_s + n\omega_0)t - \frac{4m\pi}{3}\right) \right\} \end{aligned} \quad (\text{C.128})$$

Now considering trigonometric terms in equation C.122, C.125 and C.128 we have:

$$\cos\left(m\omega_s t - \frac{2m\pi}{3}\right) = \begin{cases} \cos(m\omega_s t) & \text{if } m = 3k \\ \cos\left(m\omega_s t - \frac{2\pi}{3}\right) & \text{if } m = 3k + 1 \\ \cos\left(m\omega_s t + \frac{2\pi}{3}\right) & \text{if } m = 3k + 2 \end{cases} \quad (\text{C.129})$$

$$\sin\left(m\omega_s t - \frac{2m\pi}{3}\right) = \begin{cases} \sin(m\omega_s t) & \text{if } m = 3k \\ \sin\left(m\omega_s t - \frac{2\pi}{3}\right) & \text{if } m = 3k + 1 \\ \sin\left(m\omega_s t + \frac{2\pi}{3}\right) & \text{if } m = 3k + 2 \end{cases} \quad (\text{C.130})$$

$$\cos\left(m\omega_s t - \frac{4m\pi}{3}\right) = \begin{cases} \cos(m\omega_s t) & \text{if } m = 3k \\ \cos\left(m\omega_s t + \frac{2\pi}{3}\right) & \text{if } m = 3k + 1 \\ \cos\left(m\omega_s t - \frac{2\pi}{3}\right) & \text{if } m = 3k + 2 \end{cases} \quad (\text{C.131})$$

$$\sin\left(m\omega_s t - \frac{4m\pi}{3}\right) = \begin{cases} \sin(m\omega_s t) & \text{if } m = 3k \\ \sin\left(m\omega_s t + \frac{2\pi}{3}\right) & \text{if } m = 3k + 1 \\ \sin\left(m\omega_s t - \frac{2\pi}{3}\right) & \text{if } m = 3k + 2 \end{cases} \quad (\text{C.132})$$

$$\cos\left((m\omega_s + n\omega_0)t - \frac{2m\pi}{3}\right) = \begin{cases} \cos((m\omega_s + n\omega_0)t) & \text{if } m = 3k \\ \cos\left((m\omega_s + n\omega_0)t - \frac{2\pi}{3}\right) & \text{if } m = 3k + 1 \\ \cos\left((m\omega_s + n\omega_0)t + \frac{2\pi}{3}\right) & \text{if } m = 3k + 2 \end{cases} \quad (\text{C.133})$$

$$\sin\left((m\omega_s + n\omega_0)t - \frac{2m\pi}{3}\right) = \begin{cases} \sin((m\omega_s + n\omega_0)t) & \text{if } m = 3k \\ \sin\left((m\omega_s + n\omega_0)t - \frac{2\pi}{3}\right) & \text{if } m = 3k + 1 \\ \sin\left((m\omega_s + n\omega_0)t + \frac{2\pi}{3}\right) & \text{if } m = 3k + 2 \end{cases} \quad (\text{C.134})$$

$$\cos\left((m\omega_s + n\omega_0)t - \frac{4m\pi}{3}\right) = \begin{cases} \cos((m\omega_s + n\omega_0)t) & \text{if } m = 3k \\ \cos\left((m\omega_s + n\omega_0)t + \frac{2\pi}{3}\right) & \text{if } m = 3k + 1 \\ \cos\left((m\omega_s + n\omega_0)t - \frac{2\pi}{3}\right) & \text{if } m = 3k + 2 \end{cases} \quad (\text{C.135})$$

$$\sin\left((m\omega_s + n\omega_0)t - \frac{4m\pi}{3}\right) = \begin{cases} \sin((m\omega_s + n\omega_0)t) & \text{if } m = 3k \\ \sin\left((m\omega_s + n\omega_0)t + \frac{2\pi}{3}\right) & \text{if } m = 3k + 1 \\ \sin\left((m\omega_s + n\omega_0)t - \frac{2\pi}{3}\right) & \text{if } m = 3k + 2 \end{cases} \quad (\text{C.136})$$

Thus the phasor representation for phase A of 3-cell converter when $m_f = 3k$ is given by Figure C.20.

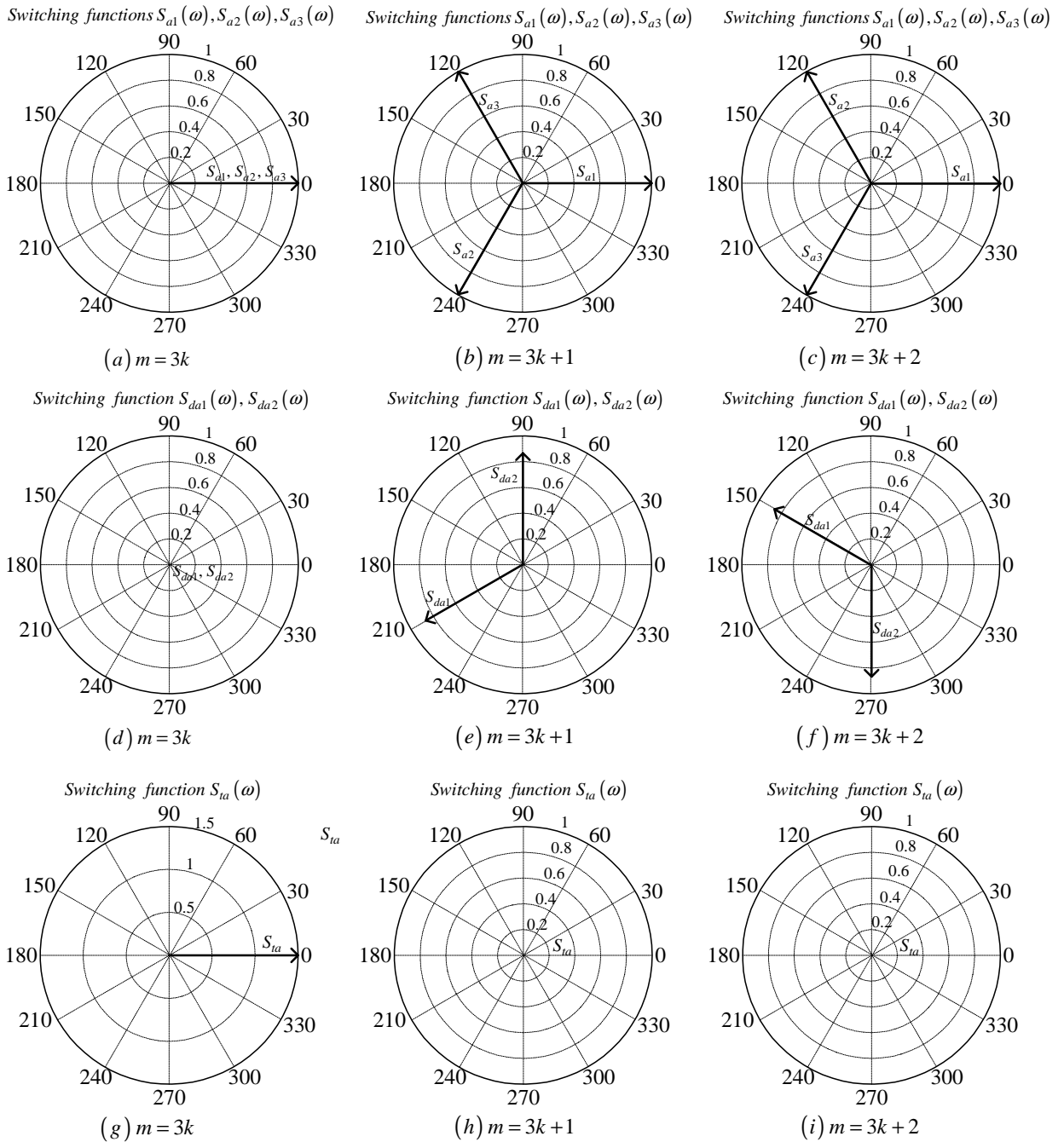


Figure C.20: Phasor representation for phase A of 3-cell converter

Phase B

From table C.2 the value of h for the background function of $s_{b1}(t)$ is given by:

$$h = \frac{2\omega_s}{\pi} t_1 \tag{C.137}$$

Substituting equation C.137 into the term $\frac{m\pi h}{2}$ of equation 3.36 we obtain:

$$\frac{m\pi h}{2} = m\omega_s t_1 \quad (\text{C.138})$$

Now substituting equation C.138 into equation 3.36 we obtain:

$$\begin{aligned} s_{b1}(t_1) &= \frac{1}{2}A_{00} + \sum_{n=1}^{\infty} (A_{0n} \cos(n\omega_0 t_1) + B_{0n} \sin(n\omega_0 t_1)) \\ &\quad + \sum_{m=1}^{\infty} (A_{m0} \cos(m\omega_s t_1) + B_{m0} \sin(m\omega_s t_1)) \\ &\quad + \sum_{m=1}^{\infty} \sum_{n=\pm 1}^{\pm\infty} \{A_{mn} \cos((m\omega_s + n\omega_0) t_1) \\ &\quad + B_{mn} \sin((m\omega_s + n\omega_0) t_1)\} \end{aligned} \quad (\text{C.139})$$

We now substitute back $t = t_1 + \frac{T_0}{3}$ into equation C.139 and obtain:

$$\begin{aligned} s_{b1}(t) &= \frac{1}{2}A_{00} + \sum_{n=1}^{\infty} \left(A_{0n} \cos\left(n\omega_0 \left(t - \frac{2\pi}{3\omega_0}\right)\right) + B_{0n} \sin\left(n\omega_0 \left(t - \frac{2\pi}{3\omega_0}\right)\right) \right) \\ &\quad + \sum_{m=1}^{\infty} \left(A_{m0} \cos\left(m\omega_s \left(t - \frac{2\pi}{3\omega_0}\right)\right) + B_{m0} \sin\left(m\omega_s \left(t - \frac{2\pi}{3\omega_0}\right)\right) \right) \\ &\quad + \sum_{m=1}^{\infty} \sum_{n=\pm 1}^{\pm\infty} \left\{ A_{mn} \cos\left((m\omega_s + n\omega_0) \left(t - \frac{2\pi}{3\omega_0}\right)\right) \right. \\ &\quad \left. + B_{mn} \sin\left((m\omega_s + n\omega_0) \left(t - \frac{2\pi}{3\omega_0}\right)\right) \right\} \end{aligned} \quad (\text{C.140})$$

From table C.2 for the background function of $s_{b2}(t)$ the value of h is given by:

$$h = \frac{2\omega_s}{\pi} t_1 - \frac{4}{3} \quad (\text{C.141})$$

Substituting equation C.141 into the term $\frac{m\pi h}{2}$ of equation 3.36 we obtain:

$$\frac{m\pi h}{2} = m\omega_s t_1 - \frac{2m\pi}{3} \quad (\text{C.142})$$

Now substituting equation C.142 into equation 3.36 we obtain:

$$\begin{aligned} s_{b2}(t_1) &= \frac{1}{2}A_{00} + \sum_{n=1}^{\infty} (A_{0n} \cos(n\omega_0 t_1) + B_{0n} \sin(n\omega_0 t_1)) \\ &\quad + \sum_{m=1}^{\infty} \left(A_{m0} \cos\left(m\omega_s t_1 - \frac{2m\pi}{3}\right) + B_{m0} \sin\left(m\omega_s t_1 - \frac{2m\pi}{3}\right) \right) \\ &\quad + \sum_{m=1}^{\infty} \sum_{n=\pm 1}^{\pm\infty} \left\{ A_{mn} \cos\left((m\omega_s + n\omega_0) t_1 - \frac{2m\pi}{3}\right) \right. \\ &\quad \left. + B_{mn} \sin\left((m\omega_s + n\omega_0) t_1 - \frac{2m\pi}{3}\right) \right\} \end{aligned} \quad (\text{C.143})$$

We now substitute back $t = t_1 + \frac{T_0}{3}$ into equation C.143 and obtain:

$$\begin{aligned}
s_{b2}(t_1) &= \frac{1}{2}A_{00} + \sum_{n=1}^{\infty} \left(A_{0n} \cos \left(n\omega_0 \left(t - \frac{2\pi}{3\omega_0} \right) \right) + B_{0n} \sin \left(n\omega_0 \left(t - \frac{2\pi}{3\omega_0} \right) \right) \right) \\
&+ \sum_{m=1}^{\infty} \left(A_{m0} \cos \left(m\omega_s \left(t - \frac{2\pi}{3\omega_0} \right) - \frac{2m\pi}{3} \right) \right. \\
&+ B_{m0} \sin \left(m\omega_s \left(t - \frac{2\pi}{3\omega_0} \right) - \frac{2m\pi}{3} \right) \\
&+ \sum_{m=1}^{\infty} \sum_{n=\pm 1}^{\pm\infty} \left\{ A_{mn} \cos \left((m\omega_s + n\omega_0) \left(t - \frac{2\pi}{3\omega_0} \right) - \frac{2m\pi}{3} \right) \right. \\
&+ B_{mn} \sin \left. \left((m\omega_s + n\omega_0) \left(t - \frac{2\pi}{3\omega_0} \right) - \frac{2m\pi}{3} \right) \right\}
\end{aligned} \tag{C.144}$$

From table C.2 for the background function of $s_{b3}(t)$ the value of h is given by:

$$h = \frac{2\omega_s}{\pi}t_1 - \frac{8}{3} \tag{C.145}$$

Substituting equation C.145 into the term $\frac{m\pi h}{2}$ of equation 3.36 we obtain:

$$\frac{m\pi h}{2} = m\omega_s t_1 - \frac{4m\pi}{3} \tag{C.146}$$

Now substituting equation C.146 into equation 3.36 we obtain:

$$\begin{aligned}
s_{b3}(t_1) &= \frac{1}{2}A_{00} + \sum_{n=1}^{\infty} (A_{0n} \cos(n\omega_0 t_1) + B_{0n} \sin(n\omega_0 t_1)) \\
&+ \sum_{m=1}^{\infty} \left(A_{m0} \cos \left(m\omega_s t_1 - \frac{4m\pi}{3} \right) + B_{m0} \sin \left(m\omega_s t_1 - \frac{4m\pi}{3} \right) \right) \\
&+ \sum_{m=1}^{\infty} \sum_{n=\pm 1}^{\pm\infty} \left\{ A_{mn} \cos \left((m\omega_s + n\omega_0) t_1 - \frac{4m\pi}{3} \right) \right. \\
&+ B_{mn} \sin \left. \left((m\omega_s + n\omega_0) t_1 - \frac{4m\pi}{3} \right) \right\}
\end{aligned} \tag{C.147}$$

We now substitute back $t = t_1 + \frac{T_0}{3}$ into equation C.147 and obtain:

$$\begin{aligned}
s_{b3}(t) &= \frac{1}{2}A_{00} + \sum_{n=1}^{\infty} \left(A_{0n} \cos \left(n\omega_0 \left(t - \frac{2\pi}{3\omega_0} \right) \right) + B_{0n} \sin \left(n\omega_0 \left(t - \frac{2\pi}{3\omega_0} \right) \right) \right) \\
&+ \sum_{m=1}^{\infty} \left(A_{m0} \cos \left(m\omega_s \left(t - \frac{2\pi}{3\omega_0} \right) - \frac{4m\pi}{3} \right) \right. \\
&+ B_{m0} \sin \left(m\omega_s \left(t - \frac{2\pi}{3\omega_0} \right) - \frac{4m\pi}{3} \right) \\
&+ \sum_{m=1}^{\infty} \sum_{n=\pm 1}^{\pm\infty} \left\{ A_{mn} \cos \left((m\omega_s + n\omega_0) \left(t - \frac{2\pi}{3\omega_0} \right) - \frac{4m\pi}{3} \right) \right. \\
&+ B_{mn} \sin \left. \left((m\omega_s + n\omega_0) \left(t - \frac{2\pi}{3\omega_0} \right) - \frac{4m\pi}{3} \right) \right\}
\end{aligned} \tag{C.148}$$

Now considering trigonometric terms in equation C.140, C.144 and C.148 we have:

$$\begin{aligned} \cos\left(n\omega_0\left(t - \frac{2\pi}{3\omega_0}\right)\right) &= \cos\left(n\omega_0 t - \frac{2n\pi}{3}\right) \\ &= \begin{cases} \cos(n\omega_0 t) & \text{if } n = 3p \\ \cos\left(n\omega_0 t - \frac{2\pi}{3}\right) & \text{if } n = 3p + 1 \\ \cos\left(n\omega_0 t + \frac{2\pi}{3}\right) & \text{if } n = 3p + 2 \end{cases} \end{aligned} \quad (\text{C.149})$$

$$\begin{aligned} \sin\left(n\omega_0\left(t - \frac{2\pi}{3\omega_0}\right)\right) &= \sin\left(n\omega_0 t - \frac{2n\pi}{3}\right) \\ &= \begin{cases} \sin(n\omega_0 t) & \text{if } n = 3p \\ \sin\left(n\omega_0 t - \frac{2\pi}{3}\right) & \text{if } n = 3p + 1 \\ \sin\left(n\omega_0 t + \frac{2\pi}{3}\right) & \text{if } n = 3p + 2 \end{cases} \end{aligned} \quad (\text{C.150})$$

$$\begin{aligned} \cos\left(m\omega_s\left(t - \frac{2\pi}{3\omega_0}\right)\right) &= \cos\left(m\omega_s t - \frac{2m\pi}{3}m_f\right) \\ &= \cos(m\omega_s t) \end{aligned} \quad (\text{C.151})$$

$$\begin{aligned} \sin\left(m\omega_s\left(t - \frac{2\pi}{3\omega_0}\right)\right) &= \sin\left(m\omega_s t - \frac{2m\pi}{3}m_f\right) \\ &= \sin(m\omega_s t) \end{aligned} \quad (\text{C.152})$$

$$\begin{aligned} \cos\left(m\omega_s\left(t - \frac{2\pi}{3\omega_0}\right) - \frac{2m\pi}{3}\right) &= \cos\left(m\omega_s t - \frac{2m\pi}{3}m_f - \frac{2m\pi}{3}\right) \\ &= \begin{cases} \cos(m\omega_s t) & \text{if } m = 3k \\ \cos\left(m\omega_s t - \frac{2\pi}{3}\right) & \text{if } m = 3k + 1 \\ \cos\left(m\omega_s t + \frac{2\pi}{3}\right) & \text{if } m = 3k + 2 \end{cases} \end{aligned} \quad (\text{C.153})$$

$$\begin{aligned} \sin\left(m\omega_s\left(t - \frac{2\pi}{3\omega_0}\right) - \frac{2m\pi}{3}\right) &= \sin\left(m\omega_s t - \frac{2m\pi}{3}m_f - \frac{2m\pi}{3}\right) \\ &= \begin{cases} \sin(m\omega_s t) & \text{if } m = 3k \\ \sin\left(m\omega_s t - \frac{2\pi}{3}\right) & \text{if } m = 3k + 1 \\ \sin\left(m\omega_s t + \frac{2\pi}{3}\right) & \text{if } m = 3k + 2 \end{cases} \end{aligned} \quad (\text{C.154})$$

$$\cos\left(m\omega_s\left(t - \frac{2\pi}{3\omega_0}\right) - \frac{4m\pi}{3}\right) = \begin{cases} \cos(m\omega_s t) & \text{if } m = 3k \\ \cos\left(m\omega_s t + \frac{2\pi}{3}\right) & \text{if } m = 3k + 1 \\ \cos\left(m\omega_s t - \frac{2\pi}{3}\right) & \text{if } m = 3k + 2 \end{cases} \quad (\text{C.155})$$

$$\sin\left(m\omega_s\left(t - \frac{2\pi}{3\omega_0}\right) - \frac{4m\pi}{3}\right) = \begin{cases} \sin(m\omega_s t) & \text{if } m = 3k \\ \sin\left(m\omega_s t + \frac{2\pi}{3}\right) & \text{if } m = 3k + 1 \\ \sin\left(m\omega_s t - \frac{2\pi}{3}\right) & \text{if } m = 3k + 2 \end{cases} \quad (\text{C.156})$$

$$\begin{aligned} & \cos\left((m\omega_s + n\omega_0)\left(t - \frac{2\pi}{3\omega_0}\right)\right) = \cos\left((m\omega_s + n\omega_0)t - \frac{2m\pi}{3}m_f - \frac{2n\pi}{3}\right) \\ = & \begin{cases} \cos((m\omega_s + n\omega_0)t) & \text{if } m = k \text{ and } n=3p \text{ or } n=-3p \\ \cos\left((m\omega_s + n\omega_0)t - \frac{2\pi}{3}\right) & \text{if } m = k \text{ and } n=3p+1 \text{ or } n=-(3p+2) \\ \cos\left((m\omega_s + n\omega_0)t + \frac{2\pi}{3}\right) & \text{if } m = k \text{ and } n=3p+2 \text{ or } n=-(3p+1) \end{cases} \end{aligned} \quad (\text{C.157})$$

$$\begin{aligned} & \sin\left((m\omega_s + n\omega_0)\left(t - \frac{2\pi}{3\omega_0}\right)\right) = \sin\left((m\omega_s + n\omega_0)t - \frac{2m\pi}{3}m_f - \frac{2n\pi}{3}\right) \\ = & \begin{cases} \sin((m\omega_s + n\omega_0)t) & \text{if } m = k \text{ and } n=3p \text{ or } n=-3p \\ \sin\left((m\omega_s + n\omega_0)t - \frac{2\pi}{3}\right) & \text{if } m = k \text{ and } n=3p+1 \text{ or } n=-(3p+2) \\ \sin\left((m\omega_s + n\omega_0)t + \frac{2\pi}{3}\right) & \text{if } m = k \text{ and } n=3p+2 \text{ or } n=-(3p+1) \end{cases} \end{aligned} \quad (\text{C.158})$$

$$\begin{aligned} & \cos\left((m\omega_s + n\omega_0)\left(t - \frac{2\pi}{3\omega_0}\right) - \frac{2m\pi}{3}\right) = \cos\left((m\omega_s + n\omega_0)t - \frac{2m\pi}{3}m_f - \frac{2n\pi}{3} - \frac{2m\pi}{3}\right) \\ = & \begin{cases} \cos((m\omega_s + n\omega_0)t) & \text{if } m = 3k \text{ and } n=3p \text{ or } n=-3p \\ \cos\left((m\omega_s + n\omega_0)t - \frac{2\pi}{3}\right) & \text{if } m = 3k \text{ and } n=3p+1 \text{ or } n=-(3p+2) \\ \cos\left((m\omega_s + n\omega_0)t + \frac{2\pi}{3}\right) & \text{if } m = 3k \text{ and } n=3p+2 \text{ or } n=-(3p+1) \\ \cos\left((m\omega_s + n\omega_0)t - \frac{2\pi}{3}\right) & \text{if } m = 3k + 1 \text{ and } n=3p \text{ or } n=-3p \\ \cos\left((m\omega_s + n\omega_0)t + \frac{2\pi}{3}\right) & \text{if } m = 3k + 1 \text{ and } n=3p+1 \text{ or } n=-(3p+2) \\ \cos((m\omega_s + n\omega_0)t) & \text{if } m = 3k + 1 \text{ and } n=3p+2 \text{ or } n=-(3p+1) \\ \cos\left((m\omega_s + n\omega_0)t + \frac{2\pi}{3}\right) & \text{if } m = 3k + 2 \text{ and } n=3p \text{ or } n=-3p \\ \cos((m\omega_s + n\omega_0)t) & \text{if } m = 3k + 2 \text{ and } n=3p+1 \text{ or } n=-(3p+2) \\ \cos\left((m\omega_s + n\omega_0)t - \frac{2\pi}{3}\right) & \text{if } m = 3k + 2 \text{ and } n=3p+2 \text{ or } n=-(3p+1) \end{cases} \end{aligned} \quad (\text{C.159})$$

$$\sin\left((m\omega_s + n\omega_0)\left(t - \frac{2\pi}{3\omega_0}\right) - \frac{2m\pi}{3}\right) = \sin\left((m\omega_s + n\omega_0)t - \frac{2m\pi}{3}m_f - \frac{2n\pi}{3} - \frac{2m\pi}{3}\right)$$

$$= \begin{cases} \sin((m\omega_s + n\omega_0)t) & \text{if } m = 3k \text{ and } n=3p \text{ or } n=-3p \\ \sin\left((m\omega_s + n\omega_0)t - \frac{2\pi}{3}\right) & \text{if } m = 3k \text{ and } n=3p+1 \text{ or } n=-(3p+2) \\ \sin\left((m\omega_s + n\omega_0)t + \frac{2\pi}{3}\right) & \text{if } m = 3k \text{ and } n=3p+2 \text{ or } n=-(3p+1) \\ \sin\left((m\omega_s + n\omega_0)t - \frac{2\pi}{3}\right) & \text{if } m = 3k + 1 \text{ and } n=3p \text{ or } n=-3p \\ \sin\left((m\omega_s + n\omega_0)t + \frac{2\pi}{3}\right) & \text{if } m = 3k + 1 \text{ and } n=3p+1 \text{ or } n=-(3p+2) \\ \sin((m\omega_s + n\omega_0)t) & \text{if } m = 3k + 1 \text{ and } n=3p+2 \text{ or } n=-(3p+1) \\ \sin\left((m\omega_s + n\omega_0)t + \frac{2\pi}{3}\right) & \text{if } m = 3k + 2 \text{ and } n=3p \text{ or } n=-3p \\ \sin((m\omega_s + n\omega_0)t) & \text{if } m = 3k + 2 \text{ and } n=3p+1 \text{ or } n=-(3p+2) \\ \sin\left((m\omega_s + n\omega_0)t - \frac{2\pi}{3}\right) & \text{if } m = 3k + 2 \text{ and } n=3p+2 \text{ or } n=-(3p+1) \end{cases} \quad (\text{C.160})$$

$$\cos\left((m\omega_s + n\omega_0)\left(t - \frac{2\pi}{3\omega_0}\right) - \frac{4m\pi}{3}\right) = \cos\left((m\omega_s + n\omega_0)t - \frac{2m\pi}{3}m_f - \frac{2n\pi}{3} - \frac{4m\pi}{3}\right)$$

$$= \begin{cases} \cos((m\omega_s + n\omega_0)t) & \text{if } m = 3k \text{ and } n=3p \text{ or } n=-3p \\ \cos\left((m\omega_s + n\omega_0)t - \frac{2\pi}{3}\right) & \text{if } m = 3k \text{ and } n=3p+1 \text{ or } n=-(3p+2) \\ \cos\left((m\omega_s + n\omega_0)t + \frac{2\pi}{3}\right) & \text{if } m = 3k \text{ and } n=3p+2 \text{ or } n=-(3p+1) \\ \cos\left((m\omega_s + n\omega_0)t + \frac{2\pi}{3}\right) & \text{if } m = 3k + 1 \text{ and } n=3p \text{ or } n=-3p \\ \cos((m\omega_s + n\omega_0)t) & \text{if } m = 3k + 1 \text{ and } n=3p+1 \text{ or } n=-(3p+2) \\ \cos\left((m\omega_s + n\omega_0)t - \frac{2\pi}{3}\right) & \text{if } m = 3k + 1 \text{ and } n=3p+2 \text{ or } n=-(3p+1) \\ \cos\left((m\omega_s + n\omega_0)t - \frac{2\pi}{3}\right) & \text{if } m = 3k + 2 \text{ and } n=3p \text{ or } n=-3p \\ \cos\left((m\omega_s + n\omega_0)t + \frac{2\pi}{3}\right) & \text{if } m = 3k + 2 \text{ and } n=3p+1 \text{ or } n=-(3p+2) \\ \cos((m\omega_s + n\omega_0)t) & \text{if } m = 3k + 2 \text{ and } n=3p+2 \text{ or } n=-(3p+1) \end{cases} \quad (\text{C.161})$$

$$\sin\left((m\omega_s + n\omega_0)\left(t - \frac{2\pi}{3\omega_0}\right) - \frac{4m\pi}{3}\right) = \sin\left((m\omega_s + n\omega_0)t - \frac{2m\pi}{3}m_f - \frac{2n\pi}{3} - \frac{4m\pi}{3}\right)$$

$$= \begin{cases} \sin((m\omega_s + n\omega_0)t) & \text{if } m = 3k \text{ and } n=3p \text{ or } n=-3p \\ \sin\left((m\omega_s + n\omega_0)t - \frac{2\pi}{3}\right) & \text{if } m = 3k \text{ and } n=3p+1 \text{ or } n=-(3p+2) \\ \sin\left((m\omega_s + n\omega_0)t + \frac{2\pi}{3}\right) & \text{if } m = 3k \text{ and } n=3p+2 \text{ or } n=-(3p+1) \\ \sin\left((m\omega_s + n\omega_0)t + \frac{2\pi}{3}\right) & \text{if } m = 3k + 1 \text{ and } n=3p \text{ or } n=-3p \\ \sin((m\omega_s + n\omega_0)t) & \text{if } m = 3k + 1 \text{ and } n=3p+1 \text{ or } n=-(3p+2) \\ \sin\left((m\omega_s + n\omega_0)t - \frac{2\pi}{3}\right) & \text{if } m = 3k + 1 \text{ and } n=3p+2 \text{ or } n=-(3p+1) \\ \sin\left((m\omega_s + n\omega_0)t - \frac{2\pi}{3}\right) & \text{if } m = 3k + 2 \text{ and } n=3p \text{ or } n=-3p \\ \sin\left((m\omega_s + n\omega_0)t + \frac{2\pi}{3}\right) & \text{if } m = 3k + 2 \text{ and } n=3p+1 \text{ or } n=-(3p+2) \\ \sin((m\omega_s + n\omega_0)t) & \text{if } m = 3k + 2 \text{ and } n=3p+2 \text{ or } n=-(3p+1) \end{cases} \quad (\text{C.162})$$

Thus the phasor representation for phase B of 3-cell converter when $m_f = 3k$ is given by Figures C.21, C.22 and C.23.

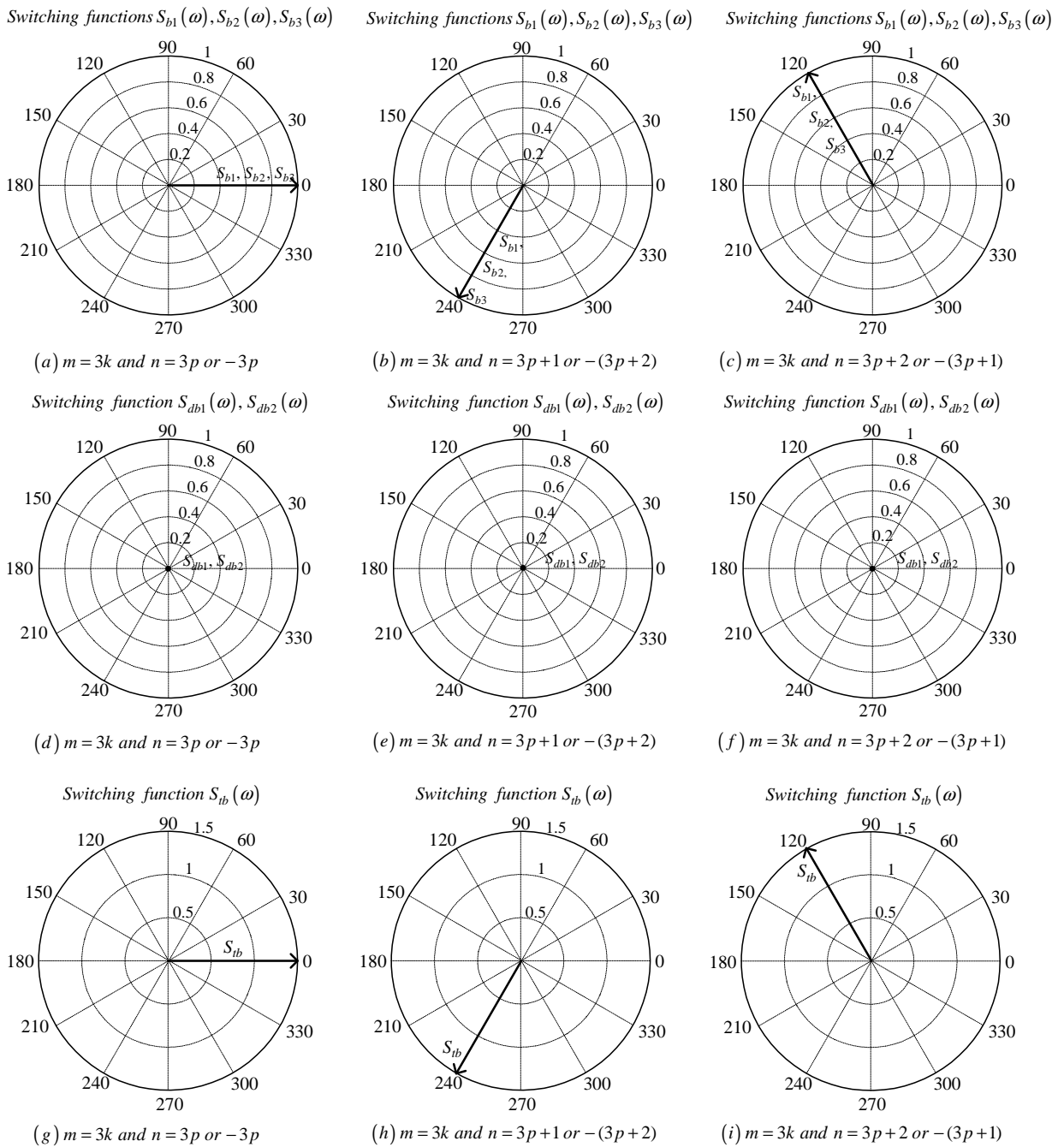


Figure C.21: Phasor representation for phase B of 3-cell converter for $m = 3k$

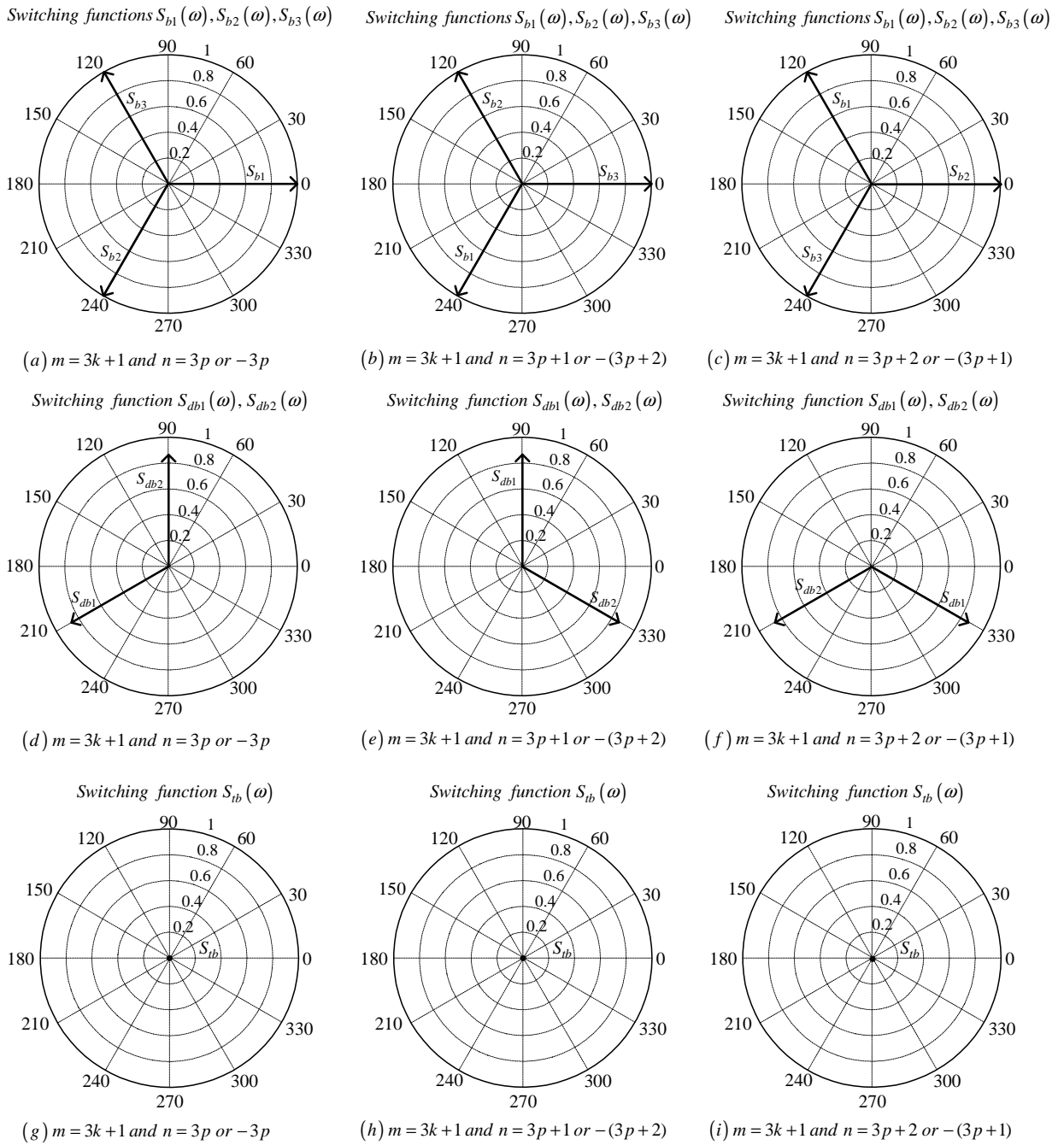


Figure C.22: Phasor representation for phase B of 3-cell converter for $m = 3k + 1$

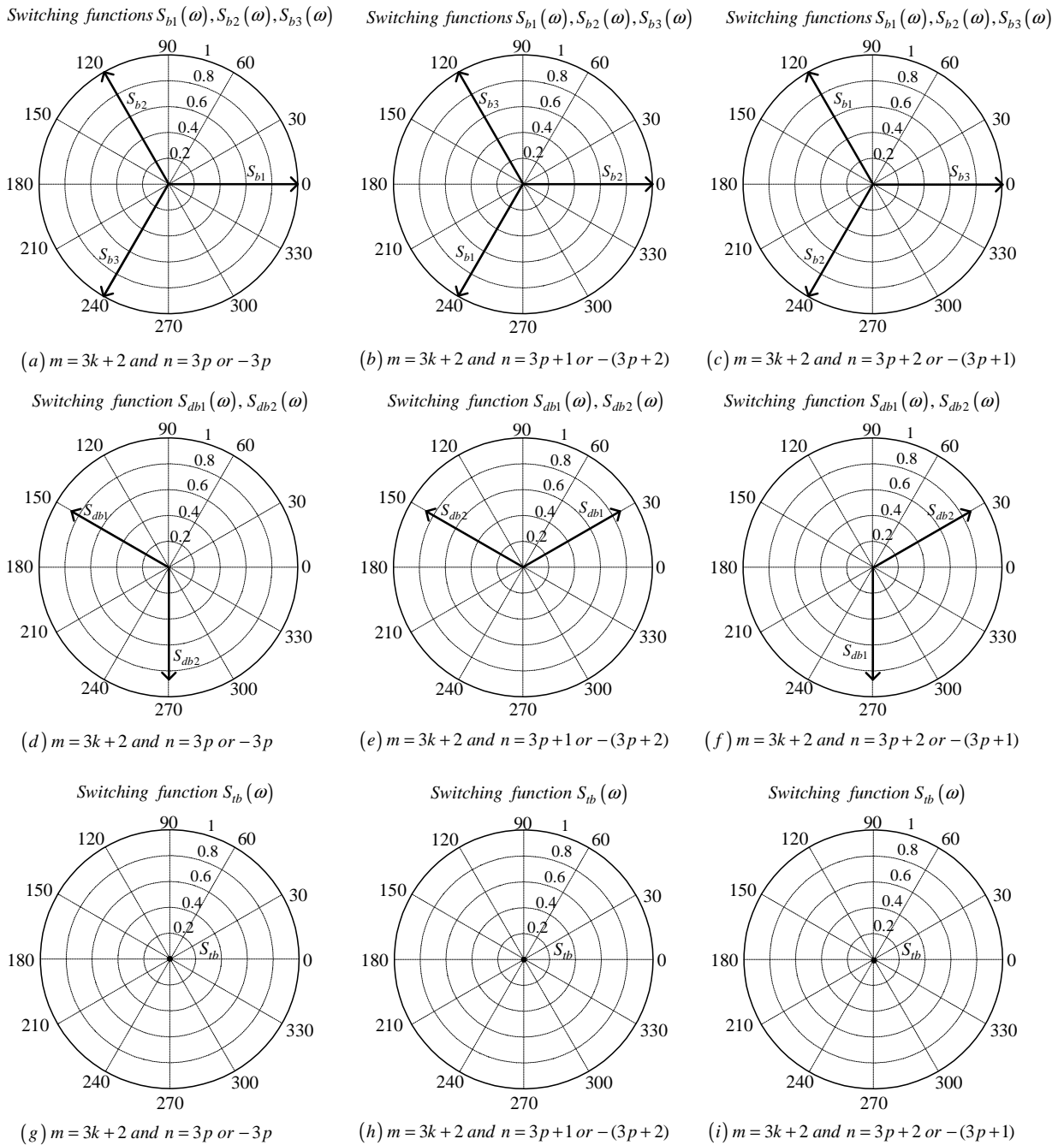


Figure C.23: Phasor representation for phase B of 3-cell converter for $m = 3k + 2$

Phase C

From table C.2 the value of h for the background function of $s_{c1}(t)$ is given by:

$$h = \frac{2\omega_s}{\pi}t_2 \quad (\text{C.163})$$

Substituting equation C.163 into the term $\frac{m\pi h}{2}$ of equation 3.36 we obtain:

$$\frac{m\pi h}{2} = m\omega_s t_2 \quad (\text{C.164})$$

Now substituting equation C.164 into equation 3.36 we obtain:

$$\begin{aligned} s_{c1}(t_2) &= \frac{1}{2}A_{00} + \sum_{n=1}^{\infty} (A_{0n} \cos(n\omega_0 t_2) + B_{0n} \sin(n\omega_0 t_2)) \\ &\quad + \sum_{m=1}^{\infty} (A_{m0} \cos(m\omega_s t_2) + B_{m0} \sin(m\omega_s t_2)) \\ &\quad + \sum_{m=1}^{\infty} \sum_{n=\pm 1}^{\pm\infty} \{A_{mn} \cos((m\omega_s + n\omega_0)t_2) \\ &\quad + B_{mn} \sin((m\omega_s + n\omega_0)t_2)\} \end{aligned} \quad (\text{C.165})$$

We now substitute back $t = t_2 + \frac{2T_0}{3}$ into equation C.165 and obtain:

$$\begin{aligned} s_{c1}(t) &= \frac{1}{2}A_{00} + \sum_{n=1}^{\infty} \left(A_{0n} \cos\left(n\omega_0 \left(t - \frac{4\pi}{3\omega_0}\right)\right) + B_{0n} \sin\left(n\omega_0 \left(t - \frac{4\pi}{3\omega_0}\right)\right) \right) \\ &\quad + \sum_{m=1}^{\infty} \left(A_{m0} \cos\left(m\omega_s \left(t - \frac{4\pi}{3\omega_0}\right)\right) + B_{m0} \sin\left(m\omega_s \left(t - \frac{4\pi}{3\omega_0}\right)\right) \right) \\ &\quad + \sum_{m=1}^{\infty} \sum_{n=\pm 1}^{\pm\infty} \left\{ A_{mn} \cos\left((m\omega_s + n\omega_0) \left(t - \frac{4\pi}{3\omega_0}\right)\right) \right. \\ &\quad \left. + B_{mn} \sin\left((m\omega_s + n\omega_0) \left(t - \frac{4\pi}{3\omega_0}\right)\right) \right\} \end{aligned} \quad (\text{C.166})$$

From table C.2 for the background function of $s_{c2}(t)$ the value of h is given by:

$$h = \frac{2\omega_s}{\pi}t_2 - \frac{4}{3} \quad (\text{C.167})$$

Substituting equation C.167 into the term $\frac{m\pi h}{2}$ of equation 3.36 we obtain:

$$\frac{m\pi h}{2} = m\omega_s t_2 - \frac{2m\pi}{3} \quad (\text{C.168})$$

Now substituting equation C.168 into equation 3.36 we obtain:

$$\begin{aligned}
s_{c2}(t_2) &= \frac{1}{2}A_{00} + \sum_{n=1}^{\infty} (A_{0n} \cos(n\omega_0 t_2) + B_{0n} \sin(n\omega_0 t_2)) \\
&+ \sum_{m=1}^{\infty} \left(A_{m0} \cos\left(m\omega_s t_2 - \frac{2m\pi}{3}\right) + B_{m0} \sin\left(m\omega_s t_2 - \frac{2m\pi}{3}\right) \right) \\
&+ \sum_{m=1}^{\infty} \sum_{n=\pm 1}^{\pm\infty} \left\{ A_{mn} \cos\left((m\omega_s + n\omega_0) t_2 - \frac{2m\pi}{3}\right) \right. \\
&\quad \left. + B_{mn} \sin\left((m\omega_s + n\omega_0) t_2 - \frac{2m\pi}{3}\right) \right\}
\end{aligned} \tag{C.169}$$

We now substitute back $t = t_2 + \frac{2T_0}{3}$ into equation C.169 and obtain:

$$\begin{aligned}
s_{c2}(t) &= \frac{1}{2}A_{00} + \sum_{n=1}^{\infty} \left(A_{0n} \cos\left(n\omega_0 \left(t - \frac{4\pi}{3\omega_0}\right)\right) + B_{0n} \sin\left(n\omega_0 \left(t - \frac{4\pi}{3\omega_0}\right)\right) \right) \\
&+ \sum_{m=1}^{\infty} \left(A_{m0} \cos\left(m\omega_s \left(t - \frac{4\pi}{3\omega_0}\right) - \frac{2m\pi}{3}\right) + B_{m0} \sin\left(m\omega_s \left(t - \frac{4\pi}{3\omega_0}\right) - \frac{2m\pi}{3}\right) \right) \\
&+ \sum_{m=1}^{\infty} \sum_{n=\pm 1}^{\pm\infty} \left\{ A_{mn} \cos\left((m\omega_s + n\omega_0) \left(t - \frac{4\pi}{3\omega_0}\right) - \frac{2m\pi}{3}\right) \right. \\
&\quad \left. + B_{mn} \sin\left((m\omega_s + n\omega_0) \left(t - \frac{4\pi}{3\omega_0}\right) - \frac{2m\pi}{3}\right) \right\}
\end{aligned} \tag{C.170}$$

From table C.2 for the background function of $s_{c3}(t)$ the value of h is given by:

$$h = \frac{2\omega_s}{\pi} t_2 - \frac{8}{3} \tag{C.171}$$

Substituting equation C.171 into the term $\frac{m\pi h}{2}$ of equation 3.36 we obtain:

$$\frac{m\pi h}{2} = m\omega_s t_2 - \frac{4m\pi}{3} \tag{C.172}$$

Now substituting equation C.172 into equation 3.36 we obtain:

$$\begin{aligned}
s_{c3}(t_2) &= \frac{1}{2}A_{00} + \sum_{n=1}^{\infty} (A_{0n} \cos(n\omega_0 t_2) + B_{0n} \sin(n\omega_0 t_2)) \\
&+ \sum_{m=1}^{\infty} \left(A_{m0} \cos\left(m\omega_s t_2 - \frac{4m\pi}{3}\right) + B_{m0} \sin\left(m\omega_s t_2 - \frac{4m\pi}{3}\right) \right) \\
&+ \sum_{m=1}^{\infty} \sum_{n=\pm 1}^{\pm\infty} \left\{ A_{mn} \cos\left((m\omega_s + n\omega_0) t_2 - \frac{4m\pi}{3}\right) \right. \\
&\quad \left. + B_{mn} \sin\left((m\omega_s + n\omega_0) t_2 - \frac{4m\pi}{3}\right) \right\}
\end{aligned} \tag{C.173}$$

We now substitute back $t = t_2 + \frac{2T_0}{3}$ into equation C.173 and obtain:

$$\begin{aligned}
s_{c3}(t) &= \frac{1}{2}A_{00} + \sum_{n=1}^{\infty} \left(A_{0n} \cos \left(n\omega_0 \left(t - \frac{4\pi}{3\omega_0} \right) \right) + B_{0n} \sin \left(n\omega_0 \left(t - \frac{4\pi}{3\omega_0} \right) \right) \right) \\
&+ \sum_{m=1}^{\infty} \left(A_{m0} \cos \left(m\omega_s \left(t - \frac{4\pi}{3\omega_0} \right) - \frac{4m\pi}{3} \right) + B_{m0} \sin \left(m\omega_s \left(t - \frac{4\pi}{3\omega_0} \right) - \frac{4m\pi}{3} \right) \right) \\
&+ \sum_{m=1}^{\infty} \sum_{n=\pm 1}^{\pm \infty} \left\{ A_{mn} \cos \left((m\omega_s + n\omega_0) \left(t - \frac{4\pi}{3\omega_0} \right) - \frac{4m\pi}{3} \right) \right. \\
&\left. + B_{mn} \sin \left((m\omega_s + n\omega_0) \left(t - \frac{4\pi}{3\omega_0} \right) - \frac{4m\pi}{3} \right) \right\} \tag{C.174}
\end{aligned}$$

Now considering trigonometric terms in equation C.166, C.170 and C.174 we have:

$$\begin{aligned}
\cos \left(n\omega_0 \left(t - \frac{4\pi}{3\omega_0} \right) \right) &= \cos \left(n\omega_0 t - \frac{4n\pi}{3} \right) \\
&= \begin{cases} \cos(n\omega_0 t) & \text{if } n = 3p \\ \cos \left(n\omega_0 t + \frac{2\pi}{3} \right) & \text{if } n = 3p + 1 \\ \cos \left(n\omega_0 t - \frac{2\pi}{3} \right) & \text{if } n = 3p + 2 \end{cases} \tag{C.175}
\end{aligned}$$

$$\begin{aligned}
\sin \left(n\omega_0 \left(t - \frac{4\pi}{3\omega_0} \right) \right) &= \sin \left(n\omega_0 t - \frac{4n\pi}{3} \right) \\
&= \begin{cases} \sin(n\omega_0 t) & \text{if } n = 3p \\ \sin \left(n\omega_0 t + \frac{2\pi}{3} \right) & \text{if } n = 3p + 1 \\ \sin \left(n\omega_0 t - \frac{2\pi}{3} \right) & \text{if } n = 3p + 2 \end{cases} \tag{C.176}
\end{aligned}$$

$$\begin{aligned}
\cos \left(m\omega_s \left(t - \frac{4\pi}{3\omega_0} \right) \right) &= \cos \left(m\omega_s t - \frac{4m\pi}{3} m_f \right) \\
&= \cos(m\omega_s t) \tag{C.177}
\end{aligned}$$

$$\begin{aligned}
\sin \left(m\omega_s \left(t - \frac{4\pi}{3\omega_0} \right) \right) &= \sin \left(m\omega_s t - \frac{4m\pi}{3} m_f \right) \\
&= \sin(m\omega_s t) \tag{C.178}
\end{aligned}$$

$$\begin{aligned}
\cos \left(m\omega_s \left(t - \frac{4\pi}{3\omega_0} \right) - \frac{2m\pi}{3} \right) &= \cos \left(m\omega_s t - \frac{4m\pi}{3} m_f - \frac{2m\pi}{3} \right) \\
&= \begin{cases} \cos(m\omega_s t) & \text{if } m = 3k \\ \cos \left(m\omega_s t - \frac{2\pi}{3} \right) & \text{if } m = 3k + 1 \\ \cos \left(m\omega_s t + \frac{2\pi}{3} \right) & \text{if } m = 3k + 2 \end{cases} \tag{C.179}
\end{aligned}$$

$$\begin{aligned} \sin\left(m\omega_s\left(t - \frac{4\pi}{3\omega_0}\right) - \frac{2m\pi}{3}\right) &= \sin\left(m\omega_s t - \frac{4m\pi}{3}m_f - \frac{2m\pi}{3}\right) \\ &= \begin{cases} \sin(m\omega_s t) & \text{if } m = 3k \\ \sin\left(m\omega_s t - \frac{2\pi}{3}\right) & \text{if } m = 3k + 1 \\ \sin\left(m\omega_s t + \frac{2\pi}{3}\right) & \text{if } m = 3k + 2 \end{cases} \end{aligned} \quad (\text{C.180})$$

$$\cos\left(m\omega_s\left(t - \frac{4\pi}{3\omega_0}\right) - \frac{4m\pi}{3}\right) = \begin{cases} \cos(m\omega_s t) & \text{if } m = 3k \\ \cos\left(m\omega_s t + \frac{2\pi}{3}\right) & \text{if } m = 3k + 1 \\ \cos\left(m\omega_s t - \frac{2\pi}{3}\right) & \text{if } m = 3k + 2 \end{cases} \quad (\text{C.181})$$

$$\sin\left(m\omega_s\left(t - \frac{4\pi}{3\omega_0}\right) - \frac{4m\pi}{3}\right) = \begin{cases} \sin(m\omega_s t) & \text{if } m = 3k \\ \sin\left(m\omega_s t + \frac{2\pi}{3}\right) & \text{if } m = 3k + 1 \\ \sin\left(m\omega_s t - \frac{2\pi}{3}\right) & \text{if } m = 3k + 2 \end{cases} \quad (\text{C.182})$$

$$\begin{aligned} \cos\left((m\omega_s + n\omega_0)\left(t - \frac{4\pi}{3\omega_0}\right)\right) &= \cos\left((m\omega_s + n\omega_0)t - \frac{4m\pi}{3}m_f - \frac{4n\pi}{3}\right) \\ &= \begin{cases} \cos((m\omega_s + n\omega_0)t) & \text{if } m = k \text{ and } n=3p \text{ or } n=-3p \\ \cos\left((m\omega_s + n\omega_0)t + \frac{2\pi}{3}\right) & \text{if } m = k \text{ and } n=3p+1 \text{ or } n=-(3p+2) \\ \cos\left((m\omega_s + n\omega_0)t - \frac{2\pi}{3}\right) & \text{if } m = k \text{ and } n=3p+2 \text{ or } n=-(3p+1) \end{cases} \end{aligned} \quad (\text{C.183})$$

$$\begin{aligned} \sin\left((m\omega_s + n\omega_0)\left(t - \frac{4\pi}{3\omega_0}\right)\right) &= \sin\left((m\omega_s + n\omega_0)t - \frac{4m\pi}{3}m_f - \frac{4n\pi}{3}\right) \\ &= \begin{cases} \sin((m\omega_s + n\omega_0)t) & \text{if } m = k \text{ and } n=3p \text{ or } n=-3p \\ \sin\left((m\omega_s + n\omega_0)t + \frac{2\pi}{3}\right) & \text{if } m = k \text{ and } n=3p+1 \text{ or } n=-(3p+2) \\ \sin\left((m\omega_s + n\omega_0)t - \frac{2\pi}{3}\right) & \text{if } m = k \text{ and } n=3p+2 \text{ or } n=-(3p+1) \end{cases} \end{aligned} \quad (\text{C.184})$$

$$\begin{aligned} \cos\left((m\omega_s + n\omega_0)\left(t - \frac{4\pi}{3\omega_0}\right) - \frac{2m\pi}{3}\right) &= \cos\left((m\omega_s + n\omega_0)t - \frac{4m\pi}{3}m_f - \frac{4n\pi}{3} - \frac{2m\pi}{3}\right) \\ &= \begin{cases} \cos((m\omega_s + n\omega_0)t) & \text{if } m = 3k \text{ and } n=3p \text{ or } n=-3p \\ \cos\left((m\omega_s + n\omega_0)t + \frac{2\pi}{3}\right) & \text{if } m = 3k \text{ and } n=3p+1 \text{ or } n=-(3p+2) \\ \cos\left((m\omega_s + n\omega_0)t - \frac{2\pi}{3}\right) & \text{if } m = 3k \text{ and } n=3p+2 \text{ or } n=-(3p+1) \\ \cos\left((m\omega_s + n\omega_0)t - \frac{2\pi}{3}\right) & \text{if } m = 3k + 1 \text{ and } n=3p \text{ or } n=-3p \\ \cos((m\omega_s + n\omega_0)t) & \text{if } m = 3k + 1 \text{ and } n=3p+1 \text{ or } n=-(3p+2) \\ \cos\left((m\omega_s + n\omega_0)t + \frac{2\pi}{3}\right) & \text{if } m = 3k + 1 \text{ and } n=3p+2 \text{ or } n=-(3p+1) \\ \cos\left((m\omega_s + n\omega_0)t + \frac{2\pi}{3}\right) & \text{if } m = 3k + 2 \text{ and } n=3p \text{ or } n=-3p \\ \cos\left((m\omega_s + n\omega_0)t - \frac{2\pi}{3}\right) & \text{if } m = 3k + 2 \text{ and } n=3p+1 \text{ or } n=-(3p+2) \\ \cos((m\omega_s + n\omega_0)t) & \text{if } m = 3k + 2 \text{ and } n=3p+2 \text{ or } n=-(3p+1) \end{cases} \end{aligned}$$

(C.185)

$$\begin{aligned} & \sin \left((m\omega_s + n\omega_0) \left(t - \frac{4\pi}{3\omega_0} \right) - \frac{2m\pi}{3} \right) = \sin \left((m\omega_s + n\omega_0) t - \frac{4m\pi}{3} m_f - \frac{4n\pi}{3} - \frac{2m\pi}{3} \right) \\ = & \begin{cases} \sin((m\omega_s + n\omega_0)t) & \text{if } m = 3k \text{ and } n=3p \text{ or } n=-3p \\ \sin\left((m\omega_s + n\omega_0)t + \frac{2\pi}{3}\right) & \text{if } m = 3k \text{ and } n=3p+1 \text{ or } n=-(3p+2) \\ \sin\left((m\omega_s + n\omega_0)t - \frac{2\pi}{3}\right) & \text{if } m = 3k \text{ and } n=3p+2 \text{ or } n=-(3p+1) \\ \sin\left((m\omega_s + n\omega_0)t - \frac{2\pi}{3}\right) & \text{if } m = 3k + 1 \text{ and } n=3p \text{ or } n=-3p \\ \sin((m\omega_s + n\omega_0)t) & \text{if } m = 3k + 1 \text{ and } n=3p+1 \text{ or } n=-(3p+2) \\ \sin\left((m\omega_s + n\omega_0)t + \frac{2\pi}{3}\right) & \text{if } m = 3k + 1 \text{ and } n=3p+2 \text{ or } n=-(3p+1) \\ \sin\left((m\omega_s + n\omega_0)t + \frac{2\pi}{3}\right) & \text{if } m = 3k + 2 \text{ and } n=3p \text{ or } n=-3p \\ \sin\left((m\omega_s + n\omega_0)t - \frac{2\pi}{3}\right) & \text{if } m = 3k + 2 \text{ and } n=3p+1 \text{ or } n=-(3p+2) \\ \sin((m\omega_s + n\omega_0)t) & \text{if } m = 3k + 2 \text{ and } n=3p+2 \text{ or } n=-(3p+1) \end{cases} \end{aligned} \quad (\text{C.186})$$

$$\begin{aligned} & \cos \left((m\omega_s + n\omega_0) \left(t - \frac{4\pi}{3\omega_0} \right) - \frac{4m\pi}{3} \right) = \cos \left((m\omega_s + n\omega_0) t - \frac{4m\pi}{3} m_f - \frac{4n\pi}{3} - \frac{4m\pi}{3} \right) \\ = & \begin{cases} \cos((m\omega_s + n\omega_0)t) & \text{if } m = 3k \text{ and } n=3p \text{ or } n=-3p \\ \cos\left((m\omega_s + n\omega_0)t + \frac{2\pi}{3}\right) & \text{if } m = 3k \text{ and } n=3p+1 \text{ or } n=-(3p+2) \\ \cos\left((m\omega_s + n\omega_0)t - \frac{2\pi}{3}\right) & \text{if } m = 3k \text{ and } n=3p+2 \text{ or } n=-(3p+1) \\ \cos\left((m\omega_s + n\omega_0)t + \frac{2\pi}{3}\right) & \text{if } m = 3k + 1 \text{ and } n=3p \text{ or } n=-3p \\ \cos\left((m\omega_s + n\omega_0)t - \frac{2\pi}{3}\right) & \text{if } m = 3k + 1 \text{ and } n=3p+1 \text{ or } n=-(3p+2) \\ \cos((m\omega_s + n\omega_0)t) & \text{if } m = 3k + 1 \text{ and } n=3p+2 \text{ or } n=-(3p+1) \\ \cos\left((m\omega_s + n\omega_0)t - \frac{2\pi}{3}\right) & \text{if } m = 3k + 2 \text{ and } n=3p \text{ or } n=-3p \\ \cos((m\omega_s + n\omega_0)t) & \text{if } m = 3k + 2 \text{ and } n=3p+1 \text{ or } n=-(3p+2) \\ \cos\left((m\omega_s + n\omega_0)t + \frac{2\pi}{3}\right) & \text{if } m = 3k + 2 \text{ and } n=3p+2 \text{ or } n=-(3p+1) \end{cases} \end{aligned} \quad (\text{C.187})$$

$$\begin{aligned}
& \sin \left((m\omega_s + n\omega_0) \left(t - \frac{4\pi}{3\omega_0} \right) - \frac{4m\pi}{3} \right) = \sin \left((m\omega_s + n\omega_0) t - \frac{4m\pi}{3} m_f - \frac{4n\pi}{3} - \frac{4m\pi}{3} \right) \\
= & \begin{cases} \sin((m\omega_s + n\omega_0)t) & \text{if } m = 3k \text{ and } n=3p \text{ or } n=-3p \\ \sin\left((m\omega_s + n\omega_0)t + \frac{2\pi}{3}\right) & \text{if } m = 3k \text{ and } n=3p+1 \text{ or } n=-(3p+2) \\ \sin\left((m\omega_s + n\omega_0)t - \frac{2\pi}{3}\right) & \text{if } m = 3k \text{ and } n=3p+2 \text{ or } n=-(3p+1) \\ \sin\left((m\omega_s + n\omega_0)t + \frac{2\pi}{3}\right) & \text{if } m = 3k + 1 \text{ and } n=3p \text{ or } n=-3p \\ \sin\left((m\omega_s + n\omega_0)t - \frac{2\pi}{3}\right) & \text{if } m = 3k + 1 \text{ and } n=3p+1 \text{ or } n=-(3p+2) \\ \sin((m\omega_s + n\omega_0)t) & \text{if } m = 3k + 1 \text{ and } n=3p+2 \text{ or } n=-(3p+1) \\ \sin\left((m\omega_s + n\omega_0)t - \frac{2\pi}{3}\right) & \text{if } m = 3k + 2 \text{ and } n=3p \text{ or } n=-3p \\ \sin((m\omega_s + n\omega_0)t) & \text{if } m = 3k + 2 \text{ and } n=3p+1 \text{ or } n=-(3p+2) \\ \sin\left((m\omega_s + n\omega_0)t + \frac{2\pi}{3}\right) & \text{if } m = 3k + 2 \text{ and } n=3p+2 \text{ or } n=-(3p+1) \end{cases}
\end{aligned} \tag{C.188}$$

Thus the phasor representation for phase C of 3-cell converter when $m_f = 3k$ is given by Figures C.24, C.25 and C.26.

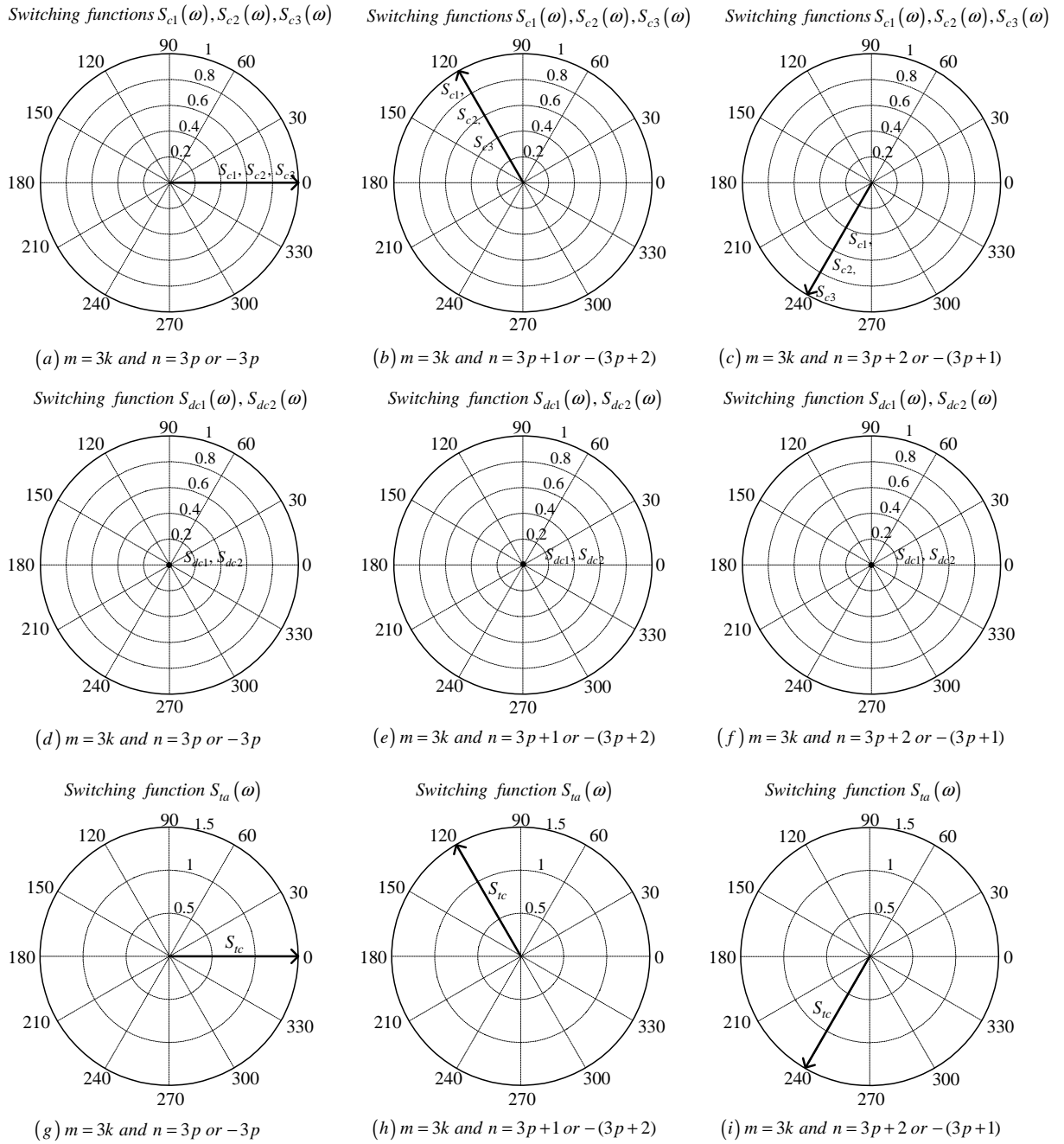


Figure C.24: Phasor representation for phase C of 3-cell converter for $m = 3k$

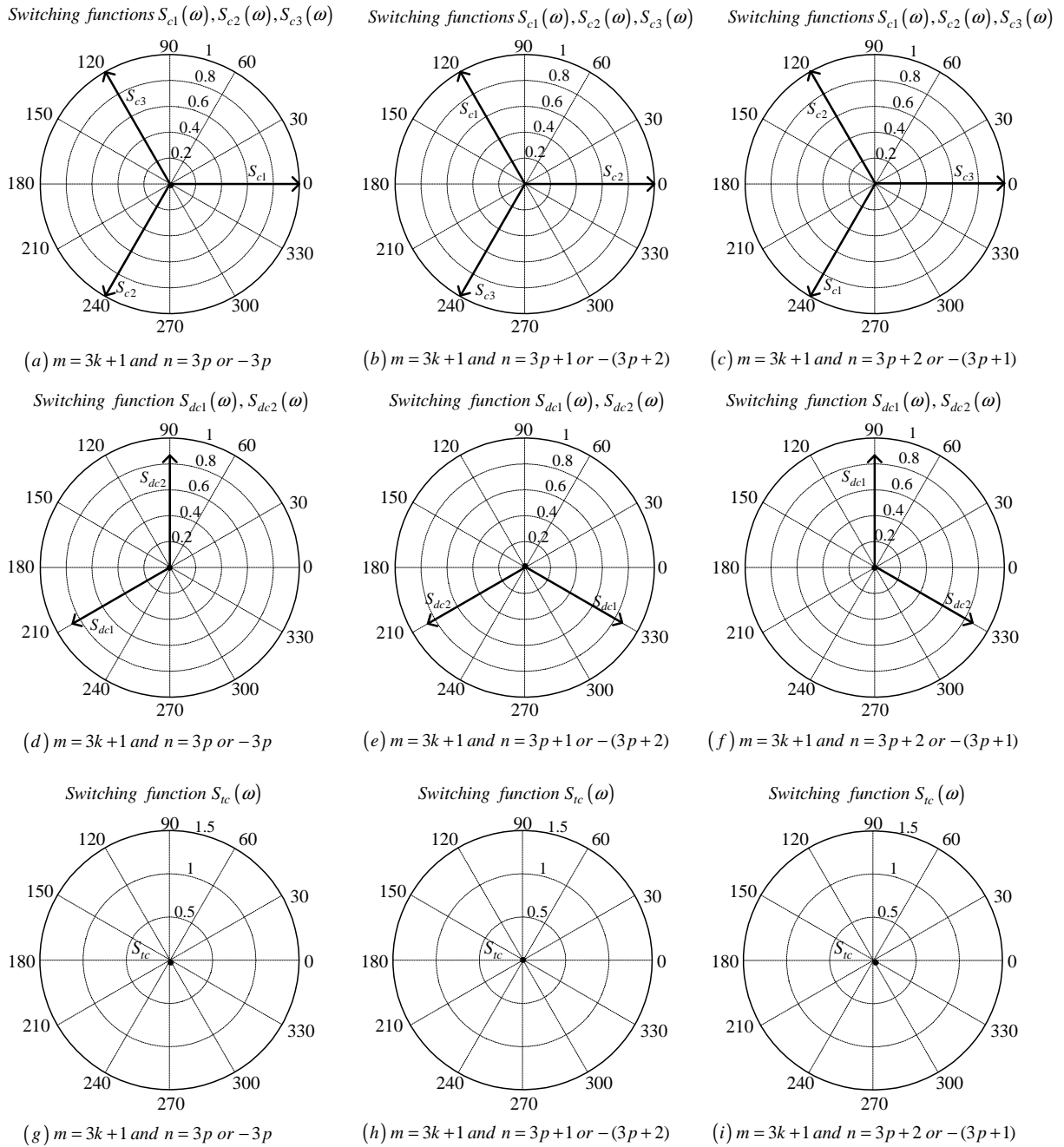


Figure C.25: Phasor representation for phase C of 3-cell converter for $m = 3k + 1$

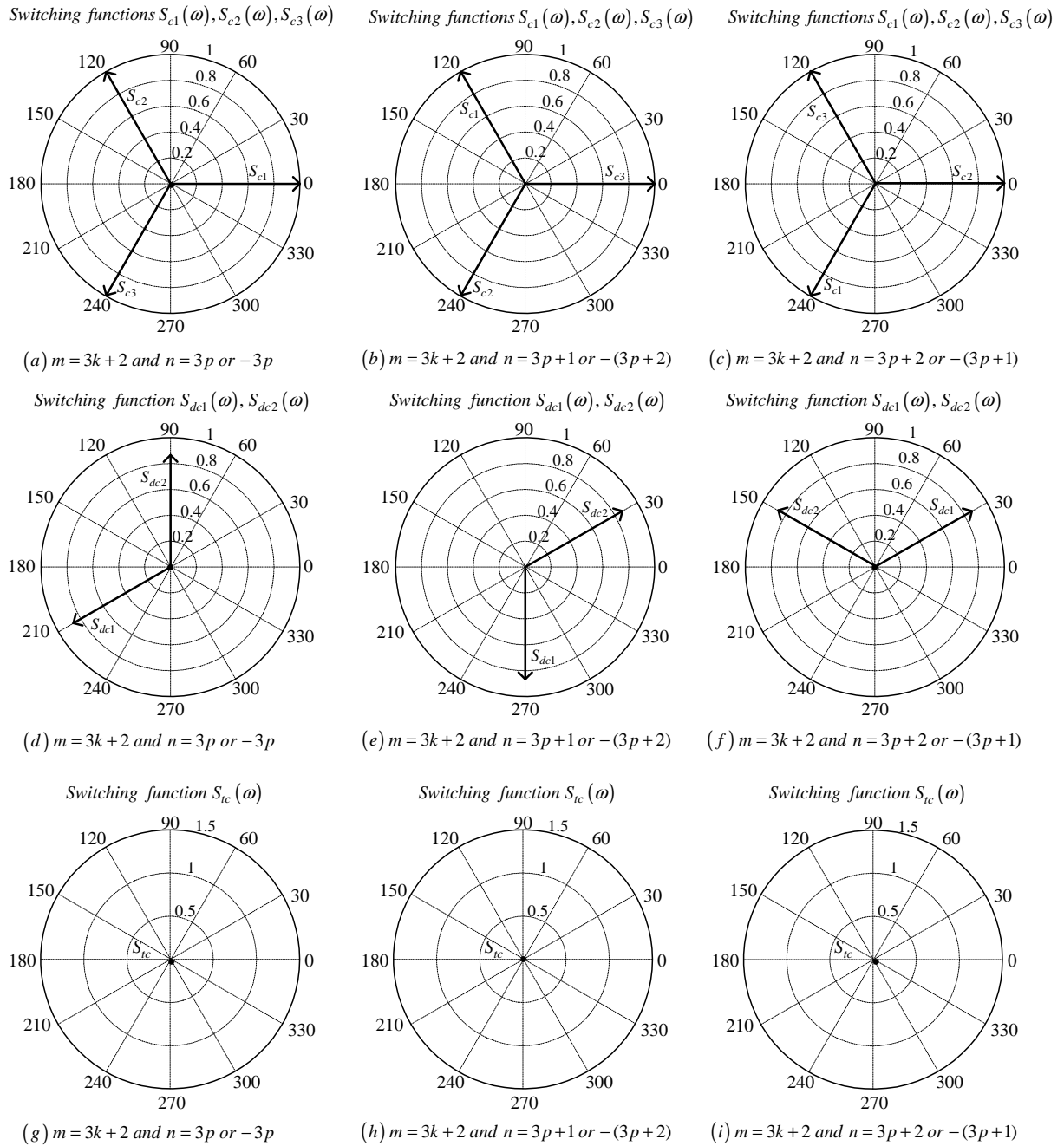


Figure C.26: Phasor representation for phase C of 3-cell converter for $m = 3k + 2$

C.2.2 For frequency modulation index $m_f = 3k + 1$

Phase A

Derivation for switching functions of phase A are the same as in subsection C.2.1 for $m_f = 3k$.

Phase B

From table C.2 the value of h for the background function of $s_{b1}(t)$ is given by:

$$h = \frac{2\omega_s}{\pi}t_1 - \frac{8}{3} \quad (\text{C.189})$$

Substituting equation C.189 into the term $\frac{m\pi h}{2}$ of equation 3.36 we obtain:

$$\frac{m\pi h}{2} = m\omega_s t_1 - \frac{4}{3}m\pi \quad (\text{C.190})$$

Now substituting equation C.190 into equation 3.36 we obtain:

$$\begin{aligned} s_{b1}(t_1) &= \frac{1}{2}A_{00} + \sum_{n=1}^{\infty} (A_{0n} \cos(n\omega_0 t_1) + B_{0n} \sin(n\omega_0 t_1)) \\ &+ \sum_{m=1}^{\infty} \left(A_{m0} \cos\left(m\omega_s t_1 - \frac{4}{3}m\pi\right) + B_{m0} \sin\left(m\omega_s t_1 - \frac{4}{3}m\pi\right) \right) \\ &+ \sum_{m=1}^{\infty} \sum_{n=\pm 1}^{\pm\infty} \left\{ A_{mn} \cos\left((m\omega_s + n\omega_0)t_1 - \frac{4}{3}m\pi\right) \right. \\ &\quad \left. + B_{mn} \sin\left((m\omega_s + n\omega_0)t_1 - \frac{4}{3}m\pi\right) \right\} \end{aligned} \quad (\text{C.191})$$

We now substitute back $t = t_1 + \frac{T_0}{3}$ into equation C.191 and obtain:

$$\begin{aligned} s_{b1}(t) &= \frac{1}{2}A_{00} + \sum_{n=1}^{\infty} \left(A_{0n} \cos\left(n\omega_0 \left(t - \frac{2\pi}{3\omega_0}\right)\right) + B_{0n} \sin\left(n\omega_0 \left(t - \frac{2\pi}{3\omega_0}\right)\right) \right) \\ &+ \sum_{m=1}^{\infty} \left(A_{m0} \cos\left(m\omega_s \left(t - \frac{2\pi}{3\omega_0}\right) - \frac{4}{3}m\pi\right) \right. \\ &\quad \left. + B_{m0} \sin\left(m\omega_s \left(t - \frac{2\pi}{3\omega_0}\right) - \frac{4}{3}m\pi\right) \right) \\ &+ \sum_{m=1}^{\infty} \sum_{n=\pm 1}^{\pm\infty} \left\{ A_{mn} \cos\left((m\omega_s + n\omega_0) \left(t - \frac{2\pi}{3\omega_0}\right) - \frac{4}{3}m\pi\right) \right. \\ &\quad \left. + B_{mn} \sin\left((m\omega_s + n\omega_0) \left(t - \frac{2\pi}{3\omega_0}\right) - \frac{4}{3}m\pi\right) \right\} \end{aligned} \quad (\text{C.192})$$

From table C.2 for the background function of $s_{b2}(t)$ the value of h is given by:

$$h = \frac{2\omega_s}{\pi}t_1 \quad (\text{C.193})$$

Substituting equation C.193 into the term $\frac{m\pi h}{2}$ of equation 3.36 we obtain:

$$\frac{m\pi h}{2} = m\omega_s t_1 \quad (\text{C.194})$$

Now substituting equation C.194 into equation 3.36 we obtain:

$$\begin{aligned} s_{b2}(t_1) &= \frac{1}{2}A_{00} + \sum_{n=1}^{\infty} (A_{0n} \cos(n\omega_0 t_1) + B_{0n} \sin(n\omega_0 t_1)) \\ &\quad + \sum_{m=1}^{\infty} (A_{m0} \cos(m\omega_s t_1) + B_{m0} \sin(m\omega_s t_1)) \\ &\quad + \sum_{m=1}^{\infty} \sum_{n=\pm 1}^{\pm\infty} \{A_{mn} \cos((m\omega_s + n\omega_0) t_1) \\ &\quad + B_{mn} \sin((m\omega_s + n\omega_0) t_1)\} \end{aligned} \quad (\text{C.195})$$

We now substitute back $t = t_1 + \frac{T_0}{3}$ into equation C.143 and obtain:

$$\begin{aligned} s_{b2}(t_1) &= \frac{1}{2}A_{00} + \sum_{n=1}^{\infty} \left(A_{0n} \cos\left(n\omega_0 \left(t - \frac{2\pi}{3\omega_0}\right)\right) + B_{0n} \sin\left(n\omega_0 \left(t - \frac{2\pi}{3\omega_0}\right)\right) \right) \\ &\quad + \sum_{m=1}^{\infty} \left(A_{m0} \cos\left(m\omega_s \left(t - \frac{2\pi}{3\omega_0}\right)\right) \right. \\ &\quad \left. + B_{m0} \sin\left(m\omega_s \left(t - \frac{2\pi}{3\omega_0}\right)\right) \right) \\ &\quad + \sum_{m=1}^{\infty} \sum_{n=\pm 1}^{\pm\infty} \left\{ A_{mn} \cos\left((m\omega_s + n\omega_0) \left(t - \frac{2\pi}{3\omega_0}\right)\right) \right. \\ &\quad \left. + B_{mn} \sin\left((m\omega_s + n\omega_0) \left(t - \frac{2\pi}{3\omega_0}\right)\right) \right\} \end{aligned} \quad (\text{C.196})$$

From table C.2 for the background function of $s_{b3}(t)$ the value of h is given by:

$$h = \frac{2\omega_s}{\pi} t_1 - \frac{4}{3} \quad (\text{C.197})$$

Substituting equation C.197 into the term $\frac{m\pi h}{2}$ of equation 3.36 we obtain:

$$\frac{m\pi h}{2} = m\omega_s t_1 - \frac{2m\pi}{3} \quad (\text{C.198})$$

Now substituting equation C.198 into equation 3.36 we obtain:

$$\begin{aligned}
s_{b3}(t_1) &= \frac{1}{2}A_{00} + \sum_{n=1}^{\infty} (A_{0n} \cos(n\omega_0 t_1) + B_{0n} \sin(n\omega_0 t_1)) \\
&+ \sum_{m=1}^{\infty} \left(A_{m0} \cos\left(m\omega_s t_1 - \frac{2m\pi}{3}\right) + B_{m0} \sin\left(m\omega_s t_1 - \frac{2m\pi}{3}\right) \right) \\
&+ \sum_{m=1}^{\infty} \sum_{n=\pm 1}^{\pm\infty} \left\{ A_{mn} \cos\left((m\omega_s + n\omega_0)t_1 - \frac{2m\pi}{3}\right) \right. \\
&\quad \left. + B_{mn} \sin\left((m\omega_s + n\omega_0)t_1 - \frac{2m\pi}{3}\right) \right\} \tag{C.199}
\end{aligned}$$

We now substitute back $t = t_1 + \frac{T_0}{3}$ into equation C.199 and obtain:

$$\begin{aligned}
s_{b3}(t) &= \frac{1}{2}A_{00} + \sum_{n=1}^{\infty} \left(A_{0n} \cos\left(n\omega_0 \left(t - \frac{2\pi}{3\omega_0}\right)\right) + B_{0n} \sin\left(n\omega_0 \left(t - \frac{2\pi}{3\omega_0}\right)\right) \right) \\
&+ \sum_{m=1}^{\infty} \left(A_{m0} \cos\left(m\omega_s \left(t - \frac{2\pi}{3\omega_0}\right) - \frac{2m\pi}{3}\right) \right. \\
&\quad \left. + B_{m0} \sin\left(m\omega_s \left(t - \frac{2\pi}{3\omega_0}\right) - \frac{2m\pi}{3}\right) \right) \\
&+ \sum_{m=1}^{\infty} \sum_{n=\pm 1}^{\pm\infty} \left\{ A_{mn} \cos\left((m\omega_s + n\omega_0) \left(t - \frac{2\pi}{3\omega_0}\right) - \frac{2m\pi}{3}\right) \right. \\
&\quad \left. + B_{mn} \sin\left((m\omega_s + n\omega_0) \left(t - \frac{2\pi}{3\omega_0}\right) - \frac{2m\pi}{3}\right) \right\} \tag{C.200}
\end{aligned}$$

Now considering trigonometric terms in equation C.192, C.196 and C.200 we have:

$$\begin{aligned}
\cos\left(n\omega_0 \left(t - \frac{2\pi}{3\omega_0}\right)\right) &= \cos\left(n\omega_0 t - \frac{2n\pi}{3}\right) \\
&= \begin{cases} \cos(n\omega_0 t) & \text{if } n = 3p \\ \cos\left(n\omega_0 t - \frac{2\pi}{3}\right) & \text{if } n = 3p + 1 \\ \cos\left(n\omega_0 t + \frac{2\pi}{3}\right) & \text{if } n = 3p + 2 \end{cases} \tag{C.201}
\end{aligned}$$

$$\begin{aligned}
\sin\left(n\omega_0 \left(t - \frac{2\pi}{3\omega_0}\right)\right) &= \sin\left(n\omega_0 t - \frac{2n\pi}{3}\right) \\
&= \begin{cases} \sin(n\omega_0 t) & \text{if } n = 3p \\ \sin\left(n\omega_0 t - \frac{2\pi}{3}\right) & \text{if } n = 3p + 1 \\ \sin\left(n\omega_0 t + \frac{2\pi}{3}\right) & \text{if } n = 3p + 2 \end{cases} \tag{C.202}
\end{aligned}$$

$$\begin{aligned}
\cos\left(m\omega_s \left(t - \frac{2\pi}{3\omega_0}\right)\right) &= \cos\left(m\omega_s t - \frac{2m\pi}{3}m_f\right) \\
&= \cos(m\omega_s t) \tag{C.203}
\end{aligned}$$

$$\begin{aligned}\sin\left(m\omega_s\left(t - \frac{2\pi}{3\omega_0}\right)\right) &= \sin\left(m\omega_s t - \frac{2m\pi}{3}m_f\right) \\ &= \sin(m\omega_s t)\end{aligned}\quad (\text{C.204})$$

$$\begin{aligned}\cos\left(m\omega_s\left(t - \frac{2\pi}{3\omega_0}\right) - \frac{2m\pi}{3}\right) &= \cos\left(m\omega_s t - \frac{2m\pi}{3}m_f - \frac{2m\pi}{3}\right) \\ &= \begin{cases} \cos(m\omega_s t) & \text{if } m = 3k \\ \cos\left(m\omega_s t - \frac{2\pi}{3}\right) & \text{if } m = 3k + 1 \\ \cos\left(m\omega_s t + \frac{2\pi}{3}\right) & \text{if } m = 3k + 2 \end{cases}\end{aligned}\quad (\text{C.205})$$

$$\begin{aligned}\sin\left(m\omega_s\left(t - \frac{2\pi}{3\omega_0}\right) - \frac{2m\pi}{3}\right) &= \sin\left(m\omega_s t - \frac{2m\pi}{3}m_f - \frac{2m\pi}{3}\right) \\ &= \begin{cases} \sin(m\omega_s t) & \text{if } m = 3k \\ \sin\left(m\omega_s t - \frac{2\pi}{3}\right) & \text{if } m = 3k + 1 \\ \sin\left(m\omega_s t + \frac{2\pi}{3}\right) & \text{if } m = 3k + 2 \end{cases}\end{aligned}\quad (\text{C.206})$$

$$\cos\left(m\omega_s\left(t - \frac{2\pi}{3\omega_0}\right) - \frac{4m\pi}{3}\right) = \begin{cases} \cos(m\omega_s t) & \text{if } m = 3k \\ \cos\left(m\omega_s t + \frac{2\pi}{3}\right) & \text{if } m = 3k + 1 \\ \cos\left(m\omega_s t - \frac{2\pi}{3}\right) & \text{if } m = 3k + 2 \end{cases}\quad (\text{C.207})$$

$$\sin\left(m\omega_s\left(t - \frac{2\pi}{3\omega_0}\right) - \frac{4m\pi}{3}\right) = \begin{cases} \sin(m\omega_s t) & \text{if } m = 3k \\ \sin\left(m\omega_s t + \frac{2\pi}{3}\right) & \text{if } m = 3k + 1 \\ \sin\left(m\omega_s t - \frac{2\pi}{3}\right) & \text{if } m = 3k + 2 \end{cases}\quad (\text{C.208})$$

$$\begin{aligned}\cos\left((m\omega_s + n\omega_0)\left(t - \frac{2\pi}{3\omega_0}\right)\right) &= \cos\left((m\omega_s + n\omega_0)t - \frac{2m\pi}{3}m_f - \frac{2n\pi}{3}\right) \\ &= \begin{cases} \cos((m\omega_s + n\omega_0)t) & \text{if } m = k \text{ and } n=3p \text{ or } n=-3p \\ \cos\left((m\omega_s + n\omega_0)t - \frac{2\pi}{3}\right) & \text{if } m = k \text{ and } n=3p+1 \text{ or } n=-(3p+2) \\ \cos\left((m\omega_s + n\omega_0)t + \frac{2\pi}{3}\right) & \text{if } m = k \text{ and } n=3p+2 \text{ or } n=-(3p+1) \end{cases}\end{aligned}\quad (\text{C.209})$$

$$\begin{aligned}\sin\left((m\omega_s + n\omega_0)\left(t - \frac{2\pi}{3\omega_0}\right)\right) &= \sin\left((m\omega_s + n\omega_0)t - \frac{2m\pi}{3}m_f - \frac{2n\pi}{3}\right) \\ &= \begin{cases} \sin((m\omega_s + n\omega_0)t) & \text{if } m = k \text{ and } n=3p \text{ or } n=-3p \\ \sin\left((m\omega_s + n\omega_0)t - \frac{2\pi}{3}\right) & \text{if } m = k \text{ and } n=3p+1 \text{ or } n=-(3p+2) \\ \sin\left((m\omega_s + n\omega_0)t + \frac{2\pi}{3}\right) & \text{if } m = k \text{ and } n=3p+2 \text{ or } n=-(3p+1) \end{cases}\end{aligned}\quad (\text{C.210})$$

$$\begin{aligned}
& \cos \left((m\omega_s + n\omega_0) \left(t - \frac{2\pi}{3\omega_0} \right) - \frac{2m\pi}{3} \right) = \cos \left((m\omega_s + n\omega_0) t - \frac{2m\pi}{3} m_f - \frac{2n\pi}{3} - \frac{2m\pi}{3} \right) \\
= & \begin{cases} \cos((m\omega_s + n\omega_0) t) & \text{if } m = 3k \text{ and } n=3p \text{ or } n=-3p \\ \cos\left((m\omega_s + n\omega_0) t - \frac{2\pi}{3}\right) & \text{if } m = 3k \text{ and } n=3p+1 \text{ or } n=-(3p+2) \\ \cos\left((m\omega_s + n\omega_0) t + \frac{2\pi}{3}\right) & \text{if } m = 3k \text{ and } n=3p+2 \text{ or } n=-(3p+1) \\ \cos\left((m\omega_s + n\omega_0) t - \frac{2\pi}{3}\right) & \text{if } m = 3k + 1 \text{ and } n=3p \text{ or } n=-3p \\ \cos\left((m\omega_s + n\omega_0) t + \frac{2\pi}{3}\right) & \text{if } m = 3k + 1 \text{ and } n=3p+1 \text{ or } n=-(3p+2) \\ \cos((m\omega_s + n\omega_0) t) & \text{if } m = 3k + 1 \text{ and } n=3p+2 \text{ or } n=-(3p+1) \\ \cos\left((m\omega_s + n\omega_0) t + \frac{2\pi}{3}\right) & \text{if } m = 3k + 2 \text{ and } n=3p \text{ or } n=-3p \\ \cos((m\omega_s + n\omega_0) t) & \text{if } m = 3k + 2 \text{ and } n=3p+1 \text{ or } n=-(3p+2) \\ \cos\left((m\omega_s + n\omega_0) t - \frac{2\pi}{3}\right) & \text{if } m = 3k + 2 \text{ and } n=3p+2 \text{ or } n=-(3p+1) \end{cases}
\end{aligned} \tag{C.211}$$

$$\begin{aligned}
& \sin \left((m\omega_s + n\omega_0) \left(t - \frac{2\pi}{3\omega_0} \right) - \frac{2m\pi}{3} \right) = \sin \left((m\omega_s + n\omega_0) t - \frac{2m\pi}{3} m_f - \frac{2n\pi}{3} - \frac{2m\pi}{3} \right) \\
= & \begin{cases} \sin((m\omega_s + n\omega_0) t) & \text{if } m = 3k \text{ and } n=3p \text{ or } n=-3p \\ \sin\left((m\omega_s + n\omega_0) t - \frac{2\pi}{3}\right) & \text{if } m = 3k \text{ and } n=3p+1 \text{ or } n=-(3p+2) \\ \sin\left((m\omega_s + n\omega_0) t + \frac{2\pi}{3}\right) & \text{if } m = 3k \text{ and } n=3p+2 \text{ or } n=-(3p+1) \\ \sin\left((m\omega_s + n\omega_0) t - \frac{2\pi}{3}\right) & \text{if } m = 3k + 1 \text{ and } n=3p \text{ or } n=-3p \\ \sin\left((m\omega_s + n\omega_0) t + \frac{2\pi}{3}\right) & \text{if } m = 3k + 1 \text{ and } n=3p+1 \text{ or } n=-(3p+2) \\ \sin((m\omega_s + n\omega_0) t) & \text{if } m = 3k + 1 \text{ and } n=3p+2 \text{ or } n=-(3p+1) \\ \sin\left((m\omega_s + n\omega_0) t + \frac{2\pi}{3}\right) & \text{if } m = 3k + 2 \text{ and } n=3p \text{ or } n=-3p \\ \sin((m\omega_s + n\omega_0) t) & \text{if } m = 3k + 2 \text{ and } n=3p+1 \text{ or } n=-(3p+2) \\ \sin\left((m\omega_s + n\omega_0) t - \frac{2\pi}{3}\right) & \text{if } m = 3k + 2 \text{ and } n=3p+2 \text{ or } n=-(3p+1) \end{cases}
\end{aligned} \tag{C.212}$$

$$\begin{aligned}
& \cos \left((m\omega_s + n\omega_0) \left(t - \frac{2\pi}{3\omega_0} \right) - \frac{4m\pi}{3} \right) = \cos \left((m\omega_s + n\omega_0) t - \frac{2m\pi}{3} m_f - \frac{2n\pi}{3} - \frac{4m\pi}{3} \right) \\
= & \begin{cases} \cos((m\omega_s + n\omega_0) t) & \text{if } m = 3k \text{ and } n=3p \text{ or } n=-3p \\ \cos\left((m\omega_s + n\omega_0) t - \frac{2\pi}{3}\right) & \text{if } m = 3k \text{ and } n=3p+1 \text{ or } n=-(3p+2) \\ \cos\left((m\omega_s + n\omega_0) t + \frac{2\pi}{3}\right) & \text{if } m = 3k \text{ and } n=3p+2 \text{ or } n=-(3p+1) \\ \cos\left((m\omega_s + n\omega_0) t + \frac{2\pi}{3}\right) & \text{if } m = 3k + 1 \text{ and } n=3p \text{ or } n=-3p \\ \cos((m\omega_s + n\omega_0) t) & \text{if } m = 3k + 1 \text{ and } n=3p+1 \text{ or } n=-(3p+2) \\ \cos\left((m\omega_s + n\omega_0) t - \frac{2\pi}{3}\right) & \text{if } m = 3k + 1 \text{ and } n=3p+2 \text{ or } n=-(3p+1) \\ \cos\left((m\omega_s + n\omega_0) t - \frac{2\pi}{3}\right) & \text{if } m = 3k + 2 \text{ and } n=3p \text{ or } n=-3p \\ \cos\left((m\omega_s + n\omega_0) t + \frac{2\pi}{3}\right) & \text{if } m = 3k + 2 \text{ and } n=3p+1 \text{ or } n=-(3p+2) \\ \cos((m\omega_s + n\omega_0) t) & \text{if } m = 3k + 2 \text{ and } n=3p+2 \text{ or } n=-(3p+1) \end{cases}
\end{aligned}$$

(C.213)

$$\sin \left((m\omega_s + n\omega_0) \left(t - \frac{2\pi}{3\omega_0} \right) - \frac{4m\pi}{3} \right) = \sin \left((m\omega_s + n\omega_0) t - \frac{2m\pi}{3} m_f - \frac{2n\pi}{3} - \frac{4m\pi}{3} \right)$$

$$= \begin{cases} \sin((m\omega_s + n\omega_0)t) & \text{if } m = 3k \text{ and } n=3p \text{ or } n=-3p \\ \sin\left((m\omega_s + n\omega_0)t - \frac{2\pi}{3}\right) & \text{if } m = 3k \text{ and } n=3p+1 \text{ or } n=-(3p+2) \\ \sin\left((m\omega_s + n\omega_0)t + \frac{2\pi}{3}\right) & \text{if } m = 3k \text{ and } n=3p+2 \text{ or } n=-(3p+1) \\ \sin\left((m\omega_s + n\omega_0)t + \frac{2\pi}{3}\right) & \text{if } m = 3k + 1 \text{ and } n=3p \text{ or } n=-3p \\ \sin((m\omega_s + n\omega_0)t) & \text{if } m = 3k + 1 \text{ and } n=3p+1 \text{ or } n=-(3p+2) \\ \sin\left((m\omega_s + n\omega_0)t - \frac{2\pi}{3}\right) & \text{if } m = 3k + 1 \text{ and } n=3p+2 \text{ or } n=-(3p+1) \\ \sin\left((m\omega_s + n\omega_0)t - \frac{2\pi}{3}\right) & \text{if } m = 3k + 2 \text{ and } n=3p \text{ or } n=-3p \\ \sin\left((m\omega_s + n\omega_0)t + \frac{2\pi}{3}\right) & \text{if } m = 3k + 2 \text{ and } n=3p+1 \text{ or } n=-(3p+2) \\ \sin((m\omega_s + n\omega_0)t) & \text{if } m = 3k + 2 \text{ and } n=3p+2 \text{ or } n=-(3p+1) \end{cases}$$

(C.214)

Thus the phasor representation for phase B of 3-cell converter when $m_f = 3k + 1$ is given by Figures C.27, C.28 and C.29.

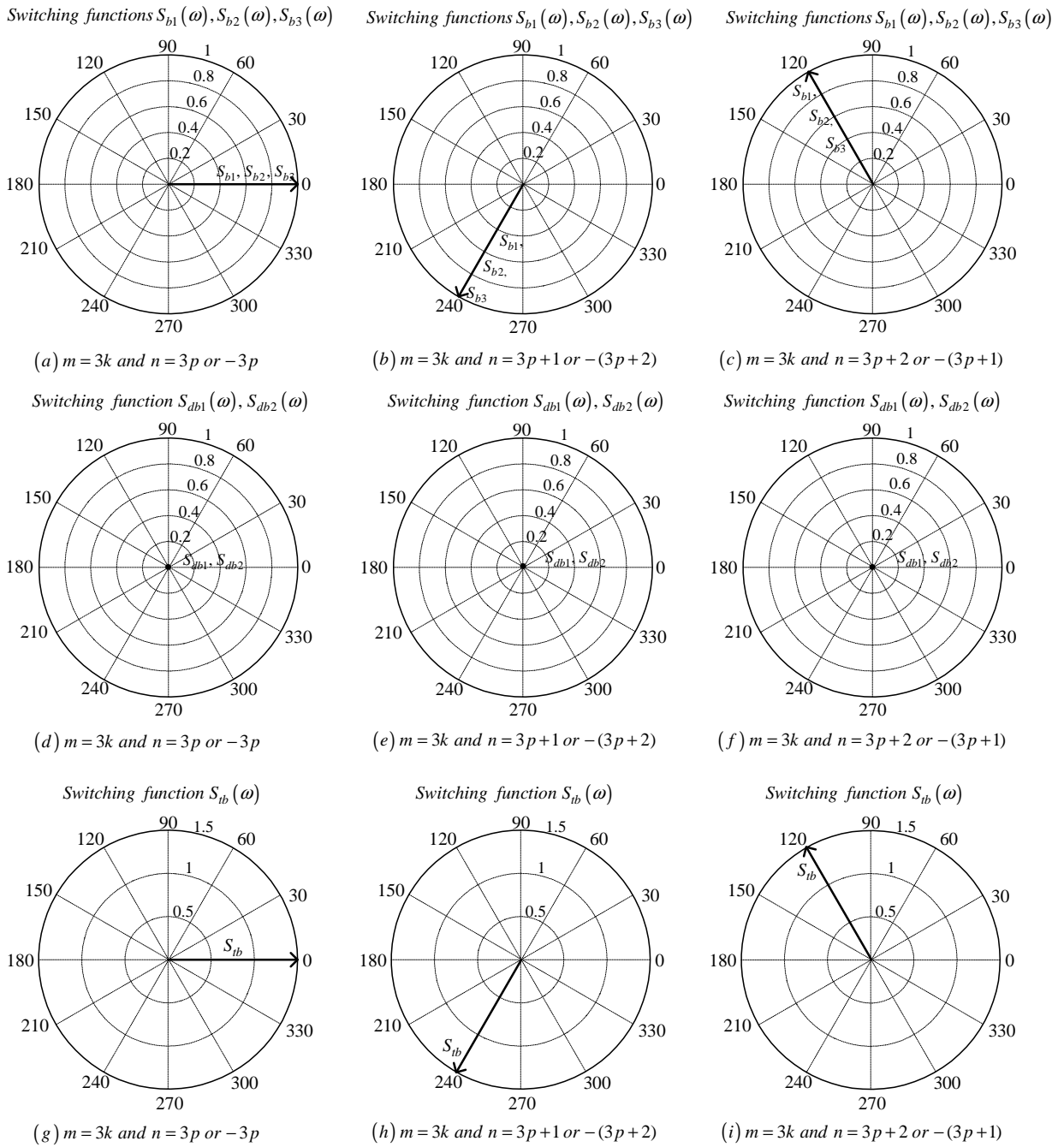


Figure C.27: Phasor representation for phase B of 3-cell converter for $m = 3k$

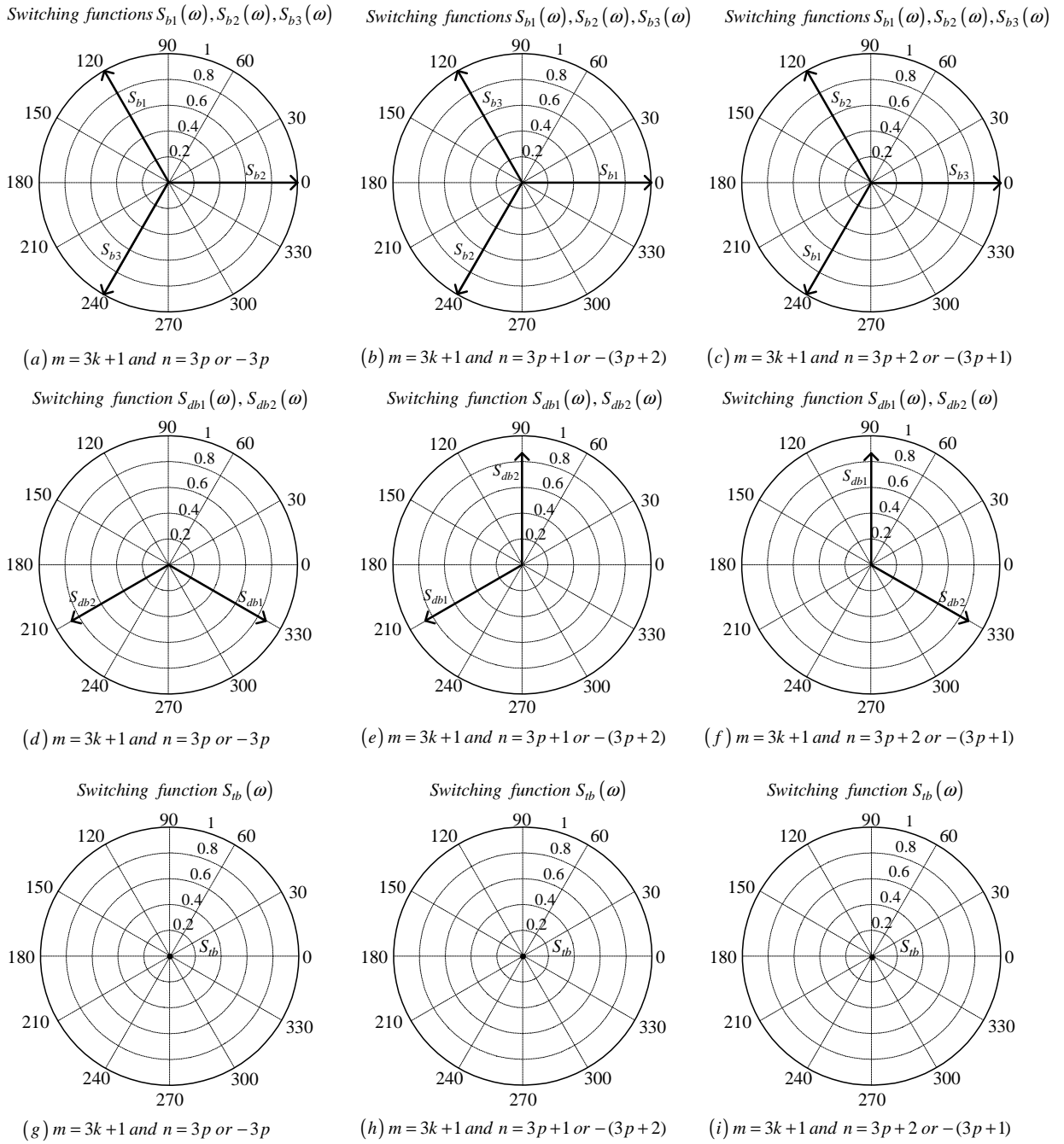


Figure C.28: Phasor representation for phase B of 3-cell converter for $m = 3k + 1$

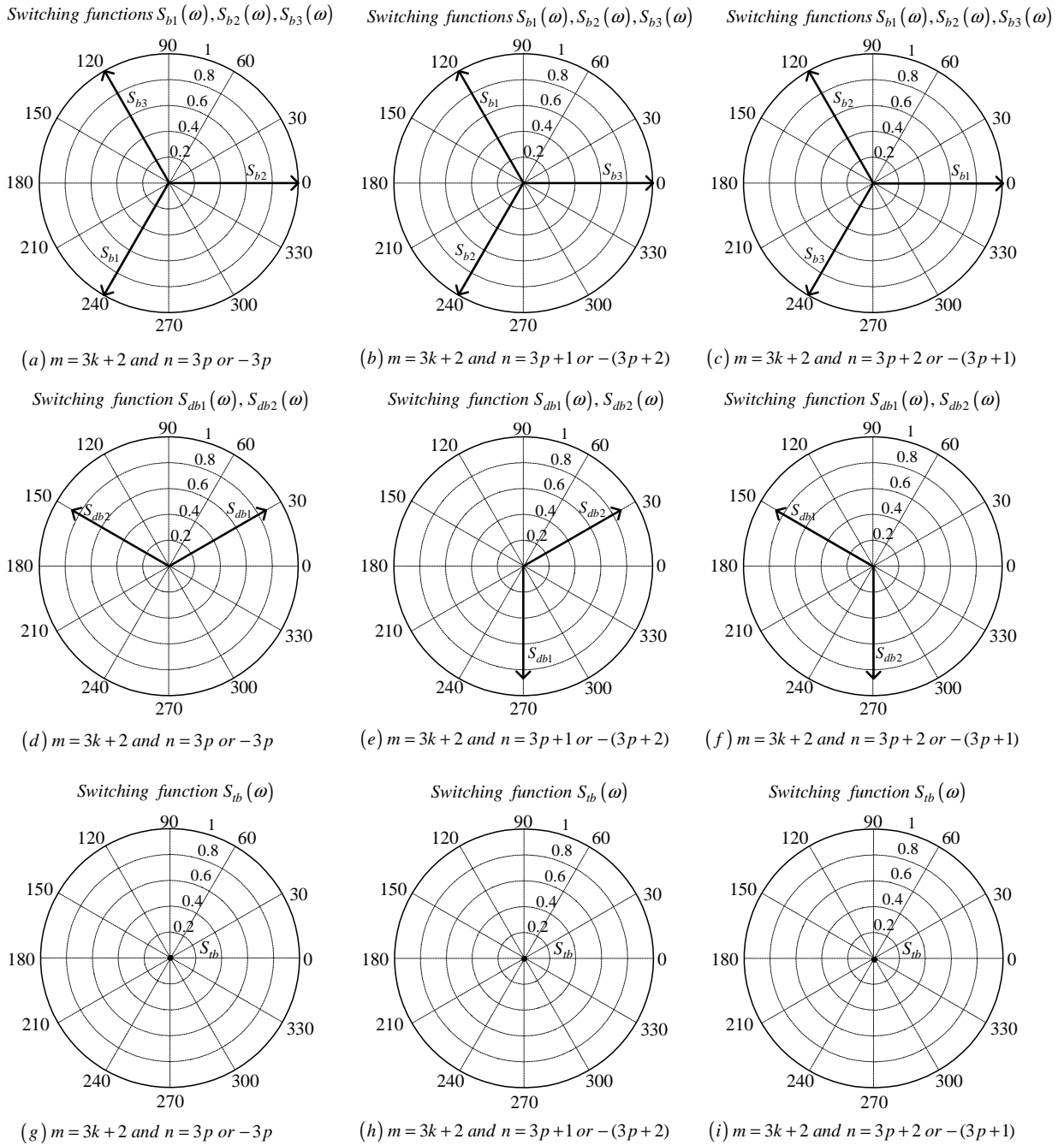


Figure C.29: Phasor representation for phase B of 3-cell converter for $m = 3k + 2$

Phase C

From table C.2 the value of h for the background function of $s_{c1}(t)$ is given by:

$$h = \frac{2\omega_s}{\pi}t_2 - \frac{4}{3} \quad (\text{C.215})$$

Substituting equation C.215 into the term $\frac{m\pi h}{2}$ of equation 3.36 we obtain:

$$\frac{m\pi h}{2} = m\omega_s t_2 - \frac{2}{3}m\pi \quad (\text{C.216})$$

Now substituting equation C.216 into equation 3.36 we obtain:

$$\begin{aligned} s_{c1}(t_2) &= \frac{1}{2}A_{00} + \sum_{n=1}^{\infty} (A_{0n} \cos(n\omega_0 t_2) + B_{0n} \sin(n\omega_0 t_2)) \\ &+ \sum_{m=1}^{\infty} \left(A_{m0} \cos\left(m\omega_s t_2 - \frac{2}{3}m\pi\right) + B_{m0} \sin\left(m\omega_s t_2 - \frac{2}{3}m\pi\right) \right) \\ &+ \sum_{m=1}^{\infty} \sum_{n=\pm 1}^{\pm\infty} \left\{ A_{mn} \cos\left((m\omega_s + n\omega_0)t_2 - \frac{2}{3}m\pi\right) \right. \\ &\left. + B_{mn} \sin\left((m\omega_s + n\omega_0)t_2 - \frac{2}{3}m\pi\right) \right\} \end{aligned} \quad (\text{C.217})$$

We now substitute back $t = t_2 + \frac{2T_0}{3}$ into equation C.217 and obtain:

$$\begin{aligned} s_{c1}(t) &= \frac{1}{2}A_{00} + \sum_{n=1}^{\infty} \left(A_{0n} \cos\left(n\omega_0 \left(t - \frac{4\pi}{3\omega_0}\right)\right) + B_{0n} \sin\left(n\omega_0 \left(t - \frac{4\pi}{3\omega_0}\right)\right) \right) \\ &+ \sum_{m=1}^{\infty} \left(A_{m0} \cos\left(m\omega_s \left(t - \frac{4\pi}{3\omega_0}\right) - \frac{2}{3}m\pi\right) \right. \\ &\left. + B_{m0} \sin\left(m\omega_s \left(t - \frac{4\pi}{3\omega_0}\right) - \frac{2}{3}m\pi\right) \right) \\ &+ \sum_{m=1}^{\infty} \sum_{n=\pm 1}^{\pm\infty} \left\{ A_{mn} \cos\left((m\omega_s + n\omega_0) \left(t - \frac{4\pi}{3\omega_0}\right) - \frac{2}{3}m\pi\right) \right. \\ &\left. + B_{mn} \sin\left((m\omega_s + n\omega_0) \left(t - \frac{4\pi}{3\omega_0}\right) - \frac{2}{3}m\pi\right) \right\} \end{aligned} \quad (\text{C.218})$$

From table C.2 for the background function of $s_{c2}(t)$ the value of h is given by:

$$h = \frac{2\omega_s}{\pi}t_2 - \frac{8}{3} \quad (\text{C.219})$$

Substituting equation C.219 into the term $\frac{m\pi h}{2}$ of equation 3.36 we obtain:

$$\frac{m\pi h}{2} = m\omega_s t_2 - \frac{4m\pi}{3} \quad (\text{C.220})$$

Now substituting equation C.220 into equation 3.36 we obtain:

$$\begin{aligned}
s_{c2}(t_2) &= \frac{1}{2}A_{00} + \sum_{n=1}^{\infty} (A_{0n} \cos(n\omega_0 t_2) + B_{0n} \sin(n\omega_0 t_2)) \\
&+ \sum_{m=1}^{\infty} \left(A_{m0} \cos\left(m\omega_s t_2 - \frac{4m\pi}{3}\right) + B_{m0} \sin\left(m\omega_s t_2 - \frac{4m\pi}{3}\right) \right) \\
&+ \sum_{m=1}^{\infty} \sum_{n=\pm 1}^{\pm\infty} \left\{ A_{mn} \cos\left((m\omega_s + n\omega_0) t_2 - \frac{4m\pi}{3}\right) \right. \\
&\quad \left. + B_{mn} \sin\left((m\omega_s + n\omega_0) t_2 - \frac{4m\pi}{3}\right) \right\} \tag{C.221}
\end{aligned}$$

We now substitute back $t = t_2 + \frac{2T_0}{3}$ into equation C.221 and obtain:

$$\begin{aligned}
s_{c2}(t) &= \frac{1}{2}A_{00} + \sum_{n=1}^{\infty} \left(A_{0n} \cos\left(n\omega_0 \left(t - \frac{4\pi}{3\omega_0}\right)\right) + B_{0n} \sin\left(n\omega_0 \left(t - \frac{4\pi}{3\omega_0}\right)\right) \right) \\
&+ \sum_{m=1}^{\infty} \left(A_{m0} \cos\left(m\omega_s \left(t - \frac{4\pi}{3\omega_0}\right) - \frac{4m\pi}{3}\right) \right. \\
&\quad \left. + B_{m0} \sin\left(m\omega_s \left(t - \frac{4\pi}{3\omega_0}\right) - \frac{4m\pi}{3}\right) \right) \\
&+ \sum_{m=1}^{\infty} \sum_{n=\pm 1}^{\pm\infty} \left\{ A_{mn} \cos\left((m\omega_s + n\omega_0) \left(t - \frac{4\pi}{3\omega_0}\right) - \frac{4m\pi}{3}\right) \right. \\
&\quad \left. + B_{mn} \sin\left((m\omega_s + n\omega_0) \left(t - \frac{4\pi}{3\omega_0}\right) - \frac{4m\pi}{3}\right) \right\} \tag{C.222}
\end{aligned}$$

From table C.2 for the background function of $s_{c3}(t)$ the value of h is given by:

$$h = \frac{2\omega_s}{\pi} t_2 \tag{C.223}$$

Substituting equation C.223 into the term $\frac{m\pi h}{2}$ of equation 3.36 we obtain:

$$\frac{m\pi h}{2} = m\omega_s t_2 \tag{C.224}$$

Now substituting equation C.224 into equation 3.36 we obtain:

$$\begin{aligned}
s_{c3}(t_2) &= \frac{1}{2}A_{00} + \sum_{n=1}^{\infty} (A_{0n} \cos(n\omega_0 t_2) + B_{0n} \sin(n\omega_0 t_2)) \\
&+ \sum_{m=1}^{\infty} (A_{m0} \cos(m\omega_s t_2) + B_{m0} \sin(m\omega_s t_2)) \\
&+ \sum_{m=1}^{\infty} \sum_{n=\pm 1}^{\pm\infty} \left\{ A_{mn} \cos((m\omega_s + n\omega_0) t_2) \right. \\
&\quad \left. + B_{mn} \sin((m\omega_s + n\omega_0) t_2) \right\} \tag{C.225}
\end{aligned}$$

We now substitute back $t = t_2 + \frac{2T_0}{3}$ into equation C.225 and obtain:

$$\begin{aligned}
s_{c3}(t) &= \frac{1}{2}A_{00} + \sum_{n=1}^{\infty} \left(A_{0n} \cos \left(n\omega_0 \left(t - \frac{4\pi}{3\omega_0} \right) \right) + B_{0n} \sin \left(n\omega_0 \left(t - \frac{4\pi}{3\omega_0} \right) \right) \right) \\
&+ \sum_{m=1}^{\infty} \left(A_{m0} \cos \left(m\omega_s \left(t - \frac{4\pi}{3\omega_0} \right) \right) + B_{m0} \sin \left(m\omega_s \left(t - \frac{4\pi}{3\omega_0} \right) \right) \right) \\
&+ \sum_{m=1}^{\infty} \sum_{n=\pm 1}^{\pm \infty} \left\{ A_{mn} \cos \left((m\omega_s + n\omega_0) \left(t - \frac{4\pi}{3\omega_0} \right) \right) \right. \\
&\left. + B_{mn} \sin \left((m\omega_s + n\omega_0) \left(t - \frac{4\pi}{3\omega_0} \right) \right) \right\} \tag{C.226}
\end{aligned}$$

Now considering trigonometric terms in equation C.218, C.222 and C.226 we have:

$$\begin{aligned}
\cos \left(n\omega_0 \left(t - \frac{4\pi}{3\omega_0} \right) \right) &= \cos \left(n\omega_0 t - \frac{4n\pi}{3} \right) \\
&= \begin{cases} \cos(n\omega_0 t) & \text{if } n = 3p \\ \cos \left(n\omega_0 t + \frac{2\pi}{3} \right) & \text{if } n = 3p + 1 \\ \cos \left(n\omega_0 t - \frac{2\pi}{3} \right) & \text{if } n = 3p + 2 \end{cases} \tag{C.227}
\end{aligned}$$

$$\begin{aligned}
\sin \left(n\omega_0 \left(t - \frac{4\pi}{3\omega_0} \right) \right) &= \sin \left(n\omega_0 t - \frac{4n\pi}{3} \right) \\
&= \begin{cases} \sin(n\omega_0 t) & \text{if } n = 3p \\ \sin \left(n\omega_0 t + \frac{2\pi}{3} \right) & \text{if } n = 3p + 1 \\ \sin \left(n\omega_0 t - \frac{2\pi}{3} \right) & \text{if } n = 3p + 2 \end{cases} \tag{C.228}
\end{aligned}$$

$$\begin{aligned}
\cos \left(m\omega_s \left(t - \frac{4\pi}{3\omega_0} \right) \right) &= \cos \left(m\omega_s t - \frac{4m\pi}{3} m_f \right) \\
&= \cos(m\omega_s t) \tag{C.229}
\end{aligned}$$

$$\begin{aligned}
\sin \left(m\omega_s \left(t - \frac{4\pi}{3\omega_0} \right) \right) &= \sin \left(m\omega_s t - \frac{4m\pi}{3} m_f \right) \\
&= \sin(m\omega_s t) \tag{C.230}
\end{aligned}$$

$$\begin{aligned}
\cos \left(m\omega_s \left(t - \frac{4\pi}{3\omega_0} \right) - \frac{2m\pi}{3} \right) &= \cos \left(m\omega_s t - \frac{4m\pi}{3} m_f - \frac{2m\pi}{3} \right) \\
&= \begin{cases} \cos(m\omega_s t) & \text{if } m = 3k \\ \cos \left(m\omega_s t - \frac{2\pi}{3} \right) & \text{if } m = 3k + 1 \\ \cos \left(m\omega_s t + \frac{2\pi}{3} \right) & \text{if } m = 3k + 2 \end{cases} \tag{C.231}
\end{aligned}$$

$$\begin{aligned} \sin\left(m\omega_s\left(t - \frac{4\pi}{3\omega_0}\right) - \frac{2m\pi}{3}\right) &= \sin\left(m\omega_s t - \frac{4m\pi}{3}m_f - \frac{2m\pi}{3}\right) \\ &= \begin{cases} \sin(m\omega_s t) & \text{if } m = 3k \\ \sin\left(m\omega_s t - \frac{2\pi}{3}\right) & \text{if } m = 3k + 1 \\ \sin\left(m\omega_s t + \frac{2\pi}{3}\right) & \text{if } m = 3k + 2 \end{cases} \end{aligned} \quad (\text{C.232})$$

$$\cos\left(m\omega_s\left(t - \frac{4\pi}{3\omega_0}\right) - \frac{4m\pi}{3}\right) = \begin{cases} \cos(m\omega_s t) & \text{if } m = 3k \\ \cos\left(m\omega_s t + \frac{2\pi}{3}\right) & \text{if } m = 3k + 1 \\ \cos\left(m\omega_s t - \frac{2\pi}{3}\right) & \text{if } m = 3k + 2 \end{cases} \quad (\text{C.233})$$

$$\sin\left(m\omega_s\left(t - \frac{4\pi}{3\omega_0}\right) - \frac{4m\pi}{3}\right) = \begin{cases} \sin(m\omega_s t) & \text{if } m = 3k \\ \sin\left(m\omega_s t + \frac{2\pi}{3}\right) & \text{if } m = 3k + 1 \\ \sin\left(m\omega_s t - \frac{2\pi}{3}\right) & \text{if } m = 3k + 2 \end{cases} \quad (\text{C.234})$$

$$\begin{aligned} \cos\left((m\omega_s + n\omega_0)\left(t - \frac{4\pi}{3\omega_0}\right)\right) &= \cos\left((m\omega_s + n\omega_0)t - \frac{4m\pi}{3}m_f - \frac{4n\pi}{3}\right) \\ &= \begin{cases} \cos((m\omega_s + n\omega_0)t) & \text{if } m = k \text{ and } n=3p \text{ or } n=-3p \\ \cos\left((m\omega_s + n\omega_0)t + \frac{2\pi}{3}\right) & \text{if } m = k \text{ and } n=3p+1 \text{ or } n=-(3p+2) \\ \cos\left((m\omega_s + n\omega_0)t - \frac{2\pi}{3}\right) & \text{if } m = k \text{ and } n=3p+2 \text{ or } n=-(3p+1) \end{cases} \end{aligned} \quad (\text{C.235})$$

$$\begin{aligned} \sin\left((m\omega_s + n\omega_0)\left(t - \frac{4\pi}{3\omega_0}\right)\right) &= \sin\left((m\omega_s + n\omega_0)t - \frac{4m\pi}{3}m_f - \frac{4n\pi}{3}\right) \\ &= \begin{cases} \sin((m\omega_s + n\omega_0)t) & \text{if } m = k \text{ and } n=3p \text{ or } n=-3p \\ \sin\left((m\omega_s + n\omega_0)t + \frac{2\pi}{3}\right) & \text{if } m = k \text{ and } n=3p+1 \text{ or } n=-(3p+2) \\ \sin\left((m\omega_s + n\omega_0)t - \frac{2\pi}{3}\right) & \text{if } m = k \text{ and } n=3p+2 \text{ or } n=-(3p+1) \end{cases} \end{aligned} \quad (\text{C.236})$$

$$\begin{aligned} \cos\left((m\omega_s + n\omega_0)\left(t - \frac{4\pi}{3\omega_0}\right) - \frac{2m\pi}{3}\right) &= \cos\left((m\omega_s + n\omega_0)t - \frac{4m\pi}{3}m_f - \frac{4n\pi}{3} - \frac{2m\pi}{3}\right) \\ &= \begin{cases} \cos((m\omega_s + n\omega_0)t) & \text{if } m = 3k \text{ and } n=3p \text{ or } n=-3p \\ \cos\left((m\omega_s + n\omega_0)t + \frac{2\pi}{3}\right) & \text{if } m = 3k \text{ and } n=3p+1 \text{ or } n=-(3p+2) \\ \cos\left((m\omega_s + n\omega_0)t - \frac{2\pi}{3}\right) & \text{if } m = 3k \text{ and } n=3p+2 \text{ or } n=-(3p+1) \\ \cos\left((m\omega_s + n\omega_0)t - \frac{2\pi}{3}\right) & \text{if } m = 3k + 1 \text{ and } n=3p \text{ or } n=-3p \\ \cos((m\omega_s + n\omega_0)t) & \text{if } m = 3k + 1 \text{ and } n=3p+1 \text{ or } n=-(3p+2) \\ \cos\left((m\omega_s + n\omega_0)t + \frac{2\pi}{3}\right) & \text{if } m = 3k + 1 \text{ and } n=3p+2 \text{ or } n=-(3p+1) \\ \cos\left((m\omega_s + n\omega_0)t + \frac{2\pi}{3}\right) & \text{if } m = 3k + 2 \text{ and } n=3p \text{ or } n=-3p \\ \cos\left((m\omega_s + n\omega_0)t - \frac{2\pi}{3}\right) & \text{if } m = 3k + 2 \text{ and } n=3p+1 \text{ or } n=-(3p+2) \\ \cos((m\omega_s + n\omega_0)t) & \text{if } m = 3k + 2 \text{ and } n=3p+2 \text{ or } n=-(3p+1) \end{cases} \end{aligned}$$

(C.237)

$$\begin{aligned} & \sin \left((m\omega_s + n\omega_0) \left(t - \frac{4\pi}{3\omega_0} \right) - \frac{2m\pi}{3} \right) = \sin \left((m\omega_s + n\omega_0) t - \frac{4m\pi}{3} m_f - \frac{4n\pi}{3} - \frac{2m\pi}{3} \right) \\ = & \begin{cases} \sin((m\omega_s + n\omega_0)t) & \text{if } m = 3k \text{ and } n=3p \text{ or } n=-3p \\ \sin\left((m\omega_s + n\omega_0)t + \frac{2\pi}{3}\right) & \text{if } m = 3k \text{ and } n=3p+1 \text{ or } n=-(3p+2) \\ \sin\left((m\omega_s + n\omega_0)t - \frac{2\pi}{3}\right) & \text{if } m = 3k \text{ and } n=3p+2 \text{ or } n=-(3p+1) \\ \sin\left((m\omega_s + n\omega_0)t - \frac{2\pi}{3}\right) & \text{if } m = 3k + 1 \text{ and } n=3p \text{ or } n=-3p \\ \sin((m\omega_s + n\omega_0)t) & \text{if } m = 3k + 1 \text{ and } n=3p+1 \text{ or } n=-(3p+2) \\ \sin\left((m\omega_s + n\omega_0)t + \frac{2\pi}{3}\right) & \text{if } m = 3k + 1 \text{ and } n=3p+2 \text{ or } n=-(3p+1) \\ \sin\left((m\omega_s + n\omega_0)t + \frac{2\pi}{3}\right) & \text{if } m = 3k + 2 \text{ and } n=3p \text{ or } n=-3p \\ \sin\left((m\omega_s + n\omega_0)t - \frac{2\pi}{3}\right) & \text{if } m = 3k + 2 \text{ and } n=3p+1 \text{ or } n=-(3p+2) \\ \sin((m\omega_s + n\omega_0)t) & \text{if } m = 3k + 2 \text{ and } n=3p+2 \text{ or } n=-(3p+1) \end{cases} \end{aligned} \quad (\text{C.238})$$

$$\begin{aligned} & \cos \left((m\omega_s + n\omega_0) \left(t - \frac{4\pi}{3\omega_0} \right) - \frac{4m\pi}{3} \right) = \cos \left((m\omega_s + n\omega_0) t - \frac{4m\pi}{3} m_f - \frac{4n\pi}{3} - \frac{4m\pi}{3} \right) \\ = & \begin{cases} \cos((m\omega_s + n\omega_0)t) & \text{if } m = 3k \text{ and } n=3p \text{ or } n=-3p \\ \cos\left((m\omega_s + n\omega_0)t + \frac{2\pi}{3}\right) & \text{if } m = 3k \text{ and } n=3p+1 \text{ or } n=-(3p+2) \\ \cos\left((m\omega_s + n\omega_0)t - \frac{2\pi}{3}\right) & \text{if } m = 3k \text{ and } n=3p+2 \text{ or } n=-(3p+1) \\ \cos\left((m\omega_s + n\omega_0)t + \frac{2\pi}{3}\right) & \text{if } m = 3k + 1 \text{ and } n=3p \text{ or } n=-3p \\ \cos\left((m\omega_s + n\omega_0)t - \frac{2\pi}{3}\right) & \text{if } m = 3k + 1 \text{ and } n=3p+1 \text{ or } n=-(3p+2) \\ \cos((m\omega_s + n\omega_0)t) & \text{if } m = 3k + 1 \text{ and } n=3p+2 \text{ or } n=-(3p+1) \\ \cos\left((m\omega_s + n\omega_0)t - \frac{2\pi}{3}\right) & \text{if } m = 3k + 2 \text{ and } n=3p \text{ or } n=-3p \\ \cos((m\omega_s + n\omega_0)t) & \text{if } m = 3k + 2 \text{ and } n=3p+1 \text{ or } n=-(3p+2) \\ \cos\left((m\omega_s + n\omega_0)t + \frac{2\pi}{3}\right) & \text{if } m = 3k + 2 \text{ and } n=3p+2 \text{ or } n=-(3p+1) \end{cases} \end{aligned} \quad (\text{C.239})$$

$$\begin{aligned}
& \sin \left((m\omega_s + n\omega_0) \left(t - \frac{4\pi}{3\omega_0} \right) - \frac{4m\pi}{3} \right) = \sin \left((m\omega_s + n\omega_0) t - \frac{4m\pi}{3} m_f - \frac{4n\pi}{3} - \frac{4m\pi}{3} \right) \\
= & \begin{cases} \sin((m\omega_s + n\omega_0)t) & \text{if } m = 3k \text{ and } n=3p \text{ or } n=-3p \\ \sin\left((m\omega_s + n\omega_0)t + \frac{2\pi}{3}\right) & \text{if } m = 3k \text{ and } n=3p+1 \text{ or } n=-(3p+2) \\ \sin\left((m\omega_s + n\omega_0)t - \frac{2\pi}{3}\right) & \text{if } m = 3k \text{ and } n=3p+2 \text{ or } n=-(3p+1) \\ \sin\left((m\omega_s + n\omega_0)t + \frac{2\pi}{3}\right) & \text{if } m = 3k + 1 \text{ and } n=3p \text{ or } n=-3p \\ \sin\left((m\omega_s + n\omega_0)t - \frac{2\pi}{3}\right) & \text{if } m = 3k + 1 \text{ and } n=3p+1 \text{ or } n=-(3p+2) \\ \sin((m\omega_s + n\omega_0)t) & \text{if } m = 3k + 1 \text{ and } n=3p+2 \text{ or } n=-(3p+1) \\ \sin\left((m\omega_s + n\omega_0)t - \frac{2\pi}{3}\right) & \text{if } m = 3k + 2 \text{ and } n=3p \text{ or } n=-3p \\ \sin((m\omega_s + n\omega_0)t) & \text{if } m = 3k + 2 \text{ and } n=3p+1 \text{ or } n=-(3p+2) \\ \sin\left((m\omega_s + n\omega_0)t + \frac{2\pi}{3}\right) & \text{if } m = 3k + 2 \text{ and } n=3p+2 \text{ or } n=-(3p+1) \end{cases}
\end{aligned} \tag{C.240}$$

Thus the phasor representation for phase C of 3-cell converter when $m_f = 3k + 1$ is given by Figures C.30, C.31 and C.32.

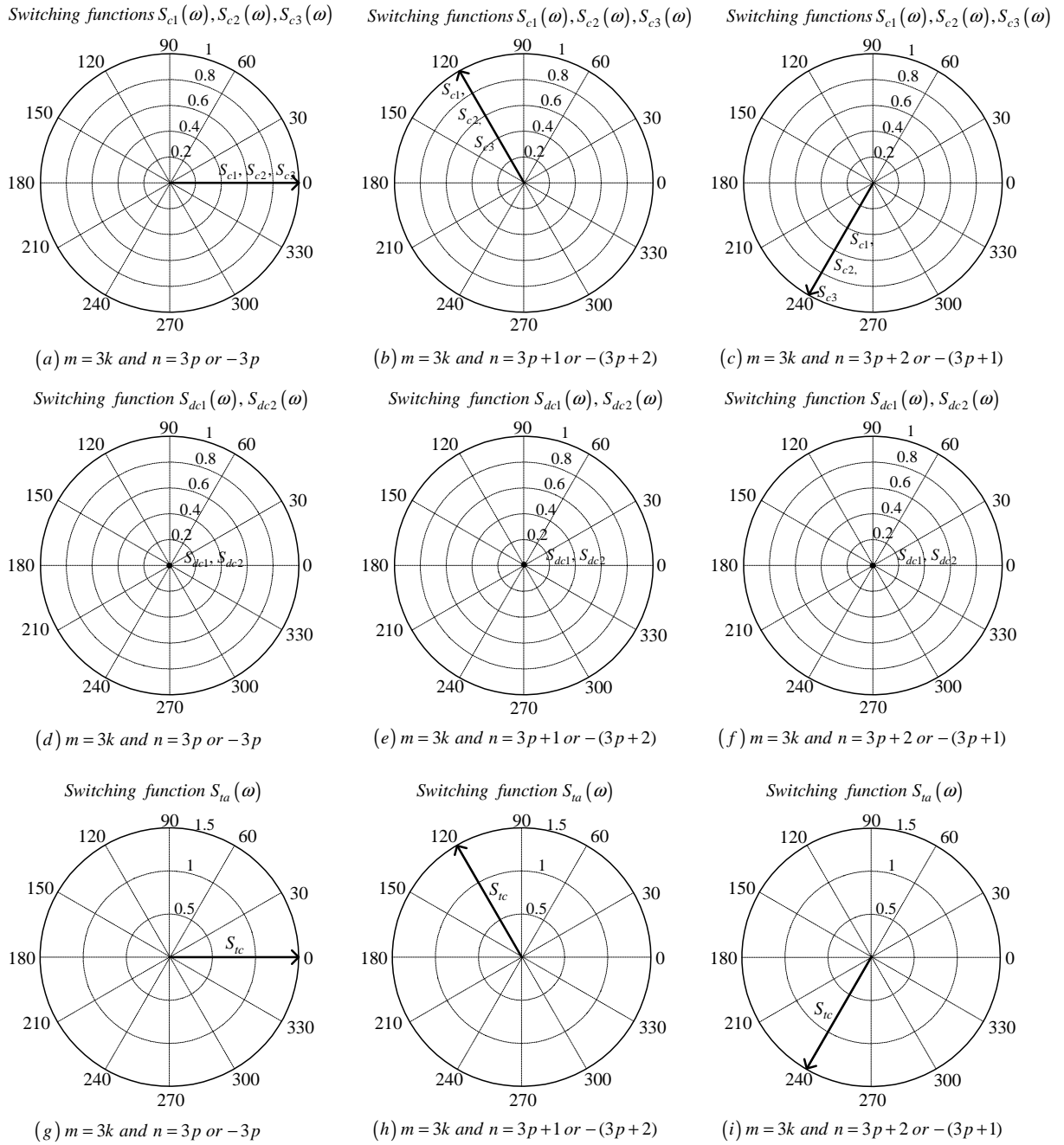


Figure C.30: Phasor representation for phase C of 3-cell converter for $m = 3k$

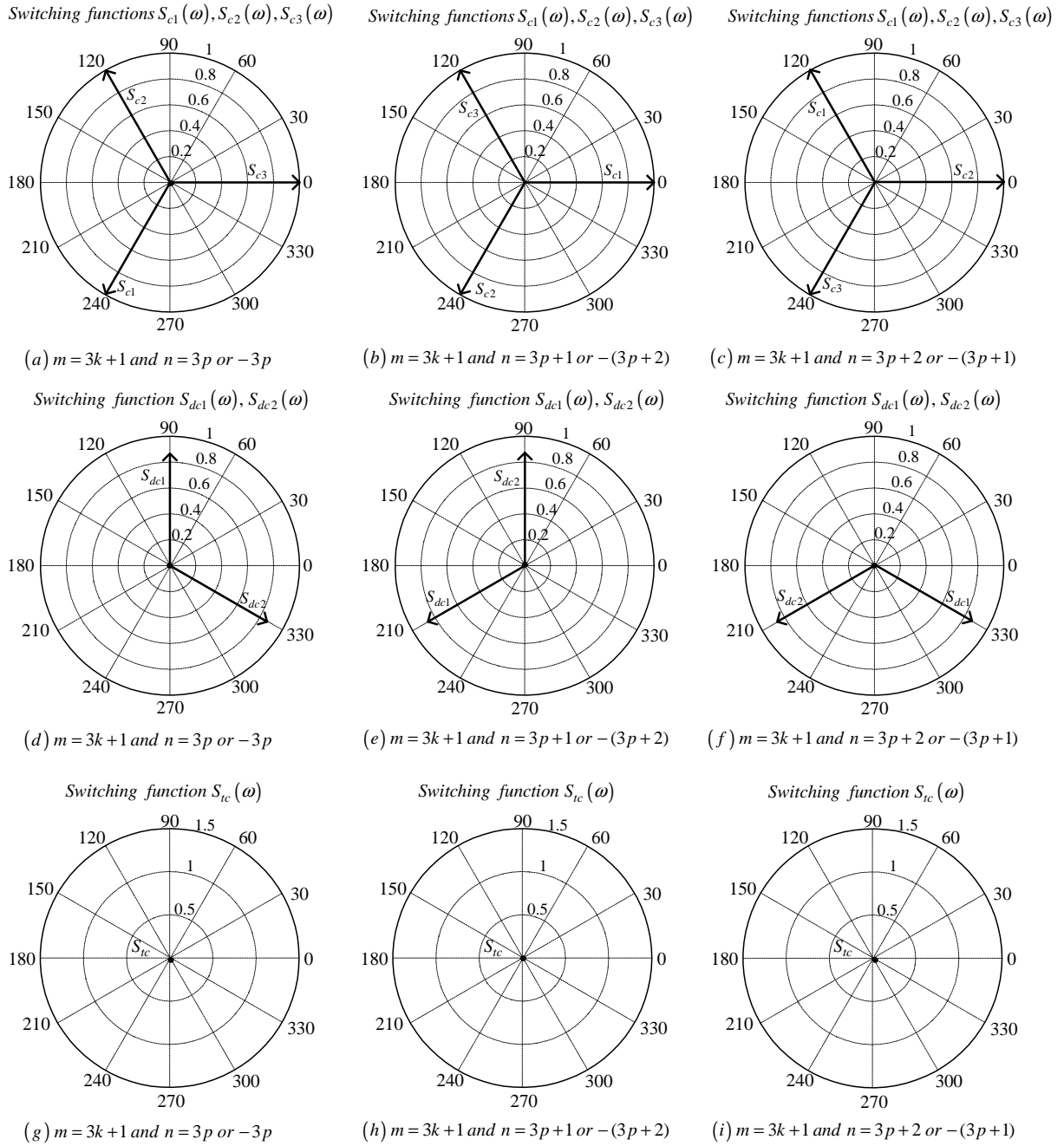


Figure C.31: Phasor representation for phase C of 3-cell converter for $m = 3k + 1$

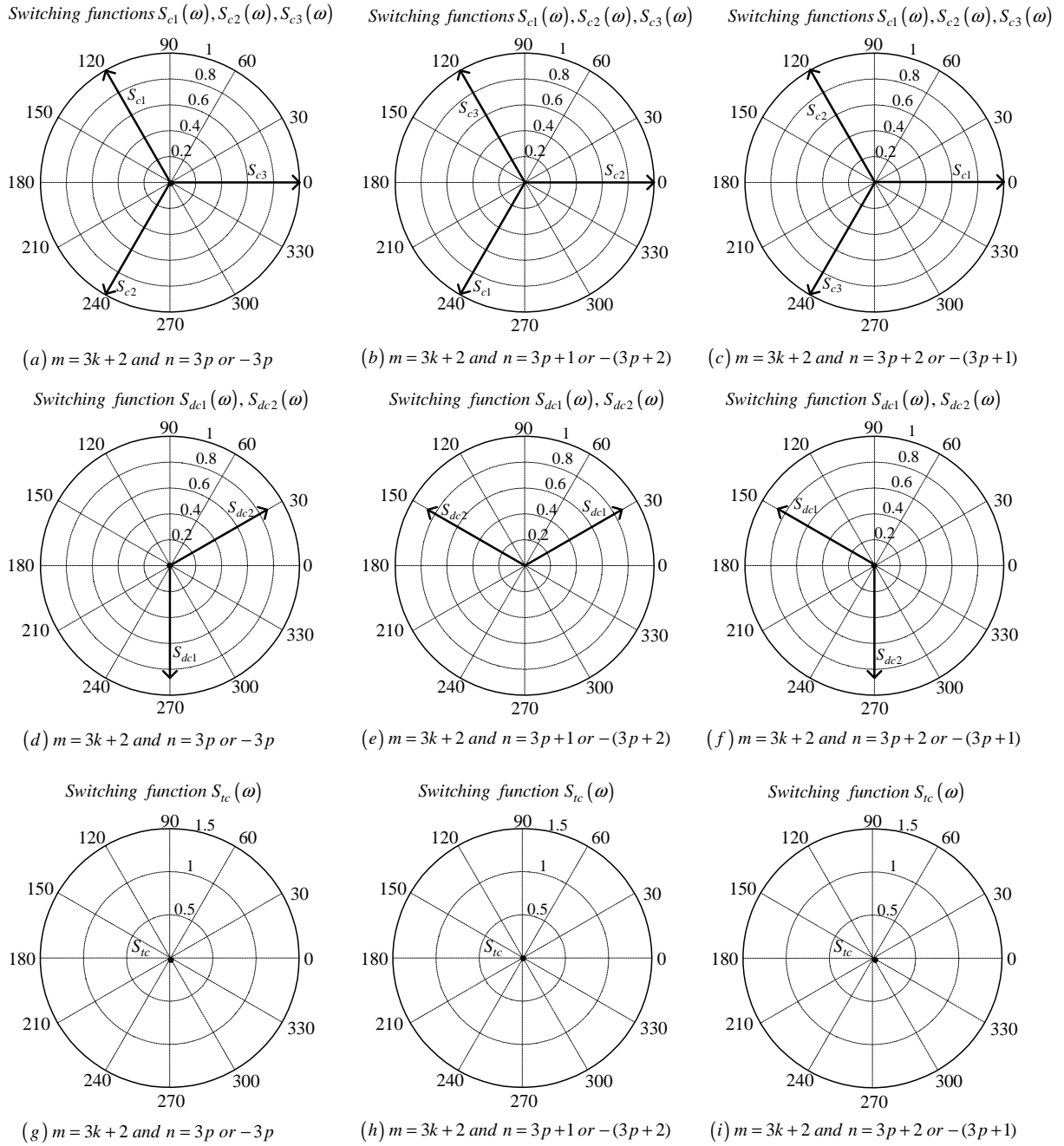


Figure C.32: Phasor representation for phase C of 3-cell converter for $m = 3k + 2$

C.2.3 For frequency modulation index $m_f = 3k + 2$

Phase A

Derivation for switching functions of phase A are the same as in subsection C.2.1 for $m_f = 3k$.

Phase B

From table C.2 the value of h for the background function of $s_{b1}(t)$ is given by:

$$h = \frac{2\omega_s}{\pi}t_1 - \frac{4}{3} \quad (\text{C.241})$$

Substituting equation C.241 into the term $\frac{m\pi h}{2}$ of equation 3.36 we obtain:

$$\frac{m\pi h}{2} = m\omega_s t_1 - \frac{2}{3}m\pi \quad (\text{C.242})$$

Now substituting equation C.242 into equation 3.36 we obtain:

$$\begin{aligned} s_{b1}(t_1) &= \frac{1}{2}A_{00} + \sum_{n=1}^{\infty} (A_{0n} \cos(n\omega_0 t_1) + B_{0n} \sin(n\omega_0 t_1)) \\ &+ \sum_{m=1}^{\infty} \left(A_{m0} \cos\left(m\omega_s t_1 - \frac{2}{3}m\pi\right) + B_{m0} \sin\left(m\omega_s t_1 - \frac{2}{3}m\pi\right) \right) \\ &+ \sum_{m=1}^{\infty} \sum_{n=\pm 1}^{\pm\infty} \left\{ A_{mn} \cos\left((m\omega_s + n\omega_0)t_1 - \frac{2}{3}m\pi\right) \right. \\ &\left. + B_{mn} \sin\left((m\omega_s + n\omega_0)t_1 - \frac{2}{3}m\pi\right) \right\} \end{aligned} \quad (\text{C.243})$$

We now substitute back $t = t_1 + \frac{T_0}{3}$ into equation C.243 and obtain:

$$\begin{aligned} s_{b1}(t) &= \frac{1}{2}A_{00} + \sum_{n=1}^{\infty} \left(A_{0n} \cos\left(n\omega_0 \left(t - \frac{2\pi}{3\omega_0}\right)\right) + B_{0n} \sin\left(n\omega_0 \left(t - \frac{2\pi}{3\omega_0}\right)\right) \right) \\ &+ \sum_{m=1}^{\infty} \left(A_{m0} \cos\left(m\omega_s \left(t - \frac{2\pi}{3\omega_0}\right) - \frac{2}{3}m\pi\right) \right. \\ &\left. + B_{m0} \sin\left(m\omega_s \left(t - \frac{2\pi}{3\omega_0}\right) - \frac{2}{3}m\pi\right) \right) \\ &+ \sum_{m=1}^{\infty} \sum_{n=\pm 1}^{\pm\infty} \left\{ A_{mn} \cos\left((m\omega_s + n\omega_0) \left(t - \frac{2\pi}{3\omega_0}\right) - \frac{2}{3}m\pi\right) \right. \\ &\left. + B_{mn} \sin\left((m\omega_s + n\omega_0) \left(t - \frac{2\pi}{3\omega_0}\right) - \frac{2}{3}m\pi\right) \right\} \end{aligned} \quad (\text{C.244})$$

From table C.2 for the background function of $s_{b2}(t)$ the value of h is given by:

$$h = \frac{2\omega_s}{\pi}t_1 - \frac{8}{3} \quad (\text{C.245})$$

Substituting equation C.245 into the term $\frac{m\pi h}{2}$ of equation 3.36 we obtain:

$$\frac{m\pi h}{2} = m\omega_s t_1 - \frac{4}{3}m\pi \quad (\text{C.246})$$

Now substituting equation C.246 into equation 3.36 we obtain:

$$\begin{aligned} s_{b2}(t_1) &= \frac{1}{2}A_{00} + \sum_{n=1}^{\infty} (A_{0n} \cos(n\omega_0 t_1) + B_{0n} \sin(n\omega_0 t_1)) \\ &+ \sum_{m=1}^{\infty} \left(A_{m0} \cos\left(m\omega_s t_1 - \frac{4}{3}m\pi\right) + B_{m0} \sin\left(m\omega_s t_1 - \frac{4}{3}m\pi\right) \right) \\ &+ \sum_{m=1}^{\infty} \sum_{n=\pm 1}^{\pm\infty} \left\{ A_{mn} \cos\left((m\omega_s + n\omega_0)t_1 - \frac{4}{3}m\pi\right) \right. \\ &\quad \left. + B_{mn} \sin\left((m\omega_s + n\omega_0)t_1 - \frac{4}{3}m\pi\right) \right\} \end{aligned} \quad (\text{C.247})$$

We now substitute back $t = t_1 + \frac{T_0}{3}$ into equation C.247 and obtain:

$$\begin{aligned} s_{b2}(t_1) &= \frac{1}{2}A_{00} + \sum_{n=1}^{\infty} \left(A_{0n} \cos\left(n\omega_0 \left(t - \frac{2\pi}{3\omega_0}\right)\right) + B_{0n} \sin\left(n\omega_0 \left(t - \frac{2\pi}{3\omega_0}\right)\right) \right) \\ &+ \sum_{m=1}^{\infty} \left(A_{m0} \cos\left(m\omega_s \left(t - \frac{2\pi}{3\omega_0}\right) - \frac{4}{3}m\pi\right) \right. \\ &\quad \left. + B_{m0} \sin\left(m\omega_s \left(t - \frac{2\pi}{3\omega_0}\right) - \frac{4}{3}m\pi\right) \right) \\ &+ \sum_{m=1}^{\infty} \sum_{n=\pm 1}^{\pm\infty} \left\{ A_{mn} \cos\left((m\omega_s + n\omega_0) \left(t - \frac{2\pi}{3\omega_0}\right) - \frac{4}{3}m\pi\right) \right. \\ &\quad \left. + B_{mn} \sin\left((m\omega_s + n\omega_0) \left(t - \frac{2\pi}{3\omega_0}\right) - \frac{4}{3}m\pi\right) \right\} \end{aligned} \quad (\text{C.248})$$

From table C.2 for the background function of $s_{b3}(t)$ the value of h is given by:

$$h = \frac{2\omega_s}{\pi} t_1 \quad (\text{C.249})$$

Substituting equation C.249 into the term $\frac{m\pi h}{2}$ of equation 3.36 we obtain:

$$\frac{m\pi h}{2} = m\omega_s t_1 \quad (\text{C.250})$$

Now substituting equation C.250 into equation 3.36 we obtain:

$$\begin{aligned}
s_{b3}(t_1) &= \frac{1}{2}A_{00} + \sum_{n=1}^{\infty} (A_{0n} \cos(n\omega_0 t_1) + B_{0n} \sin(n\omega_0 t_1)) \\
&\quad + \sum_{m=1}^{\infty} (A_{m0} \cos(m\omega_s t_1) + B_{m0} \sin(m\omega_s t_1)) \\
&\quad + \sum_{m=1}^{\infty} \sum_{n=\pm 1}^{\pm\infty} \{A_{mn} \cos((m\omega_s + n\omega_0) t_1) \\
&\quad + B_{mn} \sin((m\omega_s + n\omega_0) t_1)\}
\end{aligned} \tag{C.251}$$

We now substitute back $t = t_1 + \frac{T_0}{3}$ into equation C.251 and obtain:

$$\begin{aligned}
s_{b3}(t) &= \frac{1}{2}A_{00} + \sum_{n=1}^{\infty} \left(A_{0n} \cos\left(n\omega_0 \left(t - \frac{2\pi}{3\omega_0}\right)\right) + B_{0n} \sin\left(n\omega_0 \left(t - \frac{2\pi}{3\omega_0}\right)\right) \right) \\
&\quad + \sum_{m=1}^{\infty} \left(A_{m0} \cos\left(m\omega_s \left(t - \frac{2\pi}{3\omega_0}\right)\right) \right. \\
&\quad \left. + B_{m0} \sin\left(m\omega_s \left(t - \frac{2\pi}{3\omega_0}\right)\right) \right) \\
&\quad + \sum_{m=1}^{\infty} \sum_{n=\pm 1}^{\pm\infty} \left\{ A_{mn} \cos\left((m\omega_s + n\omega_0) \left(t - \frac{2\pi}{3\omega_0}\right)\right) \right. \\
&\quad \left. + B_{mn} \sin\left((m\omega_s + n\omega_0) \left(t - \frac{2\pi}{3\omega_0}\right)\right) \right\}
\end{aligned} \tag{C.252}$$

Now considering trigonometric terms in equation C.244, C.248 and C.252 we have:

$$\begin{aligned}
\cos\left(n\omega_0 \left(t - \frac{2\pi}{3\omega_0}\right)\right) &= \cos\left(n\omega_0 t - \frac{2n\pi}{3}\right) \\
&= \begin{cases} \cos(n\omega_0 t) & \text{if } n = 3p \\ \cos\left(n\omega_0 t - \frac{2\pi}{3}\right) & \text{if } n = 3p + 1 \\ \cos\left(n\omega_0 t + \frac{2\pi}{3}\right) & \text{if } n = 3p + 2 \end{cases}
\end{aligned} \tag{C.253}$$

$$\begin{aligned}
\sin\left(n\omega_0 \left(t - \frac{2\pi}{3\omega_0}\right)\right) &= \sin\left(n\omega_0 t - \frac{2n\pi}{3}\right) \\
&= \begin{cases} \sin(n\omega_0 t) & \text{if } n = 3p \\ \sin\left(n\omega_0 t - \frac{2\pi}{3}\right) & \text{if } n = 3p + 1 \\ \sin\left(n\omega_0 t + \frac{2\pi}{3}\right) & \text{if } n = 3p + 2 \end{cases}
\end{aligned} \tag{C.254}$$

$$\begin{aligned}
\cos\left(m\omega_s \left(t - \frac{2\pi}{3\omega_0}\right)\right) &= \cos\left(m\omega_s t - \frac{2m\pi}{3}m_f\right) \\
&= \cos(m\omega_s t)
\end{aligned} \tag{C.255}$$

$$\begin{aligned}\sin\left(m\omega_s\left(t - \frac{2\pi}{3\omega_0}\right)\right) &= \sin\left(m\omega_s t - \frac{2m\pi}{3}m_f\right) \\ &= \sin(m\omega_s t)\end{aligned}\quad (\text{C.256})$$

$$\begin{aligned}\cos\left(m\omega_s\left(t - \frac{2\pi}{3\omega_0}\right) - \frac{2m\pi}{3}\right) &= \cos\left(m\omega_s t - \frac{2m\pi}{3}m_f - \frac{2m\pi}{3}\right) \\ &= \begin{cases} \cos(m\omega_s t) & \text{if } m = 3k \\ \cos\left(m\omega_s t - \frac{2\pi}{3}\right) & \text{if } m = 3k + 1 \\ \cos\left(m\omega_s t + \frac{2\pi}{3}\right) & \text{if } m = 3k + 2 \end{cases}\end{aligned}\quad (\text{C.257})$$

$$\begin{aligned}\sin\left(m\omega_s\left(t - \frac{2\pi}{3\omega_0}\right) - \frac{2m\pi}{3}\right) &= \sin\left(m\omega_s t - \frac{2m\pi}{3}m_f - \frac{2m\pi}{3}\right) \\ &= \begin{cases} \sin(m\omega_s t) & \text{if } m = 3k \\ \sin\left(m\omega_s t - \frac{2\pi}{3}\right) & \text{if } m = 3k + 1 \\ \sin\left(m\omega_s t + \frac{2\pi}{3}\right) & \text{if } m = 3k + 2 \end{cases}\end{aligned}\quad (\text{C.258})$$

$$\cos\left(m\omega_s\left(t - \frac{2\pi}{3\omega_0}\right) - \frac{4m\pi}{3}\right) = \begin{cases} \cos(m\omega_s t) & \text{if } m = 3k \\ \cos\left(m\omega_s t + \frac{2\pi}{3}\right) & \text{if } m = 3k + 1 \\ \cos\left(m\omega_s t - \frac{2\pi}{3}\right) & \text{if } m = 3k + 2 \end{cases}\quad (\text{C.259})$$

$$\sin\left(m\omega_s\left(t - \frac{2\pi}{3\omega_0}\right) - \frac{4m\pi}{3}\right) = \begin{cases} \sin(m\omega_s t) & \text{if } m = 3k \\ \sin\left(m\omega_s t + \frac{2\pi}{3}\right) & \text{if } m = 3k + 1 \\ \sin\left(m\omega_s t - \frac{2\pi}{3}\right) & \text{if } m = 3k + 2 \end{cases}\quad (\text{C.260})$$

$$\begin{aligned}\cos\left((m\omega_s + n\omega_0)\left(t - \frac{2\pi}{3\omega_0}\right)\right) &= \cos\left((m\omega_s + n\omega_0)t - \frac{2m\pi}{3}m_f - \frac{2n\pi}{3}\right) \\ &= \begin{cases} \cos((m\omega_s + n\omega_0)t) & \text{if } m = k \text{ and } n=3p \text{ or } n=-3p \\ \cos\left((m\omega_s + n\omega_0)t - \frac{2\pi}{3}\right) & \text{if } m = k \text{ and } n=3p+1 \text{ or } n=-(3p+2) \\ \cos\left((m\omega_s + n\omega_0)t + \frac{2\pi}{3}\right) & \text{if } m = k \text{ and } n=3p+2 \text{ or } n=-(3p+1) \end{cases}\end{aligned}\quad (\text{C.261})$$

$$\begin{aligned}\sin\left((m\omega_s + n\omega_0)\left(t - \frac{2\pi}{3\omega_0}\right)\right) &= \sin\left((m\omega_s + n\omega_0)t - \frac{2m\pi}{3}m_f - \frac{2n\pi}{3}\right) \\ &= \begin{cases} \sin((m\omega_s + n\omega_0)t) & \text{if } m = k \text{ and } n=3p \text{ or } n=-3p \\ \sin\left((m\omega_s + n\omega_0)t - \frac{2\pi}{3}\right) & \text{if } m = k \text{ and } n=3p+1 \text{ or } n=-(3p+2) \\ \sin\left((m\omega_s + n\omega_0)t + \frac{2\pi}{3}\right) & \text{if } m = k \text{ and } n=3p+2 \text{ or } n=-(3p+1) \end{cases}\end{aligned}\quad (\text{C.262})$$

$$\begin{aligned}
& \cos \left((m\omega_s + n\omega_0) \left(t - \frac{2\pi}{3\omega_0} \right) - \frac{2m\pi}{3} \right) = \cos \left((m\omega_s + n\omega_0) t - \frac{2m\pi}{3} m_f - \frac{2n\pi}{3} - \frac{2m\pi}{3} \right) \\
= & \begin{cases} \cos((m\omega_s + n\omega_0)t) & \text{if } m = 3k \text{ and } n=3p \text{ or } n=-3p \\ \cos\left((m\omega_s + n\omega_0)t - \frac{2\pi}{3}\right) & \text{if } m = 3k \text{ and } n=3p+1 \text{ or } n=-(3p+2) \\ \cos\left((m\omega_s + n\omega_0)t + \frac{2\pi}{3}\right) & \text{if } m = 3k \text{ and } n=3p+2 \text{ or } n=-(3p+1) \\ \cos\left((m\omega_s + n\omega_0)t - \frac{2\pi}{3}\right) & \text{if } m = 3k + 1 \text{ and } n=3p \text{ or } n=-3p \\ \cos\left((m\omega_s + n\omega_0)t + \frac{2\pi}{3}\right) & \text{if } m = 3k + 1 \text{ and } n=3p+1 \text{ or } n=-(3p+2) \\ \cos((m\omega_s + n\omega_0)t) & \text{if } m = 3k + 1 \text{ and } n=3p+2 \text{ or } n=-(3p+1) \\ \cos\left((m\omega_s + n\omega_0)t + \frac{2\pi}{3}\right) & \text{if } m = 3k + 2 \text{ and } n=3p \text{ or } n=-3p \\ \cos((m\omega_s + n\omega_0)t) & \text{if } m = 3k + 2 \text{ and } n=3p+1 \text{ or } n=-(3p+2) \\ \cos\left((m\omega_s + n\omega_0)t - \frac{2\pi}{3}\right) & \text{if } m = 3k + 2 \text{ and } n=3p+2 \text{ or } n=-(3p+1) \end{cases}
\end{aligned} \tag{C.263}$$

$$\begin{aligned}
& \sin \left((m\omega_s + n\omega_0) \left(t - \frac{2\pi}{3\omega_0} \right) - \frac{2m\pi}{3} \right) = \sin \left((m\omega_s + n\omega_0) t - \frac{2m\pi}{3} m_f - \frac{2n\pi}{3} - \frac{2m\pi}{3} \right) \\
= & \begin{cases} \sin((m\omega_s + n\omega_0)t) & \text{if } m = 3k \text{ and } n=3p \text{ or } n=-3p \\ \sin\left((m\omega_s + n\omega_0)t - \frac{2\pi}{3}\right) & \text{if } m = 3k \text{ and } n=3p+1 \text{ or } n=-(3p+2) \\ \sin\left((m\omega_s + n\omega_0)t + \frac{2\pi}{3}\right) & \text{if } m = 3k \text{ and } n=3p+2 \text{ or } n=-(3p+1) \\ \sin\left((m\omega_s + n\omega_0)t - \frac{2\pi}{3}\right) & \text{if } m = 3k + 1 \text{ and } n=3p \text{ or } n=-3p \\ \sin\left((m\omega_s + n\omega_0)t + \frac{2\pi}{3}\right) & \text{if } m = 3k + 1 \text{ and } n=3p+1 \text{ or } n=-(3p+2) \\ \sin((m\omega_s + n\omega_0)t) & \text{if } m = 3k + 1 \text{ and } n=3p+2 \text{ or } n=-(3p+1) \\ \sin\left((m\omega_s + n\omega_0)t + \frac{2\pi}{3}\right) & \text{if } m = 3k + 2 \text{ and } n=3p \text{ or } n=-3p \\ \sin((m\omega_s + n\omega_0)t) & \text{if } m = 3k + 2 \text{ and } n=3p+1 \text{ or } n=-(3p+2) \\ \sin\left((m\omega_s + n\omega_0)t - \frac{2\pi}{3}\right) & \text{if } m = 3k + 2 \text{ and } n=3p+2 \text{ or } n=-(3p+1) \end{cases}
\end{aligned} \tag{C.264}$$

$$\begin{aligned}
& \cos \left((m\omega_s + n\omega_0) \left(t - \frac{2\pi}{3\omega_0} \right) - \frac{4m\pi}{3} \right) = \cos \left((m\omega_s + n\omega_0) t - \frac{2m\pi}{3} m_f - \frac{2n\pi}{3} - \frac{4m\pi}{3} \right) \\
= & \begin{cases} \cos((m\omega_s + n\omega_0)t) & \text{if } m = 3k \text{ and } n=3p \text{ or } n=-3p \\ \cos\left((m\omega_s + n\omega_0)t - \frac{2\pi}{3}\right) & \text{if } m = 3k \text{ and } n=3p+1 \text{ or } n=-(3p+2) \\ \cos\left((m\omega_s + n\omega_0)t + \frac{2\pi}{3}\right) & \text{if } m = 3k \text{ and } n=3p+2 \text{ or } n=-(3p+1) \\ \cos\left((m\omega_s + n\omega_0)t + \frac{2\pi}{3}\right) & \text{if } m = 3k + 1 \text{ and } n=3p \text{ or } n=-3p \\ \cos((m\omega_s + n\omega_0)t) & \text{if } m = 3k + 1 \text{ and } n=3p+1 \text{ or } n=-(3p+2) \\ \cos\left((m\omega_s + n\omega_0)t - \frac{2\pi}{3}\right) & \text{if } m = 3k + 1 \text{ and } n=3p+2 \text{ or } n=-(3p+1) \\ \cos\left((m\omega_s + n\omega_0)t - \frac{2\pi}{3}\right) & \text{if } m = 3k + 2 \text{ and } n=3p \text{ or } n=-3p \\ \cos\left((m\omega_s + n\omega_0)t + \frac{2\pi}{3}\right) & \text{if } m = 3k + 2 \text{ and } n=3p+1 \text{ or } n=-(3p+2) \\ \cos((m\omega_s + n\omega_0)t) & \text{if } m = 3k + 2 \text{ and } n=3p+2 \text{ or } n=-(3p+1) \end{cases}
\end{aligned}$$

(C.265)

$$\begin{aligned}
& \sin \left((m\omega_s + n\omega_0) \left(t - \frac{2\pi}{3\omega_0} \right) - \frac{4m\pi}{3} \right) = \sin \left((m\omega_s + n\omega_0) t - \frac{2m\pi}{3} m_f - \frac{2n\pi}{3} - \frac{4m\pi}{3} \right) \\
= & \begin{cases} \sin((m\omega_s + n\omega_0)t) & \text{if } m = 3k \text{ and } n=3p \text{ or } n=-3p \\ \sin\left((m\omega_s + n\omega_0)t - \frac{2\pi}{3}\right) & \text{if } m = 3k \text{ and } n=3p+1 \text{ or } n=-(3p+2) \\ \sin\left((m\omega_s + n\omega_0)t + \frac{2\pi}{3}\right) & \text{if } m = 3k \text{ and } n=3p+2 \text{ or } n=-(3p+1) \\ \sin\left((m\omega_s + n\omega_0)t + \frac{2\pi}{3}\right) & \text{if } m = 3k + 1 \text{ and } n=3p \text{ or } n=-3p \\ \sin((m\omega_s + n\omega_0)t) & \text{if } m = 3k + 1 \text{ and } n=3p+1 \text{ or } n=-(3p+2) \\ \sin\left((m\omega_s + n\omega_0)t - \frac{2\pi}{3}\right) & \text{if } m = 3k + 1 \text{ and } n=3p+2 \text{ or } n=-(3p+1) \\ \sin\left((m\omega_s + n\omega_0)t - \frac{2\pi}{3}\right) & \text{if } m = 3k + 2 \text{ and } n=3p \text{ or } n=-3p \\ \sin\left((m\omega_s + n\omega_0)t + \frac{2\pi}{3}\right) & \text{if } m = 3k + 2 \text{ and } n=3p+1 \text{ or } n=-(3p+2) \\ \sin((m\omega_s + n\omega_0)t) & \text{if } m = 3k + 2 \text{ and } n=3p+2 \text{ or } n=-(3p+1) \end{cases}
\end{aligned}
\tag{C.266}$$

Thus the phasor representation for phase B of 3-cell converter when $m_f = 3k + 2$ is given by Figures C.33, C.34 and C.35.

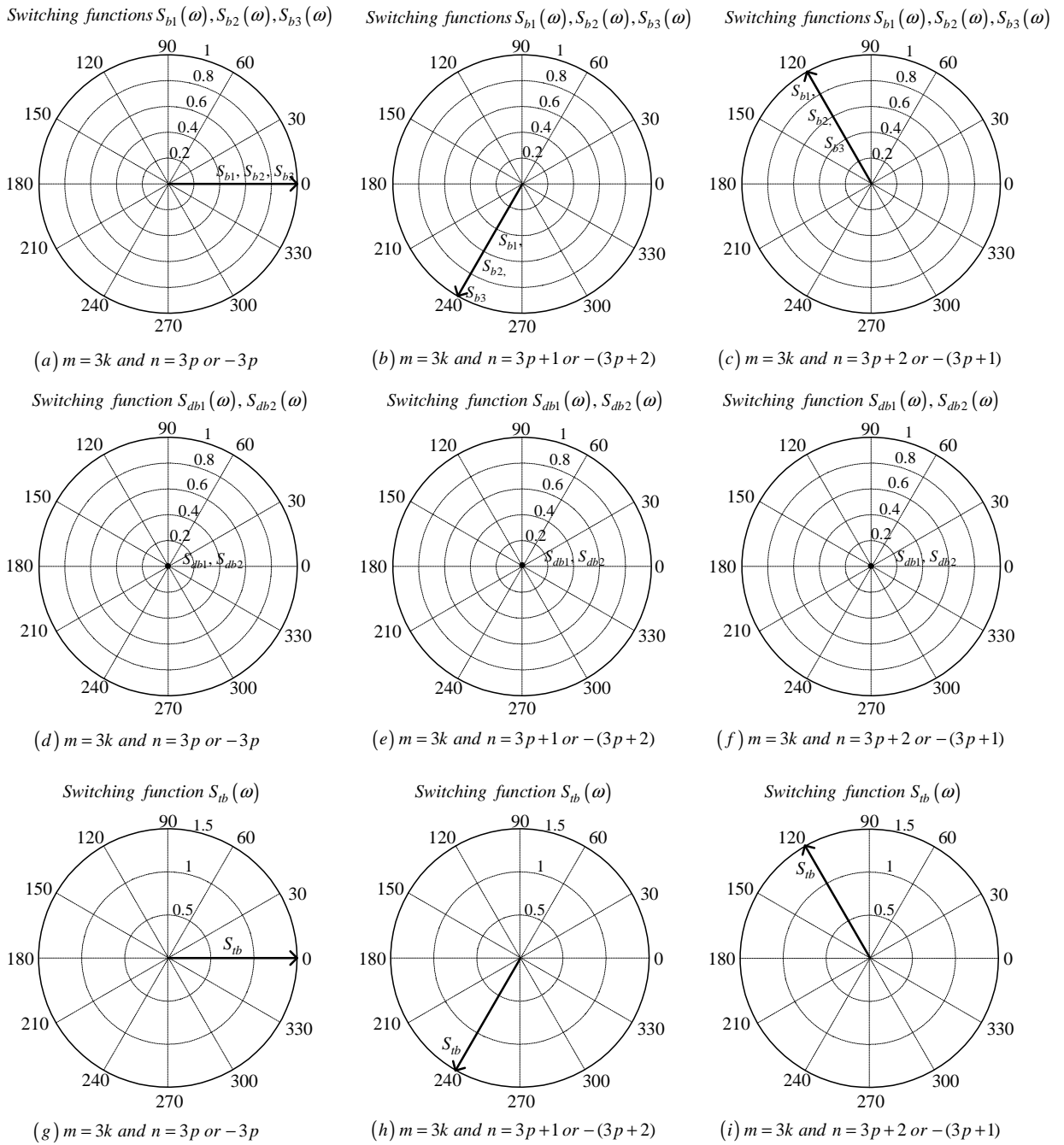


Figure C.33: Phasor representation for phase B of 3-cell converter for $m = 3k$

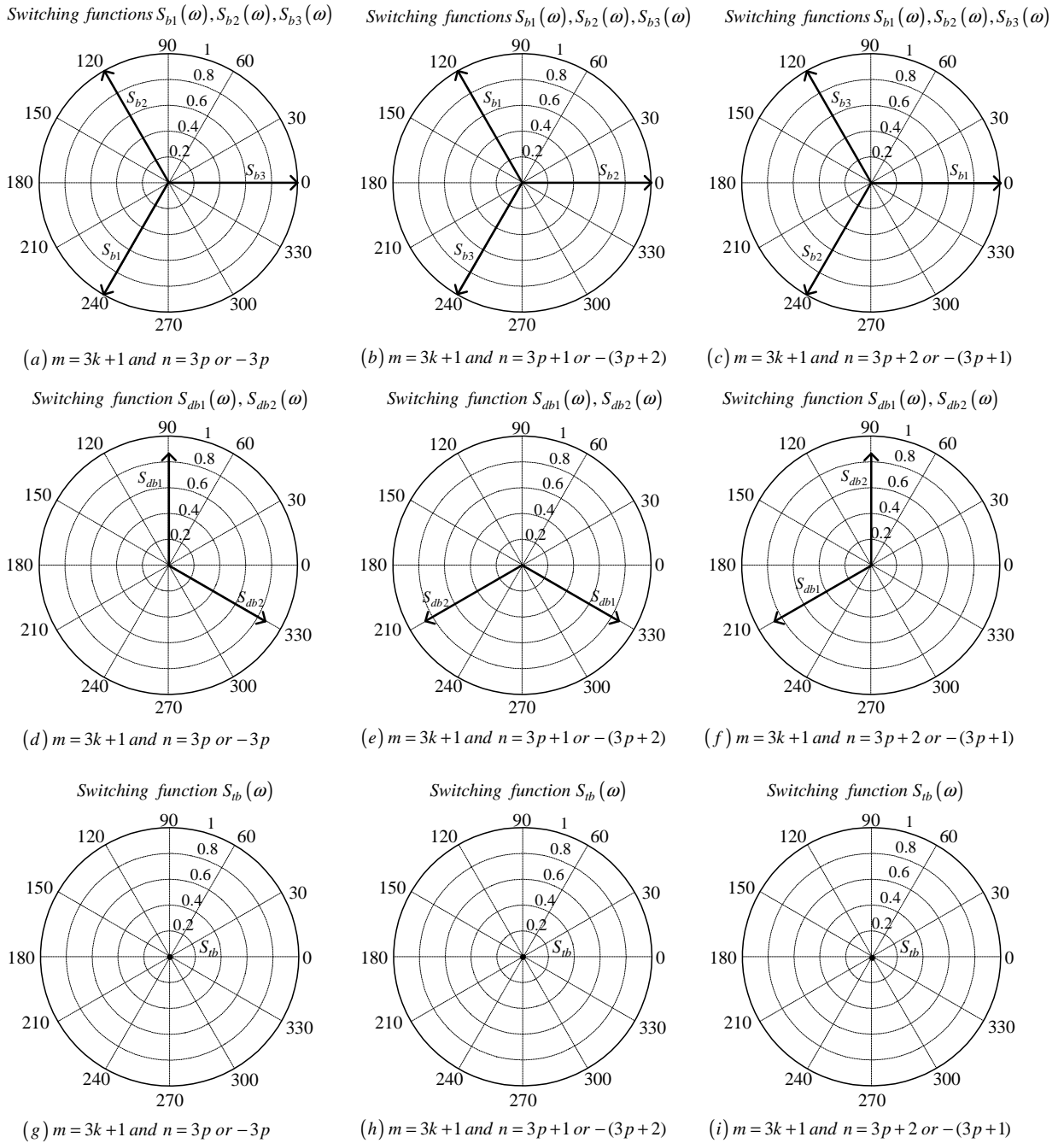


Figure C.34: Phasor representation for phase B of 3-cell converter for $m = 3k + 1$

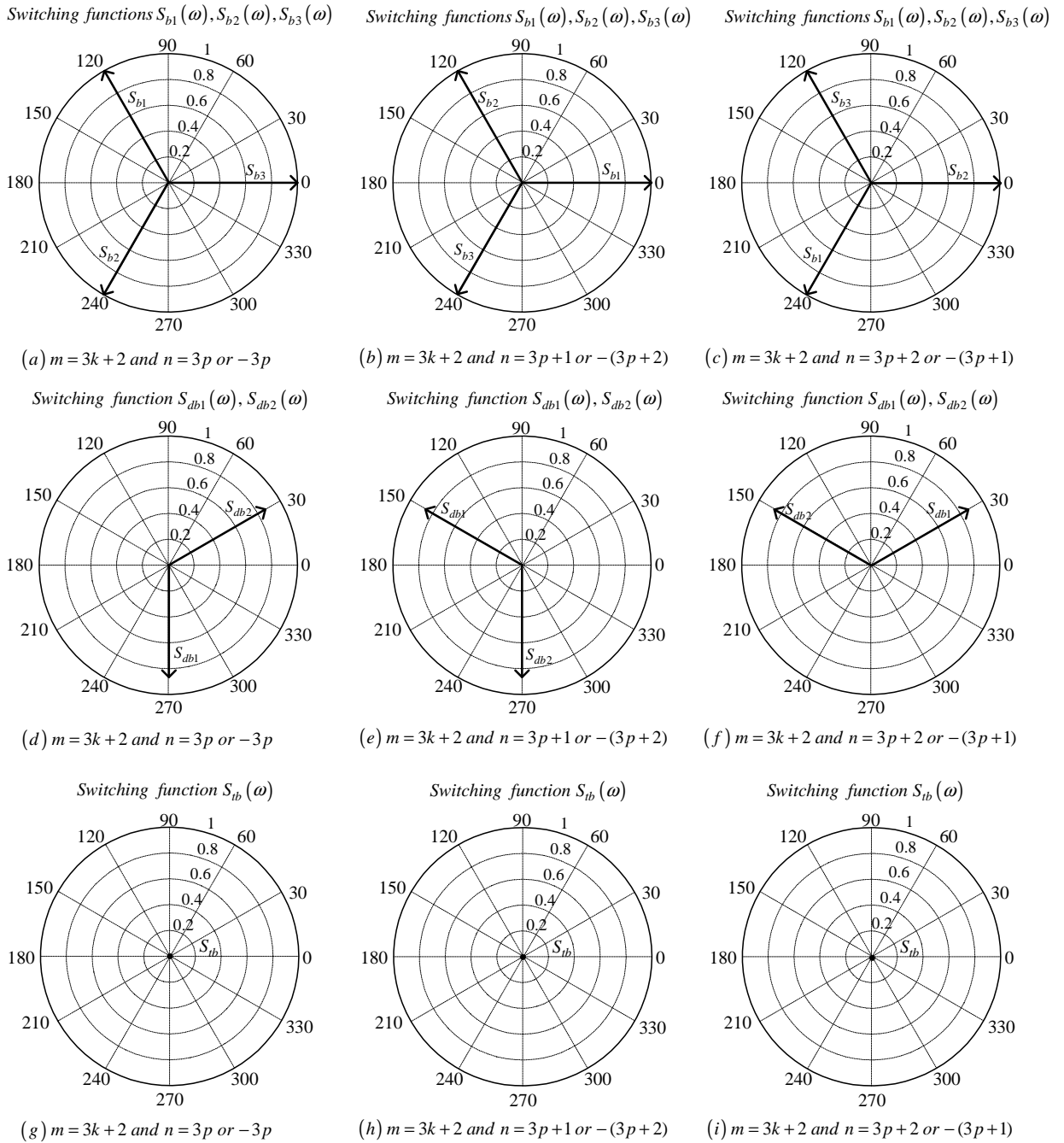


Figure C.35: Phasor representation for phase B of 3-cell converter for $m = 3k + 2$

Phase C

From table C.2 the value of h for the background function of $s_{c1}(t)$ is given by:

$$h = \frac{2\omega_s}{\pi}t_2 - \frac{8}{3} \quad (\text{C.267})$$

Substituting equation C.267 into the term $\frac{m\pi h}{2}$ of equation 3.36 we obtain:

$$\frac{m\pi h}{2} = m\omega_s t_2 - \frac{4}{3}m\pi \quad (\text{C.268})$$

Now substituting equation C.268 into equation 3.36 we obtain:

$$\begin{aligned} s_{c1}(t_2) &= \frac{1}{2}A_{00} + \sum_{n=1}^{\infty} (A_{0n} \cos(n\omega_0 t_2) + B_{0n} \sin(n\omega_0 t_2)) \\ &+ \sum_{m=1}^{\infty} \left(A_{m0} \cos\left(m\omega_s t_2 - \frac{4}{3}m\pi\right) + B_{m0} \sin\left(m\omega_s t_2 - \frac{4}{3}m\pi\right) \right) \\ &+ \sum_{m=1}^{\infty} \sum_{n=\pm 1}^{\pm\infty} \left\{ A_{mn} \cos\left((m\omega_s + n\omega_0)t_2 - \frac{4}{3}m\pi\right) \right. \\ &\quad \left. + B_{mn} \sin\left((m\omega_s + n\omega_0)t_2 - \frac{4}{3}m\pi\right) \right\} \end{aligned} \quad (\text{C.269})$$

We now substitute back $t = t_2 + \frac{2T_0}{3}$ into equation C.269 and obtain:

$$\begin{aligned} s_{c1}(t) &= \frac{1}{2}A_{00} + \sum_{n=1}^{\infty} \left(A_{0n} \cos\left(n\omega_0 \left(t - \frac{4\pi}{3\omega_0}\right)\right) + B_{0n} \sin\left(n\omega_0 \left(t - \frac{4\pi}{3\omega_0}\right)\right) \right) \\ &+ \sum_{m=1}^{\infty} \left(A_{m0} \cos\left(m\omega_s \left(t - \frac{4\pi}{3\omega_0}\right) - \frac{4}{3}m\pi\right) \right. \\ &\quad \left. + B_{m0} \sin\left(m\omega_s \left(t - \frac{4\pi}{3\omega_0}\right) - \frac{4}{3}m\pi\right) \right) \\ &+ \sum_{m=1}^{\infty} \sum_{n=\pm 1}^{\pm\infty} \left\{ A_{mn} \cos\left((m\omega_s + n\omega_0) \left(t - \frac{4\pi}{3\omega_0}\right) - \frac{4}{3}m\pi\right) \right. \\ &\quad \left. + B_{mn} \sin\left((m\omega_s + n\omega_0) \left(t - \frac{4\pi}{3\omega_0}\right) - \frac{4}{3}m\pi\right) \right\} \end{aligned} \quad (\text{C.270})$$

From table C.2 for the background function of $s_{c2}(t)$ the value of h is given by:

$$h = \frac{2\omega_s}{\pi}t_2 \quad (\text{C.271})$$

Substituting equation C.271 into the term $\frac{m\pi h}{2}$ of equation 3.36 we obtain:

$$\frac{m\pi h}{2} = m\omega_s t_2 \quad (\text{C.272})$$

Now substituting equation C.272 into equation 3.36 we obtain:

$$\begin{aligned}
s_{c2}(t_2) &= \frac{1}{2}A_{00} + \sum_{n=1}^{\infty} (A_{0n} \cos(n\omega_0 t_2) + B_{0n} \sin(n\omega_0 t_2)) \\
&+ \sum_{m=1}^{\infty} (A_{m0} \cos(m\omega_s t_2) + B_{m0} \sin(m\omega_s t_2)) \\
&+ \sum_{m=1}^{\infty} \sum_{n=\pm 1}^{\pm\infty} \{A_{mn} \cos((m\omega_s + n\omega_0) t_2) \\
&+ B_{mn} \sin((m\omega_s + n\omega_0) t_2)\}
\end{aligned} \tag{C.273}$$

We now substitute back $t = t_2 + \frac{2T_0}{3}$ into equation C.273 and obtain:

$$\begin{aligned}
s_{c2}(t) &= \frac{1}{2}A_{00} + \sum_{n=1}^{\infty} \left(A_{0n} \cos\left(n\omega_0 \left(t - \frac{4\pi}{3\omega_0}\right)\right) + B_{0n} \sin\left(n\omega_0 \left(t - \frac{4\pi}{3\omega_0}\right)\right) \right) \\
&+ \sum_{m=1}^{\infty} \left(A_{m0} \cos\left(m\omega_s \left(t - \frac{4\pi}{3\omega_0}\right)\right) \right. \\
&+ B_{m0} \sin\left(m\omega_s \left(t - \frac{4\pi}{3\omega_0}\right) - \frac{4m\pi}{3}\right) \\
&+ \sum_{m=1}^{\infty} \sum_{n=\pm 1}^{\pm\infty} \left\{ A_{mn} \cos\left((m\omega_s + n\omega_0) \left(t - \frac{4\pi}{3\omega_0}\right)\right) \right. \\
&+ B_{mn} \sin\left((m\omega_s + n\omega_0) \left(t - \frac{4\pi}{3\omega_0}\right)\right) \left. \right\}
\end{aligned} \tag{C.274}$$

From table C.2 for the background function of $s_{c3}(t)$ the value of h is given by:

$$h = \frac{2\omega_s}{\pi} t_2 - \frac{4}{3} \tag{C.275}$$

Substituting equation C.275 into the term $\frac{m\pi h}{2}$ of equation 3.36 we obtain:

$$\frac{m\pi h}{2} = m\omega_s t_2 - \frac{2}{3}m\pi \tag{C.276}$$

Now substituting equation C.276 into equation 3.36 we obtain:

$$\begin{aligned}
s_{c3}(t_2) &= \frac{1}{2}A_{00} + \sum_{n=1}^{\infty} (A_{0n} \cos(n\omega_0 t_2) + B_{0n} \sin(n\omega_0 t_2)) \\
&+ \sum_{m=1}^{\infty} \left(A_{m0} \cos\left(m\omega_s t_2 - \frac{2}{3}m\pi\right) + B_{m0} \sin\left(m\omega_s t_2 - \frac{2}{3}m\pi\right) \right) \\
&+ \sum_{m=1}^{\infty} \sum_{n=\pm 1}^{\pm\infty} \left\{ A_{mn} \cos\left((m\omega_s + n\omega_0) t_2 - \frac{2}{3}m\pi\right) \right. \\
&+ B_{mn} \sin\left((m\omega_s + n\omega_0) t_2 - \frac{2}{3}m\pi\right) \left. \right\}
\end{aligned} \tag{C.277}$$

We now substitute back $t = t_2 + \frac{2T_0}{3}$ into equation C.277 and obtain:

$$\begin{aligned}
 s_{c3}(t) &= \frac{1}{2}A_{00} + \sum_{n=1}^{\infty} \left(A_{0n} \cos \left(n\omega_0 \left(t - \frac{4\pi}{3\omega_0} \right) \right) + B_{0n} \sin \left(n\omega_0 \left(t - \frac{4\pi}{3\omega_0} \right) \right) \right) \\
 &+ \sum_{m=1}^{\infty} \left(A_{m0} \cos \left(m\omega_s \left(t - \frac{4\pi}{3\omega_0} \right) - \frac{2}{3}m\pi \right) + B_{m0} \sin \left(m\omega_s \left(t - \frac{4\pi}{3\omega_0} \right) - \frac{2}{3}m\pi \right) \right) \\
 &+ \sum_{m=1}^{\infty} \sum_{n=\pm 1}^{\pm \infty} \left\{ A_{mn} \cos \left((m\omega_s + n\omega_0) \left(t - \frac{4\pi}{3\omega_0} \right) - \frac{2}{3}m\pi \right) \right. \\
 &\left. + B_{mn} \sin \left((m\omega_s + n\omega_0) \left(t - \frac{4\pi}{3\omega_0} \right) - \frac{2}{3}m\pi \right) \right\} \tag{C.278}
 \end{aligned}$$

Now considering trigonometric terms in equation C.270, C.274 and C.278 we have:

$$\begin{aligned}
 \cos \left(n\omega_0 \left(t - \frac{4\pi}{3\omega_0} \right) \right) &= \cos \left(n\omega_0 t - \frac{4n\pi}{3} \right) \\
 &= \begin{cases} \cos(n\omega_0 t) & \text{if } n = 3p \\ \cos \left(n\omega_0 t + \frac{2\pi}{3} \right) & \text{if } n = 3p + 1 \\ \cos \left(n\omega_0 t - \frac{2\pi}{3} \right) & \text{if } n = 3p + 2 \end{cases} \tag{C.279}
 \end{aligned}$$

$$\begin{aligned}
 \sin \left(n\omega_0 \left(t - \frac{4\pi}{3\omega_0} \right) \right) &= \sin \left(n\omega_0 t - \frac{4n\pi}{3} \right) \\
 &= \begin{cases} \sin(n\omega_0 t) & \text{if } n = 3p \\ \sin \left(n\omega_0 t + \frac{2\pi}{3} \right) & \text{if } n = 3p + 1 \\ \sin \left(n\omega_0 t - \frac{2\pi}{3} \right) & \text{if } n = 3p + 2 \end{cases} \tag{C.280}
 \end{aligned}$$

$$\begin{aligned}
 \cos \left(m\omega_s \left(t - \frac{4\pi}{3\omega_0} \right) \right) &= \cos \left(m\omega_s t - \frac{4m\pi}{3}m_f \right) \\
 &= \cos(m\omega_s t) \tag{C.281}
 \end{aligned}$$

$$\begin{aligned}
 \sin \left(m\omega_s \left(t - \frac{4\pi}{3\omega_0} \right) \right) &= \sin \left(m\omega_s t - \frac{4m\pi}{3}m_f \right) \\
 &= \sin(m\omega_s t) \tag{C.282}
 \end{aligned}$$

$$\begin{aligned}
 \cos \left(m\omega_s \left(t - \frac{4\pi}{3\omega_0} \right) - \frac{2m\pi}{3} \right) &= \cos \left(m\omega_s t - \frac{4m\pi}{3}m_f - \frac{2m\pi}{3} \right) \\
 &= \begin{cases} \cos(m\omega_s t) & \text{if } m = 3k \\ \cos \left(m\omega_s t - \frac{2\pi}{3} \right) & \text{if } m = 3k + 1 \\ \cos \left(m\omega_s t + \frac{2\pi}{3} \right) & \text{if } m = 3k + 2 \end{cases} \tag{C.283}
 \end{aligned}$$

$$\begin{aligned} \sin\left(m\omega_s\left(t - \frac{4\pi}{3\omega_0}\right) - \frac{2m\pi}{3}\right) &= \sin\left(m\omega_s t - \frac{4m\pi}{3}m_f - \frac{2m\pi}{3}\right) \\ &= \begin{cases} \sin(m\omega_s t) & \text{if } m = 3k \\ \sin\left(m\omega_s t - \frac{2\pi}{3}\right) & \text{if } m = 3k + 1 \\ \sin\left(m\omega_s t + \frac{2\pi}{3}\right) & \text{if } m = 3k + 2 \end{cases} \end{aligned} \quad (\text{C.284})$$

$$\cos\left(m\omega_s\left(t - \frac{4\pi}{3\omega_0}\right) - \frac{4m\pi}{3}\right) = \begin{cases} \cos(m\omega_s t) & \text{if } m = 3k \\ \cos\left(m\omega_s t + \frac{2\pi}{3}\right) & \text{if } m = 3k + 1 \\ \cos\left(m\omega_s t - \frac{2\pi}{3}\right) & \text{if } m = 3k + 2 \end{cases} \quad (\text{C.285})$$

$$\sin\left(m\omega_s\left(t - \frac{4\pi}{3\omega_0}\right) - \frac{4m\pi}{3}\right) = \begin{cases} \sin(m\omega_s t) & \text{if } m = 3k \\ \sin\left(m\omega_s t + \frac{2\pi}{3}\right) & \text{if } m = 3k + 1 \\ \sin\left(m\omega_s t - \frac{2\pi}{3}\right) & \text{if } m = 3k + 2 \end{cases} \quad (\text{C.286})$$

$$\begin{aligned} \cos\left((m\omega_s + n\omega_0)\left(t - \frac{4\pi}{3\omega_0}\right)\right) &= \cos\left((m\omega_s + n\omega_0)t - \frac{4m\pi}{3}m_f - \frac{4n\pi}{3}\right) \\ &= \begin{cases} \cos((m\omega_s + n\omega_0)t) & \text{if } m = k \text{ and } n=3p \text{ or } n=-3p \\ \cos\left((m\omega_s + n\omega_0)t + \frac{2\pi}{3}\right) & \text{if } m = k \text{ and } n=3p+1 \text{ or } n=-(3p+2) \\ \cos\left((m\omega_s + n\omega_0)t - \frac{2\pi}{3}\right) & \text{if } m = k \text{ and } n=3p+2 \text{ or } n=-(3p+1) \end{cases} \end{aligned} \quad (\text{C.287})$$

$$\begin{aligned} \sin\left((m\omega_s + n\omega_0)\left(t - \frac{4\pi}{3\omega_0}\right)\right) &= \sin\left((m\omega_s + n\omega_0)t - \frac{4m\pi}{3}m_f - \frac{4n\pi}{3}\right) \\ &= \begin{cases} \sin((m\omega_s + n\omega_0)t) & \text{if } m = k \text{ and } n=3p \text{ or } n=-3p \\ \sin\left((m\omega_s + n\omega_0)t + \frac{2\pi}{3}\right) & \text{if } m = k \text{ and } n=3p+1 \text{ or } n=-(3p+2) \\ \sin\left((m\omega_s + n\omega_0)t - \frac{2\pi}{3}\right) & \text{if } m = k \text{ and } n=3p+2 \text{ or } n=-(3p+1) \end{cases} \end{aligned} \quad (\text{C.288})$$

$$\begin{aligned} \cos\left((m\omega_s + n\omega_0)\left(t - \frac{4\pi}{3\omega_0}\right) - \frac{2m\pi}{3}\right) &= \cos\left((m\omega_s + n\omega_0)t - \frac{4m\pi}{3}m_f - \frac{4n\pi}{3} - \frac{2m\pi}{3}\right) \\ &= \begin{cases} \cos((m\omega_s + n\omega_0)t) & \text{if } m = 3k \text{ and } n=3p \text{ or } n=-3p \\ \cos\left((m\omega_s + n\omega_0)t + \frac{2\pi}{3}\right) & \text{if } m = 3k \text{ and } n=3p+1 \text{ or } n=-(3p+2) \\ \cos\left((m\omega_s + n\omega_0)t - \frac{2\pi}{3}\right) & \text{if } m = 3k \text{ and } n=3p+2 \text{ or } n=-(3p+1) \\ \cos\left((m\omega_s + n\omega_0)t - \frac{2\pi}{3}\right) & \text{if } m = 3k + 1 \text{ and } n=3p \text{ or } n=-3p \\ \cos((m\omega_s + n\omega_0)t) & \text{if } m = 3k + 1 \text{ and } n=3p+1 \text{ or } n=-(3p+2) \\ \cos\left((m\omega_s + n\omega_0)t + \frac{2\pi}{3}\right) & \text{if } m = 3k + 1 \text{ and } n=3p+2 \text{ or } n=-(3p+1) \\ \cos\left((m\omega_s + n\omega_0)t + \frac{2\pi}{3}\right) & \text{if } m = 3k + 2 \text{ and } n=3p \text{ or } n=-3p \\ \cos\left((m\omega_s + n\omega_0)t - \frac{2\pi}{3}\right) & \text{if } m = 3k + 2 \text{ and } n=3p+1 \text{ or } n=-(3p+2) \\ \cos((m\omega_s + n\omega_0)t) & \text{if } m = 3k + 2 \text{ and } n=3p+2 \text{ or } n=-(3p+1) \end{cases} \end{aligned}$$

(C.289)

$$\sin \left((m\omega_s + n\omega_0) \left(t - \frac{4\pi}{3\omega_0} \right) - \frac{2m\pi}{3} \right) = \sin \left((m\omega_s + n\omega_0) t - \frac{4m\pi}{3} m_f - \frac{4n\pi}{3} - \frac{2m\pi}{3} \right)$$

$$= \begin{cases} \sin((m\omega_s + n\omega_0)t) & \text{if } m = 3k \text{ and } n=3p \text{ or } n=-3p \\ \sin\left((m\omega_s + n\omega_0)t + \frac{2\pi}{3}\right) & \text{if } m = 3k \text{ and } n=3p+1 \text{ or } n=-(3p+2) \\ \sin\left((m\omega_s + n\omega_0)t - \frac{2\pi}{3}\right) & \text{if } m = 3k \text{ and } n=3p+2 \text{ or } n=-(3p+1) \\ \sin\left((m\omega_s + n\omega_0)t - \frac{2\pi}{3}\right) & \text{if } m = 3k + 1 \text{ and } n=3p \text{ or } n=-3p \\ \sin((m\omega_s + n\omega_0)t) & \text{if } m = 3k + 1 \text{ and } n=3p+1 \text{ or } n=-(3p+2) \\ \sin\left((m\omega_s + n\omega_0)t + \frac{2\pi}{3}\right) & \text{if } m = 3k + 1 \text{ and } n=3p+2 \text{ or } n=-(3p+1) \\ \sin\left((m\omega_s + n\omega_0)t + \frac{2\pi}{3}\right) & \text{if } m = 3k + 2 \text{ and } n=3p \text{ or } n=-3p \\ \sin\left((m\omega_s + n\omega_0)t - \frac{2\pi}{3}\right) & \text{if } m = 3k + 2 \text{ and } n=3p+1 \text{ or } n=-(3p+2) \\ \sin((m\omega_s + n\omega_0)t) & \text{if } m = 3k + 2 \text{ and } n=3p+2 \text{ or } n=-(3p+1) \end{cases}$$

(C.290)

$$\cos \left((m\omega_s + n\omega_0) \left(t - \frac{4\pi}{3\omega_0} \right) - \frac{4m\pi}{3} \right) = \cos \left((m\omega_s + n\omega_0) t - \frac{4m\pi}{3} m_f - \frac{4n\pi}{3} - \frac{4m\pi}{3} \right)$$

$$= \begin{cases} \cos((m\omega_s + n\omega_0)t) & \text{if } m = 3k \text{ and } n=3p \text{ or } n=-3p \\ \cos\left((m\omega_s + n\omega_0)t + \frac{2\pi}{3}\right) & \text{if } m = 3k \text{ and } n=3p+1 \text{ or } n=-(3p+2) \\ \cos\left((m\omega_s + n\omega_0)t - \frac{2\pi}{3}\right) & \text{if } m = 3k \text{ and } n=3p+2 \text{ or } n=-(3p+1) \\ \cos\left((m\omega_s + n\omega_0)t + \frac{2\pi}{3}\right) & \text{if } m = 3k + 1 \text{ and } n=3p \text{ or } n=-3p \\ \cos\left((m\omega_s + n\omega_0)t - \frac{2\pi}{3}\right) & \text{if } m = 3k + 1 \text{ and } n=3p+1 \text{ or } n=-(3p+2) \\ \cos((m\omega_s + n\omega_0)t) & \text{if } m = 3k + 1 \text{ and } n=3p+2 \text{ or } n=-(3p+1) \\ \cos\left((m\omega_s + n\omega_0)t - \frac{2\pi}{3}\right) & \text{if } m = 3k + 2 \text{ and } n=3p \text{ or } n=-3p \\ \cos((m\omega_s + n\omega_0)t) & \text{if } m = 3k + 2 \text{ and } n=3p+1 \text{ or } n=-(3p+2) \\ \cos\left((m\omega_s + n\omega_0)t + \frac{2\pi}{3}\right) & \text{if } m = 3k + 2 \text{ and } n=3p+2 \text{ or } n=-(3p+1) \end{cases}$$

(C.291)

$$\begin{aligned}
& \sin \left((m\omega_s + n\omega_0) \left(t - \frac{4\pi}{3\omega_0} \right) - \frac{4m\pi}{3} \right) = \sin \left((m\omega_s + n\omega_0) t - \frac{4m\pi}{3} m_f - \frac{4n\pi}{3} - \frac{4m\pi}{3} \right) \\
= & \begin{cases} \sin((m\omega_s + n\omega_0)t) & \text{if } m = 3k \text{ and } n=3p \text{ or } n=-3p \\ \sin\left((m\omega_s + n\omega_0)t + \frac{2\pi}{3}\right) & \text{if } m = 3k \text{ and } n=3p+1 \text{ or } n=-(3p+2) \\ \sin\left((m\omega_s + n\omega_0)t - \frac{2\pi}{3}\right) & \text{if } m = 3k \text{ and } n=3p+2 \text{ or } n=-(3p+1) \\ \sin\left((m\omega_s + n\omega_0)t + \frac{2\pi}{3}\right) & \text{if } m = 3k + 1 \text{ and } n=3p \text{ or } n=-3p \\ \sin\left((m\omega_s + n\omega_0)t - \frac{2\pi}{3}\right) & \text{if } m = 3k + 1 \text{ and } n=3p+1 \text{ or } n=-(3p+2) \\ \sin((m\omega_s + n\omega_0)t) & \text{if } m = 3k + 1 \text{ and } n=3p+2 \text{ or } n=-(3p+1) \\ \sin\left((m\omega_s + n\omega_0)t - \frac{2\pi}{3}\right) & \text{if } m = 3k + 2 \text{ and } n=3p \text{ or } n=-3p \\ \sin((m\omega_s + n\omega_0)t) & \text{if } m = 3k + 2 \text{ and } n=3p+1 \text{ or } n=-(3p+2) \\ \sin\left((m\omega_s + n\omega_0)t + \frac{2\pi}{3}\right) & \text{if } m = 3k + 2 \text{ and } n=3p+2 \text{ or } n=-(3p+1) \end{cases}
\end{aligned} \tag{C.292}$$

Thus the phasor representation for phase C of 3-cell converter when $m_f = 3k + 2$ is given by Figures C.36, C.37 and C.38.

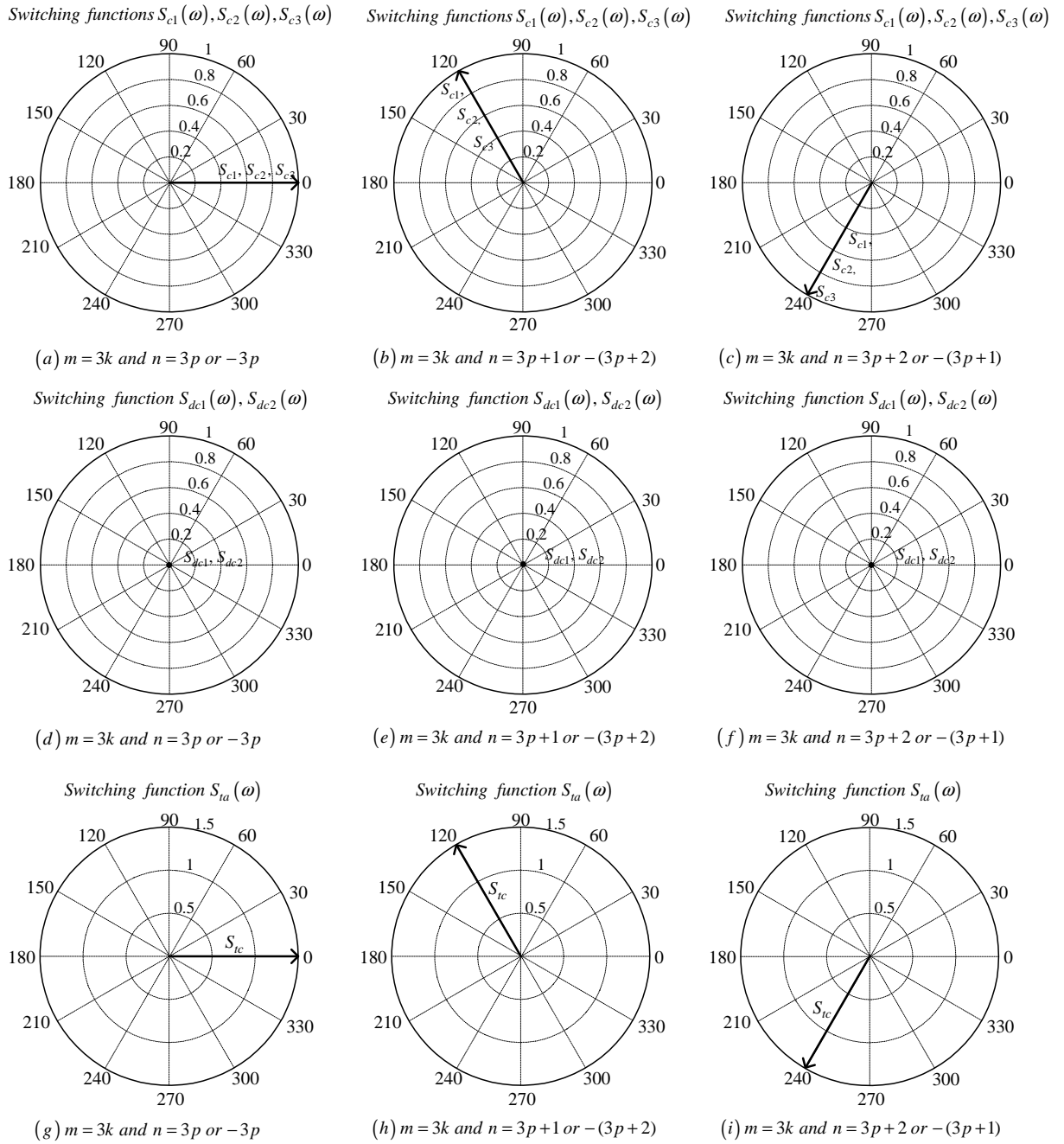


Figure C.36: Phasor representation for phase C of 3-cell converter for $m = 3k$

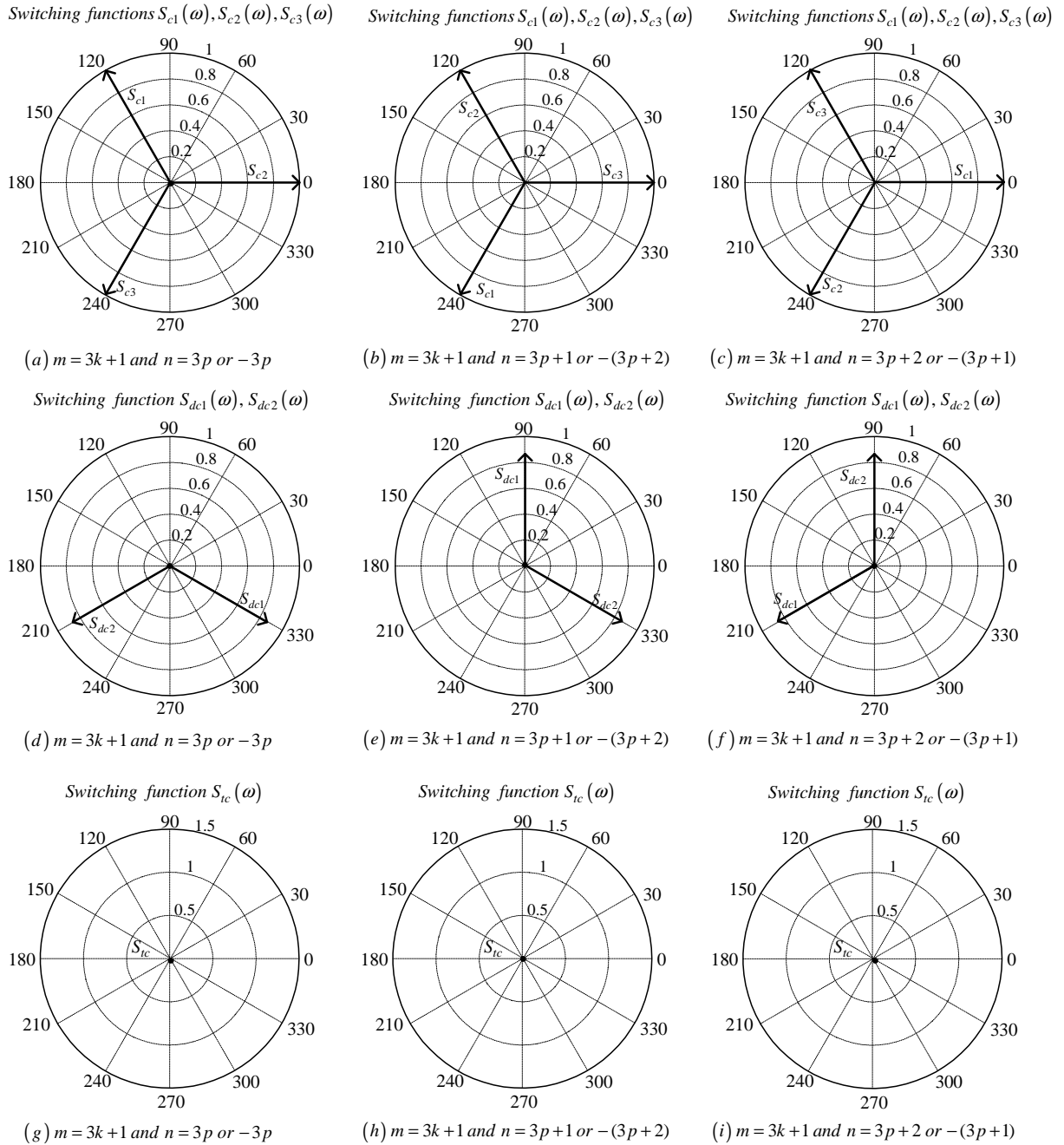


Figure C.37: Phasor representation for phase C of 3-cell converter for $m = 3k + 1$

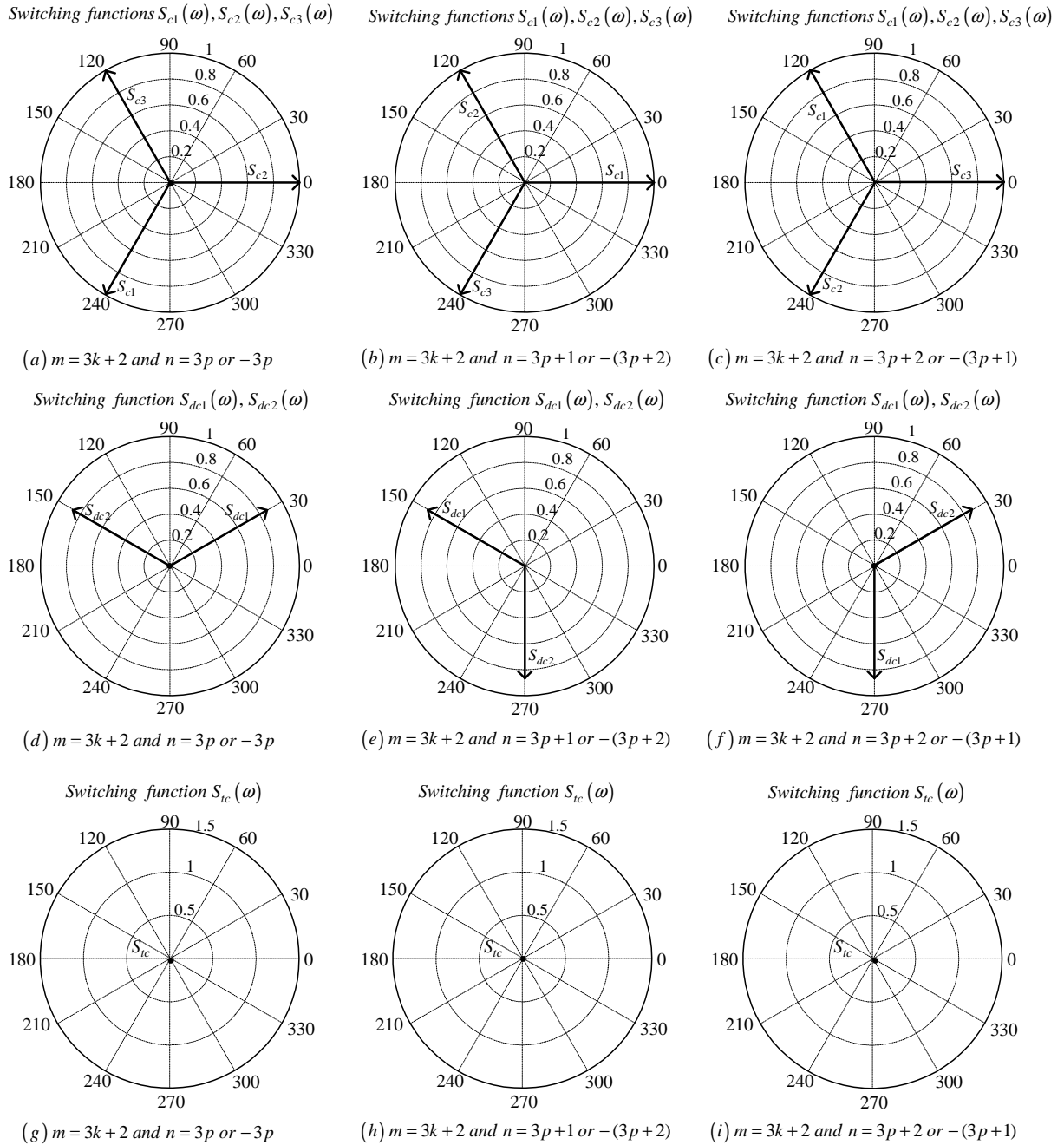


Figure C.38: Phasor representation for phase C of 3-cell converter for $3k + 2$

Appendix D

Duty Cycles for Other Five Sectors

D.1 Duty Cycles for Sector II

In this section we study the sequences and combinations of duty cycles of regions A, B, C and D of sector II. Figure D.1 show the first sector of six sectors with its regions. We show the switch combinations using all redundancy in Appendix E section E.2.

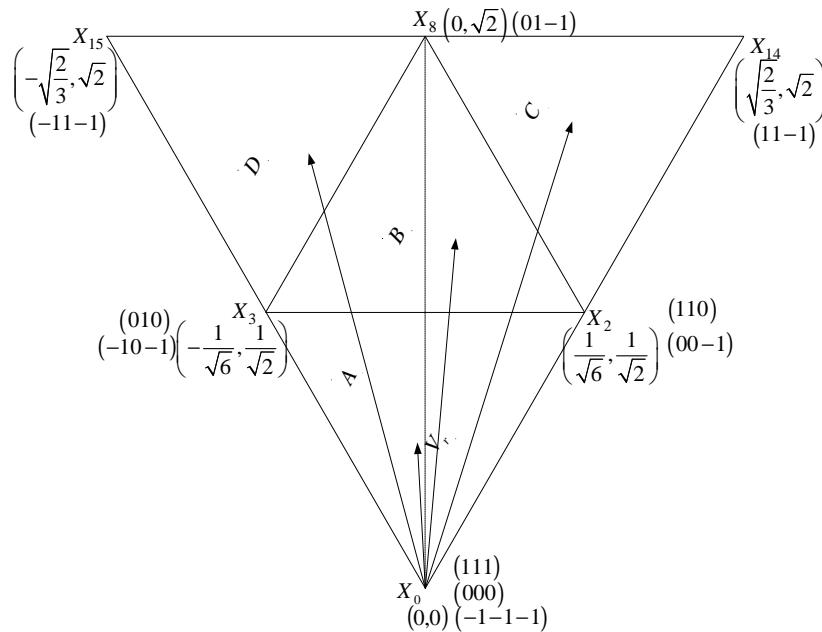


Figure D.1: *Regions of vector modulation of the 2-cell multicell converter in the second sector*

D.1.1 Region IIA

For $\theta \leq \frac{\pi}{2}$

The switch combination sequence for the nearest three vectors moving from sector IA to

IIA is given by:

$d_2(00-1)$ to $d_0(000)$ to $d_3(010)$ to $d_2(110)$ to $d_2(110)$ to $d_3(010)$ to $d_0(000)$ to $d_2(00-1)$ and the corresponding reference voltage vector waveform equations for phase A, B and C are given by equations D.1, D.2 and D.3 respectively.

$$\begin{aligned} V_{refa_{IIA1}} &= \frac{1}{4}d_2 \\ &= \frac{1}{2\sqrt{2}}m_a \cos\left(\omega t - \frac{\pi}{6}\right) \end{aligned} \quad (D.1)$$

$$\begin{aligned} V_{refb_{IIA1}} &= \frac{1}{2}d_3 + \frac{1}{4}d_2 \\ &= \frac{\sqrt{3}}{2\sqrt{2}}m_a \sin\left(\omega t - \frac{\pi}{6}\right) \end{aligned} \quad (D.2)$$

$$\begin{aligned} V_{refc_{IIA1}} &= -\frac{1}{4}d_2 \\ &= -\frac{1}{2\sqrt{2}}m_a \cos\left(\omega t - \frac{\pi}{6}\right) \end{aligned} \quad (D.3)$$

For $\theta \geq \frac{\pi}{2}$

The switch combination sequence for the nearest three vectors moving from sector IIA to $IIIA$ is given by:

$d_3(-10-1)$ to $d_2(00-1)$ to $d_0(000)$ to $d_3(010)$ to $d_3(010)$ to $d_0(000)$ to $d_2(00-1)$ to $d_3(-10-1)$

and the corresponding reference voltage vector waveform equations for phase A, B and C are given by equations D.4, D.5 and D.6 respectively.

$$\begin{aligned} V_{refa_{IIA2}} &= -\frac{1}{4}d_3 \\ &= \frac{1}{2\sqrt{2}}m_a \cos\left(\omega t + \frac{\pi}{6}\right) \end{aligned} \quad (D.4)$$

$$\begin{aligned} V_{refb_{IIA2}} &= \frac{1}{4}d_3 \\ &= -\frac{1}{2\sqrt{2}}m_a \cos\left(\omega t + \frac{\pi}{6}\right) \end{aligned} \quad (D.5)$$

$$\begin{aligned} V_{refc_{IIA2}} &= -\frac{1}{4}d_3 - \frac{1}{2}d_2 \\ &= -\frac{\sqrt{3}}{2\sqrt{2}}m_a \sin\left(\omega t + \frac{\pi}{6}\right) \end{aligned} \quad (D.6)$$

D.1.2 Region IIC

The switch combination sequence for the nearest three vector for sector *IIC* is given by: $d_2(110)$ to $d_{14}(11-1)$ to $d_8(01-1)$ to $d_2(00-1)$ to $d_2(00-1)$ to $d_8(01-1)$ to $d_{14}(11-1)$ to $d_2(110)$

and the corresponding reference voltage vector waveform equations for phase A, B and C are given by equations D.7, D.8 and D.9 respectively.

$$\begin{aligned} V_{refa_{IIC}} &= \frac{1}{4}d_2 + \frac{1}{2}d_{14} \\ &= \frac{\sqrt{3}}{2\sqrt{2}}m_a \cos \omega t \end{aligned} \quad (D.7)$$

$$\begin{aligned} V_{refb_{IIC}} &= \frac{1}{4}d_2 + \frac{1}{2}d_{14} + \frac{1}{2}d_8 \\ &= \frac{1}{2\sqrt{2}}m_a \sin \omega t \end{aligned} \quad (D.8)$$

$$\begin{aligned} V_{refc_{IIC}} &= -\frac{1}{2}d_{14} - \frac{1}{2}d_8 - \frac{1}{4}d_2 \\ &= -\frac{1}{2\sqrt{2}}m_a \sin \omega t \end{aligned} \quad (D.9)$$

D.1.3 Region IIB

For $\theta \leq \frac{\pi}{2}$

The switch combination sequence for the nearest three vectors moving from sector *IIC* to *IIB* is given by:

$d_2(00-1)$ to $d_8(01-1)$ to $d_3(010)$ to $d_2(110)$ to $d_2(110)$ to $d_3(010)$ to $d_8(01-1)$ to $d_2(00-1)$

and the reference voltage vector waveform equation is given by:

$$\begin{aligned} V_{refa_{IIB1}} &= \frac{1}{4}d_2 \\ &= \frac{1}{2\sqrt{2}}m_a \cos \left(\omega t + \frac{\pi}{6} \right) + \frac{1}{4} \end{aligned} \quad (D.10)$$

$$\begin{aligned} V_{refb_{IIB1}} &= \frac{1}{2}d_8 + \frac{1}{2}d_3 + \frac{1}{4}d_2 \\ &= -\frac{1}{2\sqrt{2}}m_a \cos \left(\omega t + \frac{\pi}{6} \right) + \frac{1}{4} \end{aligned} \quad (D.11)$$

$$\begin{aligned} V_{refc_{IIB1}} &= -\frac{1}{4}d_2 - \frac{1}{2}d_8 \\ &= -\frac{\sqrt{3}}{2\sqrt{2}}m_a \sin \left(\omega t + \frac{\pi}{6} \right) + \frac{1}{4} \end{aligned} \quad (D.12)$$

For $\theta \geq \frac{\pi}{2}$

The switch combination sequence for the nearest three vectors moving from sector *IIB* to *IID* is given by:

$d_3(-10-1)$ to $d_2(00-1)$ to $d_8(01-1)$ to $d_3(010)$ to $d_3(010)$ to $d_8(01-1)$ to $d_2(00-1)$ to $d_3(-10-1)$

and the reference voltage vector waveform equation is given by:

$$\begin{aligned} V_{refa_{IIB2}} &= -\frac{1}{4}d_3 \\ &= \frac{1}{2\sqrt{2}}m_a \cos\left(\omega t - \frac{\pi}{6}\right) - \frac{1}{4} \end{aligned} \quad (D.13)$$

$$\begin{aligned} V_{refb_{IIB2}} &= \frac{1}{4}d_3 + \frac{1}{2}d_8 \\ &= \frac{\sqrt{3}}{2\sqrt{2}}m_a \sin\left(\omega t - \frac{\pi}{6}\right) - \frac{1}{4} \end{aligned} \quad (D.14)$$

$$\begin{aligned} V_{refc_{IIB2}} &= -\frac{1}{4}d_3 - \frac{1}{2}d_2 - \frac{1}{2}d_8 \\ &= -\frac{1}{2\sqrt{2}}m_a \cos\left(\omega t - \frac{\pi}{6}\right) - \frac{1}{4} \end{aligned} \quad (D.15)$$

D.1.4 Region IID

The switch combination sequence for the nearest three vectors for sector *IID* is given by:

$d_3(010)$ to $d_8(01-1)$ to $d_{15}(-11-1)$ to $d_3(-10-1)$ to $d_3(-10-1)$ to $d_{15}(-11-1)$ to $d_8(01-1)$ to $d_3(010)$

and the reference voltage vector waveform equation is given by:

$$\begin{aligned} V_{refa_{IID}} &= -\frac{1}{4}d_3 - \frac{1}{2}d_{15} \\ &= \frac{\sqrt{3}}{2\sqrt{2}}m_a \cos \omega t \end{aligned} \quad (D.16)$$

$$\begin{aligned} V_{refb_{IID}} &= \frac{1}{4}d_3 + \frac{1}{2}d_8 + \frac{1}{2}d_{15} \\ &= \frac{1}{2\sqrt{2}}m_a \sin \omega t \end{aligned} \quad (D.17)$$

$$\begin{aligned} V_{refc_{IID}} &= -\frac{1}{2}d_8 - \frac{1}{2}d_{15} - \frac{1}{4}d_3 \\ &= -\frac{1}{2\sqrt{2}}m_a \sin \omega t \end{aligned} \quad (D.18)$$

D.2 Duty cycles for Sector III

In this section we study the sequences and combinations of duty cycles of regions A, B, C and D of sector III. Figure D.2 show the first sector of six sectors with its regions. We show the switch combinations using all redundancy in Appendix E section E.3.

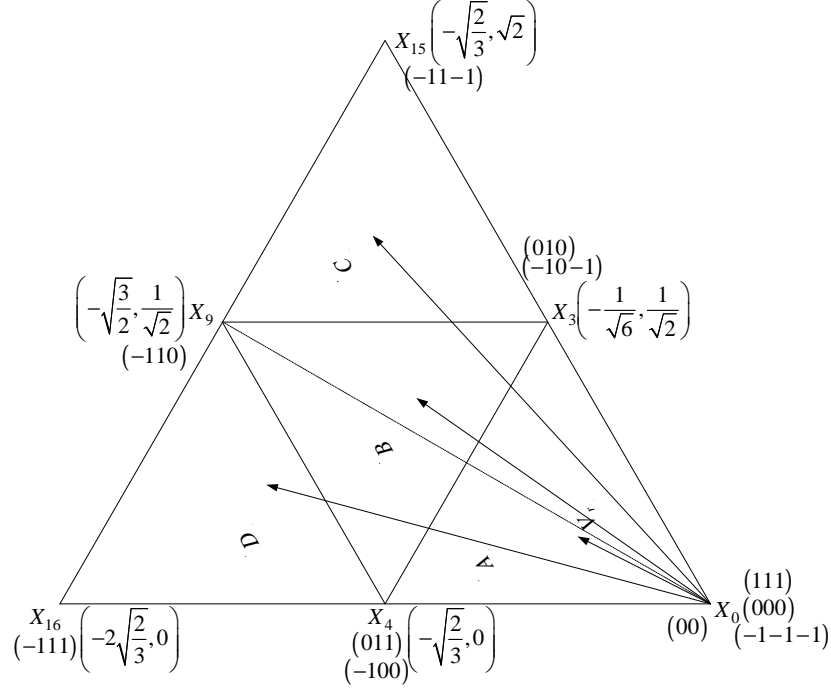


Figure D.2: Regions of vector modulation of the 2-cell multicell converter in the third sector

D.2.1 Region IIIA

For $\theta \leq \frac{5\pi}{6}$

The switch combination sequence for the nearest three vectors moving from sector *IIA* to *IIIA* is given by:

$d_3(010)$ to $d_0(000)$ to $d_4(-100)$ to $d_3(-10-1)$ to $d_3(-10-1)$ to $d_4(-100)$ to $d_0(000)$ to $d_3(010)$

and the reference voltage vector waveform equation is given by:

$$\begin{aligned} V_{refa_{IIIA1}} &= -\frac{1}{4}d_3 - \frac{1}{2}d_4 \\ &= \frac{\sqrt{3}}{2\sqrt{2}}m_a \cos \omega t \end{aligned} \quad (D.19)$$

$$V_{refb_{IIIA1}} = \frac{1}{4}d_3$$

$$= \frac{1}{2\sqrt{2}}m_a \sin \omega t \quad (\text{D.20})$$

$$\begin{aligned} V_{ref_{IIIA1}} &= -\frac{1}{4}d_3 \\ &= -\frac{1}{2\sqrt{2}}m_a \sin \omega t \end{aligned} \quad (\text{D.21})$$

For $\theta \geq \frac{5\pi}{6}$

The switch combination sequence for the nearest three vectors moving from sector *IIIA* to *IVA* is given by:

$d_4(011)$ to $d_3(010)$ to $d_0(000)$ to $d_4(-100)$ to $d_4(-100)$ to $d_0(000)$ to $d_3(010)$ to $d_4(011)$ and the reference voltage vector waveform equation is given by:

$$\begin{aligned} V_{ref_{IIIA2}} &= -\frac{1}{4}d_4 \\ &= \frac{1}{2\sqrt{2}} \cos \left(\omega t - \frac{\pi}{6} \right) \end{aligned} \quad (\text{D.22})$$

$$\begin{aligned} V_{ref_{IIIA2}} &= \frac{1}{4}d_4 + \frac{1}{2}d_3 \\ &= \frac{\sqrt{3}}{2\sqrt{2}} \sin \left(\omega t - \frac{\pi}{6} \right) \end{aligned} \quad (\text{D.23})$$

$$\begin{aligned} V_{ref_{IIIA2}} &= \frac{1}{4}d_4 \\ &= -\frac{1}{2\sqrt{2}} \cos \left(\omega t - \frac{\pi}{6} \right) \end{aligned} \quad (\text{D.24})$$

D.2.2 Region IIIC

The switch combination sequence for the nearest three vectors for sector *IIIC* is given by:

$d_3(-10-1)$ to $d_{15}(-11-1)$ to $d_9(-110)$ to $d_3(010)$ to $d_3(010)$ to $d_9(-110)$ to $d_{15}(-11-1)$ to $d_3(-10-1)$

and the reference voltage vector waveform equation is given by:

$$\begin{aligned} V_{ref_{IIIC}} &= -\frac{1}{4}d_3 - \frac{1}{2}d_{15} - \frac{1}{2}d_9 \\ &= \frac{1}{2\sqrt{2}} \cos \left(\omega t + \frac{\pi}{6} \right) \end{aligned} \quad (\text{D.25})$$

$$\begin{aligned} V_{ref_{IIIC}} &= \frac{1}{4}d_3 + \frac{1}{2}d_{15} + \frac{1}{2}d_9 \\ &= -\frac{1}{2\sqrt{2}} \cos \left(\omega t + \frac{\pi}{6} \right) \end{aligned} \quad (\text{D.26})$$

$$\begin{aligned}
V_{refc_{IIIC}} &= -\frac{1}{4}d_3 - \frac{1}{2}d_{15} \\
&= -\frac{\sqrt{3}}{2\sqrt{2}} \sin\left(\omega t + \frac{\pi}{6}\right)
\end{aligned} \tag{D.27}$$

D.2.3 Region IIIB

For $\theta \leq \frac{5\pi}{6}$

The switch combination sequence for the nearest three vectors moving from sector *IIIC* to *IIIB* is given by:

$d_3(010)$ to $d_9(-110)$ to $d_4(-100)$ to $d_3(-10-1)$ to $d_3(-10-1)$ to $d_4(-100)$ to $d_9(-110)$ to $d_3(010)$

and the reference voltage vector waveform equation is given by:

$$\begin{aligned}
V_{refa_{IIIB1}} &= -\frac{1}{4}d_3 - \frac{1}{2}d_9 - \frac{1}{2}d_4 \\
&= \frac{1}{2\sqrt{2}} \cos\left(\omega t - \frac{\pi}{6}\right) - \frac{1}{4}
\end{aligned} \tag{D.28}$$

$$\begin{aligned}
V_{refb_{IIIB1}} &= \frac{1}{4}d_3 + \frac{1}{2}d_9 \\
&= \frac{\sqrt{3}}{2\sqrt{2}} \sin\left(\omega t - \frac{\pi}{6}\right) - \frac{1}{4}
\end{aligned} \tag{D.29}$$

$$\begin{aligned}
V_{refc_{IIIB1}} &= -\frac{1}{4}d_3 \\
&= -\frac{1}{2\sqrt{2}} \cos\left(\omega t - \frac{\pi}{6}\right) - \frac{1}{4}
\end{aligned} \tag{D.30}$$

For $\theta \geq \frac{5\pi}{6}$

The switch combination sequence for the nearest three vectors moving from sector *IIIB* to *IIID* is given by:

$d_4(011)$ to $d_3(010)$ to $d_9(-110)$ to $d_4(-100)$ to $d_4(-100)$ to $d_9(-110)$ to $d_3(010)$ to $d_4(011)$

and the reference voltage vector waveform equation is given by:

$$\begin{aligned}
V_{refa_{IIIB2}} &= -\frac{1}{4}d_4 - \frac{1}{2}d_9 \\
&= \frac{\sqrt{3}}{2\sqrt{2}} \cos \omega t + \frac{1}{4}
\end{aligned} \tag{D.31}$$

$$\begin{aligned}
V_{refb_{IIIB2}} &= \frac{1}{4}d_4 + \frac{1}{2}d_3 + \frac{1}{2}d_9 \\
&= \frac{1}{2\sqrt{2}} \sin \omega t + \frac{1}{4}
\end{aligned} \tag{D.32}$$

$$\begin{aligned}
V_{refc_{IIIB2}} &= \frac{1}{4}d_4 \\
&= -\frac{1}{2\sqrt{2}} \sin \omega t + \frac{1}{4}
\end{aligned} \tag{D.33}$$

D.2.4 Region IIID

The switch combination sequence for the nearest three vectors for sector *IIID* is given by:

$d_4(-100)$ to $d_9(-110)$ to $d_{16}(-111)$ to $d_4(011)$ to $d_4(011)$ to $d_{16}(-111)$ to $d_9(-110)$ to $d_4(-100)$

and the reference voltage vector waveform equation is given by:

$$\begin{aligned} V_{refa_{IIID}} &= -\frac{1}{4}d_4 - \frac{1}{2}d_{16} - \frac{1}{2}d_9 \\ &= \frac{1}{2\sqrt{2}} \cos\left(\omega t + \frac{\pi}{6}\right) \end{aligned} \quad (\text{D.34})$$

$$\begin{aligned} V_{refb_{IIID}} &= \frac{1}{4}d_4 + \frac{1}{2}d_{16} + \frac{1}{2}d_9 \\ &= -\frac{1}{2\sqrt{2}} \cos\left(\omega t + \frac{\pi}{6}\right) \end{aligned} \quad (\text{D.35})$$

$$\begin{aligned} V_{refc_{IIID}} &= \frac{1}{2}d_{16} + \frac{1}{4}d_4 \\ &= -\frac{\sqrt{3}}{2\sqrt{2}} \sin\left(\omega t + \frac{\pi}{6}\right) \end{aligned} \quad (\text{D.36})$$

D.3 Duty cycles for Sector IV

In this section we study the sequences and combinations of duty cycles of regions A, B, C and D of sector IV. Figure D.3 show the first sector of six sectors with its regions. We show the switch combinations using all redundancy in Appendix E section E.4.

D.3.1 Region IVA

For $\theta \leq \frac{7\pi}{6}$

The switch combination sequence for the nearest three vectors moving from sector *IIIA* to *IVA* is given by:

$d_4(-100)$ to $d_0(000)$ to $d_5(001)$ to $d_4(011)$ to $d_4(011)$ to $d_5(001)$ to $d_0(000)$ to $d_4(-100)$

and the reference voltage vector waveform equation is given by:

$$\begin{aligned} V_{refa_{IVA1}} &= -\frac{1}{4}d_4 \\ &= \frac{1}{2\sqrt{2}}m_a \cos\left(\omega t + \frac{\pi}{6}\right) \end{aligned} \quad (\text{D.37})$$

$$\begin{aligned} V_{refb_{IVA1}} &= \frac{1}{4}d_4 \\ &= -\frac{1}{2\sqrt{2}}m_a \cos\left(\omega t + \frac{\pi}{6}\right) \end{aligned} \quad (\text{D.38})$$

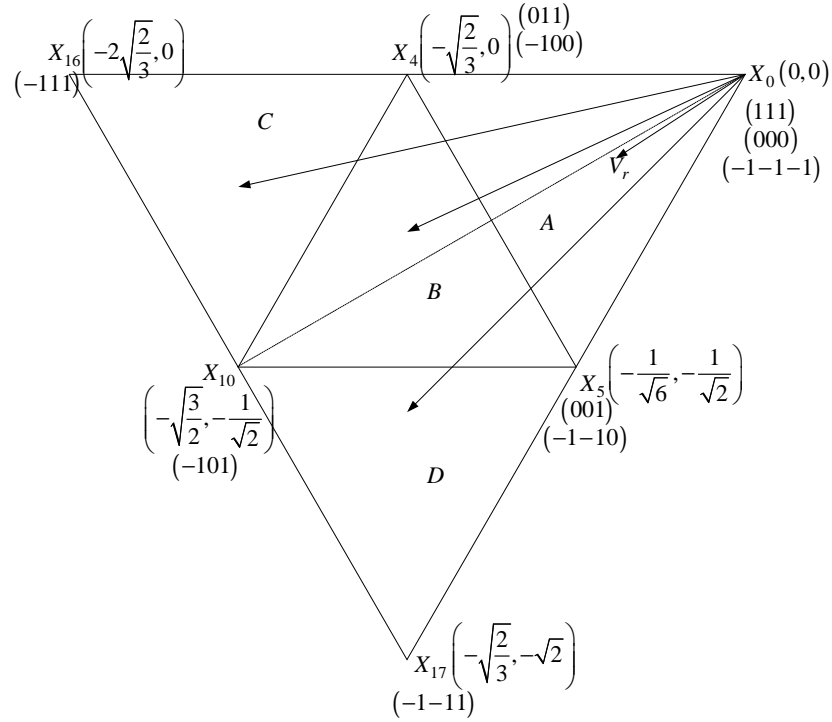


Figure D.3: Regions of vector modulation of the 2-cell multicell converter in the fourth sector

$$\begin{aligned}
 V_{ref_{IV.A1}} &= \frac{1}{2}d_5 + \frac{1}{4}d_4 \\
 &= -\frac{\sqrt{3}}{2\sqrt{2}}m_a \sin\left(\omega t + \frac{\pi}{6}\right)
 \end{aligned} \tag{D.39}$$

For $\theta \geq \frac{7\pi}{6}$

The switch combination sequence for the nearest three vectors moving from sector $IV.A$ to VA is given by:

$d_5(-1-10)$ to $d_4(-100)$ to $d_0(000)$ to $d_5(001)$ to $d_5(001)$ to $d_0(000)$ to $d_4(-100)$ to $d_5(-1-10)$

and the reference voltage vector waveform equation is given by:

$$\begin{aligned}
 V_{ref_{IV.A2}} &= -\frac{1}{4}d_5 - \frac{1}{2}d_4 \\
 &= \frac{\sqrt{3}}{2\sqrt{2}}m_a \cos \omega t
 \end{aligned} \tag{D.40}$$

$$\begin{aligned}
 V_{ref_{IV.A2}} &= -\frac{1}{4}d_5 \\
 &= \frac{1}{2\sqrt{2}}m_a \sin \omega t
 \end{aligned} \tag{D.41}$$

$$\begin{aligned}
V_{refc_{IVA2}} &= \frac{1}{4}d_5 \\
&= -\frac{1}{2\sqrt{2}}m_a \sin \omega t
\end{aligned} \tag{D.42}$$

D.3.2 Region IVC

The switch combination sequence for the nearest three vectors for sector *IVC* is given by: $d_4(011)$ to $d_{16}(-111)$ to $d_{10}(-101)$ to $d_4(-100)$ to $d_4(-100)$ to $d_{10}(-101)$ to $d_9(-111)$ to $d_4(011)$

and the reference voltage vector waveform equation is given by:

$$\begin{aligned}
V_{refa_{IVC}} &= -\frac{1}{4}d_4 - \frac{1}{2}d_{16} - \frac{1}{2}d_{10} \\
&= \frac{1}{2\sqrt{2}} \cos \left(\omega t - \frac{\pi}{6} \right)
\end{aligned} \tag{D.43}$$

$$\begin{aligned}
V_{refb_{IVC}} &= \frac{1}{4}d_4 + \frac{1}{2}d_{16} \\
&= \frac{\sqrt{3}}{2\sqrt{2}} \sin \left(\omega t - \frac{\pi}{6} \right)
\end{aligned} \tag{D.44}$$

$$\begin{aligned}
V_{refc_{IVC}} &= \frac{1}{4}d_4 + \frac{1}{2}d_{16} + \frac{1}{2}d_{10} \\
&= -\frac{1}{2\sqrt{2}} \cos \left(\omega t - \frac{\pi}{6} \right)
\end{aligned} \tag{D.45}$$

D.3.3 Region IVB

For $\theta \leq \frac{7\pi}{6}$

The switch combination sequence for the nearest three vectors moving from sector *IVC* to *IVB* is given by:

$d_4(-100)$ to $d_{10}(-101)$ to $d_5(001)$ to $d_4(011)$ to $d_4(011)$ to $d_5(001)$ to $d_{10}(-101)$ to $d_4(-100)$

and the reference voltage vector waveform equation is given by:

$$\begin{aligned}
V_{refa_{IVB1}} &= -\frac{1}{4}d_4 - \frac{1}{2}d_{10} \\
&= \frac{\sqrt{3}}{2\sqrt{2}}m_a \cos \omega t + \frac{1}{4}
\end{aligned} \tag{D.46}$$

$$\begin{aligned}
V_{refb_{IVB1}} &= \frac{1}{4}d_4 \\
&= \frac{1}{2\sqrt{2}}m_a \sin \omega t + \frac{1}{4}
\end{aligned} \tag{D.47}$$

$$\begin{aligned}
V_{refc_{IVB1}} &= \frac{1}{2}d_{10} + \frac{1}{2}d_5 + \frac{1}{4}d_4 \\
&= -\frac{1}{2\sqrt{2}}m_a \sin \omega t + \frac{1}{4}
\end{aligned} \tag{D.48}$$

For $\theta \geq \frac{7\pi}{6}$

The switch combination sequence for the nearest three vectors moving from sector IVB to IVD is given by:

$d_5(-1-10)$ to $d_4(-100)$ to $d_{10}(-101)$ to $d_5(001)$ to $d_5(001)$ to $d_{10}(-101)$ to $d_4(-100)$ to $d_5(-1-10)$

and the reference voltage vector waveform equation is given by:

$$\begin{aligned}
V_{refa_{IVB2}} &= -\frac{1}{4}d_5 - \frac{1}{2}d_4 - \frac{1}{2}d_{10} \\
&= \frac{1}{2\sqrt{2}}m_a \cos\left(\omega t + \frac{\pi}{6}\right) - \frac{1}{4}
\end{aligned} \tag{D.49}$$

$$\begin{aligned}
V_{refb_{IVB2}} &= -\frac{1}{4}d_5 \\
&= -\frac{1}{2\sqrt{2}}m_a \cos\left(\omega t + \frac{\pi}{6}\right) - \frac{1}{4}
\end{aligned} \tag{D.50}$$

$$\begin{aligned}
V_{refc_{IVB2}} &= \frac{1}{2}d_{10} + \frac{1}{4}d_5 \\
&= -\frac{\sqrt{3}}{2\sqrt{2}}m_a \sin\left(\omega t + \frac{\pi}{6}\right) - \frac{1}{4}
\end{aligned} \tag{D.51}$$

D.3.4 Region IVD

The switch combination sequence for the nearest three vectors for sector IVD is given by:

$d_5(001)$ to $d_{10}(-101)$ to $d_{17}(-1-11)$ to $d_5(-1-10)$ to $d_5(-1-10)$ to $d_{17}(-1-11)$ to $d_{10}(-101)$ to $d_5(001)$

and the reference voltage vector waveform equation is given by:

$$\begin{aligned}
V_{refa_{IVD}} &= -\frac{1}{4}d_5 - \frac{1}{2}d_{10} - \frac{1}{2}d_{17} \\
&= \frac{1}{2\sqrt{2}}\cos\left(\omega t - \frac{\pi}{6}\right)
\end{aligned} \tag{D.52}$$

$$\begin{aligned}
V_{refb_{IVD}} &= -\frac{1}{2}d_{17} - \frac{1}{4}d_5 \\
&= \frac{\sqrt{3}}{2\sqrt{2}}\sin\left(\omega t - \frac{\pi}{6}\right)
\end{aligned} \tag{D.53}$$

$$\begin{aligned}
V_{refc_{IVD}} &= \frac{1}{4}d_5 + \frac{1}{2}d_{10} + \frac{1}{2}d_{17} \\
&= -\frac{1}{2\sqrt{2}}\cos\left(\omega t - \frac{\pi}{6}\right)
\end{aligned} \tag{D.54}$$

D.4 Duty cycles for Sector V

In this section we study the sequences and combinations of duty cycles of regions A, B, C and D of sector V. Figure D.4 show the first sector of six sectors with its regions. We show the switch combinations using all redundancy in Appendix E section E.5.

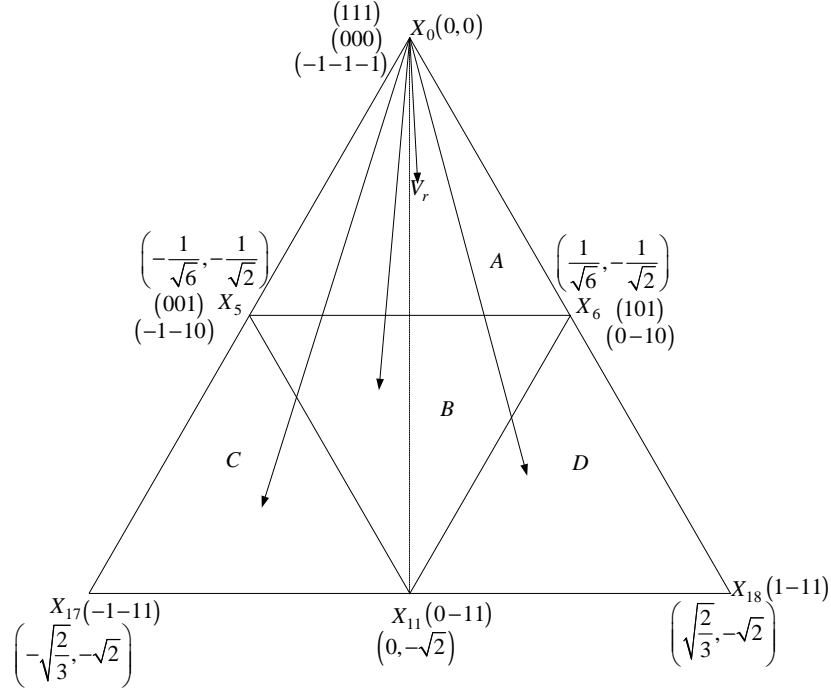


Figure D.4: Regions of vector modulation of the 2-cell multicell converter in the fifth sector

D.4.1 Region VA

For $\theta \leq \frac{3\pi}{2}$

The switch combination sequence for the nearest three vectors moving from sector IVA to VA is given by:

$d_5(001)$ to $d_0(000)$ to $d_6(0-10)$ to $d_5(-1-10)$ to $d_5(-1-10)$ to $d_6(0-10)$ to $d_0(000)$ to $d_5(001)$

and the reference voltage vector waveform equation is given by:

$$\begin{aligned} V_{refv_{A1}} &= -\frac{1}{4}d_5 \\ &= \frac{1}{2\sqrt{2}}m_a \cos\left(\omega t - \frac{\pi}{6}\right) \end{aligned} \quad (\text{D.55})$$

$$V_{refv_{A1}} = -\frac{1}{2}d_6 - \frac{1}{4}d_5$$

$$= \frac{\sqrt{3}}{2\sqrt{2}}m_a \sin\left(\omega t - \frac{\pi}{6}\right) \quad (\text{D.56})$$

$$\begin{aligned} V_{refcVA1} &= \frac{1}{4}d_5 \\ &= -\frac{1}{2\sqrt{2}}m_a \cos\left(\omega t - \frac{\pi}{6}\right) \end{aligned} \quad (\text{D.57})$$

For $\theta \geq \frac{3\pi}{2}$

The switch combination sequence for the nearest three vectors moving from sector VA to VIA is given by:

$d_6(101)$ to $d_5(001)$ to $d_0(000)$ to $d_6(0-10)$ to $d_6(0-10)$ to $d_0(000)$ to $d_5(001)$ to $d_6(101)$ and the reference voltage vector waveform equation is given by:

$$\begin{aligned} V_{refaVA2} &= \frac{1}{4}d_6 \\ &= \frac{1}{2\sqrt{2}}m_a \cos\left(\omega t + \frac{\pi}{6}\right) \end{aligned} \quad (\text{D.58})$$

$$\begin{aligned} V_{refbVA2} &= -\frac{1}{4}d_6 \\ &= -\frac{1}{2\sqrt{2}}m_a \cos\left(\omega t + \frac{\pi}{6}\right) \end{aligned} \quad (\text{D.59})$$

$$\begin{aligned} V_{refcVA2} &= \frac{1}{4}d_6 + \frac{1}{2}d_5 \\ &= -\frac{\sqrt{3}}{2\sqrt{2}}m_a \sin\left(\omega t + \frac{\pi}{6}\right) \end{aligned} \quad (\text{D.60})$$

D.4.2 Region VC

The switch combination sequence for the nearest three vectors for sector VC is given by: $d_5(-1-10)$ to $d_{17}(-1-11)$ to $d_{11}(0-11)$ to $d_5(001)$ to $d_5(001)$ to $d_{11}(0-11)$ to $d_{17}(-1-11)$ to $d_5(-1-10)$

and the reference voltage vector waveform equation is given by:

$$\begin{aligned} V_{refaVC} &= -\frac{1}{4}d_5 - \frac{1}{2}d_{17} \\ &= \frac{\sqrt{3}}{2\sqrt{2}}\cos\omega t \end{aligned} \quad (\text{D.61})$$

$$\begin{aligned} V_{refbVC} &= -\frac{1}{4}d_5 - \frac{1}{2}d_{17} - \frac{1}{2}d_{11} \\ &= \frac{1}{2\sqrt{2}}\sin\omega t \end{aligned} \quad (\text{D.62})$$

$$\begin{aligned} V_{refcVC} &= \frac{1}{2}d_{17} + \frac{1}{2}d_{11} + \frac{1}{4}d_5 \\ &= -\frac{1}{2\sqrt{2}}\sin\omega t \end{aligned} \quad (\text{D.63})$$

D.4.3 Region VB

For $\theta \leq \frac{3\pi}{2}$

The switch combination sequence for the nearest three vectors moving from sector VC to VB is given by:

$d_5(001)$ to $d_{11}(0-11)$ to $d_6(0-10)$ to $d_5(-1-10)$ to $d_5(-1-10)$ to $d_6(0-10)$ to $d_{11}(0-11)$ to $d_5(001)$

and the reference voltage vector waveform equation is given by:

$$\begin{aligned} V_{ref_{aVB1}} &= -\frac{1}{4}d_5 \\ &= \frac{1}{2\sqrt{2}}m_a \cos\left(\omega t + \frac{\pi}{6}\right) - \frac{1}{4} \end{aligned} \quad (\text{D.64})$$

$$\begin{aligned} V_{ref_{bVB1}} &= -\frac{1}{2}d_{11} - \frac{1}{2}d_6 - \frac{1}{4}d_5 \\ &= -\frac{1}{2\sqrt{2}}m_a \cos\left(\omega t + \frac{\pi}{6}\right) - \frac{1}{4} \end{aligned} \quad (\text{D.65})$$

$$\begin{aligned} V_{ref_{cVB1}} &= \frac{1}{4}d_5 + \frac{1}{2}d_{11} \\ &= -\frac{\sqrt{3}}{2\sqrt{2}}m_a \sin\left(\omega t + \frac{\pi}{6}\right) - \frac{1}{4} \end{aligned} \quad (\text{D.66})$$

For $\theta \geq \frac{3\pi}{2}$

The switch combination sequence for the nearest three vectors moving from sector VB to VD is given by:

$d_6(101)$ to $d_5(001)$ to $d_{11}(0-11)$ to $d_6(0-10)$ to $d_6(0-10)$ to $d_{11}(0-11)$ to $d_5(001)$ to $d_6(101)$

and the reference voltage vector waveform equation is given by:

$$\begin{aligned} V_{ref_{aVB2}} &= \frac{1}{4}d_6 \\ &= \frac{1}{2\sqrt{2}}m_a \cos\left(\omega t - \frac{\pi}{6}\right) + \frac{1}{4} \end{aligned} \quad (\text{D.67})$$

$$\begin{aligned} V_{ref_{bVB2}} &= -\frac{1}{2}d_{11} - \frac{1}{4}d_6 \\ &= \frac{\sqrt{3}}{2\sqrt{2}}m_a \sin\left(\omega t - \frac{\pi}{6}\right) + \frac{1}{4} \end{aligned} \quad (\text{D.68})$$

$$\begin{aligned} V_{ref_{cVB2}} &= \frac{1}{4}d_6 + \frac{1}{2}d_5 + \frac{1}{2}d_{11} \\ &= -\frac{1}{2\sqrt{2}}m_a \cos\left(\omega t - \frac{\pi}{6}\right) + \frac{1}{4} \end{aligned} \quad (\text{D.69})$$

D.4.4 Region VD

The switch combination sequence for the nearest three vectors for sector VD is given by: $d_6(0-10)$ to $d_{11}(0-11)$ to $d_{18}(1-11)$ to $d_6(101)$ to $d_6(101)$ to $d_{18}(1-11)$ to $d_{11}(0-11)$ to $d_6(0-10)$

and the reference voltage vector waveform equation is given by:

$$\begin{aligned} V_{refa_{VD}} &= \frac{1}{4}d_6 + \frac{1}{2}d_{18} \\ &= \frac{\sqrt{3}}{2\sqrt{2}} \cos \omega t \end{aligned} \quad (D.70)$$

$$\begin{aligned} V_{refb_{VD}} &= -\frac{1}{4}d_6 - \frac{1}{2}d_{11} - \frac{1}{2}d_{18} \\ &= \frac{1}{2\sqrt{2}} \sin \omega t \end{aligned} \quad (D.71)$$

$$\begin{aligned} V_{refc_{VD}} &= \frac{1}{2}d_{11} + \frac{1}{2}d_{18} + \frac{1}{4}d_6 \\ &= -\frac{1}{2\sqrt{2}} \sin \omega t \end{aligned} \quad (D.72)$$

D.5 Duty cycles for Sector VI

In this section we study the sequences and combinations of duty cycles of regions A, B, C and D of sector VI. Figure D.5 show the first sector of six sectors with its regions. We show the switch combinations using all redundancy in Appendix E section E.6.

D.5.1 Region VIA

For $\theta \leq \frac{11\pi}{6}$

The switch combination sequence for the nearest three vectors moving from sector VA to VIA is given by:

$d_6(0-10)$ to $d_0(000)$ to $d_1(100)$ to $d_6(101)$ to $d_6(101)$ to $d_1(100)$ to $d_0(000)$ to $d_6(0-10)$ and the reference voltage vector waveform equation is given by:

$$\begin{aligned} V_{refa_{VIA1}} &= \frac{1}{4}d_6 + \frac{1}{2}d_1 \\ &= \frac{\sqrt{3}}{2\sqrt{2}} m_a \cos(\omega t) \end{aligned} \quad (D.73)$$

$$\begin{aligned} V_{refb_{VIA1}} &= -\frac{1}{4}d_6 \\ &= \frac{1}{2\sqrt{2}} m_a \sin(\omega t) \end{aligned} \quad (D.74)$$

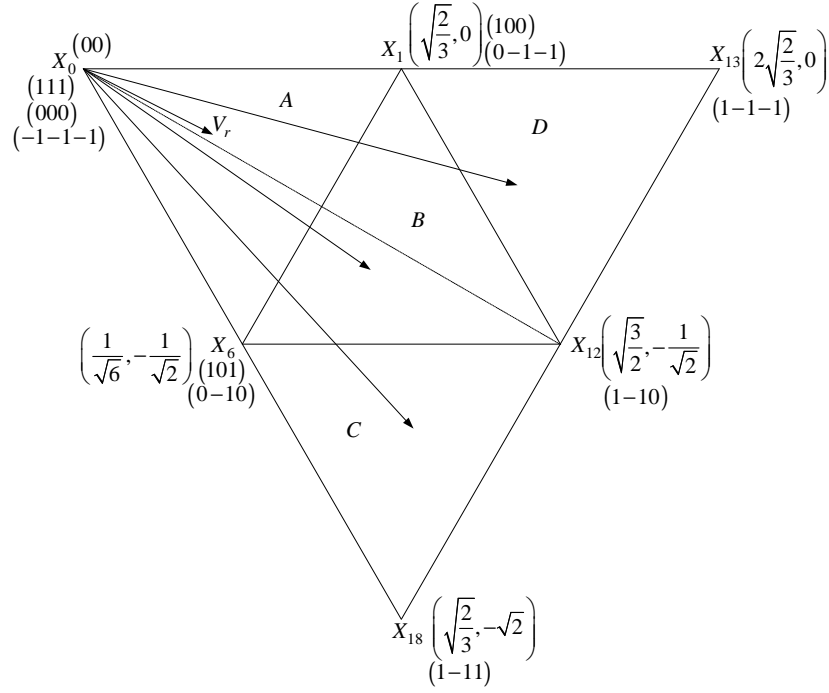


Figure D.5: Regions of vector modulation of the 2-cell multicell converter in the sixth sector

$$\begin{aligned}
 V_{refcvIA1} &= \frac{1}{4}d_6 \\
 &= -\frac{1}{2\sqrt{2}}m_a \sin(\omega t)
 \end{aligned} \tag{D.75}$$

For $\theta \geq \frac{11\pi}{6}$

The switch combination sequence for the nearest three vectors moving from sector VIA to IA is given by:

$d_1(0-1-1)$ to $d_6(0-10)$ to $d_0(000)$ to $d_1(100)$ to $d_1(100)$ to $d_0(000)$ to $d_6(0-10)$ to $d_1(0-1-1)$

and the reference voltage vector waveform equation is given by:

$$\begin{aligned}
 V_{refavIA2} &= \frac{1}{4}d_1 \\
 &= \frac{1}{2\sqrt{2}} \left(\frac{\sqrt{3}}{2}m_a \cos \omega t + \frac{1}{2}m_a \sin \omega t \right) \\
 &= \frac{1}{2\sqrt{2}}m_a \cos \left(\omega t - \frac{\pi}{6} \right)
 \end{aligned} \tag{D.76}$$

$$\begin{aligned}
 V_{refbvIA2} &= -\frac{1}{4}d_1 - \frac{1}{2}d_6 \\
 &= \frac{\sqrt{3}}{2\sqrt{2}}m_a \sin \left(\omega t - \frac{\pi}{6} \right)
 \end{aligned} \tag{D.77}$$

$$\begin{aligned}
V_{refc_{VIA2}} &= -\frac{1}{4}d_1 \\
&= -\frac{1}{2\sqrt{2}}m_a \cos\left(\omega t - \frac{\pi}{6}\right)
\end{aligned} \tag{D.78}$$

D.5.2 Region VIC

The switch combination sequence for the nearest three vectors for sector *VIC* is given by: $d_6(101)$ to $d_{18}(1-11)$ to $d_{12}(1-10)$ to $d_6(0-10)$ to $d_6(0-10)$ to $d_{12}(1-10)$ to $d_{18}(1-11)$ to $d_6(101)$

and the reference voltage vector waveform equation is given by:

$$\begin{aligned}
V_{refa_{VIC}} &= \frac{1}{4}d_6 + \frac{1}{2}d_{18} + \frac{1}{2}d_{12} \\
&= \frac{1}{2\sqrt{2}}m_a \cos\left(\omega t + \frac{\pi}{6}\right)
\end{aligned} \tag{D.79}$$

$$\begin{aligned}
V_{refb_{VIC}} &= -\frac{1}{4}d_6 - \frac{1}{2}d_{18} - \frac{1}{2}d_{12} \\
&= -\frac{1}{2\sqrt{2}}m_a \cos\left(\omega t + \frac{\pi}{6}\right)
\end{aligned} \tag{D.80}$$

$$\begin{aligned}
V_{refc_{VIC}} &= \frac{1}{4}d_6 + \frac{1}{2}d_{18} \\
&= -\frac{\sqrt{3}}{2\sqrt{2}}m_a \sin\left(\omega t + \frac{\pi}{6}\right)
\end{aligned} \tag{D.81}$$

D.5.3 Region VIB

For $\theta \leq \frac{11\pi}{6}$

The switch combination sequence for the nearest three vectors moving from sector *VIC* to *VIB* is given by:

$d_6(0-10)$ to $d_{12}(1-10)$ to $d_1(100)$ to $d_6(101)$ to $d_6(101)$ to $d_1(100)$ to $d_{12}(1-10)$ to $d_6(0-10)$

and the reference voltage vector waveform equation is given by:

$$\begin{aligned}
V_{refa_{VIB1}} &= \frac{1}{4}d_6 + \frac{1}{2}d_{12} + \frac{1}{2}d_1 \\
&= \frac{1}{2\sqrt{2}}m_a \cos\left(\omega t - \frac{\pi}{6}\right) + \frac{1}{4}
\end{aligned} \tag{D.82}$$

$$\begin{aligned}
V_{refb_{VIB1}} &= -\frac{1}{4}d_6 - \frac{1}{2}d_{12} \\
&= \frac{\sqrt{3}}{2\sqrt{2}}m_a \sin\left(\omega t - \frac{\pi}{6}\right) + \frac{1}{4}
\end{aligned} \tag{D.83}$$

$$\begin{aligned}
V_{refcVIB1} &= \frac{1}{4}d_6 \\
&= -\frac{1}{2\sqrt{2}}m_a \cos\left(\omega t - \frac{\pi}{6}\right) + \frac{1}{4}
\end{aligned} \tag{D.84}$$

For $\theta \geq \frac{11\pi}{6}$

The switch combination sequence for the nearest three vectors moving from sector VIB to VID is given by:

$d_1(0-1-1)$ to $d_6(0-10)$ to $d_{12}(1-10)$ to $d_1(100)$ to $d_1(100)$ to $d_{12}(1-10)$ to $d_6(0-10)$ to $d_1(0-1-1)$

and the reference voltage vector waveform equation is given by:

$$\begin{aligned}
V_{refaVIB2} &= \frac{1}{4}d_1 + \frac{1}{2}d_{12} \\
&= \frac{\sqrt{3}}{2\sqrt{2}}m_a \cos\omega t - \frac{1}{4}
\end{aligned} \tag{D.85}$$

$$\begin{aligned}
V_{refbVIB2} &= -\frac{1}{4}d_1 - \frac{1}{2}d_6 - \frac{1}{2}d_{12} \\
&= \frac{1}{2\sqrt{2}}m_a \sin\omega t - \frac{1}{4}
\end{aligned} \tag{D.86}$$

$$\begin{aligned}
V_{refcVIB2} &= -\frac{1}{4}d_1 \\
&= -\frac{1}{2\sqrt{2}}m_a \sin\omega t - \frac{1}{4}
\end{aligned} \tag{D.87}$$

D.5.4 Region VID

The switch combination sequence for the nearest three vectors for sector VID is given by:

$d_1(100)$ to $d_{12}(1-10)$ to $d_{13}(1-1-1)$ to $d_1(0-1-1)$ to $d_1(0-1-1)$ to $d_{13}(1-1-1)$ to $d_{12}(1-10)$ to $d_1(100)$

and the reference voltage vector waveform equation is given by:

$$\begin{aligned}
V_{refaVID} &= \frac{1}{4}d_1 + \frac{1}{2}d_{12} + \frac{1}{2}d_{13} \\
&= \frac{1}{2\sqrt{2}}m_a \cos\left(\omega t + \frac{\pi}{6}\right)
\end{aligned} \tag{D.88}$$

$$\begin{aligned}
V_{refbVID} &= -\frac{1}{2}d_{12} - \frac{1}{2}d_{13} - \frac{1}{4}d_1 \\
&= -\frac{1}{2\sqrt{2}}m_a \cos\left(\omega t + \frac{\pi}{6}\right)
\end{aligned} \tag{D.89}$$

$$\begin{aligned}
V_{refcVID} &= -\frac{1}{2}d_{13} - \frac{1}{4}d_1 \\
&= -\frac{\sqrt{3}}{2\sqrt{2}}m_a \sin\left(\omega t + \frac{\pi}{6}\right)
\end{aligned} \tag{D.90}$$

Appendix E

Switching Combinations

E.1 Sector I

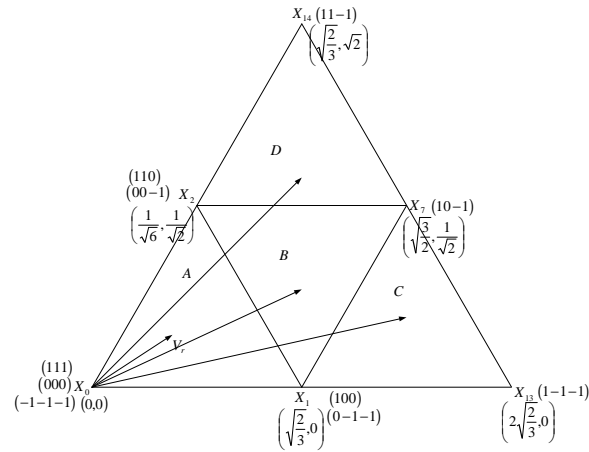


Figure E.1: *Regions of vector modulation of the 2-cell multicell converter in the first sector*

E.1.1 Region A

Duty Cycles

$$V_r = d_0 X_0 + d_1 X_1 + d_2 X_2$$

$$(m_a \cos \omega t, m_a \sin \omega t) = d_0(0, 0) + d_1\left(\sqrt{\frac{2}{3}}, 0\right) + d_2\left(\frac{1}{\sqrt{6}}, \frac{1}{\sqrt{2}}\right)$$

where m_a is modulation index.

$$m_a \cos \omega t = \sqrt{\frac{2}{3}}d_1 + \frac{1}{\sqrt{6}}d_2$$

$$m_a \sin \omega t = \frac{1}{\sqrt{2}} d_2$$

$$d_2 = \sqrt{2} m_a \sin \omega t$$

$$m_a \cos \omega t = \sqrt{\frac{2}{3}} d_1 + \frac{1}{\sqrt{3}} m_a \sin \omega t$$

$$d_1 = \sqrt{\frac{3}{2}} m_a \cos \omega t - \frac{1}{\sqrt{2}} m_a \sin \omega t$$

$$\begin{aligned} d_0 &= 1 - \sqrt{2} m_a \sin \omega t - \sqrt{\frac{3}{2}} m_a \cos \omega t + \frac{1}{\sqrt{2}} m_a \sin \omega t \\ &= 1 - \frac{1}{\sqrt{2}} m_a \sin \omega t - \sqrt{\frac{3}{2}} m_a \cos \omega t \end{aligned}$$

For $\theta \leq \frac{\pi}{6}$

The switch combination sequence for the nearest three vector moving from sector *VIA* to *IA* for 2-cell is given by:

$d_1(100)$ ([1, 1], [1, -1], [1, -1]) to $d_0(000)$ ([1, -1], [1, -1], [1, -1]) to $d_2(00-1)$ ([1, -1], [1, -1], [-1, -1]) to $d_1(0-1-1)$ ([1, -1], [-1, -1], [-1-1])

or

$d_1(100)$ ([1, 1], [1, -1], [1, -1]) to $d_0(000)$ ([-1, 1], [1, -1], [1, -1]) to $d_2(00-1)$ ([-1, 1], [1, -1], [-1, -1]) to $d_1(0-1-1)$ ([-1, 1], [-1, -1], [-1-1])

or

$d_1(100)$ ([1, 1], [-1, 1], [-1, 1]) to $d_0(000)$ ([1, -1], [-1, 1], [-1, 1]) to $d_2(00-1)$ ([1, -1], [-1, 1], [-1, -1]) to $d_1(0-1-1)$ ([1, -1], [-1, -1], [-1-1])

or

$d_1(100)$ ([1, 1], [-1, 1], [-1, 1]) to $d_0(000)$ ([-1, 1], [-1, 1], [-1, 1]) to $d_2(00-1)$ ([-1, 1], [-1, 1], [-1, -1]) to $d_1(0-1-1)$ ([-1, 1], [-1, -1], [-1-1])

or

$d_1(100)$ ([1, 1], [-1, 1], [1, -1]) to $d_0(000)$ ([1, -1], [-1, 1], [1, -1]) to $d_2(00-1)$ ([1, -1], [-1, 1], [-1, -1]) to $d_1(0-1-1)$ ([1, -1], [-1, -1], [-1-1])

or

$d_1(100)$ ([1, 1], [-1, 1], [1, -1]) to $d_0(000)$ ([-1, 1], [-1, 1], [1, -1]) to $d_2(00-1)$ ([-1, 1], [-1, 1], [-1, -1]) to $d_1(0-1-1)$ ([-1, 1], [-1, -1], [-1-1])

or

$d_1(100)$ ([1, 1], [1, -1], [-1, 1]) to $d_0(000)$ ([1, -1], [1, -1], [-1, 1]) to $d_2(00-1)$ ([1, -1], [1, -1], [-1, -1]) to $d_1(0-1-1)$ ([1, -1], [-1, -1], [-1-1])

or

$d_1(100)$ $([1, 1], [1, -1], [-1, 1])$ to $d_0(000)$ $([-1, 1], [1, -1], [-1, 1])$ to
 $d_2(00 - 1)$ $([-1, 1], [1, -1], [-1, -1])$ to $d_1(0 - 1 - 1)$ $([-1, 1], [-1, -1], [-1 - 1])$

For $\theta \geq \frac{\pi}{6}$

The switch combination sequence for the nearest three vector moving from sector IA to IIA for 2-cell is given by:

$d_2(110)$ $([1, 1], [1, 1], [1, -1])$ to $d_1(100)$ $([1, 1], [1, -1], [1, -1])$ to
 $d_0(000)$ $([1, -1], [1, -1], [1, -1])$ to $d_2(00 - 1)$ $([1, -1], [1, -1], [-1 - 1])$

or

$d_2(110)$ $([1, 1], [1, 1], [1, -1])$ to $d_1(100)$ $([1, 1], [1, -1], [1, -1])$ to
 $d_0(000)$ $([-1, 1], [1, -1], [1, -1])$ to $d_2(00 - 1)$ $([-1, 1], [1, -1], [-1 - 1])$

or

$d_2(110)$ $([1, 1], [1, 1], [-1, 1])$ to $d_1(100)$ $([1, 1], [-1, 1], [-1, 1])$ to
 $d_0(000)$ $([1, -1], [-1, 1], [-1, 1])$ to $d_2(00 - 1)$ $([1, -1], [-1, 1], [-1 - 1])$

or

$d_2(110)$ $([1, 1], [1, 1], [-1, 1])$ to $d_1(100)$ $([1, 1], [-1, 1], [-1, 1])$ to
 $d_0(000)$ $([-1, 1], [-1, 1], [-1, 1])$ to $d_2(00 - 1)$ $([-1, 1], [-1, 1], [-1 - 1])$

or

$d_2(110)$ $([1, 1], [1, 1], [1, -1])$ to $d_1(100)$ $([1, 1], [-1, 1], [1, -1])$ to
 $d_0(000)$ $([1, -1], [-1, 1], [1, -1])$ to $d_2(00 - 1)$ $([1, -1], [-1, 1], [-1 - 1])$

or

$d_2(110)$ $([1, 1], [1, 1], [1, -1])$ to $d_1(100)$ $([1, 1], [-1, 1], [1, -1])$ to
 $d_0(000)$ $([-1, 1], [-1, 1], [1, -1])$ to $d_2(00 - 1)$ $([-1, 1], [-1, 1], [-1 - 1])$

or

$d_2(110)$ $([1, 1], [1, 1], [-1, 1])$ to $d_1(100)$ $([1, 1], [1, -1], [-1, 1])$ to
 $d_0(000)$ $([1, -1], [1, -1], [-1, 1])$ to $d_2(00 - 1)$ $([1, -1], [1, -1], [-1 - 1])$

or

$d_2(110)$ $([1, 1], [1, 1], [-1, 1])$ to $d_1(100)$ $([1, 1], [1, -1], [-1, 1])$ to
 $d_0(000)$ $([-1, 1], [1, -1], [-1, 1])$ to $d_2(00 - 1)$ $([-1, 1], [1, -1], [-1 - 1])$

E.1.2 Region B

Duty Cycles

$$V_r = d_1 X_1 + d_7 X_7 + d_2 X_2$$

$$(m_a \cos \omega t, m_a \sin \omega) = d_1 \left(\sqrt{\frac{2}{3}}, 0 \right) + d_7 \left(\sqrt{\frac{3}{2}}, \frac{1}{\sqrt{2}} \right) + d_2 \left(\frac{1}{\sqrt{6}}, \frac{1}{\sqrt{2}} \right)$$

$$m_a \cos \omega t = \sqrt{\frac{2}{3}}d_1 + \sqrt{\frac{3}{2}}d_7 + \frac{1}{\sqrt{6}}d_2$$

$$m_a \sin \omega t = \frac{1}{\sqrt{2}}d_7 + \frac{1}{\sqrt{2}}d_2$$

$$d_2 = \sqrt{2}m_a \sin \omega t - d_7$$

$$\begin{aligned} m_a \cos \omega t &= \sqrt{\frac{2}{3}}d_1 + \sqrt{\frac{3}{2}}d_7 + \frac{1}{\sqrt{6}}\sqrt{2}m_a \sin \omega t - \frac{1}{\sqrt{6}}d_7 \\ &= \sqrt{\frac{2}{3}}d_1 + \sqrt{\frac{2}{3}}d_7 + \frac{1}{\sqrt{3}}m_a \sin \omega t \end{aligned}$$

$$d_1 + d_7 + d_2 = 1$$

$$\begin{aligned} d_1 &= 1 - \sqrt{2}m_a \sin \omega t + d_7 - d_7 \\ &= 1 - \sqrt{2}m_a \sin \omega t \end{aligned}$$

$$m_a \cos \omega t = \sqrt{\frac{2}{3}} - \frac{2}{\sqrt{3}}m_a \sin \omega t + \sqrt{\frac{2}{3}}d_7 + \frac{1}{\sqrt{3}}m_a \sin \omega t$$

$$d_7 = \sqrt{\frac{3}{2}}m_a \cos \omega t - 1 + \frac{1}{\sqrt{2}}m_a \sin \omega t$$

$$\begin{aligned} d_2 &= \sqrt{2}m_a \sin \omega t + 1 - \sqrt{\frac{3}{2}}m_a \cos \omega t - \frac{1}{\sqrt{2}}m_a \sin \omega t \\ &= 1 + \frac{1}{\sqrt{2}}m_a \sin \omega t - \sqrt{\frac{3}{2}}m_a \cos \omega t \end{aligned}$$

For $\theta \leq \frac{\pi}{6}$

The switch combination sequence for the nearest three vector moving from sector IC to IB for 2-cell is given by:

$$d_1(100) ([1, 1], [1, -1], [1, -1]) \text{ to } d_7(10-1) ([1, 1], [1, -1], [-1, -1]) \text{ to } d_2(00-1) ([1, -1], [1, -1], [-1, -1]) \text{ to } d_1(0-1-1) ([1, -1], [-1, -1], [-1-1])$$

or

$$d_1(100) ([1, 1], [1, -1], [1, -1]) \text{ to } d_7(10-1) ([1, 1], [1, -1], [-1, -1]) \text{ to } d_2(00-1) ([-1, 1], [1, -1], [-1, -1]) \text{ to } d_1(0-1-1) ([-1, 1], [-1, -1], [-1-1])$$

or

$$d_1(100) ([1, 1], [-1, 1], [-1, 1]) \text{ to } d_7(10-1) ([1, 1], [-1, 1], [-1, -1]) \text{ to}$$

$d_2(00-1) ([1, -1], [-1, 1], [-1, -1])$ to $d_1(0-1-1) ([1, -1], [-1, -1], [-1-1])$
 or
 $d_1(100) ([1, 1], [-1, 1], [-1, 1])$ to $d_7(10-1) ([1, 1], [-1, 1], [-1, -1])$ to
 $d_2(00-1) ([-1, 1], [-1, 1], [-1, -1])$ to $d_1(0-1-1) ([-1, 1], [-1, -1], [-1-1])$
 or
 $d_1(100) ([1, 1], [-1, 1], [1, -1])$ to $d_7(10-1) ([1, 1], [-1, 1], [-1, -1])$ to
 $d_2(00-1) ([1, -1], [-1, 1], [-1, -1])$ to $d_1(0-1-1) ([1, -1], [-1, -1], [-1-1])$
 or
 $d_1(100) ([1, 1], [-1, 1], [1, -1])$ to $d_7(10-1) ([1, 1], [-1, 1], [-1, -1])$ to
 $d_2(00-1) ([-1, 1], [-1, 1], [-1, -1])$ to $d_1(0-1-1) ([-1, 1], [-1, -1], [-1-1])$
 or
 $d_1(100) ([1, 1], [1, -1], [-1, 1])$ to $d_7(10-1) ([1, 1], [1, -1], [-1, -1])$ to
 $d_2(00-1) ([1, -1], [1, -1], [-1, -1])$ to $d_1(0-1-1) ([1, -1], [-1, -1], [-1-1])$
 or
 $d_1(100) ([1, 1], [1, -1], [-1, 1])$ to $d_7(10-1) ([1, 1], [1, -1], [-1, -1])$ to
 $d_2(00-1) ([-1, 1], [1, -1], [-1, -1])$ to $d_1(0-1-1) ([-1, 1], [-1, -1], [-1-1])$

For $\theta \geq \frac{\pi}{6}$

The switch combination sequence for the nearest three vector moving from sector IB to ID for 2-cell is given by:

$d_2(110) ([1, 1], [1, 1], [1, -1])$ to $d_1(100) ([1, 1], [1, -1], [1, -1])$ to
 $d_7(10-1) ([1, 1], [1, -1], [-1, -1])$ to
 $d_2(00-1) ([1, -1], [1, -1], [-1-1])$
 or
 $d_2(110) ([1, 1], [1, 1], [1, -1])$ to $d_1(100) ([1, 1], [1, -1], [1, -1])$ to
 $d_7(10-1) ([1, 1], [1, -1], [-1, -1])$ to
 $d_2(00-1) ([-1, 1], [1, -1], [-1-1])$
 or
 $d_2(110) ([1, 1], [1, 1], [1, -1])$ to $d_1(100) ([1, 1], [-1, 1], [1, -1])$ to
 $d_7(10-1) ([1, 1], [-1, 1], [-1, -1])$ to
 $d_2(00-1) ([1, -1], [-1, 1], [-1-1])$
 or
 $d_2(110) ([1, 1], [1, 1], [1, -1])$ to $d_1(100) ([1, 1], [-1, 1], [1, -1])$ to
 $d_7(10-1) ([1, 1], [-1, 1], [-1, -1])$ to
 $d_2(00-1) ([-1, 1], [-1, 1], [-1-1])$
 or
 $d_2(110) ([1, 1], [1, 1], [-1, 1])$ to $d_1(100) ([1, 1], [-1, 1], [-1, 1])$ to

$d_7(10 - 1) ([1, 1], [-1, 1], [-1, -1])$ to

$d_2(00 - 1) ([1, -1], [-1, 1], [-1 - 1])$

or

$d_2(110) ([1, 1], [1, 1], [-1, 1])$ to $d_1(100) ([1, 1], [-1, 1], [-1, 1])$ to

$d_7(10 - 1) ([1, 1], [-1, 1], [-1, -1])$ to

$d_2(00 - 1) ([-1, 1], [-1, 1], [-1 - 1])$

or

$d_2(110) ([1, 1], [1, 1], [-1, 1])$ to $d_1(100) ([1, 1], [1, -1], [-1, 1])$ to

$d_7(10 - 1) ([1, 1], [1, -1], [-1, -1])$ to

$d_2(00 - 1) ([1, -1], [1, -1], [-1 - 1])$

or

$d_2(110) ([1, 1], [1, 1], [-1, 1])$ to $d_1(100) ([1, 1], [1, -1], [-1, 1])$ to

$d_7(10 - 1) ([1, 1], [1, -1], [-1, -1])$ to

$d_2(00 - 1) ([-1, 1], [1, -1], [-1 - 1])$

E.1.3 Region C

Duty Cycles

$$V_r = d_1 X_1 + d_{13} X_{13} + d_7 X_7$$

$$(m_a \cos \omega t, m_a \sin \omega t) = d_1 \left(\sqrt{\frac{2}{3}}, 0 \right) + d_{13} \left(2\sqrt{\frac{2}{3}}, 0 \right) + d_7 \left(\sqrt{\frac{3}{2}}, \frac{1}{\sqrt{2}} \right)$$

$$m_a \cos \omega t = \sqrt{\frac{2}{3}} d_1 + 2\sqrt{\frac{2}{3}} d_{13} + \sqrt{\frac{3}{2}} d_7$$

$$m_a \sin \omega t = \frac{1}{\sqrt{2}} d_7$$

$$d_7 = \sqrt{2} m_a \sin \omega t$$

$$m_a \cos \omega t = \sqrt{\frac{2}{3}} d_1 + 2\sqrt{\frac{2}{3}} d_{13} + \sqrt{\frac{3}{2}} \sqrt{2} m_a \sin \omega t$$

$$d_1 + d_{13} + d_4 = 1$$

$$d_1 = 1 - d_{13} - \sqrt{2} m_a \sin \omega t$$

$$m_a \cos \omega t = \sqrt{\frac{2}{3}} - \sqrt{\frac{2}{3}} d_{13} - \sqrt{2} \sqrt{\frac{2}{3}} m_a \sin \omega t + 2\sqrt{\frac{2}{3}} d_{13} + \sqrt{3} m_a \sin \omega t$$

$$\sqrt{\frac{2}{3}} d_{13} = m_a \cos \omega t - \frac{1}{\sqrt{3}} m_a \sin \omega t - \sqrt{\frac{2}{3}}$$

$$d_{13} = \sqrt{\frac{3}{2}}m_a \cos \omega t - \frac{1}{\sqrt{2}}m_a \sin \omega t - 1$$

$$\begin{aligned} d_1 &= 1 - \sqrt{\frac{3}{2}}m_a \cos \omega t + \frac{1}{\sqrt{2}}m_a \sin \omega t + 1 - \sqrt{2}m_a \sin \omega t \\ &= 2 - \sqrt{\frac{3}{2}}m_a \cos \omega t - \frac{1}{\sqrt{2}}m_a \sin \omega t \end{aligned}$$

Switch Combination

The switch combination sequence for the nearest three vector moving from sector IC for 2-cell is given by:

$d_1(0-1-1)$ ($[1, -1], [-1, -1], [-1, -1]$) to $d_{13}(1-1-1)$ ($[1, 1], [-1, -1], [-1, -1]$) to $d_7(10-1)$ ($[1, 1], [1, -1], [-1, -1]$) to $d_1(100)$ ($[1, 1], [1, -1], [1, -1]$)

or

$d_1(0-1-1)$ ($[1, -1], [-1, -1], [-1, -1]$) to $d_{13}(1-1-1)$ ($[1, 1], [-1, -1], [-1, -1]$) to $d_7(10-1)$ ($[1, 1], [1, -1], [-1, -1]$) to $d_1(100)$ ($[1, 1], [1, -1], [-1, 1]$)

or

$d_1(0-1-1)$ ($[1, -1], [-1, -1], [-1, -1]$) to $d_{13}(1-1-1)$ ($[1, 1], [-1, -1], [-1, -1]$) to $d_7(10-1)$ ($[1, 1], [-1, 1], [-1, -1]$) to $d_1(100)$ ($[1, 1], [-1, 1], [-1, 1]$)

or

$d_1(0-1-1)$ ($[1, -1], [-1, -1], [-1, -1]$) to $d_{13}(1-1-1)$ ($[1, 1], [-1, -1], [-1, -1]$) to $d_7(10-1)$ ($[1, 1], [-1, 1], [-1, -1]$) to $d_1(100)$ ($[1, 1], [-1, 1], [1, -1]$)

or

$d_1(0-1-1)$ ($[-1, 1], [-1, -1], [-1, -1]$) to $d_{13}(1-1-1)$ ($[1, 1], [-1, -1], [-1, -1]$) to $d_7(10-1)$ ($[1, 1], [1, -1], [-1, -1]$) to $d_1(100)$ ($[1, 1], [1, -1], [1, -1]$)

or

$d_1(0-1-1)$ ($[-1, 1], [-1, -1], [-1, -1]$) to $d_{13}(1-1-1)$ ($[1, 1], [-1, -1], [-1, -1]$) to $d_7(10-1)$ ($[1, 1], [1, -1], [-1, -1]$) to $d_1(100)$ ($[1, 1], [1, -1], [-1, 1]$)

or

$d_1(0-1-1)$ ($[-1, 1], [-1, -1], [-1, -1]$) to $d_{13}(1-1-1)$ ($[1, 1], [-1, -1], [-1, -1]$) to $d_7(10-1)$ ($[1, 1], [-1, 1], [-1, -1]$) to $d_1(100)$ ($[1, 1], [-1, 1], [-1, 1]$)

or

$d_1(0-1-1)$ ($[-1, 1], [-1, -1], [-1, -1]$) to $d_{13}(1-1-1)$ ($[1, 1], [-1, -1], [-1, -1]$) to $d_7(10-1)$ ($[1, 1], [-1, 1], [-1, -1]$) to $d_1(100)$ ($[1, 1], [-1, 1], [1, -1]$)

E.1.4 Region D

Duty Cycles

$$V_r = d_2 X_2 + d_7 X_7 + d_{14} X_{14}$$

$$(m_a \cos \omega t, m_a \sin \omega t) = d_2 \left(\frac{1}{\sqrt{6}}, \frac{1}{\sqrt{2}} \right) + d_7 \left(\sqrt{\frac{3}{2}}, \frac{1}{\sqrt{2}} \right) + d_{14} \left(\sqrt{\frac{2}{3}}, \sqrt{2} \right)$$

$$m_a \cos \omega t = \frac{1}{\sqrt{6}} d_2 + \sqrt{\frac{3}{2}} d_7 + \sqrt{\frac{2}{3}} d_{14}$$

$$m_a \sin \omega t = \frac{1}{\sqrt{2}} d_2 + \frac{1}{\sqrt{2}} d_7 + \sqrt{2} d_{14}$$

$$d_2 + d_7 + d_{14} = 1$$

$$d_2 = \sqrt{2} m_a \sin \omega t - d_7 - 2d_{14}$$

$$\begin{aligned} m_a \cos \omega t &= \frac{1}{\sqrt{6}} \sqrt{2} m_a \sin \omega t - \frac{1}{\sqrt{6}} d_7 - \frac{1}{\sqrt{6}} 2d_{14} + \sqrt{\frac{3}{2}} d_7 + \frac{2}{3} d_{14} \\ &= \frac{1}{\sqrt{3}} m_a \sin \omega t - \frac{1}{\sqrt{6}} d_7 - \sqrt{\frac{2}{3}} d_{14} + \sqrt{\frac{3}{2}} d_7 + \sqrt{\frac{2}{3}} d_{14} \\ &= \frac{1}{\sqrt{3}} m_a \sin \omega t + \sqrt{\frac{2}{3}} d_7 \end{aligned}$$

$$d_7 = \sqrt{\frac{3}{2}} m_a \cos \omega t - \frac{1}{\sqrt{2}} m_a \sin \omega t$$

$$\begin{aligned} d_2 &= \sqrt{2} m_a \sin \omega t - \sqrt{\frac{3}{2}} m_a \cos \omega t + \frac{1}{\sqrt{2}} m_a \sin \omega t - 2d_{14} \\ &= \frac{3}{\sqrt{2}} m_a \sin \omega t - \sqrt{\frac{3}{2}} m_a \cos \omega t - 2d_{14} \end{aligned}$$

$$\begin{aligned} d_{14} &= 1 - d_4 - d_2 \\ &= 1 - \sqrt{\frac{3}{2}} m_a \cos \omega t + \frac{1}{\sqrt{2}} m_a \sin \omega t - \frac{3}{\sqrt{2}} m_a \sin \omega t + \sqrt{\frac{3}{2}} m_a \cos \omega t + 2d_{14} \\ &= 1 - \sqrt{2} m_a \sin \omega t + 2d_{14} \end{aligned}$$

$$d_{14} = \sqrt{2} m_a \sin \omega t - 1$$

$$\begin{aligned} d_2 &= \frac{3}{2} m_a \sin \omega t - \sqrt{\frac{3}{2}} m_a \cos \omega t - 2\sqrt{2} m_a \sin \omega t + 2 \\ &= -\frac{1}{\sqrt{2}} m_a \sin \omega t - \sqrt{\frac{3}{2}} m_a \cos \omega t + 2 \end{aligned}$$

Switch Combination

The switch combination sequence for the nearest three vector moving from sector ID for 2-cell is given by:

$d_2(00 - 1) ([1, -1], [1, -1], [-1, -1])$ to $d_7(10 - 1) ([1, 1], [1, -1], [-1, -1])$ to $d_{14}(11 - 1) ([1, 1], [1, 1], [-1, -1])$ to $d_2(110) ([1, 1], [1, 1], [1, -1])$

or

$d_2(00 - 1) ([1, -1], [1, -1], [-1, -1])$ to $d_7(10 - 1) ([1, 1], [1, -1], [-1, -1])$ to $d_{14}(11 - 1) ([1, 1], [1, 1], [-1, -1])$ to $d_2(110) ([1, 1], [1, 1], [-1, 1])$

or

$d_2(00 - 1) ([-1, 1], [1, -1], [-1, -1])$ to $d_7(10 - 1) ([1, 1], [1, -1], [-1, -1])$ to $d_{14}(11 - 1) ([1, 1], [1, 1], [-1, -1])$ to $d_2(110) ([1, 1], [1, 1], [1, -1])$

or

$d_2(00 - 1) ([-1, 1], [1, -1], [-1, -1])$ to $d_7(10 - 1) ([1, 1], [1, -1], [-1, -1])$ to $d_{14}(11 - 1) ([1, 1], [1, 1], [-1, -1])$ to $d_2(110) ([1, 1], [1, 1], [-1, 1])$

or

$d_2(00 - 1) ([1, -1], [-1, 1], [-1, -1])$ to $d_7(10 - 1) ([1, 1], [-1, 1], [-1, -1])$ to $d_{14}(11 - 1) ([1, 1], [1, 1], [-1, -1])$ to $d_2(110) ([1, 1], [1, 1], [1, -1])$

or

$d_2(00 - 1) ([1, -1], [-1, 1], [-1, -1])$ to $d_7(10 - 1) ([1, 1], [-1, 1], [-1, -1])$ to $d_{14}(11 - 1) ([1, 1], [1, 1], [-1, -1])$ to $d_2(110) ([1, 1], [1, 1], [-1, 1])$

or

$d_2(00 - 1) ([-1, 1], [-1, 1], [-1, -1])$ to $d_7(10 - 1) ([1, 1], [-1, 1], [-1, -1])$ to $d_{14}(11 - 1) ([1, 1], [1, 1], [-1, -1])$ to $d_2(110) ([1, 1], [1, 1], [1, -1])$

or

$d_2(00 - 1) ([-1, 1], [-1, 1], [-1, -1])$ to $d_7(10 - 1) ([1, 1], [-1, 1], [-1, -1])$ to $d_{14}(11 - 1) ([1, 1], [1, 1], [-1, -1])$ to $d_2(110) ([1, 1], [1, 1], [-1, 1])$

E.2 Sector II

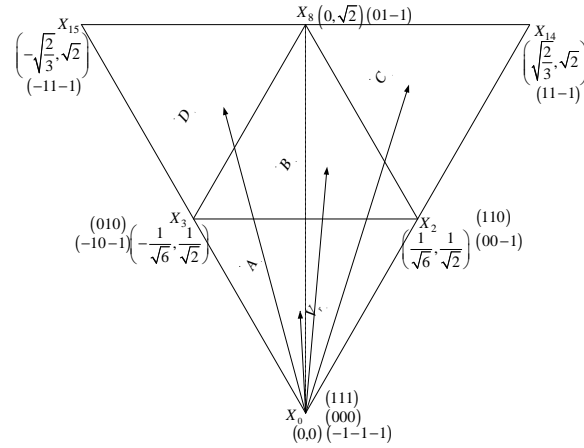


Figure E.2: Regions of vector modulation of the 2-cell multicell converter in the second sector

E.2.1 Region A

Duty Cycles

$$V_r = d_0 X_0 + d_2 X_2 + d_3 X_3$$

$$(m_a \cos \omega t, m_a \sin \omega t) = d_0 (0, 0) + d_2 \left(\frac{1}{\sqrt{6}}, \frac{1}{\sqrt{2}} \right) + d_3 \left(-\frac{1}{\sqrt{6}}, \frac{1}{\sqrt{2}} \right)$$

$$m_a \cos \omega t = \frac{1}{\sqrt{6}} d_2 - \frac{1}{\sqrt{6}} d_3$$

$$m_a \sin \omega t = \frac{1}{\sqrt{2}} d_2 + \frac{1}{\sqrt{2}} d_3$$

$$d_0 + d_2 + d_3 = 1$$

$$d_0 = -\sqrt{2} m_a \sin \omega t + 1$$

$$d_2 = \sqrt{\frac{3}{2}} m_a \cos \omega t + \frac{1}{\sqrt{2}} m_a \sin \omega t$$

$$d_3 = -\sqrt{\frac{3}{2}} m_a \cos \omega t + \frac{1}{\sqrt{2}} m_a \sin \omega t$$

For $\theta \leq \frac{\pi}{2}$

The switch combination sequence for the nearest three vector moving from sector IA to IIA for 2-cell is given by:

$d_2(00-1) ([1, -1], [1, -1], [-1, -1])$ to $d_0(000) ([1, -1], [1, -1], [1, -1])$ to

$d_3(010) ([1, -1], [1, 1], [1, -1])$ to $d_2(110) ([1, 1], [1, 1], [1, -1])$

or

$d_2(00-1) ([-1, 1], [1, -1], [-1, -1])$ to $d_0(000) ([-1, 1], [1, -1], [1, -1])$ to

$d_3(010) ([-1, 1], [1, 1], [1, -1])$ to $d_2(110) ([1, 1], [1, 1], [1, -1])$

or

$d_2(00-1) ([1, -1], [-1, 1], [-1, -1])$ to $d_0(000) ([1, -1], [-1, 1], [-1, 1])$ to

$d_3(010) ([1, -1], [1, 1], [-1, 1])$ to $d_2(110) ([1, 1], [1, 1], [-1, 1])$

or

$d_2(00-1) ([-1, 1], [-1, 1], [-1, -1])$ to $d_0(000) ([-1, 1], [-1, 1], [-1, 1])$ to

$d_3(010) ([-1, 1], [1, 1], [-1, 1])$ to $d_2(110) ([1, 1], [1, 1], [-1, 1])$

or

$d_2(00-1) ([1, -1], [-1, 1], [-1, -1])$ to $d_0(000) ([1, -1], [-1, 1], [1, -1])$ to

$d_3(010) ([1, -1], [1, 1], [1, -1])$ to $d_2(110) ([1, 1], [1, 1], [1, -1])$

or

$d_2(00-1) ([-1, 1], [-1, 1], [-1, -1])$ to $d_0(000) ([-1, 1], [-1, 1], [1, -1])$ to

$d_3(010) ([-1, 1], [1, 1], [1, -1])$ to $d_2(110) ([1, 1], [1, 1], [1, -1])$

or

$d_2(00-1) ([1, -1], [1, -1], [-1, -1])$ to $d_0(000) ([1, -1], [1, -1], [-1, 1])$ to

$d_3(010) ([1, -1], [1, 1], [-1, 1])$ to $d_2(110) ([1, 1], [1, 1], [-1, 1])$

or

$d_2(00-1) ([-1, 1], [1, -1], [-1, -1])$ to $d_0(000) ([-1, 1], [1, -1], [-1, 1])$ to

$d_3(010) ([-1, 1], [1, 1], [-1, 1])$ to $d_2(110) ([1, 1], [1, 1], [-1, 1])$

For $\theta \geq \frac{\pi}{2}$

The switch combination sequence for the nearest three vector moving from sector IIA to $IIIA$ for 2-cell is given by:

$d_3(-10-1) ([-1, -1], [1, -1], [-1, -1])$ to $d_2(00-1) ([1, -1], [1, -1], [-1, -1])$ to

$d_0(000) ([1, -1], [1, -1], [1, -1])$ to $d_3(010) ([1, -1], [1, 1], [1, -1])$

or

$d_3(-10-1) ([-1, -1], [1, -1], [-1, -1])$ to $d_2(00-1) ([-1, 1], [1, -1], [-1, -1])$ to

$d_0(000) ([-1, 1], [1, -1], [1, -1])$ to $d_3(010) ([-1, 1], [1, 1], [1, -1])$

or

$d_3(-10-1) ([-1, -1], [-1, 1], [-1, -1])$ to $d_2(00-1) ([1, -1], [-1, 1], [-1, -1])$ to

$d_0(000)$ $([1, -1], [-1, 1], [-1, 1])$ to $d_3(010)$ $([1, -1], [1, 1], [-1, 1])$

or

$d_3(-10 - 1)$ $([-1, -1], [-1, 1], [-1, -1])$ to $d_2(00 - 1)$ $([-1, 1], [-1, 1], [-1, -1])$ to $d_0(000)$ $([-1, 1], [-1, 1], [-1, 1])$ to $d_3(010)$ $([-1, 1], [1, 1], [-1, 1])$

or

$d_3(-10 - 1)$ $([-1, -1], [-1, 1], [-1, -1])$ to $d_2(00 - 1)$ $([1, -1], [-1, 1], [-1, -1])$ to $d_0(000)$ $([1, -1], [-1, 1], [1, -1])$ to $d_3(010)$ $([1, -1], [1, 1], [1, -1])$

or

$d_3(-10 - 1)$ $([-1, -1], [-1, 1], [-1, -1])$ to $d_2(00 - 1)$ $([-1, 1], [-1, 1], [-1, -1])$ to $d_0(000)$ $([-1, 1], [-1, 1], [1, -1])$ to $d_3(010)$ $([-1, 1], [1, 1], [1, -1])$

or

$d_3(-10 - 1)$ $([-1, -1], [1, -1], [-1, -1])$ to $d_2(00 - 1)$ $([1, -1], [1, -1], [-1, -1])$ to $d_0(000)$ $([1, -1], [1, -1], [-1, 1])$ to $d_3(010)$ $([1, -1], [1, 1], [-1, 1])$

or

$d_3(-10 - 1)$ $([-1, -1], [1, -1], [-1, -1])$ to $d_2(00 - 1)$ $([-1, 1], [1, -1], [-1, -1])$ to $d_0(000)$ $([-1, 1], [1, -1], [-1, 1])$ to $d_3(010)$ $([-1, 1], [1, 1], [-1, 1])$

E.2.2 Region C

Duty Cycles

$$V_r = d_2 X_2 + d_{14} X_{14} + d_8 X_8$$

$$(m_a \cos \omega t, m_a \sin \omega t) = d_2 \left(\frac{1}{\sqrt{6}}, \frac{1}{\sqrt{2}} \right) + d_{14} \left(\sqrt{\frac{2}{3}}, \sqrt{2} \right) + d_8 (0, \sqrt{2})$$

$$m_a \cos \omega t = \frac{1}{\sqrt{6}} d_2 + \sqrt{\frac{2}{3}} d_{14}$$

$$m_a \sin \omega t = \frac{1}{\sqrt{2}} d_2 + \sqrt{2} d_{14} + \sqrt{2} d_8$$

$$d_2 + d_{14} + d_8 = 1$$

$$d_{14} = \sqrt{\frac{3}{2}} m_a \cos \omega t + \frac{1}{\sqrt{2}} m_a \sin \omega t - 1$$

$$d_2 = -\sqrt{2} m_a \sin \omega t + 2$$

$$d_8 = -\sqrt{\frac{3}{2}} m_a \cos \omega t + \frac{1}{\sqrt{2}} m_a \sin \omega t$$

Switching Combinations

The switch combination sequence for the nearest three vector for sector *IIC* for 2-cell is given by:

$$d_2(110) ([1, 1], [1, 1], [1, -1]) \text{ to } d_{14}(11 - 1) ([1, 1], [1, 1], [-1, -1]) \text{ to } d_8(01 - 1) ([1, -1], [1, 1], [-1, -1]) \text{ to } d_2(00 - 1) ([1, -1], [1, -1], [-1, -1])$$

or

$$d_2(110) ([1, 1], [1, 1], [1, -1]) \text{ to } d_{14}(11 - 1) ([1, 1], [1, 1], [-1, -1]) \text{ to } d_8(01 - 1) ([1, -1], [1, 1], [-1, -1]) \text{ to } d_2(00 - 1) ([1, -1], [-1, 1], [-1, -1])$$

or

$$d_2(110) ([1, 1], [1, 1], [1, -1]) \text{ to } d_{14}(11 - 1) ([1, 1], [1, 1], [-1, -1]) \text{ to } d_8(01 - 1) ([-1, 1], [1, 1], [-1, -1]) \text{ to } d_2(00 - 1) ([-1, 1], [1, -1], [-1, -1])$$

or

$$d_2(110) ([1, 1], [1, 1], [1, -1]) \text{ to } d_{14}(11 - 1) ([1, 1], [1, 1], [-1, -1]) \text{ to } d_8(01 - 1) ([-1, 1], [1, 1], [-1, -1]) \text{ to } d_2(00 - 1) ([-1, 1], [-1, 1], [-1, -1])$$

or

$$d_2(110) ([1, 1], [1, 1], [-1, 1]) \text{ to } d_{14}(11 - 1) ([1, 1], [1, 1], [-1, -1]) \text{ to } d_8(01 - 1) ([1, -1], [1, 1], [-1, -1]) \text{ to } d_2(00 - 1) ([1, -1], [1, -1], [-1, -1])$$

or

$$d_2(110) ([1, 1], [1, 1], [-1, 1]) \text{ to } d_{14}(11 - 1) ([1, 1], [1, 1], [-1, -1]) \text{ to } d_8(01 - 1) ([1, -1], [1, 1], [-1, -1]) \text{ to } d_2(00 - 1) ([1, -1], [-1, 1], [-1, -1])$$

or

$$d_2(110) ([1, 1], [1, 1], [-1, 1]) \text{ to } d_{14}(11 - 1) ([1, 1], [1, 1], [-1, -1]) \text{ to } d_8(01 - 1) ([-1, 1], [1, 1], [-1, -1]) \text{ to } d_2(00 - 1) ([-1, 1], [1, -1], [-1, -1])$$

or

$$d_2(110) ([1, 1], [1, 1], [-1, 1]) \text{ to } d_{14}(11 - 1) ([1, 1], [1, 1], [-1, -1]) \text{ to } d_8(01 - 1) ([-1, 1], [1, 1], [-1, -1]) \text{ to } d_2(00 - 1) ([-1, 1], [-1, 1], [-1, -1])$$

E.2.3 Region B

Duty Cycles

$$m_a \cos \omega t = \frac{1}{\sqrt{6}}d_2 - \frac{1}{\sqrt{6}}d_3$$

$$m_a \sin \omega t = \frac{1}{\sqrt{2}}d_2 + \sqrt{2}d_8 + \frac{1}{\sqrt{2}}d_3$$

$$d_2 + d_8 + d_3 = 1$$

$$d_2 = \sqrt{\frac{3}{2}}m_a \cos \omega t - \frac{1}{\sqrt{2}}m_a \sin \omega t + 1$$

$$d_8 = \sqrt{2}m_a \sin \omega t - 1$$

$$d_3 = -\sqrt{\frac{3}{2}}m_a \cos \omega t - \frac{1}{\sqrt{2}}m_a \sin \omega t + 1$$

For $\theta \leq \frac{\pi}{2}$

The switch combination sequence for the nearest three vector moving from sector *IIC* to *IIB* for 2-cell is given by:

$$d_2(00-1) ([1, -1], [1, -1], [-1, -1]) \text{ to } d_8(01-1) ([1, -1], [1, 1], [-1, -1]) \text{ to}$$

$$d_3(010) ([1, -1], [1, 1], [1, -1]) \text{ to } d_2(110) ([1, 1], [1, 1], [1, -1])$$

or

$$d_2(00-1) ([1, -1], [1, -1], [-1, -1]) \text{ to } d_8(01-1) ([1, -1], [1, 1], [-1, -1]) \text{ to}$$

$$d_3(010) ([1, -1], [1, 1], [-1, 1]) \text{ to } d_2(110) ([1, 1], [1, 1], [-1, 1])$$

or

$$d_2(00-1) ([1, -1], [-1, 1], [-1, -1]) \text{ to } d_8(01-1) ([1, -1], [1, 1], [-1, -1]) \text{ to}$$

$$d_3(010) ([1, -1], [1, 1], [1, -1]) \text{ to } d_2(110) ([1, 1], [1, 1], [1, -1])$$

or

$$d_2(00-1) ([1, -1], [-1, 1], [-1, -1]) \text{ to } d_8(01-1) ([1, -1], [1, 1], [-1, -1]) \text{ to}$$

$$d_3(010) ([1, -1], [1, 1], [-1, 1]) \text{ to } d_2(110) ([1, 1], [1, 1], [-1, 1])$$

or

$$d_2(00-1) ([-1, 1], [1, -1], [-1, -1]) \text{ to } d_8(01-1) ([-1, 1], [1, 1], [-1, -1]) \text{ to}$$

$$d_3(010) ([-1, 1], [1, 1], [1, -1]) \text{ to } d_2(110) ([1, 1], [1, 1], [1, -1])$$

or

$$d_2(00-1) ([-1, 1], [1, -1], [-1, -1]) \text{ to } d_8(01-1) ([-1, 1], [1, 1], [-1, -1]) \text{ to}$$

$$d_3(010) ([-1, 1], [1, 1], [-1, 1]) \text{ to } d_2(110) ([1, 1], [1, 1], [-1, 1])$$

or

$$d_2(00-1) ([-1, 1], [-1, 1], [-1, -1]) \text{ to } d_8(01-1) ([-1, 1], [1, 1], [-1, -1]) \text{ to}$$

$$d_3(010) ([-1, 1], [1, 1], [1, -1]) \text{ to } d_2(110) ([1, 1], [1, 1], [1, -1])$$

or

$$d_2(00-1) ([-1, 1], [-1, 1], [-1, -1]) \text{ to } d_8(01-1) ([-1, 1], [1, 1], [-1, -1]) \text{ to}$$

$$d_3(010) ([-1, 1], [1, 1], [-1, 1]) \text{ to } d_2(110) ([1, 1], [1, 1], [-1, 1])$$

For $\theta \geq \frac{\pi}{2}$

The switch combination sequence for the nearest three vector moving from sector *IIB* to *IID* for 2-cell is given by:

$$d_3(-10-1) ([-1, -1], [1, -1], [-1, -1]) \text{ to } d_2(00-1) ([1, -1], [1, -1], [-1, -1]) \text{ to}$$

$$d_8(01-1) ([1, -1], [1, 1], [-1, -1]) \text{ to } d_3(010) ([1, -1], [1, 1], [1, -1])$$

or

$d_3(-10 - 1) ([-1, -1], [1, -1], [-1, -1])$ to $d_2(00 - 1) ([1, -1], [1, -1], [-1, -1])$ to $d_8(01 - 1) ([1, -1], [1, 1], [-1, -1])$ to $d_3(010) ([1, -1], [1, 1], [-1, 1])$

or

$d_3(-10 - 1) ([-1, -1], [1, -1], [-1, -1])$ to $d_2(00 - 1) ([-1, 1], [1, -1], [-1, -1])$ to $d_8(01 - 1) ([-1, 1], [1, 1], [-1, -1])$ to $d_3(010) ([-1, 1], [1, 1], [1, -1])$

or

$d_3(-10 - 1) ([-1, -1], [1, -1], [-1, -1])$ to $d_2(00 - 1) ([-1, 1], [1, -1], [-1, -1])$ to $d_8(01 - 1) ([-1, 1], [1, 1], [-1, -1])$ to $d_3(010) ([-1, 1], [1, 1], [-1, 1])$

or

$d_3(-10 - 1) ([-1, -1], [-1, 1], [-1, -1])$ to $d_2(00 - 1) ([1, -1], [-1, 1], [-1, -1])$ to $d_8(01 - 1) ([1, -1], [1, 1], [-1, -1])$ to $d_3(010) ([1, -1], [1, 1], [1, -1])$

or

$d_3(-10 - 1) ([-1, -1], [-1, 1], [-1, -1])$ to $d_2(00 - 1) ([1, -1], [-1, 1], [-1, -1])$ to $d_8(01 - 1) ([1, -1], [1, 1], [-1, -1])$ to $d_3(010) ([1, -1], [1, 1], [-1, 1])$

or

$d_3(-10 - 1) ([-1, -1], [-1, 1], [-1, -1])$ to $d_2(00 - 1) ([-1, 1], [-1, 1], [-1, -1])$ to $d_8(01 - 1) ([-1, 1], [1, 1], [-1, -1])$ to $d_3(010) ([-1, 1], [1, 1], [1, -1])$

or

$d_3(-10 - 1) ([-1, -1], [-1, 1], [-1, -1])$ to $d_2(00 - 1) ([-1, 1], [-1, 1], [-1, -1])$ to $d_8(01 - 1) ([-1, 1], [1, 1], [-1, -1])$ to $d_3(010) ([-1, 1], [1, 1], [-1, 1])$

E.2.4 Region D

Duty Cycles

$$m_a \cos \omega t = -\frac{1}{\sqrt{6}}d_3 - \sqrt{\frac{2}{3}}d_{15}$$

$$m_a \sin \omega t = \frac{1}{\sqrt{2}}d_3 + \sqrt{2}d_8 + \sqrt{2}d_{15}$$

$$d_3 + d_8 + d_{15} = 1$$

$$d_3 = -\sqrt{2}m_a \sin \omega t + 2$$

$$d_8 = \sqrt{\frac{3}{2}}m_a \cos \omega t + \frac{1}{\sqrt{2}}m_a \sin \omega t$$

$$d_{15} = -\sqrt{\frac{3}{2}}m_a \cos \omega t + \frac{1}{\sqrt{2}}m_a \sin \omega t - 1$$

Switch Combinations

The switch combination sequence for the nearest three vector for sector *IID* for 2-cell is given by:

$$d_3(010) ([1, -1], [1, 1], [1, -1]) \text{ to } d_8(01 - 1) ([1, -1], [1, 1], [-1, -1]) \text{ to } \\ d_{15}(-11 - 1) ([-1, -1], [1, 1], [-1, -1]) \text{ to } d_3(-10 - 1) ([-1, -1], [1, -1], [-1, -1])$$

or

$$d_3(010) ([1, -1], [1, 1], [1, -1]) \text{ to } d_8(01 - 1) ([1, -1], [1, 1], [-1, -1]) \text{ to } \\ d_{15}(-11 - 1) ([-1, -1], [1, 1], [-1, -1]) \text{ to } d_3(-10 - 1) ([-1, -1], [-1, 1], [-1, -1])$$

or

$$d_3(010) ([1, -1], [1, 1], [-1, 1]) \text{ to } d_8(01 - 1) ([1, -1], [1, 1], [-1, -1]) \text{ to } \\ d_{15}(-11 - 1) ([-1, -1], [1, 1], [-1, -1]) \text{ to } d_3(-10 - 1) ([-1, -1], [1, -1], [-1, -1])$$

or

$$d_3(010) ([1, -1], [1, 1], [-1, 1]) \text{ to } d_8(01 - 1) ([1, -1], [1, 1], [-1, -1]) \text{ to } \\ d_{15}(-11 - 1) ([-1, -1], [1, 1], [-1, -1]) \text{ to } d_3(-10 - 1) ([-1, -1], [-1, 1], [-1, -1])$$

or

$$d_3(010) ([-1, 1], [1, 1], [1, -1]) \text{ to } d_8(01 - 1) ([-1, 1], [1, 1], [-1, -1]) \text{ to } \\ d_{15}(-11 - 1) ([-1, -1], [1, 1], [-1, -1]) \text{ to } d_3(-10 - 1) ([-1, -1], [1, -1], [-1, -1])$$

or

$$d_3(010) ([-1, 1], [1, 1], [1, -1]) \text{ to } d_8(01 - 1) ([-1, 1], [1, 1], [-1, -1]) \text{ to } \\ d_{15}(-11 - 1) ([-1, -1], [1, 1], [-1, -1]) \text{ to } d_3(-10 - 1) ([-1, -1], [-1, 1], [-1, -1])$$

or

$$d_3(010) ([-1, 1], [1, 1], [-1, 1]) \text{ to } d_8(01 - 1) ([-1, 1], [1, 1], [-1, -1]) \text{ to } \\ d_{15}(-11 - 1) ([-1, -1], [1, 1], [-1, -1]) \text{ to } d_3(-10 - 1) ([-1, -1], [1, -1], [-1, -1])$$

or

$$d_3(010) ([-1, 1], [1, 1], [-1, 1]) \text{ to } d_8(01 - 1) ([-1, 1], [1, 1], [-1, -1]) \text{ to } \\ d_{15}(-11 - 1) ([-1, -1], [1, 1], [-1, -1]) \text{ to } d_3(-10 - 1) ([-1, -1], [-1, 1], [-1, -1])$$

E.3 Sector III

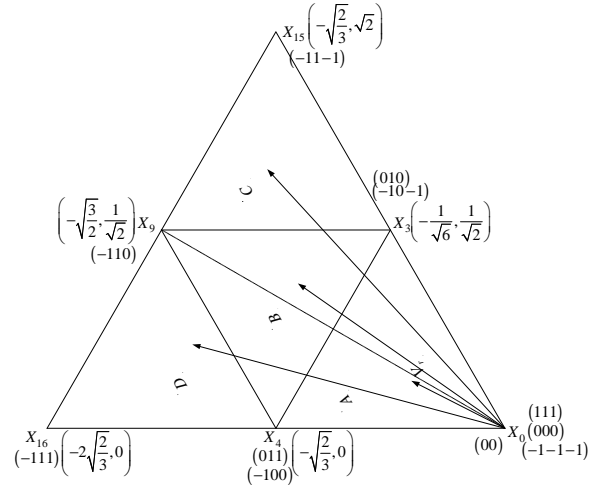


Figure E.3: Regions of vector modulation of the 2-cell multicell converter in the third sector

E.3.1 Region A

Duty Cycles

$$m_a \cos \omega t = -\frac{1}{\sqrt{6}}d_3 - \sqrt{\frac{2}{3}}d_4$$

$$m_a \sin \omega t = \frac{1}{\sqrt{2}}d_3$$

$$d_3 + d_4 + d_0 = 1$$

$$d_0 = -\frac{1}{\sqrt{2}}m_a \sin \omega t + \sqrt{\frac{3}{2}}m_a \cos \omega t + 1$$

$$d_4 = -\sqrt{\frac{3}{2}}m_a \cos \omega t - \frac{1}{\sqrt{2}}m_a \sin \omega t$$

$$d_3 = \sqrt{2}m_a \sin \omega t$$

For $\theta \leq \frac{5\pi}{6}$

The switch combination sequence for the nearest three vector moving from sector *IIA* to *IIIA* for 2-cell is given by:

$d_3(010)$ $([1, -1], [1, 1], [1, -1])$ to $d_0(000)$ $([1, -1], [1, -1], [1, -1])$ to

$d_4(-100)$ $([-1, -1], [1, -1], [1, -1])$ to $d_3(-10-1)$ $([-1, -1], [1, -1], [-1, -1])$

or

$d_3(010)$ $([-1, 1], [1, 1], [1, -1])$ to $d_0(000)$ $([-1, 1], [1, -1], [1, -1])$ to
 $d_4(-100)$ $([-1, -1], [1, -1], [1, -1])$ to $d_3(-10 - 1)$ $([-1, -1], [1, -1], [-1, -1])$

or

$d_3(010)$ $([1, -1], [1, 1], [-1, 1])$ to $d_0(000)$ $([1, -1], [-1, 1], [-1, 1])$ to
 $d_4(-100)$ $([-1, -1], [-1, 1], [-1, 1])$ to $d_3(-10 - 1)$ $([-1, -1], [-1, 1], [-1, -1])$

or

$d_3(010)$ $([-1, 1], [1, 1], [-1, 1])$ to $d_0(000)$ $([-1, 1], [-1, 1], [-1, 1])$ to
 $d_4(-100)$ $([-1, -1], [-1, 1], [-1, 1])$ to $d_3(-10 - 1)$ $([-1, -1], [-1, 1], [-1, -1])$

or

$d_3(010)$ $([1, -1], [1, 1], [1, -1])$ to $d_0(000)$ $([1, -1], [-1, 1], [1, -1])$ to
 $d_4(-100)$ $([-1, -1], [-1, 1], [1, -1])$ to $d_3(-10 - 1)$ $([-1, -1], [-1, 1], [-1, -1])$

or

$d_3(010)$ $([-1, 1], [1, 1], [1, -1])$ to $d_0(000)$ $([-1, 1], [-1, 1], [1, -1])$ to
 $d_4(-100)$ $([-1, -1], [-1, 1], [1, -1])$ to $d_3(-10 - 1)$ $([-1, -1], [-1, 1], [-1, -1])$

or

$d_3(010)$ $([1, -1], [1, 1], [-1, 1])$ to $d_0(000)$ $([1, -1], [1, -1], [-1, 1])$ to
 $d_4(-100)$ $([-1, -1], [1, -1], [-1, 1])$ to $d_3(-10 - 1)$ $([-1, -1], [1, -1], [-1, -1])$

or

$d_3(010)$ $([-1, 1], [1, 1], [-1, 1])$ to $d_0(000)$ $([-1, 1], [1, -1], [-1, 1])$ to
 $d_4(-100)$ $([-1, -1], [1, -1], [-1, 1])$ to $d_3(-10 - 1)$ $([-1, -1], [1, -1], [-1, -1])$

For $\theta \geq \frac{5\pi}{6}$

The switch combination sequence for the nearest three vector moving from sector *IIIA* to *IVA* for 2-cell is given by:

$d_4(011)$ $([1, -1], [1, 1], [1, 1])$ to $d_3(010)$ $([1, -1], [1, 1], [1, -1])$ to
 $d_0(000)$ $([1, -1], [1, -1], [1, -1])$ to $d_4(-100)$ $([-1, -1], [1, -1], [1, -1])$

or

$d_4(011)$ $([-1, 1], [1, 1], [1, 1])$ to $d_3(010)$ $([-1, 1], [1, 1], [1, -1])$ to
 $d_0(000)$ $([-1, 1], [1, -1], [1, -1])$ to $d_4(-100)$ $([-1, -1], [1, -1], [1, -1])$

or

$d_4(011)$ $([1, -1], [1, 1], [1, 1])$ to $d_3(010)$ $([1, -1], [1, 1], [-1, 1])$ to
 $d_0(000)$ $([1, -1], [-1, 1], [-1, 1])$ to $d_4(-100)$ $([-1, -1], [-1, 1], [-1, 1])$

or

$d_4(011)$ $([-1, 1], [1, 1], [1, 1])$ to $d_3(010)$ $([-1, 1], [1, 1], [-1, 1])$ to
 $d_0(000)$ $([-1, 1], [-1, 1], [-1, 1])$ to $d_4(-100)$ $([-1, -1], [-1, 1], [-1, 1])$

or

$d_4(011)$ ($[1, -1], [1, 1], [1, 1]$) to $d_3(010)$ ($[1, -1], [1, 1], [1, -1]$) to
 $d_0(000)$ ($[1, -1], [-1, 1], [1, -1]$) to $d_4(-100)$ ($[-1, -1], [-1, 1], [1, -1]$)
 or
 $d_4(011)$ ($[-1, 1], [1, 1], [1, 1]$) to $d_3(010)$ ($[-1, 1], [1, 1], [1, -1]$) to
 $d_0(000)$ ($[-1, 1], [-1, 1], [1, -1]$) to $d_4(-100)$ ($[-1, -1], [-1, 1], [1, -1]$)
 or
 $d_4(011)$ ($[1, -1], [1, 1], [1, 1]$) to $d_3(010)$ ($[1, -1], [1, 1], [-1, 1]$) to
 $d_0(000)$ ($[1, -1], [1, -1], [-1, 1]$) to $d_4(-100)$ ($[-1, -1], [1, -1], [-1, 1]$)
 or
 $d_4(011)$ ($[-1, 1], [1, 1], [1, 1]$) to $d_3(010)$ ($[-1, 1], [1, 1], [-1, 1]$) to
 $d_0(000)$ ($[-1, 1], [1, -1], [-1, 1]$) to $d_4(-100)$ ($[-1, -1], [1, -1], [-1, 1]$)

E.3.2 Region C

Duty Cycles

$$m_a \cos \omega t = -\frac{1}{\sqrt{6}}d_3 - \sqrt{\frac{2}{3}}d_{15} - \sqrt{\frac{3}{2}}d_9$$

$$m_a \sin \omega t = \frac{1}{\sqrt{2}}d_3 + \sqrt{2}d_{15} + \frac{1}{\sqrt{2}}d_9$$

$$d_3 + d_{15} + d_9 = 1$$

$$d_{15} = \sqrt{2}m_a \sin \omega t - 1$$

$$d_3 = -\frac{1}{\sqrt{2}}m_a \sin \omega t + \sqrt{\frac{3}{2}}m_a \cos \omega t + 2$$

$$d_9 = -\frac{1}{\sqrt{2}}m_a \sin \omega t - \sqrt{\frac{3}{2}}m_a \cos \omega t$$

Switch Combinations

The switch combination sequence for the nearest three vector for sector *IIIC* for 2-cell is given by:

$d_3(-10 - 1)$ ($[-1, -1], [1, -1], [-1, -1]$) to $d_{15}(-11 - 1)$ ($[-1, -1], [1, 1], [-1, -1]$) to
 $d_9(-110)$ ($[-1, -1], [1, 1], [1, -1]$) to $d_3(010)$ ($[1, -1], [1, 1], [1, -1]$)
 or
 $d_3(-10 - 1)$ ($[-1, -1], [1, -1], [-1, -1]$) to $d_{15}(-11 - 1)$ ($[-1, -1], [1, 1], [-1, -1]$) to
 $d_9(-110)$ ($[-1, -1], [1, 1], [1, -1]$) to $d_3(010)$ ($[-1, 1], [1, 1], [1, -1]$)
 or
 $d_3(-10 - 1)$ ($[-1, -1], [1, -1], [-1, -1]$) to $d_{15}(-11 - 1)$ ($[-1, -1], [1, 1], [-1, -1]$) to

$d_9(-110) ([-1, -1], [1, 1], [-1, 1])$ to $d_3(010) ([1, -1], [1, 1], [-1, 1])$

or

$d_3(-10 - 1) ([-1, -1], [1, -1], [-1, -1])$ to $d_{15}(-11 - 1) ([-1, -1], [1, 1], [-1, -1])$ to $d_9(-110) ([-1, -1], [1, 1], [-1, 1])$ to $d_3(010) ([-1, 1], [1, 1], [-1, 1])$

or

$d_3(-10 - 1) ([-1, -1], [-1, 1], [-1, -1])$ to $d_{15}(-11 - 1) ([-1, -1], [1, 1], [-1, -1])$ to $d_9(-110) ([-1, -1], [1, 1], [1, -1])$ to $d_3(010) ([1, -1], [1, 1], [1, -1])$

or

$d_3(-10 - 1) ([-1, -1], [-1, 1], [-1, -1])$ to $d_{15}(-11 - 1) ([-1, -1], [1, 1], [-1, -1])$ to $d_9(-110) ([-1, -1], [1, 1], [1, -1])$ to $d_3(010) ([-1, 1], [1, 1], [1, -1])$

or

$d_3(-10 - 1) ([-1, -1], [-1, 1], [-1, -1])$ to $d_{15}(-11 - 1) ([-1, -1], [1, 1], [-1, -1])$ to $d_9(-110) ([-1, -1], [1, 1], [-1, 1])$ to $d_3(010) ([1, -1], [1, 1], [-1, 1])$

or

$d_3(-10 - 1) ([-1, -1], [-1, 1], [-1, -1])$ to $d_{15}(-11 - 1) ([-1, -1], [1, 1], [-1, -1])$ to $d_9(-110) ([-1, -1], [1, 1], [-1, 1])$ to $d_3(010) ([-1, 1], [1, 1], [-1, 1])$

E.3.3 Region B

Duty Cycles

$$m_a \cos \omega t = -\frac{1}{\sqrt{6}}d_3 - \sqrt{\frac{3}{2}}d_9 - \sqrt{\frac{2}{3}}d_4$$

$$m_a \sin \omega t = \frac{1}{\sqrt{2}}d_3 + \frac{1}{\sqrt{2}}d_9$$

$$d_3 + d_9 + d_4 = 1$$

$$d_3 = \frac{1}{\sqrt{2}}m_a \sin \omega t + \sqrt{\frac{3}{2}}\cos \omega t + 1$$

$$d_4 = -\sqrt{2}m_a \sin \omega t + 1$$

$$d_9 = -\sqrt{\frac{3}{2}}\cos \omega t + \frac{1}{\sqrt{2}}\sin \omega t - 1$$

For $\theta \leq \frac{5\pi}{6}$

The switch combination sequence for the nearest three vector moving from sector *IIIC* to *IIIB* for 2-cell is given by:

$d_3(010) ([1, -1], [1, 1], [1, -1])$ to $d_9(-110) ([-1, -1], [1, 1], [1, -1])$ to

$d_4(-100) ([-1, -1], [1, -1], [1, -1])$ to $d_3(-10 - 1) ([-1, -1], [1, -1], [-1, -1])$

or

$d_3(010)$ $([1, -1], [1, 1], [1, -1])$ to $d_9(-110)$ $([-1, -1], [1, 1], [1, -1])$ to
 $d_4(-100)$ $([-1, -1], [-1, 1], [1, -1])$ to $d_3(-10 - 1)$ $([-1, -1], [-1, 1], [-1, -1])$

or

$d_3(010)$ $([-1, 1], [1, 1], [1, -1])$ to $d_9(-110)$ $([-1, -1], [1, 1], [1, -1])$ to
 $d_4(-100)$ $([-1, -1], [1, -1], [1, -1])$ to $d_3(-10 - 1)$ $([-1, -1], [1, -1], [-1, -1])$

or

$d_3(010)$ $([-1, 1], [1, 1], [1, -1])$ to $d_9(-110)$ $([-1, -1], [1, 1], [1, -1])$ to
 $d_4(-100)$ $([-1, -1], [-1, 1], [1, -1])$ to $d_3(-10 - 1)$ $([-1, -1], [-1, 1], [-1, -1])$

or

$d_3(010)$ $([1, -1], [1, 1], [-1, 1])$ to $d_9(-110)$ $([-1, -1], [1, 1], [-1, 1])$ to
 $d_4(-100)$ $([-1, -1], [1, -1], [-1, 1])$ to $d_3(-10 - 1)$ $([-1, -1], [1, -1], [-1, -1])$

or

$d_3(010)$ $([1, -1], [1, 1], [-1, 1])$ to $d_9(-110)$ $([-1, -1], [1, 1], [-1, 1])$ to
 $d_4(-100)$ $([-1, -1], [-1, 1], [-1, 1])$ to $d_3(-10 - 1)$ $([-1, -1], [-1, 1], [-1, -1])$

or

$d_3(010)$ $([-1, 1], [1, 1], [-1, 1])$ to $d_9(-110)$ $([-1, -1], [1, 1], [-1, 1])$ to
 $d_4(-100)$ $([-1, -1], [1, -1], [-1, 1])$ to $d_3(-10 - 1)$ $([-1, -1], [1, -1], [-1, -1])$

or

$d_3(010)$ $([-1, 1], [1, 1], [-1, 1])$ to $d_9(-110)$ $([-1, -1], [1, 1], [-1, 1])$ to
 $d_4(-100)$ $([-1, -1], [-1, 1], [-1, 1])$ to $d_3(-10 - 1)$ $([-1, -1], [-1, 1], [-1, -1])$

For $\theta \geq \frac{5\pi}{6}$

The switch combination sequence for the nearest three vector moving from sector *IIIB* to *IIID* for 2-cell is given by:

$d_4(011)$ $([1, -1], [1, 1], [1, 1])$ to $d_3(010)$ $([1, -1], [1, 1], [1, -1])$ to
 $d_9(-110)$ $([-1, -1], [1, 1], [1, -1])$ to $d_4(-100)$ $([-1, -1], [1, -1], [1, -1])$

or

$d_4(011)$ $([1, -1], [1, 1], [1, 1])$ to $d_3(010)$ $([1, -1], [1, 1], [1, -1])$ to
 $d_9(-110)$ $([-1, -1], [1, 1], [1, -1])$ to $d_4(-100)$ $([-1, -1], [-1, 1], [1, -1])$

or

$d_4(011)$ $([1, -1], [1, 1], [1, 1])$ to $d_3(010)$ $([1, -1], [1, 1], [-1, 1])$ to
 $d_9(-110)$ $([-1, -1], [1, 1], [-1, 1])$ to $d_4(-100)$ $([-1, -1], [1, -1], [-1, 1])$

or

$d_4(011)$ $([1, -1], [1, 1], [1, 1])$ to $d_3(010)$ $([1, -1], [1, 1], [-1, 1])$ to
 $d_9(-110)$ $([-1, -1], [1, 1], [-1, 1])$ to $d_4(-100)$ $([-1, -1], [-1, 1], [-1, 1])$

or

$d_4(011) ([-1, 1], [1, 1], [1, 1])$ to $d_3(010) ([-1, 1], [1, 1], [1, -1])$ to
 $d_9(-110) ([-1, -1], [1, 1], [1, -1])$ to $d_4(-100) ([-1, -1], [1, -1], [1, -1])$
 or
 $d_4(011) ([-1, 1], [1, 1], [1, 1])$ to $d_3(010) ([-1, 1], [1, 1], [1, -1])$ to
 $d_9(-110) ([-1, -1], [1, 1], [1, -1])$ to $d_4(-100) ([-1, -1], [-1, 1], [1, -1])$
 or
 $d_4(011) ([-1, 1], [1, 1], [1, 1])$ to $d_3(010) ([-1, 1], [1, 1], [-1, 1])$ to
 $d_9(-110) ([-1, -1], [1, 1], [-1, 1])$ to $d_4(-100) ([-1, -1], [1, -1], [-1, 1])$
 or
 $d_4(011) ([-1, 1], [1, 1], [1, 1])$ to $d_3(010) ([-1, 1], [1, 1], [-1, 1])$ to
 $d_9(-110) ([-1, -1], [1, 1], [-1, 1])$ to $d_4(-100) ([-1, -1], [-1, 1], [-1, 1])$

E.3.4 Region D

Duty Cycles

$$m_a \cos \omega t = -\sqrt{\frac{2}{3}}d_4 - \sqrt{\frac{3}{2}}d_9 - 2\sqrt{\frac{2}{3}}d_{16}$$

$$m_a \sin \omega t = \frac{1}{\sqrt{2}}d_9$$

$$d_4 + d_9 + d_{16} = 1$$

$$d_{16} = -\sqrt{\frac{3}{2}}m_a \cos \omega t - \frac{1}{\sqrt{2}}m_a \sin \omega t - 1$$

$$d_4 = \sqrt{\frac{3}{2}}m_a \cos \omega t - \frac{1}{\sqrt{2}}m_a \cos \omega t + 2$$

$$d_9 = \sqrt{2}m_a \sin \omega t$$

Switching Combinations

The switch combination sequence for the nearest three vector for sector *IIID* for 2-cell is given by:

$d_4(-100) ([-1, -1], [1, -1], [1, -1])$ to $d_9(-110) ([-1, -1], [1, 1], [1, -1])$ to
 $d_{16}(-111) ([-1, -1], [1, 1], [1, 1])$ to $d_4(011) ([1, -1], [1, 1], [1, 1])$

or

$d_4(-100) ([-1, -1], [1, -1], [1, -1])$ to $d_9(-110) ([-1, -1], [1, 1], [1, -1])$ to
 $d_{16}(-111) ([-1, -1], [1, 1], [1, 1])$ to $d_4(011) ([-1, 1], [1, 1], [1, 1])$

or

$d_4(-100) ([-1, -1], [-1, 1], [1, -1])$ to $d_9(-110) ([-1, -1], [1, 1], [1, -1])$ to $d_{16}(-111) ([-1, -1], [1, 1], [1, 1])$ to $d_4(011) ([1, -1], [1, 1], [1, 1])$
 or
 $d_4(-100) ([-1, -1], [-1, 1], [1, -1])$ to $d_9(-110) ([-1, -1], [1, 1], [1, -1])$ to $d_{16}(-111) ([-1, -1], [1, 1], [1, 1])$ to $d_4(011) ([-1, 1], [1, 1], [1, 1])$
 or
 $d_4(-100) ([-1, -1], [1, -1], [-1, 1])$ to $d_9(-110) ([-1, -1], [1, 1], [-1, 1])$ to $d_{16}(-111) ([-1, -1], [1, 1], [1, 1])$ to $d_4(011) ([1, -1], [1, 1], [1, 1])$
 or
 $d_4(-100) ([-1, -1], [1, -1], [-1, 1])$ to $d_9(-110) ([-1, -1], [1, 1], [-1, 1])$ to $d_{16}(-111) ([-1, -1], [1, 1], [1, 1])$ to $d_4(011) ([-1, 1], [1, 1], [1, 1])$
 or
 $d_4(-100) ([-1, -1], [-1, 1], [-1, 1])$ to $d_9(-110) ([-1, -1], [1, 1], [-1, 1])$ to $d_{16}(-111) ([-1, -1], [1, 1], [1, 1])$ to $d_4(011) ([1, -1], [1, 1], [1, 1])$
 or
 $d_4(-100) ([-1, -1], [-1, 1], [-1, 1])$ to $d_9(-110) ([-1, -1], [1, 1], [-1, 1])$ to $d_{16}(-111) ([-1, -1], [1, 1], [1, 1])$ to $d_4(011) ([1, -1], [1, 1], [1, 1])$

E.4 Sector IV

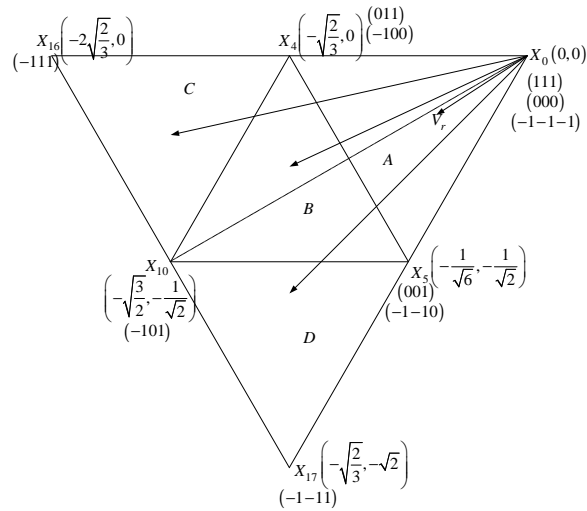


Figure E.4: *Regions of vector modulation of the 2-cell multicell converter in the fourth sector*

E.4.1 Region A

Duty Cycles

$$m_a \cos \omega t = -\sqrt{\frac{2}{3}}d_4 - \frac{1}{\sqrt{6}}d_5$$

$$m_a \sin \omega t = -\frac{1}{\sqrt{2}}d_5$$

$$d_0 + d_4 + d_5 = 1$$

$$d_0 = \frac{1}{\sqrt{2}}m_a \sin \omega t + \sqrt{\frac{3}{2}}m_a \cos \omega t + 1$$

$$d_4 = -\sqrt{\frac{3}{2}}m_a \cos \omega t + \frac{1}{\sqrt{2}}m_a \sin \omega t$$

$$d_5 = -\sqrt{2}m_a \sin \omega t$$

For $\theta \leq \frac{7\pi}{6}$

The switch combination sequence for the nearest three vector moving from sector *IIIA* to *IVA* for 2-cell is given by:

$d_4(-100)$ ($[-1, -1], [1, -1], [1, -1]$) to $d_0(000)$ ($[1, -1], [1, -1], [1, -1]$) to $d_5(001)$ ($[1, -1], [1, -1], [1, 1]$) to $d_4(011)$ ($[1, -1], [1, 1], [1, 1]$)

or

$d_4(-100)$ ($[-1, -1], [1, -1], [1, -1]$) to $d_0(000)$ ($[-1, 1], [1, -1], [1, -1]$) to $d_5(001)$ ($[-1, 1], [1, -1], [1, 1]$) to $d_4(011)$ ($[-1, 1], [1, 1], [1, 1]$)

or

$d_4(-100)$ ($[-1, -1], [-1, 1], [-1, 1]$) to $d_0(000)$ ($[1, -1], [-1, 1], [-1, 1]$) to $d_5(001)$ ($[1, -1], [-1, 1], [1, 1]$) to $d_4(011)$ ($[1, -1], [1, 1], [1, 1]$)

or

$d_4(-100)$ ($[-1, -1], [-1, 1], [-1, 1]$) to $d_0(000)$ ($[-1, 1], [-1, 1], [-1, 1]$) to $d_5(001)$ ($[-1, 1], [-1, 1], [1, 1]$) to $d_4(011)$ ($[-1, 1], [1, 1], [1, 1]$)

or

$d_4(-100)$ ($[-1, -1], [-1, 1], [1, -1]$) to $d_0(000)$ ($[1, -1], [-1, 1], [1, -1]$) to $d_5(001)$ ($[1, -1], [-1, 1], [1, 1]$) to $d_4(011)$ ($[1, -1], [1, 1], [1, 1]$)

or

$d_4(-100)$ ($[-1, -1], [-1, 1], [1, -1]$) to $d_0(000)$ ($[-1, 1], [-1, 1], [1, -1]$) to $d_5(001)$ ($[-1, 1], [-1, 1], [1, 1]$) to $d_4(011)$ ($[-1, 1], [1, 1], [1, 1]$)

or

$d_4(-100)$ ($[-1, -1], [1, -1], [-1, 1]$) to $d_0(000)$ ($[1, -1], [1, -1], [-1, 1]$) to $d_5(001)$ ($[1, -1], [1, -1], [1, 1]$) to $d_4(011)$ ($[1, -1], [1, 1], [1, 1]$)

or

$d_4(-100)$ ($[-1, -1], [1, -1], [-1, 1]$) to $d_0(000)$ ($[-1, 1], [1, -1], [-1, 1]$) to $d_5(001)$ ($[-1, 1], [1, -1], [1, 1]$) to $d_4(011)$ ($[-1, 1], [1, 1], [1, 1]$)

For $\theta \geq \frac{7\pi}{6}$

The switch combination sequence for the nearest three vector moving from sector IVA to $IV A$ for 2-cell is given by:

$d_5(-1 - 10)$ ($[-1, -1], [-1, -1], [1, -1]$) to $d_4(-100)$ ($[-1, -1], [1, -1], [1, -1]$) to $d_0(000)$ ($[1, -1], [1, -1], [1, -1]$) to $d_5(001)$ ($[1, -1], [1, -1], [1, 1]$)

or

$d_5(-1 - 10)$ ($[-1, -1], [-1, -1], [1, -1]$) to $d_4(-100)$ ($[-1, -1], [1, -1], [1, -1]$) to $d_0(000)$ ($[-1, 1], [1, -1], [1, -1]$) to $d_5(001)$ ($[-1, 1], [1, -1], [1, 1]$)

or

$d_5(-1 - 10)$ ($[-1, -1], [-1, -1], [-1, 1]$) to $d_4(-100)$ ($[-1, -1], [-1, 1], [-1, 1]$) to $d_0(000)$ ($[1, -1], [-1, 1], [-1, 1]$) to $d_5(001)$ ($[1, -1], [-1, 1], [1, 1]$)

or

$d_5(-1 - 10)$ ($[-1, -1], [-1, -1], [-1, 1]$) to $d_4(-100)$ ($[-1, -1], [-1, 1], [-1, 1]$) to $d_0(000)$ ($[-1, 1], [-1, 1], [-1, 1]$) to $d_5(001)$ ($[-1, 1], [-1, 1], [1, 1]$)

or

$d_5(-1 - 10)$ ($[-1, -1], [-1, -1], [1, -1]$) to $d_4(-100)$ ($[-1, -1], [-1, 1], [1, -1]$) to $d_0(000)$ ($[1, -1], [-1, 1], [1, -1]$) to $d_5(001)$ ($[1, -1], [-1, 1], [1, 1]$)

or

$d_5(-1 - 10)$ ($[-1, -1], [-1, -1], [1, -1]$) to $d_4(-100)$ ($[-1, -1], [-1, 1], [1, -1]$) to $d_0(000)$ ($[-1, 1], [-1, 1], [1, -1]$) to $d_5(001)$ ($[-1, 1], [-1, 1], [1, 1]$)

or

$d_5(-1 - 10)$ ($[-1, -1], [-1, -1], [-1, 1]$) to $d_4(-100)$ ($[-1, -1], [1, -1], [-1, 1]$) to $d_0(000)$ ($[1, -1], [1, -1], [-1, 1]$) to $d_5(001)$ ($[1, -1], [1, -1], [1, 1]$)

or

$d_5(-1 - 10)$ ($[-1, -1], [-1, -1], [-1, 1]$) to $d_4(-100)$ ($[-1, -1], [1, -1], [-1, 1]$) to $d_0(000)$ ($[-1, 1], [1, -1], [-1, 1]$) to $d_5(001)$ ($[-1, 1], [1, -1], [1, 1]$)

E.4.2 Region C

Duty Cycles

$$m_a \cos \omega t = -\sqrt{\frac{2}{3}}d_4 - 2\sqrt{\frac{2}{3}}d_{16} - \sqrt{\frac{3}{2}}d_{10}$$

$$m_a \sin \omega t = -\frac{1}{\sqrt{2}}d_{10}$$

$$d_4 + d_{16} + d_{10} = 1$$

$$d_{16} = -\sqrt{\frac{3}{2}}m_a \cos \omega t + \frac{1}{\sqrt{2}}m_a \sin \omega t - 1$$

$$d_4 = \sqrt{\frac{3}{2}}m_a \cos \omega t + \frac{1}{\sqrt{2}}m_a \cos \omega t + 2$$

$$d_{10} = -\sqrt{2}m_a \sin \omega t$$

Switching Combinations

The switch combination sequence for the nearest three vector for sector *IVC* for 2-cell is given by:

$d_4(011)$ ($[1, -1], [1, 1], [1, 1]$) to $d_{16}(-111)$ ($[-1, -1], [1, 1], [1, 1]$) to $d_{10}(-101)$ ($[-1, -1], [1, -1], [1, 1]$) to $d_4(-100)$ ($[-1, -1], [1, -1], [1, -1]$)

or

$d_4(011)$ ($[1, -1], [1, 1], [1, 1]$) to $d_{16}(-111)$ ($[-1, -1], [1, 1], [1, 1]$) to $d_{10}(-101)$ ($[-1, -1], [1, -1], [1, 1]$) to $d_4(-100)$ ($[-1, -1], [1, -1], [-1, 1]$)

or

$d_4(011)$ ($[1, -1], [1, 1], [1, 1]$) to $d_{16}(-111)$ ($[-1, -1], [1, 1], [1, 1]$) to $d_{10}(-101)$ ($[-1, -1], [-1, 1], [1, 1]$) to $d_4(-100)$ ($[-1, -1], [-1, 1], [1, -1]$)

or

$d_4(011)$ ($[1, -1], [1, 1], [1, 1]$) to $d_{16}(-111)$ ($[-1, -1], [1, 1], [1, 1]$) to $d_{10}(-101)$ ($[-1, -1], [-1, 1], [1, 1]$) to $d_4(-100)$ ($[-1, -1], [-1, 1], [-1, 1]$)

or

$d_4(011)$ ($[-1, 1], [1, 1], [1, 1]$) to $d_{16}(-111)$ ($[-1, -1], [1, 1], [1, 1]$) to $d_{10}(-101)$ ($[-1, -1], [1, -1], [1, 1]$) to $d_4(-100)$ ($[-1, -1], [1, -1], [1, -1]$)

or

$d_4(011)$ ($[-1, 1], [1, 1], [1, 1]$) to $d_{16}(-111)$ ($[-1, -1], [1, 1], [1, 1]$) to $d_{10}(-101)$ ($[-1, -1], [1, -1], [1, 1]$) to $d_4(-100)$ ($[-1, -1], [1, -1], [-1, 1]$)

or

$d_4(011)$ ($[-1, 1], [1, 1], [1, 1]$) to $d_{16}(-111)$ ($[-1, -1], [1, 1], [1, 1]$) to $d_{10}(-101)$ ($[-1, -1], [-1, 1], [1, 1]$) to $d_4(-100)$ ($[-1, -1], [-1, 1], [1, -1]$)

or

$d_4(011)$ ($[-1, 1], [1, 1], [1, 1]$) to $d_{16}(-111)$ ($[-1, -1], [1, 1], [1, 1]$) to $d_{10}(-101)$ ($[-1, -1], [-1, 1], [1, 1]$) to $d_4(-100)$ ($[-1, -1], [-1, 1], [-1, 1]$)

or

E.4.3 Region B

Duty Cycles

$$m_a \cos \omega t = -\sqrt{\frac{2}{3}}d_4 - \sqrt{\frac{3}{2}}d_{10} - \frac{1}{\sqrt{6}}d_5$$

$$m_a \sin \omega t = -\frac{1}{\sqrt{2}}d_{10} - \frac{1}{\sqrt{2}}d_5$$

$$d_4 + d_{10} + d_5 = 1$$

$$d_4 = \sqrt{2}m_a \sin \omega t + 1$$

$$d_{10} = -\frac{1}{\sqrt{2}}m_a \sin \omega t - \sqrt{\frac{3}{2}}m_a \cos \omega t - 1$$

$$d_5 = \sqrt{\frac{3}{2}}m_a \cos \omega t - \frac{1}{\sqrt{2}}m_a \sin \omega t + 1$$

For $\theta \leq \frac{7\pi}{6}$

The switch combination sequence for the nearest three vector moving from sector *IVC* to *IVB* for 2-cell is given by:

$d_4(-100)$ ($[-1, -1], [1, -1], [1, -1]$) to $d_{10}(-101)$ ($[-1, -1], [1, -1], [1, 1]$) to $d_5(001)$ ($[1, -1], [1, -1], [1, 1]$) to $d_4(011)$ ($[1, -1], [1, 1], [1, 1]$)

or

$d_4(-100)$ ($[-1, -1], [1, -1], [1, -1]$) to $d_{10}(-101)$ ($[-1, -1], [1, -1], [1, 1]$) to $d_5(001)$ ($[-1, 1], [1, -1], [1, 1]$) to $d_4(011)$ ($[-1, 1], [1, 1], [1, 1]$)

or

$d_4(-100)$ ($[-1, -1], [1, -1], [-1, 1]$) to $d_{10}(-101)$ ($[-1, -1], [1, -1], [1, 1]$) to $d_5(001)$ ($[1, -1], [1, -1], [1, 1]$) to $d_4(011)$ ($[1, -1], [1, 1], [1, 1]$)

or

$d_4(-100)$ ($[-1, -1], [1, -1], [-1, 1]$) to $d_{10}(-101)$ ($[-1, -1], [1, -1], [1, 1]$) to $d_5(001)$ ($[-1, 1], [1, -1], [1, 1]$) to $d_4(011)$ ($[-1, 1], [1, 1], [1, 1]$)

or

$d_4(-100)$ ($[-1, -1], [-1, 1], [1, -1]$) to $d_{10}(-101)$ ($[-1, -1], [-1, 1], [1, 1]$) to $d_5(001)$ ($[1, -1], [-1, 1], [1, 1]$) to $d_4(011)$ ($[1, -1], [1, 1], [1, 1]$)

or

$d_4(-100)$ ($[-1, -1], [-1, 1], [1, -1]$) to $d_{10}(-101)$ ($[-1, -1], [-1, 1], [1, 1]$) to $d_5(001)$ ($[-1, 1], [-1, 1], [1, 1]$) to $d_4(011)$ ($[-1, 1], [1, 1], [1, 1]$)

or

$d_4(-100)$ ($[-1, -1], [-1, 1], [-1, 1]$) to $d_{10}(-101)$ ($[-1, -1], [-1, 1], [1, 1]$) to $d_5(001)$ ($[1, -1], [-1, 1], [1, 1]$) to $d_4(011)$ ($[1, -1], [1, 1], [1, 1]$)

or

$d_4(-100)$ $([-1, -1], [-1, 1], [-1, 1])$ to $d_{10}(-101)$ $([-1, -1], [-1, 1], [1, 1])$ to $d_5(001)$ $([-1, 1], [-1, 1], [1, 1])$ to $d_4(011)$ $([-1, 1], [1, 1], [1, 1])$

For $\theta \geq \frac{7\pi}{6}$

The switch combination sequence for the nearest three vector moving from sector IVB to IVD for 2-cell is given by:

$d_5(-1-10)$ $([-1, -1], [-1, -1], [1, -1])$ to $d_4(-100)$ $([-1, -1], [1, -1], [1, -1])$ to $d_{10}(-101)$ $([-1, -1], [1, -1], [1, 1])$ to $d_5(001)$ $([1, -1], [1, -1], [1, 1])$

or

$d_5(-1-10)$ $([-1, -1], [-1, -1], [1, -1])$ to $d_4(-100)$ $([-1, -1], [1, -1], [1, -1])$ to $d_{10}(-101)$ $([-1, -1], [1, -1], [1, 1])$ to $d_5(001)$ $([-1, 1], [1, -1], [1, 1])$

or

$d_5(-1-10)$ $([-1, -1], [-1, -1], [1, -1])$ to $d_4(-100)$ $([-1, -1], [-1, 1], [1, -1])$ to $d_{10}(-101)$ $([-1, -1], [-1, 1], [1, 1])$ to $d_5(001)$ $([1, -1], [-1, 1], [1, 1])$

or

$d_5(-1-10)$ $([-1, -1], [-1, -1], [1, -1])$ to $d_4(-100)$ $([-1, -1], [-1, 1], [1, -1])$ to $d_{10}(-101)$ $([-1, -1], [-1, 1], [1, 1])$ to $d_5(001)$ $([-1, 1], [-1, 1], [1, 1])$

or

$d_5(-1-10)$ $([-1, -1], [-1, -1], [-1, 1])$ to $d_4(-100)$ $([-1, -1], [1, -1], [-1, 1])$ to $d_{10}(-101)$ $([-1, -1], [1, -1], [1, 1])$ to $d_5(001)$ $([1, -1], [1, -1], [1, 1])$

or

$d_5(-1-10)$ $([-1, -1], [-1, -1], [-1, 1])$ to $d_4(-100)$ $([-1, -1], [1, -1], [-1, 1])$ to $d_{10}(-101)$ $([-1, -1], [1, -1], [1, 1])$ to $d_5(001)$ $([-1, 1], [1, -1], [1, 1])$

or

$d_5(-1-10)$ $([-1, -1], [-1, -1], [-1, 1])$ to $d_4(-100)$ $([-1, -1], [-1, 1], [-1, 1])$ to $d_{10}(-101)$ $([-1, -1], [-1, 1], [1, 1])$ to $d_5(001)$ $([1, -1], [-1, 1], [1, 1])$

or

$d_5(-1-10)$ $([-1, -1], [-1, -1], [-1, 1])$ to $d_4(-100)$ $([-1, -1], [-1, 1], [-1, 1])$ to $d_{10}(-101)$ $([-1, -1], [-1, 1], [1, 1])$ to $d_5(001)$ $([-1, 1], [-1, 1], [1, 1])$

E.4.4 Region D

Duty Cycles

$$m_a \cos \omega t = -\frac{1}{\sqrt{6}}d_5 - \frac{1}{\sqrt{2}}d_{10} - \sqrt{\frac{2}{3}}d_{17}$$

$$m_a \sin \omega t = -\frac{1}{\sqrt{2}}d_5 - \frac{1}{\sqrt{2}}d_{10} - \sqrt{2}d_{17}$$

$$d_5 + d_{10} + d_{17} = 1$$

$$d_{17} = -\sqrt{2}m_a \sin \omega t - 1$$

$$d_5 = \sqrt{\frac{3}{2}}m_a \cos \omega t + \frac{1}{\sqrt{2}}m_a \cos \omega t + 2$$

$$d_{10} = -\sqrt{\frac{3}{2}}m_a \cos \omega t + \frac{1}{\sqrt{2}}m_a \sin \omega t$$

Switch Combinations

The switch combination sequence for the nearest three vector for sector *IVC* for 2-cell is given by:

$d_5(001)$ ($[1, -1], [1, -1], [1, 1]$) to $d_{10}(-101)$ ($[-1, -1], [1, -1], [1, 1]$) to $d_{17}(-1 - 11)$ ($[-1, -1], [-1, -1], [1, 1]$) to $d_5(-1 - 10)$ ($[-1, -1], [-1, -1], [1, -1]$)

or

$d_5(001)$ ($[1, -1], [1, -1], [1, 1]$) to $d_{10}(-101)$ ($[-1, -1], [1, -1], [1, 1]$) to $d_{17}(-1 - 11)$ ($[-1, -1], [-1, -1], [1, 1]$) to $d_5(-1 - 10)$ ($[-1, -1], [-1, -1], [-1, 1]$)

or

$d_5(001)$ ($[-1, 1], [1, -1], [1, 1]$) to $d_{10}(-101)$ ($[-1, -1], [1, -1], [1, 1]$) to $d_{17}(-1 - 11)$ ($[-1, -1], [-1, -1], [1, 1]$) to $d_5(-1 - 10)$ ($[-1, -1], [-1, -1], [1, -1]$)

or

$d_5(001)$ ($[-1, 1], [1, -1], [1, 1]$) to $d_{10}(-101)$ ($[-1, -1], [1, -1], [1, 1]$) to $d_{17}(-1 - 11)$ ($[-1, -1], [-1, -1], [1, 1]$) to $d_5(-1 - 10)$ ($[-1, -1], [-1, -1], [-1, 1]$)

or

$d_5(001)$ ($[1, -1], [-1, 1], [1, 1]$) to $d_{10}(-101)$ ($[-1, -1], [-1, 1], [1, 1]$) to $d_{17}(-1 - 11)$ ($[-1, -1], [-1, -1], [1, 1]$) to $d_5(-1 - 10)$ ($[-1, -1], [-1, -1], [1, -1]$)

or

$d_5(001)$ ($[1, -1], [-1, 1], [1, 1]$) to $d_{10}(-101)$ ($[-1, -1], [-1, 1], [1, 1]$) to $d_{17}(-1 - 11)$ ($[-1, -1], [-1, -1], [1, 1]$) to $d_5(-1 - 10)$ ($[-1, -1], [-1, -1], [-1, 1]$)

or

$d_5(001)$ ($[-1, 1], [-1, 1], [1, 1]$) to $d_{10}(-101)$ ($[-1, -1], [-1, 1], [1, 1]$) to $d_{17}(-1 - 11)$ ($[-1, -1], [-1, -1], [1, 1]$) to $d_5(-1 - 10)$ ($[-1, -1], [-1, -1], [1, -1]$)

or

$d_5(001)$ ($[-1, 1], [-1, 1], [1, 1]$) to $d_{10}(-101)$ ($[-1, -1], [-1, 1], [1, 1]$) to $d_{17}(-1 - 11)$ ($[-1, -1], [-1, -1], [1, 1]$) to $d_5(-1 - 10)$ ($[-1, -1], [-1, -1], [-1, 1]$)

E.5 Sector V

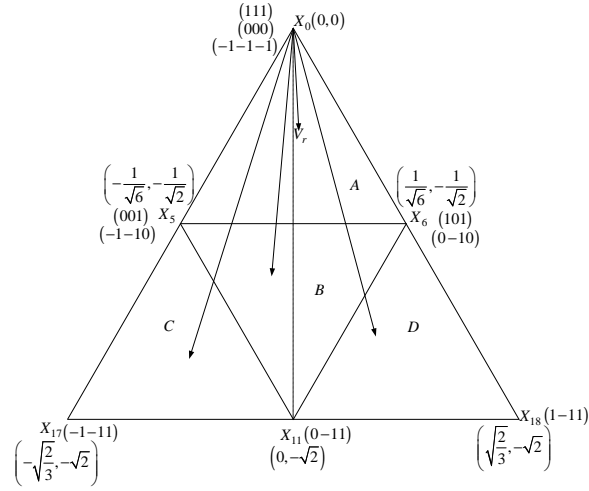


Figure E.5: Regions of vector modulation of the 2-cell multicell converter in the fifth sector

E.5.1 Region A

Duty Cycles

$$m_a \cos \omega t = -\frac{1}{\sqrt{6}}d_5 + \frac{1}{\sqrt{6}}d_6$$

$$m_a \sin \omega t = -\frac{1}{\sqrt{2}}d_5 - \frac{1}{\sqrt{2}}d_6$$

$$d_0 + d_5 + d_6 = 1$$

$$d_0 = \sqrt{2}m_a \sin \omega t + 1$$

$$d_5 = -\frac{1}{\sqrt{2}}m_a \sin \omega t - \sqrt{\frac{3}{2}}m_a \cos \omega t$$

$$d_6 = \sqrt{\frac{3}{2}}m_a \cos \omega t - \frac{1}{\sqrt{2}}m_a \sin \omega t$$

For $\theta \leq \frac{3\pi}{2}$

The switch combination sequence for the nearest three vector moving from sector *IVA* to *VA* for 2-cell is given by:

$d_5(001)$ $([1, -1], [1, -1], [1, 1])$ to $d_0(000)$ $([1, -1], [1, -1], [1, -1])$ to

$d_6(0-10)$ $([1, -1], [-1, -1], [1, -1])$ to $d_5(-1-10)$ $([-1, -1], [-1, -1], [1, -1])$

or

$d_5(001) ([-1, 1], [1, -1], [1, 1])$ to $d_0(000) ([-1, 1], [1, -1], [1, -1])$ to
 $d_6(0 - 10) ([-1, 1], [-1, -1], [1, -1])$ to $d_5(-1 - 10) ([-1, -1], [-1, -1], [1, -1])$

or

$d_5(001) ([1, -1], [-1, 1], [1, 1])$ to $d_0(000) ([1, -1], [-1, 1], [-1, 1])$ to
 $d_6(0 - 10) ([1, -1], [-1, -1], [-1, 1])$ to $d_5(-1 - 10) ([-1, -1], [-1, -1], [-1, 1])$

or

$d_5(001) ([-1, 1], [-1, 1], [1, 1])$ to $d_0(000) ([-1, 1], [-1, 1], [-1, 1])$ to
 $d_6(0 - 10) ([-1, 1], [-1, -1], [-1, 1])$ to $d_5(-1 - 10) ([-1, -1], [-1, -1], [-1, 1])$

or

$d_5(001) ([1, -1], [-1, 1], [1, 1])$ to $d_0(000) ([1, -1], [-1, 1], [1, -1])$ to
 $d_6(0 - 10) ([1, -1], [-1, -1], [1, -1])$ to $d_5(-1 - 10) ([-1, -1], [-1, -1], [1, -1])$

or

$d_5(001) ([-1, 1], [-1, 1], [1, 1])$ to $d_0(000) ([-1, 1], [-1, 1], [1, -1])$ to
 $d_6(0 - 10) ([-1, 1], [-1, -1], [1, -1])$ to $d_5(-1 - 10) ([-1, -1], [-1, -1], [1, -1])$

or

$d_5(001) ([1, -1], [1, -1], [1, 1])$ to $d_0(000) ([1, -1], [1, -1], [-1, 1])$ to
 $d_6(0 - 10) ([1, -1], [-1, -1], [-1, 1])$ to $d_5(-1 - 10) ([-1, -1], [-1, -1], [-1, 1])$

or

$d_5(001) ([-1, 1], [1, -1], [1, 1])$ to $d_0(000) ([-1, 1], [1, -1], [-1, 1])$ to
 $d_6(0 - 10) ([-1, 1], [-1, -1], [-1, 1])$ to $d_5(-1 - 10) ([-1, -1], [-1, -1], [-1, 1])$

For $\theta \geq \frac{3\pi}{2}$

The switch combination sequence for the nearest three vector moving from sector VA to VIA for 2-cell is given by:

$d_6(101) ([1, 1], [1, -1], [1, 1])$ to $d_5(001) ([1, -1], [1, -1], [1, 1])$ to
 $d_0(000) ([1, -1], [1, -1], [1, -1])$ to $d_6(0 - 10) ([1, -1], [-1, -1], [1, -1])$

or

$d_6(101) ([1, 1], [1, -1], [1, 1])$ to $d_5(001) ([-1, 1], [1, -1], [1, 1])$ to
 $d_0(000) ([-1, 1], [1, -1], [1, -1])$ to $d_6(0 - 10) ([-1, 1], [-1, -1], [1, -1])$

or

$d_6(101) ([1, 1], [-1, 1], [1, 1])$ to $d_5(001) ([1, -1], [-1, 1], [1, 1])$ to
 $d_0(000) ([1, -1], [-1, 1], [-1, 1])$ to $d_6(0 - 10) ([1, -1], [-1, -1], [-1, 1])$

or

$d_6(101) ([1, 1], [-1, 1], [1, 1])$ to $d_5(001) ([-1, 1], [-1, 1], [1, 1])$ to
 $d_0(000) ([-1, 1], [-1, 1], [-1, 1])$ to $d_6(0 - 10) ([-1, 1], [-1, -1], [-1, 1])$

or

$d_6(101) ([1, 1], [-1, 1], [1, 1])$ to $d_5(001) ([1, -1], [-1, 1], [1, 1])$ to
 $d_0(000) ([1, -1], [-1, 1], [1, -1])$ to $d_6(0-10) ([1, -1], [-1, -1], [1, -1])$
 or
 $d_6(101) ([1, 1], [-1, 1], [1, 1])$ to $d_5(001) ([-1, 1], [-1, 1], [1, 1])$ to
 $d_0(000) ([-1, 1], [-1, 1], [1, -1])$ to $d_6(0-10) ([-1, 1], [-1, -1], [1, -1])$
 or
 $d_6(101) ([1, 1], [1, -1], [1, 1])$ to $d_5(001) ([1, -1], [1, -1], [1, 1])$ to
 $d_0(000) ([1, -1], [1, -1], [-1, 1])$ to $d_6(0-10) ([1, -1], [-1, -1], [-1, 1])$
 or
 $d_6(101) ([1, 1], [1, -1], [1, 1])$ to $d_5(001) ([-1, 1], [1, -1], [1, 1])$ to
 $d_0(000) ([-1, 1], [1, -1], [-1, 1])$ to $d_6(0-10) ([-1, 1], [-1, -1], [-1, 1])$

E.5.2 Region C

Duty Cycles

$$m_a \cos \omega t = -\frac{1}{\sqrt{6}}d_5 - \sqrt{\frac{2}{3}}d_{17}$$

$$m_a \sin \omega t = -\frac{1}{\sqrt{2}}d_5 - \sqrt{2}d_{17} - \sqrt{2}d_{11}$$

$$d_5 + d_{17} + d_{11} = 1$$

$$d_{17} = -\sqrt{\frac{3}{2}}m_a \cos \omega t - \frac{1}{\sqrt{2}}m_a \sin \omega t - 1$$

$$d_5 = \sqrt{2}m_a \sin \omega t + 2$$

$$d_{11} = \sqrt{\frac{3}{2}}m_a \cos \omega t - \frac{1}{\sqrt{2}}m_a \sin \omega t$$

Switch Combinations

The switch combination sequence for the nearest three vector for sector VC for 2-cell is given by:

$d_5(-1-10) ([1, 1], [-1, -1], [1, -1])$ to $d_{17}(-1-11) ([-1, -1], [-1, -1], [1, 1])$ to
 $d_{11}(0-11) ([1, -1], [-1, -1], [1, 1])$ to $d_5(001) ([1, -1], [1, -1], [1, 1])$

or

$d_5(-1-10) ([1, 1], [-1, -1], [1, -1])$ to $d_{17}(-1-11) ([-1, -1], [-1, -1], [1, 1])$ to
 $d_{11}(0-11) ([1, -1], [-1, -1], [1, 1])$ to $d_5(001) ([1, -1], [-1, 1], [1, 1])$

or

$d_5(-1-10) ([-1, -1], [-1, -1], [1, -1])$ to $d_{17}(-1-11) ([-1, -1], [-1, -1], [1, 1])$ to

$d_{11}(0 - 11) ([-1, 1], [-1, -1], [1, 1])$ to $d_5(001) ([-1, 1], [1, -1], [1, 1])$

or

$d_5(-1 - 10) ([1, 1], [-1, -1], [1, -1])$ to $d_{17}(-1 - 11) ([-1, -1], [-1, -1], [1, 1])$ to $d_{11}(0 - 11) ([-1, 1], [-1, -1], [1, 1])$ to $d_5(001) ([-1, 1], [-1, 1], [1, 1])$

or

$d_5(-1 - 10) ([1, 1], [-1, -1], [-1, 1])$ to $d_{17}(-1 - 11) ([-1, -1], [-1, -1], [1, 1])$ to $d_{11}(0 - 11) ([1, -1], [-1, -1], [1, 1])$ to $d_5(001) ([1, -1], [1, -1], [1, 1])$

or

$d_5(-1 - 10) ([1, 1], [-1, -1], [-1, 1])$ to $d_{17}(-1 - 11) ([-1, -1], [-1, -1], [1, 1])$ to $d_{11}(0 - 11) ([1, -1], [-1, -1], [1, 1])$ to $d_5(001) ([1, -1], [-1, 1], [1, 1])$

or

$d_5(-1 - 10) ([1, 1], [-1, -1], [-1, 1])$ to $d_{17}(-1 - 11) ([-1, -1], [-1, -1], [1, 1])$ to $d_{11}(0 - 11) ([-1, 1], [-1, -1], [1, 1])$ to $d_5(001) ([-1, 1], [1, -1], [1, 1])$

or

$d_5(-1 - 10) ([1, 1], [-1, -1], [-1, 1])$ to $d_{17}(-1 - 11) ([-1, -1], [-1, -1], [1, 1])$ to $d_{11}(0 - 11) ([-1, 1], [-1, -1], [1, 1])$ to $d_5(001) ([-1, 1], [-1, 1], [1, 1])$

E.5.3 Region B

Duty Cycles

$$m_a \cos \omega t = -\frac{1}{\sqrt{6}}d_5 + \frac{1}{\sqrt{6}}d_6$$

$$m_a \sin \omega t = -\frac{1}{\sqrt{2}}d_5 - \sqrt{2}d_{11} - \frac{1}{\sqrt{2}}d_6$$

$$d_5 + d_{11} + d_6 = 1$$

$$d_5 = \frac{1}{\sqrt{2}}m_a \sin \omega t - \sqrt{\frac{3}{2}}m_a \cos \omega t + 1$$

$$d_{11} = -\sqrt{2}m_a \sin \omega t$$

$$d_6 = \sqrt{\frac{3}{2}}m_a \cos \omega t + \frac{1}{\sqrt{2}}m_a \sin \omega t + 1$$

For $\theta \leq \frac{3\pi}{2}$

The switch combination sequence for the nearest three vector moving from sector VC to VB for 2-cell is given by:

$d_5(001) ([1, -1], [1, -1], [1, 1])$ to $d_{11}(0 - 11) ([1, -1], [-1, -1], [1, 1])$ to $d_6(0 - 10) ([1, -1], [-1, -1], [1, -1])$ to $d_5(-1 - 10) ([-1, -1], [-1, -1], [1, -1])$

or

$d_5(001) ([1, -1], [1, -1], [1, 1])$ to $d_{11}(0 - 11) ([1, -1], [-1, -1], [1, 1])$ to
 $d_6(0 - 10) ([1, -1], [-1, -1], [-1, 1])$ to $d_5(-1 - 10) ([-1, -1], [-1, -1], [-1, 1])$

or

$d_5(001) ([1, -1], [-1, 1], [1, 1])$ to $d_{11}(0 - 11) ([1, -1], [-1, -1], [1, 1])$ to
 $d_6(0 - 10) ([1, -1], [-1, -1], [1, -1])$ to $d_5(-1 - 10) ([-1, -1], [-1, -1], [1, -1])$

or

$d_5(001) ([1, -1], [-1, 1], [1, 1])$ to $d_{11}(0 - 11) ([1, -1], [-1, -1], [1, 1])$ to
 $d_6(0 - 10) ([1, -1], [-1, -1], [-1, 1])$ to $d_5(-1 - 10) ([-1, -1], [-1, -1], [-1, 1])$

or

$d_5(001) ([-1, 1], [1, -1], [1, 1])$ to $d_{11}(0 - 11) ([-1, 1], [-1, -1], [1, 1])$ to
 $d_6(0 - 10) ([-1, 1], [-1, -1], [1, -1])$ to $d_5(-1 - 10) ([-1, -1], [-1, -1], [1, -1])$

or

$d_5(001) ([-1, 1], [1, -1], [1, 1])$ to $d_{11}(0 - 11) ([-1, 1], [-1, -1], [1, 1])$ to
 $d_6(0 - 10) ([-1, 1], [-1, -1], [-1, 1])$ to $d_5(-1 - 10) ([-1, -1], [-1, -1], [-1, 1])$

or

$d_5(001) ([-1, 1], [-1, 1], [1, 1])$ to $d_{11}(0 - 11) ([-1, 1], [-1, -1], [1, 1])$ to
 $d_6(0 - 10) ([-1, 1], [-1, -1], [1, -1])$ to $d_5(-1 - 10) ([-1, -1], [-1, -1], [1, -1])$

or

$d_5(001) ([-1, 1], [-1, 1], [1, 1])$ to $d_{11}(0 - 11) ([-1, 1], [-1, -1], [1, 1])$ to
 $d_6(0 - 10) ([-1, 1], [-1, -1], [-1, 1])$ to $d_5(-1 - 10) ([-1, -1], [-1, -1], [-1, 1])$

For $\theta \geq \frac{3\pi}{2}$

The switch combination sequence for the nearest three vector moving from sector VB to VD for 2-cell is given by:

$d_6(101) ([1, 1], [1, -1], [1, 1])$ to $d_5(001) ([1, -1], [1, -1], [1, 1])$ to
 $d_{11}(0 - 11) ([1, -1], [-1, -1], [1, 1])$ to $d_6(0 - 10) ([1, -1], [-1, -1], [1, -1])$

or

$d_6(101) ([1, 1], [1, -1], [1, 1])$ to $d_5(001) ([1, -1], [1, -1], [1, 1])$ to
 $d_{11}(0 - 11) ([1, -1], [-1, -1], [1, 1])$ to $d_6(0 - 10) ([1, -1], [-1, -1], [-1, 1])$

or

$d_6(101) ([1, 1], [1, -1], [1, 1])$ to $d_5(001) ([-1, 1], [1, -1], [1, 1])$ to
 $d_{11}(0 - 11) ([-1, 1], [-1, -1], [1, 1])$ to $d_6(0 - 10) ([-1, 1], [-1, -1], [1, -1])$

or

$d_6(101) ([1, 1], [1, -1], [1, 1])$ to $d_5(001) ([-1, 1], [1, -1], [1, 1])$ to
 $d_{11}(0 - 11) ([-1, 1], [-1, -1], [1, 1])$ to $d_6(0 - 10) ([-1, 1], [-1, -1], [-1, 1])$

or

$d_6(101) ([1, 1], [-1, 1], [1, 1])$ to $d_5(001) ([1, -1], [-1, 1], [1, 1])$ to
 $d_{11}(0 - 11) ([1, -1], [-1, -1], [1, 1])$ to $d_6(0 - 10) ([1, -1], [-1, -1], [1, -1])$
 or
 $d_6(101) ([1, 1], [-1, 1], [1, 1])$ to $d_5(001) ([1, -1], [-1, 1], [1, 1])$ to
 $d_{11}(0 - 11) ([1, -1], [-1, -1], [1, 1])$ to $d_6(0 - 10) ([1, -1], [-1, -1], [-1, 1])$
 or
 $d_6(101) ([1, 1], [-1, 1], [1, 1])$ to $d_5(001) ([-1, 1], [-1, 1], [1, 1])$ to
 $d_{11}(0 - 11) ([-1, 1], [-1, -1], [1, 1])$ to $d_6(0 - 10) ([-1, 1], [-1, -1], [1, -1])$
 or
 $d_6(101) ([1, 1], [-1, 1], [1, 1])$ to $d_5(001) ([-1, 1], [-1, 1], [1, 1])$ to
 $d_{11}(0 - 11) ([-1, 1], [-1, -1], [1, 1])$ to $d_6(0 - 10) ([-1, 1], [-1, -1], [-1, 1])$

E.5.4 Region D

Duty Cycles

$$m_a \cos \omega t = \frac{1}{\sqrt{6}}d_6 + \sqrt{\frac{2}{3}}d_{18}$$

$$m_a \sin \omega t = -\frac{1}{\sqrt{2}}d_6 - \sqrt{2}d_{11} - \sqrt{2}d_{18}$$

$$d_6 + d_{11} + d_{18} = 1$$

$$d_{18} = \sqrt{\frac{3}{2}}m_a \cos \omega t - \frac{1}{\sqrt{2}}m_a \sin \omega t - 1$$

$$d_6 = \sqrt{2}m_a \sin \omega t + 2$$

$$d_{11} = -\sqrt{\frac{3}{2}}m_a \cos \omega t - \frac{1}{\sqrt{2}}m_a \sin \omega t$$

Switch Combinations

The switch combination sequence for the nearest three vector for sector VD for 2-cell is given by:

$d_6(0 - 10) ([1, -1], [-1, -1], [1, -1])$ to $d_{11}(0 - 11) ([1, -1], [-1, -1], [1, 1])$ to
 $d_{18}(1 - 11) ([1, 1], [-1, -1], [1, 1])$ to $d_6(101) ([1, 1], [1, -1], [1, 1])$

or

$d_6(0 - 10) ([1, -1], [-1, -1], [1, -1])$ to $d_{11}(0 - 11) ([1, -1], [-1, -1], [1, 1])$ to
 $d_{18}(1 - 11) ([1, 1], [-1, -1], [1, 1])$ to $d_6(101) ([1, 1], [-1, 1], [1, 1])$

or

$d_6(0 - 10) ([1, -1], [-1, -1], [-1, 1])$ to $d_{11}(0 - 11) ([1, -1], [-1, -1], [1, 1])$ to

$d_{18}(1 - 11) ([1, 1], [-1, -1], [1, 1])$ to $d_6(101) ([1, 1], [1, -1], [1, 1])$

or

$d_6(0 - 10) ([1, -1], [-1, -1], [-1, 1])$ to $d_{11}(0 - 11) ([1, -1], [-1, -1], [1, 1])$ to

$d_{18}(1 - 11) ([1, 1], [-1, -1], [1, 1])$ to $d_6(101) ([1, 1], [-1, 1], [1, 1])$

or

$d_6(0 - 10) ([-1, 1], [-1, -1], [1, -1])$ to $d_{11}(0 - 11) ([-1, 1], [-1, -1], [1, 1])$ to

$d_{18}(1 - 11) ([1, 1], [-1, -1], [1, 1])$ to $d_6(101) ([1, 1], [1, -1], [1, 1])$

or

$d_6(0 - 10) ([-1, 1], [-1, -1], [1, -1])$ to $d_{11}(0 - 11) ([-1, 1], [-1, -1], [1, 1])$ to

$d_{18}(1 - 11) ([1, 1], [-1, -1], [1, 1])$ to $d_6(101) ([1, 1], [-1, 1], [1, 1])$

or

$d_6(0 - 10) ([-1, 1], [-1, -1], [-1, 1])$ to $d_{11}(0 - 11) ([-1, 1], [-1, -1], [1, 1])$ to

$d_{18}(1 - 11) ([1, 1], [-1, -1], [1, 1])$ to $d_6(101) ([1, 1], [1, -1], [1, 1])$

or

$d_6(0 - 10) ([-1, 1], [-1, -1], [-1, 1])$ to $d_{11}(0 - 11) ([-1, 1], [-1, -1], [1, 1])$ to

$d_{18}(1 - 11) ([1, 1], [-1, -1], [1, 1])$ to $d_6(101) ([1, 1], [-1, 1], [1, 1])$

E.6 Sector VI

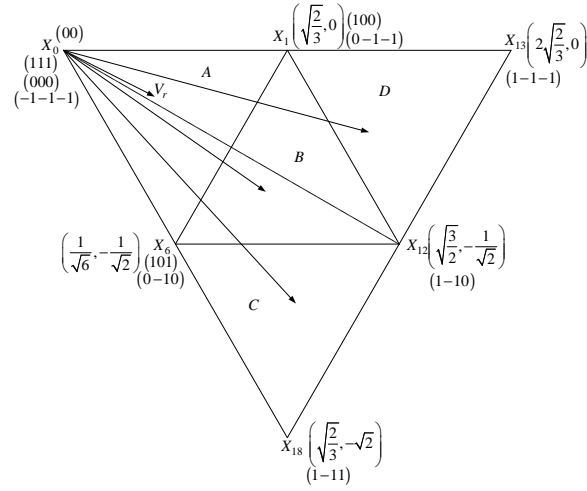


Figure E.6: Regions of vector modulation of the 2-cell multicell converter in the sixth sector

E.6.1 Region A

Duty Cycles

$$m_a \cos \omega t = \frac{1}{\sqrt{6}} d_6 + \sqrt{\frac{2}{3}} d_1$$

$$m_a \sin \omega t = -\frac{1}{\sqrt{2}} d_6$$

$$d_6 + d_1 + d_0 = 1$$

$$d_0 = -\sqrt{\frac{3}{2}} m_a \cos \omega t + \frac{1}{\sqrt{2}} m_a \sin \omega t + 1$$

$$d_1 = \frac{1}{\sqrt{2}} m_a \sin \omega t + \sqrt{\frac{3}{2}} m_a \cos \omega t$$

$$d_6 = -\sqrt{2} m_a \sin \omega t$$

For $\theta \leq \frac{11\pi}{6}$

The switch combination sequence for the nearest three vector moving from sector VA to VIA for 2-cell is given by:

$d_6(0-10)$ ($[1, -1], [-1, -1], [1, -1]$) to $d_0(000)$ ($[1, -1], [1, -1], [1, -1]$) to $d_1(100)$ ($[1, 1], [1, -1], [1, -1]$) to $d_6(101)$ ($[1, 1], [1, -1], [1, 1]$)

or

$d_6(0 - 10) ([-1, 1], [-1, -1], [1, -1])$ to $d_0(000) ([-1, 1], [1, -1], [1, -1])$ to $d_1(100) ([1, 1], [1, -1], [1, -1])$ to $d_6(101) ([1, 1], [1, -1], [1, 1])$

or

$d_6(0 - 10) ([1, -1], [-1, -1], [-1, 1])$ to $d_0(000) ([1, -1], [-1, 1], [-1, 1])$ to $d_1(100) ([1, 1], [-1, 1], [-1, 1])$ to $d_6(101) ([1, 1], [-1, 1], [1, 1])$

or

$d_6(0 - 10) ([-1, 1], [-1, -1], [-1, 1])$ to $d_0(000) ([-1, 1], [-1, 1], [-1, 1])$ to $d_1(100) ([1, 1], [-1, 1], [-1, 1])$ to $d_6(101) ([1, 1], [-1, 1], [1, 1])$

or

$d_6(0 - 10) ([1, -1], [-1, -1], [1, -1])$ to $d_0(000) ([1, -1], [-1, 1], [1, -1])$ to $d_1(100) ([1, 1], [-1, 1], [1, -1])$ to $d_6(101) ([1, 1], [-1, 1], [1, 1])$

or

$d_6(0 - 10) ([-1, 1], [-1, -1], [1, -1])$ to $d_0(000) ([-1, 1], [-1, 1], [1, -1])$ to $d_1(100) ([1, 1], [-1, 1], [1, -1])$ to $d_6(101) ([1, 1], [-1, 1], [1, 1])$

or

$d_6(0 - 10) ([1, -1], [-1, -1], [-1, 1])$ to $d_0(000) ([1, -1], [1, -1], [-1, 1])$ to $d_1(100) ([1, 1], [1, -1], [-1, 1])$ to $d_6(101) ([1, 1], [1, -1], [1, 1])$

or

$d_6(0 - 10) ([-1, 1], [-1, -1], [-1, 1])$ to $d_0(000) ([-1, 1], [1, -1], [-1, 1])$ to $d_1(100) ([1, 1], [1, -1], [-1, 1])$ to $d_6(101) ([1, 1], [1, -1], [1, 1])$

For $\theta \geq \frac{11\pi}{6}$

The switch combination sequence for the nearest three vector moving from sector VIA to IA for 2-cell is given by:

$d_1(0 - 1 - 1) ([1, -1], [-1, -1], [-1, -1])$ to $d_6(0 - 10) ([1, -1], [-1, -1], [1, -1])$ to $d_0(000) ([1, -1], [1, -1], [1, -1])$ to $d_1(100) ([1, 1], [1, -1], [1, -1])$

or

$d_1(0 - 1 - 1) ([-1, 1], [-1, -1], [-1, -1])$ to $d_6(0 - 10) ([-1, 1], [-1, -1], [1, -1])$ to $d_0(000) ([-1, 1], [1, -1], [1, -1])$ to $d_1(100) ([1, 1], [1, -1], [1, -1])$

or

$d_1(0 - 1 - 1) ([1, -1], [-1, -1], [-1, -1])$ to $d_6(0 - 10) ([1, -1], [-1, -1], [-1, 1])$ to $d_0(000) ([1, -1], [-1, 1], [-1, 1])$ to $d_1(100) ([1, 1], [-1, 1], [-1, 1])$

or

$d_1(0 - 1 - 1) ([-1, 1], [-1, -1], [-1, -1])$ to $d_6(0 - 10) ([-1, 1], [-1, -1], [-1, 1])$ to $d_0(000) ([-1, 1], [-1, 1], [-1, 1])$ to $d_1(100) ([1, 1], [-1, 1], [-1, 1])$

or

$d_1(0 - 1 - 1)$ ($[1, -1], [-1, -1], [-1, -1]$) to $d_6(0 - 10)$ ($[1, -1], [-1, -1], [1, -1]$) to $d_0(000)$ ($[1, -1], [-1, 1], [1, -1]$) to $d_1(100)$ ($[1, 1], [-1, 1], [1, -1]$)

or

$d_1(0 - 1 - 1)$ ($[-1, 1], [-1, -1], [-1, -1]$) to $d_6(0 - 10)$ ($[-1, 1], [-1, -1], [1, -1]$) to $d_0(000)$ ($[-1, 1], [-1, 1], [1, -1]$) to $d_1(100)$ ($[1, 1], [-1, 1], [1, -1]$)

or

$d_1(0 - 1 - 1)$ ($[1, -1], [-1, -1], [-1, -1]$) to $d_6(0 - 10)$ ($[1, -1], [-1, -1], [-1, 1]$) to $d_0(000)$ ($[1, -1], [1, -1], [-1, 1]$) to $d_1(100)$ ($[1, 1], [1, -1], [-1, 1]$)

or

$d_1(0 - 1 - 1)$ ($[-1, 1], [-1, -1], [-1, -1]$) to $d_6(0 - 10)$ ($[-1, 1], [-1, -1], [-1, 1]$) to $d_0(000)$ ($[-1, 1], [1, -1], [-1, 1]$) to $d_1(100)$ ($[1, 1], [1, -1], [-1, 1]$)

E.6.2 Region C

Duty Cycles

$$m_a \cos \omega t = \frac{1}{\sqrt{6}}d_6 + \sqrt{\frac{2}{3}}d_{18} + \sqrt{\frac{3}{2}}d_{12}$$

$$m_a \sin \omega t = -\frac{1}{\sqrt{2}}d_6 - \sqrt{2}d_{18} - \frac{1}{\sqrt{2}}d_{12}$$

$$d_6 + d_{18} + d_{12} = 1$$

$$d_{18} = -\sqrt{2}m_a \sin \omega t - 1$$

$$d_6 = -\sqrt{\frac{3}{2}}m_a \cos \omega t + \frac{1}{\sqrt{2}}m_a \sin \omega t + 2$$

$$d_{12} = \sqrt{\frac{3}{2}}m_a \cos \omega t + \frac{1}{\sqrt{2}}m_a \sin \omega t$$

Switching Combinations

The switch combination sequence for the nearest three vector for sector VIC for 2-cell is given by:

$d_6(101)$ ($[1, 1], [1, -1], [1, 1]$) to $d_{18}(1 - 11)$ ($[1, 1], [-1, -1], [1, 1]$) to $d_{12}(1 - 10)$ ($[1, 1], [-1, -1], [1, -1]$) to $d_6(0 - 10)$ ($[1, -1], [-1, -1], [1, -1]$)

or

$d_6(101)$ ($[1, 1], [1, -1], [1, 1]$) to $d_{18}(1 - 11)$ ($[1, 1], [-1, -1], [1, 1]$) to $d_{12}(1 - 10)$ ($[1, 1], [-1, -1], [1, -1]$) to $d_6(0 - 10)$ ($[-1, 1], [-1, -1], [1, -1]$)

or

$d_6(101)$ ($[1, 1], [1, -1], [1, 1]$) to $d_{18}(1 - 11)$ ($[1, 1], [-1, -1], [1, 1]$) to

$d_{12}(1 - 10) ([1, 1], [-1, -1], [-1, 1])$ to $d_6(0 - 10) ([1, -1], [-1, -1], [-1, 1])$
 or
 $d_6(101) ([1, 1], [1, -1], [1, 1])$ to $d_{18}(1 - 11) ([1, 1], [-1, -1], [1, 1])$ to
 $d_{12}(1 - 10) ([1, 1], [-1, -1], [-1, 1])$ to $d_6(0 - 10) ([-1, 1], [-1, -1], [-1, 1])$
 or
 $d_6(101) ([1, 1], [-1, 1], [1, 1])$ to $d_{18}(1 - 11) ([1, 1], [-1, -1], [1, 1])$ to
 $d_{12}(1 - 10) ([1, 1], [-1, -1], [1, -1])$ to $d_6(0 - 10) ([1, -1], [-1, -1], [1, -1])$
 or
 $d_6(101) ([1, 1], [-1, 1], [1, 1])$ to $d_{18}(1 - 11) ([1, 1], [-1, -1], [1, 1])$ to
 $d_{12}(1 - 10) ([1, 1], [-1, -1], [1, -1])$ to $d_6(0 - 10) ([-1, 1], [-1, -1], [1, -1])$
 or
 $d_6(101) ([1, 1], [-1, 1], [1, 1])$ to $d_{18}(1 - 11) ([1, 1], [-1, -1], [1, 1])$ to
 $d_{12}(1 - 10) ([1, 1], [-1, -1], [-1, 1])$ to $d_6(0 - 10) ([1, -1], [-1, -1], [-1, 1])$
 or
 $d_6(101) ([1, 1], [-1, 1], [1, 1])$ to $d_{18}(1 - 11) ([1, 1], [-1, -1], [1, 1])$ to
 $d_{12}(1 - 10) ([1, 1], [-1, -1], [-1, 1])$ to $d_6(0 - 10) ([-1, 1], [-1, -1], [-1, 1])$

E.6.3 Region B

Duty Cycles

$$m_a \cos \omega t = \frac{1}{\sqrt{6}}d_6 + \sqrt{\frac{3}{2}}d_{12} + \sqrt{\frac{2}{3}}d_1$$

$$m_a \sin \omega t = -\frac{1}{\sqrt{2}}d_6 - \frac{1}{\sqrt{2}}d_{12}$$

$$d_6 + d_{12} + d_1 = 1$$

$$d_6 = -\sqrt{\frac{3}{2}}m_a \cos \omega t - \frac{1}{\sqrt{2}}m_a \sin \omega t + 1$$

$$d_{12} = -\frac{1}{\sqrt{2}}m_a \sin \omega t + \sqrt{\frac{3}{2}}m_a \cos \omega t - 1$$

$$d_1 = \sqrt{2}m_a \sin \omega t + 1$$

For $\theta \leq \frac{11\pi}{6}$

The switch combination sequence for the nearest three vector moving from sector *VIB* to *VIC* for 2-cell is given by:

$d_6(0 - 10) ([1, -1], [-1, -1], [1, -1])$ to $d_{12}(1 - 10) ([1, 1], [-1, -1], [1, -1])$ to

$d_1(100)$ $([1, 1], [1, -1], [1, -1])$ to $d_6(101)$ $([1, 1], [1, -1], [1, 1])$

or

$d_6(0 - 10)$ $([1, -1], [-1, -1], [1, -1])$ to $d_{12}(1 - 10)$ $([1, 1], [-1, -1], [1, -1])$ to $d_1(100)$ $([1, 1], [-1, 1], [1, -1])$ to $d_6(101)$ $([1, 1], [-1, 1], [1, 1])$

or

$d_6(0 - 10)$ $([-1, 1], [-1, -1], [1, -1])$ to $d_{12}(1 - 10)$ $([1, 1], [-1, -1], [1, -1])$ to $d_1(100)$ $([1, 1], [1, -1], [1, -1])$ to $d_6(101)$ $([1, 1], [1, -1], [1, 1])$

or

$d_6(0 - 10)$ $([-1, 1], [-1, -1], [1, -1])$ to $d_{12}(1 - 10)$ $([1, 1], [-1, -1], [1, -1])$ to $d_1(100)$ $([1, 1], [-1, 1], [1, -1])$ to $d_6(101)$ $([1, 1], [-1, 1], [1, 1])$

or

$d_6(0 - 10)$ $([1, -1], [-1, -1], [-1, 1])$ to $d_{12}(1 - 10)$ $([1, 1], [-1, -1], [-1, 1])$ to $d_1(100)$ $([1, 1], [1, -1], [-1, 1])$ to $d_6(101)$ $([1, 1], [1, -1], [1, 1])$

or

$d_6(0 - 10)$ $([1, -1], [-1, -1], [-1, 1])$ to $d_{12}(1 - 10)$ $([1, 1], [-1, -1], [-1, 1])$ to $d_1(100)$ $([1, 1], [-1, 1], [-1, 1])$ to $d_6(101)$ $([1, 1], [-1, 1], [1, 1])$

or

$d_6(0 - 10)$ $([-1, 1], [-1, -1], [-1, 1])$ to $d_{12}(1 - 10)$ $([1, 1], [-1, -1], [-1, 1])$ to $d_1(100)$ $([1, 1], [1, -1], [-1, 1])$ to $d_6(101)$ $([1, 1], [1, -1], [1, 1])$

or

$d_6(0 - 10)$ $([-1, 1], [-1, -1], [-1, 1])$ to $d_{12}(1 - 10)$ $([1, 1], [-1, -1], [-1, 1])$ to $d_1(100)$ $([1, 1], [-1, 1], [-1, 1])$ to $d_6(101)$ $([1, 1], [-1, 1], [1, 1])$

For $\theta \geq \frac{11\pi}{6}$

The switch combination sequence for the nearest three vector moving from sector VIB to VIC for 2-cell is given by:

$d_1(0 - 1 - 1)$ $([1, -1], [-1, -1], [-1, -1])$ to $d_6(0 - 10)$ $([1, -1], [-1, -1], [1, -1])$ to $d_{12}(1 - 10)$ $([1, 1], [-1, -1], [1, -1])$ to $d_1(100)$ $([1, 1], [1, -1], [1, -1])$

or

$d_1(0 - 1 - 1)$ $([1, -1], [-1, -1], [-1, -1])$ to $d_6(0 - 10)$ $([1, -1], [-1, -1], [1, -1])$ to $d_{12}(1 - 10)$ $([1, 1], [-1, -1], [1, -1])$ to $d_1(100)$ $([1, 1], [-1, 1], [1, -1])$

or

$d_1(0 - 1 - 1)$ $([1, -1], [-1, -1], [-1, -1])$ to $d_6(0 - 10)$ $([1, -1], [-1, -1], [-1, 1])$ to $d_{12}(1 - 10)$ $([1, 1], [-1, -1], [-1, 1])$ to $d_1(100)$ $([1, 1], [1, -1], [-1, 1])$

or

$d_1(0 - 1 - 1)$ $([1, -1], [-1, -1], [-1, -1])$ to $d_6(0 - 10)$ $([1, -1], [-1, -1], [-1, 1])$ to $d_{12}(1 - 10)$ $([1, 1], [-1, -1], [-1, 1])$ to $d_1(100)$ $([1, 1], [-1, 1], [-1, 1])$

or

$d_1(0 - 1 - 1) ([-1, 1], [-1, -1], [-1, -1])$ to $d_6(0 - 10) ([-1, 1], [-1, -1], [1, -1])$ to $d_{12}(1 - 10) ([1, 1], [-1, -1], [1, -1])$ to $d_1(100) ([1, 1], [1, -1], [1, -1])$

or

$d_1(0 - 1 - 1) ([-1, 1], [-1, -1], [-1, -1])$ to $d_6(0 - 10) ([-1, 1], [-1, -1], [1, -1])$ to $d_{12}(1 - 10) ([1, 1], [-1, -1], [1, -1])$ to $d_1(100) ([1, 1], [-1, 1], [1, -1])$

or

$d_1(0 - 1 - 1) ([-1, 1], [-1, -1], [-1, -1])$ to $d_6(0 - 10) ([-1, 1], [-1, -1], [-1, 1])$ to $d_{12}(1 - 10) ([1, 1], [-1, -1], [-1, 1])$ to $d_1(100) ([1, 1], [1, -1], [-1, 1])$

or

$d_1(0 - 1 - 1) ([-1, 1], [-1, -1], [-1, -1])$ to $d_6(0 - 10) ([-1, 1], [-1, -1], [-1, 1])$ to $d_{12}(1 - 10) ([1, 1], [-1, -1], [-1, 1])$ to $d_1(100) ([1, 1], [-1, 1], [-1, 1])$

E.6.4 Region D

Duty Cycles

$$m_a \cos \omega t = \sqrt{\frac{2}{3}}d_1 + \sqrt{\frac{3}{2}}d_{12} + 2\sqrt{\frac{2}{3}}d_{13}$$

$$m_a \sin \omega t = -\frac{1}{\sqrt{2}}d_{12}$$

$$d_1 + d_{12} + d_{13} = 1$$

$$d_{12} = -\sqrt{2}m_a \sin \omega t$$

$$d_1 = -\sqrt{\frac{3}{2}}m_a \cos \omega t + \frac{1}{\sqrt{2}}m_a \sin \omega t + 2$$

$$d_{13} = \sqrt{\frac{3}{2}}m_a \cos \omega t + \frac{1}{\sqrt{2}}m_a \sin \omega t - 1$$

Switching Combinations

The switch combination sequence for the nearest three vector for sector VID for 2-cell is given by:

$d_1(100) ([1, 1], [1, -1], [1, -1])$ to $d_{12}(1 - 10) ([1, 1], [-1, -1], [1, -1])$ to $d_{13}(1 - 1 - 1) ([1, 1], [-1, -1], [-1, -1])$ to $d_1(0 - 1 - 1) ([1, -1], [-1, -1], [-1, -1])$

or

$d_1(100) ([1, 1], [1, -1], [1, -1])$ to $d_{12}(1 - 10) ([1, 1], [-1, -1], [1, -1])$ to $d_{13}(1 - 1 - 1) ([1, 1], [-1, -1], [-1, -1])$ to $d_1(0 - 1 - 1) ([-1, 1], [-1, -1], [-1, -1])$

or

$d_1(100) ([1, 1], [-1, 1], [1, -1])$ to $d_{12}(1 - 10) ([1, 1], [-1, -1], [1, -1])$ to
 $d_{13}(1 - 1 - 1) ([1, 1], [-1, -1], [-1, -1])$ to $d_1(0 - 1 - 1) ([1, -1], [-1, -1], [-1, -1])$
 or
 $d_1(100) ([1, 1], [-1, 1], [1, -1])$ to $d_{12}(1 - 10) ([1, 1], [-1, -1], [1, -1])$ to
 $d_{13}(1 - 1 - 1) ([1, 1], [-1, -1], [-1, -1])$ to $d_1(0 - 1 - 1) ([-1, 1], [-1, -1], [-1, -1])$
 or
 $d_1(100) ([1, 1], [1, -1], [-1, 1])$ to $d_{12}(1 - 10) ([1, 1], [-1, -1], [-1, 1])$ to
 $d_{13}(1 - 1 - 1) ([1, 1], [-1, -1], [-1, -1])$ to $d_1(0 - 1 - 1) ([1, -1], [-1, -1], [-1, -1])$
 or
 $d_1(100) ([1, 1], [1, -1], [-1, 1])$ to $d_{12}(1 - 10) ([1, 1], [-1, -1], [-1, 1])$ to
 $d_{13}(1 - 1 - 1) ([1, 1], [-1, -1], [-1, -1])$ to $d_1(0 - 1 - 1) ([-1, 1], [-1, -1], [-1, -1])$
 or
 $d_1(100) ([1, 1], [-1, 1], [-1, 1])$ to $d_{12}(1 - 10) ([1, 1], [-1, -1], [-1, 1])$ to
 $d_{13}(1 - 1 - 1) ([1, 1], [-1, -1], [-1, -1])$ to $d_1(0 - 1 - 1) ([1, -1], [-1, -1], [-1, -1])$
 or
 $d_1(100) ([1, 1], [-1, 1], [-1, 1])$ to $d_{12}(1 - 10) ([1, 1], [-1, -1], [-1, 1])$ to
 $d_{13}(1 - 1 - 1) ([1, 1], [-1, -1], [-1, -1])$ to $d_1(0 - 1 - 1) ([-1, 1], [-1, -1], [-1, -1])$

E.7 Combination of switching states

In this section we show the first and third switching states combinations only since the second and the fourth combination follow directly from first and third combinations respectively. Also we only show combinations for reference vector moving through regions C, B and D and region A since the combinations for reference vector moving through regions C and D and region B can be derived from the combinations for reference vector moving through regions C, B and D.

E.7.1 First Combination for reference vector moving through regions C, B and D

IC

$d_1(0-1-1) ([1, -1], [-1, -1], [-1, -1])$ to $d_{13}(1-1-1) ([1, 1], [-1, -1], [-1, -1])$ to $d_7(10-1) ([1, 1], [1, -1], [-1, -1])$ to $d_1(100) ([1, 1], [1, -1], [1, -1])$

to IB1

$d_1(100) ([1, 1], [1, -1], [1, -1])$ to $d_7(10-1) ([1, 1], [1, -1], [-1, -1])$ to $d_2(00-1) ([1, -1], [1, -1], [-1, -1])$ to $d_1(0-1-1) ([1, -1], [-1, -1], [-1-1])$

to

$d_1(0-1-1) ([1, -1], [-1, -1], [-1-1])$ to $d_2(00-1) ([1, -1], [1, -1], [-1, -1])$ to $d_7(10-1) ([1, 1], [1, -1], [-1, -1])$ to $d_1(100) ([1, 1], [1, -1], [1, -1])$

to IB2

$d_2(110) ([1, 1], [1, 1], [1, -1])$ to $d_1(100) ([1, 1], [1, -1], [1, -1])$ to $d_7(10-1) ([1, 1], [1, -1], [-1, -1])$

to

$d_2(00-1) ([1, -1], [1, -1], [-1-1])$

to ID

$d_2(00-1) ([1, -1], [1, -1], [-1, -1])$ to $d_7(10-1) ([1, 1], [1, -1], [-1, -1])$ to $d_{14}(11-1) ([1, 1], [1, 1], [-1, -1])$ to $d_2(110) ([1, 1], [1, 1], [1, -1])$

to IIC

$d_2(110) ([1, 1], [1, 1], [1, -1])$ to $d_{14}(11-1) ([1, 1], [1, 1], [-1, -1])$ to $d_8(01-1) ([1, -1], [1, 1], [-1, -1])$ to $d_2(00-1) ([1, -1], [1, -1], [-1, -1])$

to IIB1

$d_2(00-1) ([1, -1], [1, -1], [-1, -1])$ to $d_8(01-1) ([1, -1], [1, 1], [-1, -1])$ to $d_3(010) ([1, -1], [1, 1], [1, -1])$ to $d_2(110) ([1, 1], [1, 1], [1, -1])$

to

$d_2(110) ([1, 1], [1, 1], [1, -1])$ to $d_3(010) ([1, -1], [1, 1], [1, -1])$ to $d_8(01-1) ([1, -1], [1, 1], [-1, -1])$ to $d_2(00-1) ([1, -1], [1, -1], [-1, -1])$

to IIB2

$d_3(-10-1) ([-1, -1], [1, -1], [-1, -1])$ to $d_2(00-1) ([1, -1], [1, -1], [-1, -1])$ to

$d_8(01-1) ([1, -1], [1, 1], [-1, -1])$ to $d_3(010) ([1, -1], [1, 1], [1, -1])$
 to IID
 $d_3(010) ([1, -1], [1, 1], [1, -1])$ to $d_8(01-1) ([1, -1], [1, 1], [-1, -1])$ to
 $d_{15}(-11-1) ([-1, -1], [1, 1], [-1, -1])$ to $d_3(-10-1) ([-1, -1], [1, -1], [-1, -1])$
 to IIIC
 $d_3(-10-1) ([-1, -1], [1, -1], [-1, -1])$ to $d_{15}(-11-1) ([-1, -1], [1, 1], [-1, -1])$ to
 $d_9(-110) ([-1, -1], [1, 1], [1, -1])$ to $d_3(010) ([1, -1], [1, 1], [1, -1])$
 to IIIB1
 $d_3(010) ([1, -1], [1, 1], [1, -1])$ to $d_9(-110) ([-1, -1], [1, 1], [1, -1])$ to
 $d_4(-100) ([-1, -1], [1, -1], [1, -1])$ to $d_3(-10-1) ([-1, -1], [1, -1], [-1, -1])$
 to
 $d_3(-10-1) ([-1, -1], [1, -1], [-1, -1])$ to $d_4(-100) ([-1, -1], [1, -1], [1, -1])$ to
 $d_9(-110) ([-1, -1], [1, 1], [1, -1])$ to $d_3(010) ([1, -1], [1, 1], [1, -1])$
 to IIIB2
 $d_4(011) ([1, -1], [1, 1], [1, 1])$ to $d_3(010) ([1, -1], [1, 1], [1, -1])$ to
 $d_9(-110) ([-1, -1], [1, 1], [1, -1])$ to $d_4(-100) ([-1, -1], [1, -1], [1, -1])$
 to IIID
 $d_4(-100) ([-1, -1], [1, -1], [1, -1])$ to $d_9(-110) ([-1, -1], [1, 1], [1, -1])$ to
 $d_{16}(-111) ([-1, -1], [1, 1], [1, 1])$ to $d_4(011) ([1, -1], [1, 1], [1, 1])$
 to IVC
 $d_4(011) ([-1, 1], [1, 1], [1, 1])$ to $d_{16}(-111) ([-1, -1], [1, 1], [1, 1])$ to
 $d_{10}(-101) ([-1, -1], [-1, 1], [1, 1])$ to $d_4(-100) ([-1, -1], [-1, 1], [-1, 1])$
 to IVB1
 $d_4(-100) ([-1, -1], [-1, 1], [-1, 1])$ to $d_{10}(-101) ([-1, -1], [-1, 1], [1, 1])$ to
 $d_5(001) ([-1, 1], [-1, 1], [1, 1])$ to $d_4(011) ([-1, 1], [1, 1], [1, 1])$
 to
 $d_4(011) ([-1, 1], [1, 1], [1, 1])$ to $d_5(001) ([-1, 1], [-1, 1], [1, 1])$ to
 $d_{10}(-101) ([-1, -1], [-1, 1], [1, 1])$ to $d_4(-100) ([-1, -1], [-1, 1], [-1, 1])$
 to IVB2
 $d_5(-1-10) ([-1, -1], [-1, -1], [-1, 1])$ to $d_4(-100) ([-1, -1], [-1, 1], [-1, 1])$ to
 $d_{10}(-101) ([-1, -1], [-1, 1], [1, 1])$ to $d_5(001) ([-1, 1], [-1, 1], [1, 1])$
 to IVD
 $d_5(001) ([-1, 1], [-1, 1], [1, 1])$ to $d_{10}(-101) ([-1, -1], [-1, 1], [1, 1])$ to
 $d_{17}(-1-11) ([-1, -1], [-1, -1], [1, 1])$ to $d_5(-1-10) ([-1, -1], [-1, -1], [-1, 1])$
 to VC
 $d_5(-1-10) ([1, 1], [-1, -1], [-1, 1])$ to $d_{17}(-1-11) ([-1, -1], [-1, -1], [1, 1])$ to
 $d_{11}(0-11) ([-1, 1], [-1, -1], [1, 1])$ to $d_5(001) ([-1, 1], [-1, 1], [1, 1])$
 to VB1

$d_5(001)$ $([-1, 1], [-1, 1], [1, 1])$ to $d_{11}(0 - 11)$ $([-1, 1], [-1, -1], [1, 1])$ to
 $d_6(0 - 10)$ $([-1, 1], [-1, -1], [-1, 1])$ to $d_5(-1 - 10)$ $([-1, -1], [-1, -1], [-1, 1])$
to
 $d_5(-1 - 10)$ $([-1, -1], [-1, -1], [-1, 1])$ to $d_6(0 - 10)$ $([-1, 1], [-1, -1], [-1, 1])$ to
 $d_{11}(0 - 11)$ $([-1, 1], [-1, -1], [1, 1])$ to $d_5(001)$ $([-1, 1], [-1, 1], [1, 1])$
to VB2
 $d_6(101)$ $([1, 1], [-1, 1], [1, 1])$ to $d_5(001)$ $([-1, 1], [-1, 1], [1, 1])$ to
 $d_{11}(0 - 11)$ $([-1, 1], [-1, -1], [1, 1])$ to $d_6(0 - 10)$ $([-1, 1], [-1, -1], [-1, 1])$
to VD
 $d_6(0 - 10)$ $([-1, 1], [-1, -1], [-1, 1])$ to $d_{11}(0 - 11)$ $([-1, 1], [-1, -1], [1, 1])$ to
 $d_{18}(1 - 11)$ $([1, 1], [-1, -1], [1, 1])$ to $d_6(101)$ $([1, 1], [-1, 1], [1, 1])$
to VIC
 $d_6(101)$ $([1, 1], [-1, 1], [1, 1])$ to $d_{18}(1 - 11)$ $([1, 1], [-1, -1], [1, 1])$ to
 $d_{12}(1 - 10)$ $([1, 1], [-1, -1], [-1, 1])$ to $d_6(0 - 10)$ $([-1, 1], [-1, -1], [-1, 1])$
to VIB1
 $d_6(0 - 10)$ $([-1, 1], [-1, -1], [-1, 1])$ to $d_{12}(1 - 10)$ $([1, 1], [-1, -1], [-1, 1])$ to
 $d_1(100)$ $([1, 1], [-1, 1], [-1, 1])$ to $d_6(101)$ $([1, 1], [-1, 1], [1, 1])$
to
 $d_6(101)$ $([1, 1], [-1, 1], [1, 1])$ to $d_1(100)$ $([1, 1], [-1, 1], [-1, 1])$ to
 $d_{12}(1 - 10)$ $([1, 1], [-1, -1], [-1, 1])$ to $d_6(0 - 10)$ $([-1, 1], [-1, -1], [-1, 1])$
to VIB2
 $d_1(0 - 1 - 1)$ $([-1, 1], [-1, -1], [-1, -1])$ to $d_6(0 - 10)$ $([-1, 1], [-1, -1], [-1, 1])$ to
 $d_{12}(1 - 10)$ $([1, 1], [-1, -1], [-1, 1])$ to $d_1(100)$ $([1, 1], [-1, 1], [-1, 1])$
to VID
 $d_1(100)$ $([1, 1], [-1, 1], [-1, 1])$ to $d_{12}(1 - 10)$ $([1, 1], [-1, -1], [-1, 1])$ to
 $d_{13}(1 - 1 - 1)$ $([1, 1], [-1, -1], [-1, -1])$ to $d_1(0 - 1 - 1)$ $([-1, 1], [-1, -1], [-1, -1])$

E.7.2 Third Combination for reference vector moving through regions C, B and D

IC
 $d_1(0 - 1 - 1)$ $([1, -1], [-1, -1], [-1, -1])$ to $d_{13}(1 - 1 - 1)$ $([1, 1], [-1, -1], [-1, -1])$ to
 $d_7(10 - 1)$ $([1, 1], [1, -1], [-1, -1])$ to $d_1(100)$ $([1, 1], [1, -1], [1, -1])$
to IB1
 $d_1(100)$ $([1, 1], [1, -1], [1, -1])$ to $d_7(10 - 1)$ $([1, 1], [1, -1], [-1, -1])$ to
 $d_2(00 - 1)$ $([1, -1], [1, -1], [-1, -1])$ to $d_1(0 - 1 - 1)$ $([1, -1], [-1, -1], [-1, -1])$
to
 $d_1(0 - 1 - 1)$ $([1, -1], [-1, -1], [-1, -1])$ to $d_2(00 - 1)$ $([1, -1], [1, -1], [-1, -1])$ to

$d_7(10 - 1) ([1, 1], [1, -1], [-1, -1])$ to $d_1(100) ([1, 1], [1, -1], [1, -1])$
 to IB2
 $d_2(110) ([1, 1], [1, 1], [1, -1])$ to $d_1(100) ([1, 1], [1, -1], [1, -1])$ to $d_7(10-1) ([1, 1], [1, -1], [-1, -1])$
 to
 $d_2(00 - 1) ([1, -1], [1, -1], [-1 - 1])$
 to ID
 $d_2(00 - 1) ([1, -1], [1, -1], [-1, -1])$ to $d_7(10 - 1) ([1, 1], [1, -1], [-1, -1])$ to
 $d_{14}(11 - 1) ([1, 1], [1, 1], [-1, -1])$ to $d_2(110) ([1, 1], [1, 1], [1, -1])$
 to IIC
 $d_2(110) ([1, 1], [1, 1], [-1, 1])$ to $d_{14}(11 - 1) ([1, 1], [1, 1], [-1, -1])$ to
 $d_8(01 - 1) ([-1, 1], [1, 1], [-1, -1])$ to $d_2(00 - 1) ([-1, 1], [-1, 1], [-1, -1])$
 to IIB1
 $d_2(00 - 1) ([-1, 1], [-1, 1], [-1, -1])$ to $d_8(01 - 1) ([-1, 1], [1, 1], [-1, -1])$ to
 $d_3(010) ([-1, 1], [1, 1], [-1, 1])$ to $d_2(110) ([1, 1], [1, 1], [-1, 1])$
 to
 $d_2(110) ([1, 1], [1, 1], [-1, 1])$ to $d_3(010) ([-1, 1], [1, 1], [-1, 1])$ to
 $d_8(01 - 1) ([-1, 1], [1, 1], [-1, -1])$ to $d_2(00 - 1) ([-1, 1], [-1, 1], [-1, -1])$
 to IIB2
 $d_3(-10 - 1) ([-1, -1], [-1, 1], [-1, -1])$ to $d_2(00 - 1) ([-1, 1], [-1, 1], [-1, -1])$ to
 $d_8(01 - 1) ([-1, 1], [1, 1], [-1, -1])$ to $d_3(010) ([-1, 1], [1, 1], [-1, 1])$
 to IID
 $d_3(010) ([-1, 1], [1, 1], [-1, 1])$ to $d_8(01 - 1) ([-1, 1], [1, 1], [-1, -1])$ to
 $d_{15}(-11 - 1) ([-1, -1], [1, 1], [-1, -1])$ to $d_3(-10 - 1) ([-1, -1], [-1, 1], [-1, -1])$
 to IIIC
 $d_3(-10 - 1) ([-1, -1], [1, -1], [-1, -1])$ to $d_{15}(-11 - 1) ([-1, -1], [1, 1], [-1, -1])$ to
 $d_9(-110) ([-1, -1], [1, 1], [1, -1])$ to $d_3(010) ([1, -1], [1, 1], [1, -1])$
 to IIIB1
 $d_3(010) ([1, -1], [1, 1], [1, -1])$ to $d_9(-110) ([-1, -1], [1, 1], [1, -1])$ to
 $d_4(-100) ([-1, -1], [1, -1], [1, -1])$ to $d_3(-10 - 1) ([-1, -1], [1, -1], [-1, -1])$
 to
 $d_3(-10 - 1) ([-1, -1], [1, -1], [-1, -1])$ to $d_4(-100) ([-1, -1], [1, -1], [1, -1])$ to
 $d_9(-110) ([-1, -1], [1, 1], [1, -1])$ to $d_3(010) ([1, -1], [1, 1], [1, -1])$
 to IIIB2
 $d_4(011) ([1, -1], [1, 1], [1, 1])$ to $d_3(010) ([1, -1], [1, 1], [1, -1])$ to
 $d_9(-110) ([-1, -1], [1, 1], [1, -1])$ to $d_4(-100) ([-1, -1], [1, -1], [1, -1])$
 to IIID
 $d_4(-100) ([-1, -1], [1, -1], [1, -1])$ to $d_9(-110) ([-1, -1], [1, 1], [1, -1])$ to
 $d_{16}(-111) ([-1, -1], [1, 1], [1, 1])$ to $d_4(011) ([1, -1], [1, 1], [1, 1])$

to IVC

$d_4(011)$ $([-1, 1], [1, 1], [1, 1])$ to $d_{16}(-111)$ $([-1, -1], [1, 1], [1, 1])$ to
 $d_{10}(-101)$ $([-1, -1], [-1, 1], [1, 1])$ to $d_4(-100)$ $([-1, -1], [-1, 1], [-1, 1])$

to IVB1

$d_4(-100)$ $([-1, -1], [-1, 1], [-1, 1])$ to $d_{10}(-101)$ $([-1, -1], [-1, 1], [1, 1])$ to
 $d_5(001)$ $([-1, 1], [-1, 1], [1, 1])$ to $d_4(011)$ $([-1, 1], [1, 1], [1, 1])$

to

$d_4(011)$ $([-1, 1], [1, 1], [1, 1])$ to $d_5(001)$ $([-1, 1], [-1, 1], [1, 1])$ to
 $d_{10}(-101)$ $([-1, -1], [-1, 1], [1, 1])$ to $d_4(-100)$ $([-1, -1], [-1, 1], [-1, 1])$

to IVB2

$d_5(-1 - 10)$ $([-1, -1], [-1, -1], [-1, 1])$ to $d_4(-100)$ $([-1, -1], [-1, 1], [-1, 1])$ to
 $d_{10}(-101)$ $([-1, -1], [-1, 1], [1, 1])$ to $d_5(001)$ $([-1, 1], [-1, 1], [1, 1])$

to IVD

$d_5(001)$ $([-1, 1], [-1, 1], [1, 1])$ to $d_{10}(-101)$ $([-1, -1], [-1, 1], [1, 1])$ to
 $d_{17}(-1 - 11)$ $([-1, -1], [-1, -1], [1, 1])$ to $d_5(-1 - 10)$ $([-1, -1], [-1, -1], [-1, 1])$

to VC

$d_5(-1 - 10)$ $([1, 1], [-1, -1], [1, -1])$ to $d_{17}(-1 - 11)$ $([-1, -1], [-1, -1], [1, 1])$ to
 $d_{11}(0 - 11)$ $([1, -1], [-1, -1], [1, 1])$ to $d_5(001)$ $([1, -1], [1, -1], [1, 1])$

to VB1

$d_5(001)$ $([1, -1], [1, -1], [1, 1])$ to $d_{11}(0 - 11)$ $([1, -1], [-1, -1], [1, 1])$ to
 $d_6(0 - 10)$ $([1, -1], [-1, -1], [1, -1])$ to $d_5(-1 - 10)$ $([-1, -1], [-1, -1], [1, -1])$

to

$d_5(-1 - 10)$ $([-1, -1], [-1, -1], [1, -1])$ to $d_6(0 - 10)$ $([1, -1], [-1, -1], [1, -1])$ to
 $d_{11}(0 - 11)$ $([1, -1], [-1, -1], [1, 1])$ to $d_5(001)$ $([1, -1], [1, -1], [1, 1])$

to VB2

$d_6(101)$ $([1, 1], [1, -1], [1, 1])$ to $d_5(001)$ $([1, -1], [1, -1], [1, 1])$ to
 $d_{11}(0 - 11)$ $([1, -1], [-1, -1], [1, 1])$ to $d_6(0 - 10)$ $([1, -1], [-1, -1], [1, -1])$

to VD

$d_6(0 - 10)$ $([1, -1], [-1, -1], [1, -1])$ to $d_{11}(0 - 11)$ $([1, -1], [-1, -1], [1, 1])$ to
 $d_{18}(1 - 11)$ $([1, 1], [-1, -1], [1, 1])$ to $d_6(101)$ $([1, 1], [1, -1], [1, 1])$

to VIC

$d_6(101)$ $([1, 1], [-1, 1], [1, 1])$ to $d_{18}(1 - 11)$ $([1, 1], [-1, -1], [1, 1])$ to
 $d_{12}(1 - 10)$ $([1, 1], [-1, -1], [-1, 1])$ to $d_6(0 - 10)$ $([-1, 1], [-1, -1], [-1, 1])$

to VIB1

$d_6(0 - 10)$ $([-1, 1], [-1, -1], [-1, 1])$ to $d_{12}(1 - 10)$ $([1, 1], [-1, -1], [-1, 1])$ to
 $d_1(100)$ $([1, 1], [-1, 1], [-1, 1])$ to $d_6(101)$ $([1, 1], [-1, 1], [1, 1])$

to

$d_6(101)$ $([1, 1], [-1, 1], [1, 1])$ to $d_1(100)$ $([1, 1], [-1, 1], [-1, 1])$ to

$d_{12}(1-10) ([1, 1], [-1, -1], [-1, 1])$ to $d_6(0-10) ([-1, 1], [-1, -1], [-1, 1])$
 to VIB2
 $d_1(0-1-1) ([-1, 1], [-1, -1], [-1, -1])$ to $d_6(0-10) ([-1, 1], [-1, -1], [-1, 1])$ to
 $d_{12}(1-10) ([1, 1], [-1, -1], [-1, 1])$ to $d_1(100) ([1, 1], [-1, 1], [-1, 1])$
 to VID
 $d_1(100) ([1, 1], [-1, 1], [-1, 1])$ to $d_{12}(1-10) ([1, 1], [-1, -1], [-1, 1])$ to
 $d_{13}(1-1-1) ([1, 1], [-1, -1], [-1, -1])$ to $d_1(0-1-1) ([-1, 1], [-1, -1], [-1, -1])$

E.7.3 First Combination for reference vector moving through region A

IA

$d_1(100) ([1, 1], [1, -1], [1, -1])$ to $d_0(000) ([1, -1], [1, -1], [1, -1])$ to $d_2(00-1) ([1, -1], [1, -1], [-1, -1])$
 to $d_1(0-1-1) ([1, -1], [-1, -1], [-1-1])$

to

$d_1(0-1-1) ([1, -1], [-1, -1], [-1-1])$ to $d_2(00-1) ([1, -1], [1, -1], [-1, -1])$ to $d_0(000) ([1, -1], [1, -1], [1, -1])$
 to $d_1(100) ([1, 1], [1, -1], [1, -1])$

to IA2

$d_2(110) ([1, 1], [1, 1], [1, -1])$ to $d_1(100) ([1, 1], [1, -1], [1, -1])$ to $d_0(000) ([1, -1], [1, -1], [1, -1])$
 to $d_2(00-1) ([1, -1], [1, -1], [-1-1])$

to IIA1

$d_2(00-1) ([1, -1], [1, -1], [-1, -1])$ to $d_0(000) ([1, -1], [1, -1], [1, -1])$ to
 $d_3(010) ([1, -1], [1, 1], [1, -1])$ to $d_2(110) ([1, 1], [1, 1], [1, -1])$ to
 $d_2(110) ([1, 1], [1, 1], [1, -1])$ to $d_3(010) ([1, -1], [1, 1], [1, -1])$ to
 $d_0(000) ([1, -1], [1, -1], [1, -1])$ to $d_2(00-1) ([1, -1], [1, -1], [-1, -1])$

to IIA2

$d_3(-10-1) ([-1, -1], [1, -1], [-1, -1])$ to $d_2(00-1) ([1, -1], [1, -1], [-1, -1])$ to
 $d_0(000) ([1, -1], [1, -1], [1, -1])$ to $d_3(010) ([1, -1], [1, 1], [1, -1])$

to IIIA1

$d_3(010) ([1, -1], [1, 1], [1, -1])$ to $d_0(000) ([1, -1], [1, -1], [1, -1])$ to
 $d_4(-100) ([-1, -1], [1, -1], [1, -1])$ to $d_3(-10-1) ([-1, -1], [1, -1], [-1, -1])$ to
 $d_3(-10-1) ([-1, -1], [1, -1], [-1, -1])$ to $d_4(-100) ([-1, -1], [1, -1], [1, -1])$ to
 $d_0(000) ([1, -1], [1, -1], [1, -1])$ to $d_3(010) ([1, -1], [1, 1], [1, -1])$

to IIIA2

$d_4(011) ([1, -1], [1, 1], [1, 1])$ to $d_3(010) ([1, -1], [1, 1], [1, -1])$ to
 $d_0(000) ([1, -1], [1, -1], [1, -1])$ to $d_4(-100) ([-1, -1], [1, -1], [1, -1])$

to IVA1

$d_4(-100) ([-1, -1], [-1, 1], [-1, 1])$ to $d_0(000) ([-1, 1], [-1, 1], [-1, 1])$ to

$d_5(001)$ $([-1, 1], [-1, 1], [1, 1])$ to $d_4(011)$ $([-1, 1], [1, 1], [1, 1])$ to
 $d_4(011)$ $([-1, 1], [1, 1], [1, 1])$ to $d_5(001)$ $([-1, 1], [-1, 1], [1, 1])$ to
 $d_0(000)$ $([-1, 1], [-1, 1], [-1, 1])$ to $d_4(-100)$ $([-1, -1], [-1, 1], [-1, 1])$
to IVA2
 $d_5(-1-10)$ $([-1, -1], [-1, -1], [-1, 1])$ to $d_4(-100)$ $([-1, -1], [-1, 1], [-1, 1])$ to
 $d_0(000)$ $([-1, 1], [-1, 1], [-1, 1])$ to $d_5(001)$ $([-1, 1], [-1, 1], [1, 1])$
to VA1
 $d_5(001)$ $([-1, 1], [-1, 1], [1, 1])$ to $d_0(000)$ $([-1, 1], [-1, 1], [-1, 1])$ to
 $d_6(0-10)$ $([-1, 1], [-1, -1], [-1, 1])$ to $d_5(-1-10)$ $([-1, -1], [-1, -1], [-1, 1])$ to
 $d_5(-1-10)$ $([-1, -1], [-1, -1], [-1, 1])$ to $d_6(0-10)$ $([-1, 1], [-1, -1], [-1, 1])$ to
 $d_0(000)$ $([-1, 1], [-1, 1], [-1, 1])$ to $d_5(001)$ $([-1, 1], [-1, 1], [1, 1])$
to VA2
 $d_6(101)$ $([1, 1], [-1, 1], [1, 1])$ to $d_5(001)$ $([-1, 1], [-1, 1], [1, 1])$ to
 $d_0(000)$ $([-1, 1], [-1, 1], [-1, 1])$ to $d_6(0-10)$ $([-1, 1], [-1, -1], [-1, 1])$
to VIA1
 $d_6(0-10)$ $([-1, 1], [-1, -1], [-1, 1])$ to $d_0(000)$ $([-1, 1], [-1, 1], [-1, 1])$ to
 $d_1(100)$ $([1, 1], [-1, 1], [-1, 1])$ to $d_6(101)$ $([1, 1], [-1, 1], [1, 1])$ to
 $d_6(101)$ $([1, 1], [-1, 1], [1, 1])$ to $d_1(100)$ $([1, 1], [-1, 1], [-1, 1])$ to
 $d_0(000)$ $([-1, 1], [-1, 1], [-1, 1])$ to $d_6(0-10)$ $([-1, 1], [-1, -1], [-1, 1])$
to VIA2
 $d_1(0-1-1)$ $([-1, 1], [-1, -1], [-1, -1])$ to $d_6(0-10)$ $([-1, 1], [-1, -1], [-1, 1])$ to
 $d_0(000)$ $([-1, 1], [-1, 1], [-1, 1])$ to $d_1(100)$ $([1, 1], [-1, 1], [-1, 1])$

E.7.4 Third Combination for reference vector moving through region A

IA
 $d_1(100)$ $([1, 1], [1, -1], [1, -1])$ to $d_0(000)$ $([1, -1], [1, -1], [1, -1])$ to $d_2(00-1)$ $([1, -1], [1, -1], [-1, -1])$
to $d_1(0-1-1)$ $([1, -1], [-1, -1], [-1, -1])$
to
 $d_1(0-1-1)$ $([1, -1], [-1, -1], [-1, -1])$ to $d_2(00-1)$ $([1, -1], [1, -1], [-1, -1])$ to $d_0(000)$ $([1, -1], [1, -1], [1, -1])$
to $d_1(100)$ $([1, 1], [1, -1], [1, -1])$
to IA2
 $d_2(110)$ $([1, 1], [1, 1], [1, -1])$ to $d_1(100)$ $([1, 1], [1, -1], [1, -1])$ to $d_0(000)$ $([1, -1], [1, -1], [1, -1])$
to $d_2(00-1)$ $([1, -1], [1, -1], [-1, -1])$
to IIA1
 $d_2(00-1)$ $([-1, 1], [-1, 1], [-1, -1])$ to $d_0(000)$ $([-1, 1], [-1, 1], [-1, 1])$ to
 $d_3(010)$ $([-1, 1], [1, 1], [-1, 1])$ to $d_2(110)$ $([1, 1], [1, 1], [-1, 1])$ to

$d_2(110)$ $([1, 1], [1, 1], [-1, 1])$ to $d_3(010)$ $([-1, 1], [1, 1], [-1, 1])$ to
 $d_0(000)$ $([-1, 1], [-1, 1], [-1, 1])$ to $d_2(00 - 1)$ $([-1, 1], [-1, 1], [-1, -1])$
to IIA2
 $d_3(-10 - 1)$ $([-1, -1], [-1, 1], [-1, -1])$ to $d_2(00 - 1)$ $([-1, 1], [-1, 1], [-1, -1])$ to
 $d_0(000)$ $([-1, 1], [-1, 1], [-1, 1])$ to $d_3(010)$ $([-1, 1], [1, 1], [-1, 1])$
to IIIA1
 $d_3(010)$ $([1, -1], [1, 1], [1, -1])$ to $d_0(000)$ $([1, -1], [1, -1], [1, -1])$ to
 $d_4(-100)$ $([-1, -1], [1, -1], [1, -1])$ to $d_3(-10 - 1)$ $([-1, -1], [1, -1], [-1, -1])$ to
 $d_3(-10 - 1)$ $([-1, -1], [1, -1], [-1, -1])$ to $d_4(-100)$ $([-1, -1], [1, -1], [1, -1])$ to
 $d_0(000)$ $([1, -1], [1, -1], [1, -1])$ to $d_3(010)$ $([1, -1], [1, 1], [1, -1])$
to IIIA2
 $d_4(011)$ $([1, -1], [1, 1], [1, 1])$ to $d_3(010)$ $([1, -1], [1, 1], [1, -1])$ to
 $d_0(000)$ $([1, -1], [1, -1], [1, -1])$ to $d_4(-100)$ $([-1, -1], [1, -1], [1, -1])$
to IVA1
 $d_4(-100)$ $([-1, -1], [-1, 1], [-1, 1])$ to $d_0(000)$ $([-1, 1], [-1, 1], [-1, 1])$ to
 $d_5(001)$ $([-1, 1], [-1, 1], [1, 1])$ to $d_4(011)$ $([-1, 1], [1, 1], [1, 1])$ to
 $d_4(011)$ $([-1, 1], [1, 1], [1, 1])$ to $d_5(001)$ $([-1, 1], [-1, 1], [1, 1])$ to
 $d_0(000)$ $([-1, 1], [-1, 1], [-1, 1])$ to $d_4(-100)$ $([-1, -1], [-1, 1], [-1, 1])$
to IVA2
 $d_5(-1 - 10)$ $([-1, -1], [-1, -1], [-1, 1])$ to $d_4(-100)$ $([-1, -1], [-1, 1], [-1, 1])$ to
 $d_0(000)$ $([-1, 1], [-1, 1], [-1, 1])$ to $d_5(001)$ $([-1, 1], [-1, 1], [1, 1])$
to VA1
 $d_5(001)$ $([1, -1], [1, -1], [1, 1])$ to $d_0(000)$ $([1, -1], [1, -1], [1, -1])$ to
 $d_6(0 - 10)$ $([1, -1], [-1, -1], [1, -1])$ to $d_5(-1 - 10)$ $([-1, -1], [-1, -1], [1, -1])$ to
 $d_5(-1 - 10)$ $([-1, -1], [-1, -1], [1, -1])$ to $d_6(0 - 10)$ $([1, -1], [-1, -1], [1, -1])$ to
 $d_0(000)$ $([1, -1], [1, -1], [1, -1])$ to $d_5(001)$ $([1, -1], [1, -1], [1, 1])$
to VA2
 $d_6(101)$ $([1, 1], [1, -1], [1, 1])$ to $d_5(001)$ $([1, -1], [1, -1], [1, 1])$ to
 $d_0(000)$ $([1, -1], [1, -1], [1, -1])$ to $d_6(0 - 10)$ $([1, -1], [-1, -1], [1, -1])$
to VIA1
 $d_6(0 - 10)$ $([-1, 1], [-1, -1], [-1, 1])$ to $d_0(000)$ $([-1, 1], [-1, 1], [-1, 1])$ to
 $d_1(100)$ $([1, 1], [-1, 1], [-1, 1])$ to $d_6(101)$ $([1, 1], [-1, 1], [1, 1])$ to
 $d_6(101)$ $([1, 1], [-1, 1], [1, 1])$ to $d_1(100)$ $([1, 1], [-1, 1], [-1, 1])$ to
 $d_0(000)$ $([-1, 1], [-1, 1], [-1, 1])$ to $d_6(0 - 10)$ $([-1, 1], [-1, -1], [-1, 1])$
to VIA2
 $d_1(0 - 1 - 1)$ $([-1, 1], [-1, -1], [-1, -1])$ to $d_6(0 - 10)$ $([-1, 1], [-1, -1], [-1, 1])$ to
 $d_0(000)$ $([-1, 1], [-1, 1], [-1, 1])$ to $d_1(100)$ $([1, 1], [-1, 1], [-1, 1])$